Manitoba
Energy and Mines
Geological Services

Geological Report GR 87-1

Geology of the Flin Flon-White Lake Area

By A.H. Bailes and E.C. Syme

Winnipeg, 1989

Energy and Mines

Hon. Harold J. Neufeld
Minister

Ian Haugh
Deputy Minister

Minerals Division

Sobharam Singh
Assistant Deputy Minister

Geological Services
W.D. McRitchie
Director

90-02362/

TABLE OF CONTENTS

Page

INTRODUCTION 1
  GEOLOGICAL SETTING 1
  TERMINOLOGY 3
  PREVIOUS WORK 3
  PRESENT WORK AND ACKNOWLEDGEMENTS 4
  REPORT STRUCTURE 5

BEAR LAKE BLOCK 6
  INTRODUCTION 6
  BEAR LAKE BASALTIC ANDESITE (UNIT 1) 6
    Introduction 6
    Flows 7
      Flow organization 7
      Primary structures in flows 7
      Petrography of flows 16
      Stratigraphic variation in flow type and thickness 18
    Pillow fragment breccias 20
    Synvolcanic sills, dykes and irregular bodies 23
    Alteration and deformation 26
    Geochemistry 26
    Interpretation 29
  HETEROLITHOLOGIC BRECCIA, LAPILLI TUFF, TUFF (UNIT 30) 29
    Interpretation 29
  SOLODIUK LAKE RHYOLITE (UNIT 13) 29
    Interpretation 31
  WHITE LAKE DACITIC TUFF (UNIT 26) 31
    Unit 26a: Dacitic tuff with weakly defined layering 32
    Unit 26b: Pumice-block-bearing dacitic tuff and tuff breccia 32
    Unit 26c: Reworked dacitic tuff or greywacke 32
    Unit 26d: Dacitic tuff with sporadic pumice clasts 33
    Interpretation 33
  LITTLE SPRUCE LAKE ANDESITIC LAPILLI TUFF (UNIT 24) 33
    Interpretation 34
  MUDSTONE, MASSIVE SULPHIDE (UNIT 36) 34
  TWO PORTAGE LAKE FERROBASALT (UNIT 5) 34
    Geochemistry 34
    Interpretation 37
  TWO PORTAGE LAKE RHYOLITE CRYSTAL TUFF (UNIT 27) 37
    Interpretation 38
  VICK LAKE ANDESITIC TUFF (UNIT 25) 38
    Petrography 40
      Shards 40
      Pumice 40
      Plagioclase crystals and crystal fragments 40
      Brown "vitric" microclasts 40
      Microlitic lithics 40
      Amphibole crystals 40
      Recrystallized matrix 40
    Bedforms 40
    Members 42
    Deformation structures 53
    Geochemistry 53
    Interpretation 53
  DACITE, TUFF (UNITS 18a and 28b) 53

Page
INTERMEDIATE TUFF, BRECCIA (UNIT 29), MAFIC FLOWS (UNIT 7) 54
VOLCANIC RECONSTRUCTION OF THE BEAR LAKE BLOCK 54
Shield building stage 54
Rhyolite volcanism and deposition of volcaniclastics 55
Ferrobasalt lava plain 55
Andesitic phreatomagmatic and plinian eruptions 56

SCOTTY LAKE BLOCK 57
INTRODUCTION 57
FELSIC VOLCANIC ROCKS (UNIT 18) 57
SCOTTY LAKE BASALT (UNIT 4) 57
Flows 57
Petrography of flows 65
Synvolcanic dykes, sills and related intrusions 65
Minor units 66
Geochemistry 76
Interpretation 76
NORTHEAST ARM MAFIC VOLCANICLASTIC ROCKS (UNIT 19) 78
Interpretation 79
MAFIC MUDSTONE AND WACKE, BASALT, GABBRO (UNIT 34a) 79
ANKERITE-QUARTZ-CHLORITE-SERICITE SCHIST (UNIT 37a) 81
MUDSTONE, SILTSTONE, GREYWACKE (UNIT 33) 81
SUMMARY 81

WHITEFISH LAKE-MIKANAGAN LAKE BLOCK 84
INTRODUCTION 84
BASALTS (UNITS 7 and 9) 84
MIKANAGAN LAKE MAFIC VOLCANICLASTIC ROCKS (UNIT 20) 84
Tuff (units 20a and 20b) 84
Lapilli tuff and tuff breccia (unit 20c) 84
Interpretation 84
INTERMEDIATE TO MAFIC TUFF, LAPILLI TUFF, TUFF BRECCIA (UNITS 21 and 22) 88
Sawmill Lake 88
North Star Road 88
Other occurrences 88
DACITE, RHYOLITE (UNIT 18a) 89
NORTH STAR ROAD VOLCANIC CONGLOMERATE (UNIT 31) 89
Interpretation 91
GREYWACKE, SILTSTONE, MUDSTONE (UNITS 33 and 34) 91
VOLCANIC ENVIRONMENT 91

BAKERS NARROWS BLOCK 93
INTRODUCTION 93
BASALT, BASALTIC ANDESITE (UNITS 7-9) 93
Unit B_A (Thompson Bay basalt) 93
Unit B_B (Wright Bay basalt) 93
Unit B_C 95
Unit B_D (Sharpe Bay basalt) 95
Unit B_E 96
Geochemistry 96
FELSIC FLOWS (UNIT 18) 96
Unit F_A (Wright Bay rhyolite) 96
Unit F_B 96
Unit F_C 97
Unit F_D (Sharpe Bay rhyolite) 97
Interpretation 99
INTERPRETATION 99

SOURDOUGH BAY BLOCK 100
INTRODUCTION 100
MAFIC TO INTERMEDIATE FLOWS AND PILLOW FRAGMENT BRECCIA (UNITS 7-9) 100
Southern section 100
Northern section 100

Page
PLAGIOCLASE-QUARTZ-PHYRIC INTERMEDIATE FLOWS (UNIT 12) 100
PLAGIOCLASE CRYSTAL-RICH MAFIC TUFF AND LAPILLI TUFF (UNITS 22a and 21b) 100
BAKER PATTON FELSIC COMPLEX (UNIT 17) 101
  Tuff, lapilli tuff (unit 17a) 102
  Undivided massive felsic rocks and possible flows (unit 17b) 102
  Felsic dykes (unit 17c) 102
  Interpretation 102
FELSIC VOLCANIC ROCKS (UNITS 18 and 28) 102
VOLCANICLASTIC AND SEDIMENTARY ROCKS (UNITS 29, 30, 33, 36 and 38) 103
  Northern section 103
  Southern section 103
  Interpretation 104
VOLCANIC ENVIRONMENT 104

GRASSY NARROWS ZONE 105
INTRODUCTION 105
GRASSY NARROWS BASALT (UNITS 7 and 8) 105
  Geochemistry 105
  Interpretation 108
RHYOLITE (UNIT 18) 108
  Northern body 108
  Southern body 110
  Other rhyolite bodies 110
SILTSTONE, GREYWACKE (UNIT 33) 110
FELSIC SANDSTONE AND PEBBLE CONGLOMERATE (UNIT 32) 114

MANISTIKWAN LAKE BLOCK 115
INTRODUCTION 115
STEEVES LAKE PORTION 115
  Mafic flows and related rocks (unit 7) 115
  Pyritic mudstone (unit 36) 115
  Felsic sandstone, pebbly conglomerate, pyritic mudstone (units 32 and 36) 115
BIG ISLAND PORTION 115
  Pillow fragment breccia (unit 8a) 115
  Porphyritic basalt and basaltic andesite (unit 8) 117
SUMMARY 117

COPE LAKE BLOCK 119
INTRODUCTION 119
MAFIC FLOWS 119
  Aphyric to sparsely porphyritic flows (unit 7) 119
  Strongly porphyritic flows (unit 9) 119
  Aphyric to sparsely porphyritic flows (units 7 and 9) 119
  Strongly porphyritic flows (units 8 and 9) 119
  Aphyric flows (unit 7) 119
  Porphyritic flows (unit 8) 119
SUMMARY 119

HOOK LAKE BLOCK 120
INTRODUCTION 120
PLAGIOCLASE-PHYRIC PILLOW FRAGMENT BRECCIA (A) 121
APHYRIC BASALTIC ANDESITE (B) 121
PORPHYRITIC MAFIC FLOWS (C) 122
PORPHYRITIC PILLOW FRAGMENT BRECCIA (D) 122
APHYRIC AND SPARSELY PORPHYRITIC BASALT (E) 124
PORPHYRITIC SCORIA TUFF AND BRECCIA, PORPHYRITIC FLOWS (F) 124
PLAGIOCLASE-PHYRIC MAFIC FLOWS (G) 126
SCORIA TUFF AND BRECCIA (H) 126
APHYRIC BASALT (I) 126
PORPHYRITIC BASALT FLOWS, SCORIA TUFF, PILLOW FRAGMENT BRECCIA (J) 128
PLAGIOCLASE-GLOMEROPHYRIC MAFIC TO INTERMEDIATE FLOWS (K) 128
APHYRIC TO SPARSELY PORPHYRITIC BASALT (L) 128

Page
PLAGIOCLASE-GLOMEROPHYRIC BASALTIC ANDESITE AND ANDESITE (M) 133
SCHIST LAKE SECTION 133
GRANT LAKE SECTION 135
SUMMARY AND INTERPRETATION 135

FLIN FLON BLOCK 137
INTRODUCTION 137
HAPNOT LAKE SUB-BLOCK 137
South Main basalt (unit 6) 137
Flows (unit 6a) 137
Pillow fragment breccia (unit 6b) 137
Plagioclase-phyric mafic volcaniclastic rocks (unit 22) 142
South Main rhyolite domes (unit 16) 145
Mine rhyolite (unit 15) 145
Railway volcaniclastic rocks (unit 30a) 146
Hidden Lake-Burley Lake mafic flows (units 2 and 3) 146
Hidden Lake basalt (unit 2) 147
Burley Lake basaltic andesite (unit 3) and related rocks 148
Geochemistry 151
Summary and interpretation 151
MANDY SUB-BLOCK 153
Basalt, basaltic andesite (units 3 and 7) 154
Pillow fragment breccia (units 3c and 11) 154
Heterolithologic breccia (units 29 and 30) 156
Mafic scoria-rich tuff and tuff breccia (unit 23b) 157
Stitt Island dacite (unit 14) 157
Volcaniclastic sedimentary rocks (units 33 and 34) 157
Geochemistry and summary 158
LEDGE LAKE SUB-BLOCK 160
Plagioclase-glomerophyric mafic flows (unit 10) 160
Aphyric mafic flows (unit 7) 160
Rhyolite (unit 18) 160
GREEN LAKE SUB-BLOCK 161
Mafic flows 161
Mafic tuff and lapilli tuff 162
Sedimentary rocks 162
MITT LAKE SUB-BLOCK 162
RAILWAY LINE SUB-BLOCK 163
Mafic volcaniclastic rocks and sediments (units 22b, 23b and 33) 163
Aphyric mafic flows (unit 7) 163
Pillow fragment breccia, pillowed flows (units 7a and 8b) 164
Mafic scoria-rich tuff and tuff breccia (unit 23b) 164
FLIN FLON BLOCK: SUMMARY AND COMPARISON TO OTHER BLOCKS 169

AMISK GROUP GEOCHEMISTRY 170
TECTONIC SETTING 172

PRE-MISSI INTRUSIVE ROCKS, INTRUSIONS OF UNKNOWN AGE 175
INTRODUCTION 175
WHITE LAKE SILL AND RELATED INTRUSIONS (UNIT 39) 175
White Lake Sill 175
Brown gabbro (unit 39a) 177
Green ferrogabbro (unit 39b) 177
Ferrodiorite, quartz ferrodiorite, tonalite (unit 39c) 178
Pyroxene-phyric gabbro (unit 39d) 178
Johnson Lake Sill 178
Brown gabbro (unit 39a) 179
Green ferrogabbro, ferrodiorite (unit 39b) 179
Geochemistry 179
WHITEFISH LAKE MAFIC INTRUSIONS (UNIT 40) 180
One Portage Lake Intrusion 180
Wehrlite (unit 40a) 180

Page
Pyroxenite (unit 40b) ... 180
Gabbro (unit 40c) ... 181
Quartz diorite (unit 40d) ... 181
South Whitefish Lake Intrusion ... 181
MIKANAGAN LAKE SILL AND RELATED INTRUSIONS (UNIT 41) ... 181
Mikanagan Lake Sill ... 184
Gabbronorite zone (unit 41a) ... 185
Gabbro zone (unit 41b) ... 185
Oikocrystic gabbronorite zone (unit 41c) ... 185
Transition gabbro (unit 41d), gabbro pegmatite (unit 41e) zone ... 187
Ferrogabbro zone (unit 41f) ... 189
Quartz ferrodiorite, ferrotonalite zone (unit 41g) ... 189
Micrographic leucotonalite zone (unit 41h) ... 192
Upper margin zone (unit 41i) ... 192
Recrystallized country rocks ... 192
Geochemistry ... 193
Benn Lake Intrusion ... 193
Contact relationships ... 193
Gabbronorite (unit 41a) ... 199
Gabbro (unit 41b) ... 200
Oikocrystic gabbronorite ... 200
Geochemistry ... 200
Hook Lake Intrusion ... 200
Shore Lake Intrusions ... 202
Embury Lake Intrusion ... 202
GABBRO, DIORITE, QUARTZ DIORITE (UNIT 42) ... 202
ROSENBERG LAKE INTRUSIVE COMPLEX (UNIT 43) ... 203
CHANNING TONALITE (UNIT 44) ... 208
CLIFF LAKE PLUTON (UNIT 45) ... 208
Quartz diorite (unit 45a) ... 209
Quartz-phyric tonalite with abundant large xenoliths (unit 45b) ... 209
Quartz-phyric tonalite with abundant small, highly digested xenoliths (unit 45c) ... 212
Quartz-phyric leucotonalite and micrographic leucotonalite with few small, highly assimilated xenoliths (unit 45d) ... 212
Fine grained, quartz-phyric micrographic tonalite (unit 45e) ... 212
Leucotonalite marginal phase (unit 45f) ... 214
Micrographic aplite dykes ... 214
Post-Cliff Lake Pluton mafic intrusive rocks ... 214
Geochemistry ... 214
TONALITE, LEUCOTONALITE (UNIT 46) ... 216
CENTENNIAL MINE LEUCOGRANITE/LEUCOGRANODIORITE (UNIT 47) ... 216
QUARTZ PORPHYRY, QUARTZ-PLAGIOCLASE PORPHYRY (UNIT 48) ... 216
Quartz porphyry (unit 48a) ... 216
Quartz-plagioclase porphyry (unit 48b) ... 216
RHYOLITE (UNIT 49) ... 217
Borne Lake rhyolite ... 217
Hook Lake area ... 217
South of Cliff Lake Pluton ... 219
Steeves Lake area ... 219
AGE RELATIONSHIPS ... 219
Manistikwan Lake, Hook Lake and Cope Lake Blocks ... 219
Bear Lake Block ... 220
Scotty Lake Block ... 224
Whitefish-Mikanagan Lakes Block, Sourdough Bay Block ... 224

MISSI GROUP ... 225
INTRODUCTION ... 225
RELATIONSHIP TO AMISK GROUP AND CONTAINED INTRUSIONS ... 225
STRATIGRAPHY OF THE MISSI GROUP ... 225
PROVENANCE ... 237
INTERPRETATION ... 239

Page
POST-MISSI INTRUSIVE ROCKS 243
  MELADIORITE AND PYROXENITE (BOUNDARY INTRUSIONS) (UNIT 51) 243
  PYROXENITE DYKES (UNIT 52) 243
  GABBRO, DIORITE, QUARTZ DIORITE (UNIT 53) 243
  WHITEFISH LAKE QUARTZ MONZODIORITE AND RELATED INTRUSIONS (UNIT 54) 243
    Whitefish Lake quartz monzodiorite (unit 54a) 243
    Related intrusions 245
  QUARTZ-MEGACRYSTIC TONALITE (UNIT 55) 245
  QUARTZ-PLAGIOCLASE PORPHYRY DYKES (UNIT 56) 245
  PORPHYRITIC GRANODIORITE (UNIT 57) 246

FOLDS 247
  INTRODUCTION 247
  BURLEY LAKE SYNCLINE 247
  COPE LAKE SYNCLINE 247
  HIDDEN LAKE SYNFORM 247
  NORTHEAST ARM SYNCLINE 252
  MILLIKEN LAKE SYNCLINE 254
  FOLDS SOUTHEAST OF STITT ISLAND 255

FAULTS 256
  INTRODUCTION 256
  BLOCK-BOUNDING FAULTS 256
    Cliff Lake Fault 256
    Manistikwan Lake Fault 257
    Big Island Fault 257
    Rosenberg Lake Fault 257
    Inlet Arm Fault 257
    Northeast Arm Fault 257
    Boundary between Scotty Lake and Whitefish-Mikanagan Lakes Blocks 258
    Sourdough Bay Fault 258
    North Arm Fault 258
  INTERNAL FAULTS 258
    Flin Flon Block 258
    Hook Lake Block 259
    Manistikwan Lake Block 260
    Grassy Narrows Zone 260
    Bear Lake Block 260
    Scotty Lake Block 260
    Whitefish-Mikanagan Lakes Block 261

METAMORPHISM 262
  INTRODUCTION 262
  CONTACT METAMORPHISM 262
  REGIONAL METAMORPHISM 262
    Subgreenschist facies (prehnite-pumpellyite) 262
    Lower greenschist facies 265
    Middle greenschist facies 265

ECONOMIC GEOLOGY 266
  INTRODUCTION 266
  VOLCANOGENIC MASSIVE SULPHIDE DEPOSITS 266
    Flin Flon Mine 266
    Schist Lake and Mandy mines 268
    Centennial Mine 268
    White Lake and Cuprus mines 268
    Other deposits and showings 271
  Cu-Mo MINERALIZATION IN FELSIC INTRUSIONS 271
    Whitefish Lake quartz monzodiorite 271
    Cliff Lake Pluton 272
  GOLD DEPOSITS 272
    Gold potential in the Flin Flon-White Lake area 272

Page
ALTERATION 272
CONTROLS ON DEPOSITION OF BASE METAL MASSIVE SULPHIDE DEPOSITS 275

REGIONAL CONSIDERATIONS 278
INTRODUCTION 278
AMISK LAKE 278
SNOW LAKE 278
SIGNIFICANCE OF FLIN FLON BELT IN TRANS-HUDSON OROGEN 278

REFERENCES 280

APPENDIX

TABLES OF PRECISIONS AND DETECTION LIMITS FOR ANALYSES 285
TABLE OF WHOLE ROCK CHEMICAL ANALYSES 287

FIGURES

Figure 1: Tectonic elements of the Trans-Hudson Orogen as exposed in northern Manitoba and Saskatchewan. 1

Figure 2: Location of the Flin Flon-White Lake area on a generalized geology map of north central Manitoba and Saskatchewan. . . . 2

Figure 3: Structural blocks, major faults and folds, and metamorphic isograds in the Flin Flon-White Lake area. 4

Figure 4: Mixture and end member terms for pyroclastic deposits and fragments (from Fisher, 1966) adopted for use in this report. . 5

Figure 5: Schematic diagram showing main stratigraphic elements of the Bear Lake Block. 6

Figure 6: Stratigraphic subdivisions, flow directions and areas of intense epidotization, Bear Lake basaltic andesite (unit 1). 7

Figure 7: Laminated interflow tuff or sediment between two Bear Lake basaltic andesite pillowed flows (unit 1). 8

Figure 8: Interpretation of the lateral facies sequence in an idealized subaqueous Bear Lake basaltic andesite flow. 8

Figure 9: Typical features and zonation in: (a) pillowed and (b) massive and compound Bear Lake basaltic andesite flows. 9

Figure 10: Sections from Bear Lake area showing organization and vertical sequence of typical Bear Lake basaltic andesite flows and stratified pillow fragment breccia. 10

Figure 11: Contact between massive part of a Bear Lake basaltic andesite flow (unit 1) and its amoeboid pillow breccia flow top. 11

Figure 12: Contact between massive division of a Bear Lake flow and overlying, amoeboid pillow (flow top) breccia. 11

Figure 13: Contact between pillowed division of a Bear Lake flow and the overlying, amoeboid pillow (flow top) breccia. 12

Figure 14: Spherulitic pillow, Bear Lake basaltic andesite (unit 1). 12

Figure 15: Involuted pillow with well developed quartz-filled radial pipe vesicles, Bear Lake basaltic andesite (unit 1a). 13

Figure 16: Bun-shaped pillow (unit 1a) with quartz-filled radial pipe vesicles around margin. 14

Figure 17: Concentration of large, oval, quartz-filled gas cavities near the top of a 4 m thick massive Bear Lake basaltic andesite flow (unit 1). 14

Figure 18: Pillow with radial and concentric contraction fractures, Bear Lake basaltic andesite (unit 1). 15

Figure 19: Radial contraction fractures perpendicular to concentric cooling cracks in a pillow, resulting in angular and wedge-shaped fracture-bounded domains. 15

Figure 20: Partly recrystallized Bear Lake basaltic andesite (unit 1) with well preserved plagioclase microlites. 16

Figure 21: Fan-radial epidote filling vesicles in Bear Lake basaltic andesite (unit 1). 17

Figure 22: Polymineralic amygdale in Bear Lake basaltic andesite flow (unit 1). 17

Figure 23: Flow thickness in zones 1, 2, 3 and 4 of the Bear Lake basaltic andesite. 19

Figure 24: Flow thickness, by flow type, in the lower (zones 1 and 2) and upper (zones 3 and 4) portions of Bear Lake basaltic andesite. 19

Figure 25: Frequency of flow types in zones 1, 2, 3 and 4 of the Bear Lake basaltic andesite. 19

Figure 26: Crudely stratified Bear Lake pillow fragment breccia (unit 1e). 20

Figure 27: Pillow fragment breccia (unit 1e). 21

Figure 28: Pillow fragment breccia (unit 1e). 21

Page

Figure 29: Pillow fragment breccia (unit 1e). 22

Figure 30: Intact complete pillow as clast in Bear Lake pillow fragment breccia (unit 1e). 22

Figure 31: Contact between a pillowed flow and overlying, redeposited, pillow fragment breccia. 23

Figure 32: Pillow fragment with curvilinear pillow margin and quartz-filled radial pipe vesicles, Bear Lake pillow breccia (unit 1e). 24

Figure 33: Stratified pillow fragment breccia (unit 1e) containing a large fragment of amoeboid pillow flow top breccia. 24

Figure 34: Synvolcanic dyke 17 cm wide cutting Bear Lake basaltic andesite (unit 1). 25

Figure 35: Rose diagram displaying the orientation of 80 synvolcanic dykes emplaced in Bear Lake basaltic andesite. 25

Figure 36: Synvolcanic mafic dyke (unit 1f) intruding Bear Lake basaltic andesite flow-top breccia (unit 1). 26

Figure 37: Banded epidosite derived from pillowed Bear Lake basaltic andesite. 27

Figure 38: Tectonically flattened epidosite-bearing Bear Lake pillowed flow (unit 1). 27

Figure 39: Illustrations showing tectonite structures developed during strong flattening of more altered Bear Lake pillowed flows containing rigid epidosite domains. 28

Figure 40: FeO*/MgO vs. SiO_2 and MgO vs. SiO_2, Bear Lake basaltic andesite. 28

Figure 41: Jensen (1976) cation plot, Bear Lake basaltic andesite. 28

Figure 42: Element mobility during epidotization of Bear Lake basaltic andesite pillow. 29

Figure 43: Small irregular massive rhyolite lobes and intervening microbreccia in the subaqueous Solodiuk Lake rhyolite (unit 13). 31

Figure 44: Tectonically flattened pumice fragments in White Lake dacite tuff (unit 26b). 32

Figure 45: Tectonically flattened fragments in foliated Little Spruce Lake andesitic lapilli tuff (unit 24). 33

Figure 46: FeO*/MgO vs. SiO_2 and MgO vs. SiO_2 for the Two Portage Lake ferrobasalt. 35

Figure 47: TiO_2 vs. FeO*/MgO; Two Portage Lake ferrobasalt. 35

Figure 48: Jensen cation plot, Two Portage ferrobasalts. 35

Figure 49: Outcrop stratigraphy south of Two Portage Lake showing upper two-thirds of Two Portage Lake ferrobasalt and members 1 and 2 of Vick Lake andesitic tuff. 36

Figure 50: Photomicrograph of rhyolite crystal tuff (unit 27). 37

Figure 51: Three examples of bed organization displayed by rhyolite crystal tuff (unit 27) in Two Portage Lake area. 38

Figure 52: Distribution of stratigraphic members of the Vick Lake andesitic tuff. 39

Figure 53: Large shard displaying conchoidal boundaries cutting through vesicles. Vick Lake andesitic tuff. 41

Figure 54: Shard with one vesicle cut by a straight fracture boundary and another cut by a conchoidal fracture boundary, Vick Lake andesitic tuff. 42

Figure 55: Size, shape and distribution of pumice granules and plagioclase crystal fragments in a pumice-rich bed, member 2, Vick Lake andesitic tuff. 42

Figure 56: Long-tube pumice fragment in Vick Lake andesitic tuff. 43

Figure 57: Pumice fragment with high vesicularity, Vick Lake andesitic tuff. 43

Figure 58: Pumice granule replaced by mosaic of polygranular sutured quartz and albite, Vick Lake andesitic tuff. 44

Page

Figure 59: Plagioclase-phyric brown microlitic lithic granule in Vick Lake andesitic tuff. 44

Figure 60: Juvenile tan brown granule with irregular boundary dominated by vesicle margins, Vick Lake andesitic tuff. 45

Figure 61: Thickness of A division plotted against total bed thickness, Vick Lake andesitic tuff. 45

Figure 62: Bed organization and distribution of megascopic pumice granules and blocks in three thick beds, Vick Lake andesitic tuff. 46

Figure 63: Flame structures in Vick Lake andesitic tuff. 47

Figure 64: Photograph of bed shown in Fig. 65. 48

Figure 65: Vick Lake andesitic tuff bed with Bouma B, C and D divisions. 48

Figure 66: Single bed in Vick Lake andesitic tuff (unit 25e) with Bouma A, B, C, D and E divisions. 49

Figure 67: Sketch of Vick Lake andesitic tuff bed with Bouma A, B, C, D and E divisions. 49

Figure 68: Schematic diagram of typical Vick Lake andesitic tuff AB bed. 50

Figure 69: Disrupted pumice layer in very thick bedded Vick Lake andesitic tuff, member 5. 50

Figure 70: Height of pumice layers in A divisions, divided by thickness of A division, versus total bed thickness, Vick Lake andesite tuff. 51

Figure 71: Pumice-rich bed, Vick Lake andesitic tuff (unit 25c). 51

Figure 72: Pumice-rich bed, Vick lake andesitic tuff (unit 25c). 52

Figure 73: Thinly bedded mudstone, tuff and chert (unit 25d), Vick Lake andesitic tuff. 52

Figure 74: P_2O_5 vs. TiO_2, Vick Lake andesitic tuff. 53

Figure 75: Model for eruptive mechanism and depositional environment of the Vick Lake andesitic tuff (diagram after Heinrichs, 1984). 54

Figure 76: Reconstruction of stages of volcanic development of the Bear Lake Block sequence. 55

Figure 77: Distribution of massive and pillowed flows, Scotty Lake basalt. 58

Figure 78: Distribution of synvolcanic intrusions, Scotty Lake basalt. 59

Figure 79: Massive Scotty Lake basalt flow. 60

Figure 80: Tracing of polished slab of amoeboid pillow breccia taken from top of massive flow (Fig. 79), Scotty Lake basalt. 61

Figure 81: Photograph of part of polished slab traced in Figure 80. 61

Figure 82: Spherulites in interior of amoeboid pillow shown in Figures 80 and 81. 62

Figure 83: Spherulitic amoeboid pillow and its thermally shattered sideromelane rim, Scotty Lake basalt. 62

Figure 84: Outer part of thermally fractured rim on an amoeboid pillow transitional to matrix hyaloclastite, Scotty Lake basalt. 63

Figure 85: Schematic diagram of textures in a Cenozoic, palagonitized hyaloclastite granule. 63

Figure 86: Relict textures in pseudomorphed palagonite rims on an amoeboid pillow fragment in hyaloclastite, Scotty Lake basalt flow top. 64

Figure 87: Massive Scotty Lake basalt flow with flow top hyaloclastite and amoeboid pillows. 64

Figure 88: Distribution patterns of spherulites in the margins of pillows, Scotty Lake basalt. 65

Figure 89: Photomicrographs in Figures 89-93 show variation in texture across massive division of Scotty Lake basalt flow (Fig. 79). In this photomicrograph the chilled base of flow (C1) displays fine grained intergranular texture with elongate clinopyroxene pseudomorphs interstitial to randomly oriented tabular plagioclase. 67

Page

Figure 90: Lower part of flow (C3). Coarse intergranular texture with elongate, skeletal clinopyroxene pseudomorphs randomly oriented or in crude radiate arrays with plagioclase. 67

Figure 91: Interior of flow (C4). Fan-like arrays of plagioclase laths intergrown with skeletal clinopyroxene pseudomorphs. 68

Figure 92: Upper flow margin (C6). Intergranular texture with elongate clinopyroxene pseudomorphs and randomly oriented tabular plagioclase. 68

Figure 93: Chilled flow top (C7). (a) Random and branching, acicular and ornamented skeletal chains of clinopyroxene; (b) Detail of ornamented skeletal clinopyroxene chains in (a). 69

Figure 94: Linear chains of skeletal clinopyroxene crystals in chilled upper margin of massive Scotty Lake basalt flow 70

Figure 95: Intrafasciculate texture, Scotty Lake basalt. 71

Figure 96: Coarse fan spherulite of plagioclase (white) in massive Scotty Lake basalt. 71

Figure 97: Subophitic massive Scotty Lake basalt. 72

Figure 98: Intersertal texture, pillowed Scotty Lake basalt. 72

Figure 99: Interpillow hyaloclastite, Scotty Lake basalt. 73

Figure 100: Detail of internal structure of an interpillow hyaloclastite granule, Scotty Lake basalt. 74

Figure 101: Partly silicified hyaloclastite granules with relict textures of former palagonite, Scotty Lake basalt. 74

Figure 102: Replacement of palagonitized hyaloclastite granules by botryoidal saponite (pseudomorphed by chlorite and subsequent epidote). 75

Figure 103: Spherulites nucleated on perlitic cracks in a hyaloclastite granule. 75

Figure 104: Rose diagram of orientation of 34 synvolcanic dykes, Scotty Lake basalt. 76

Figure 105: FeO*/MgO vs. SiO_2 and MgO vs. SiO_2, Scotty Lake basalt. 76

Figure 106: TiO_2 vs. FeO*/MgO, Scotty Lake basalt. 77

Figure 107: Jensen cation plot, Scotty Lake basalt. 77

Figure 108: Element variation with stratigraphic elevation, Scotty Lake basalt. 78

Figure 109: Thin bedded Northeast Arm mafic volcaniclastics (unit 19). 79

Figure 110: Sequence in Northeast Arm volcaniclastic rocks (unit 19), east shore of Schist Lake. 80

Figure 111: Laminated felsic tuff and mudstone (unit 35), northeast end of Northeast Arm. 81

Figure 112: Stratigraphic section through Northeast Arm intermediate to mafic volcanclastic sequence (unit 19), north end of Schist Lake. 82

Figure 113: Location and distribution of major basalt bodies, Whitefish Lake-Mikanagan Lake Block. 85

Figure 114: Plagioclase-pyroxene-phyric mafic lapilli tuff, Mikanagan Lake mafic volcaniclastics (unit 20c). 88

Figure 115: North Star Road volcanic conglomerate (unit 31). 89

Figure 116: Heterolithologic, framework-supported North Star Road volcanic conglomerate (unit 31). 90

Figure 117: Angular joint-bounded boulder of hypabyssal pyroxene-phyric intermediate intrusive rock in North Star Road volcanic conglomerate (unit 31). 90

Figure 118: Maximum clast size distribution in the North Star Road volcanic conglomerate (unit 31). 91

Figure 119: Clast-supported, poorly sorted North Star Road volcanic conglomerate (unit 31). 92

Page

Figure 120: Distribution of major basalt-basaltic andesite and felsic units, Bakers Narrows Block. 93

Figure 121: Stratigraphic sequence through Bakers Narrows Block. 94

Figure 122: Sequence of structures through a typical Wright Bay basalt (B_B) flow. 94

Figure 123: Contact between massive lava and flow top amoeboid pillow breccia in unit 7, Bakers Narrows Block. 95

Figure 124: TiO_2 vs. FeO^*/MgO, Bakers Narrows Block basalt and basaltic andesite. 96

Figure 125: FeO^*/MgO vs. SiO_2 and MgO vs. SiO_2, Bakers Narrows Block basalt and basaltic andesite. 97

Figure 126: Jensen cation plot of the Bakers Narrows Block basalts and basaltic andesites. 97

Figure 127: Measured sequence through a series of thin massive intermediate to felsic lava flows, unit F_B between Wright and Sharpe Bays. 98

Figure 128: Flow-top breccia on thin felsic flow (unit 18c, b), Bakers Narrows Block. 98

Figure 129: Schematic diagram of primary structures in three successive rhyolite flows, Sharpe Bay rhyolite. 98

Figure 130: Representative stratigraphic sections, Sourdough Bay Block, with gabbro intrusions omitted. 101

Figure 131: Inclusions in a quartz-plagioclase-phyric rhyolite dyke (unit 17c), north shore of Thompson Bay, Athapapuskow Lake. 102

Figure 132: Facing direction of Grassy Narrows basalt flows and location of major rhyolite bodies, Grassy Narrows Zone. 105

Figure 133: Tectonically flattened pillows from tightly folded Grassy Narrows basalt flow (unit 7). 106

Figure 134: Primary facing direction of mafic flows in deformed terrains can be ascertained from bullet-, crescent-, and pear-shaped pillows, formed by tectonic flattening of bun, draped and downward protruding types at a high angle to their primary orientation. 106

Figure 135: TiO_2 vs. FeO^*/MgO, Grassy Narrows basalt-basaltic andesite. 107

Figure 136: FeO^*/MgO vs. SiO_2 and MgO vs. SiO_2, Grassy Narrows basalt-basaltic andesite. 107

Figure 137: Distribution of rock types in the northern massive and brecciated rhyolite body and the southern rhyolite lobe-microbreccia body, Grassy Narrows, Manistikwan Lake. 108

Figure 138: Microfractured, massive spherulitic rhyolite (unit 18b), transition zone of northern flow, Grassy Narrows zone. 109

Figure 139: Columnar joints in massive phase of Grassy Narrows rhyolite (unit 18b) 109

Figure 140: Breccia zone, Northern rhyolite body, Grassy Narrows Zone. 111

Figure 141: Large tongue of massive rhyolite in microbreccia, subaqueous Grassy Narrows rhyolite flow (unit 18a). 112

Figure 142: Subaqueous rhyolite flow (unit 18a), Grassy Narrows Zone. 112

Figure 143: Contact between a massive rhyolite lobe and intraflow unit of reworked rhyolite microbreccia and mudstone, Grassy Narrows rhyolite (unit 18a, d). 113

Figure 144: Rounded to well rounded pebble- and cobble-sized fragments in heterolithologic felsic pebble conglomerate (unit 32), Grassy Narrows Zone. 113

Figure 145: Crossbedding in felsic sandstone and pebble conglomerate (unit 32), south end of Embury Lake. 116

Figure 146: Heterolithologic felsic pebble conglomerate (unit 32) with angular, laminated intermediate fragments. 116

Fiugre 147: Pillow fragment breccia (unit 8a), Big Island, Manistikwan Lake. 117

Figure 148: Stratified pillow fragment breccia (unit 8a), Big Island, Manistikwan Lake. 118

Figure 149: Pillowed mafic flow (unit 8), Big Island, Manistikwan Lake. 118

Page

Figure 150: Stratigraphic sections contained in sub-blocks of the Hook Lake Block. 120

Figure 151: Lithologic and stratigraphic subdivisions, Hook Lake Block. 121

Figure 152: Jensen cation plot, Hook Lake Block mafic flows. 122

Figure 153: FeO^*/MgO and MgO vs. SiO_2, Hook Lake Block mafic flows. 122

Figure 154: TiO_2 vs. FeO^*/MgO, Hook Lake Block mafic flows. 123

Figure 155: Pillow fragment breccia (unit 11), 180 m northeast of Milliken Lake. 123

Figure 156: Amoeboid pillow breccia top of pillowed basalt flow (unit 7), 600 m south southeast of Insole Lake. 124

Figure 157: Pillow fragment breccia (unit 7) containing crescentic pillow fragment with bands of vesicles parallel to pillow selvage and truncated at fragment margin. 125

Figure 158: Centimetre-scale amygdale banding in an aphyric pillow (unit 7). 125

Figure 159: Amoeboid pillow breccia (unit 7b), between Borne and Rennie Lakes, Hook Lake Block. 127

Figure 160: Lath-shaped plagioclase microlites in aphyric mafic flow (unit 7), north of Borne Lake. 127

Figure 161: Stratigraphic sequence in a portion of unit "J", Hook Lake Block. 129

Figure 162: Pillow fragment breccia (unit 9a) within stratigraphic unit J, Hook Lake Block. 130

Figure 163: Large, porphyritic scoria lapillus in scoria-rich plagioclase-phyric mafic tuff (unit 23b). 130

Figure 164: Layering in mafic, scoria-rich lapilli tuff (unit 23a), east of Borne Lake. 131

Figure 165: Grading displayed by three scoria-rich tuff beds, unit "J", Hook Lake Block. 131

Figure 166: Tracings of scoria particles in scoria-rich mafic tuff, unit "J", Hook Lake Block. 132

Figure 167: Accessory clasts of pillowed basalt in mafic scoria-rich tuff (unit 23b), east of Kinsella Lake. 133

Figure 168: Well-bedded mafic scoria-rich tuff (unit 23), 900 m west of Hook Lake. 134

Figure 169: Structural sub-blocks, major faults and folds and location of Ledge Lake and Mandy stratigraphic sections, Flin Flon Block. 138

Figure 170: Simplified geology of the Flin Flon Mine area. 139

Figure 171: Distribution of major mafic flow units in the Hapnot Lake and Mandy sub-blocks. 140

Figure 172: Pillowed South Main basalt (unit 6a). 141

Figure 173: South Main pillow fragment breccia (unit 6b). 141

Figure 174: Schematic illustration depicting the stratigraphic sequence northwest of HBMS smelter, through the stratigraphic footwall and hanging wall of the Flin Flon Cu-Zn sulphide orebody. 142

Figure 175: Overview of the unconformity contact between plagioclase-phyric mafic tuff (unit 22b) and overlying South Main pillow fragment breccia (unit 6b), 300 m northwest of HBMS smelter. 143

Figure 176: Unconformable contact between plagioclase-phyric mafic tuff (unit 22b) and overlying South Main pillow fragment breccia (unit 6b), 300 m northwest of HBMS smelter. 143

Figure 177: Graded beds of plagioclase crystal tuff (unit 22b). 144

Figure 178: Plagioclase-phyric mafic crystal-lapilli tuff (unit 22b), 1160 m northwest of HBMS smelter, by Flin Flon Lake. 144

Figure 179: Mine rhyolite, upper breccia (unit 15c), 330 m northwest of HBMS smelter. 145

Page

Figure 180: Railway volcaniclastics (unit 30a), 330 m northwest of HBMS smelter. 146

Figure 181: FeO*/MgO and MgO vs. SiO_2, South Main basalt, Hidden Lake basalt and Burley Lake basaltic andesite. 147

Figure 182: Cross-section of tube-shaped, banded, concentrically zoned structure interpreted to be a lava tube, Hidden Lake basalt (unit 2), 100 m north of Hidden Lake. 147

Figure 183: Large protrusion from the top of the pillowed portion of a flow into amoeboid pillow breccia flow top, Hidden Lake basalt (unit 2a) 148

Figure 184: Contact between the pillowed portion of a basalt flow and amoeboid pillow breccia flow top, Hidden Lake basalt (unit 2a). 149

Figure 185: Flow top breccia, same locality as Fig. 184. 149

Figure 186: Sketch showing primary features and internal organization in two massive mafic flows (unit 3b) northeast of Potter Bay on Phantom Lake, Hapnot Lake sub-block. 150

Figure 187: Pie-shaped and crescentic pillow fragments, pillow fragment breccia (unit 3c), 750 m west of Mandy Mine. 151

Figure 188: Sketch showing lateral and vertical variation in flow morphology and thickness, Burley Lake, Hapnot Lake sub-block. 152

Figure 189: Contorted flow-folds defined by flow banding in rhyolite flow (unit 18a), Burley Lake. 152

Figure 190: Chondrite-normalized REE plot, South Main basalt, Hidden Lake basalt and Burley Lake basaltic andesite. 153

Figure 191: Burley Lake section, Hapnot Lake sub-block, and Carlisle Lake section, Mandy sub-block. 154

Figure 192: Basalt pillows (unit 3b) with dark oxidized selvages, 300 m southeast of Carlisle Lake. 155

Figure 193: Amoeboid pillow breccia, Burley Lake basaltic andesite (unit 3b). 155

Figure 194: Pillowed basaltic andesite (unit 3b), 200 m southeast of Carlisle Lake. Pillows have no selvages and shapes are defined by quartz-filled thermal contraction cracks. 156

Figure 195: Large oscillatory zoned plagioclase phenocrysts characteristic of mafic scoria tuffs (unit 23b) exposed 570 m west of Mandy Mine. 157

Figure 196: Well defined primary columnar joints in Stitt Island dacite (unit 14). 158

Figure 197: Thin-bedded greywacke, mudstone and felsic mudstone, unit 33, west shore of Northwest Arm. 159

Figure 198: FeO*/MgO and MgO vs. SiO_2, Carlisle Lake basalts, Mandy sub-block. 159

Figure 199: TiO_2 vs. FeO*/MgO, Carlisle Lake basalts, Mandy sub-block. 160

Figure 200: Ledge Lake section, Ledge Lake sub-block. 161

Figure 201: Contact between two massive mafic flows, 200 m west of Ledge Lake. 161

Figure 202: Bedded mafic volcanic wacke or tuff (unit 22), 300 m southwest of Burley Lake. 162

Figure 203: Glomerophyric mafic flow (unit 10), Mitt Lake area. 163

Figure 204: Clast in pillow fragment breccia (unit 7a), west of Hook Lake. The clast has a well preserved plagioclase microlitic texture identical to that in mafic flows. 164

Figure 205: Scoria tuff (unit 23b) bed 1.2 m thick. 165

Figure 206: Measured section through thinly bedded mafic, scoria-rich tuff (unit 23b), Railway Line sub-block, about 1900 m southeast of Stitt Island. 165

Figure 207: Tracings of scoria particles in bedded, mafic, scoria-rich tuff (unit 23b), Railway Line sub-block. 166

Figure 208: Trains of accessory fragments defining crude layers in mafic scoria-rich tuff (unit 23b), 100 m east of northwest arm of Schist Lake. 167

Figure 209: Possible bomb sag in bedded mafic scoria-rich tuff (unit 23b), 100 m east of northwest arm of Schist Lake. 167

Page

Figure 210: Plagioclase-glomerophyric fragment in mafic tuff breccia (unit 23b), west of Hook Lake. 168

Figure 211: Heterolithologic breccia (unit 29) with large boulder of a banded, synvolcanic mafic dyke. 168

Figure 212: Chondrite normalized REE plots of Amisk Group mafic rocks, showing ranges for basalt, basaltic andesite and ferrobasalt. 170

Figure 213: Chondrite normalized REE plots of Amisk Group rhyolites. 170

Figure 214: Amisk Group basalts plotted on tectonic discrimination diagram using Ti, Zr and Sr (Pearce and Cann, 1973). 173

Figure 215: MORB-normalized trace element patterns for representative Amisk Group rocks (Syme, 1988). 173

Figure 216: Ti vs. Zr, Amisk Group (Flin Flon metavolcanic belt) and Wasekwan Group (Lynn Lake metavolcanic belt) (Syme, 1988). . . 174

Figure 217: Ti vs. Zr comparing parental magmas of major gabbro intrusions with fields of Amisk Group basalt/basaltic andesite and ferrobasalt. 175

Figure 218: Zr/Y vs. Zr comparing parental magmas of major gabbro intrusions with fields of Amisk Group basalt/basaltic andesite and ferrobasalt. 176

Figure 219: P_2O_5 vs. TiO_2 comparing parental magmas of major gabbro intrusions with fields of Amisk Group basalt/basaltic andesite and ferrobasalt. 176

Figure 220: Location of major mafic intrusive bodies, Flin Flon area. 177

Figure 221: Igneous layering in gabbro (unit 39a), White Lake Sill at White Lake. 178

Figure 222: Disposition of lithologic units in the Whitefish Lake Intrusion (unit 40). 180

Figure 223: Gabbronorite (unit 41a), Mikanagan Lake Sill. 185

Figure 224: Gabbro (unit 41b), Mikanagan Lake Sill. 186

Figure 225: Oikocrystic gabbronorite (unit 41c), Mikanagan Lake Sill. 186

Figure 226: Schematic diagram showing characteristic features of the transition Gabbro zone (unit 41d) as exposed at two widely separated localities in the Mikanagan Lake Sill. 187

Figure 227: Contact between transition gabbro (unit 41d) and ferrogabbro (unit 41f). 188

Figure 228: Detail of transition gabbro — ferrogabbro contact shown in Fig. 227. 188

Figure 229: Irregular pod of gabbroic pegmatite (unit 41e) emplaced in layered transition gabbro (unit 41d), Mikanagan Lake Sill. 189

Figure 230: Igneous lamination of plagioclase in ferrograbbro (unit 41f), Mikanagan Lake Sill. 190

Figure 231: Ferrogabbro (unit 41f), Mikangan Lake Sill. 190

Figure 232: Ferrotonalite (unit 41g), Mikanagan Lake Sill, showing micrographic intergrowths of quartz and plagioclase. 191

Figure 233: Ferrotonalite (unit 41g), Mikanagan Lake Sill. 191

Figure 234: Micrographic leucotonalite (unit 41h), Mikanagan Lake Sill. 192

Figure 235: Mineralogical and chemical variation in the differentiated, zoned Mikanagan Lake Sill (unit 41). 194

Figure 236: Ternary AFM diagram showing tholeiitic character and extreme Fe-enrichment trend of the Mikanagan Lake Sill. 195

Figure 237: Jensen cation plot, Mikanagan Lake Sill. 195

Figure 238: Chondrite normalized REE plot of sample from chilled margin of Mikanagan Lake Sill with range for Amisk Group basalts/basaltic andesites and ferrobasalts for comparison. 198

Figure 239: Ni vs. Cr comparing parental magmas of major gabbro intrusions with fields of Amisk Group basalt/basaltic andesite and ferrobasalt. 198

Page

Figure 240: Ternary AFM diagram, mafic intrusions, Flin Flon area. 199

Figure 241: TiO_2 vs. FeO*/MgO, mafic intrusions, Flin Flon area. 200

Figure 242: Banded, fine grained mafic dyke emplaced in Hook Lake gabbronorite (unit 41a). 201

Figure 243: Gabbro pegmatite vein emplaced in Hook Lake gabbronorite (unit 41a). 201

Figure 244: Magnetiferous quartz diorite (unit 42j), Manistikwan Lake. 203

Figure 245: Western contact of Cliff Lake Pluton (unit 45b) with host pillowed basalt (unit 7). 210

Figure 246: Contact zone of the Cliff Lake Pluton (unit 49) showing apophyses of tonalite intruding a pillowed mafic flow. 210

Figure 247: Xenoliths of basalt in unit 45b, Cliff Lake Pluton. 211

Figure 248: Intrusive contact between tonalite with abundant large mafic xenoliths (unit 45b) and younger tonalite with fewer and smaller xenoliths (unit 45c), Cliff Lake Pluton. 211

Figure 249: Aligned, partially assimilated mafic xenoliths in Cliff Lake tonalite (unit 45b). 212

Figure 250: Small mafic xenoliths in quartz-phyric tonalite (unit 45c), Cliff Lake Pluton. 213

Figure 251: Cliff Lake tonalite (unit 45c) displaying envelopes of epidotization around rusty chloritic fractures. 213

Figure 252: Chlorite-rich alteration along fractures in quartz-phyric leucotonalite (unit 45d), Cliff Lake Pluton. 214

Figure 253: Ternary AFM diagram showing various phases of the Cliff Lake Pluton and samples of contained mafic volcanic xenoliths. 215

Figure 254: FeO*, MgO, CaO, TiO_2 plotted against SiO_2 showing various phases of the Cliff Lake Pluton and samples of contained mafic xenoliths. 215

Figure 255: Spherulitic quartz porphyry (unit 48a), Manistikwan Lake. 217

Figure 256: Curvilinear perlitic cracks in Borne Lake rhyolite (unit 49c). 218

Figure 257: Spherulites in Borne Lake rhyolite intrusion (unit 49c). 218

Figure 258: Spherulitic rhyolite dyke (unit 49d), Manistikwan Lake. 219

Figure 259: Measured section through Missi Group in vicinity of the town of Flin Flon. 226

Figure 260: Hematiferous, "onionskin" weathering in unit 7 Amisk Group pillowed flows within the sub-Missi regolith; old Highway 10 at Northstar Road. 236

Figure 261: Hematiferous regolith developed on Amisk Group basalt (unit 7) beneath unconformably overlying Missi Group fluviatile pebble and cobble conglomerate (unit 52c, b). 236

Figure 262: Missi Group conglomerate (unit 50b) containing a clast of Amisk Group volcanic rock displaying hematiferous, onionskin weathering characteristic of the Amisk regolith. 237

Figure 263: Crossbedding in Missi Group pebbly sandstone (unit 50b). 238

Figure 264: Missi Group crossbedded, quartz-rich coarse sandstone (unit 50a). 238

Figure 265: Sandstone (unit 50a), Missi Group, composed of subangular to subround clasts of quartz, plagioclase and lithic fragments. 239

Figure 266: Heavy mineral placers/lamellae, Missi Group sandstone (unit 50a). 240

Figure 267: Trough crossbedding in Missi Group sandstone (unit 50c). 240

Figure 268: Unusually thick heavy mineral placers in Missi Group trough crossbedded pebbly sandstone (unit 50b, c). 241

Figure 269: Missi Group trough crossbedded coarse pebbly sandstone (unit 50b, c), old Highway 10 at Northstar Road. 241

Page

Figure 270: Schematic diagram depicting four stages leading up to and including deposition of the Missi Group. 242

Figure 271: Hypidiomorphic phase of Whitefish Lake quartz monzodiorite (unit 54). 244

Figure 272: Porphyritic phase of Whitefish Lake quartz monzodiorite (unit 54a). 244

Figure 273: Porphyritic granodiorite (unit 57). 245

Figure 274: Disposition of folds, faults and the prehnite-pumpellyite isograd. 249

Figure 275: Lower hemisphere stereographic plots of structural fabric elements of the pre-Missi, P1 Burley Lake syncline. 250

Figure 276: Lower hemisphere stereographic plots of structural fabric elements of the P3 Hidden Lake synform. 250

Figure 277: Deformed pillow in Hidden Lake basalt (unit 2a), near the axial trace of Hidden Lake synform. 251

Figure 278: Deformed pillows in Hidden Lake basalt (unit 2a), south end of Hidden Lake. 251

Figure 279: Deformed pillowed flow (unit 9) and interflow sediments, near axial trace of Milliken Lake syncline. 252

Figure 280: Lower hemisphere stereographic plots of structural fabric elements of the P3 Northeast Arm syncline. 253

Figure 281: Tight, chevron-shaped minor folds developed in Vick Lake andesitic tuff (unit 25c), 1370 m northeast of White Lake mine, on the shore of Northeast Arm. 253

Figure 282: Isoclinal folds in axial trace of Northeast Arm syncline, 400 m south of Highway 10. 254

Figure 283: Lower hemisphere stereograhic plots of structural fabric elements of the P3 Milliken Lake syncline. 254

Figure 284: Lower hemisphere stereographic plots of structural fabric elements of the P3 folds southeast of Stitt Island. 255

Figure 285: Fault breccia associated with late brittle deformation of strongly foliated White Lake dacite tuff, 200 m west of Little Spruce Lake. 256

Figure 286: Trace of the Club Lake fault, separating schistose Amisk Group rocks and foliated Missi Group pebbly sandstone. 259

Figure 287: Subgreenschist and greenschist facies metamorphic mineral assemblages in the Hook Lake area. 263

Figure 288: Plagioclase-pyroxene-phyric mafic flow (unit 9), west of Hook Lake. 264

Figure 289: Detail of amygdale in porphyritic mafic flow (unit 9), west of Hook Lake. 264

Figure 290: Cross-section of the Centennial Mine (from Provins, 1982). 269

Figure 291: Generalized distribution of alteration types in host rocks of the Centennial Cu-Zn massive sulphide orebody (from Provins, 1982). 269

Figure 292: Major element distribution in host rocks of the Centennial Cu-Zn massive sulphide orebody (from Provins, 1982). 270

Figure 293: Zoned polymineralic alteration structures in unit 7 mafic flow; island in Manistikwan Lake, 640 m west of Steeves Lake. . . 273

Figure 294: Spherical hydrothermal alteration structures of uncertain genesis in fine grained quartz diorite dyke 1200 m north of Cope Lake. 273

Figure 295: Anastomosing chlorite-filled veins in foliated, heterolithologic felsic breccias, Schist Lake Mine area. 274

Figure 296: South Embury alteration zone. 274

Figure 297: Rusty-brown weathering carbonate vein cutting Stitt Island dacite (unit 14). 275

Figure 298: Spherulitic pillowed mafic flow (unit 7), 700 m south southeast of Insole Lake. 276

Figure 299: Spherulitic alteration structures nucleated on fractures and selvages in unit 7 mafic pillowed flow, 300 m northwest of Hook Lake. 276

Figure 300: Tourmalinization adjacent to vein in gabbro; north end of Big Charlie Lake. 277

TABLES

Page

Table 1: U-Pb zircon age determinations, Flin Flon and Kisseynew belts. 3

Table 2: Average flow thickness in zones 1, 2, 3 and 4 of the Bear Lake basaltic andesite. 18

Table 3: Flow thickness, by flow type, in the lower (zones 1 and 2) and upper (zones 3 and 4) portions of the Bear Lake basaltic andesite. . . . 18

Table 4: Frequency of flow types in zones 1, 2, 3 and 4 of the Bear Lake basaltic andesite. 18

Table 5: Summary of criteria used to estimate depth of effusion of basalt magmas. 30

Table 6: Textural variation through Scotty Lake basalt flow. 66

Table 7: Basalt units in the Whitefish Lake-Mikanagan Lake Block. 86

Table 8: Average compositions of some major mafic flow units. 171

Table 9: Average compositions of some major volcaniclastic and rhyolite units. 172

Table 10: Comparison of compositions in the White Lake Sill (unit 39) and an average of 5 analyses of the Two Portage Lake ferrobasalt (unit 5). 179

Table 11: Alteration sequence in the Mikanagan Lake Sill (unit 41). 182

Table 12: Estimated primary mineral modes, Mikanagan Lake Sill and related intrusions. 184

Table 13: Average chemical composition of zones and chilled margins in the Mikanagan Lake Sill, calculated bulk composition of the Mikanagan Lake Sill, and comparative data from the Josland Lake Sill. 196

Table 14: Chemical analyses of chilled margins of major gabbro intrusions. 197

Table 15: Colour, mineralogy, texture and general characteristics of various gabbro, diorite and quartz diorite intrusions (unit 42). 204

Table 16: Age relationships of intrusive rocks in the southern Hook Lake Block. 220

Table 17: Age relationships of intrusive rocks in the northern Hook Lake Block. 221

Table 18: Age relationships of intrusive rocks in the southern Manistikwan Lake Block. 221

Table 19: Age relationships of intrusive rocks in the Hook Lake Block and Manistikwan Lake Block, compiled from Tables 16, 17 and 18. . . . 222

Table 20: Age relationships of intrusive rocks in the Bear Lake Block. 223

Table 21: Age relationships of intrusive rocks in the Scotty Lake Block. 223

Table 22: Age relationships of intrusive rocks in the Whitefish-Mikanagan Lakes Block and Sourdough Bay Block. 224

Table 23: Summary of main features of sandstone and conglomerate units in the measured section through the Missi Group. 227

Table 24: Framework clast percentages in Missi Group conglomerates. 235

Table 25: Summary of major deformational events. 248

Table 26: Copper-zinc and gold deposits, Flin Flon district. 267

MAPS

Map GR87-1-1: Geology of the Flin Flon-White Lake area. . . . . (in pocket)

Map GR87-1-2: Geology of the Flin Flon-White Lake area showing mineral occurrences, alteration, and location of analyzed samples.(in pocket)

INTRODUCTION

GEOLOGICAL SETTING

The Flin Flon belt comprises an assemblage of early Proterozoic subaqueous and subordinate subaerial volcanic rocks and associated sediments, an overlying sequence of terrestrial sediments, and a complex array of intrusive rocks. It is bounded to the north by metasedimentary gneisses of the Kisseynew belt to the south by a gneissic terrain of uncertain origin. Flat-lying Ordovician dolomitic limestones of the Western Interior Platform cover the Precambrian rocks south of Athapapuskow Lake (Fig. 1 and 2). The Flin Flon belt has a length of 250 km and an exposed width of 32-48 km, but its total width, including the area covered by Paleozoic rocks, may be considerably larger (Green et al., 1985). The Flin Flon-White Lake area, located in the west central portion of the belt, covers more than 200 km² in the region adjacent to and including the town of Flin Flon (Fig. 2).

The Flin Flon and Kisseynew belts are part of the southern Churchill Structural Province and are elements of the Trans-Hudson Orogen (Hoffman, 1988, 1989). Supracrustal and intrusive rocks in these belts have been dated by U-Pb zircon techniques (Gordon et al., 1987, 1989; Syme et al., 1987) and by a variety of other radiometric methods (references in Sangster, 1978). U-Pb zircon ages suggest that volcanism in the Flin Flon belt occurred at approximately 1886 Ma, followed by various intru-

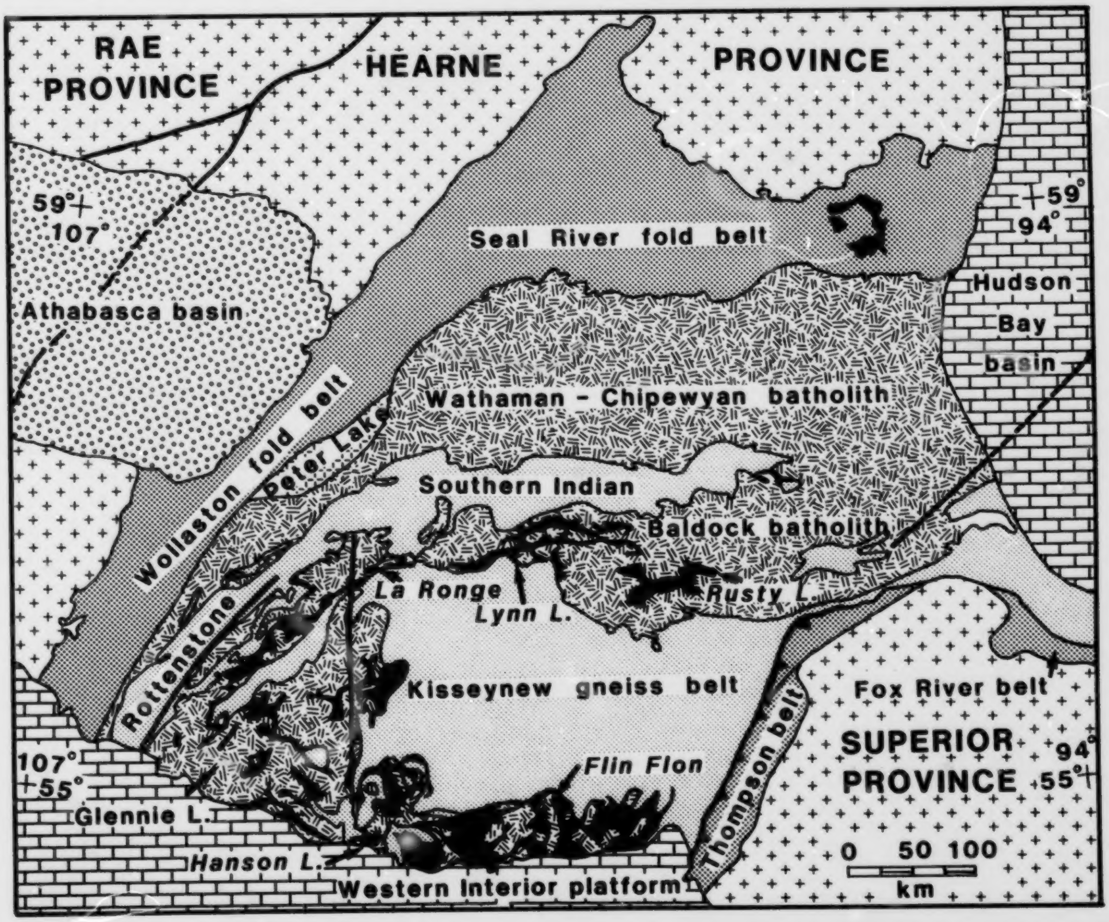
RAE PROVINCE
HEARNE
PROVINCE
59°
107°
59°
94°
Seal River fold belt
Athabasca basin
Hudson Bay basin
Wathaman - Chipewyan batholith
Wollaston fold belt
Peter Lake
Southern Indian
Baldock batholith
La Ronge
Lynn L.
Rusty L.
Rottenstone
Kisseynew gneiss belt
Fox River belt
SUPERIOR PROVINCE
107°
55°
94°
55°
Flin Flon
Thompson belt
Glennie L.
Hanson L.
Western Interior platform
0 50 100
km

Figure i: *Tectonic elements of the Trans-Hudson Orogen as exposed in northern Manitoba and Saskatchewan (from Hoffman, 1988). Volcanic belts are shown in black. Major faults are indicated by bold lines.*

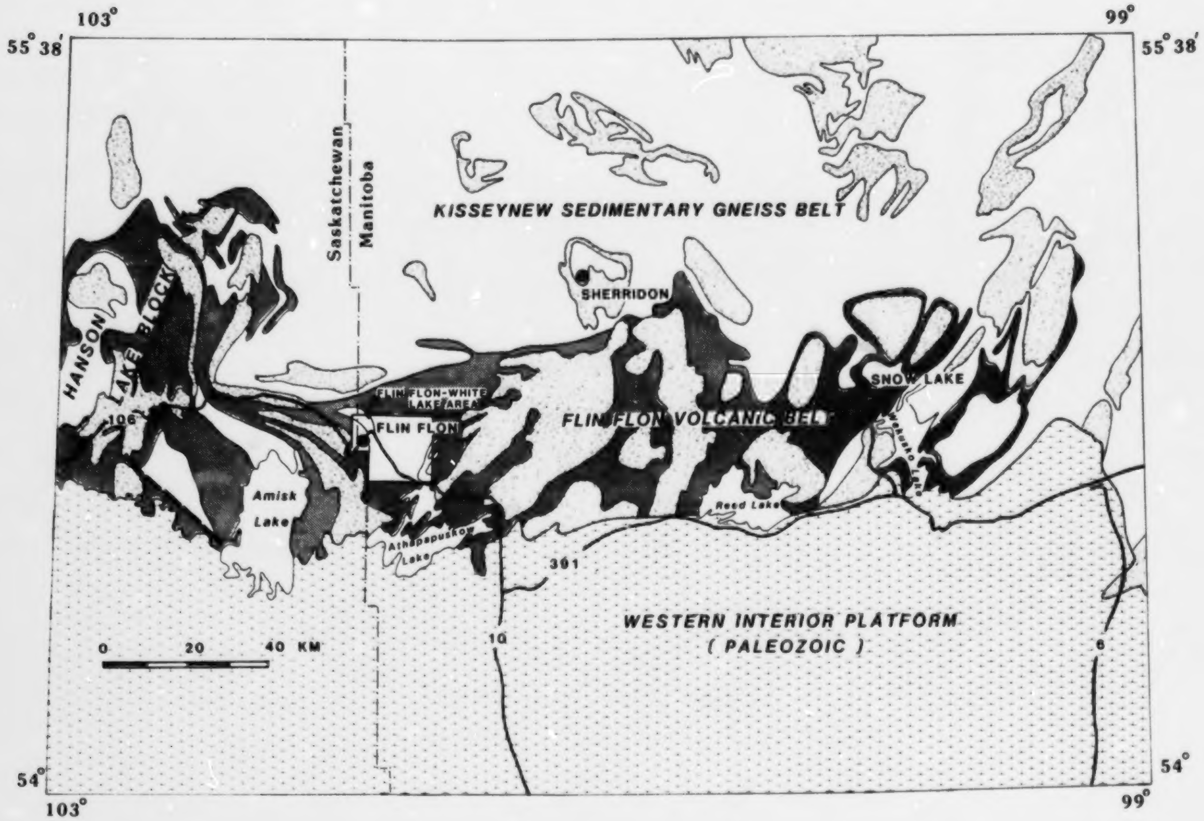

Figure 2: Location of the Flin Flon-White Lake area on a generalized geology map of north central Manitoba and Saskatchewan. Dark dot pattern represents volcanic rocks, light dot pattern represents sedimentary rocks, paragneiss and orthogneiss, and hachured pattern represents granitic plutons.

sive magmatic events between 1886 and 1830 Ma and by younger terrestrial sedimentation and minor volcanic activity at approximately 1830 Ma. Metamorphism and anatexis in the Kisseynew belt peaked at about 1815 Ma and continued to approximately 1780 Ma (Table 1).

The volcanic rocks are the oldest lithologies in the belt, and were assigned to the Amisk Group by Bruce (1918) who named them for their type locality on Amisk Lake, Saskatchewan. The Amisk Group includes a wide variety of rock types, representing several distinct stratigraphic sequences. Most were deposited in a shallow to moderately deep marine environment but locally, as at Amisk Lake in Saskatchewan, subaerial environments have been recognized (Ayres, 1978). Some pyroclastic rocks in the Flin Flon-White Lake area are interpreted to have been erupted in a subaerial environment but deposited underwater. The Amisk Group is dominated by basalt and basaltic andesite, which occur in units up to 3.3 km thick and are interpreted as portions of subaqueous shield volcanoes. Rhyolite flows, a minor component of the Amisk Group, occur as sporadic, discrete bodies, some of which have aprons of reworked felsic tuff. Mafic and intermediate volcaniclastic rocks vary widely in phenocryst type and abundance, texture, grain size and bedding characteristics; most were deposited from subaqueous density currents. Minor rock types include felsic volcaniclastic rocks, volcanic conglomerate, oxide facies iron formation, greywacke-siltstone-mudstone, and carbonate-rich sedimentary rocks. The thickest reconstructed Amisk section in the Flin Flon area is 7.5 km. The chemical and physical characteristics of the Amisk Group are consistent with deposition in an island arc type of environment. Locally, as at east Amisk Lake (Parslow and Gaskarth, 1984) and Athapapuskow Lake (Syme, 1987), deposition may have been in an ocean floor or back arc environment.

The Missi Group, named by Bruce (1918), is the youngest supracrustal succession in the Flin Flon belt. It is more than 1900 m thick at Flin Flon and consists of metamorphosed sandstone, pebbly sandstone and polymictic conglomerate that lies with profound angular unconformity on previously folded Amisk Group rocks and contained intrusions. At least 2.5-3 km of Amisk section is truncated at this basal Missi unconformity and a hematiferous weathered zone (regolith) several metres thick is developed on underlying Amisk volcanic and intrusive rocks. Missi Group rocks contain primary structures such as trough crossbedding, pebble lags, heavy mineral placers, conglomerate lenses and multiple scours consistent with deposition by fluvial processes, probably within a subaerial alluvial fan. Provenance of the detrital material in the Missi is from Amisk Group volcanic and intrusive rocks, and post-Amisk granitoid rocks. The presence of granitic clasts in the Missi and the basal angular unconformity indicates that the Missi Group postdates a major period of plutonism, deformation, uplift and erosion that affected the Amisk Group.

A wide variety of intrusive rocks cut the Amisk Group but are not present in the unconformably overlying Missi Group. Some intrusions are

Table 1:
U-Pb zircon age determinations, Flin Flon and Kisseynew belts

Flin Flon Belt	
FLIN FLON AREA	
Amisk Group rhyolite tuff (unit 27)[1]	1886 +/-2 Ma
Cliff Lake pluton (unit 45)[2]	1874 +32/-25 Ma
Lynx Lake pluton[1]	1847 +/-4 Ma
SNOW LAKE AREA	
Herblet gneiss dome[2]	1890 +12/-9 Ma
Richard Lake pluton[3]	1889 +8/-6 Ma
Wekusko granite[2]	1834 +8/-6 Ma
Rex Lake pluton[2]	1832 +/-4 Ma
Ham Lake pluton[2]	1830 +27/-19 Ma
Missi Group volcanic rocks[2]	1832 +/-2 Ma
Kisseynew Belt	
Enderbite sills[2]	1830 +11/-5 Ma
Anatectic granitoids[2]	
Highrock Lake tonalite	1841 +35/-15 Ma
Burntwood Lake granodiorite	1814 +17/-11 Ma
Burntwood Lake granite (migmatite)	1816 +23/-12 Ma

References:

[1] Syme et al., 1987
[2] Gordon et al., 1989
[3] Bailes et al., 1988

syn-Amisk, some were emplaced in folded Amisk rocks and thus postdate volcanism, and others occur as isolated intrusions whose age relative to Amisk volcanism and the Missi Group are unknown. Major intrusion types include ubiquitous fine- to medium-grained diorites, small porphyritic felsic stocks and several large differentiated gabbroic intrusions.

Five phases of folding are recognized in the Flin Flon-White Lake area (P1 to P5). One phase predates, and four phases postdate the Missi Group.

Faults dominate the structural fabric of the Flin Flon-White Lake area. Two groups of faults are recognized, those that bound major stratigraphic blocks and those that occur within the blocks (Fig. 3; map GR87-1-1). Stratigraphic correlations cannot be made across block-bounding faults, whereas sequences can be traced or correlated across internal faults. In other respects (e.g. physical expression, age) block bounding and internal faults are indistinguishable. Many are not simple isolated structures, but tend to splay or occur in clusters, resulting in numerous lens-shaped fault-bounded domains of all sizes. Most faults appear to have been initiated at different times during the P5 deformation, and as a result display different degrees of flexure about the P5 Embury Lake Antiform. Implications of the fault-block style of deformation are far-reaching. For example, each block comprises a more or less intact, definable stratigraphic succession that is unique to that block. A direct consequence of this is that a comprehensive, composite or regional Amisk Group stratigraphy cannot be reconstructed.

Regional metamorphism in the Flin Flon belt increases in grade northwards, towards the Kisseynew metasedimentary gneiss belt. In the Flin Flon-White Lake area, metamorphic grade increases from subgreenschist (prehnite-pumpellyite) at Hook Lake (Fig. 3) to middle greenschist (biotite present) at Ross Lake. The dominant, lower greenschist mineral assemblages are characterized by chlorite, tremolite-actinolite, epidote, albite, muscovite and quartz. Metamorphism postdated deposition of the Missi Group and emplacement of all intrusions, and accompanied development of schistosity during the third and fourth phases of deformation. Metamorphic zones are offset by faults developed during P5, implying that faults and P5 deformation are younger than 1815 Ma, the estimated age for peak regional metamorphism (Gordon et al., 1988).

The Flin Flon area is well known for its volcanogenic stratabound massive Cu-Zn sulphide deposits. Seven current and past producing mines occur in the map area: Flin Flon, Callinan and Centennial are still in production whereas Mandy, Schist Lake, Cuprus and White Lake are not. Interest in Au has recently been fueled by the opening of the Tartan Lake gold mine, just north of the map area, and discovery of the Au-rich Westfield Zn sulphide deposit.

TERMINOLOGY

Volcanic rock types in the Flin Flon-White Lake area are classified according to SiO_2 content (volatile free basis): basalt (46-53% SiO_2), basaltic andesite (53-57% SiO_2), andesite (57-62% SiO_2), dacite (62-70% SiO_2), and rhyolite (70-80% SiO_2). Basaltic andesite is volumetrically the most common rock type in the area, followed closely by basalt. Andesite and dacite are very rare; rhyolite occurs locally. Classification as to magma series (tholeiitic, calc-alkaline) is generally after Jensen (1976) and Irvine and Baragar (1971).

Terminology for volcaniclastic rocks generally follows that of Fisher and Schmincke (1984). *Pyroclastic* rocks are produced by many processes connected with volanic eruptions. They are composed of "particles expelled from volcanic vents without reference to the causes of eruption or origin of the particles" (Fisher and Schmincke, op. cit.; p. 89). Redeposited unconsolidated pyroclastic debris, for example tuff redeposited by subaqueous density contents, is similarly termed pyroclastic. The size classification of pyroclastic fragments is after Fisher (1966) (Fig. 4). *Hyaloclastite* is defined (after Rittmann, 1958; 1962) as comprising glassy particles produced by nonexplosive spalling and granulation of lava that comes in contact with water. *Autoclastic* rocks are produced by fragmentation produced by mechanical friction or gaseous explosion during movement of a lava flow. If the origin of fragments is unknown, due to obliteration of primary textures, these deposits are referred to with the general term *volcaniclastic* (Fisher, 1961).

Intrusive rocks are classified and named according to mineral content (Streckeisen, 1976). Epiclastic rocks, produced by weathering and erosion of volcanic and plutonic rocks, are classified by grain size according to the Wentworth scale (Wentworth, 1922). The general term greywacke is used in this report to denote a poorly sorted, sand-sized sedimentary rock derived mainly from volcanic rocks.

PREVIOUS WORK

The Flin Flon-White Lake area was mapped previously at a scale of 1 inch to 1 mile (1:63 360) by Tanton (1941a, b), Bateman and Harrison (1945) and Buckham (1944). More detailed mapping at a scale of 1 inch to 1000 feet (1:12 000) was carried out by Stockwell (1960) and Heywood (1966), in the vicinity of Flin Flon and Ledge Lake.

Contributions to the understanding of the Amisk Group have been made by Byers and Dahlstrom (1954), Byers et al. (1965), Stauffer et al. (1975), Ayres (1978, 1982) and Van Wagoner and Van Wagoner (1982). The Missi Group has been described by Bruce (1918), Ambrose (1936a, b), Buckham (1944), Byers (1953), Byers and Dahlstrom (1954), Byers et al. (1965), Stauffer and Mukherjee (1971) and Stauffer (1974). Recent work on the base metal deposits in the area includes that of Sangster (1972),

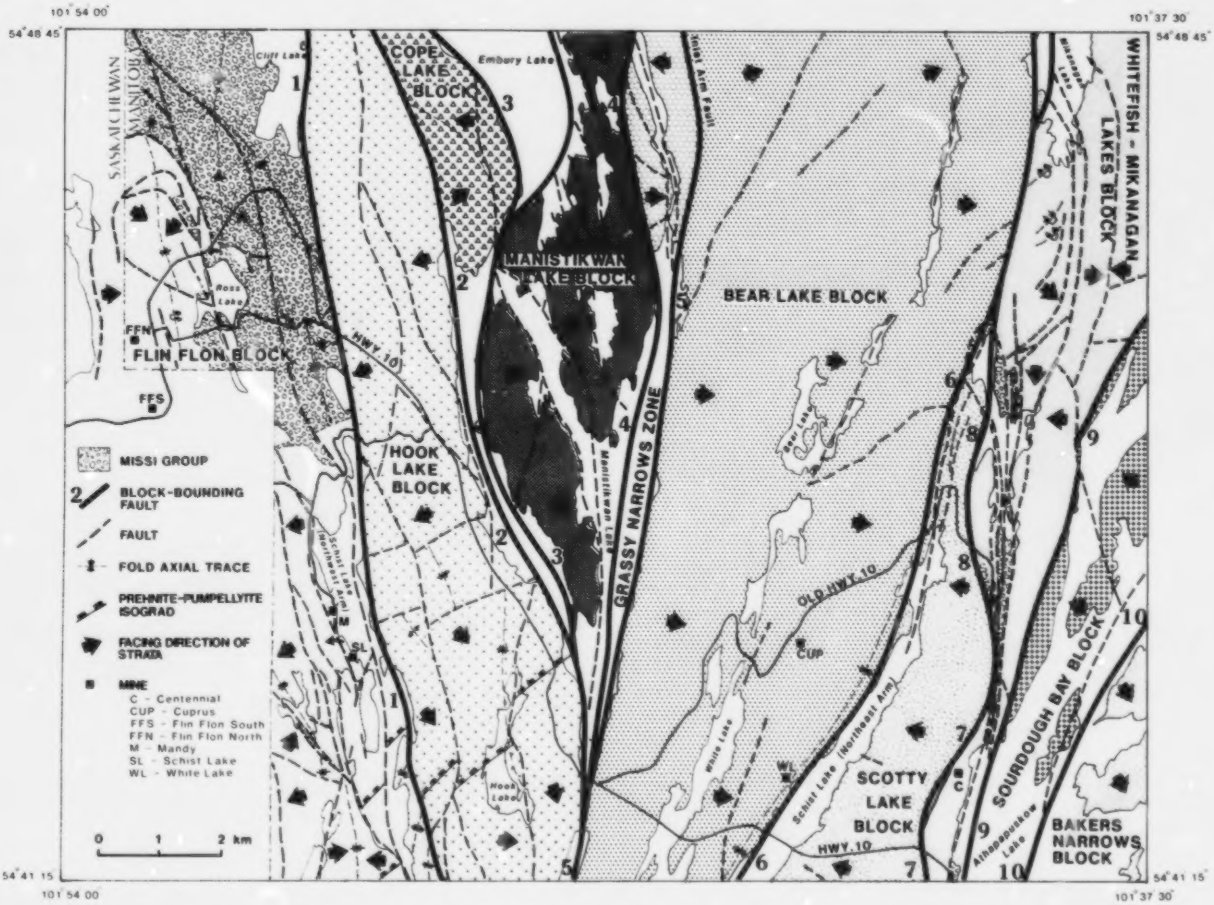

101°54'00"
54°48'45"
101°37'30"
54°48'45"
SASKATCHEWAN
MANITOBA
Cliff Lake
Embury Lake
COPE LAKE BLOCK
MANISTIKWAN LAKE BLOCK
Inlet Arm Fault
BEAR LAKE BLOCK
Mikanagan Lake
WHITEFISH - MIKANAGAN LAKES BLOCK
Ross Lake
FFN
FLIN FLON BLOCK
HWY. 10
FFS
HOOK LAKE BLOCK
Manistikwan Lake
GRASSY NARROWS ZONE
Bear Lake
OLD HWY. 10
CUP
Schist Lake (Northwest Arm)
M
SL
Hook Lake
White Lake
WL
Schist Lake (Northeast Arm)
SCOTTY LAKE BLOCK
C
SOURDOUGH BAY BLOCK
Athapapuskow Lake
BAKERS NARROWS BLOCK
HWY. 10
1
2
3
4
5
6
7
8
9
10
MISSI GROUP
BLOCK-BOUNDING FAULT
FAULT
FOLD AXIAL TRACE
PREHNITE-PUMPELLYITE ISOGRAD
FACING DIRECTION OF STRATA
MINE
C - Centennial
CUP - Cuprus
FFS - Flin Flon South
FFN - Flin Flon North
M - Mandy
SL - Schist Lake
WL - White Lake
0
1
2 km
54°41'15"
101°54'00"
54°41'15"
101°37'30"

Figure 3: Structural blocks, major faults and folds, and metamorphic isograds in the Flin Flon-White Lake area. Structure in the Missi Group is from Stauffer and Mukherjee (1971). Block-bounding faults are: 1 — Cliff Lake fault, 2 — Manistikwan Lake fault, 3 — Big Island and Embury Lake faults, 4 — Rosenberg Lake fault, 5 — Inlet Arm fault, 6 — Northeast Arm fault, 7 — Old Highway 10 fault, 8 — Scotty Lake fault, 9 — Sourdough Bay fault, 10 — North Arm fault.

Koo and Mossman (1975), and Gale et al. (1980). Byers et al. (1965) include descriptions and early references for many deposits in Saskatchewan.

PRESENT WORK AND ACKNOWLEDGEMENTS

Field work in the Flin Flon-White Lake area was conducted in 1979, 1980, 1982 and 1983, with short field sessions in 1981 and 1984. Standard pace and compass traverses from lakes and roads provided access to most of the area, and fly-in traverses were set out in the less accessible northern part of the area. Outcrop locations and geology were plotted on 1:15 840 scale aerial photographs, and subsequently transferred to topographic base maps of the same scale. The published scale of the final geological map (GR87-1-1) is 1:20 000.

In areas underlain by volcanic rocks, virtually every major outcrop was examined. In areas underlain by large intrusive bodies the traverse spacing was expanded, but nevertheless all major outcrop areas were visited. Approximately two thousand thin sections were cut and examined to establish the petrographic character of every unit. Two hundred and fifteen whole rock chemical analyses (Appendix) document the compositional variations of volcanic flows, volcaniclastic rocks, sedimentary rocks and intrusions. Nearly all of the analyzed samples were collected by drill or with a sledge hammer, after the mapping in a particular area had been completed and the stratigraphy established. This permitted selection of the best material from least altered outcrops.

Field work was facilitated by the able and cheerful assistance of a number of students from the Universities of Manitoba and Brandon: C. Alexander and T. Conlin (1979), R. Ambrosie, S. Peloquin and G. Carter (1980), J. Young, L. Wood and M. Cooper (1982), and J. Young, D. Seneshen and S. Boden (1983).

The authors wish to extend their appreciation to colleaques with whom they have had many fruitful discussions regarding the geology of the area: D. Price, A. Walker, J. Pickell and N. Provins (HBMS/HBED); M.T. Corkery, P.G. Lenton and H.V. Zwanzig (Manitoba Geological Survey); E. Froese and T. Gordon (GSC). Earlier drafts benefited from editing by W. Weber, B.B. Bannatyne and W.D. McRitchie. Thin sections and slabs were prepared by staff of the rock preparation lab under the direction of D. Berk. Chemical analyses were supervised by J. Gregorchuk at the Energy and Mines Analytical Laboratory. Careful drafting of the final geological map was done by D. Bagwell, assisted by M. McFarlane. Figures were drafted by L. Villeneuve and N. Barton. Report layout and

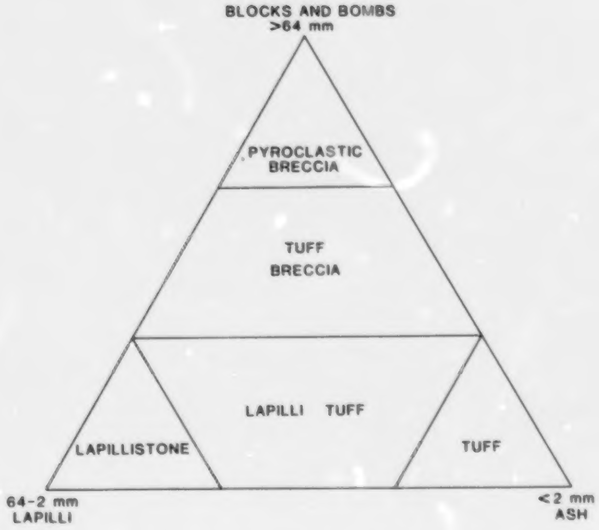

Figure 4: *Mixture and end member terms for pyroclastic deposits and fragments (from Fisher, 1966) adopted for use in this report.*

map preparation were supervised by R. Sales. Data on the mineral deposit map was provided in part by G.H. Gale and R. Eccles. Expediting for the field operation was handled by N. Brandson. Special thanks are due to B. Rigby for typing the original manuscript and to L. Chudy and S. Weselak for making subsequent revisions and additions.

REPORT STRUCTURE

This report contains complete descriptions of all supracrustal and intrusive units, as well as separate chapters on 'Structure', 'Metamorphism', 'Geochemistry' and 'Economic Geology'. Separate unit descriptions are given for each fault-bounded block (Fig. 3), because units and stratigraphic sequences are different and unique to each block; there is, for example, no "typical" basaltic andesite.

Each block description begins with an 'Introduction' summarizing the stratigraphy. Descriptions of more important units include geochemical characteristics and/or an interpretation of origin of the unit. Final sections in each block description summarize data and interpretations for each included unit and synthesize an interpretation or volcanic reconstruction for the entire block. Readers who wish only to get an overview of the geology of each block can do so by omitting the unit descriptions and going directly to block summaries.

Intrusive rocks are subdivided into those which predate the Missi Group or are of unknown age, and those which postdate the Missi Group. Cross-cutting relationships providing relative ages of different intrusions are not common; consequently it is not possible to determine the chronological order of all intrusions nor their age relative to the Missi Group. The post-Missi intrusive group includes *only* those bodies that either cut the Missi or intrude post-Missi faults. Placement of units in the map legend, and their order of description in the report, is based on composition (mafic to felsic) and does not imply relative age.

Most of the Missi Group was not remapped during this project because an adequate map (Stockwell, 1960) already exists. The location of folds and faults in the Missi is derived from Stauffer and Mukherjee (1971) and Stockwell (1960). A composite stratigraphic section through the Missi Group was measured to provide detailed information on upward variation in sedimentology of this sandstone-conglomerate unit.

Structure of the Flin Flon-White Lake area is described in two chapters — one on 'Folds' and another on 'Faults'. Each chapter begins with an introductory section summarizing main features. Major structures (folds, faults) are described in detail in following sections of the chapters.

The chapter on 'Metamorphism' is a summary of petrographic features in the subgreenschist, lower greenschist and middle greenschist facies in the area. More specific details on petrography are included in descriptions of individual units.

Geochemistry of volcanic and intrusive units is discussed first within the detailed unit descriptions, where geochemical characteristics of units are documented and compared with related units, and secondly in the chapter on 'Geochemistry', which is an overview that summarizes main geochemical characteristics and discusses probable tectonic environments into which the Amisk Group was emplaced. Sample locations are shown on map GR87-1-2.

Stratigraphic settings of volcanogenic base metal deposits are most thoroughly described in chapters on block descriptions. The chapter on 'Economic Geology' summarizes the setting and description for each major deposit as well as for significant, but uneconomic, deposits and showings. Map GR87-1-2 shows information obtained from cancelled assessment files (as of December 1986), and displays features related to hydrothermal alteration.

The section entitled 'Regional Considerations' compares the Amisk Group at Flin Flon with similar rocks at Amisk Lake (Saskatchewan) and Snow Lake. It also discusses the significance of the Amisk Group in the context of Trans-Hudson Orogen.

BEAR LAKE BLOCK

INTRODUCTION

The Bear Lake Block (Fig. 3) is bounded on the east by the Northeast Arm Fault and on the west by the Inlet Arm Fault. In this block a 5 km thick, mainly homoclinal east-facing sequence of lava flows and volcaniclastic rocks is exposed. Near the eastern margin of the block units are folded about the tight, northerly plunging Northeast Arm Syncline.

Preservation of primary structures in this block is generally moderate to good, rock outcrops are large and lichen-free, and stratigraphic units can be readily mapped. The Bear Lake Block comprises one of the thickest intact stratigraphic sequences in the map area and contains a suite of rocks that is diverse in composition and mode of deposition. The stratigraphic position and volcanic setting of two Cu-Zn massive sulphide deposits, Cuprus Mine and White Lake Mine, can be determined in this block with a degree of certainty seldom achieved elsewhere in the Flin Flon area. The recently discovered Westfield Au-rich Zn sulphide deposit also occurs in this block.

Eleven discrete units compose the stratigraphic section in the Bear Lake Block (Fig. 5). They are listed below in stratigraphic order from top to base, accompanied by their maximum stratigraphic thicknesses. Some of the units are lens- or wedge-shaped so the cumulative thickness exceeds the true stratigraphic thickness of the sequence.

Unit	
29	Intermediate tuff, breccia (30 m)
18a, 28b	Dacite, tuff (100 m)
25	Vick Lake andesitic tuff (900 m)
5, 27	Two Portage Lake ferrobasalt and rhyolite crystal tuff (200 m)
36	Mudstone, massive sulphides (25 m)
24	Little Spruce Lake andesitic lapilli tuff (350 m)
26	White Lake dacitic tuff (300 m)
13	Solodiuk Lake rhyolite (250 m)
30	Heterolithologic breccia (150 m)
1	Bear Lake basaltic andesite (3300 m)

BEAR LAKE BASALTIC ANDESITE (UNIT 1)

Introduction

The stratigraphic base of the east-facing Bear Lake Block consists of Bear Lake basaltic andesite, a 3.3 km thick unit of buff-weathering flows, related breccias and dykes. The lower part of this unit is removed by the Inlet Arm Fault, so its true thickness is in excess of 3.3 km. The basaltic andesite is overlain in the south by White Lake dacitic tuff (unit 26) and in the north by felsic heterolithologic breccia (unit 30) and Solodiuk Lake rhyolite (unit 13). The unit has a very large lateral extent that extends beyond the northern and southern boundaries of the map area.

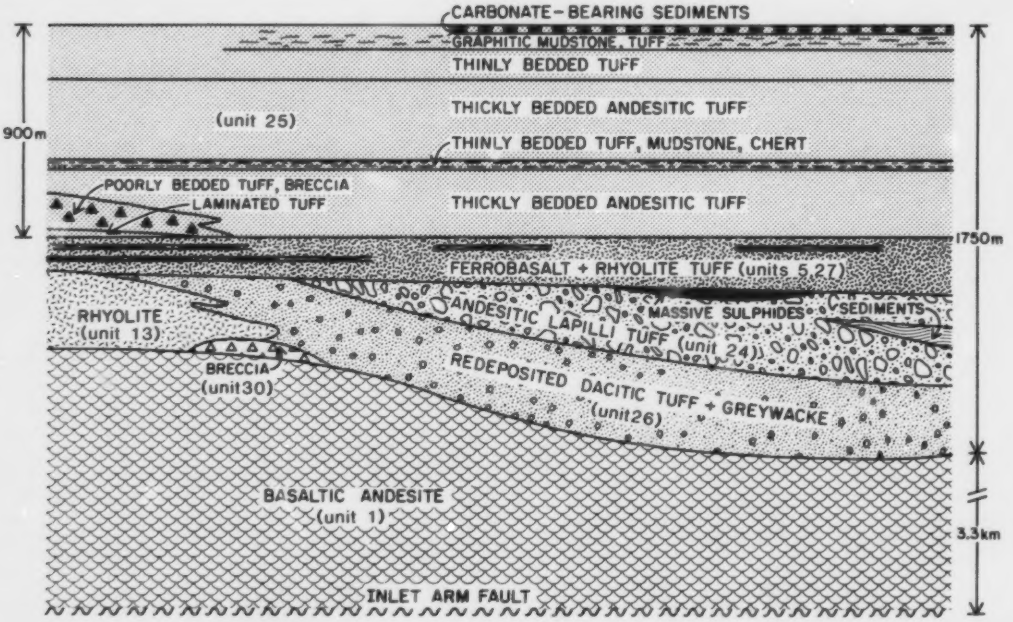
CARBONATE-BEARING SEDIMENTS
GRAPHITIC MUDSTONE, TUFF
THINLY BEDDED TUFF
THICKLY BEDDED ANDESITIC TUFF
(unit 25)
900m
THINLY BEDDED TUFF, MUDSTONE, CHERT
POORLY BEDDED TUFF, BRECCIA
LAMINATED TUFF
THICKLY BEDDED ANDESITIC TUFF
1750m
FERROBASALT + RHYOLITE TUFF (units 5,27)
RHYOLITE (unit 13)
ANDESITIC LAPILLI TUFF (unit 24)
MASSIVE SULPHIDES
SEDIMENTS
BRECCIA (unit30)
REDEPOSITED DACITIC TUFF + GREYWACKE (unit26)
BASALTIC ANDESITE (unit 1)
3.3km
INLET ARM FAULT

Figure 5: Schematic diagram showing main stratigraphic elements of the Bear Lake Block.

For convenience Bear Lake basaltic andesite is subdivided into four stratigraphic zones (Fig. 6). Systematic variation in flow thickness and organization can be demonstrated using this four-fold subdivision, as discussed later in this section.

Pervasive epidotization has affected a large part of the southern and western portions of the unit (Fig. 6). This epidotization has largely destroyed primary structures and rendered flow contacts unrecognizable. Outside the area of strong epidotization primary structures and flow contacts are well preserved and readily identified.

The basaltic andesite includes aphyric to sparsely pyroxene- and plagioclase-phyric lava flows, breccias composed of pillow fragments, abundant syn-volcanic dykes and sills, and very minor interflow tuff (Fig. 7). There is an almost complete absence of intercalated pyroclastic or sedimentary material.

Flows

Flow organization

Flow thickness ranges from less than 1 to more than 80 m and averages about 10 m; most flows are between 5 and 15 m thick. Pillowed flows are usually the thickest. Flows are organized in a manner comparable to that described by Dimroth et al. (1978), comprising one or more of the following divisions (from base to top): massive lava, pillowed lava and amoeboid pillow breccia ("flow top" breccia). Idealized flow types and an interpretation of the relationship between flow types (Fig. 8 and 9) are based on detailed examination of more than 200 individual flows. Specific examples of measured flow sequences are shown in Fig. 10.

Massive flows (Fig. 9) are generally the thinnest flow type. They have chilled bases, a few centimetres thick, which may in some flows contain thermal contraction fractures. Grain size increases towards the centres of flows but microgabbroic textures are not attained. Up to 15% amygdales commonly occur in the lowermost part of flows. Amygdale content and size decrease to the typically non-vesicular centre of the massive division and then increases upwards to the contact with the overlying flow or the amoeboid pillow breccia flow top. The uppermost part of the massive division is generally amygdaloidal and may contain large quartz-filled cavities (Fig. 11); these large gas cavities near the flow top are useful in identifying facing direction in altered or deformed flows. Tops of massive flows may include a division of amoeboid pillow breccia; those which do not are marked by an upper chilled contact with thermal contraction fractures. The contact between massive lava and amoeboid pillow breccia is commonly involuted (Fig. 12). Amoeboid pillows are interpreted to be derived by budding of irregular protruberances from the underlying massive lava. The size of the protruberances and amoeboid pillows ranges from a few centimetres to several metres.

Compound flows (Fig. 9) are generally intermediate in thickness between massive and pillowed types. Massive divisions of these flows share the characteristics of simple massive flows; however, the upper part of the massive division is transitional into an overlying pillowed division. This transitional contact is first marked by incipient selvages in the massive lava, succeeded by an abrupt upward budding into bun to elongate pillows. Pillow size commonly decreases to the top of the pillowed division with a concomitant increase in amygdale abundance. Elongate megapillows several metres in length may characterize the base of the pillowed division whereas smaller podiform pillows less than 1 m long occur at the top. Compound flows may include amoeboid pillow breccia tops similar to the flow tops on massive flows.

Pillowed flows (Fig. 3) are generally the thickest flow type, ranging to an observed maximum of 82 m. The lowermost portions of pillowed flows are commonly composed of elongate megapillows (5 — 15 m by less than 2 m) with low vesicularity. Amygdales typically occur in megapillow tops. In some flows the basal megapillows are imbricated and can be used to determine flow direction. Pillow size decreases upwards and vesicularity increases upwards as in compound flows. The contact between the pillowed division and amoeboid pillow breccia in pillowed and compound flows is similar to that in massive flows, with small involuted protruberances budding from the topmost layer of pillows (Fig. 13).

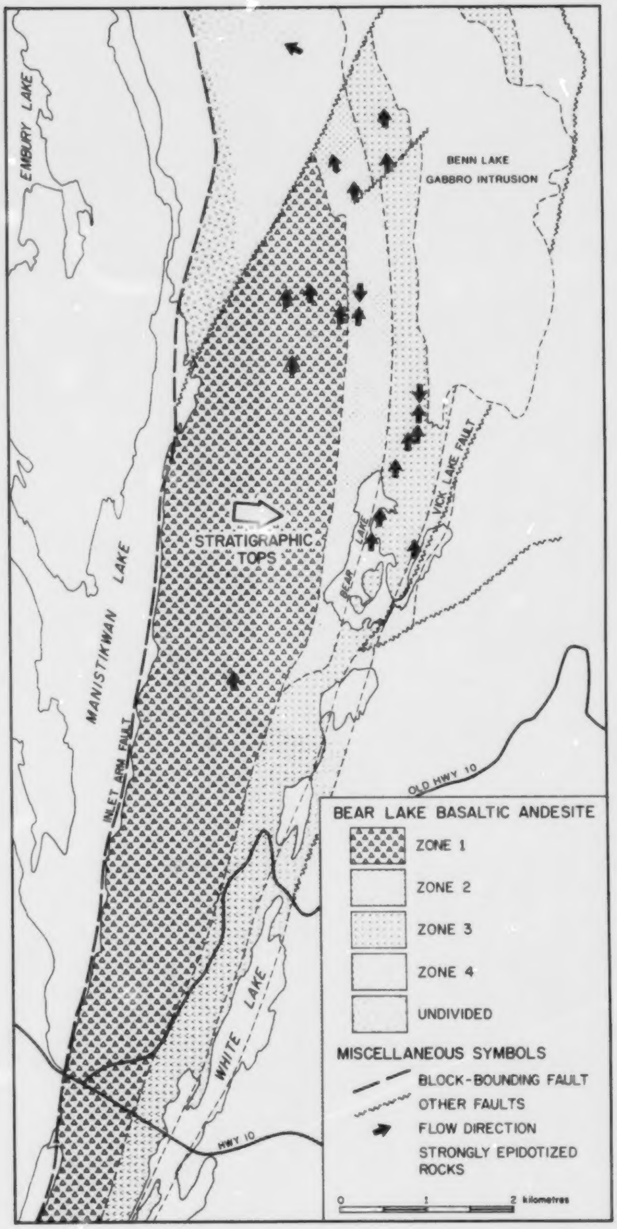

Figure 6: *Stratigraphic subdivisions, flow directions and areas of intense epidotization, Bear Lake basaltic andesite (unit 1).*

Primary structures in flows

Large, lichen-free outcrops on and north of Bear Lake permit ready identification of a wide variety of primary flow structures. These structures are described briefly below and are shown in accompanying photographs.

Figure 7: Laminated interflow tuff or sediment marking the contact between two Bear Lake basaltic andesite pillowed flows (unit 1). Benn Lake.

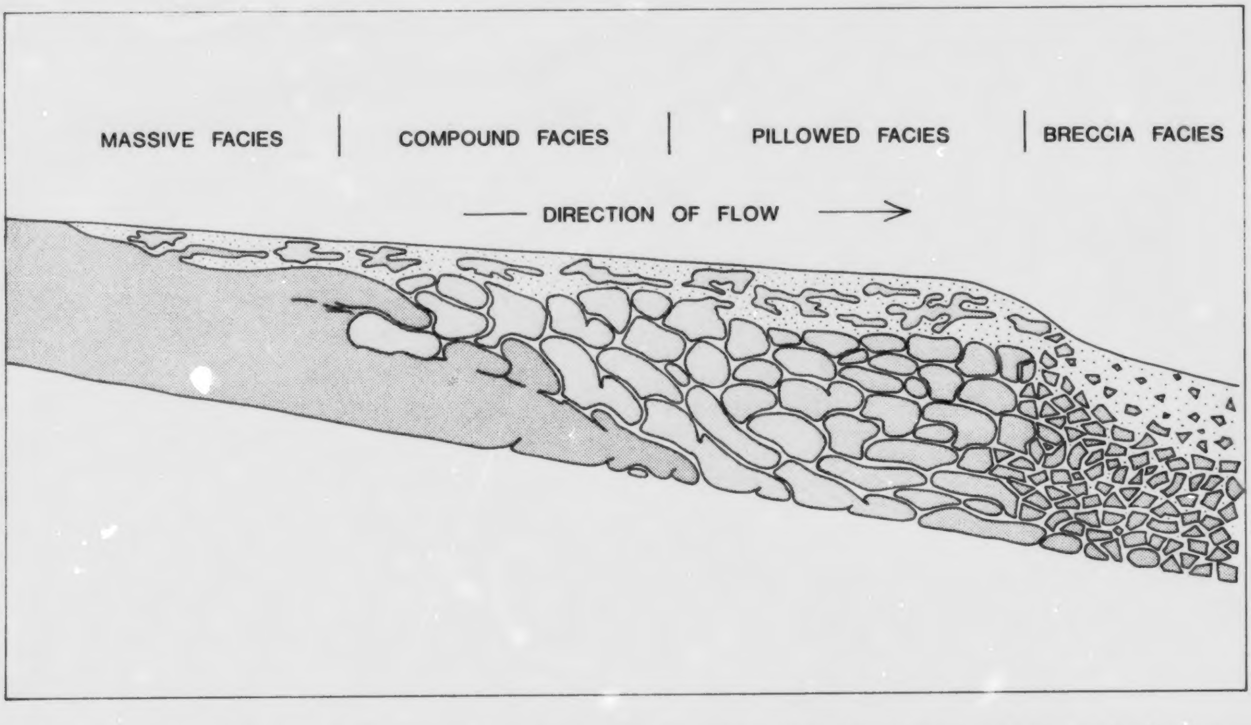
MASSIVE FACIES
COMPOUND FACIES
PILLOWED FACIES
BRECCIA FACIES
DIRECTION OF FLOW

Figure 8: Interpretation of the lateral facies sequence in an idealized subaqueous Bear Lake basaltic andesite flow, showing relationships between various flow types (Fig. 9). Not to scale; horizontal axis is compressed.

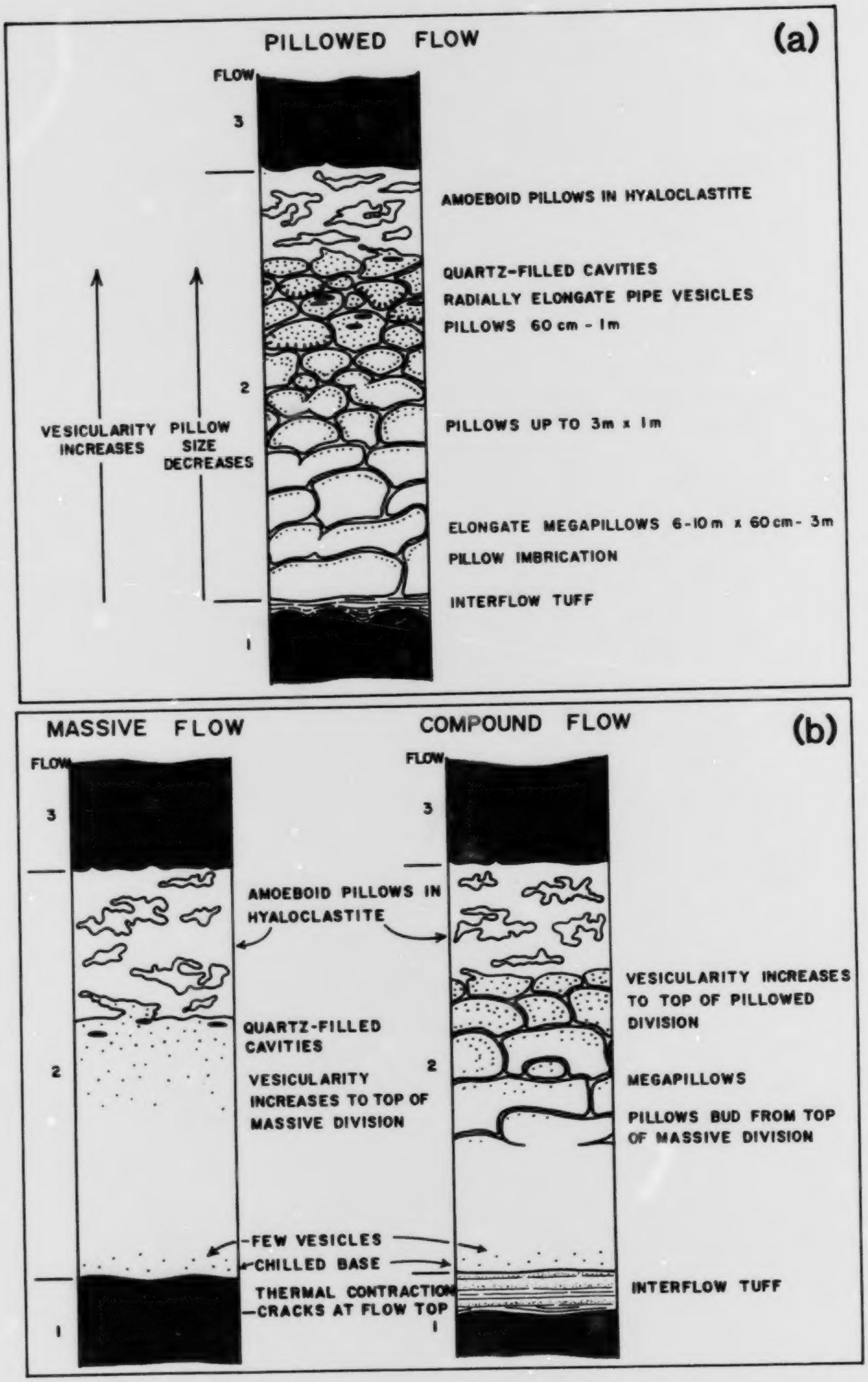
PILLOWED FLOW
(a)
FLOW
3
2
1
AMOEBOID PILLOWS IN HYALOCLASTITE
QUARTZ-FILLED CAVITIES
RADIALLY ELONGATE PIPE VESICLES
PILLOWS 60 cm - 1m
PILLOWS UP TO 3m x 1m
ELONGATE MEGAPILLOWS 6-10m x 60cm- 3m
PILLOW IMBRICATION
INTERFLOW TUFF
VESICULARITY INCREASES
PILLOW SIZE DECREASES
MASSIVE FLOW
COMPOUND FLOW
(b)
FLOW
3
2
1
FLOW
3
2
1
AMOEBOID PILLOWS IN HYALOCLASTITE
QUARTZ-FILLED CAVITIES
VESICULARITY INCREASES TO TOP OF MASSIVE DIVISION
VESICULARITY INCREASES TO TOP OF PILLOWED DIVISION
MEGAPILLOWS
PILLOWS BUD FROM TOP OF MASSIVE DIVISION
FEW VESICLES
CHILLED BASE
THERMAL CONTRACTION CRACKS AT FLOW TOP
INTERFLOW TUFF

Figure 9: *Typical features and zonation in: (a) pillowed and (b) massive and compound Bear Lake basaltic andesite flows. Numbers beside columns refer to individual flows.*

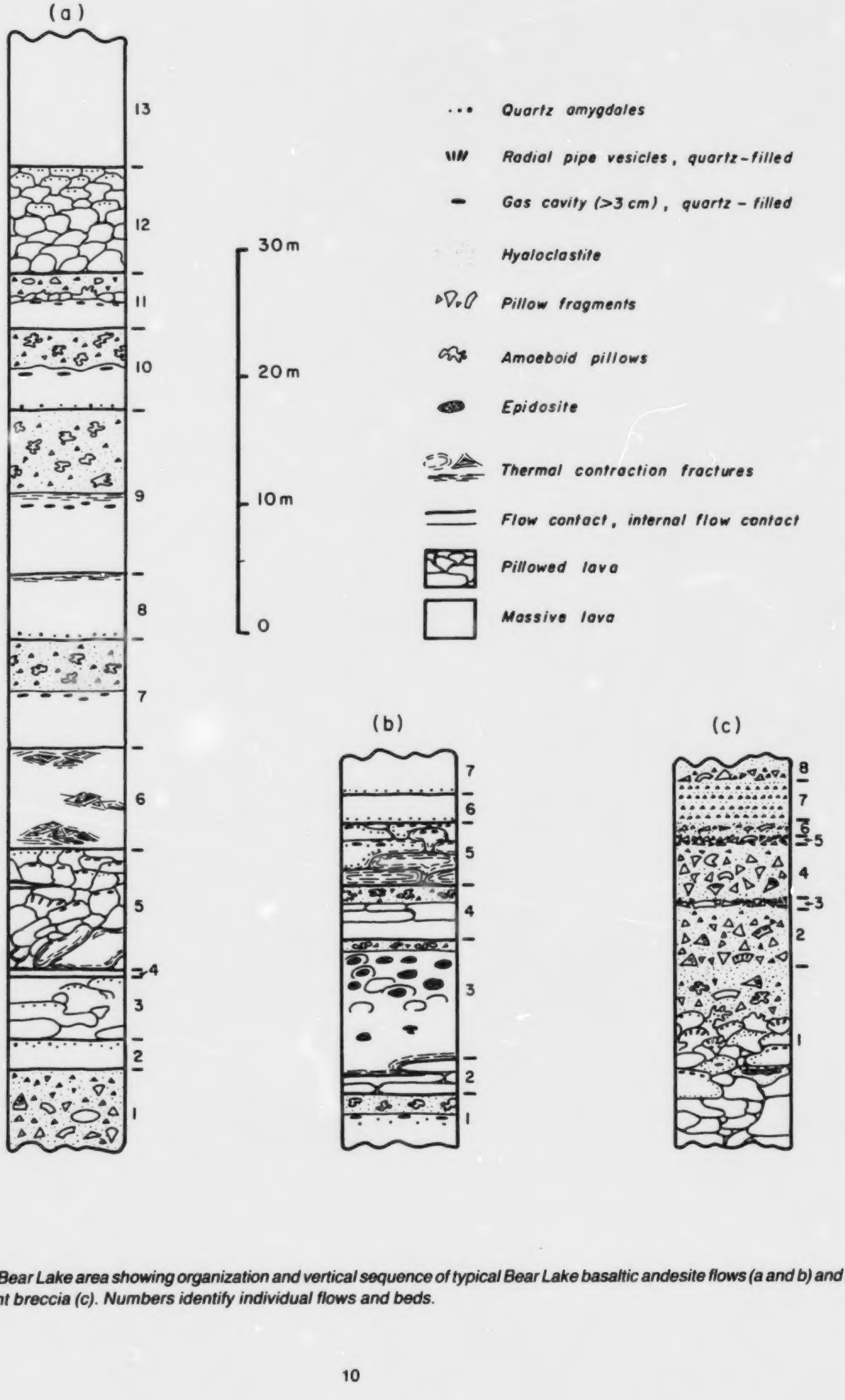
(a)
13
12
11
10
9
8
7
6
5
4
3
2
1
30m
20m
10m
0
Quartz amygdales
Radial pipe vesicles, quartz-filled
Gas cavity (>3 cm), quartz - filled
Hyaloclastite
Pillow fragments
Amoeboid pillows
Epidosite
Thermal contraction fractures
Flow contact, internal flow contact
Pillowed lava
Massive lava
(b)
7
6
5
4
3
2
1
(c)
8
7
6
5
4
3
2
1

Figure 10: *Sections from Bear Lake area showing organization and vertical sequence of typical Bear Lake basaltic andesite flows (a and b) and stratified pillow fragment breccia (c). Numbers identify individual flows and beds.*

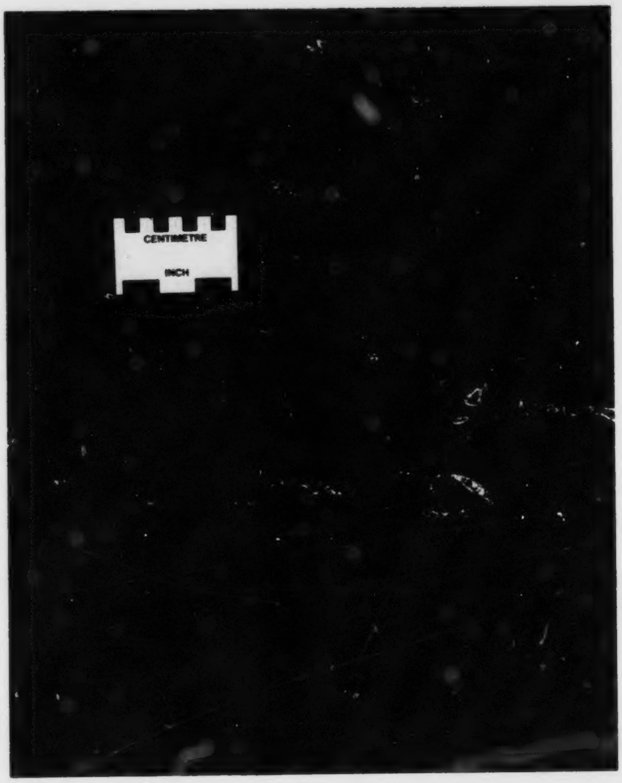
CENTIMETRE
INCH

Figure 11: *Contact between massive part of a Bear Lake basaltic andesite flow (unit 1) and its amoeboid pillow breccia flow top. Note the large, quartz-filled amygdales and oval gas cavities in top of massive lava. Flow number 7, Fig. 10a; Bear Lake.*

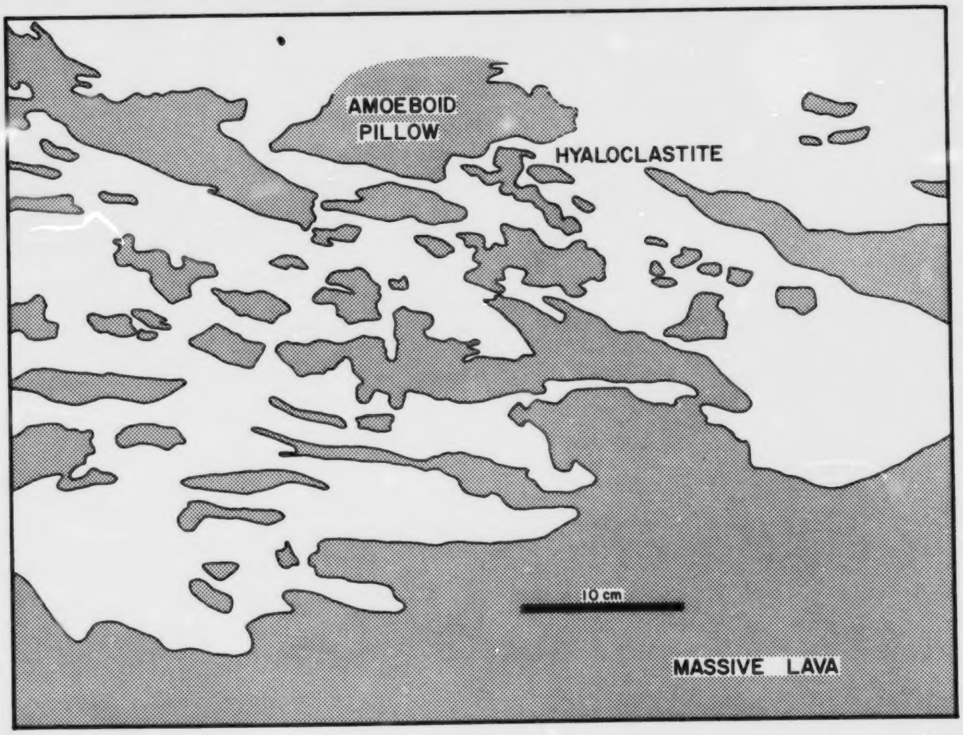
AMOEBOID PILLOW
HYALOCLASTITE
10 cm
MASSIVE LAVA

Figure 12: *Contact between massive division of a Bear Lake flow and overlying, amoeboid pillow (flow top) breccia; traced from a photograph. Note highly involuted protruberances from the massive lava into the breccia, which itself is composed of involuted, amoeboid lava pods (pillows) in a matrix of hyaloclastite.*

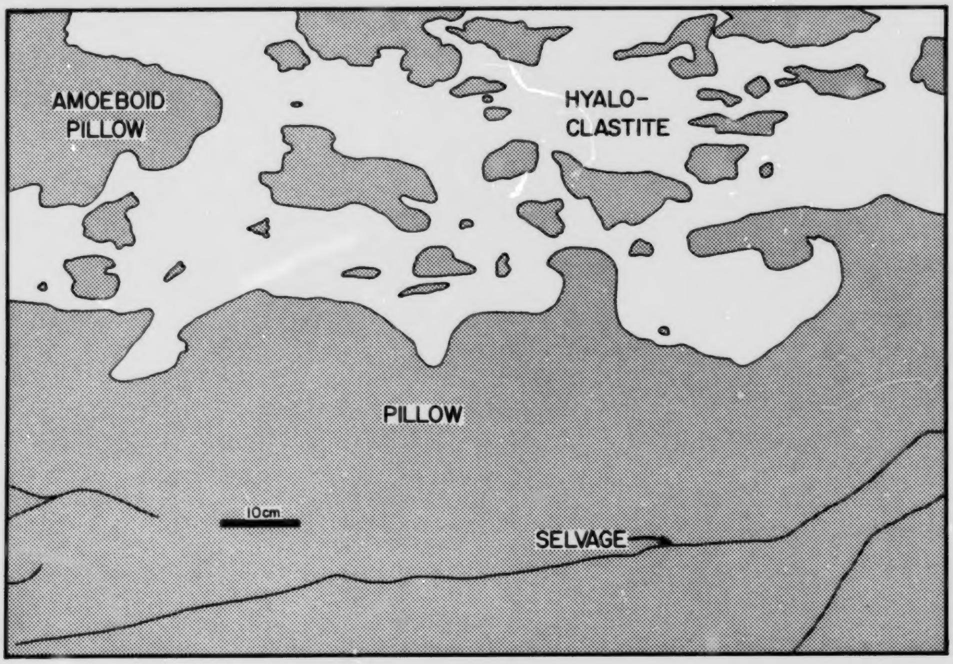
AMOEBOID PILLOW
HYALO-CLASTITE
PILLOW
10cm
SELVAGE

Figure 13: *Contact between pillowed division of a Bear Lake flow and the overlying, amoeboid pillow (flow top) breccia; traced from a photograph. Note irregular lava protrusions from topmost pillow into the breccia.*

CENTIMETRE
INCH

Figure 14: *Spherulitic pillow, Bear Lake basaltic andesite (unit 1), 1650 m north of Bear Lake. Outer margin of the pillow is not spherulitic; spherulites increase in abundance towards the core of the pillow, where they form a coalesced mass (light).*

Pillows, the most obvious primary structure in most exposures, range in length from less than 1 m to 15 m, as previously discussed (Fig. 14). Selvages are 2 — 10 mm wide and weather dark rusty brown in contrast to the light buff pillow interiors. Pillow morphology varies widely from elongate shapes to classic bun and podiform shapes, as well as to local large irregular bodies that may have acted as the distributary system in the flow. Some pillows are draped over underlying pillows and may form an imbrication giving flow direction. Amygdales are concentrated either in the pillow margin or the core, or both. In general, amygdales are most abundant and largest in the upper parts of pillows. Concentric amygdaloidal bands a few centimetres thick occur in some pillows. Radial pipe vesicles up to 1 cm in diameter by 10 cm long occur locally in pillow margins (Fig. 15); these can occur at tops, or completely around densely vesicular pillows. Vesicularity varies both within and between flows, with individual pillows attaining up to 40% total vesicularity. Secondary epidotization is commonly localized in the most vesicular portions of pillows (Fig. 16). Interpillow voids are filled with hyaloclastite that is largely altered to epidote and quartz. Clastic material between pillows varies in thickness (0 — 5 cm) from flow to flow but is relatively constant within a single pillowed flow and assists in identifying individual flows in the sequence.

Amoeboid pillow breccias which form flow tops (Fig. 9) range in thickness from less than 1 m to 20 m. They occur less commonly as lenses within the pillowed division. The breccias consist of amoeboid pillows, spalled pillow selvages, small pillow fragments, and hyaloclastite matrix. Amoeboid pillows are highly irregular in shape, have complete selvages, and are characterized by high vesicularity. They range from 10 cm to 4 m long, and are elongate parallel to flow contacts. The matrix is composed of brownish green selvage fragments, light buff to light green epidotized hyaloclastite granules, rusty chocolate brown granules, and an intergranular "cement" of chlorite, quartz and epidote. As demonstrated later (see section on Scotty Lake basalt) the matrix was derived from *in situ* quenching and thermal fragmentation of glassy rims of amoeboid pillows (Fig. 9). Although amoeboid pillows appear on an outcrop surface to be discrete matrix-supported bodies they can locally be shown to be interconnected.

Gas cavities up to 25 cm long by 4 cm wide, some with cupola shapes, preferentially occur at the top of massive divisions of flows (Fig. 17) and in the upper parts of some pillows. These cavities parallel the flow contacts or pillow elongation and are filled with coarse quartz or quartz and pink feldspar.

Thermal contraction cracks occur within some pillows and at margins of some massive flows. The fractures are paper thin, parallel, filled with quartz, and spaced 1 mm to tens of centimetres apart. In pillows the cracks are parallel to the rim and occur in the outer margin and, more rarely, in the outer part of the pillow core. In massive flows the fractures parallel the flow contact, including protruberances and irregularities. In both pillows and massive flows the spacing of thermal contraction cracks increases with distance from the cooling surface. Thermal contraction cracks are developed preferentially in weakly vesicular or non-vesicular portions of massive flows or pillows. Radial contraction cracks in pillows are perpendicular to cooling surfaces (Fig. 18 and 19) and break pillows into wedge-shaped domains.

CENTIMETRE
INCH

Figure 15: *Involuted pillow with well developed quartz-filled radial pipe vesicles, Bear Lake basaltic andesite (unit 1a), 1900 m north of Bear Lake. Budding from pillow structure, through influx of additional magma, is responsible for irregular shape of pillow.*

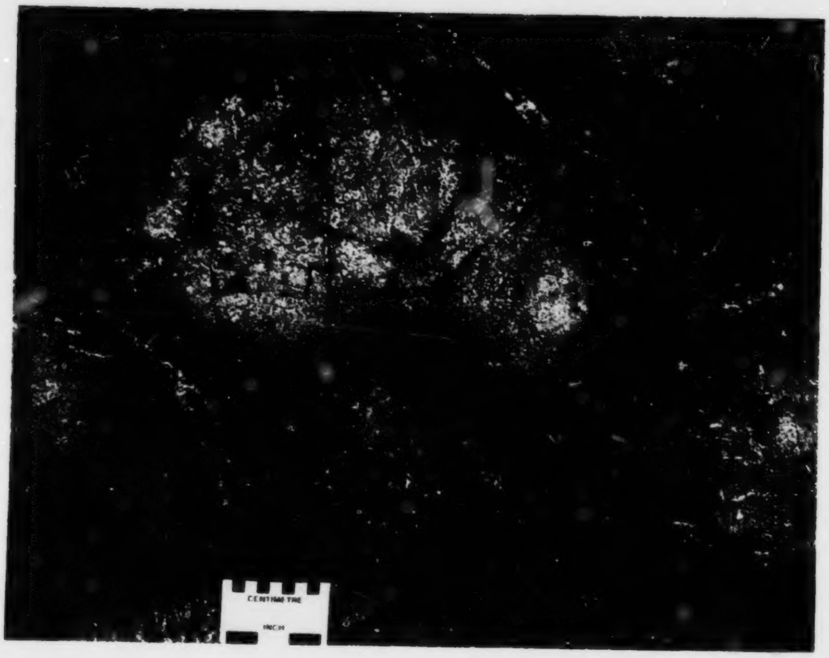

Figure 16: *Bun-shaped pillow (unit 1a) with quartz-filled radial pipe vesicles around margin, 2 km north of Bear Lake. Light coloured, epidote-rich domains, such as that in upper half of pillow, are common in pillowed Bear Lake basaltic andesite flows.*

Figure 17: *Concentration of large, oval, quartz-filled gas cavities near the top of a 4 m thick massive Bear Lake basaltic andesite flow (unit 1), 400 m east of the north end of Bear Lake. The gas cavities, up to 45 cm long and 10 cm wide, are elongate parallel to flow contacts and occur in the top 2 m of the flow.*

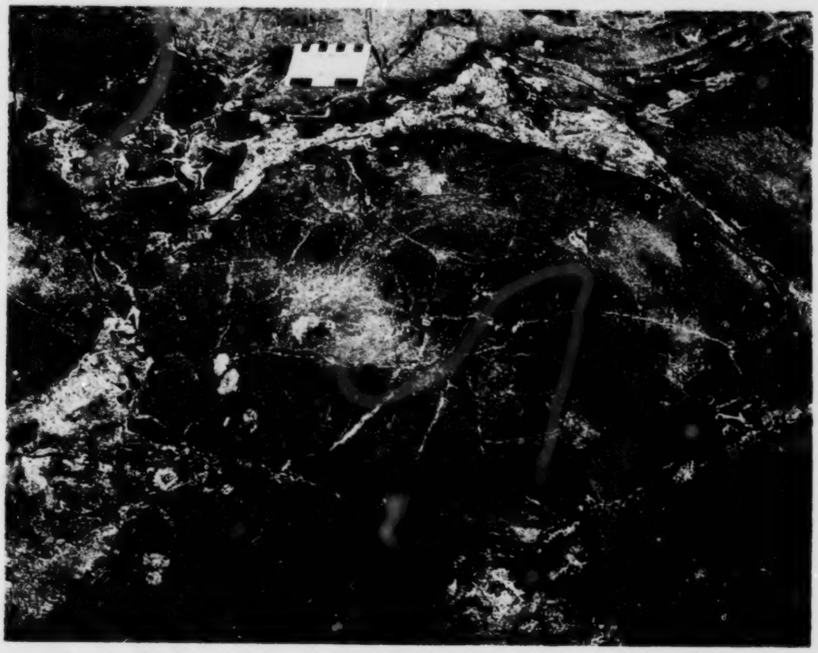

Figure 18: *Pillowed flow, Bear Lake basaltic andesite (unit 1), 1130 m southwest of Benn Lake. This pillow contains two sets of primary contraction fractures — a radial and a concentric set (Fig. 19). It also contains a well developed set of fine-scale thermal contraction cracks. Bits of spalled selvage and fragments of pillow margin occur in interstices between pillows; hyaloclastite matrix (light) is recrystallized to epidote and quartz.*

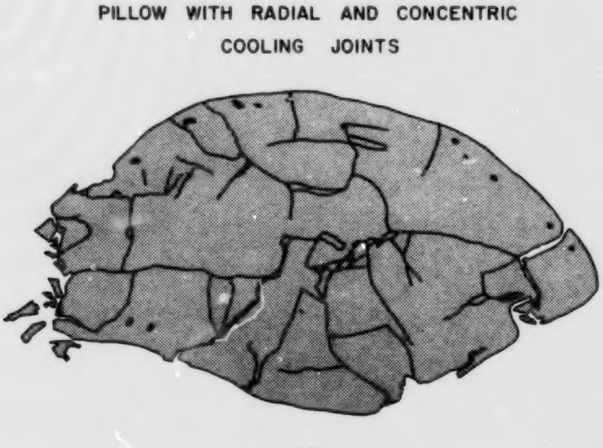

Figure 19: *Radial contraction fractures perpendicular to concentric cooling cracks in a pillow, resulting in angular and wedge-shaped fracture-bounded domains. Traced from pillow in Fig. 18.*

Petrography of flows

Aphyric, plagioclase-phyric, pyroxene-phyric, and pyroxene + plagioclase-phyric flows occur in each of the four stratigraphic subdivisions (Fig. 6). Zone 1 is dominantly aphyric, zone 2 is dominantly pyroxene-phyric, zone 3 is dominantly aphyric, and zone 4 is a mixture of aphyric and porphyritic types with no single type dominating.

Pyroxene phenocrysts range in size from 0.4 to 4 mm and in abundance from 1 to 10%. Some flows in zone 4 on White Lake contain up to 25% pyroxene phenocrysts. Pyroxene phenocrysts are locally concentrated at the base of massive divisions and in the lower halves of pillows. Primary subhedral pyroxene is pseudomorphed by tremolite-actinolite and chlorite; rare clinopyroxene relicts occur in flows on Bear Lake.

Plagioclase phenocrysts are euhedral, equant to tabular in shape, 0.2 to 2 mm long, and form less than 1 to 5% of the flows. Some flows northeast of Shore Lake are more prominently plagioclase-phyric with up to 15% phenocrysts. Plagioclase is albite-twinned, in areas of best preservation, but generally the polysynthetic twinning has been destroyed and plagioclase is overprinted by fibrous tremolite-actinolite, epidote and chlorite.

Groundmass in the best preserved flows consists of felted plagioclase microlites (0.2 — 0.4 mm long, up to 50%; Fig. 20) and fine grained fibrous tremolite-actinolite, chlorite, and epidote after groundmass clinopyroxene. Minor interstitial quartz occurs in some flows. In moderately to strongly recrystallized rocks there is no preservation of primary textures and the groundmass consists of a foliated fine grained mass of tremolite-actinolite, chlorite, epidote, albite, minor quartz, leucoxene, pyrite, magnetite, carbonate and rare stilpnomelane and sericite.

Amygdales, 0.1 — 10 mm in diameter, are filled with epidote, quartz, carbonate, chlorite and rare pumpellyite. A common type consists of radiating sheaves of elongate epidote crystals which have nucleated at or near the margins of the amygdale (Fig. 21, 22). Some polymineralic amygdales are concentrically zoned and have textures that pseudomorph primary zeolite(?) infillings.

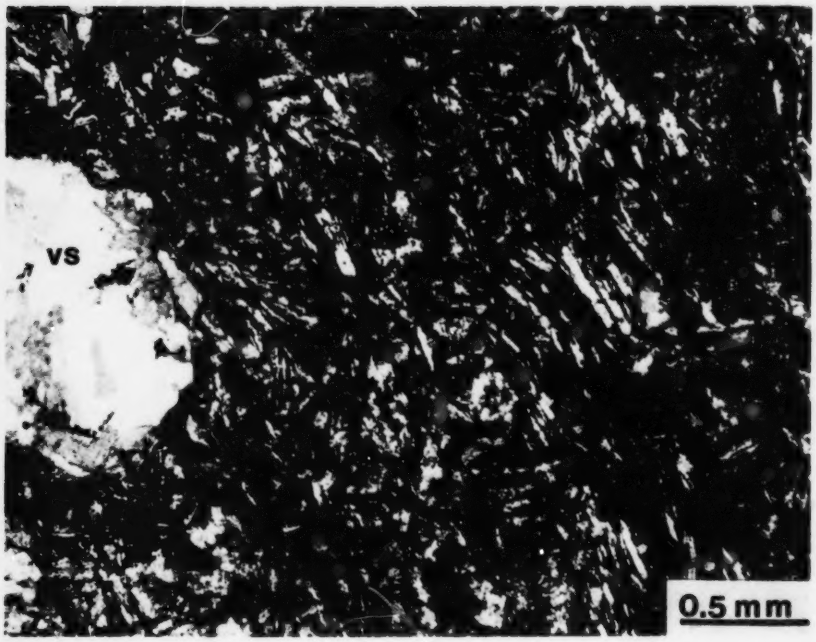

Figure 20: *Partly recrystallized Bear Lake basaltic andesite (unit 1) with well preserved plagioclase microlites. Vesicle (vs) is filled with quartz and chlorite. Sample 3269-1, plane polarized light.*

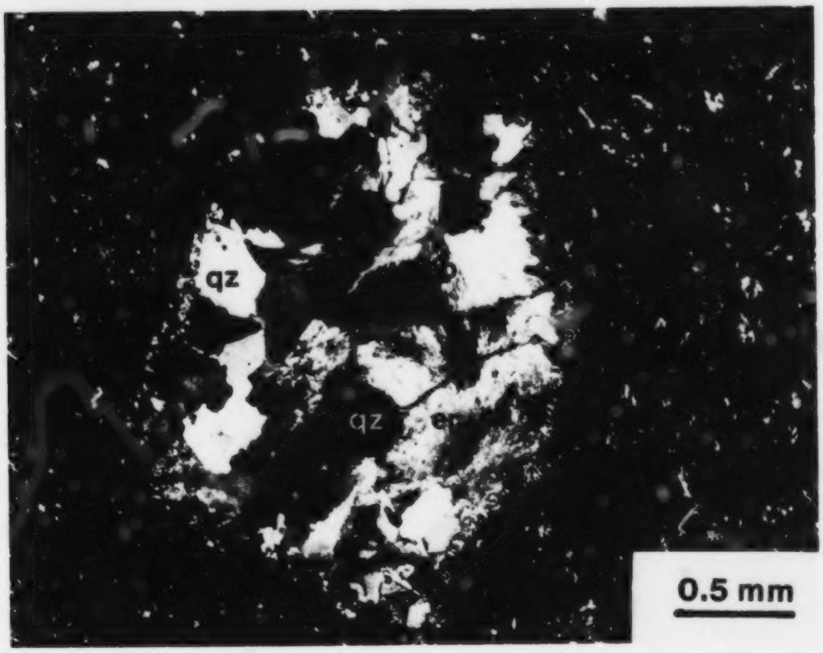

Figure 21: Fan-radial epidote after unknown mineral (probably a zeolite) filling vesicles (vs) in Bear Lake basaltic andesite (unit 1). Fans have typically nucleated from a single site on vesicle walls. Sample 348-1, polarized light.

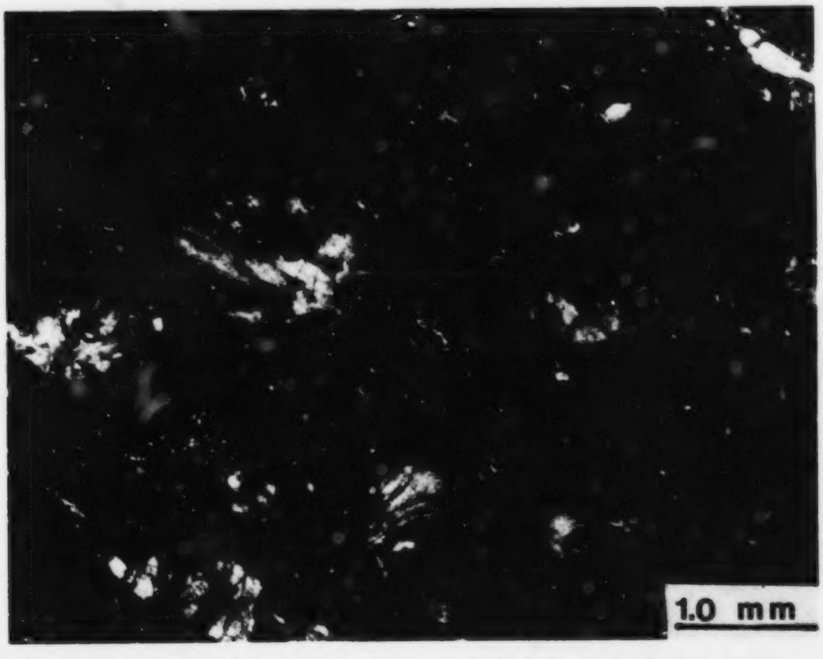

Figure 22: Polymineralic amygdale in Bear Lake basaltic andesite flow (unit 1). Euhedral quartz (qz) commonly occurs at the margin of the amygdale. Epidote (ep) has a fibro-radial habit; plumose crystal clusters are nucleated at or near the amygdale margin. Sample 1474-1, crossed polarizers.

Stratigraphic variation in flow type and thickness

In this 3.3 km thick unit 219 individual flows have been measured and examined in detail; of these, 144 are completely exposed from base to top. From these data some limited statistical observations have been made on stratigraphic variations in flow thickness and flow organization (Fig. 23-25, Tables 2-4).

The average thickness of flows (of all types) decreases upward from 16.9 m in zone 1 to 4.2 m in zone 4. There is a an attendant upward decrease in the proportion of thick (greater than 15 m) flows, and increase in the proportion of thin (less than 5 m) flows. The systematic upward decrease in average flow thickness is shown by each flow type (massive, compound and pillowed; Fig. 24). The proportion of massive flows increases upwards and is accompanied by a parallel decrease in the proportion of pillowed flows; the proportion of compound flows remains relatively constant (Fig. 25).

Table 2: Average flow thickness in zones 1, 2, 3 and 4 of Bear Lake basaltic andesite (unit 1)

Stratigraphic Zone	Number of Measured Flows	Average Thickness (metres)	Standard Deviation
4	16	4.2	5.1
3	68	7.1	5.5
2	35	12.3	14.6
1	25	16.9	17.8
Total	144	9.7	

Table 3: Flow thickness, by flow type, in the lower (zones 1 and 2) and upper (zones 3 and 4) portions of Bear Lake basaltic andesite (unit 1)

Flow Type	Stratigraphic Zone	Number of Measured Flows	Average Thickness (metres)	Standard Deviation
Massive	3 + 4	31	3.8	3.7
	1 + 2	13	6.1	3.0
Compound	3 + 4	28	9.9	5.5
	1 + 2	11	13.9	10.7
Pillowed	3 + 4	19	6.3	5.5
	1 + 2	30	22.0	22.2

Table 4: Frequency of flow types in zones 1, 2, 3 and 4 of Bear Lake basaltic andesite (unit 1) (M — massive division, P — pillowed division, B — amoeboid pillow (flow top) breccia)

Stratigraphic Zone	Number of Measured Flows	Massive flows		Compound flows		Pillowed flows	
		M	MB	MP	MPB	P	PB
4	18	9 (50%)	3 (17%)	2 (11%)	0 (0%)	2 (11%)	2 (11%)
3	78	19 (24%)	11 (14%)	19 (24%)	11 (14%)	17 (22%)	1 (1%)
2	35	5 (14%)	6 (17%)	2 (6%)	5 (14%)	9 (26%)	8 (23%)
1	33	4 (12%)	0 (0%)	5 (15%)	3 (9%)	4 (12%)	17 (52%)
Total	164	37 (23%)	20 (12%)	28 (17%)	19 (12%)	32 (19%)	28 (17%)

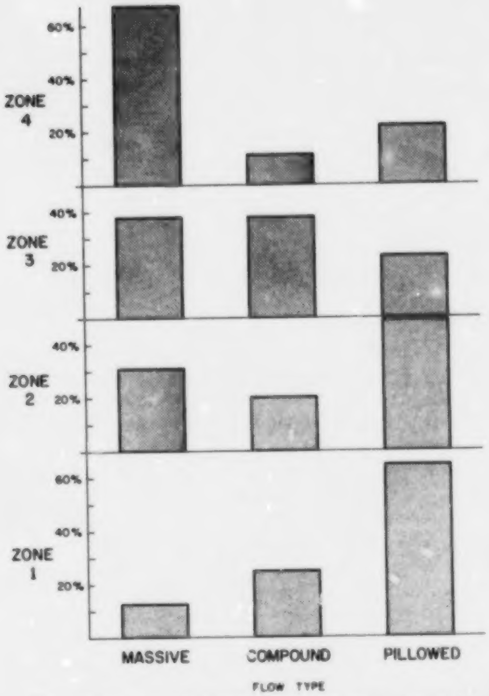

Figure 23: *Frequency of flow types (massive, compound and pillowed; see Fig. 8) in zones 1, 2, 3 and 4 of the Bear Lake basaltic andesite. The proportion of massive to pillowed flows increases steadily up section through the unit. N = 164 flows (33 from zone 1, 35 from zone 2, 78 from zone 3, and 18 from zone 4).*

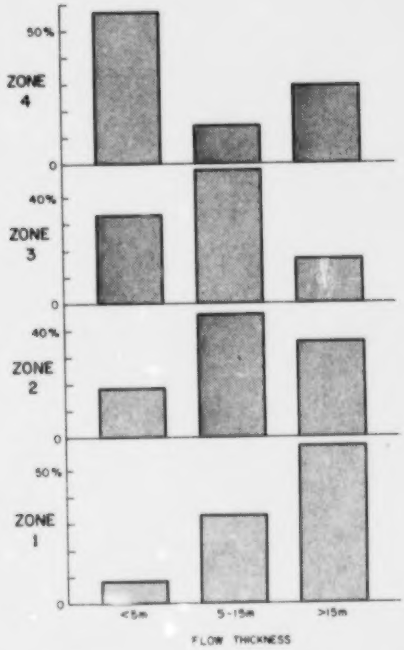

Figure 25: *Flow thickness in zones 1, 2, 3 and 4 of the Bear Lake basaltic andesite. Flows become progressively thinner upwards through the section. N = 219 flows.*

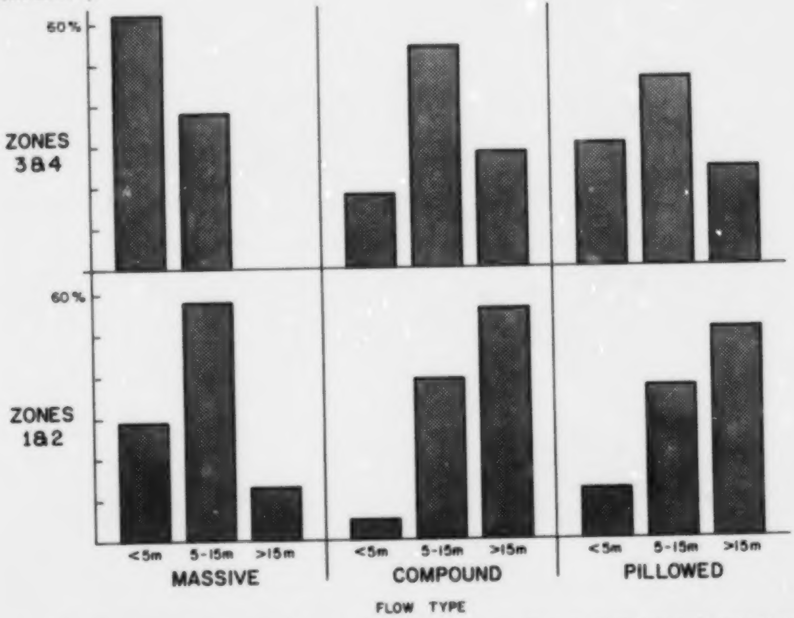

Figure 24: *Flow thickness, by flow type, in the lower (zones 1 and 2) and upper (zones 3 and 4) portions of Bear Lake basaltic andesite. A shift to thinner flows is displayed by all three flow types, in the upper part of the unit. N = 216 flows.*

Pillow fragment breccias

Units of breccia composed of pillow fragments range from single beds within flow sequences, to the large irregular body at Bear Lake which is 300 m thick by 4 km long. Mappable bodies of pillow fragment breccia (unit 1e) occur at the top of zone 2 and within zone 4 (Fig. 6). Fragments in the breccias are petrographically similar to associated lava flows, and locally breccias can be shown to be laterally equivalent to pillowed flows. Thick units of pillow fragment breccia (such as that north of Bear Lake) commonly contain thin (1 — 3 m) pillowed flows which locally compose up to 50% of the sequence.

Bedding in pillow fragment breccia ranges in thickness from less than 1 m to greater than 20 m; most beds are less than 6 m thick (Fig. 26). Bed contacts vary from sharp to subtle; they are defined by abrupt changes in fragment size and proportion of fragments to matrix. The lower three-quarters of most beds are clast supported, unsorted, non-graded to weakly normally graded. The upper one-quarter of the beds are typically matrix supported, contain smaller fragments, and display grading in both fragment size and matrix grain size. Reverse grading at the base of beds is rare. These bedforms suggest that the pillow fragment breccias were deposited from subaqueous debris flows.

Fragments are angular to subrounded, slabby to equant (Fig. 27, 28). Some are clearly hemispherical or crescentic pillow margin fragments (Fig. 29), some with radial pipe vesicles and remnant selvages. Subordinate complete, oval to bun-shaped pillows (generally less than 60 cm; Fig. 30) occur in thicker beds, where they overlie pillowed flows. Fragments of amoeboid pillow breccia, found in some thicker beds, further demonstrate derivation from cold flows. Fragments are variably vesicular (less than 5 to 40% amygdales) and some have vesicularity comparable to associated pillowed flows. Wedge-shaped fragments, crescentic fragments and complete pillows are diagnostic, as they indicate that these breccias were formed from disintegration of pillows along radial and concentric thermal contraction fractures (e.g. Fig. 19). Fragment size ranges from 2 mm to 80 cm; the base of most beds contains fragments up to 40 cm across whereas tops of beds have fragments in the 5 — 10 cm range.

Matrix of the breccias is composed of pillow granules, dark brown pillow selvage fragments, and fine grained light brown material largely replaced by epidote (Fig. 27, 28). The matrix is the same composition as fragments and was derived, like the fragments, from break-up, disintegration and granulation of consolidated pillowed flows.

Most beds are monolithologic but fragment types may vary between beds. Rare beds are heterolithologic, indicating mixing of fragments from more than one flow.

Intercalated thin pillowed flows have sharp basal and top contacts with enclosing pillow fragment breccia (Fig. 31). In some breccia beds topmost pillows have been plucked from the underlying flow and locally breccia fills hollows and voids between pillows at the flow top. In the thick breccia unit north of Bear Lake some flows grade laterally northwards from medium (60 — 100 cm), to small pillows (30 cm), to pillow fragment breccia. In one exposure this lateral gradation takes place over 45 m.

Pillow fragment breccia differs significantly from amoeboid pillow breccia, which is the other major breccia type in the Bear Lake sequence. Pillow fragment breccias are demonstrably transported and form thick mappable units, whereas amoeboid pillow breccias are integral parts of individual lava flows and consequently do not form mappable units at this scale. Amoeboid pillows formed during extrusion of the flow, by budding from the underlying massive or pillowed lava (Fig. 12, 13). In contrast to pillow fragment breccias that formed by the cold fragmentation of pillows to form pillow fragment breccias.

The large irregular body of pillow fragment breccia north of Bear Lake has been studied in considerable detail by Dolozi and Ayres (1987). They found the vesicularity of fragments to be significantly higher (average 35%, range 10—50%) than enclosing and intercalated pillowed flows (average 20%, range 0—35%). On this basis they concluded that the fragments had a shallow water, magmatic explosive origin, with subsequent slumping to produce downslope debris flows.

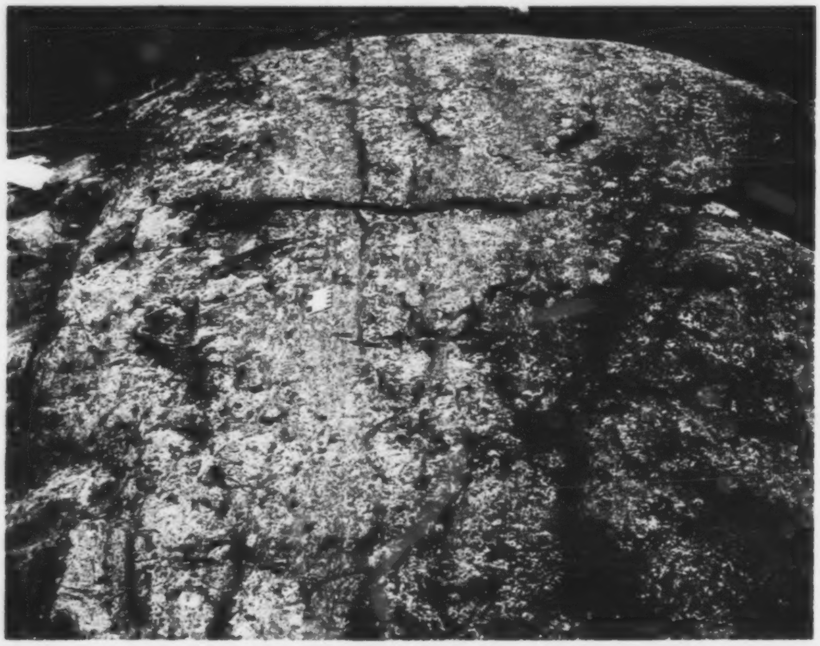

Figure 26: Crudely stratified Bear Lake pillow fragment breccia (unit 1e), 250 m north of Bear Lake.

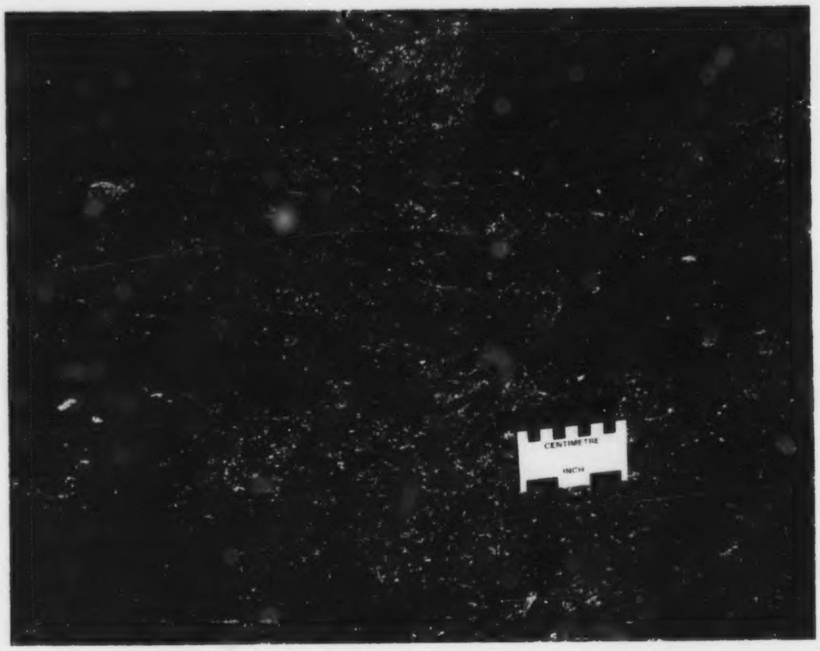

Figure 27: Pillow fragment breccia (unit 1e), 700 m north of Bear Lake, containing angular fragments, some with remnants of selvage and bands of amygdales.

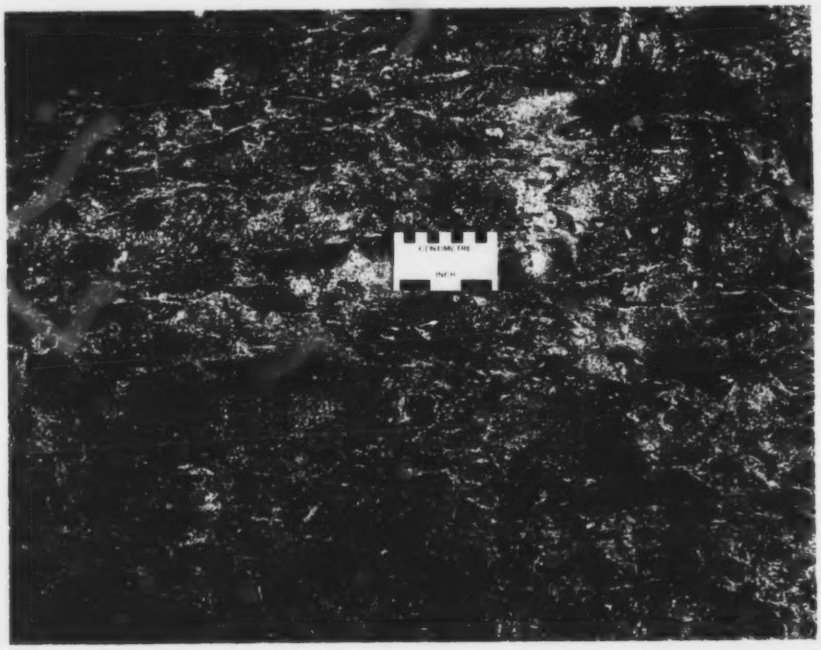

Figure 28: Pillow fragment breccia (unit 1e), 1070 m north of Bear Lake. Angular, pie-shaped to crescentic fragments vary in amygdale content. Bands of amygdales and bits of selvage identify fragments as derived from pillows.

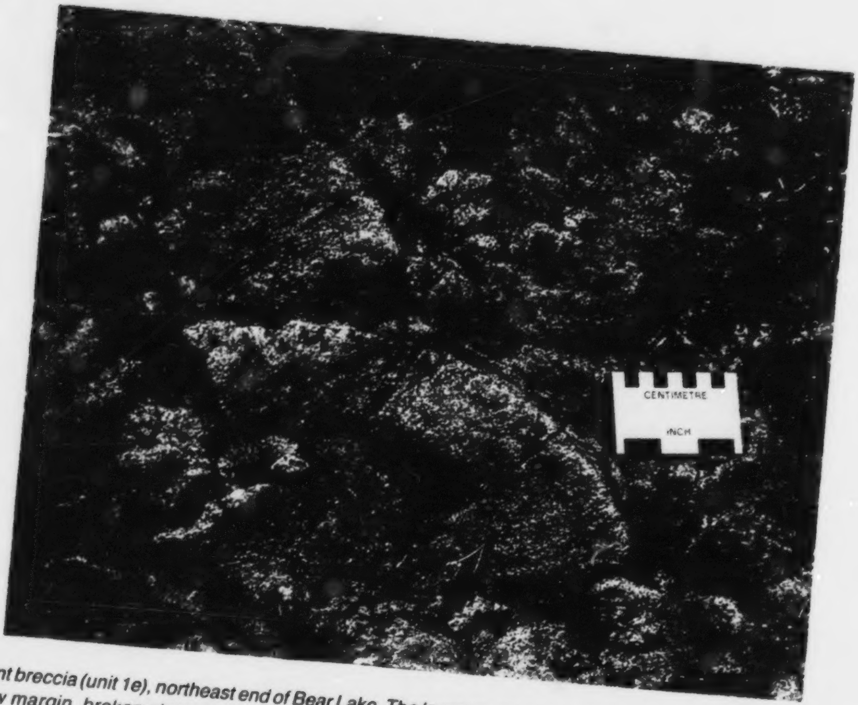

Figure 29: *Pillow fragment breccia (unit 1e), northeast end of Bear Lake. The large crescentic fragment is diagnostic for this type of breccia: it represents part of a pillow margin, broken along primary radial and concentric cooling fractures (see Fig. 19).*

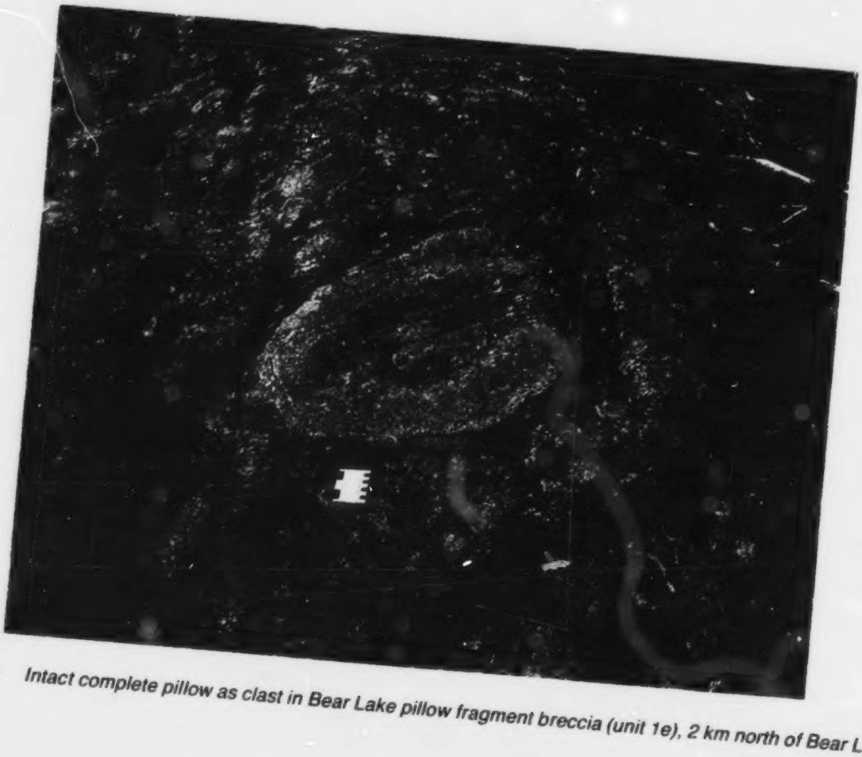

Figure 30: *Intact complete pillow as clast in Bear Lake pillow fragment breccia (unit 1e), 2 km north of Bear Lake.*

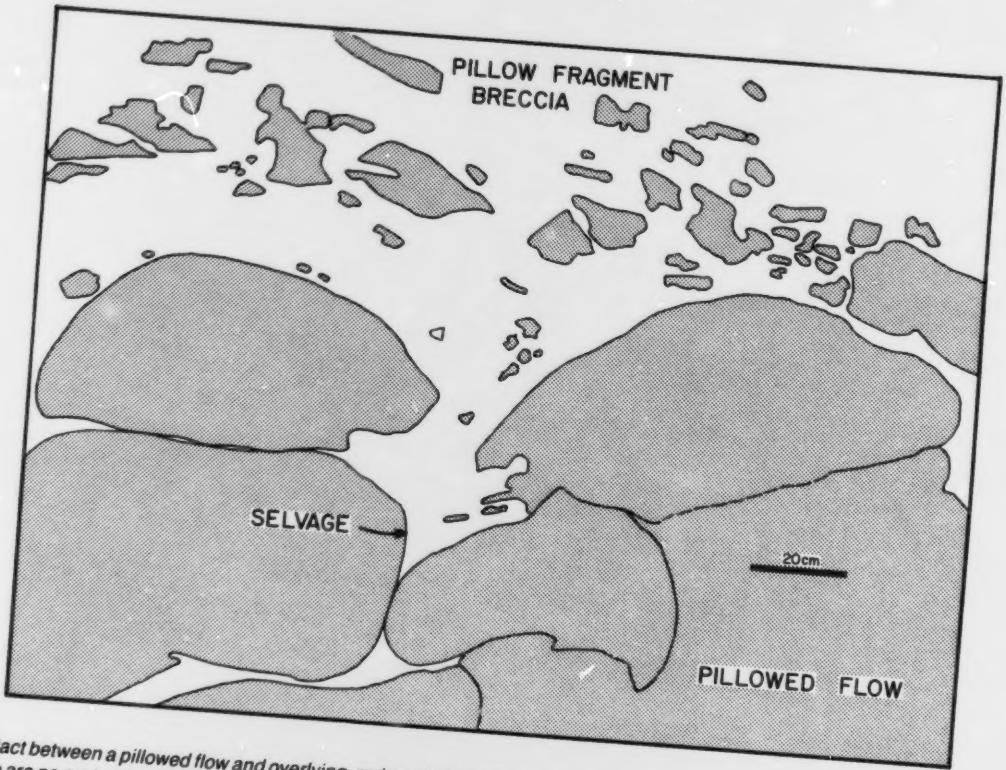

Figure 31: Contact between a pillowed flow and overlying, redeposited, pillow fragment breccia; traced from a photograph. Note that, unlike Fig. 13, there are no protrusions from the topmost pillows into the breccia. The breccia is composed of pillow fragments which were derived from cold fragmentation of pillowed flows elsewhere in the section.

Our work, although not as detailed, is consistent with the interpretation of Dolozi and Ayres (1987) that the breccias were deposited from debris flows. The fragment shapes, however, lead us to conclude that they formed by either: 1) cold fragmentation of pillowed flows, and subsequent mass movement and deposition, or 2) *in situ* fragmentation of pillows during extrusion. Our reasons for this interpretation are evident from the preceding description of these deposits and are supported by the description, and similar interpretation, of identical pillow fragment breccias in a Pliocene seamount exposed at La Palma in the Canary Islands (Staudigel and Schmincke, 1984). Staudigel and Schmincke (1984) conclude that "pillow fragment breccias" at La Palma comprise "remobilized debris that accumulated on the higher slopes of the volcano rather than direct results of an eruption". Additional support for an origin of fragments in the Bear Lake basaltic andesite by cold fragmentation or *in situ* fragmentation of pillowed flows is (a) the presence of radial pipe vesicles in some fragments (Fig. 32), including the highly vesicular varieties, and (b) fragments of flow top breccia in some beds (Fig. 33). Philpotts and Lewis (1987) have suggested that radial pipe vesicles are products of gas exsolution into bubbles attached to the solidification front of cooling lava. Radial pipe vesicles are unlikely to form by this mechanism under the rapid cooling conditions accompanying subaqueous magmatic explosions, but are consistent with slower cooling rates in a lava flow; fragments with radial pipe vesicles must therefore be pillow fragments.

Staudigel and Schmincke (1984) estimate that pillow fragment breccias at La Palma travelled between 3 to 6 km downslope from their source before deposition. Similar downslope redeposition may explain the higher average vesicularity of pillow breccia fragments as compared with associated pillowed flows in the Bear Lake basaltic andesite noted by Dolozi and Ayres (1987). If the Bear Lake pillow breccias travelled similar downslope distances from their source it is possible that they originated from more highly vesiculated, less degassed flows deposited in shallower water, closer to the volcano summit.

Synvolcanic sills, dykes and irregular bodies

Synvolcanic dykes occur throughout the Bear Lake basaltic andesite. Their abundance is highly variable. Dykes are typically 0.5 to 3 m thick, but are locally several metres wide; an average thickness on 96 measured dykes is 2.7 m. They range from straight-walled, steeply dipping sills and dykes to irregular bodies which wind through pillowed flows and breccias without cross-cutting pillows or fragments. Two large, mappable lenticular sill-like bodies occur in the sequence; the largest, between Bear Lake and McBratney Lake, is 3 km long and up to 300 m wide.

Smaller dykes invariably have chilled contacts against host flows. Margins of the intrusions are commonly banded; bands are 5 to 15 cm thick and are interpreted as chilled phases deposited by successive pulses of magma that passed through the dyke. Individual bands have an outer buff-

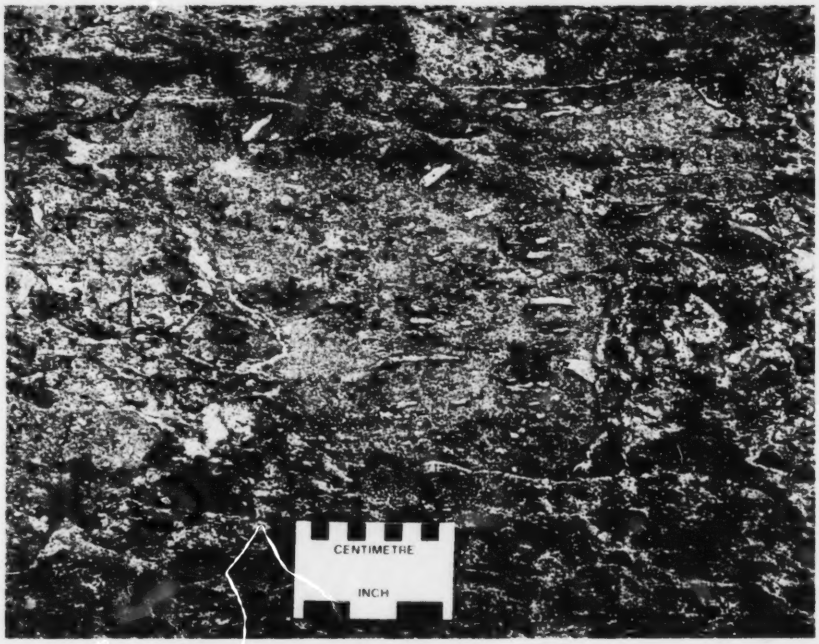

Figure 32: *Pillow fragment (above scale card) with curvilinear pillow margin and quartz-filled radial pipe vesicles, Bear Lake pillow breccia (unit 1e), 250 m north of Bear Lake.*

Figure 33: *Stratified pillow fragment breccia (unit 1e) containing a large fragment of amoeboid pillow flow top breccia (a: amoeboid pillow, h: recrystallized hyaloclastite). The presence of fragments such as this within pillow fragment breccia indicates the breccias were derived from the fragmentation of cold pillowed flows; the debris was redeposited from subaqueous density currents. 1740 m north of Bear Lake.*

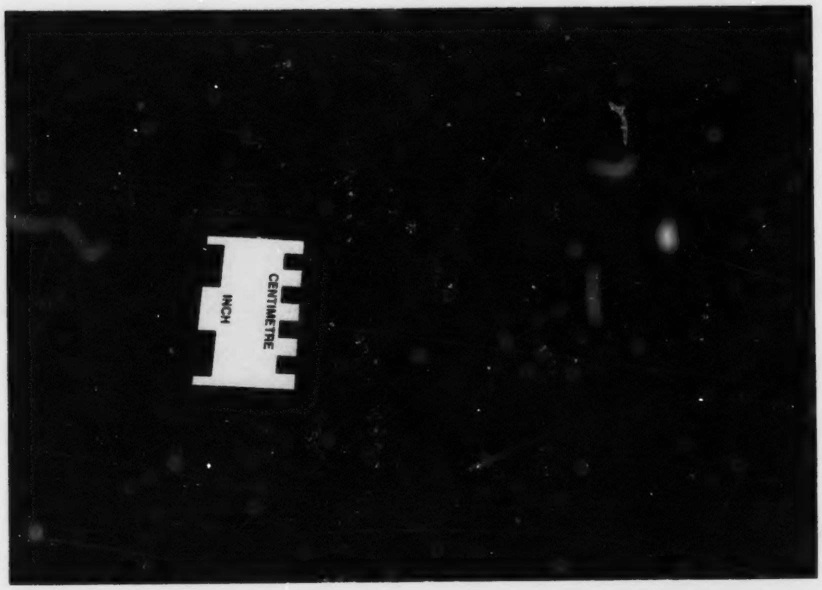

Figure 34: *Synvolcanic dyke 17 cm wide cutting Bear Lake basaltic andesite (unit 1), Benn Lake area. Dyke has chilled margins (arrows) and characteristic bands in the margins. Core of the dyke is non-banded and amygdaloidal.*

brown zone that grades to a darker brown inner zone. Sharp contacts occur between the dark brown material of one band and the light brown material in the next band towards the centre of the dykes (Fig. 34). Thickness of individual bands increases gradually from dyke margins to centres.

Most dykes weather buff brown, similar to massive basaltic andesite flows. They are typically equigranular and fine grained (0.25 — 1 mm) and may contain up to 20% quartz (up to 2 mm). Most dykes are aphyric but a minority contain pyroxene or plagioclase phenocrysts up to 2 mm across and forming 10 — 30% of the rock. Some dykes are composite with up to 3 individual phases; most are aphyric but some composite dykes include both aphyric and porphyritic phases. Pyroxene phenocrysts are selectively concentrated on the stratigraphic footwalls of some porphyritic sills.

Amygdales up to 10 mm in diameter (generally less than 5 mm) occur in a variety of positions within some dykes: (1) at margins, (2) in cores, (3) sporadically throughout, (4) in massive central portions of banded dykes and (5) in bands of some banded dykes. Locally amygdales are concentrated at the tops of sills. Vesicularity in one dyke, trending at a high angle to stratigraphy, increases up-section, from negligible to 25%.

Most intrusions strike slightly east of north (Fig. 35), parallel to their host lava flows, and can be interpreted as synvolcanic sills. Some have both sill and dyke components. Some exhibit involuted margins in flow top breccia (Fig. 36) suggesting intrusion shortly after extrusion of the flows, prior to lithification.

The two mappable bodies of quartz diorite are typically fine grained and texturally identical to thinner sills and dykes. They are composed of numerous individual intrusions containing, near the margins, screens of pillowed lavas. In one outcrop, where the contact is well exposed, the intrusion displays a vague layering, about 8 m from its contact with flows. Grain size in the intrusions is generally less than 0.5 — 1 mm, with quartz locally up to 4 mm diameter.

Dykes and sills are texturally similar to the centres of thick massive flows. They are hypidiomorphic granular with equant amphibole pseudomorphs after primary pyroxene (40—60%) and stubby tabular epidote + plagioclase pseudomorphs after primary calcic plagioclase.

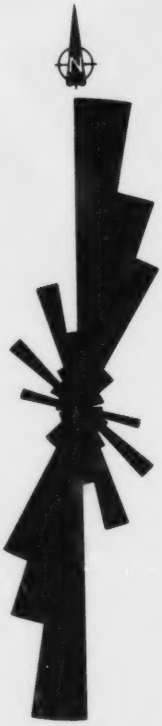

Figure 35: *Rose diagram displaying the orientation of 80 synvolcanic dykes emplaced in Bear Lake basaltic andesite; most dykes strike slightly east of north, approximately conformable with host lava flows.*

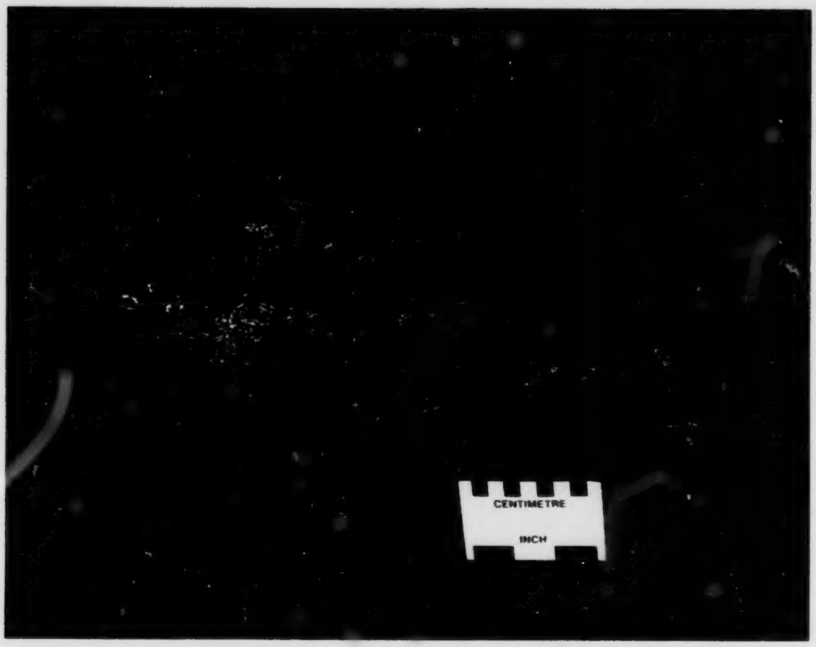

Figure 36: Synvolcanic mafic dyke (unit 1f) intruding Bear Lake basaltic andesite flow-top breccia (unit 1). Amoeboid protrusions (A) of dyke into host breccia attests to unconsolidated nature of breccia and synvolcanic character of dyke.

Quartz is anhedral, equant, and interstitial; it ranges in abundance from negligible to approximately 20%. Iron oxides include secondary magnetite and hematite and up to 4% leucoxene after primary Fe-Ti oxides.

Several features indicate that the intrusive suite is high-level and synvolcanic. For example, dykes are not present in overlying dacite tuff (unit 26) and rhyolite (unit 13), and are compositionally similar to host basaltic andesite flows. In addition, vesicles, thermal contraction fractures, local spherulites, and irregular contacts with breccia all indicate a high level of intrusion essentially synchronous with volcanism.

Alteration and deformation

An area of approximately 6 km² south of Sleep Lake and west of McBratney Lake is characterized by strongly epidotized flows (Fig. 6). These altered flows grade into well preserved varieties on and north of Bear Lake; however, *all* flows in unit 1 are affected, to some degree, by secondary epidotization.

In the area of least alteration, hyaloclastite and highly vesicular portions of flows are most strongly affected by epidote replacement. In pillows epidotization generally follows the distribution of vesicles, i.e. variably along pillow margins or in pillow cores (Fig. 16). In massive flows the most common alteration style is that of long, linear epidosite bands a few centimetres wide that parallel flow contacts. These bands do not necessarily coincide with vesicular zones in the flow.

In strongly epidotized zones the degree of alteration is an order of magnitude greater than in the better preserved zones. Epidosite domains are typically oval to slightly irregular in shape, weather pale yellow-green to white, and compose 40—60% of outcrops. They are 10—70 cm long and locally up to 2 x 1 m. They have sharp to gradational contacts (over about 2 cm) with the unepidotized, brown weathering, schistose material that occurs between epidosite masses. Pillow selvages are locally preserved between epidosite domains; they are marked by darker weathering zones, locally further defined by yellow-green interpillow filling, and in some places by interpillow chert. More commonly, strong schistosity has destroyed pillow selvages.

The relationship between vesicularity and epidotization is variable. In amygdaloidal pillows, large quartz amygdales are commonly preserved in the epidosite domains; however, amygdales do not occur in *all* epidosites and thus the process of epidotization is not strongly related to primary pillow porosity. For example, in some flows amygdales are in the schistose material and not in the epidosite. Random selective epidotization of certain fragments in breccias produced an apparent heterogeneity in clast composition.

The zone of epidotization is also characterized by more intense deformation (Fig. 37). Deformation is essentially a flattening process perpendicular to foliation and has produced a number of typical tectonite structures. Due to ductility contrast between resistant epidosite domains and unepidotized portions of flows the pillow margins develop a strong schistosity which is wrapped around epidosite masses. Epidosite domains act as rigid bodies which display pull-aparts and shear-step fractures (Figs. 38 and 39). Quartz amygdales are flattened into pancake-shaped forms, and pillows, where recognizable, are flattened approximately 5-10:1. Synvolcanic dykes at a high angle to foliation are ptygmatically folded whereas those parallel to foliation are boudinaged.

Geochemistry

Nine analyses of relatively unaltered Bear Lake flows are listed in the Appendix (analyses 1 — 9). The average silica content (calculated H_2O and CO_2 free) is 54.71%. The analyses range in SiO_2 content from about 52 to 57% and in MgO content from about 4 to 9% (Fig. 40). On a Jenson cation plot (Fig. 41) the suite straddles the tholeiite-calc-alkaline boundary and does not display Fe-enrichment.

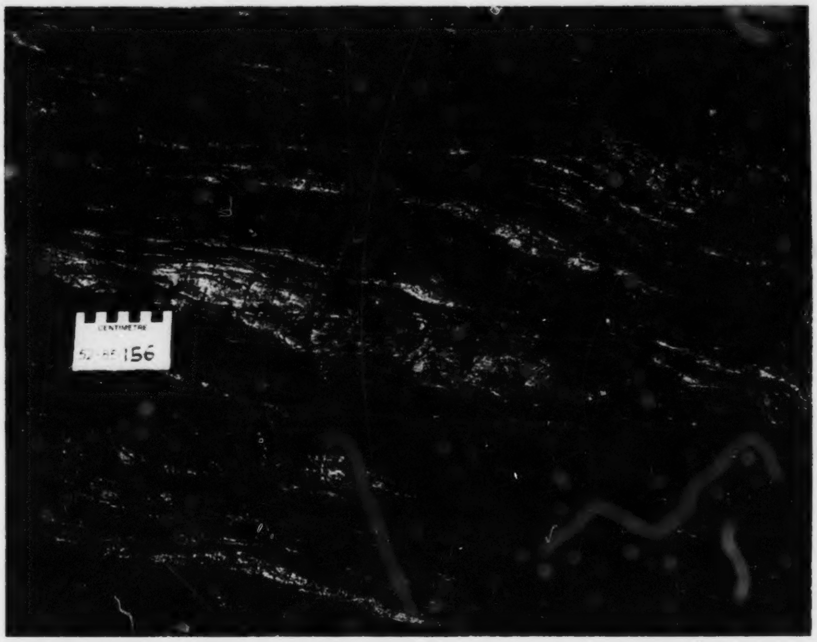

Figure 37: *Banded epidosite derived from pillowed Bear Lake basaltic andesite; typical of deformation observed adjacent to the Inlet Arm fault. South end of Schist Lake.*

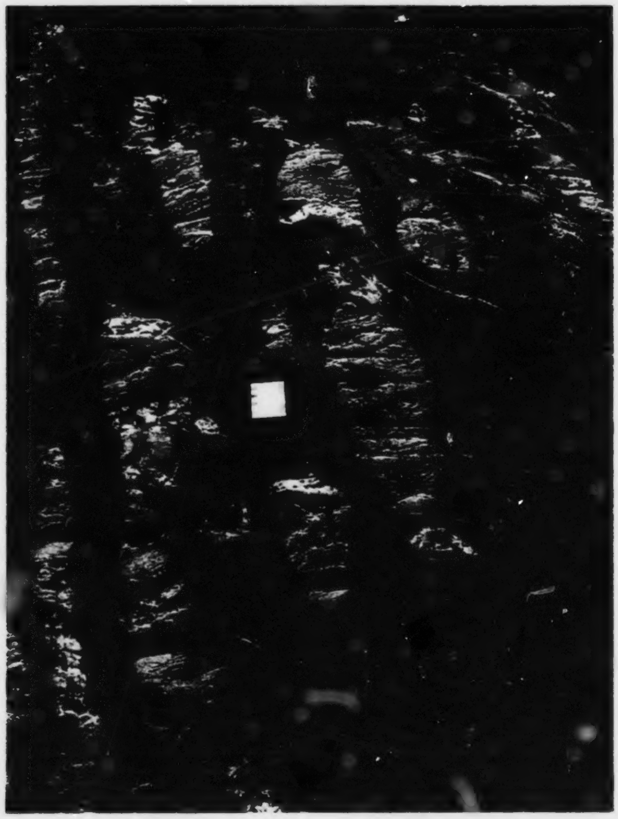

Figure 38: *Tectonically flattened epidosite-bearing Bear Lake pillowed flow (unit 1), island near north end of White Lake. Pillow selvages are destroyed, basaltic andesite is strongly foliated, and rigid epidosite domains are flattened with quartz-filled pull-apart structures (refer also to Figure 39).*

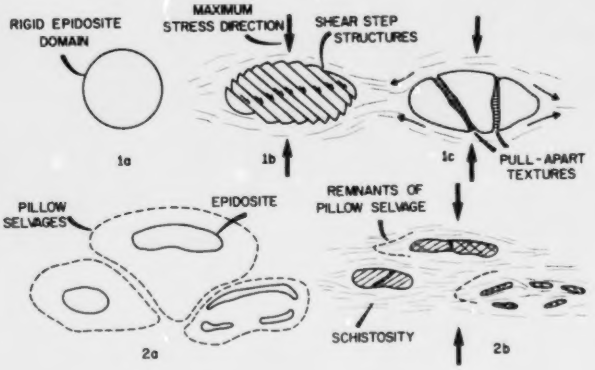
RIGID EPIDOSITE DOMAIN
MAXIMUM STRESS DIRECTION
SHEAR STEP STRUCTURES
1a
1b
1c
PULL-APART TEXTURES
PILLOW SELVAGES
EPIDOSITE
REMNANTS OF PILLOW SELVAGE
SCHISTOSITY
2a
2b

Figure 39: Tectonite structures developed during strong flattening of more altered Bear Lake pillowed flows containing rigid epidosite domains. Illustrations 1b and 1c show shear-step fractures and pull-apart structures formed during flattening of rigid epidosite domain in 1a. Illustration 2b shows development of tectonite fabrics formed during flattening of pillows containing one or more epidosite domains.

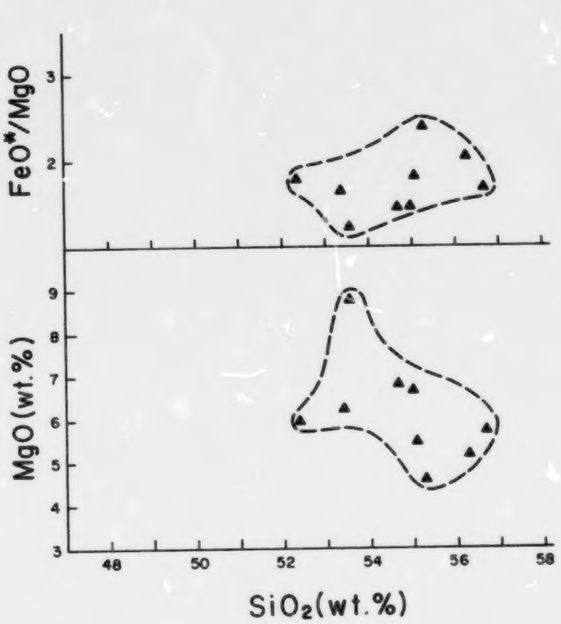

Figure 40: FeO*/MgO vs. SiO_2 and MgO vs. SiO_2, Bear Lake basaltic andesite. Note the small variation in FeO*/MgO ratio for the range of SiO_2. In this plot, and succeeding plots like it, oxides are reported recalculated H_2O- and CO_2- free. Throughout this report, FeO* represents total iron expressed as FeO (i.e. FeO + 0.9 Fe_2O_3 reported in the analysis).

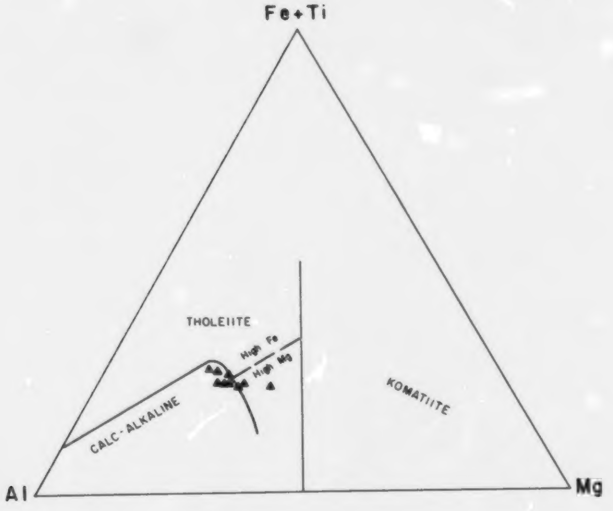

Figure 41: Jensen (1976) cation plot, Bear Lake basaltic andesite. Analyses straddle the tholeiite/calc-alkaline field boundary and do not define a significant Fe-enrichment trend.

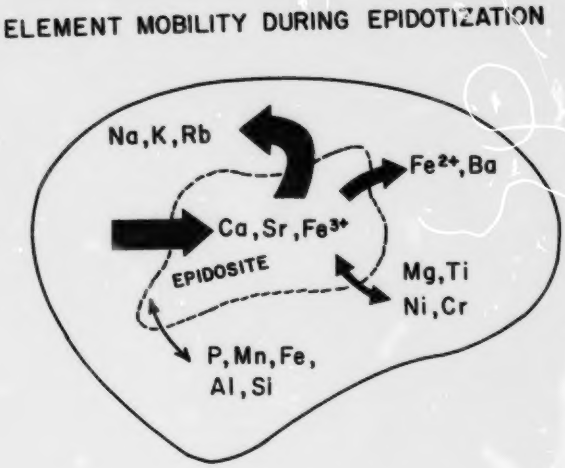

Figure 42: Element mobility during epidotization of Bear Lake basaltic andesite pillow, with relative mobilities shown by width of arrows.

Three flows (two pillowed and one massive) were sampled to investigate the mobility of elements during epidotization (analyses 10 — 13). Relative to less altered portions of flows, epidosite domains are enriched in Ca, Sr and Fe^{3+}, and are depleted in Na, K, Rb, Fe^{2+}, Ba, Zn, Si and Mg (Fig. 42). Al and Ti show no consistent trends and Ni, Cr and P are commonly unchanged.

Interpretation

Several criteria suggest that this major basaltic andesite unit is a remnant of a shield volcano. The unit is composed entirely of subaqueous lava flows and related breccias with a complete absence of intercalated, genetically unrelated pyroclastic and sedimentary rocks. Flow direction indicators (Fig. 6) show a uniform northerly component of transport, indicating a source area an unknown distance south of Sleep Lake.

The unit displays systematic vertical variation in vesicularity, flow thickness, and flow types. There is a gradual overall increase in vesicularity in flows, from faulted base of the unit to its top. Flows within the basal 2 km generally do not contain more than 5% vesicles and commonly contain less than 2%. Flows above 2 km typically contain between 5 and 20% vesicles and locally up to 40%. Gas cavities and vesicles larger than 1 cm are rare in the basal 1 km and are not abundant until 2 km above the faulted base. The thickness of all types of flows shows a regular upward decrease (Fig. 24), and the proportion of massive to pillowed flows increases upwards (Fig. 25). This suggests that, during construction of the volcanic edifice, flows were extruded under progressively shallower water conditions and lower effusion rates. Subaerial conditions were not attained as pillowed flows are present throughout the entire section. However, the abundance and large size of vesicles in the upper 1.3 km of the unit suggests a very shallow water environment (Table 5), probably significantly less than 1 km. Assuming a 10° slope profile the Bear Lake shield volcano would have a minimum diameter of 37 km; assuming an 8° slope profile the minimum diameter would be 47 km.

HETEROLITHOLOGIC BRECCIA, LAPILLI TUFF, TUFF (UNIT 30)

A unit of stratified breccia, lapilli tuff, and tuff overlies Bear Lake basaltic andesite (unit 1) between Bear Lake and Sleep Lake. It is 150 m thick at Bear Lake and has a mapped lateral extent of 2.8 km; it is truncated, at a low angle, in the north by the Vick Lake fault. At Bear Lake this mixed unit is overlain by, and occurs within, basal portions of the Solodiuk Lake rhyolite (unit 13). East of Sleep Lake it is overlain by dacitic tuff (unit 26a) whereas south of Sleep Lake it apparently interfingers with, or is laterally gradational to, dacitic tuff.

The contact with underlying Bear Lake basaltic andesite is exposed at only one locality, on the south shore of Sleep Lake. At this locality the contact between basaltic andesite flow breccia and the overlying sequence of heterolithologic breccias is sharp and abrupt. The basal member of unit 30 comprises 2 m of breccia with abundant 1 — 30 cm white felsic fragments close-packed in a darker tuffaceous matrix. It is in turn overlain by 10 m of heterolithologic breccia. This breccia contains two fragment types: (1) abundant grey to white, lenticular, variably vesicular "dacitic" fragments 2 mm — 40 cm long, and (2) about 30% white rhyolite blocks up to more than 3 x 0.5 m in size. Rhyolite blocks are aphyric, flow banded, and were originally angular; flow banding is tightly folded. The basal sequence at this locality is topped by more than 10 m of light brown, fine grained intermediate tuff with sporadic lapilli-sized intermediate fragments.

The main body of unit 30 comprises a stratified sequence of breccia, tuff, lapilli tuff, and pumice-lump breccia. Beds are 0.2 — 2 m thick with sharp to gradational bed contacts. Breccias contain intermediate to felsic, buff weathering fragments 2 — 40 cm long in a fine grained grey-green foliated matrix. Tuff beds are fine grained and contain variable amounts of 0.2 — 0.5 mm quartz (up to 20%). A few white felsic tuff beds 5 — 10 cm thick contain 3% 1 mm quartz. Lapilli tuff beds contain about 10% fragments, 2 — 20 cm long by up to 1.5 cm wide, in a granular tuff matrix. The fragments are vesicular, aphyric, and include buff intermediate as well as smaller felsic types. The top of the unit at Bear Lake comprises massive intermediate tuff with less than 5% intermediate lapilli in a matrix of feldspar crystals, lithic granules and fine grained material.

On the south shore of Solodiuk Lake approximately 20 m of stratified breccias occurs within the basal portion of the Solodiuk Lake rhyolite (unit 13; the breccias are both underlain and overlain by the rhyolite-lobe facies of this rhyolite flow. The breccias contain fragments of rhyolite and amygdaloidal intermediate rocks.

Interpretation

Deposition of this unit marks abrupt termination of basaltic andesite volcanism (unit 1) and onset of felsic volcanism; the latter includes this unit, the Solodiuk Lake rhyolite (unit 13), and the White Lake dacite tuffs (unit 26). Contemporaneity with rhyolite volcanism is displayed by large to small rhyolite clasts in breccia units and by the unit of mixed breccia within the basal portion of the Solodiuk Lake rhyolite.

SOLODIUK LAKE RHYOLITE (UNIT 13)

A large rhyolite flow(s) occurs east of Bear Lake; it has a maximum thickness of 250 m but pinches out to the south. North of Solodiuk Lake it is intruded by a large gabbro plug (unit 41a) and cut by the Vick Lake Fault. The rhyolite overlies Bear Lake basaltic andesite (unit 1), heterolithologic breccia (unit 30), and dacite tuff (unit 26a). It is overlain by the Two Portage Lake ferrobasalt (unit 5), and intruded by the White Lake gabbro sill (unit 39) and a younger gabbro sill (unit 42a).

The Solodiuk Lake rhyolite is composed of massive, white rhyolite "lobes", monolithologic rhyolite breccia, and light brown-weathering microbreccia. These lithologies are interpreted to be parts of a subaqueous rhyolite extrusive complex by analogy to descriptions of such deposits given by De Rosen-Spence et al. (1980) and Furnes et al. (1980).

Table 5:
Summary of criteria used to estimate depth of effusion of basaltic magmas

Depth	Eruptive Style/Vesicle Content In Various Magma Types	Reference
< 100 m	Explosive distintegration of tholeiitic basalt magma	Moore and Schilling, 1973
200 m	Transition from effusion of pillow lava to phreatomagmatic explosive phase; subglacial basalts, Iceland	Sigvaldason, 1968; Jones, 1970; Allen, 1979; Sigurdsson, 1982
< 500 m	Pillow lava sequence shows progressive increase in vesicularity with decreasing water depth, ranging from 5-10% vesicles at 400-500 m to 30-40% vesicles at 100-300 m; subglacial basalt, Iceland	Jones, 1969
< 700 m	Pipe vesicles in ocean ridge basalts	Moore and Schilling, 1973
780 m	Critical depth for explosive volcanism, alkali basalt magma	Staudigel and Schmincke, 1984
< 1250 m	Pipe vesicles, alkali basalt	as above
1140-1800 m	Large range in vesicle content (5-40%), alkali basalt. Increase in vesicle content with decreasing eruption depth.	as above
2-4 km	Vesicle content ranges from 1-5% in pillow basalt at depths of 2-4 km. Vesicularity shows a marked increase in basalts erupted at less than: 500 m (K-poor tholeiites) 800 m (Kilauean tholeiites) 1800 m (alkali basalts)	Moore, 1970
	Pillow interiors cool more slowly than the rinds and consequently undergo significant crystallization; as a result, the concentration of volatiles increases in the residual melt. Result: pillow interiors more vesicular than rinds.	MacPherson, 1984
	LREE-enriched lavas are more vesicular at moderate depths (1.5-3.0 km) than LREE-depleted lavas	as above
	Significant variations occur in the initial volatile contents of basalts that are otherwise similar in bulk composition	as above

Massive rhyolite forms lobes, pods and narrow tongues enveloped by breccia and microbreccia (Fig. 43). Bodies of massive rhyolite are typically elongate parallel to stratigraphy and range from bands 15 cm wide to domains 4.5 m wide by more than 12 m long. Contacts with microbreccia are dominated by irregularities, brecciation of lobe margins, and bifurcation of larger lobes into smaller lobes. Contacts vary from sharp to gradational (brecciated) over about 15 cm. Lateral, northward gradation of large rhyolite lobes into rhyolite breccia and microbreccia was observed in several, widely separated localities. Larger rhyolite lobes commonly have envelopes 1 — 3 m wide in which brown microbreccia contains abundant granule- to block-sized rhyolite fragments identical to, and derived from, adjacent massive rhyolite lobes. The fragment-rich envelopes underlie and overlie lobes. These rhyolite-fragment-rich microbreccias grade over a few centimetres to fragment-free or fragment-poor brown microbreccia. These features are taken as clear evidence of intense *in situ* fragmentation of lobe margins. The massive rhyolite is locally flow banded and contains sporadic vesicles 0.1 to 2 mm in diameter. In some outcrops lobes are imbricated at a high angle to regional stratigraphy and suggest a northerly component of flow transport.

Massive rhyolite varies considerably due to devitrification, silicification, metamorphic recrystallization, and carbonate/sericite alteration. There is no clear evidence to indicate the presence of more than one flow. All massive rhyolite lobes have similar phenocryst populations. Quartz phenocrysts (0.1 — 0.5 mm, less than 1% to 4%) are subrounded with weakly corroded margins; some larger crystals have dipyramidal forms. Plagioclase phenocrysts (0.5 — 1.5 mm, glomerocrysts to 2 mm; 1 to 3%) are tabular to equant and recrystallized to albite (plus rare microcline), epidote, sericite and carbonate. The groundmass is dominated by 0.1 — 0.3 mm spherulites composed of quartz and feldspar and locally replaced entirely by monocrystalline quartz. The spherulites are in a matrix of very fine grained feldspar, chlorite and epidote. Rare lithoidal textures (felted elongate plagioclase to 0.2 mm) were observed as patches a few centimetres across, within non-lithoidal rhyolite. Chlorite is the only mafic phase present, generally forming less than 1%, but up to about 15% of some altered rocks. Alteration takes a variety of forms including carbonate blastesis, sericitization, chloritization, and pyritization (as disseminated grains and fracture fillings).

Rhyolite microbreccia weathers light brown to brown. It resembles dacite tuff (unit 26a) but is somewhat more siliceous and does not contain intermediate rock fragments. The microbreccia is fine grained, moderately foliated, with variable content of 0.2 — 0.5 mm quartz. Content of white rhyolite granules and blocks varies, commonly increasing with proximity to massive rhyolite lobes. In thin section two main types of microbreccia are recognized. One is composed largely of close-packed, deformed long-tube pumice, accompanied by sporadic granules of white rhyolite. The other comprises non-pumiceous spherulitic rhyolite granules in a matrix of foliated chlorite, epidote, quartz and feldspar. The microbreccia contains quartz and plagioclase phenocrysts similar in size and abundance to those in the associated lobes.

Angular white rhyolite blocks are present in various proportions in the microbreccia. They are most abundant in proximity to areas with abundant lobes of massive rhyolite. The microbreccia and breccia range from unsorted, chaotic deposits to crudely stratified types. Stratification, where observed, is several centimetres to several metres in thickness and is defined by rhyolite fragment abundance and rare normal abundance grading.

Interpretation

Considered as a single entity the Solodiuk Lake rhyolite contains many of the structures and relationships described by Furnes et al. (1980) in a Cenozoic subglacial (subaqueous) rhyolite complex in Iceland. The Icelandic microbreccia comprises two phases also found in the Solodiuk Lake rhyolite. The first is pumiceous and is considered by Furnes et al. (1980) to have been produced by violent magmatic explosive events. The second phase is composed of obsidian and lithic rhyolite granules derived directly from break-up of rhyolite lava by a continuous process of construction and destruction (by quenching and thermal fragmentation) of massive lobes. On the basis of these similarities the Solodiuk Lake rhyolite is considered to be a subaqueous rhyolite extrusive complex. It was probably emplaced in shallow water as indicated by the presence of pumiceous fragments. The dacitic tuff (unit 26a) is probably an epiclastic/pyroclastic apron derived, in part, from the fine grained microbreccia component of the rhyolite body.

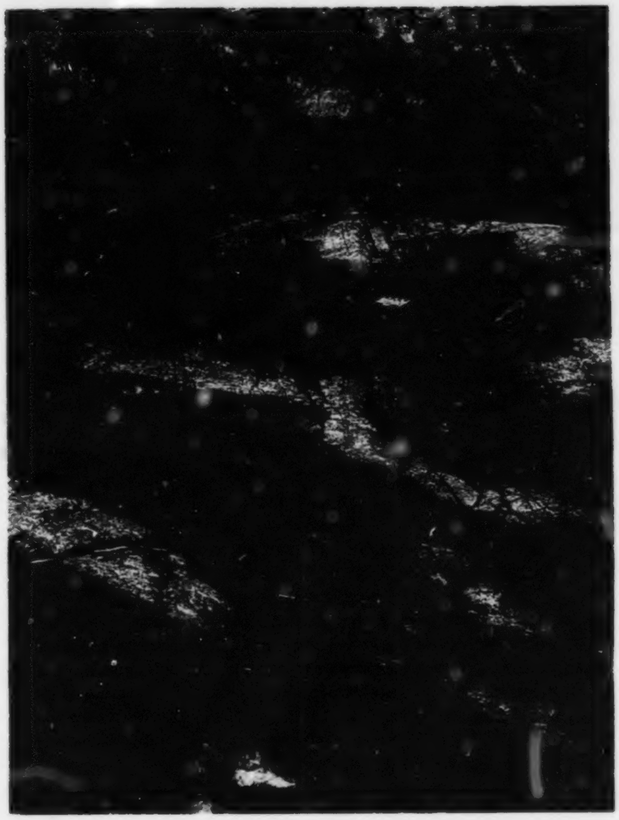

Figure 43: Small irregular massive rhyolite lobes (light) and intervening microbreccia (dark) in the subaqueous Solodiuk Lake rhyolite (unit 13), 500 m northeast of Sleep Lake.

WHITE LAKE DACITIC TUFF (UNIT 26)

A heterolithologic unit comprising rocks of dacitic bulk composition conformably overlies Bear Lake basaltic andesite (unit 1) between Sleep Lake and White Lake. South of Bear Lake the unit presumably interdigitates with heterolithologic breccia and tuff (unit 30) whereas west of Bear Lake it occurs as mappable lenses within the Solodiuk Lake rhyolite (unit 13). The dacitic sequence forms a southward thickening, wedge-shaped deposit with a maximum thickness of 300 m at White Lake; its complete lateral extent is unknown but is at least 6.7 km within the map area.

The dacitic unit comprises four distinct members. Contact relationships between members are not exposed; however, constituents of the members are locally interlayered and their distribution indicates that they are laterally equivalent. The members form a series of wedge-shaped deposits which include, from north to south: (1) dacitic tuff with weakly defined layering (unit 26a), (2) dacitic tuff and tuff breccia characterized by abundant pumice blocks (unit 26b), (3) reworked dacitic tuff or greywacke (unit 26c), and (4) dacitic tuff with subtle bedding and sporadic pumice clasts (unit 26d). These members are described individually in the following sections.

Unit 26a: Dacitic tuff with weakly defined layering

Dacitic tuff weathers a characteristic buff to rusty red brown and is dark green on fresh surface. It is massive to subtly layered, with bedding marked by slight changes in weathering colour and quartz content. Bedding thickness ranges from 2 to 40 cm. Intercalated felsic tuff beds, up to 40 cm thick, are white, light buff to greenish buff and internally laminated.

Quartz grains commonly comprise 2 — 5% of the rock and are 0.1-0.7 mm in diameter. They are subrounded and monocrystalline, probably derived from quartz-phyric felsic volcanic rocks. Microcline, possibly after primary plagioclase, ranges in size from 0.2 — 1.7 mm and comprises 1 — 2% (rarely up to 5%). Rock fragments (from 1 mm to 2 cm long) include (1) quartz- and plagioclase-phyric rhyolite, in which the phenocrysts are the same general size range and shape as in the matrix, and (2) plagioclase-phyric intermediate fragments, some with amygdales to 0.3 mm. The matrix contains fine grained epidote, dark green actinolite, chlorite, feldspar and quartz. A strong foliation and tectonic flattening of component rock fragments is typical for rocks of this unit.

The lens of unit 26a within the Solodiuk Lake rhyolite contains the "normal" dacite tuff and intercalcated white felsic tuff beds; in addition it contains abundant pumice-rich beds 5 — 60 cm thick and local angular white rhyolite granules and blocks. Bedding is somewhat better defined in this lens of unit 26a than in outcrops of unit 26a south of Sleep Lake.

Unit 26b: Pumice-block-bearing dacitic tuff and tuff breccia

This unit weathers buff and is dark grey on fresh surface; it is crudely layered, and is characterized by pumice fragments in many beds. Primary textures and structures are not well preserved due to recrystallization, tectonic flattening and the imposition of a foliation. Platy jointing parallel to schistosity is characteristic.

Beds are between 0.5 to 20 m thick and are defined by variation in abundance and size of contained pumice fragments and quartz grains. There is no recognizable bed organization and bed contacts are poorly defined. Pumice-bearing beds are interlayered with up to 20 — 30% dacite tuffs of the type described in unit 26a.

Pumice fragments range from small lapilli to blocks up to 30 cm by 1 m. They are strongly altered to a mixture of epidote and quartz; primary vesicularity is generally poorly preserved. Most pumice is flattened into the plane of foliation; length to width ratios range from 5:1 to 20:1 but are locally up to 200:1 (Fig. 44). Where flattening is intense the rock develops a pseudolamination. Pumice fragments contain phenocrysts of microcline (after plagioclase?) up to 0.6 mm and quartz up to 0.5 mm.

Unit 26c: Reworked dacitic tuff or greywacke

Reworked, volcanogenic rocks of dacitic composition weather medium grey, light grey-green to orange-buff, and are dark grey to dark grey-green on fresh surface. Bedding ranges from indistinct to moderately well defined, and from 0.5 to 60 cm thick. Variation in the abundance of fine grained (0.5 mm) quartz defines stratification: quartz-rich (20%) and quartz-poor (5%) types are generally intergradational but sharp bedding plane contacts do occur.

Quartz grains are subrounded to rounded, monocrystalline, and up to 0.8 mm across in rocks with greatest quartz content. Grain size is seriate with very fine grained quartz in the matrix. Plagioclase crystals

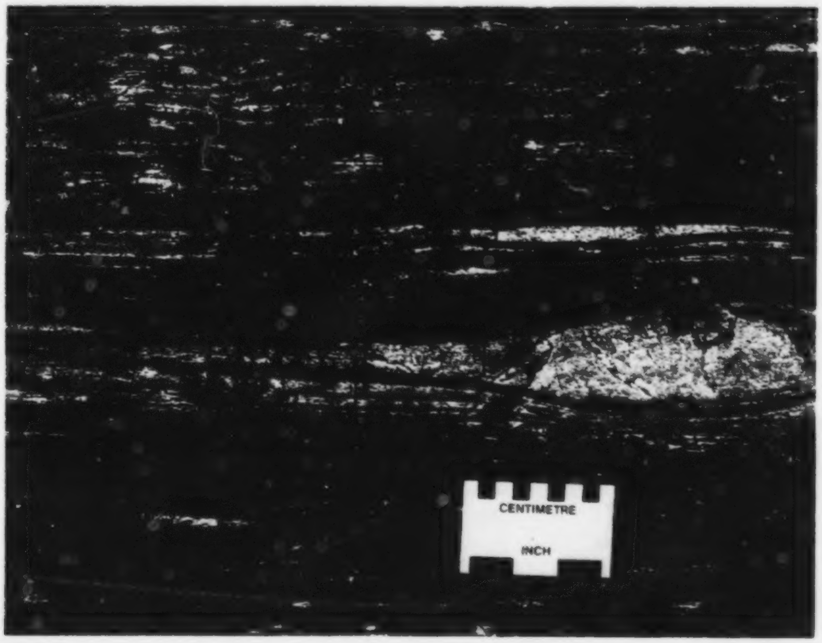

Figure 44: Tectonically flattened pumice fragments in White Lake dacite tuff (unit 26b), 100 m west of Little Spruce Lake. Length to width ratios of fragments at this locality are up to 230:1 and produce a striking psuedo-lamination.

include subhedral crystals, crystal fragments and some phenocrysts. They compose up to 3% of the rock, are typically less than 1 mm long, and are identical to phenocrysts in plagioclase-phyric rock fragments.

A variety of rock fragments, up to 3 cm long and strongly flattened, occur in these beds. They are readily identified in thin sections and stained rock slabs, but are generally not observed on outcrops. Rock fragment types include plagioclase-phyric intermediate volcanic rocks (some with amygdales), and quartz-phyric and aphyric rhyolite similar to the Solodiuk Lake rhyolite (unit 13). The matrix contains a very fine grained mosaic of feldspar, quartz, epidote, chlorite, stilpnomelane and white mica; total mafics range from 30 to 60%.

Unit 26d: Dacitic tuff with sporadic pumice clasts

These rocks are similar to unit 26c but differ in that they are less mafic, coarser grained, and contain sporadic pumice blocks and lapilli. In general bedding is subtle and defined by variation in quartz content, but locally pumice-rich strata forms well defined beds.

The contact between this unit and underlying Bear Lake basaltic andesite flows (south of Highway 10) is sharp. The basal member of the dacite tuff at this locality comprises about 15 m of fine grained, finely layered intermediate tuff.

Interpretation

Quartz and feldspar microclast population of the tuff, and contact relations with the Solodiuk Lake rhyolite, imply a genetic relationship between the two units. The dacitic bulk composition is a consequence of incorporation, of common fine grained, plagioclase-phyric lithic fragments of intermediate to mafic composition in the felsic tuff. The presence and local abundance of pumice suggests a significant pyroclastic component. Several features, including bedding, abundance of lithic clasts, compositional variation between beds, and heterolithologic rock fragment populations in individual beds, suggest that these originally felsic pyroclastic deposits were transported, reworked and mixed before being redeposited.

LITTLE SPRUCE LAKE ANDESITIC LAPILLI TUFF (UNIT 24)

Volcaniclastic rocks of andesitic composition form a southward-thickening deposit that is up to about 350 m thick east of White Lake. The unit has a 5 km strike length within the map area but its total extent is unknown. These fragmental rocks overlie dacitic tuff (unit 26) and are overlain by a thin unit of graphitic mudstone (unit 36) which hosts the Cuprus and White Lake massive sulphide deposits.

The unit is composed predominantly of tuff, lapilli tuff, and local tuff breccia (unit 24). South of White Lake Mine, it also includes a strongly folded, tectonically transposed group of fine grained sediments and tuff (unit 24e). Primary structures and textures are generally not well preserved due to recrystallization and tectonic flattening (Fig. 45). In best preserved portions (e.g. east shore of Little Spruce Lake) unit 24 is composed largely of scoria clasts and rare blocks in a granular tuffaceous matrix.

Weathered andesitic tuff and lapilli tuff is highly variable in shades of buff, brown and green; fresh surfaces are medium to dark green. Bed thickness ranges from a few centimetres to 13 m but is commonly 1 — 5 m. Bed contacts are typically poorly defined although abrupt changes in fragment size have been observed. Individual beds generally are monolithologic but may appear heterolithologic due to selective alteration of fragments. Many beds display normal size and abundance grading in contained fragments. Some thick tuff breccia beds have fine grained tops devoid of large fragments. Reverse size grading occurs rarely at bases of beds.

Fragments are plagioclase-phyric andesite variably replaced by epidote, quartz and chlorite. They are flattened, lensoid, and up to 40 by 2 cm. Fragments are supported by a foliated matrix composed of abundant 1 — 6 mm equant granules, subordinate blocky euhedral plagioclase crystals and fine grained epidote, actinolite and chlorite. Some fragments are microvesicular scoria but commonly the rock is too recrystallized to permit recognition of small-scale structures.

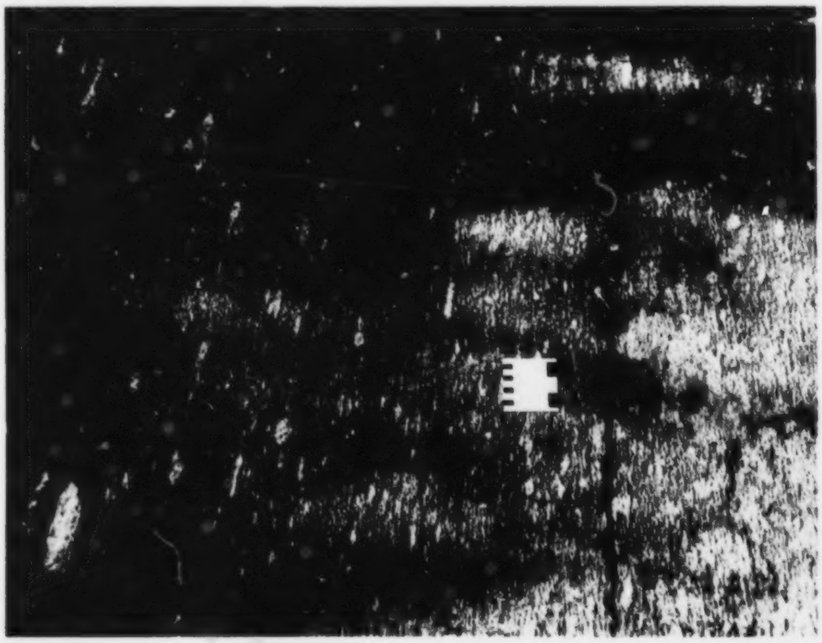

Figure 45: Tectonically flattened fragments in foliated Little Spruce Lake andesitic lapilli tuff (unit 24), east shore of White Lake.

Fine grained sediments and tuff (unit 24a) are exposed south of White Lake Mine in the hinge area of the Northeast Arm syncline. The sediments are tightly chevron folded, contain a strong imposed foliation, and are locally transposed. Consequently, thickness, lateral extent and stratigraphic order are uncertain. Major components of the subunit are intermediate to mafic mudstones and siltstones; minor components are feldspar-rich greywacke, white felsic tuff layers, chert, jasper and pyritic mudstone. Beds are thin and laterally continuous. Isolated pumice blocks occur sporadically in some beds and quartz crystals to 2 mm occur in some felsic tuff layers.

An extensive hydrothermal alteration zone is not developed in the andesitic lapilli tuff even though it forms the footwall of the Cuprus and White Lake Cu-Zn sulphide deposits. The single known exception is a small exposure, 5 m wide, of strongly chloritized lapilli tuff adjacent to an exploration pit south of the Cuprus Mine. An analysis of this altered rock (see Appendix) displays high MgO and FeO, and low Na_2O and CaO relative to unaltered andesitic lapilli tuff.

Interpretation

This volcaniclastic sequence is interpreted as a resedimented, andesitic pyroclastic deposit that fills a southward-deepening basin. The primary pyroclastic origin of contained clasts and granules is shown by their monolithologic and microvesicular to scoriaceous nature. Bedforms and bed organization indicate that this pyroclastic material was transported from its place of origin, probably as subaqueous debris flows. Finally, the deposit is wedge-shaped, thick in the south and tapering to a pinch-out south of the Solodiuk Lake rhyolite, suggesting that these transported materials fill a paleobasin which was deep in the south and shallow in the north. The occurrence of sub-basins within the larger basinal structure is indicated by local fine grained detrital sediments, chemical sediments, and massive sulphide deposits (at the top of the unit).

MUDSTONE, MASSIVE SULPHIDE (UNIT 36)

In the White Lake area 25 m of sulphide-bearing fine grained sediments occur at the contact between the andesitic lapilli tuff (unit 24) and overlying Two Portage Lake ferrobasalt (unit 5). This unit is not exposed (and may not occur) north of old Highway 10 but its stratigraphic position is eqivalent to the contact between the Solodiuk Lake rhyolite and the Two Portage Lake ferrobasalt.

Rock types that outcrop in exploration pits south of Cuprus Mine constitute two poorly defined subunits; a lower zone of laminated graphitic mudstone with sulphide layers and minor chert laminae, and an upper zone of siliceous argillite, chert and sulphide.

Two massive sulphide deposits (White Lake Mine and Cuprus Mine) occur within this formation. Both deposits are stratiform, lensoid, and strongly folded along with enclosing sedimentary rocks. In the White Lake Mine the NNE plunge of ore lenses shallows with depth from 35-40° at surface to 23° at the 2110 foot level, parallel to the axis of the Northeast Arm syncline. The White Lake orebody is associated with graphitic argillite, which completely encloses the massive sulphides at depth. Neither the Cuprus nor White Lake deposits have extensive footwall alteration zones. Mineralogical banding (chalcopyrite-sphalerite-pyrrhotite) occurs in the White Lake deposit; these define repetitive Cu-rich and Zn-rich cycles but Cu content is highest in the stratigraphic footwall of the mine.

TWO PORTAGE LAKE FERROBASALT (UNIT 5)

A distinctive, 120-200 m thick, Fe-rich basaltic unit overlies, successively from north to south, the Solodiuk Lake rhyolite (unit 13), White Lake dacitic tuff (unit 26a), Little Spruce Lake andesitic lapilli tuff (unit 24) and graphitic mudstones (unit 36). It is overlain by the Vick Lake andesitic tuff (unit 25). Within the map area its strike length is 11.5 km, but it extends an unknown distance to the north, and is terminated to the south by the Northeast Arm Fault.

At Two Portage Lake, where these ferrobasalt flows are best preserved, they weather dark grey, medium brown through greenish brown, and are locally rusty brown. Of 19 measured partial and complete flows, 79% are massive, 16% are pillowed, and 5% are compound. An average flow thickness of about 13 m is obtained from 8 completely exposed flows. Well over half the flows are greater than 15 m thick. Massive flows have microgabbroic textures (to 1 mm grain size) with 10-50 cm thick aphanitic, chilled bases and tops. Hyaloclastite was observed at the top of only one flow. Rhyolite crystal tuff (unit 27) commonly occurs as interflow layers and assists demarcation of flow contacts. Approximately half of the flows have 2 to 30% amygdales (1 — 3 mm) in a narrow zone near the flow top, beneath the chilled crust. Pillowed flows are characterized by very narrow (1 — 2 mm) pillow selvages. They do not contain amygdales and pillows are small (less than 50 cm).

South of Johnson Lake, where the flows are schistose and poorly preserved, they weather brown, brownish green and dark rusty brown. Flow contacts are not recognized and outcrops are generally massive and featureless. Flattened pillow structures are recognized north of White Lake Mine.

Estimated primary modal mineralogy includes 45 — 55% pyroxene, 40 — 50% plagioclase, 2 — 7% Fe-Ti oxides and nil to trace apatite. Pyroxene is pseudomorphed by actinolite and subordinate epidote, plagioclase is replaced by albite, epidote, chlorite and carbonate, and Fe-Ti oxides are altered to leucoxene and magnetite. There is considerable textural variation within flows, from aphanitic or very fine grained intersertal flow tops and bases, to broadly microgabbroic interiors. Microgabbroic textures vary between flows and include the following:

(1) *Subophitic*, with anhedral to subhedral pyroxene (to 0.7 mm) partially enclosing euhedral plagioclase tablets (0.3 — 1.5 mm); anhedral Fe-Ti oxides (to 2 mm) enclose pyroxene and plagioclase.

(2) *Hypidiomorphic*, with subhedral to euhedral stubby pyroxene prisms (to 0.4 mm) interlocking with randomly oriented plagioclase laths (to 1 mm); skeletal octahedral Fe-Ti oxides occur as inclusions in pyroxene.

(3) *Diabasic*, with anhedral pyroxene oikocrysts (to 2 mm) enclosing many stubby plagioclase laths (to 0.7 mm); subhedral Fe-Ti oxides (to 0.5 mm) partially enclose plagioclase and have pyroxene inclusions.

(4) *Coarse hypidiomorphic*, with stubby subhedral pyroxene (to 0.8 mm) enclosed by large stubby plagioclase tablets (to 3 mm); Fe-Ti oxides (to 0.3 mm) are subhedral to euhedral octahedra enclosed by, or interstitial to, pyroxene.

In areas of increased strain, these rocks show a strong foliation, primary structures are obliterated, and flows are composed simply of a strongly foliated mass of very fine grained actinolite, chlorite and epidote in which there are isolated epidote blasts.

Two Portage Lake ferrobasalt flows are texturally and compositionally similar to chilled margins of the White Lake differentiated gabbro sills. Although these sills intrude Solodiuk Lake rhyolite, White Lake dacitic tuff, Little Spruce Lake andesitic lapilli tuff and Two Portage ferrobasalt, they are not present in units stratigraphically above the ferrobasalt.

Geochemistry

Two Portage Lake ferrobasalt has a distinctive compositional range (Fig. 46 to 48) characterized by high Fe contents (FeO 12.90 to 18.05%), high TiO_2 contents (1.49 to 2.65%), a wide range of FeO /MgO ratios (1.71 — 4.25), and relatively high P_2O_5 (0.13 — 0.31%). On a Jensen diagram (Fig. 48) analyses plot well within the iron tholeiite field. Chilled samples from the White Lake sill share these distinctive geochemical characteristics (Fig. 47).

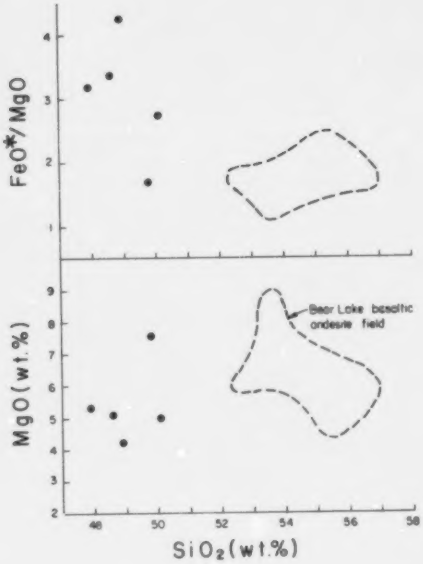

Figure 46: *FeO*/MgO vs. SiO_2 and MgO vs. SiO_2 for the Two Portage Lake ferrobasalt, with the Bear Lake basaltic andesite field shown for comparison. Note wide range of FeO*/MgO at almost constant SiO_2 in the ferrobasalt, indicating tholeiitic affinity.*

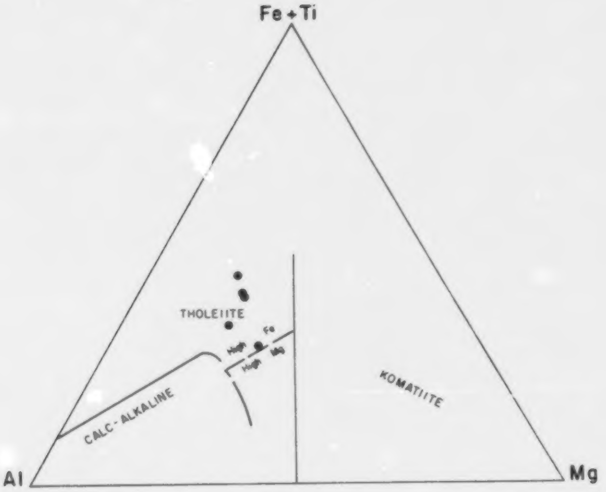

Figure 48: *Jensen cation plot, Two Portage ferrobasalts. Flows are well within the Fe-tholeiite field and define a trend of Fe-enrichment.*

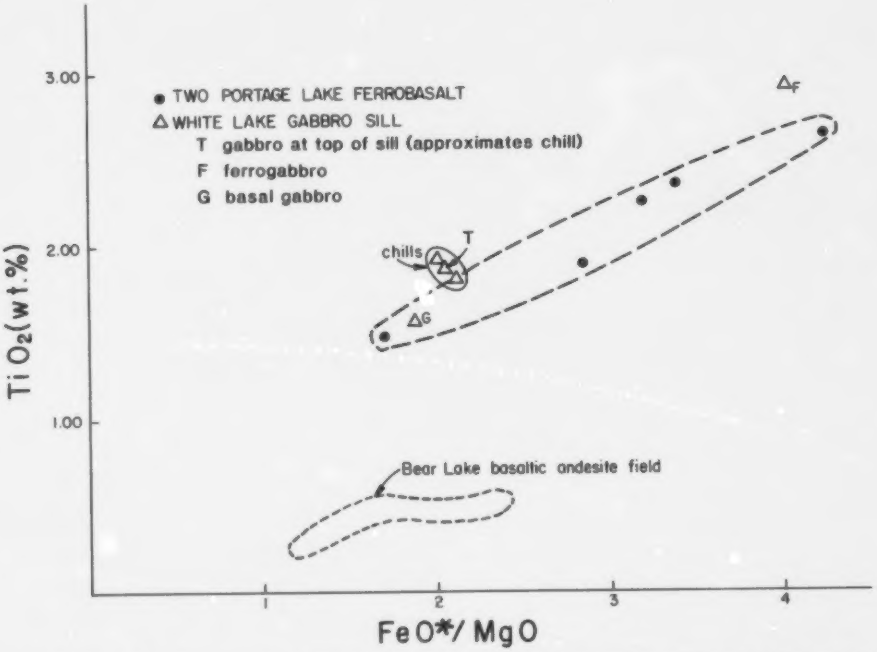

Figure 47: *TiO_2 vs. FeO*/MgO; Two Portage Lake ferrobasalt, compared to Bear Lake basaltic andesite and components of the differentiated White Lake gabbro-ferrogabbro sill. The range of compositions in the sill parallels the compositional variation displayed by the ferrobasalts, suggesting that the sill is synvolcanic and related to the same magma source as the ferrobasalt.*

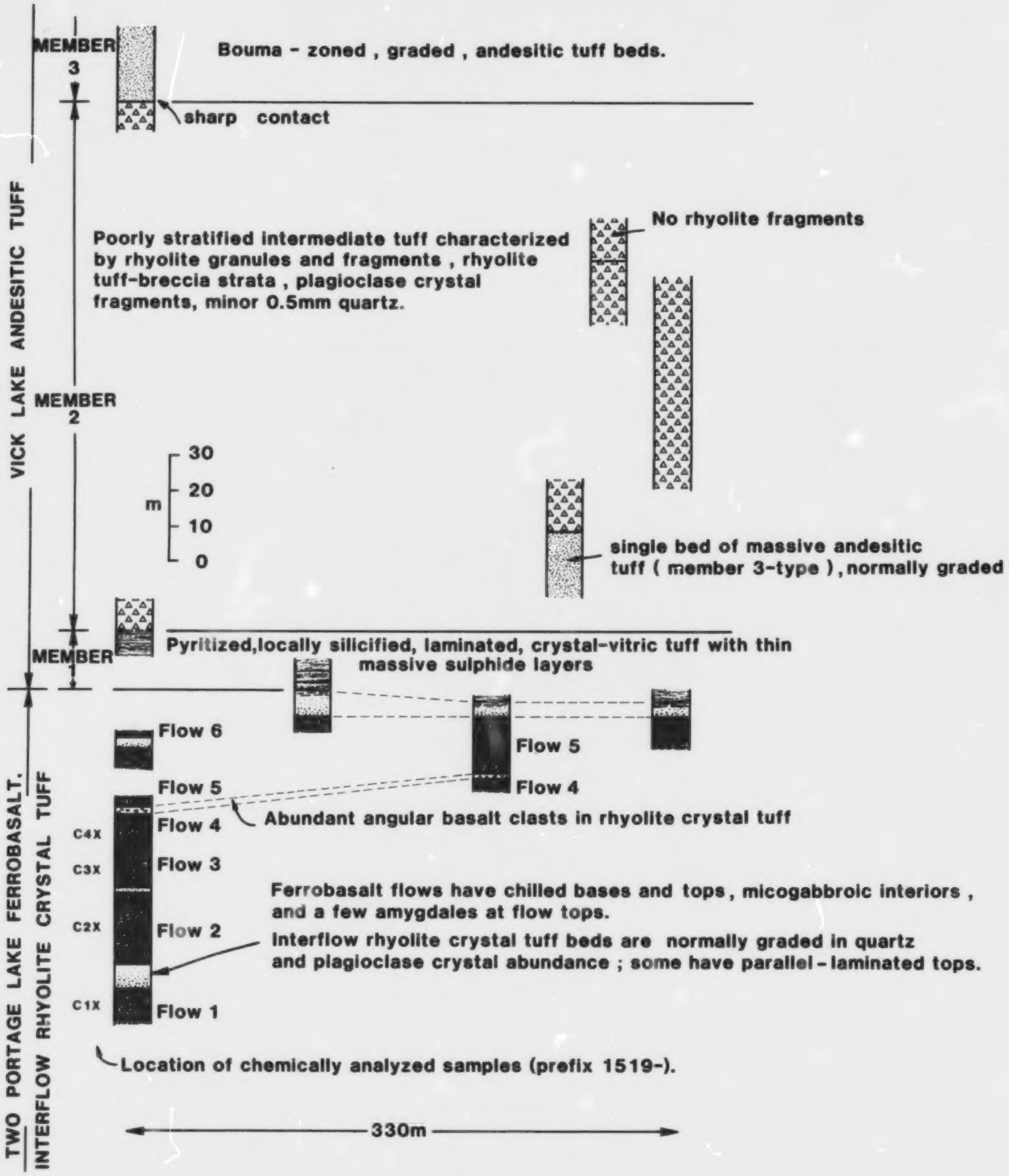
VICK LAKE ANDESITIC TUFF
MEMBER 3
Bouma - zoned , graded , andesitic tuff beds.
sharp contact
No rhyolite fragments
Poorly stratified intermediate tuff characterized by rhyolite granules and fragments , rhyolite tuff-breccia strata , plagioclase crystal fragments, minor 0.5mm quartz.
MEMBER 2
30
20
m
10
0
single bed of massive andesitic tuff (member 3-type) , normally graded
MEMBER 1
Pyritized, locally silicified, laminated, crystal-vitric tuff with thin massive sulphide layers
Flow 6
Flow 5
Flow 4
Flow 5
Flow 4
Abundant angular basalt clasts in rhyolite crystal tuff
C4X
C3X
Flow 3
Ferrobasalt flows have chilled bases and tops , micogabbroic interiors , and a few amygdales at flow tops.
C2X
Flow 2
Interflow rhyolite crystal tuff beds are normally graded in quartz and plagioclase crystal abundance ; some have parallel - laminated tops.
C1X
Flow 1
Location of chemically analyzed samples (prefix 1519-).
330m
TWO PORTAGE LAKE FERROBASALT.
INTERFLOW RHYOLITE CRYSTAL TUFF

Figure 49: *Outcrop stratigraphy south of Two Portage Lake. Upper two-thirds of Two Portage Lake ferrobasalt and members 1 and 2 of Vick Lake andesitic tuff are exposed in a series of outcrops extending about 330 m south of lake. Only the vertical axis is to scale.*

Interpretation

The Two Portage Lake ferrobasalt and the intercalated rhyolite crystal tuff (unit 27) form a bimodal suite that can be interpreted in terms of periodic eruption from a high level, chemically zoned magma chamber. In such a chamber high-SiO_2 rhyolitic liquids occur at the top, underlain by fractionated basalt magma. The eruption sequence would begin with rhyolitic pyroclastic volcanism followed by quiet effusion of less volatile-rich, fractionated basalt, producing cycles of the type observed in Fig. 49. The White Lake ferrogabbro sills are considered to be intrusive equivalents of the fractionated basalt (*not* the chamber from which the basalts were erupted).

The presence of pillowed flows and the uniform, laterally extensive nature of the unit suggests it formed a subaqueous lava plain. It overlaps several different basin-fill volcaniclastic units and provides an approximate time-stratigraphic marker within the basin.

TWO PORTAGE LAKE RHYOLITE CRYSTAL TUFF (UNIT 27)

Graded rhyolite crystal tuff beds, 30 cm to 8.5 m thick, occur as interflow markers in Two Portage Lake ferrobasalt. At least six of these beds are exposed in the section at Two Portage Lake; individual beds thin to the south. Rhyolite crystal tuff beds occur throughout the lateral extent of the ferrobasalt unit. These rhyolite tuffs are found *only* within and at the top of the ferrobasalt unit; together these rocks form an excellent time-stratigraphic marker which is readily recognized in highly deformed rocks.

Rhyolite crystal tuff beds are white weathering, graded and laminated (Bouma type A and AB). They contain varying amounts of crystals and crystal fragments (quartz maximum 3 — 4 mm, plagioclase typical maximum 2 mm, to 6 mm in one bed) and a heterolithologic suite of rock fragments (Fig. 50). The latter include ferrobasalt (0.2 — 50 cm), porphyritic rhyolite (0.2 — 6 cm), and minor "plagioclasite", tonalite and slabby mudstone. Normal grading is defined by upward decrease in crystal fragment and rock fragment size and abundance (Fig. 51). Bed tops, especially in the thicker beds, are parallel laminated, very fine grained, with each layer or lamina itself graded. Fine grained tops of beds commonly contain disseminated very fine grained pyrite.

Quartz crystals are subhedral to euhedral and some are embayed; in deformed rocks they are flattened ellipses elongate parallel to foliation. Crystal fragments are angular to subrounded. Plagioclase crystals (An_3) are euhedral stubby laths with sharply defined albite twinning and weak sericitic alteration; most are angular crystal fragments.

Basalt rock fragments have the texture of chilled ferrobasalt flow tops, some with actinolite-filled amygdales (Fig. 50); commonly they are represented by discrete patches of fine grained actinolite, chlorite and sphene. Porphyritic rhyolite clasts have quartz and plagioclase phenocrysts of the size and shape observed in the tuffaceous matrix. Some rhyolite clasts are spherulitic, some are vesicular, and in general they have a coarser texture than the tuff matrix. "Plagioclasite" fragments are composed of a mosaic of elongate plagioclase microlites (0.2 mm) and subordinate interstitial fine grained epidote or sphene. Tonalite clasts are a medium grained (0.5 — 1.5 mm), leucocratic mosaic of subhedral tabular plagioclase and large anhedral equant quartz.

The matrix is a very fine grained mosaic of feldspar, quartz, minor chlorite, epidote, and shreds of sericite. Trace amounts of brown euhedral zircon occur in the matrix and in one plagioclasite rock fragment. Zircon crystals separated from one of the rhyolite crystal tuff beds yields a U-Pb age of 1886 +/- 1.3 Ma (Syme et al., 1987).

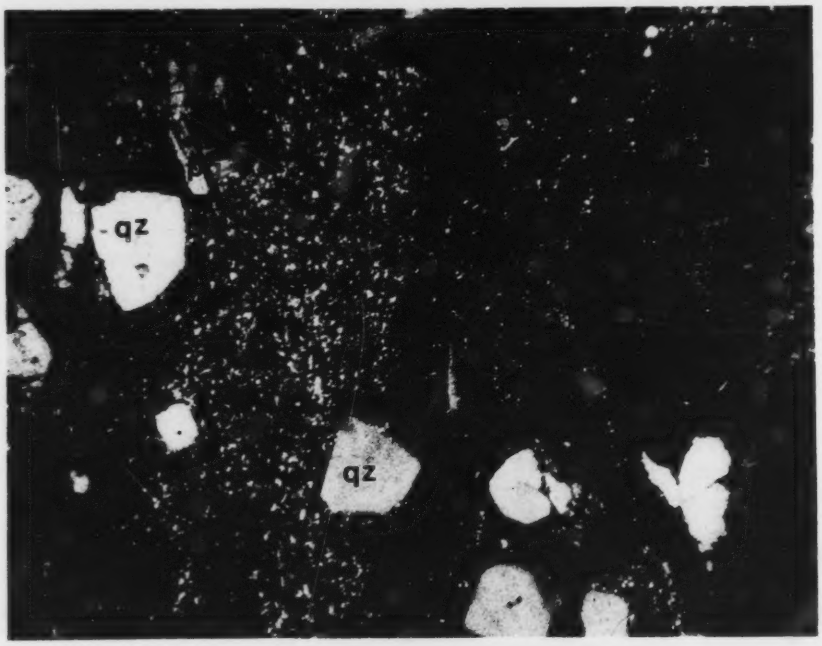

Figure 50: *Rhyolite crystal tuff (unit 27), west of Two Portage Lake. Quartz (qz) and plagioclase (pg) crystals and crystal fragments occur in a fine grained recrystallized quartzofeldspathic groundmass. A rip-up (FB) of vesicular Two Portage Lake ferrobasalt (unit 5) occurs in the tuff.*

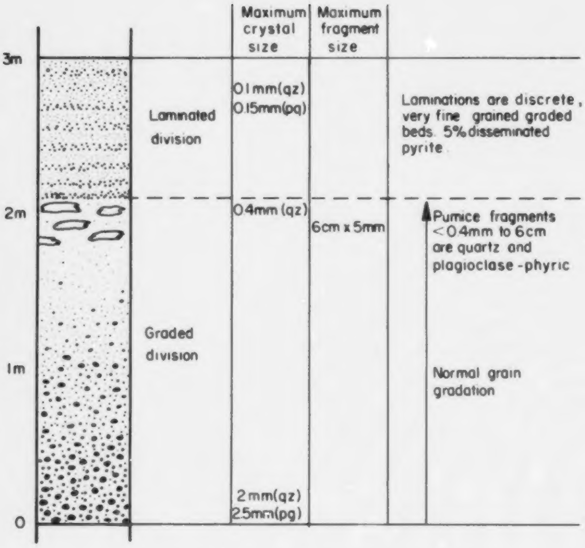
Maximum crystal size
Maximum fragment size
3m
2m
1m
0
Laminated division
Graded division
0.1mm(qz)
0.15mm(pg)
0.4mm (qz)
2mm(qz)
2.5mm(pg)
6cm x 5mm
Laminations are discrete, very fine grained graded beds. 5% disseminated pyrite.
Pumice fragments <0.4mm to 6cm are quartz and plagioclase-phyric
Normal grain gradation

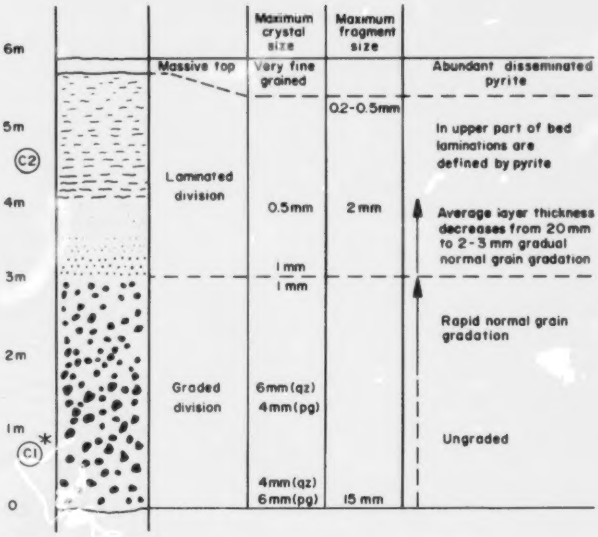
Maximum crystal size
Maximum fragment size
6m
5m
4m
3m
2m
1m
0
C2
C1
Massive top
Very fine grained
Abundant disseminated pyrite
0.2-0.5mm
In upper part of bed laminations are defined by pyrite
Laminated division
0.5mm
2mm
Average layer thickness decreases from 20mm to 2-3mm gradual normal grain gradation
1mm
1mm
Rapid normal grain gradation
Graded division
6mm(qz)
4mm(pg)
Ungraded
4mm(qz)
6mm(pg)
15 mm

* Stratigraphic position of chemically analyzed samples (see Appendix, samples 453-C1 and C2)

Figure 51: Three examples of bed organization displayed by rhyolite crystal tuff (unit 27) in Two Portage Lake area.

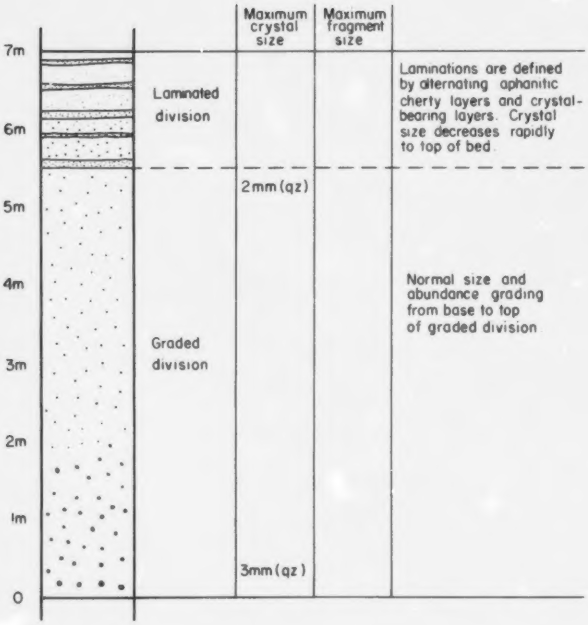
Maximum crystal size
Maximum fragment size
7m
6m
5m
4m
3m
2m
1m
0
Laminated division
Graded division
Laminations are defined by alternating aphanitic cherty layers and crystal-bearing layers. Crystal size decreases rapidly to top of bed.
2mm (qz)
Normal size and abundance grading from base to top of graded division
3mm (qz)

Interpretation

This unit is interpreted as a tuff despite recrystallization which has obliterated primary textures in what was presumably an ash matrix. Porphyritic rhyolite clasts are probably cogenetic with the rhyolite tuff matrix. Some rhyolite clasts have textures suggesting that they were pumiceous; most were originally glassy or lithoidal.

Bed organization is consistent with deposition from turbulent subaqueous density currents. Ferrobasalt and mudstone clasts are considered to be rip-ups incorporated into the body of the density current as it flowed over underlying ferrobasalt lavas.

VICK LAKE ANDESITIC TUFF (UNIT 25)

A 900 m thick unit of andesitic tuff conformably overlies the Two Portage Lake ferrobasalt (unit 5) and is overlain by dacitic flows and mixed pyroclastics (units 18a and 18b). The sequence is broadly upward fining and is interlayered near the top with pyritic, graphitic mudstones. Local excellent preservation of shards, pumice clasts and juvenile lithics permit unambiguous interpretation of this unit as a pyroclastic deposit. Turbidite bedforms, ubiquitous throughout the unit, indicate deposition from turbulent subaqueous density currents.

Vick Lake andesitic tuff has a lateral extent within the map area of 11.5 km. It is terminated at its southern end by the Northeast Arm Fault and extends an unknown distance north of the area. South of old Highway 10 it is tightly folded in the shallow north-plunging Northeast Arm Syncline. The tuff is intruded by the Mikanagan Lake Sill (unit 41), plagioclase porphyry sill (unit 42c), and axial planar dykes of gabbro (unit 42a) and quartz porphyry (unit 56). The unit is subdivided into eight stratigraphic members (Fig. 52).

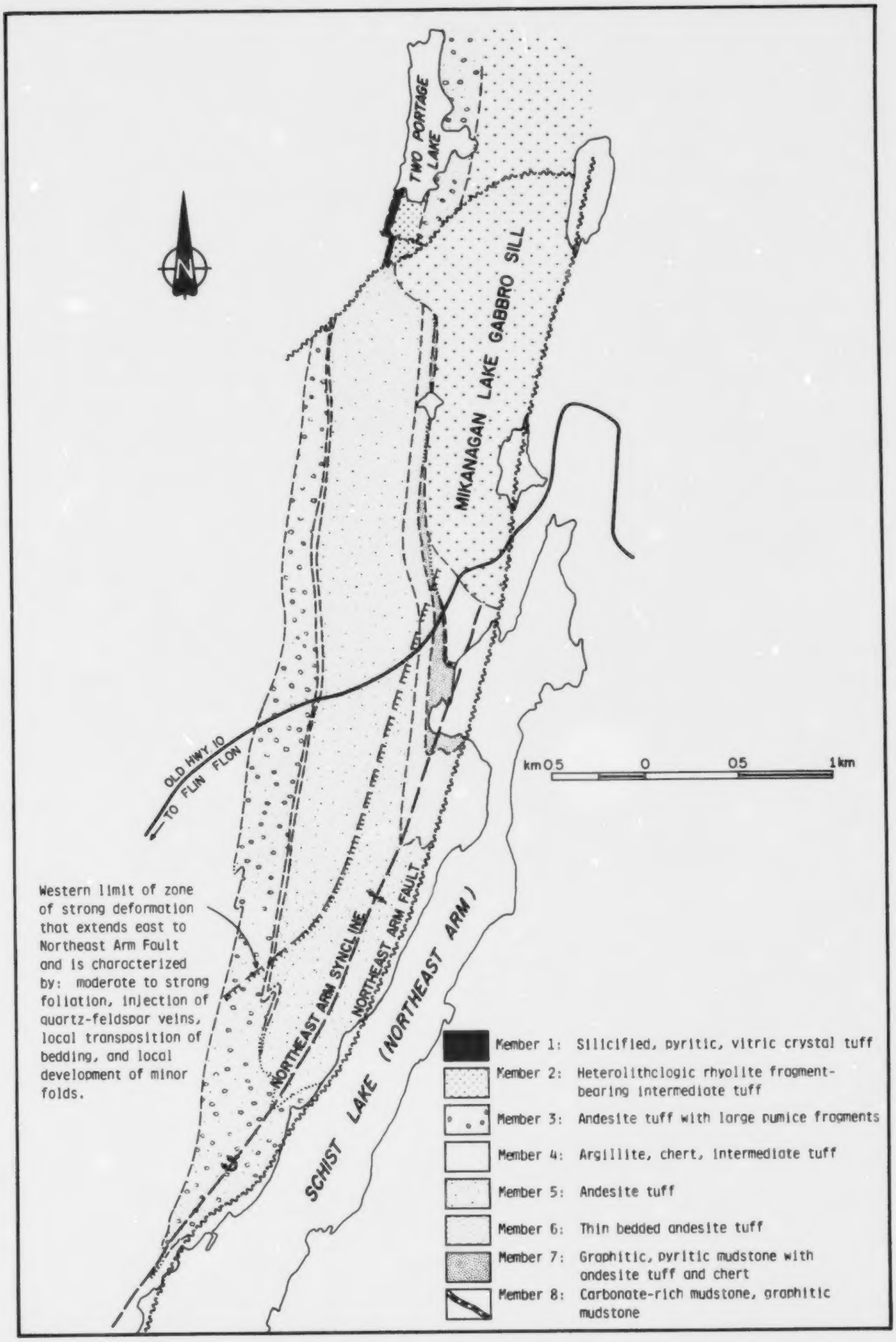
TWO PORTAGE LAKE
N
MIKANAGAN LAKE GABBRO SILL
OLD HWY 10
TO FLIN FLON
km 0.5 0 0.5 1 km
Western limit of zone of strong deformation that extends east to Northeast Arm Fault and is characterized by: moderate to strong foliation, injection of quartz-feldspar veins, local transposition of bedding, and local development of minor folds.
NORTHEAST ARM SYNCLINE
NORTHEAST ARM FAULT
SCHIST LAKE (NORTHEAST ARM)
Member 1: Silicified, pyritic, vitric crystal tuff
Member 2: Heterolithologic rhyolite fragment-bearing intermediate tuff
Member 3: Andesite tuff with large pumice fragments
Member 4: Argillite, chert, intermediate tuff
Member 5: Andesite tuff
Member 6: Thin bedded andesite tuff
Member 7: Graphitic, pyritic mudstone with andesite tuff and chert
Member 8: Carbonate-rich mudstone, graphitic mudstone

Figure 52: Distribution of stratigraphic members of the Vick Lake andesitic tuff.

Petrography

With the exception of members 4, 7 and 8 the Vick Lake tuff is composed entirely of pyroclastic materials with a conspicuous absence of interbeds of epiclastic material. The tuff is composed of shards, pumice, plagioclase crystals and crystal fragments, brown "vitric" microclasts, microlitic lithics, and amphibole crystals and crystal fragments. Areas of good preservation include Two Portage Lake and portions of the area traversed by old Highway 10. Farther south a strong foliation accompanied by metamorphic recrystallization obliterates fine-scale features in these rocks.

Shards

Shards are 0.05 — 0.4 mm across, and are generally smaller than 0.2 mm. They have equant to tabular shapes; boundaries are defined by a combination of straight to conchoidal fracture surfaces and vesicle walls (Figs. 53 and 54). Fracture surfaces at grain boundaries commonly cut through vesicles. Some ash particles are completely controlled by vesicle walls but these are generally small and appear to be shreds of pumice. The shards are aphyric and non-vesicular to weakly vesicular. Vesicles are generally less than 0.05 mm across, and are round, oval or tube-shaped, and filled with very fine grained epidote, chlorite, feldspar or quartz.

Shards are replaced by a mixture of albite, subordinate quartz, and a dusting of epidote, chlorite and sericite. They are recrystallized, with sutured grain boundaries; devitrification structures such as axiolites are not preserved (Fig. 53).

Pumice

Pumice in the ash-sized matrix of most beds ranges from 0.4 to 6 mm. As observed in outcrop it is typically less than 3 cm long but can be up to 30 cm in maximum dimension in some pumice-rich beds in member 3. The shape of pumice granules and blocks is variable from oval, equant to irregular (Fig. 55 and 56). Vesicularity ranges from 50 to 80%; vesicles are round, oval or tube-shaped, less than 0.4 mm in diameter. Pumice fragments contain plagioclase phenocrysts similar in size and shape to complete crystals in the matrix (Fig. 55).

Pumice is replaced by a polygranular mosaic of feldspar and quartz, similar to shards. Very fine grained chlorite and epidote outline vesicle walls (Fig. 57 and 58). Strongly recrystallized and altered pumice is represented by a coarse grained mixture of epidote, carbonate, quartz and feldspar in which vesicles are poorly preserved or obliterated.

Plagioclase crystals and crystal fragments

Tabular euhedral plagioclase crystals and angular to subangular crystal fragments form approximately 15 — 40% of tuff beds; they range in size from 0.1 to 2 mm. Normal size and abundance grading in plagioclase is typical of most beds. Best preserved crystals are monocrystalline, albite-twinned, slightly turbid, with patchy replacement by green chlorite, epidote, carbonate and sericite. Other, more altered plagioclase crystals are untwinned and variably annealed to an irregular fine grained mosaic with associated secondary replacement minerals.

Plagioclase crystals are identical in size and form to those in pumice and lithic fragments. Broken crystals predominate in the matrix.

Brown "vitric" microclasts

Distinctive, tan-brown microclasts up to 2 mm, but generally less than 1 mm across, are common in the lower parts of graded beds where they constitute up to 15% of the tuff. Shapes vary from subrounded to subangular but larger granules may have ragged margins, a few vesicles and irregular amoeboid shapes (Fig. 59 and 60). They are aphyric or plagioclase-phyric; large phenocrysts are typically broken at clast margins. The groundmass is composed of very fine grained, brownish, semi-opaque material (largely epidote) with or without randomly oriented acicular plagioclase microlites (0.05 — 0.1 mm). Some granules contain a few small (0.08 mm) round to tube-shaped vesicles. These clasts are interpreted as juvenile glass fragments, bounded largely by conchoidal fracture surfaces, with shapes subsequently smoothed by abrasion.

Microlitic lithics

In contrast to the juvenile brown vitric clasts these lithics are coloured shades of grey and contain abundant lath-shaped plagioclase microlites (0.05 — 0.1 mm) in felted to pilotaxitic texture. They are subrounded, non-vesicular to weakly vesicular, and are generally less than 0.5 mm across. Some contain stubby plagioclase phenocrysts 0.1 — 0.25 mm long. The groundmass, interstitial to microlites, is composed of very fine grained epidote, tremolite-actinolite or chlorite. These microclasts are interpreted as accidental lithics derived from flows or a dome.

Amphibole crystals

Broken euhedral prisms of magmatic hornblende compose 0 — 3% of the tuff and are selectively concentrated at the bases of beds. Some are unaltered, strongly pleochroic (yellow green to deep olive green) crystals; others are variably altered, from minor replacement by colourless tremolite-actinolite at crystal rims to complete pseudomorphic replacement by secondary amphibole plus chlorite.

Recrystallized matrix

In rocks with best preservation of fine textures, the matrix between shards consists of a very fine grained mixture of brown epidote with subordinate feldspar, tremolite-actinolite or chlorite, quartz and sphene. In more recrystallized and foliated rocks the secondary assemblage completely overprints shards and microclasts; epidote has recrystallized from very fine grained brownish aggregates to well defined yellow-green crystals. In highly recrystallized tuff even the pumice fragments are obliterated.

Bedforms

In members 3, 5 and 6, which dominate this unit, turbidite bedforms are ubiquitous. Individual beds range from 0.3 to 18 m and average about 1 m thick. Beds contain one or more of the following Bouma-type internal zones: a graded A division; parallel laminated B division; ripple laminated C division; parallel laminated D division; and very fine grained, white, structureless E division. Most of the beds are AB with a thick A division and thin B division; in these beds B division thickness is relatively constant, regardless of bed thickness (Fig. 61). Examples of typical, measured beds are shown in Fig. 62.

These tuffs contain structures typical associated with "classical" greywacke turbidite structures. Shallow scours with high width to depth ratios occur at the bases of many beds and have eroded as deeply as the A division of the underlying bed. Flame structures have been observed locally associated with thin beds (e.g. Fig. 63). Some flames show apparent opposing transport directions on a single bed indicating that transport direction may have been approximately perpendicular to the outcrop surface. Size and abundance grading in plagioclase crystal fragments is continuous from base to top of beds (Fig. 62). The majority of "lithic" fragments and amphibole crystals occur at the bases of beds. Parallel laminations in the B division are very fine grained, and in some places are internally graded. Ripple laminations (Figs. 64, 65, 66, 67) are relatively rare with some showing convoluted forms suggesting penecontemporaneous soft-sediment deformation. Rare rip-ups of the very fine grained white E division tuff occur in the A division of overlying beds.

Features not associated with epiclastic turbidites, but which are common in this pyroclastic sequence, include pumice granule strata *within* turbidite beds and pumice-lump beds within the sequence. Pumice granule strata form layers 5 mm — 1 m thick within the graded A division of many beds (Fig. 62). One to several pumice layers may occur within a single bed, with thicker beds generally containing up to 4 — 6 individual pumice layers. Layers are commonly sharply defined and pumice-supported, and contain fragments less than 0.1 to 3 cm long. Thicker layers

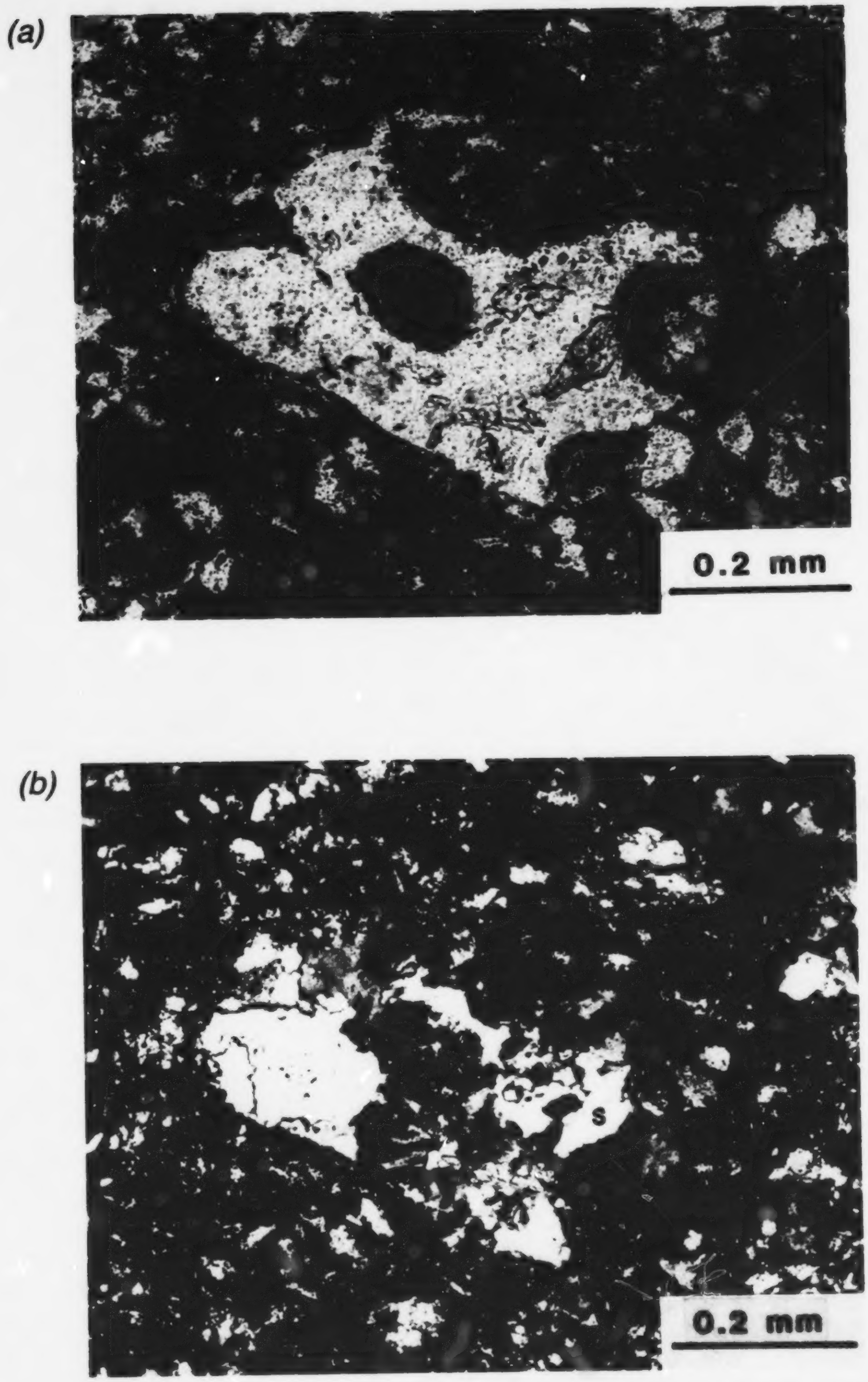

Figure 53: *Large shard displaying conchoidal boundaries cutting through vesicles, in plane polarized light (a) and crossed polarizers (b). Secondary sericite (s) and epidote (e) overprints sutured polygranular albite comprising the greater portion of the shard (b). Vick Lake andesitic tuff, sample 1420-3.*

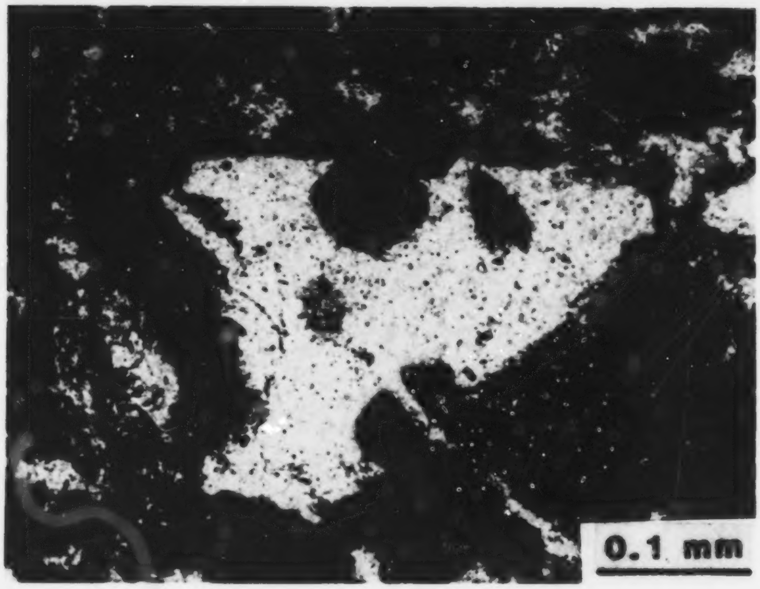

Figure 54: *Shard with one vesicle cut by a straight fracture boundary and another cut by a conchoidal fracture boundary. A small tectonic fracture filled with quartz (v) cuts through the shard. Vick Lake andesitic tuff sample 1420-3, plane polarized light.*

tend to contain largest pumice and in places, contain large aggregates of smaller pumice (to 3 m long). Layers are laterally continuous to discontinuous: thinner layers tend to be lensoid, in trough-like forms with planar tops and bases that are concave upwards (Fig. 68) whereas thicker layers are continuous laterally for several metres, usually extending across individual outcrops with only minor variation in thickness. Thin beds (less than 50 cm), beginning with a B division in some instances, contain pumice granule laminae; some of these occur at the base of the bed (Fig. 64, 65). Highly disrupted pumice layers are interpreted as once-continuous layers subsequently disrupted by dewatering of the unconsolidated turbidite (Fig. 69). Pumice layers, which generally occur in the upper part or top of the A division (Fig. 66, 67, 70), are interpreted to reflect a density sorting in a pumice population characterized by variable vesicularity.

Large pumice lumps (to 25 cm long) occur in beds within the Bouma-bedded sequence, mainly in member 3 (Fig. 71, 72). They occur in unsorted, 0.1 — 5 m thick pumice beds and as isolated fragments throughout, or at the top of, A divisions of graded beds.

Members

Member 1 (Fig. 49 and 52) is an altered, pyritized and variably silicified, 20 m thick tuff which directly overlies a thick rhyolite crystal tuff (unit 27) south of Two Portage Lake (Fig. 49). It contains abundant fine grained pyrite, is thinly laminated, with massive pyrite layers up to 5 cm thick. Graded, crystal-vitric tuff laminae contain slabby vitric shards, with plagioclase crystal fragments and amphibole crystal fragments concentrated at the bases of laminae.

Member 2 is 150 m thick south of Two Portage Lake (Fig. 49). It is distinctly different from the overlying Bouma-zoned andesitic tuff in that it is not well stratified, contains abundant aphyric and quartz-phyric rhyolite fragments, and contains (1%) fine grained quartz crystals. Rhyolite fragments weather white and are up to 60 cm across; they occur concentrated in beds up to 2 m thick or as sporadic clasts in an intermediate tuff matrix. Shapes of rhyolite clasts range from angular to rounded. A sharp contact occurs between the poorly stratified tuff of member 2 and overlying Bouma-zoned tuff of member 3.

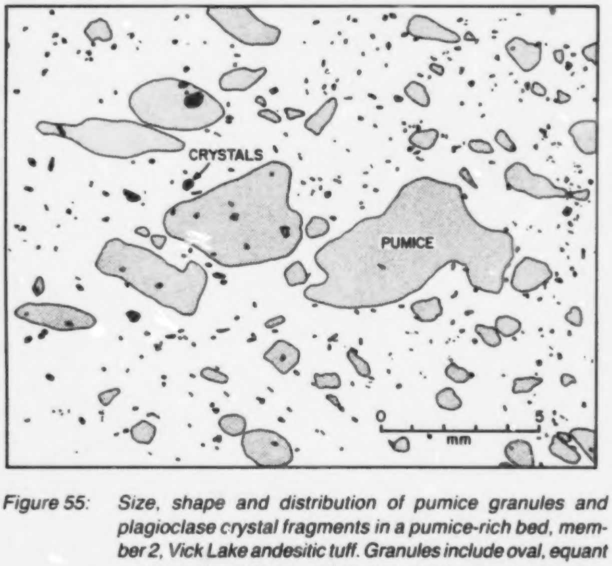

Figure 55: *Size, shape and distribution of pumice granules and plagioclase crystal fragments in a pumice-rich bed, member 2, Vick Lake andesitic tuff. Granules include oval, equant and irregular shapes, and display plagioclase phenocrysts similar in size and shape to crystals in matrix. Traced from a photomicrograph.*

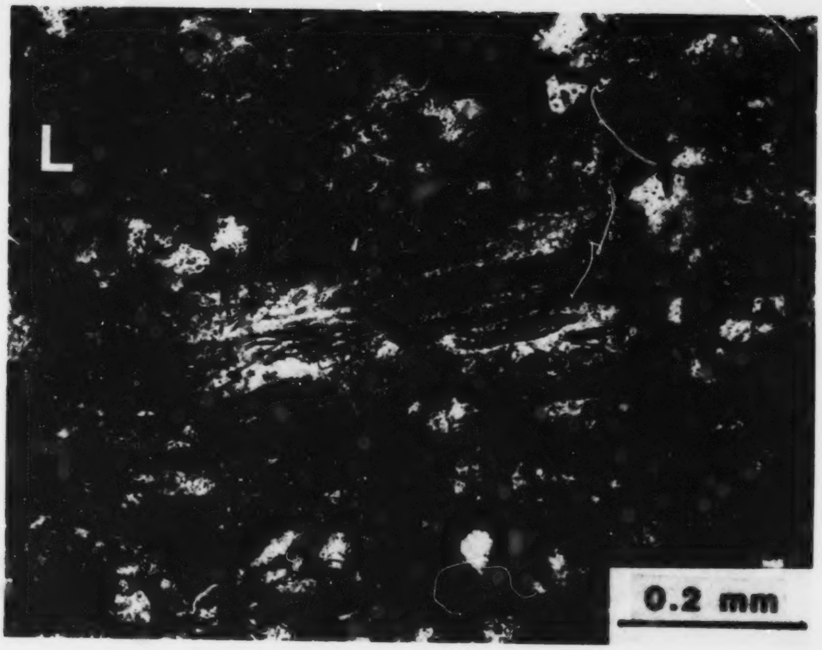

Figure 56: Long-tube pumice fragment in a matrix of shards, small plagioclase crystal fragments, secondary epidote (dark) and small lithic granules (l). Vesicles in pumice are filled with chlorite (light grey) and very fine grained epidote (dark). Vick Lake andesitic tuff, sample 1420-1, plane polarized light.

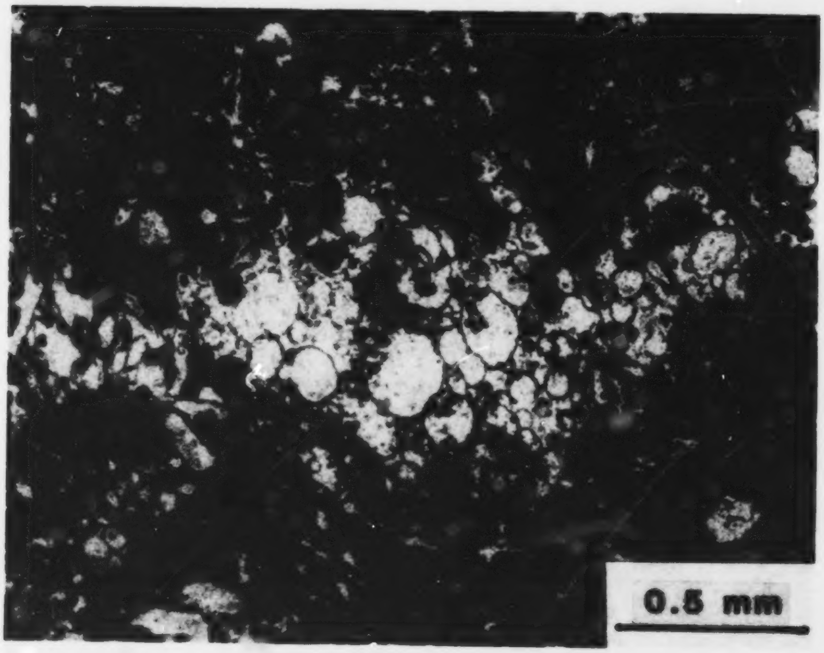

Figure 57: Pumice fragment with high vesicularity. Vesicles are filled with quartz and albite and are separated by septa composed of very fine grained seconary chlorite and epidote. Vick Lake andesitic tuff, sample 1420-3, plane polarized light.

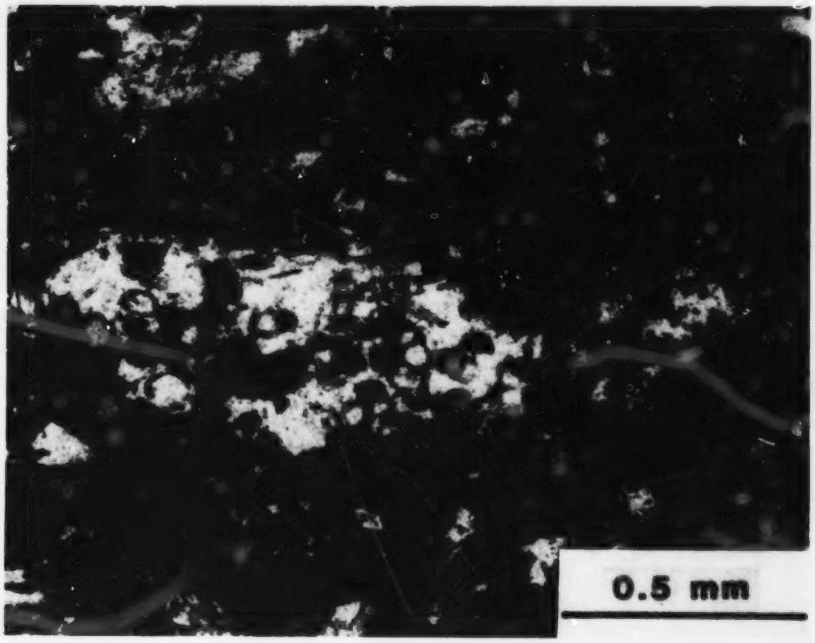

Figure 58: *Pumice granule replaced by mosaic of polygranular sutured quartz and albite. Vesicles are outlined by very fine grained chlorite and minor epidote. Vesicles are filled with quartz, albite (white), chlorite (light grey) and epidote (dark). Vick Lake andesitic tuff, sample 1420-3, plane polarized light.*

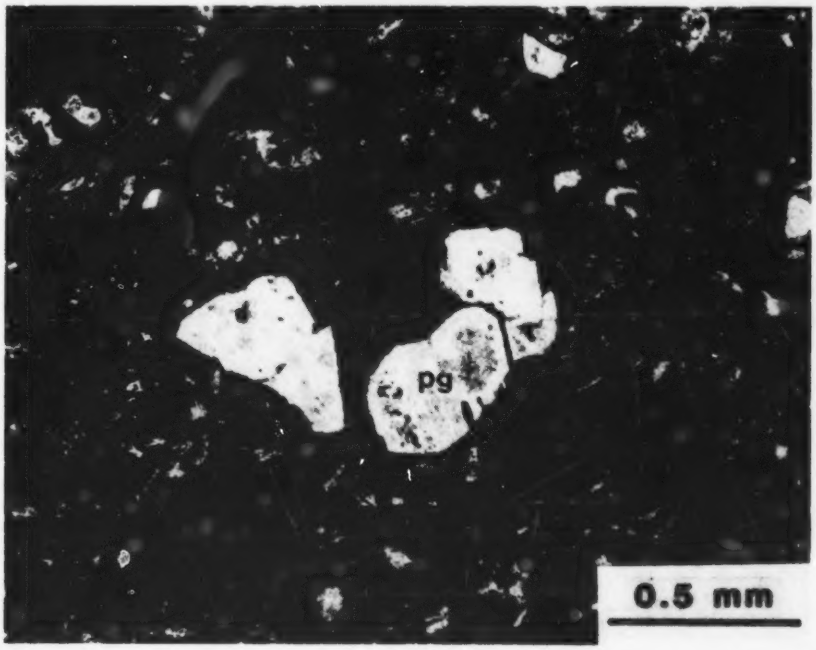

Figure 59: *Plagioclase-phyric brown microlitic lithic granules in a fine grained matrix of shards. Note subrounded form of granule and truncation of phenocrysts at clast boundaries. Vick Lake andesitic tuff, sample 1420-3, plane polarized light.*

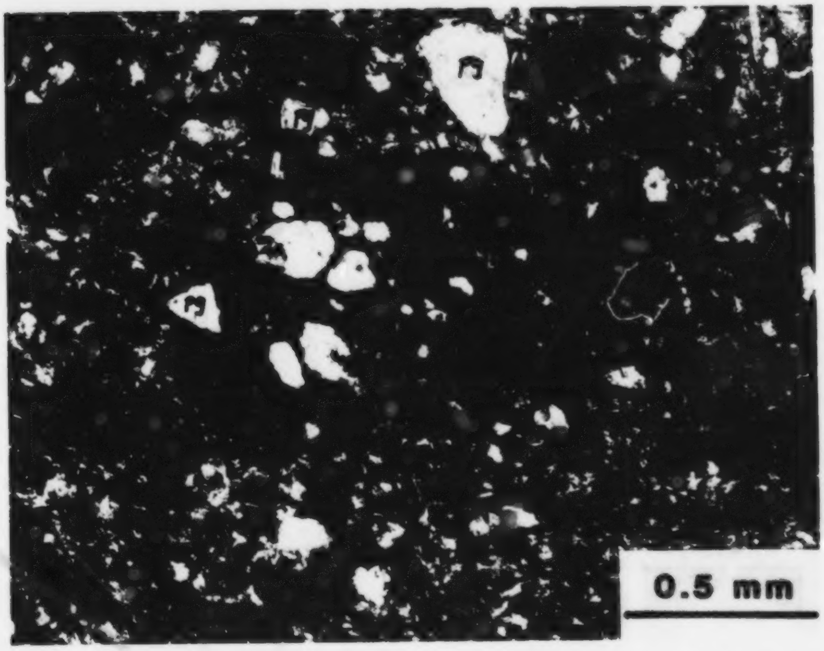

Figure 60: *Juvenile tan brown granule with irregular boundary dominated by vesicle margins. Vesicles are filled with untwinned feldspar, quartz, minor chlorite, actinolite and epidote. Matrix consists of very fine grained shards (white), plagioclase crystal fragments (pg) and secondary epidote (dark). Vick Lake andesitic tuff, sample 1420-1, plane polarized light.*

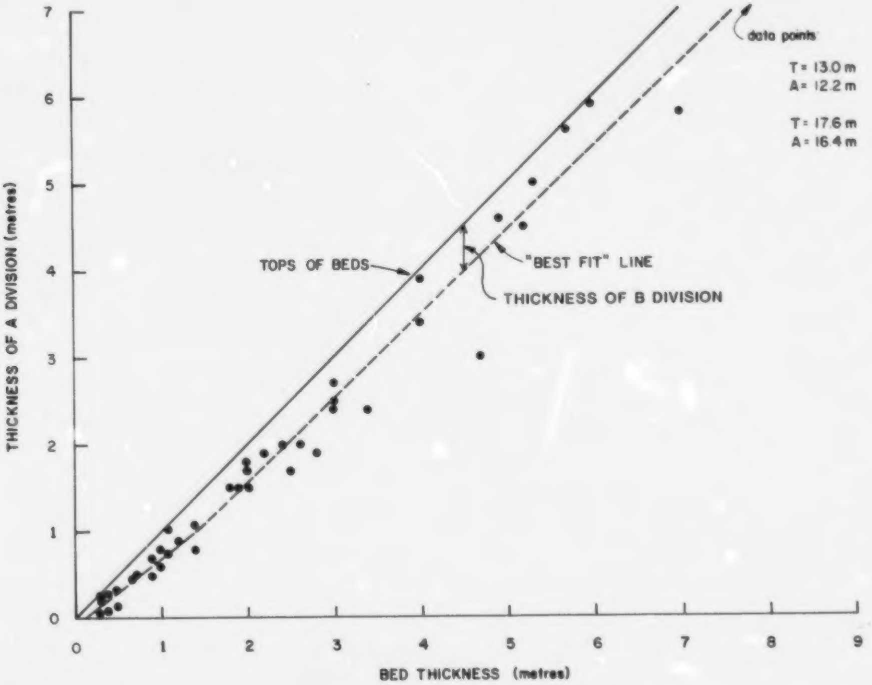

Figure 61: *Thickness of A division plotted against total bed thickness, Vick Lake andesitic tuff. Note that the thickness of the B division is virtually constant, regardless of bed thickness, particularly for beds thicker than 1.5 m.*

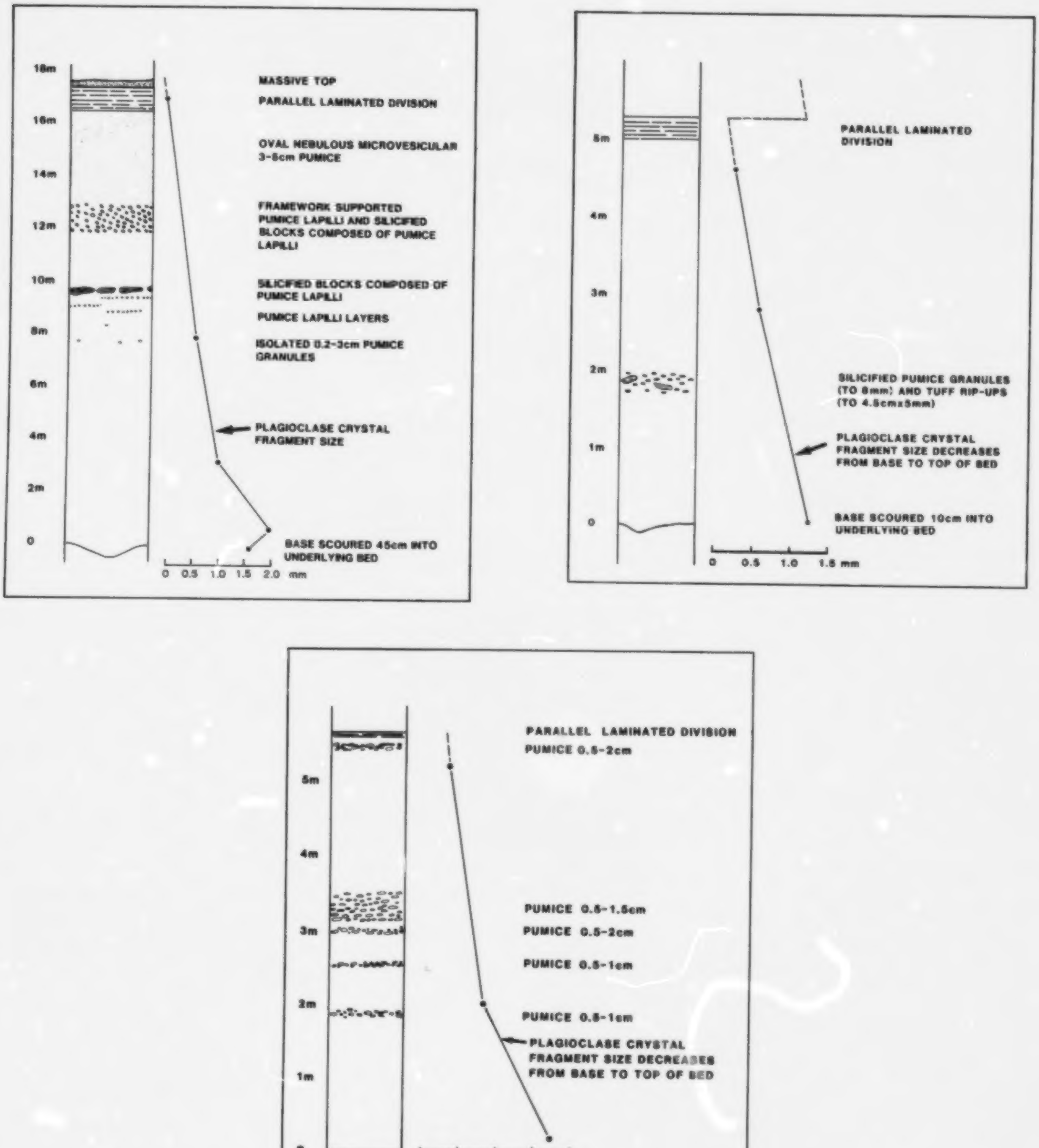
18m
16m
14m
12m
10m
8m
6m
4m
2m
0
MASSIVE TOP
PARALLEL LAMINATED DIVISION
OVAL NEBULOUS MICROVESICULAR 3-5cm PUMICE
FRAMEWORK SUPPORTED PUMICE LAPILLI AND SILICIFIED BLOCKS COMPOSED OF PUMICE LAPILLI
SILICIFIED BLOCKS COMPOSED OF PUMICE LAPILLI
PUMICE LAPILLI LAYERS
ISOLATED 0.2-3cm PUMICE GRANULES
PLAGIOCLASE CRYSTAL FRAGMENT SIZE
BASE SCOURED 45cm INTO UNDERLYING BED
0 0.5 1.0 1.5 2.0 mm
5m
4m
3m
2m
1m
0
PARALLEL LAMINATED DIVISION
SILICIFIED PUMICE GRANULES (TO 8mm) AND TUFF RIP-UPS (TO 4.5cmx5mm)
PLAGIOCLASE CRYSTAL FRAGMENT SIZE DECREASES FROM BASE TO TOP OF BED
BASE SCOURED 10cm INTO UNDERLYING BED
0 0.5 1.0 1.5 mm
5m
4m
3m
2m
1m
0
PARALLEL LAMINATED DIVISION
PUMICE 0.5-2cm
PUMICE 0.5-1.5cm
PUMICE 0.5-2cm
PUMICE 0.5-1cm
PUMICE 0.5-1cm
PLAGIOCLASE CRYSTAL FRAGMENT SIZE DECREASES FROM BASE TO TOP OF BED
0 0.5 1.0 1.5 2.0 mm

Figure 62: *Bed organization and distribution of megascopic pumice granules and blocks in three thick beds, Vick Lake andesitic tuff. Note continuous size grading of plagioclase crystal fragments across pumice granule layers, indicating these pumice layers are integral parts of beds and do not represent separate depositional events.*

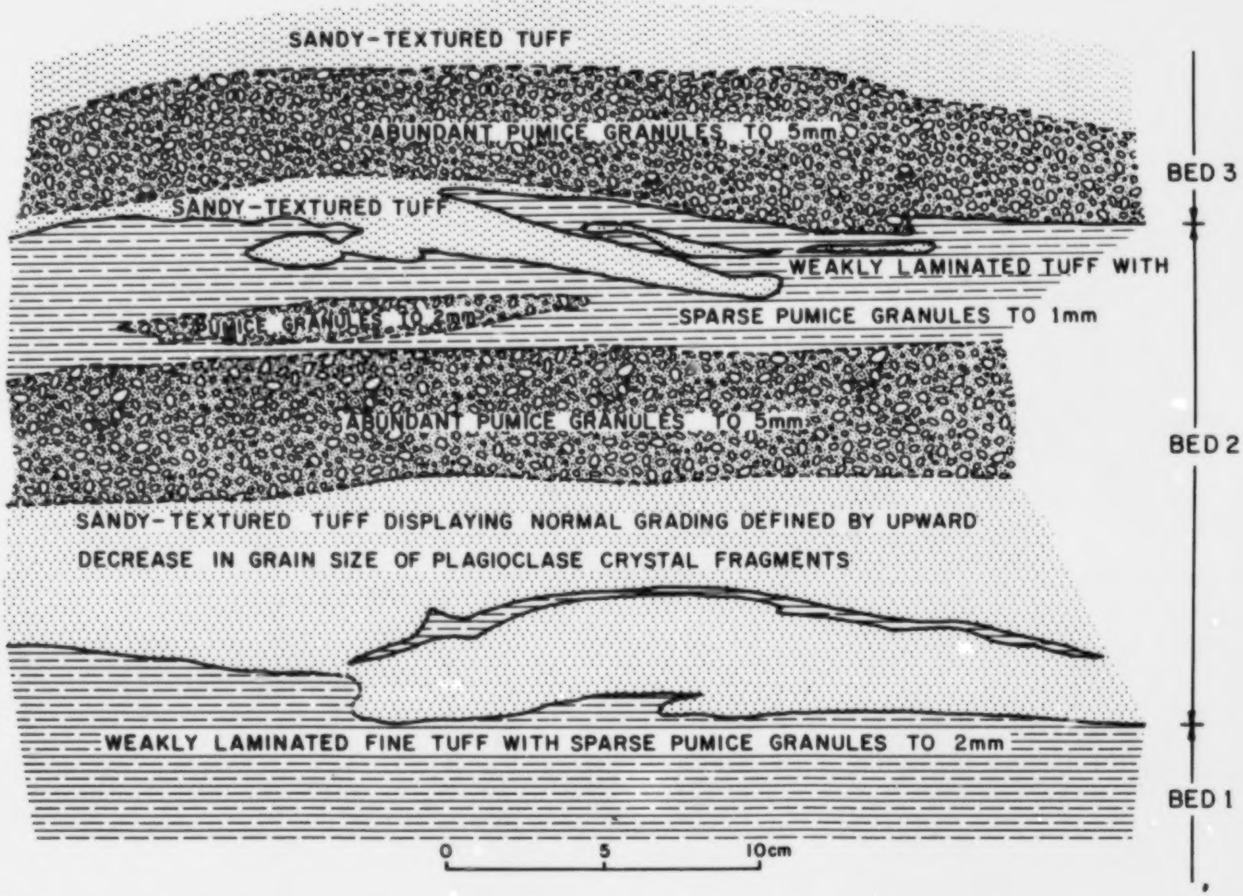
SANDY-TEXTURED TUFF
ABUNDANT PUMICE GRANULES TO 5mm
BED 3
SANDY-TEXTURED TUFF
WEAKLY LAMINATED TUFF WITH
SPARSE PUMICE GRANULES TO 1mm
PUMICE GRANULES TO 2mm
ABUNDANT PUMICE GRANULES TO 5mm
BED 2
SANDY-TEXTURED TUFF DISPLAYING NORMAL GRADING DEFINED BY UPWARD
DECREASE IN GRAIN SIZE OF PLAGIOCLASE CRYSTAL FRAGMENTS
WEAKLY LAMINATED FINE TUFF WITH SPARSE PUMICE GRANULES TO 2mm
BED 1
0
5
10cm

Figure 63: Flame structures in Vick Lake andesitic tuff, traced from a photograph. Note "detached" flame structure at top of bed 1 and flames with opposing directions at top of bed 2.

Members 3, 5 and 6 are all broadly similar and form more than 80% of the Vick Lake tuff. Bedforms and constituents have been discussed above. Member 3 contains more large pumice fragments than members 5 and 6, and member 6 is distinctly thinner bedded.

Member 4 forms a thin (30 m), laterally continuous subunit composed of interbedded buff, fine grained tuff, dark grey argillite and white chert (Fig. 73). Many of the argillite beds are weakly pyritic. Bedding thickness ranges from laminae to 30 cm. This member is significant in that it forms a readily identifiable marker unit that is composed largely of non-pyroclastic material.

Member 7 is approximately 60 m thick and is best exposed adjacent to old Highway 10. It is composed of dark grey to black, graphitic, pyritic mudstone with interbeds of buff andesitic tuff and chert. There is an upward decrease in abundance of andesitic tuff beds such that midway through the member the section is completely composed of mudstone. Chert beds occur only in the upper part of the member.

Member 8 is approximately 20 m thick. It is composed of alternating layers of grey graphitic mudstone and white to pale brown, carbonate-rich beds. Beds are less than 3 m thick; some contain up to 5% disseminated pyrite and 30 — 40% rusty weathering Fe-carbonate(?) blasts.

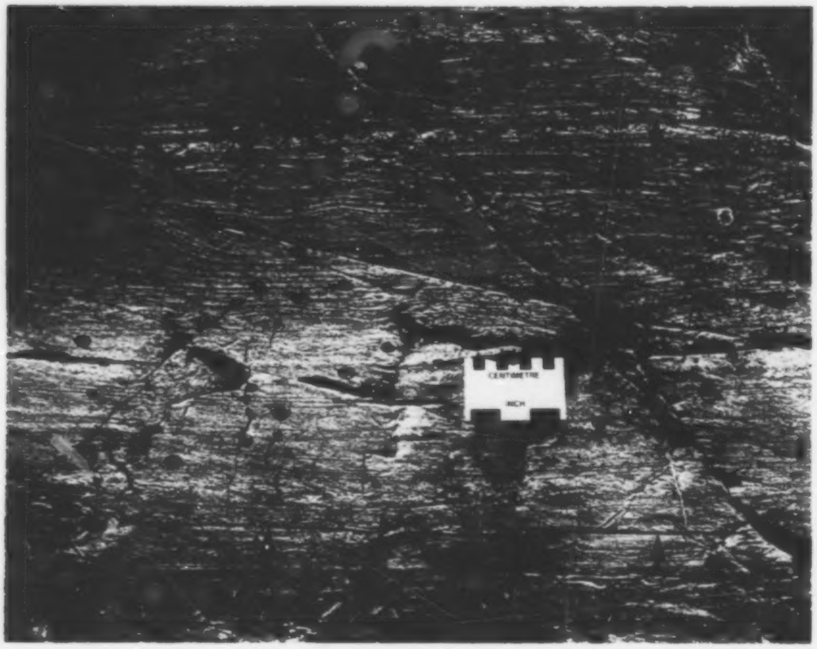

Figure 64: Vick Lake andesitic tuff (unit 25e) with Bouma B, C and D divisions, 300 m west of north end of Northeast Arm. Base and top of bed marked by arrows and highlighted with felt pen.

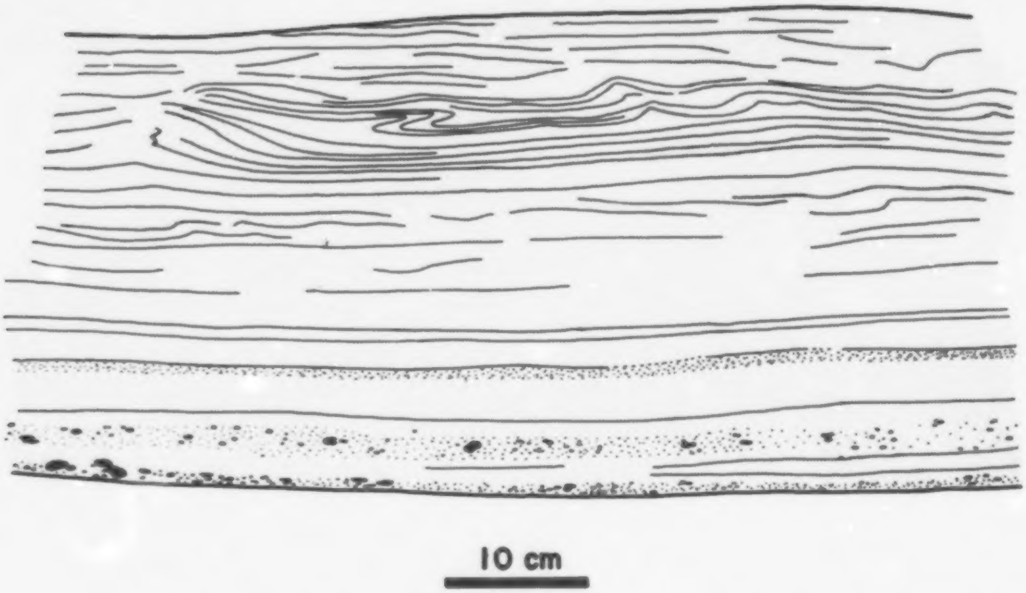

Figure 65: Tracing of bed shown in Fig. 64, showing Bouma B, C and D divisions. Pumiceous grains and granules in black.

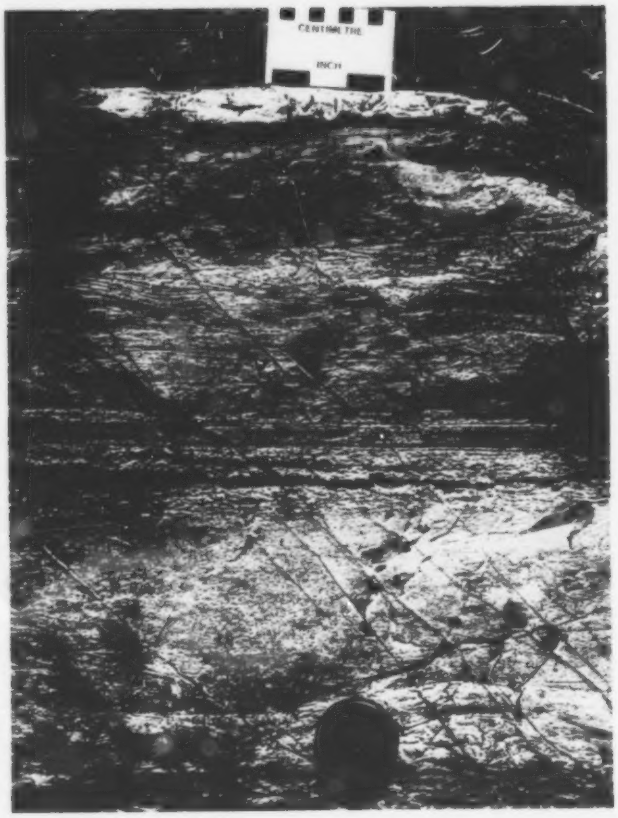

Figure 66: *Single bed in Vick Lake andesitic tuff (unit 25e) with Bouma A, B, C, D and E divisions. Base of the bed is at the top of the lens cap, top of the bed is at the scale card. Note pumice granules in upper part of A division and lower part of B division. 430 west of the north end of Northeast Arm, north of old Highway 10.*

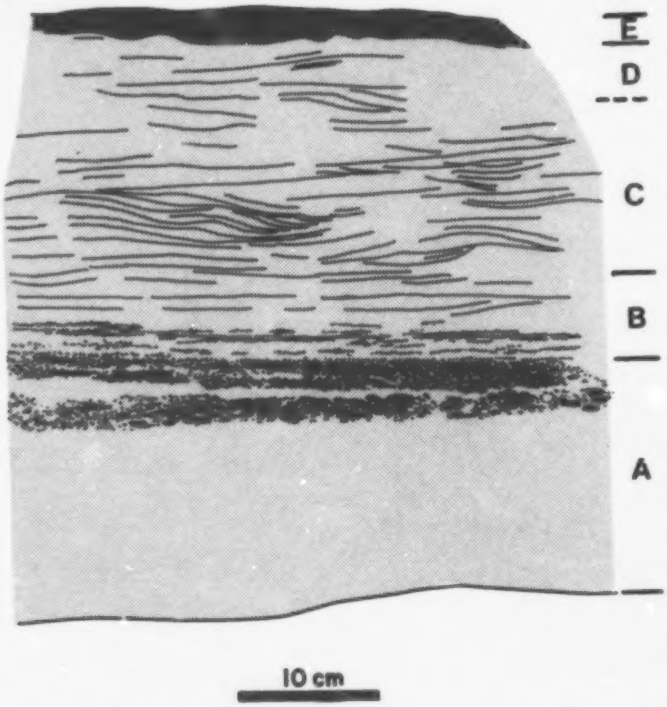

Figure 67: *Tracing of bed shown in Fig. 66. Pumice granules (black) occur in the upper part of the A division and lower part of the B division.*

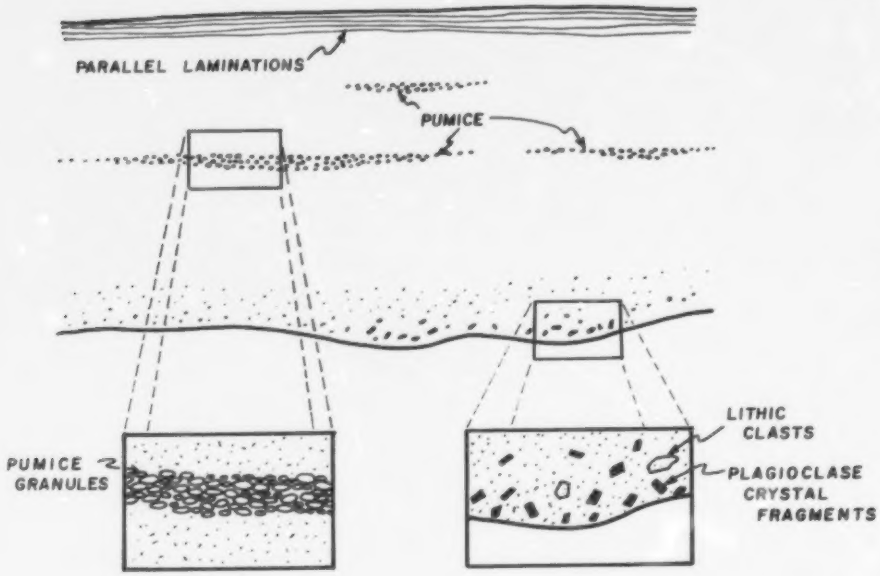
PARALLEL LAMINATIONS
PUMICE
PUMICE GRANULES
LITHIC CLASTS
PLAGIOCLASE CRYSTAL FRAGMENTS

Figure 68: *Schematic diagram of typical Vick Lake andesitic tuff AB bed, showing concentration of lithic granules and plagioclase crystal fragments at base of bed and the lensoid nature of narrow pumice-rich internal layers.*

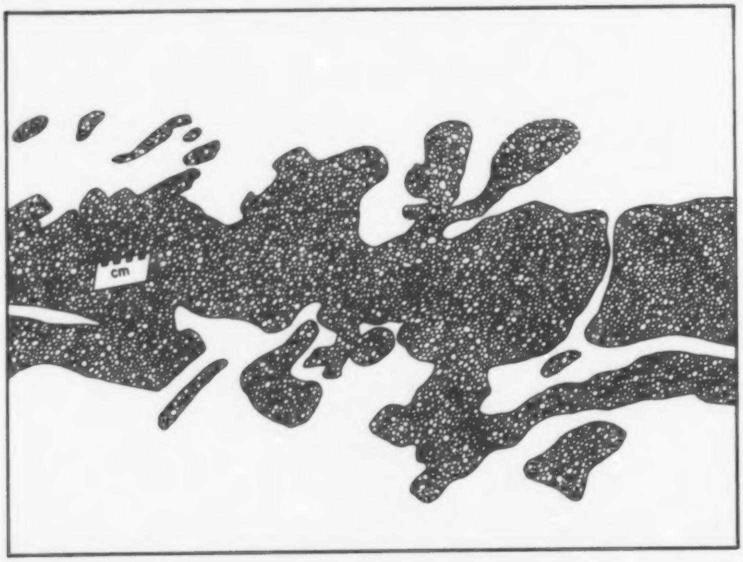

Figure 69: *Disrupted pumice layer in very thick bedded Vick Lake andesitic tuff, member 5, 400 m south of Two Portage Lake. In these beds pumice occurs in poorly defined layers, in "lumps" (pumice aggregates) to 5 cm diameter, and in disrupted layers as shown (traced from photograph). Disruption of the pumice layer is interpreted to be the result of dewatering of the tuff bed shortly after deposition from a turbulent gravity flow.*

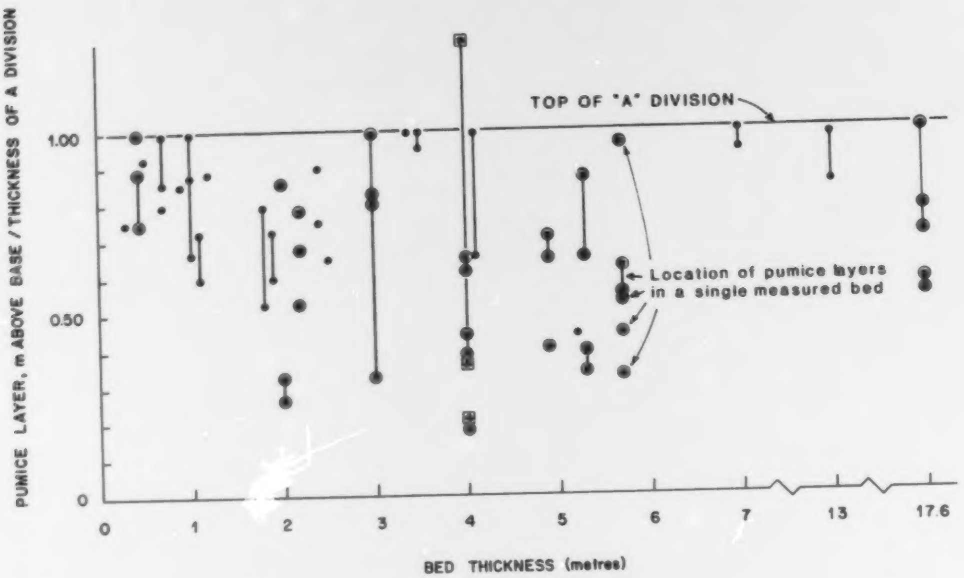

Figure 70: *Height of pumice layers in A divisions, divided by thickness of A division, versus total bed thickness. Vertical lines between points indicate limits of thicker layers. In single beds containing more than one pumice layer the data points are circled (e.g. 2 layers in 2 m bed, 4 layers in 3 m bed). Pumice layers tend to occur in the upper parts of A divisions.*

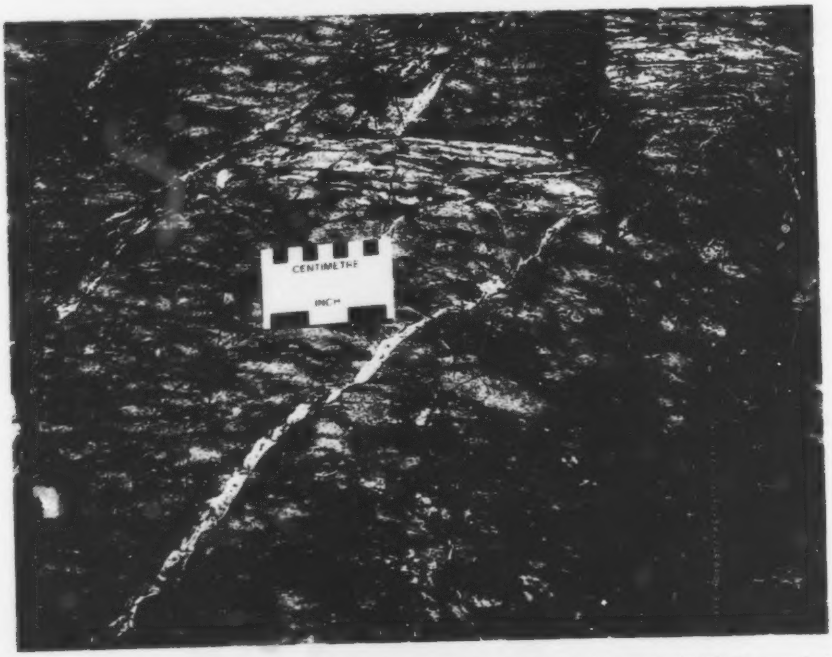

Figure 71: *Pumice-rich bed, Vick Lake andesitic tuff (unit 25c), 640 m east of Little Spruce Lake.*

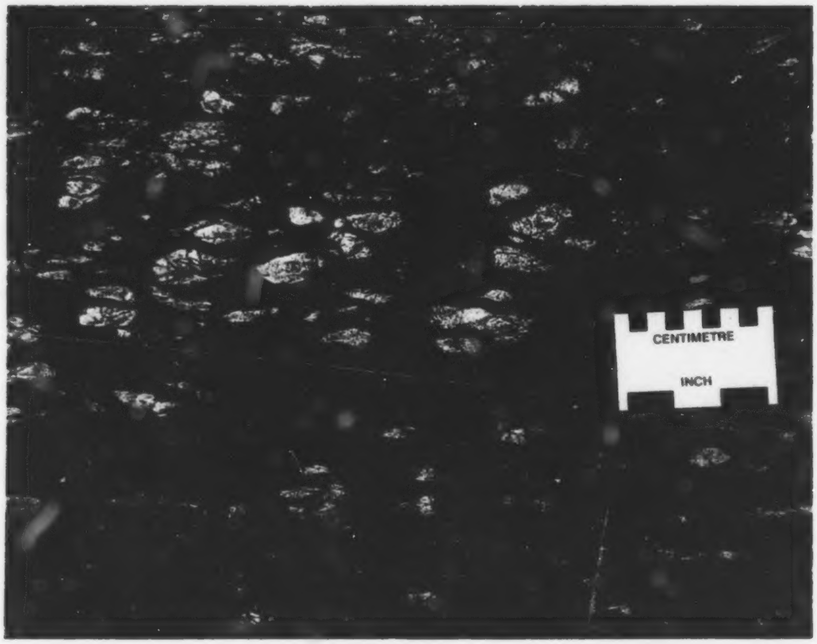
CENTIMETRE
INCH

Figure 72: *Pumice-rich bed, Vick lake andesitic tuff (unit 25c), 730 m east of Little Spruce Lake. Pumice lumps (white) average 4 cm long and are deformed into the plane of schistosity.*

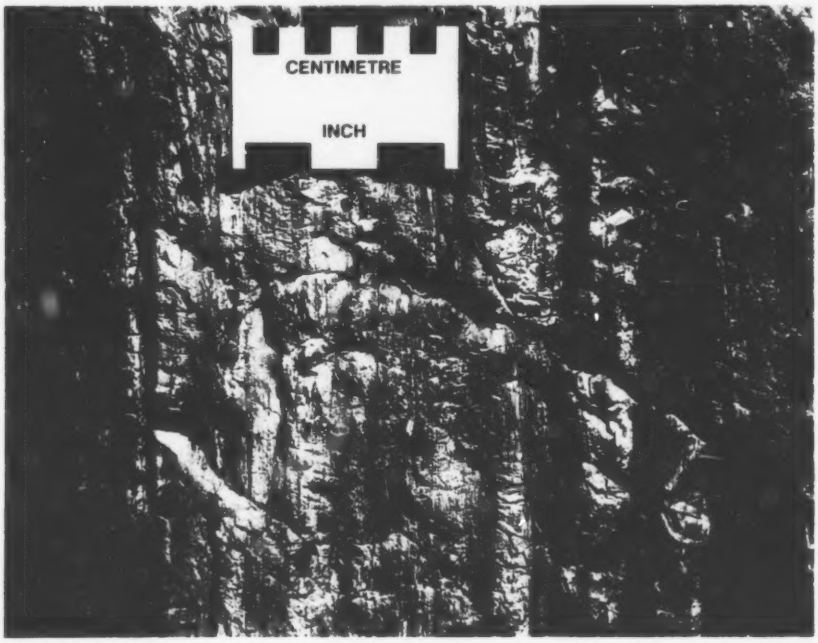
CENTIMETRE
INCH

Figure 73: *Thinly bedded mudstone, tuff and chert (unit 25d), Vick Lake andesitic tuff, 980 m northeast of Little Spruce Lake.*

Deformation structures

In the hinge zone of the Northeast Arm Syncline (Fig. 52) the tuffs are characterized by a strong axial plane foliation, obliteration of shard structures and bedforms, broken and rotated plagioclase crystals and chevron folds. This area is also characterized by abundant 0.1 — 15 cm wide pink granitoid veinlets composed of quartz, feldspar, and minor carbonate and pyrite. The veinlets are typically axial planar, but larger irregular pegmatoid masses and stockworks are locally abundant.

Geochemistry

The tuff is andesitic in composition (56.3% SiO_2 — average of six analyses calculated volatile-free) and is characterized by high contents of K_2O, Na_2O and Al_2O_3 and very high Rb, Sr and Ba contents. Relative to Bear Lake basaltic andesite it also has elevated P_2O_5 and TiO_2 (Fig. 74). LIL elements, which are all abundant in this unit, are highly mobile during seafloor alteration and metamorphism. Limited data from this unit (serial samples through three beds in the lower, middle and upper part of the sequence) indicate that *all* of the tuff is similarly characterized by high LIL element, P_2O_5 and TiO_2 concentrations. This compositional homogeneity suggests that the abundance of these elements approximates primary values. If this is true then the andesitic magma was alkalic in character.

Interpretation

The local exceptional state of preservation and well defined stratigraphic setting of the Vick Lake andesitic tuff permits the following constraints for modelling its origin:

(1) The unit was deposited upon a subaqueous lava plain (Two Portage Lake ferrobasalt).

(2) The thickness of the Vick Lake tuff (900 m) indicates that the lava plain floored a large, deep basin.

(3) Ash morphology, with shard boundaries controlled largely by fracture surfaces, indicates an eruptive style which was dominated by a phreatomagmatic component (c.f. Heiken, 1972; Heinrichs, 1984), implying relatively shallow water or subaerial conditions.

(4) Presence and abundance of pumice, in ash to block-size fractions, indicates that eruptions also had plinian components, again emphasizing a very shallow water or subaerial environment.

(5) Bouma organization of beds indicates that the pyroclastic materials were deposited from turbulent density currents.

(6) Absence of welding is consistent with both a phreatomagmatic eruption mechanism and deposition from subaqueous density currents.

(7) Absence of interbeds of extraneous sedimentary or volcanic material indicates that the eruptions were closely spaced in time.

(8) General upward fining of the sequence, and gradual increase and ultimate dominance of pelagic sedimentary components in the upper 180 m of the unit indicates a gradual cessation of pyroclastic volcanism, with eruptions becoming more widely spaced with smaller volume of ejected material.

(9) Presence of thick beds (up to 18 m) indicates proximity to source vents.

(10) Presence of amphibole phenocrysts and alkalic bulk compositions is consistent with high volatile contents in the magma, and explosive eruption styles.

(11) Absence of exotic clasts or particles in the tuff beds indicates that mixing of the pyroclastic material with foreign detritus was virtually non existent.

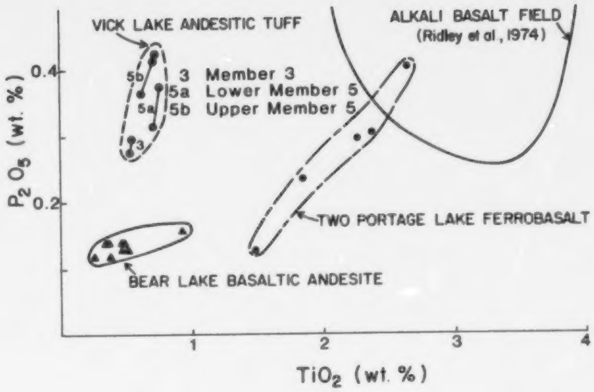

Figure 74: P_2O_5 vs. TiO_2, Vick Lake andesitic tuff and, for comparison, Bear Lake basaltic andesite and Two Portage Lake ferrobasalt. The lower, middle and upper parts of 3 Vick Lake andesitic tuff beds (from members 3 and 5) were analyzed; lines join analyses from the same bed. In each analyzed bed P_2O_5 content is greatest in its upper part; P_2O_5 content also increases upwards through the unit as a whole.

A model which is consistent with the above constraints (Fig. 75) is similar to that proposed by Heinrichs (1984) for an Archean volcaniclastic turbidite deposit. Shallow water or subaerial phreatomagmatic and plinian eruptions produced ash, pumice and crystal fragments that entered the water column from base surges, pyroclastic flows(?) and fallout. The absence of exotic fragments suggests immediate gravity flow transport of these pyroclastic materials from the flanks of the subaqueous portion of the cone into the adjacent deeper water basin. Similarly the gravity flows are not considered to have been initiated as lahars, mudflows, landslides nor subaqueous slumps of more or less consolidated material. In this model a number of individual beds may have been deposited during a single eruption event. The entire deposit represents a large number of eruption events relatively closely spaced in time; the white, very fine grained tuff E division layers probably represent settling of the finest ash through the water column between eruption events. Sedimentary units (e.g. member 4) represent longer quiescent periods during which pelagic shales and cherts were also deposited. As the andesitic pyroclastic volcanism waned, increasing proportions of pelagic graphitic shales were deposited between eruptions (members 7 and 8).

DACITE, TUFF (UNITS 18a and 28b)

Approximately 100 m of decite flows and poorly exposed intermediate and felsic tuff occurs in the hinge of the Northeast Arm Syncline, in the vicinity of old Highway 10. Exposures are small and the unit is extremely limited in its present extent; it is truncated to the north by the Mikanagan Lake Sill and to the east by the Northeast Arm Fault. The main significance of this unit is its stratigraphic setting: it overlies member 8 of the Vick Lake andesitic tuff and signals the onset of a new and completely different phase of volcanism in the Bear Lake Block sequence.

The dacite weathers light grey-buff and is apparently a massive flow. The only primary structures include rare flow laminations (less than 1 to 3 mm wide) and recrystallized, feldspar-epidote spherulites (to 2 mm). The groundmass is recrystallized to fine grained feldspar, epidote and leucoxene. Gossan zones in the dacite reflect oxidation of disseminated and fracture-filling pyrite. Other alteration features include black chlorite veinlet stockworks and black amphibole veins to 10 cm wide. Gossan zones and chloritic alteration cut across flow layering at a high angle.

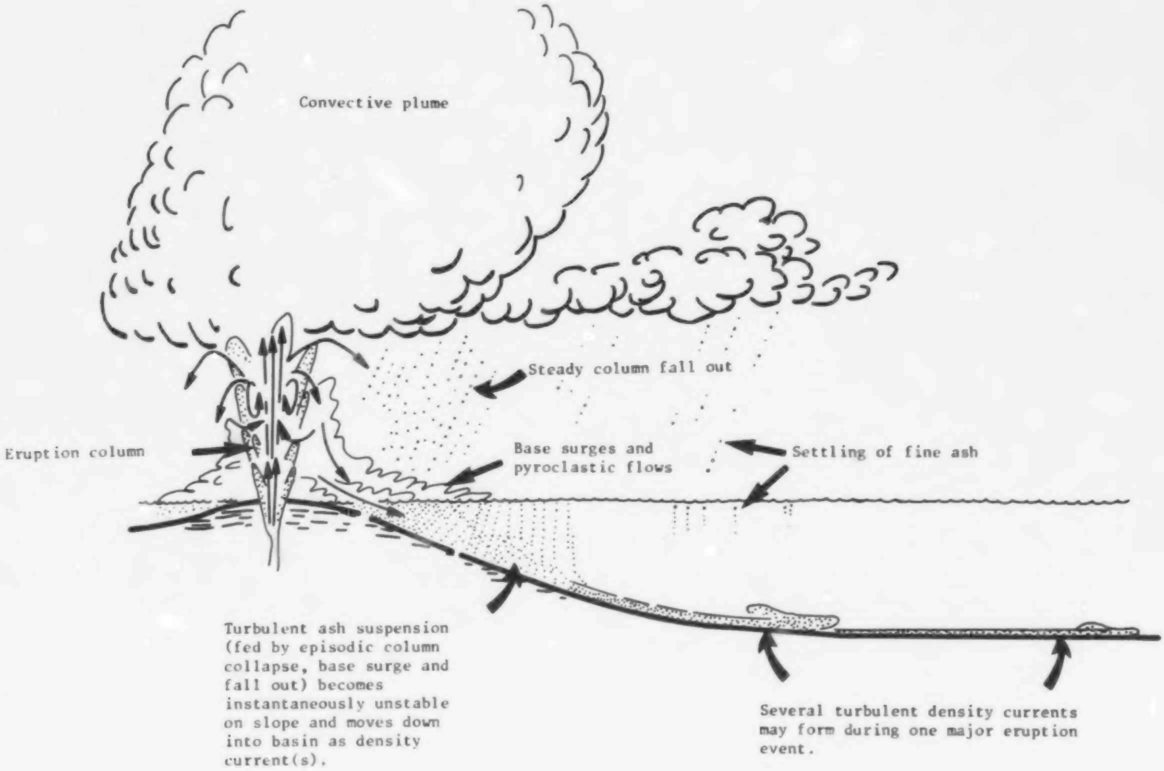
Convective plume
Steady column fall out
Eruption column
Base surges and pyroclastic flows
Settling of fine ash
Turbulent ash suspension (fed by episodic column collapse, base surge and fall out) becomes instantaneously unstable on slope and moves down into basin as density current(s).
Several turbulent density currents may form during one major eruption event.

Figure 75: Model for eruptive mechanism and depositional environment of the Vick Lake andesitic tuff (diagram after Heinrichs, 1984).

Intermediate and felsic tuffs are poorly exposed. They weather brown, greenish brown and white and form an apparently thinly stratified (1 — 3 m) sequence. Some of the laminated dacite may be tuffaceous.

INTERMEDIATE TUFF, BRECCIA (UNIT 29), MAFIC FLOWS (UNIT 7)

A 30 m thick unit of heterogeneous volcaniclastic rocks overlies dacite (unit 18a) in the hinge zone of the Northeast Arm Syncline. The tuff is well bedded (1 — 25 cm) with interlayers of breccia (10 — 50 cm); locally it is cut by probable intrusive breccias. The tuff and breccia has a heterogeneous clast population including microlitic intermediate-mafic flow rocks, laminated to massive aphyric felsic rocks, dark green basalt, amphibole pseudomorphs after pyroxene crystals, and plagioclase crystals. Fragments are framework supported, with a matrix of fine grained quartz. Some beds are normally graded.

The tuff is overlain by an unknown thickness (less than 40 m) of medium green weathering aphyric mafic flows.

VOLCANIC RECONSTRUCTION OF THE BEAR LAKE BLOCK

The major volcanic events which produced the sequence of rock units exposed in the Bear Lake Block can be subdivided into four stages (Fig. 76): (1) construction of a subaqueous basaltic andesite shield volcano, (2) rhyolite volcanism and deposition of volcaniclastics in an adjacent basin, (3) eruption of ferrobasalt to form a subaqueous lava plain, and (4) deposition of andesitic tuff in a deep basin.

Shield building stage

The Bear Lake shield volcano has a minimum thickness of 3.3 km; assuming a profile slope of 10° the minimum diameter of this volcano would be 37 km. There is a clear upward decrease in average flow thickness and an increase in the proportion of massive to pillowed flows (Fig. 23 to 25) suggesting a progressively lower effusion rate as the volcano matured. A parallel upward increase in overall flow vesicularity indicates that the volcano was constructed into progressively shallower water. Flows in the upper part of the Bear Lake volcano are characterized by 15 — 20% vesicles (locally up to 40%), radial pipe vesicles, and abundant amygdales up to and larger than 1 cm in diameter. In modern ocean ridge basalts abundant large vesicles occur only at depths less than 300 m (Jones, 1969) and pipe vesicles are confined to flows emplaced at depths less than 700 m (Moore and Schilling, 1973; see also Table 5). The absence of pyroclastic material, even in the uppermost part, indicates eruption in water depth of more than 300 m based on studies Icelandic subglacial basaltic volcanoes where a phreatomagmatic style dominates eruptions when water depth is less than about 300 m (Jones, 1979, 1970; Sigval-

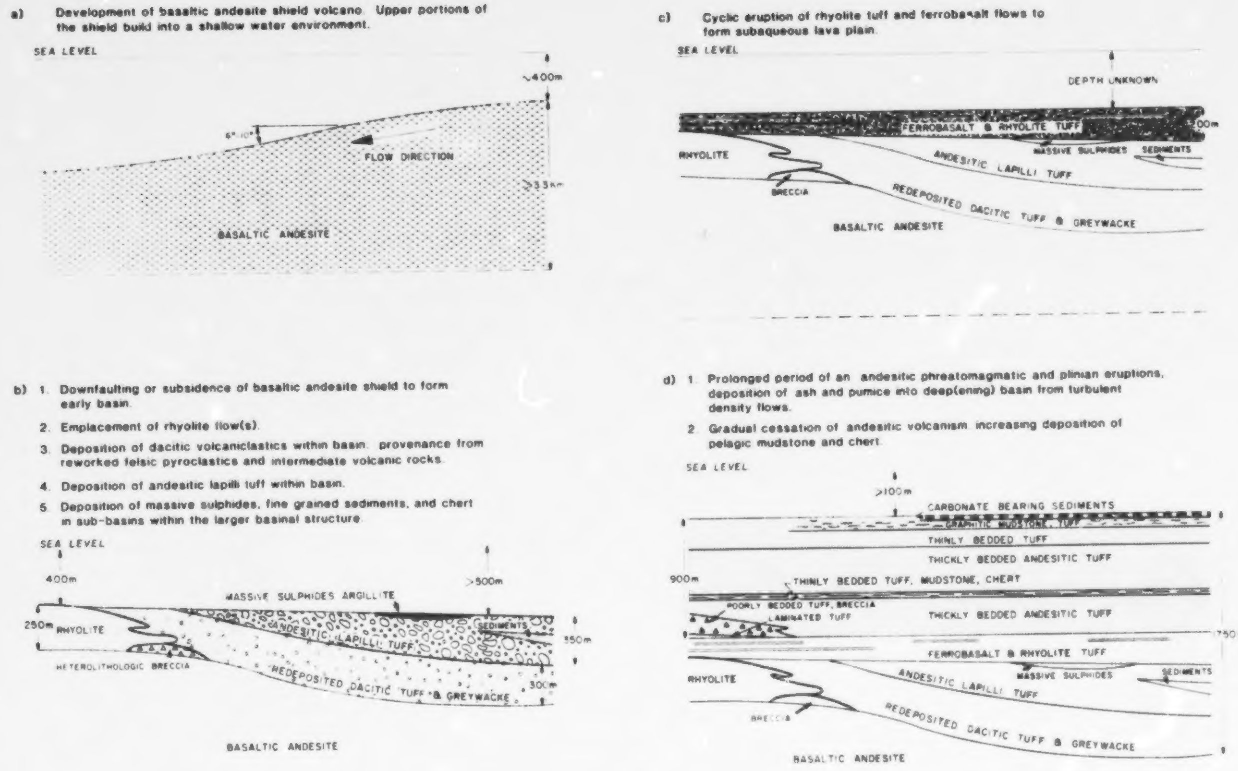
a) Development of basaltic andesite shield volcano. Upper portions of the shield build into a shallow water environment.

b) 1. Downfaulting or subsidence of basaltic andesite shield to form early basin.
2. Emplacement of rhyolite flow(s).
3. Deposition of dacitic volcaniclastics within basin: provenance from reworked felsic pyroclastics and intermediate volcanic rocks.
4. Deposition of andesitic lapilli tuff within basin.
5. Deposition of massive sulphides, fine grained sediments, and chert in sub-basins within the larger basinal structure.

c) Cyclic eruption of rhyolite tuff and ferrobasalt flows to form subaqueous lava plain.

d) 1. Prolonged period of an andesitic phreatomagmatic and plinian eruptions, deposition of ash and pumice into deep(ening) basin from turbulent density flows.
2. Gradual cessation of andesitic volcanism increasing deposition of pelagic mudstone and chert.

SEA LEVEL
~400m
6°-10°
FLOW DIRECTION
>3.3km
BASALTIC ANDESITE
SEA LEVEL
400m
>500m
MASSIVE SULPHIDES ARGILLITE
250m
RHYOLITE
SEDIMENTS
ANDESITIC LAPILLI TUFF
350m
HETEROLITHOLOGIC BRECCIA
REDEPOSITED DACITIC TUFF & GREYWACKE
300m
BASALTIC ANDESITE
SEA LEVEL
DEPTH UNKNOWN
FERROBASALT & RHYOLITE TUFF
200m
RHYOLITE
MASSIVE SULPHIDES
SEDIMENTS
ANDESITIC LAPILLI TUFF
BRECCIA
REDEPOSITED DACITIC TUFF & GREYWACKE
BASALTIC ANDESITE
SEA LEVEL
>100m
CARBONATE BEARING SEDIMENTS
GRAPHITIC MUDSTONE, TUFF
THINLY BEDDED TUFF
THICKLY BEDDED ANDESITIC TUFF
900m
THINLY BEDDED TUFF, MUDSTONE, CHERT
POORLY BEDDED TUFF, BRECCIA
LAMINATED TUFF
THICKLY BEDDED ANDESITIC TUFF
750m
FERROBASALT & RHYOLITE TUFF
RHYOLITE
MASSIVE SULPHIDES
SEDIMENTS
ANDESITIC LAPILLI TUFF
BRECCIA
REDEPOSITED DACITIC TUFF & GREYWACKE
BASALTIC ANDESITE

Figure 76: Reconstruction of stages of volcanic development of the Bear Lake Block sequence.

dason, 1968; Allen, 1969). Consequently, it is unlikely that the Bear Lake volcano grew into depths less than 300 m. With these constraints it is possible to place the top of the Bear Lake shield at between 300 and 400 m below sea level.

Flow direction indicators show a uniform northerly component of transport, placing the source area of the flows an unknown distance south of Sleep Lake. More than 1650 m of subaqueous volcaniclastics and lava flows were subsequently deposited on top of the Bear Lake volcano in this area, indicating that a minimum of about 1.5 km of subsidence must have occurred, between the end of Bear Lake shield volcanism and the end of Vick Lake andesitic pyroclastic volcanism. The exact nature of this subsidence is unknown. Two possibilities are: formation of a summit caldera in the final stages of Bear Lake volcanism, and isostatic sinking of the entire volcano under its own weight (as in oceanic islands; Williams and McBirney, 1979).

Rhyolite volcanism and deposition of volcaniclastics

The cessation of Bear Lake basaltic andesite volcanism was marked by the abrupt eruption of Solodiuk Lake subaqueous rhyolite flows and contemporaneous infilling of a southward-deepening basin with volcaniclastic rocks. The volcaniclastic rocks include: (1) heterolithologic breccia derived in part from the rhyolite, (2) dacite tuff and reworked tuff in large part derived from pyroclastic components of rhyolitic volcanism, (3) and redeposited andesite lapilli tuff derived from a centre not exposed in the present sequence. The upper part of the sequence contains fine grained sedimentary rocks and stratabound massive sulphide deposits which are interpreted to represent smaller subbasins within the larger structure.

Rhyolite volcanism and deposition of dacitic and overlying andesitic volcaniclastic rocks ended in a period of volcanic quiescence, during which the graphitic mudstones, cherts and stratabound massive sulphides were deposited. The massive sulphides at Cuprus and White Lake Mines are not associated directly with a hydrothermal alteration zone. This suite of mudstones and chemical sedimentary rocks at the top of the section indicates that at this time the basin was starved of detrital material.

The Cu-Zn massive sulphide deposits are unlikely to have been deposited at water depths less than 500 m (Guber and Ohmoto, 1978). These sulphide deposits are underlain by 650 m of volcaniclastic rocks, implying that total basin depth (to the top of the Bear Lake shield) was a minimum of 1150 m. Since the Bear Lake summit, when active, was probably no more than 400 m below sea level, a minimum of 750 m basin subsidence is required before the sulphides were deposited.

Ferrobasalt lava plain

The period of volcanic quiescence, during which the Cuprus and White Lake massive sulphide deposits were formed, ended with effusion of ferrobasalt flows and intercalated rhyolite crystal tuffs, and intrusion of large, shallow ferrogabbro sills. This bimodal suite, 120 — 200 m thick, is best interpreted as a lava plain because of its relatively constant thickness throughout its 12 km lateral extent. The close association between highly fractionated basalt flows and rhyolite tuff suggests cyclic eruption of rhyolite-basalt pairs from a compositionally zoned, fractionated subvolcanic reservoir. Each cycle is interpreted to have begun with felsic pyroclastic eruptions from the volatile-rich top of the magma chamber and to have ended with quiet effusion of fractionated, volatile-poor basalt from lower in the chamber.

Andesitic phreatomagmatic and plinian eruptions

Shallow water or subaerial phreatomagmatic and plinian eruptions produced the pyroclastic components of this 900 m thick unit. Immediate gravity flow transport of these materials from the flanks of the subaqueous portion of the andesite cone, into an adjacent deep-water basin, produced pyroclastic turbidite flows which deposited Bouma-zoned beds. These andesitic pyroclastic rocks signal a major compositional and depositional change from the conditions which produced the underlying bimodal basalt-rhyolite lava plain.

The unit represents a large number of closely timed eruption events, between which, with few exceptions, extraneous sedimentary or volcanic material was not deposited. In the uppermost 80 m of the unit increasing proportions of pelagic mudstone were deposited between tuff beds, recording the gradual waning of andesitic pyroclastic activity. This stage of volcanism was terminated by the onset of dacitic and intermediate volcanism, resulting in deposition of flows and heterogeneous tuffs.

By the time andesitic pyroclastic volcanism had ceased approximately 1750 m of volcaniclastic rocks and lava flows had been deposited on top of the Bear Lake basaltic andesite shield. Assuming a water depth in excess of 100 m at this stage (in order to preserve sedimentary structures) and a water depth of 400 m at the top of the active shield, minimum subsidence of the basaltic andesite shield would be on the order of 1450 m.

SCOTTY LAKE BLOCK

INTRODUCTION

The Scotty Lake Block (Fig. 3) is bounded on the east by the old Highway 10 fault and on the west by the Northeast Arm Fault. In this block a 2 km thick homoclinal west-facing sequence of lava flows and volcaniclastic rocks is exposed. The One Portage Lake fault occurs within the Block; formations on either side of this strike fault are not necessarily part of a single, unbroken stratigraphic sequence.

Preservation of primary structures is good in the centre of the block but poor along the shoreline of Schist Lake, due to considerable flattening and imposition of a strong foliation.

Seven discrete units compose the stratigraphic section in the Scotty Lake Block. They are listed below in stratigraphic order from top to base (maximum stratigraphic thicknesses in brackets):

Unit	
33	Mudstone, siltstone, greywacke (90 m)
37a	Ankerite-quartz-chlorite-sericite schist (30 m)
34a	Mafic mudstone and wacke (150 m)
	One Portage Lake fault
19	Northeast Arm volcaniclastic rocks (365 m)
4	Scotty Lake basalt (1350 m)
18	Felsic volcanic rocks (300 m)

FELSIC VOLCANIC ROCKS (UNIT 18)

Pale buff to white weathering felsic volcanic rocks (unit 18) of uncertain genesis outcrop in four discrete bodies near the faulted base of the Scotty Lake Block. The largest of these is 300 m by more than 600 m. The most northerly body consists of monolithologic breccia composed of angular, vesicular, aphyric felsic blocks set in rusty brown weathering matrix. The next body to the south, located 1 km north of the Centennial Mine, consists of iron oxide stained, fractured, sheared, strongly altered aphyric and quartz-phyric felsic rocks exposed in several large trenches. These rocks are strongly sericitized with abundant pyrite and minor silica and carbonate introduced along fractures. Some Au values have been reported for assayed samples. The body 600 m north of the junction of Highway 10 and old Highway 10 is a massive white to pale buff weathering felsic volcanic rock characterized by abundant (approximately 60%) 0.2 mm spherulites and 1 — 2% 0.2 mm phenocrysts of quartz and plagioclase. The most southerly body consists of massive aphyric and quartz-phyric rhyolite, the latter containing up to 5%, 0.5 — 1 mm quartz phenocrysts. Close-spaced fractures in this body impart a rubbly appearance to most outcrop surfaces. Some of this fracturing may be pre-tectonic (rare polygonal cooling fractures were observed) but most is probably a product of deformation.

SCOTTY LAKE BASALT (UNIT 4)

Scotty Lake basalt forms a large, homoclinal, west-facing body with a maximum thickness of 1350 m. To the east and southeast the unit is truncated by the old Highway 10 fault and to the northeast, at Whitefish Lake, it is terminated by the Scotty Lake Fault. Andesitic to basaltic volcaniclastic rocks (unit 19) overlie Scotty Lake basalt in exposures on the east shore of Schist Lake.

Aphyric, rusty brown weathering, Fe-rich basalts (unit 4a) and related synvolcanic dykes and sills (unit 4b) dominate the unit. Pyroxene-plagioclase-phyric flows (units 8 and 9) are also present as discrete subunits in the extreme north and south. The basalt flows are typically massive, but include local zones where pillowed varieties are common (Fig. 77). The flows are intruded by related dykes which commonly form over 60% of many exposures (Fig. 78) and locally are present as mappable bodies (unit 4b). A single member of fine grained volcanogenic sediments (unit 33), up to 60 m thick, occurs within the upper 150 m of the Scotty Lake basalt unit.

Flows

Flows range in thickness from 3 m to more than 38 m; 16 completely exposed flows average 9.2 m. The abundance of texturally similar synvolcanic dykes, plus the small size and lichen-covered nature of most rock outcrops, makes measurement of flows or sequences of flows very difficult.

Three main flow types are encountered: simple massive flows, massive flows with hyaloclastite tops (with or without related amoeboid pillows), and compound flows with massive bases overlain by narrow pillowed divisions and hyaloclastite tops. Pillowed flows appear to be thicker than massive and compound flows, but this is difficult to document as their flow contacts are rarely exposed. Pillowed flows are restricted to particular stratigraphic subunits, and are best exposed at Scotty Lake and along Highway 10 (Fig. 77). Contacts between massive flows are subtle; in the absence of interflow hyaloclastite or chert they are defined by dark rusty brown, aphanitic, chilled zones 10 — 20 cm thick at flow tops and flow bases.

Flow top hyaloclastite ranges in thickness from a few centimetres to 7.5 m. It is typically thickest in depressions on hummocky tops of massive divisions (Fig. 79). Hyaloclastite is composed of brown, green, or white weathering angular granules and fragments of altered basaltic glass in a fine grained matrix. Flow top breccia commonly includes involuted amoeboid pillows; in areas of best preservation it is evident that the hyaloclastite was derived from the *in situ* quenching and thermal fragmentation of glassy rims on amoeboid pillows (Fig. 80 to 86). Granules in the hyaloclastite are slabby to equant, 1 mm to 2 cm long, bounded by curviplanar thermal fractures, and are internally intensely fractured. They are identical to the thermally fractured rims which remain in place on amoeboid pillows. In areas where there is a strong foliation developed in the rocks the hyaloclastite comprises recessive, schistose zones between massive portions of flows.

The grain size in massive flows increases from margins to centres (Fig. 79 and 87); this variation is readily identifiable in the field and assists in the identification of flow contacts. Synvolcanic dykes in the sequence have a similar grain size to massive flows but they contain stubby tabular plagioclase crystals in contrast to acicular plagioclase microlites in flows.

Pillows are 0.3 — 2 m in maximum dimension and are ovoid, bun-shaped or irregular in shape. Selvages are narrow; in best preserved exposures they are 0.5 — 1 cm thick and thermally fractured as in amoeboid pillows. Some pillows have spherulitic margins (Fig. 88). Pillow structures are not well preserved in the northern half of the unit due to epidotization (especially of pillow cores) and imposition of a foliation which is strongest in pillow margins and selvages.

Amygdales generally compose less than 2% (0.2 — 2 mm) of massive flows. They occur in the chilled zones of some flows and the coarser portions of others. Gas cavities, up to 4 by 1 cm in size, also occur in the interiors of some massive flows (Fig. 79 and 87). Vesicularity is more pronounced in pillowed flows than in massive flows, but nevertheless amygdales compose only 10% or less of pillows. They occur in the spherulitic marginal zones of some pillows and in the cores of others, and range in size from 1 to 5 mm. There is no systematic variation in amygdale size or abundance through the Scotty Lake basalt sequence.

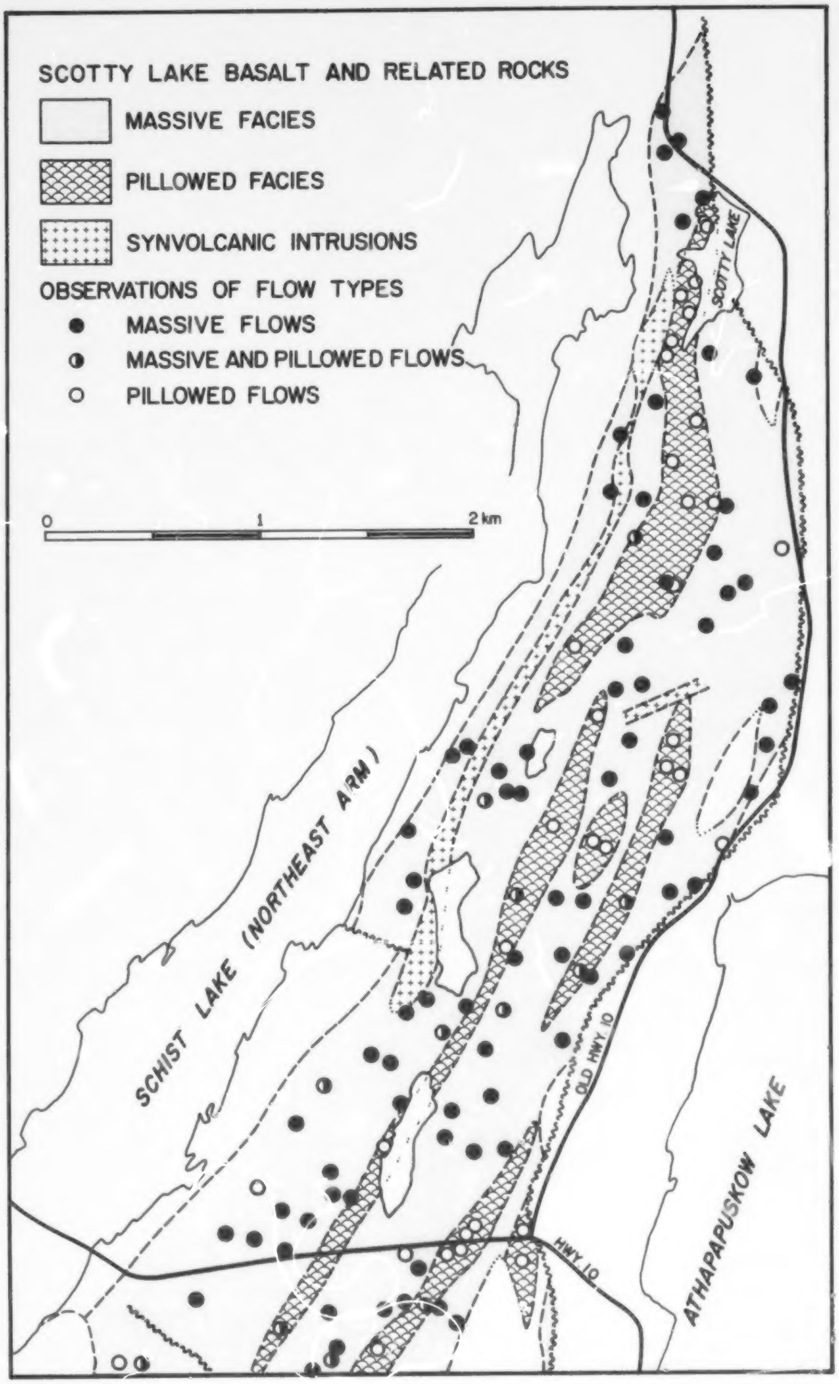
SCOTTY LAKE BASALT AND RELATED ROCKS
MASSIVE FACIES
PILLOWED FACIES
SYNVOLCANIC INTRUSIONS
OBSERVATIONS OF FLOW TYPES
● MASSIVE FLOWS
◐ MASSIVE AND PILLOWED FLOWS
○ PILLOWED FLOWS
0
1
2 km
SCOTTY LAKE
SCHIST LAKE (NORTHEAST ARM)
OLD HWY 10
HWY 10
ATHAPAPUSKOW LAKE

Figure 77: *Distribution of massive and pillowed flows, Scotty Lake basalt. Predominance of massive flows suggests high effusion rates.*

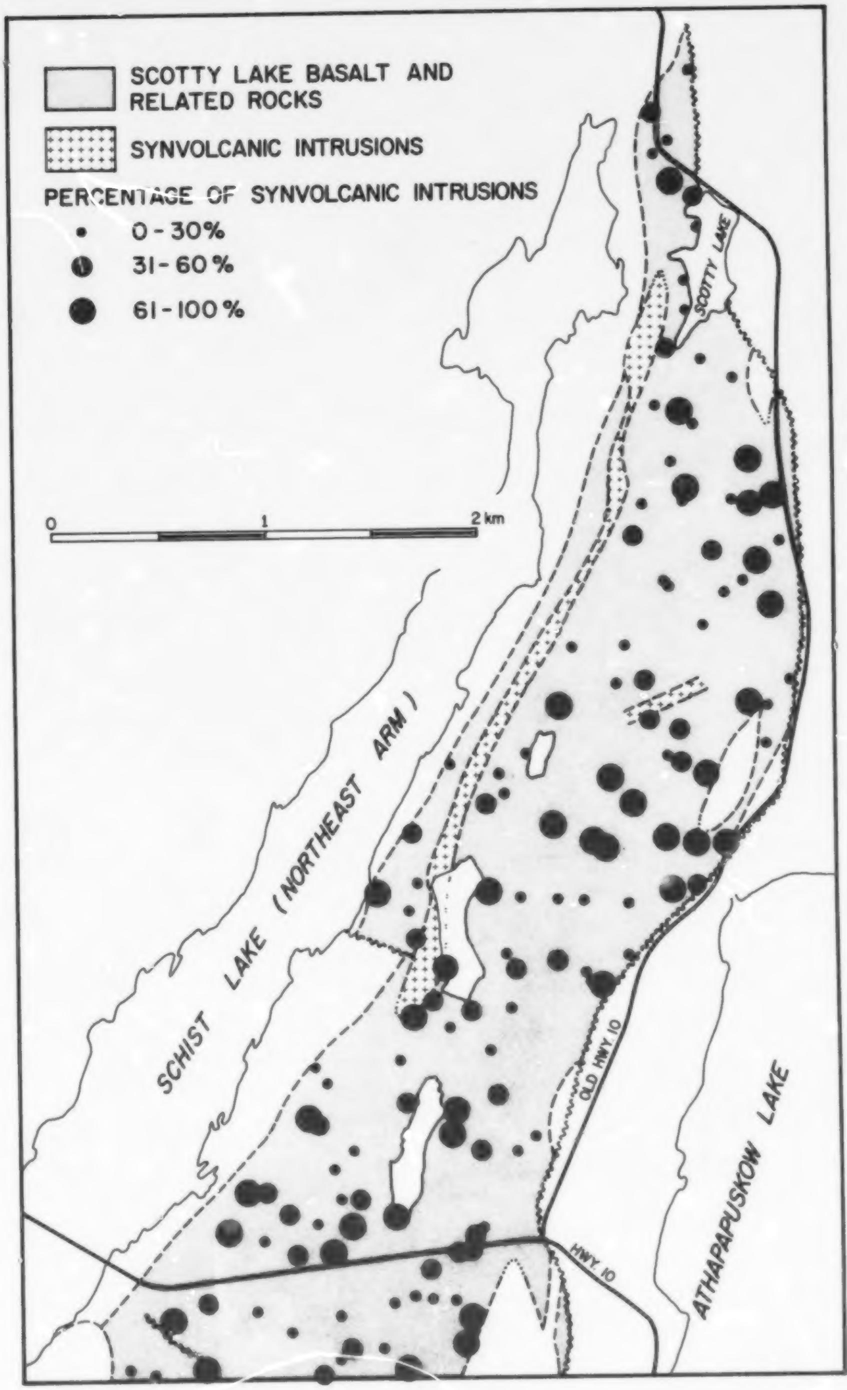
SCOTTY LAKE BASALT AND RELATED ROCKS
SYNVOLCANIC INTRUSIONS
PERCENTAGE OF SYNVOLCANIC INTRUSIONS
0-30%
31-60%
61-100%
0
1
2 km
SCOTTY LAKE
SCHIST LAKE (NORTHEAST ARM)
OLD HWY. 10
HWY. 10
ATHAPAPUSKOW LAKE

Figure 78: Distribution of synvolcanic intrusions, Scotty Lake basalt. High average abundance of synvolcanic dykes is characteristic of this formation.

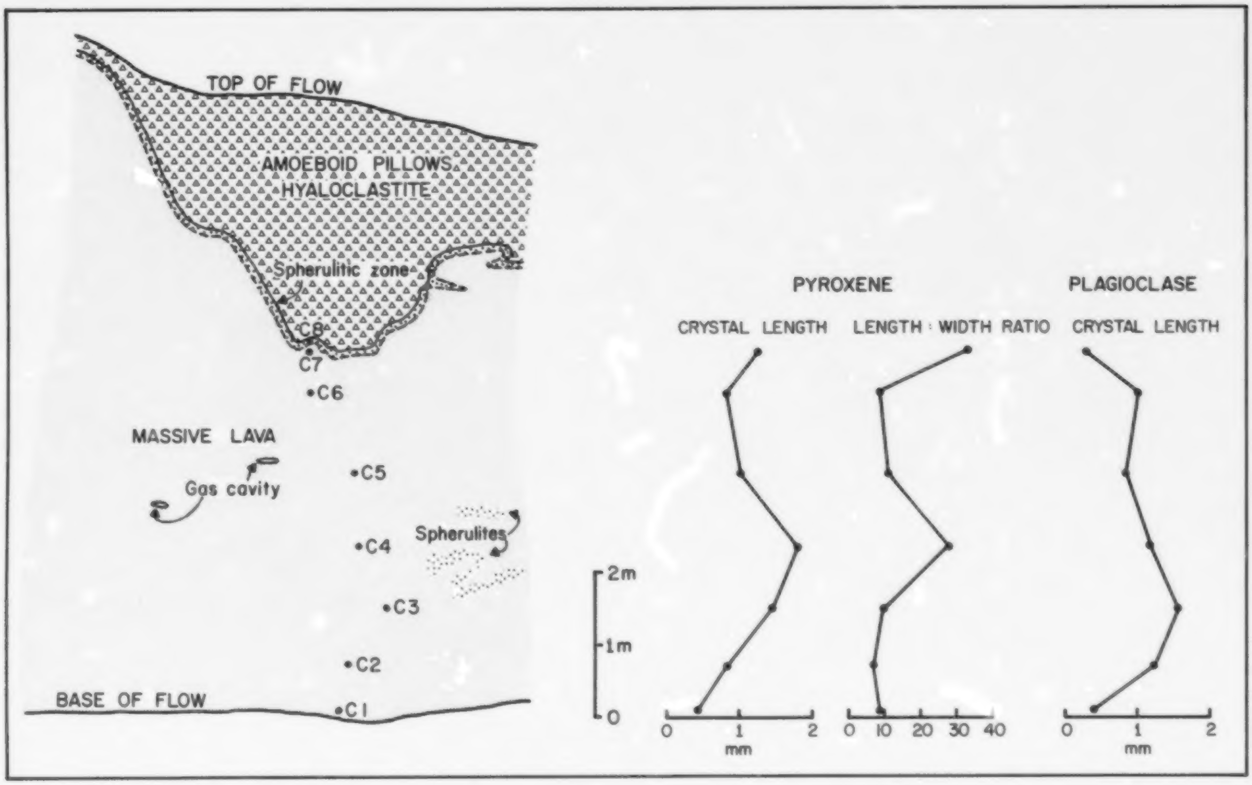
TOP OF FLOW
AMOEBOID PILLOWS
HYALOCLASTITE
Spherulitic zone
C8
C7
C6
MASSIVE LAVA
Gas cavity
C5
Spherulites
C4
C3
C2
BASE OF FLOW
C1
2m
1m
0
PYROXENE
PLAGIOCLASE
CRYSTAL LENGTH
LENGTH : WIDTH RATIO
CRYSTAL LENGTH
0 1 2
mm
0 10 20 30 40
0 1 2
mm

Figure 79: *Massive Scotty Lake basalt flow (map location 1112). Minor cross-cutting faults omitted. Dots are sample locations (thin sections and chemical analyses). See Table 5 for description of basalt textures, Figures 89 to 93 for photomicrographs of massive lava, Figures 81 to 84 for details of hyaloclastite and amoeboid pillows, and Appendix for chemical analyses. Primary pyroxene and plagioclase are pseudomorphed by actinolite and albite + sericite + epidote, respectively.*

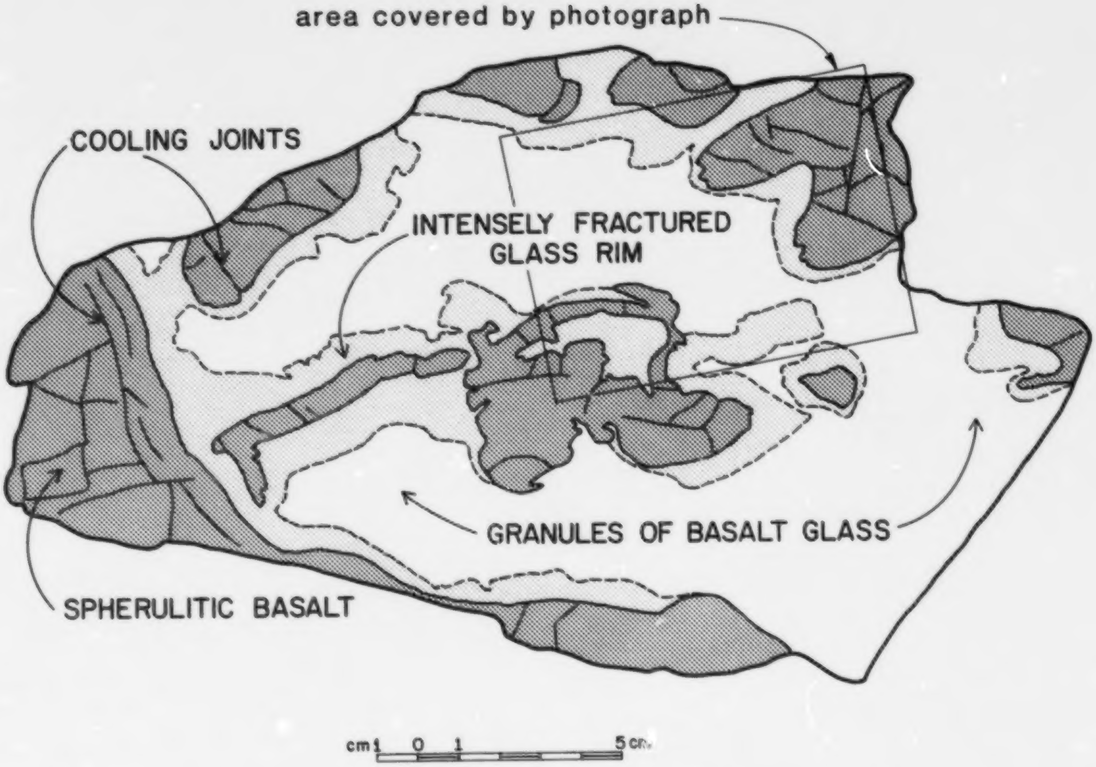
area covered by photograph
COOLING JOINTS
INTENSELY FRACTURED GLASS RIM
GRANULES OF BASALT GLASS
SPHERULITIC BASALT
cm 1 0 1 5 cm

Figure 80: *Tracing of polished slab of amoeboid pillow breccia taken from top of massive flow (1112, Fig. 79), Scotty Lake basalt. Amoeboid pillows have involuted shapes and are composed of spherulitic basalt with radial and concentric cooling/contraction fractures. Amoeboid pillows have 0.5 — 1 cm thick rims composed of intensely fractured, spherulitic altered glass (Fig. 81 to 84). Granules derived by spalling from this thermally fractured rim compose the hyaloclastite matrix of the amoeboid pillow breccia.*

Figure 81: *Photograph of part of polished slab traced in Fig. 80. Amoeboid pillows (upper right and lower left) in the breccia have two components: (1) an interior of spherulitic basalt (light in colour) crossed by thermal fractures and (2) a 0.5 — 1 cm thick rim composed of thermally shattered sideromelane (dark in colour, pseudomorphed by epidote). Hyaloclastite granules in the matrix are identical to the shattered rim and clearly formed by spalling from the glassy amoeboid pillow margin. Note that spherulites in interior of amoeboid pillows form concentric distribution patterns paralleling margins of thermal fractures. Scale bar represents 2 cm.*

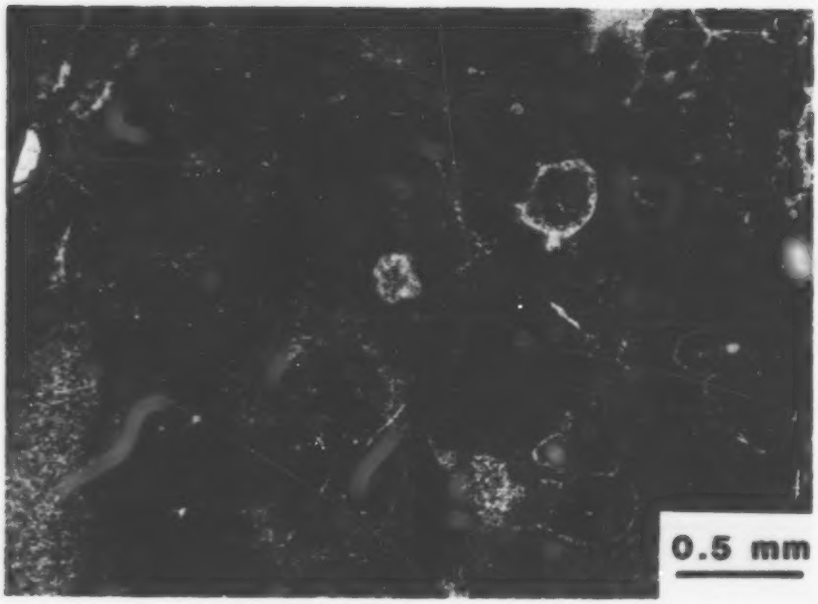

Figure 82: *Spherulites in interior of amoeboid pillow shown in Figures 80 and 81. Contact with thermally shattered sideromelane rim is at "r". Spherulites are homogeneous or concentrically zoned, the latter are defined by variable abundance of secondary chlorite, epidote and leucoxene. Large spherulites have an exclusion rim of leucoxene. An iron oxide crust (dark coloured and composed of leucoxene and sphene) occurs at the contact between amoeboid pillow interior and its thermally fractured rim. Sample 1112, plane polarized light.*

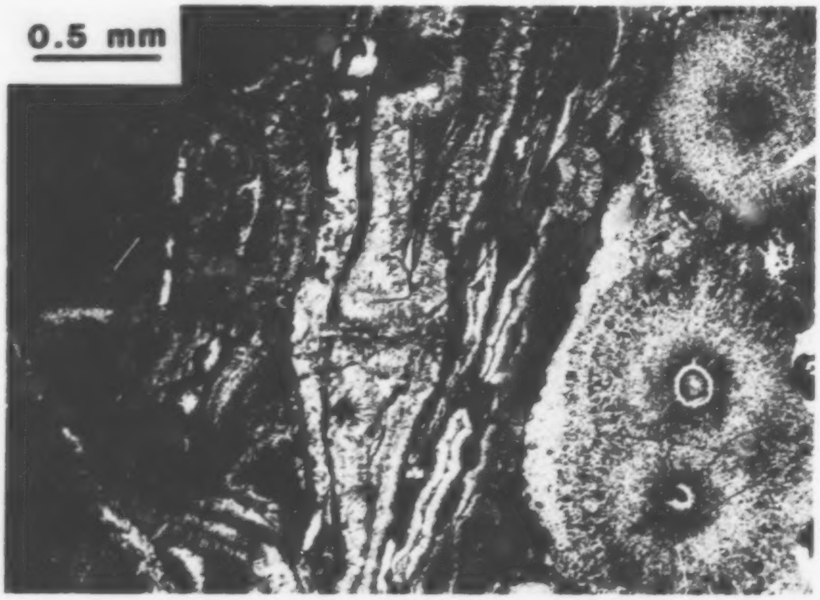

Figure 83: *Spherulitic amoeboid pillow and its thermally shattered sideromelane rim (Fig. 80 and 81); contact (r) is marked by a crust of Fe-oxide. Spherulites in amoeboid pillow interior have fibro-radial textures and Liesegang-like rings of Fe-oxide granules; some spherulites are coalescent. Thermal fractures (t) in the rim are predominantly subparallel (concentric) or perpendicular (radial) to the contact (r). Margins of fracture-bounded domains have fibro-radial textures and are composed of chlorite and finely divided epidote; the texture is interpreted as pseudomorphic after zeolites which replaced a palagonite rim. Cores of the fracture-bounded domains are replaced by chlorite and epidote interpreted to be after primary sideromelane. Fe-oxide crusts occur along thermal fractures and between the palagonite rim and sideromelane cores of fracture-bounded domains (eg. C). Sequence of replacement is interpreted to have been as follows: 1) sideromelane to fibro-palagonite rims to zeolites to fibro-radial chlorite rims, and 2) sideromelane core to chlorite and epidote. Sample 1112, plane polarized light.*

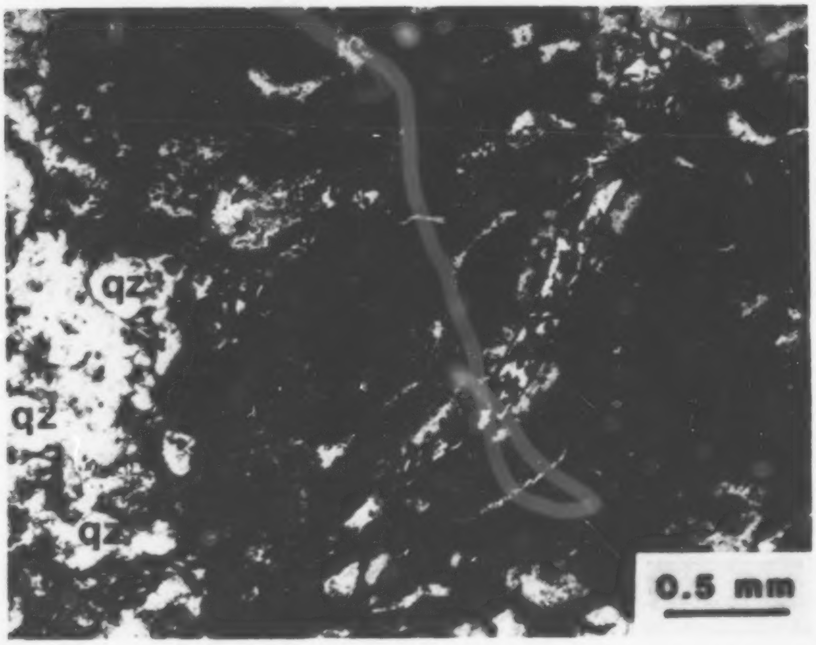
qz
qz
qz
0.5 mm

Figure 84: *Outer part of thermally fractured rim on an amoeboid pillow (Figs. 80 and 81), transitional to matrix hyaloclastite. Hyaloclastite granule is detached from rim of amoeboid pillow along curviplanar thermal fractures (t), now filled by quartz, actinolite and chlorite. Fibro-radial chlorite and finely divided epidote occur adjacent to thermal fractures that rim the granule and are interpreted as replacement of palagonite (Fig. 85). Cores of granules are chlorite + epidote + actinolite (after sideromelane?). Fibro-radial texture and Leisegang-like rings (arrow) may represent former smectites or zeolites. Pore-space filling comprises quartz after chalcedony spherulites (qz), feldspar, epidote and actinolite. Sample 1112, plane polarized light.*

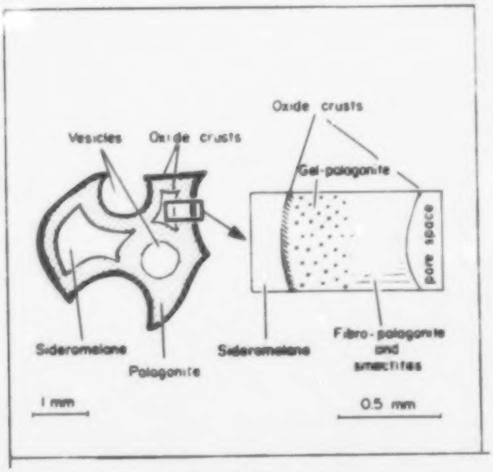
Oxide crusts
Vesicles
Oxide crusts
Gel-palagonite
pore space
Sideromelane
Palagonite
Sideromelane
Fibro-palagonite and smectites
1 mm
0.5 mm

Figure 85: *Schematic diagram of textures in a Cenozoic, palagonitized hyaloclastite granule (from Dimroth and Lichtblau, 1979, after Honorez, 1972).*

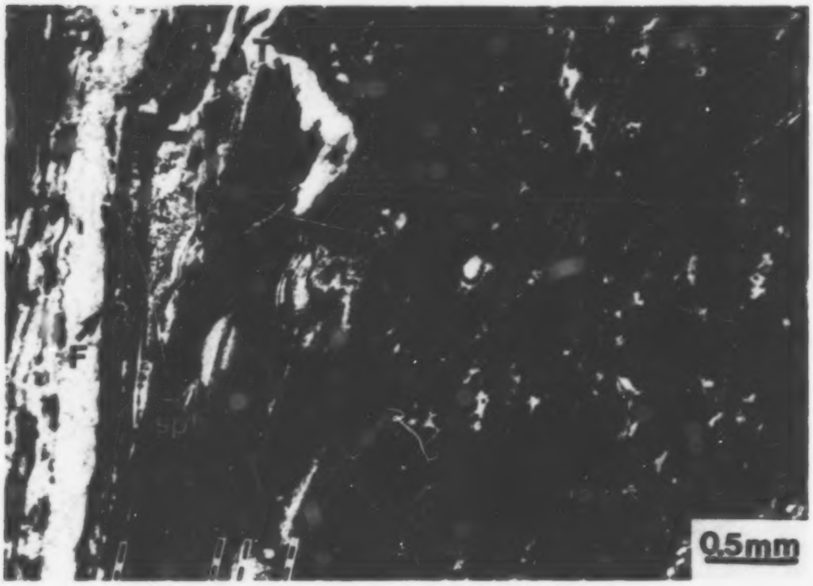

Figure 86: *Relict textures in pseudomorphed palagonite rims on an amoeboid pillow fragment in hyaloclastite, Scotty Lake basalt flow top (117, Fig. 87). Palagonite pseudomorph comprises: 1) an outer zone of fine grained epidote (dark) with thermal fractures (T), parallel to fragment margin, and spherulites (sph), centred on fractures, 2) a zone characterized by Leisegang-like rings (L), defined by fine grained Fe-Ti oxides, in a matrix of fine grained silica and grey epidote, 3) a band of finely disseminated epidote, and 4) an inner zone characterized by 0.05 — 0.1 mm Fe-Ti oxide granules replaced by leucoxene (ox). Note spalled slabby fragment of palagonite rim (F) and the oxide-coated perlitic cracks (P). Fine grained quartz, epidote and colourless chlorite form the voids between fragments in the hyaloclastite. Plane polarized light.*

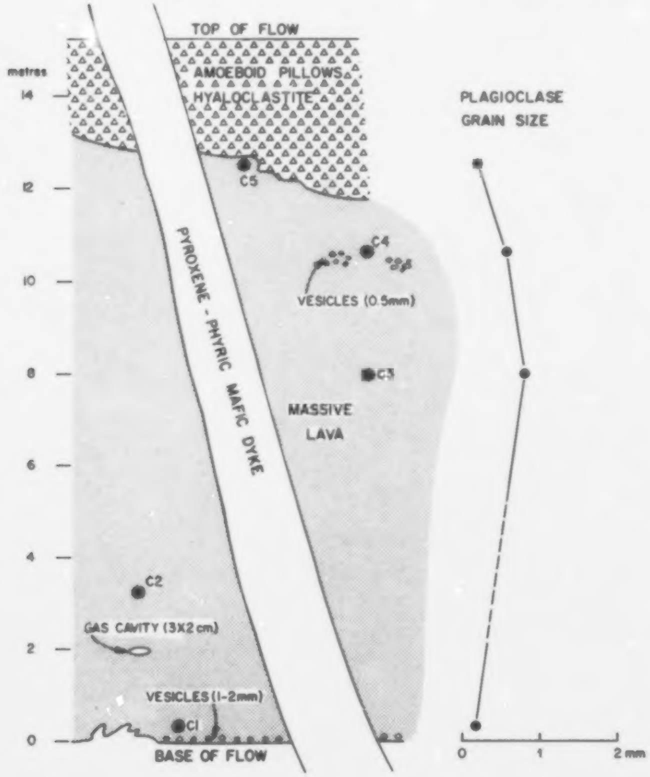
TOP OF FLOW
AMOEBOID PILLOWS
HYALOCLASTITE
metres
14
12
10
8
6
4
2
0
C5
C4
VESICLES (0.5mm)
C3
PYROXENE - PHYRIC MAFIC DYKE
MASSIVE LAVA
C2
GAS CAVITY (3X2 cm)
VESICLES (1-2mm)
C1
BASE OF FLOW
PLAGIOCLASE GRAIN SIZE
0
1
2 mm

Figure 87: *Massive Scotty Lake basalt flow with flow top hyaloclastite and amoeboid pillows (117). Dots are sample locations (thin sections and chemical analyses). See Appendix for chemical analyses. Primary plagioclase, pseudomorphed by albite, varies in grain size across flow.*

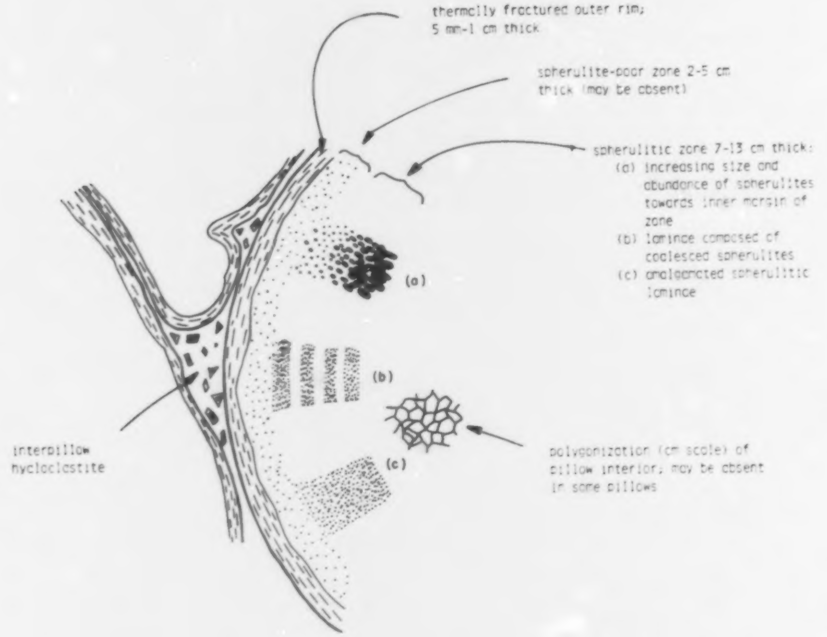

Figure 88: *Distribution patterns of spherulites in the margins of pillows, Scotty Lake basalt. Sporadic amygdales may occur along the inner margin of the spherulitic zone. Centimetre-scale polygonization begins about 2 cm inside the inner margin of the spherulitic zone, but sporadic small spherulites can also occur within the polygonized material. The polygonization occurs throughout the pillow interior. Details of interpillow hyaloclastite shown in Figures 99 and 100.*

Petrography of flows

Preservation of delicate primary textures is best in two areas: 1—2 km south of Scotty Lake, and adjacent to Highway 10. Textural variation occurs within individual flows as well as between different flows. One example of within-flow variation is described in Table 6 and Fig. 89-93. This example appears to be representative since many flows contain zones that are characterized by acicular skeletal plagioclase and pyroxene. Textures dominated by skeletal crystals (Fig. 94 to 96) indicate that many of these lava flows, some of which are up to 15 m thick, crystallized rapidly from supercooled magmas (e.g. Lofgren, 1974, 1983). Other flows display non-skeletal intergranular to subophitic textures (Fig. 97) indicating less rapid crystallization and a smaller degree of supercooling. Some pillowed flows have intersertal texture (Fig. 98).

With few exceptions primary minerals have been pseudomorphed by secondary metamorphic assemblages. Clinopyroxene is replaced by single crystals of green tremolite-actinolite, plagioclase is pseudomorphed by albite, sericite, epidote and chlorite, and Fe-Ti oxides are now represented by magnetite and leucoxene. Deuteric brown hornblende occurs in some flows, as an overgrowth on primary clinopyroxene. In more recrystallized and deformed rocks primary textures are largely destroyed, epidote is more abundant, and sheaves of strongly pleochroic golden brown stilpnomelane overprint all other secondary minerals.

Hyaloclastite petrography is similar to that described by Dimroth and Lichtblau (1979). Hyaloclastite granules are bounded by curviplanar thermal fracture surfaces and are replaced by quartz, epidote, chlorite, actinolite and leucoxene. These secondary minerals occur in zones that pseudomorph the pre-metamorphic distribution of sideromelane glass and secondary palagonite (Fig. 99 to 103).

Synvolcanic dykes, sills and related intrusions

Scotty Lake basalt contains a suite of aphyric and porphyritic, mafic to intermediate, non-vesicular dykes which locally compose up to 100% of exposures (Fig. 78). These dykes range in size from a few centimetres wide, to a large, composite body 3.3 km long and up to 150 m wide. Although many are subconcordant to flow attitude, cross-cutting relationships are common (Fig. 104). These dykes are interpreted to be synvolcanic as they are not present in the overlying volcaniclastics (unit 19); however, they have a wider range of composition than is observed in flows. The most common dyke type is equigranular, fine grained and weathers buff to rusty brown similar to the flow rocks. Porphyritic varieties include pyroxene-phyric, plagioclase-phyric and pyroxene-plagioclase-phyric types. Aphyric plagioclase-rich dykes are a minor component of the suite. Equigranular dykes generally cut the porphyritic varieties.

Equigranular dykes are superficially similar to host basalts in that they have comparable weathering colours, grain size and composition. However, dykes have chilled margins, and are both megascopically and microscopically distinguishable from basalt by their stubby plagioclase crystal morphology and the presence of quartz. They have a hypidiomorphic granular texture comprising a mosaic of tabular, randomly oriented plagioclase, stubby pyroxene, interstitial quartz, and disseminated subhedral Fe-Ti oxides. The plagioclase is partly altered to fine grained epidote, chlorite and sericite, pyroxene is replaced by early deuteric green-brown hornblende and subsequent tremolite-actinolite and chlorite, and Fe-Ti oxides are replaced by magnetite, leucoxene and sphene. Quartz abundance ranges from 5 to 25% (commonly less than 10%); quartz-rich varieties contain extensive quartz-plagioclase micrographic intergrowths.

Table 6:
Textural variation through Scotty Lake basalt flow shown in Fig. 79

Sample	Zone	Texture	Description
1112-C8	Spherulitic chilled top	Spherulitic	Discrete orbicular feldspar spherulites 2-15 mm in diameter in a matrix of dominantly pyroxene fan-spherulites. Feldspar spherulites composed of coalesced round to fan-shaped spherulites, disseminated Fe-oxides, and subordinate acicular pyroxene chains.
1112-C7	Chilled top	Radiate to hyalopilitic	Pyroxene acicular skeletal, random to radiate. Plagioclase forms fan-radiate groundmass to pyroxene. Fe-oxides disseminated, equant. This texture grades to patches in which acicular pyroxene chains occur in structureless glass groundmass (up to 40% glass).
1112-C6	Upper margin	Intergranular	Pyroxene coarsely elongate, locally intergrown with plagioclase. Plagioclase elongate tabular, felted. Fe-oxides disseminated, equant. Quartz amygdales (0.2-3 mm, 3%) are large and spherical to small, irregular interstitial.
1112-C5	Interior	Radiate	Pyroxene skeletal, coarsely elongate to acicular, random; also intergrown with plagioclase in fan-spherulites. Plagioclase very fine grained, acicular, intergrown with pyroxene; groundmass to larger acicular pyroxene. Fe-oxides disseminated, equant. Quartz amygdales to 1.5 mm, 2%.
1112-C4	Interior	Radiate	Pyroxene acicular skeletal. Plagioclase acicular, skeletal, intrafasciculate. Fan- and plumose-spherulites of pyroxene and plagioclase. Fe-oxides very fine grained, disseminated.
1112-C3	Lower margin	Intergranular	Pyroxene elongate skeletal, intergranular to coarsely radiate intergrown with plagioclase. Plagioclase elongate tabular, intrafasciculate. Fe-oxides disseminated, equant. Quartz amygdales to 0.5 mm, 5%.
1112-C2	Lower margin	Intergranular	Pyroxene elongate, some skeletal, intergranular to subophitic to coarsely radiate intergrown with plagioclase. Plagioclase elongate tabular, random and in coarse radiate intergrowths with pyroxene.
1112-C1	Chilled base	Intergranular	Pyroxene fine grained elongate interstitial to plagioclase. Plagioclase fine grained, tabular, random. Fe-oxides disseminated equant. Chlorite amygdales to 0.4 mm, 2%.

Porphyritic dykes contain 10 — 40%, 1 — 4 mm, euhedral equant phenocrysts set in a hypidiomorphic equigranular 0.1 — 0.4 mm groundmass. The groundmass is composed of tabular plagioclase laths, equant pyroxene grains, interstitial quartz and 2 — 4% subhedral oxides. Different porphyritic types locally crosscut each other.

Minor units

South of Highway 10 approximately 400 m of pyroxene and plagioclase-phyric and sparsely porphyritic flows (units 8 and 9) form the top of the Scotty Lake sequence. These rocks are significantly different in composition, texture and colour from typical aphyric Scotty Lake basalts and are probably unrelated to the underlying aphyric basalt sequence. Flows are light brown to light green and include massive and pillowed varieties. They are cut by equigranular and porphyritic dykes that are similar to dykes elsewhere in the Scotty Lake suite. Flows contain up to 15% phenocrysts up to 4 mm across, and quartz amygdales occur in the upper portions of some pillows. In most of the western part of the subunit rocks are foliated, outcrops are poor, and flow structures are not preserved.

A single member of fine grained volcanogenic sedimentary rocks (unit 33) occurs within the upper 150 m of the Scotty Lake basalt. The unit is discontinuously exposed for 5.3 km. It directly underlies the porphyritic flows (units 8 and 9) in the area of Highway 10, and occurs *within* the

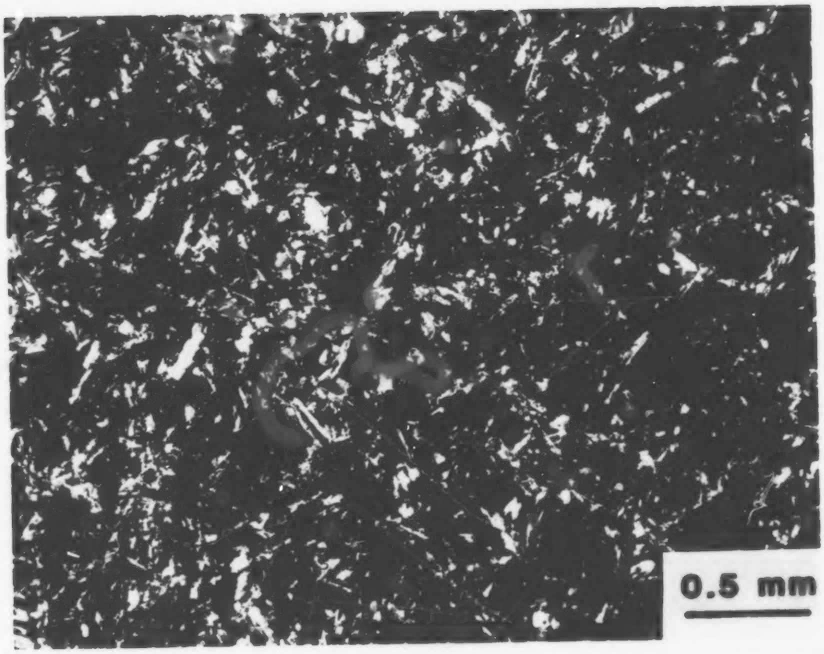

Figure 89: *Photomicrographs in Figures 89-93 show variation in texture across massive division of Scotty Lake basalt flow (1112, Fig. 79). In this photomicrograph the chilled base of flow (C1) displays fine grained intergranular texture with elongate clinopyroxene pseudomorphs (white) interstitial to randomly oriented tabular plagioclase (mottled grey). Crossed polarizers.*

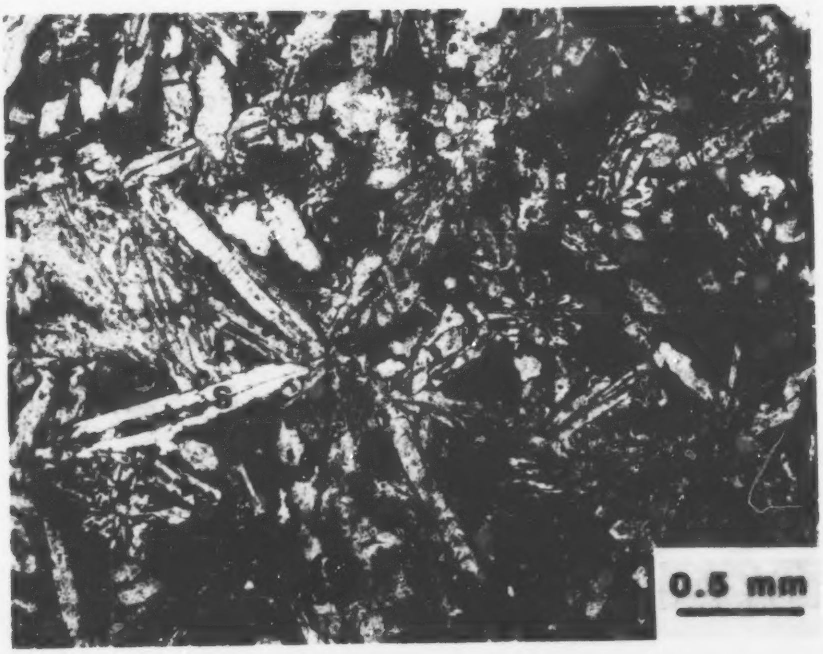

Figure 90: *Lower part of flow (C3). Coarse intergranular texture with elongate, skeletal (e.g. at s) clinopyroxene pseudomorphs randomly oriented or in crude radiate arrays with plagioclase. Plagioclase laths (light mottled grey) are tabular; some are intrafasciculate. Some small plagioclase-clinopyroxene spherulitic intergrowths (i). Disseminated oxides are black. Plane polarized light.*

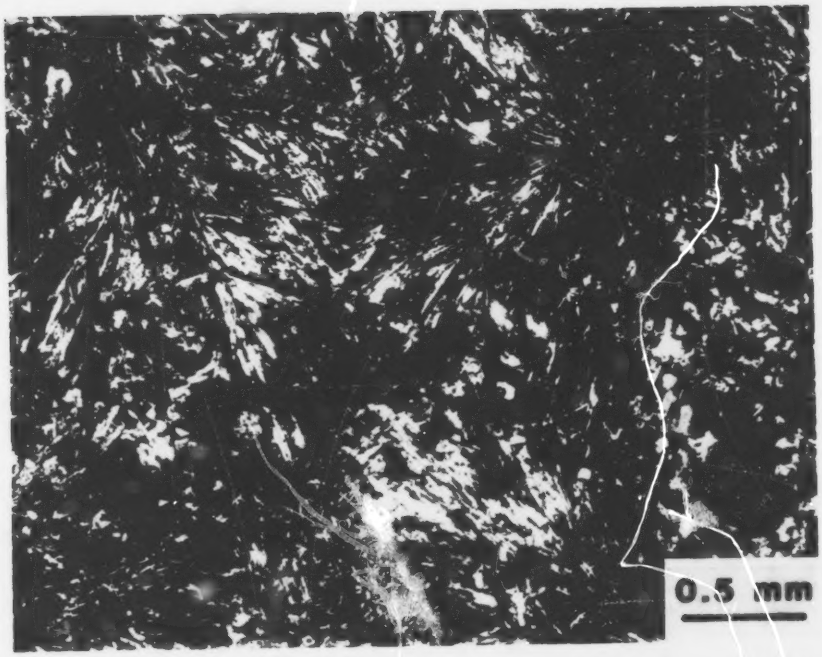

Figure 91: Interior of flow (C4). Fan-like arrays of plagioclase laths (white) intergrown with skeletal clinopyroxene pseudomorphs (grey, white). Some plagioclase laths are hollow, with clinopyroxene cores (intrafasciculate texture). Polarized light.

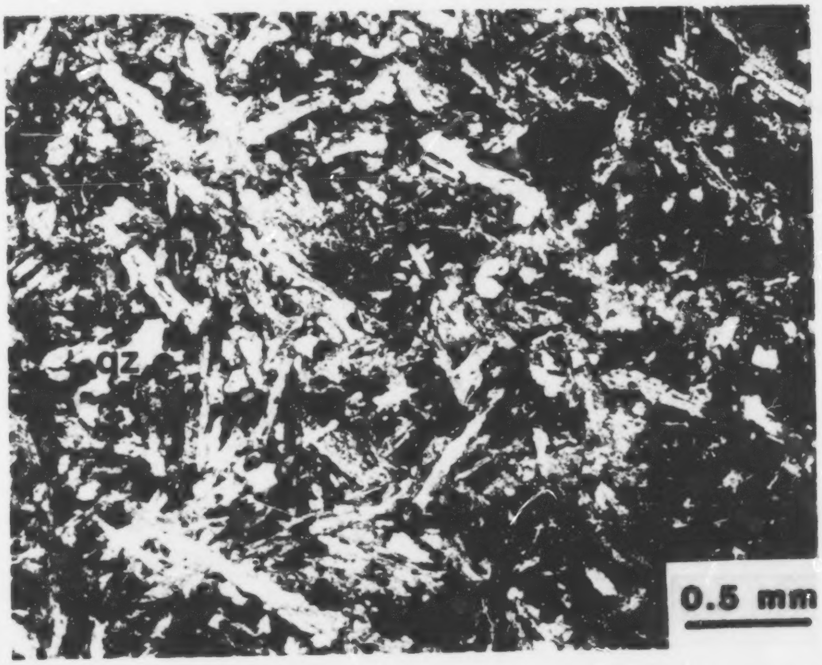

Figure 92: Upper flow margin (C6). Intergranular texture with elongate clinopyroxene pseudomorphs (white) and randomly oriented tabular plagioclase (mottled gray). Small interstitial amygdales are filled with quartz (qz) and chlorite (c). Polarized light.

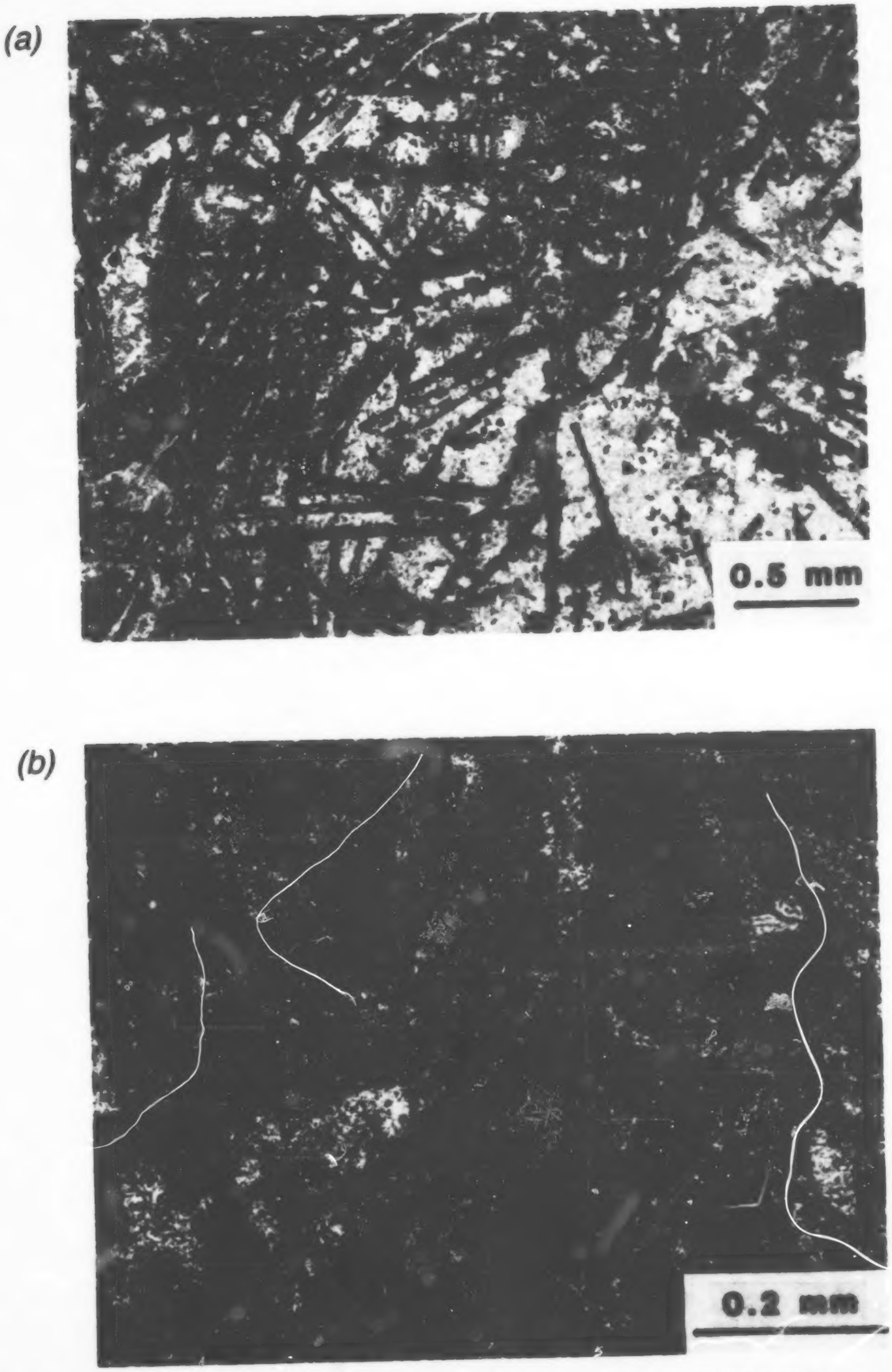

Figure 93: *Chilled flow top (C7). (a) Random and branching, acicular and ornamented skeletal chains of clinopyroxene pseudomorphs in a groundmass of frond-like clinopyroxene (upper right) and structureless former glass. Fe-Ti oxides (black) occur as aggregates and linear arrays. Clinopyroxene is pseudomorphed by tremolite-actinolite and "glass" is replaced by feldspar + chlorite + sericite. (b) Detail of ornamented skeletal clinopyroxene pseudomorph chains in (a). Chains are composed of M-shaped crystal segments. Groundmass is altered "glass" and fine, frond-like sprays of former clinopyroxene. Plane polarized light.*

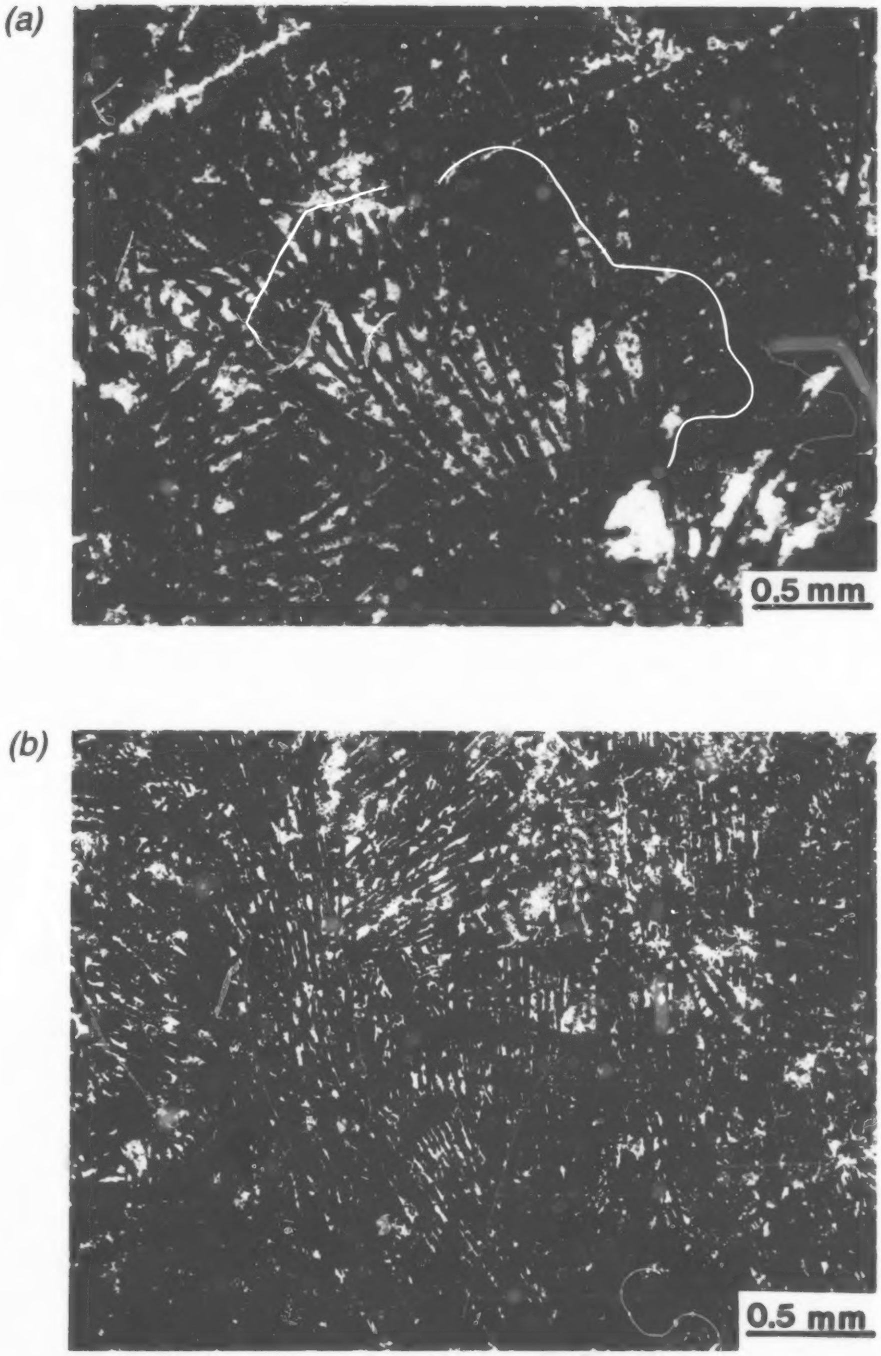

Figure 94: *Linear chains of skeletal clinopyroxene crystals in chilled upper margin of massive Scotty Lake basalt flow. Chains vary in morphology and include large chains originating from point sources (a), smaller chains which branch from larger ones and form irregular mesh-like arrays (b), and arcuate, spoke-like open arrays with intervening plumose spherulitic clinopyroxene (not shown). Such clinopyroxene morphologies indicate very rapid crystallization under high rates of cooling. Clinopyroxene is replaced by tremolite-actinolite. Individual skeletal clinopyroxene crystal morphologies in the chain are not well preserved in this sample but are clearly seen in Figure 93. Sample 125-2, plane polarized light.*

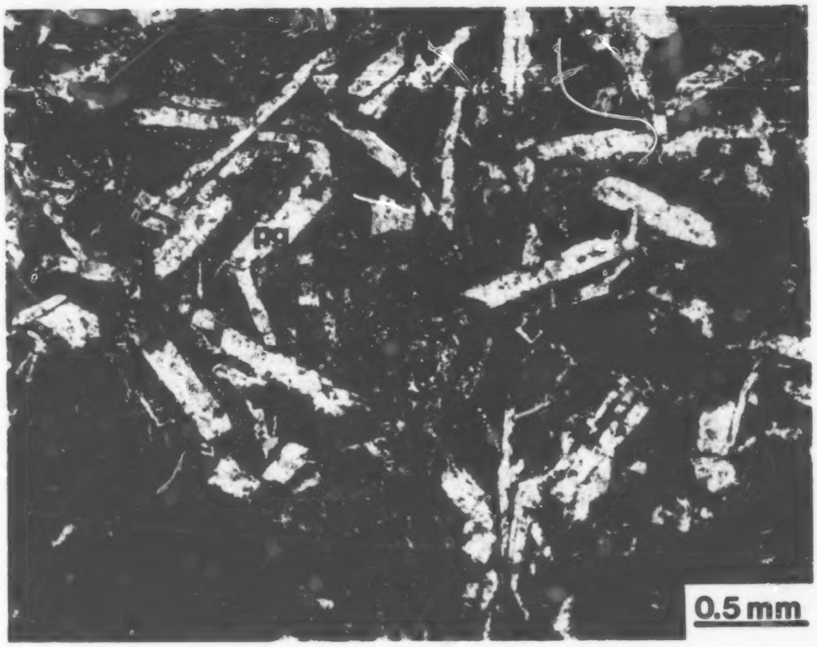

Figure 95: *Intrafasciculate texture, Scotty Lake basalt. Note longtitudinal and cross sections of plagioclase crystals showing hollow skeletal character (arrows). Hollow dark cores of plagioclase crystals are filled with actinolite after primary clinopyroxene. Dark grey to black grains are magnetite and leucoxene after primary Fe-Ti oxide. Intrafasciculate texture, in this sample, occurs at the boundary between domains with subophitic texture and those with finer grain size and spherulitic plagioclase and clinopyroxene. Sample 149-1, plane polarized light.*

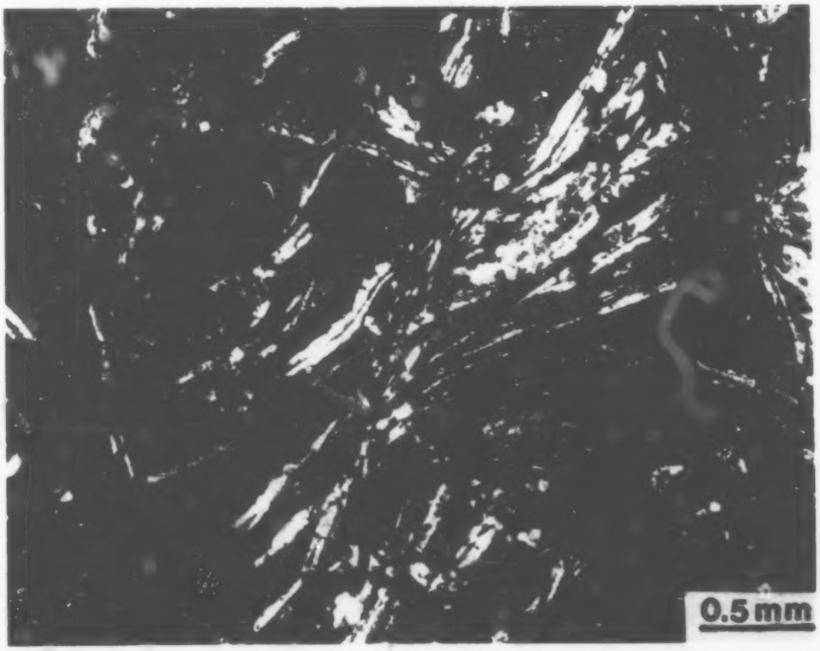

Figure 96: *Coarse fan spherulite of plagioclase (white) in massive Scotty Lake basalt. Note arcuate shape and hollow skeletal form of individual plagioclase crystals. Sample 125-1, polarized light.*

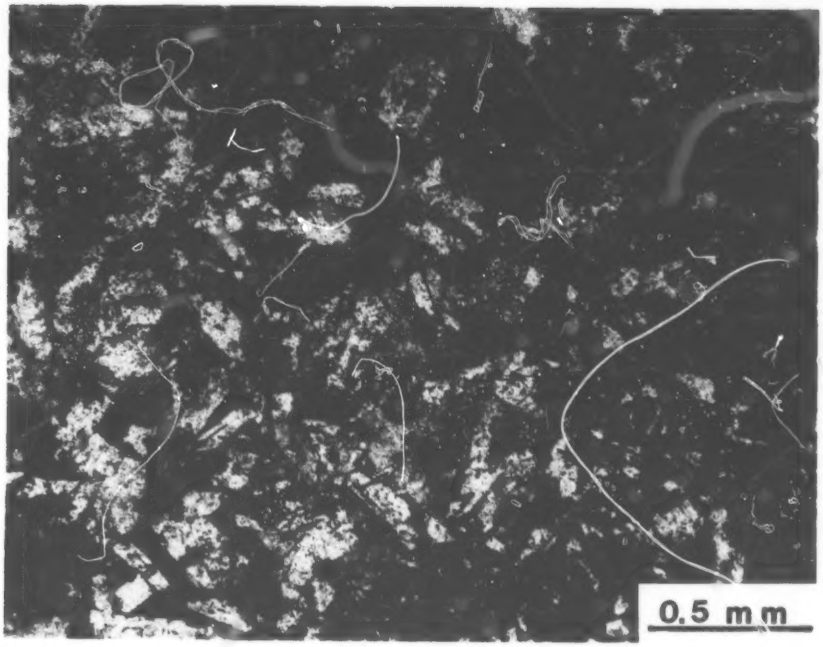

Figure 97: Subophitic massive Scotty Lake basalt. Stubby, tabular plagioclase crystals (pg) are partly enclosed by interstitial actinolite after clinopyroxene (cpx). Elongate, skeletal (hollow) crystal morphologies are displayed by some plagioclase (arrows). Dark grey to black grains are magnetite and leucoxene after primary Fe-Ti oxide. Sample 149-2, plane polarized light.

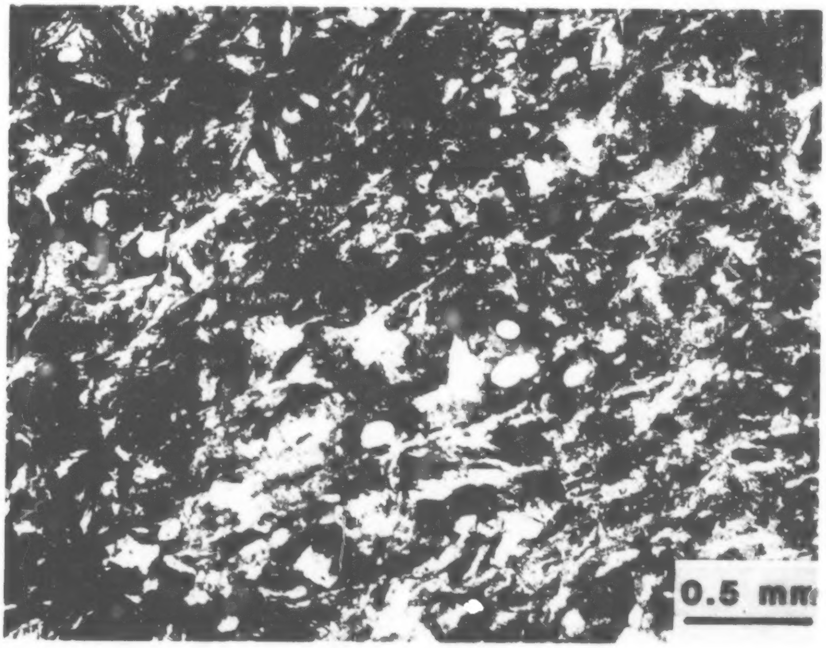

Figure 98: Intersertal texture, pillowed Scotty Lake basalt. Patches of "glass" (replaced by epidote; outlined) are interstitial to plagioclase laths and to chlorite after groundmass pyroxene. Oval, quartz-filled vesicles occur within many of the "glass" patches. Sample 1117-C1, plane polarized light.

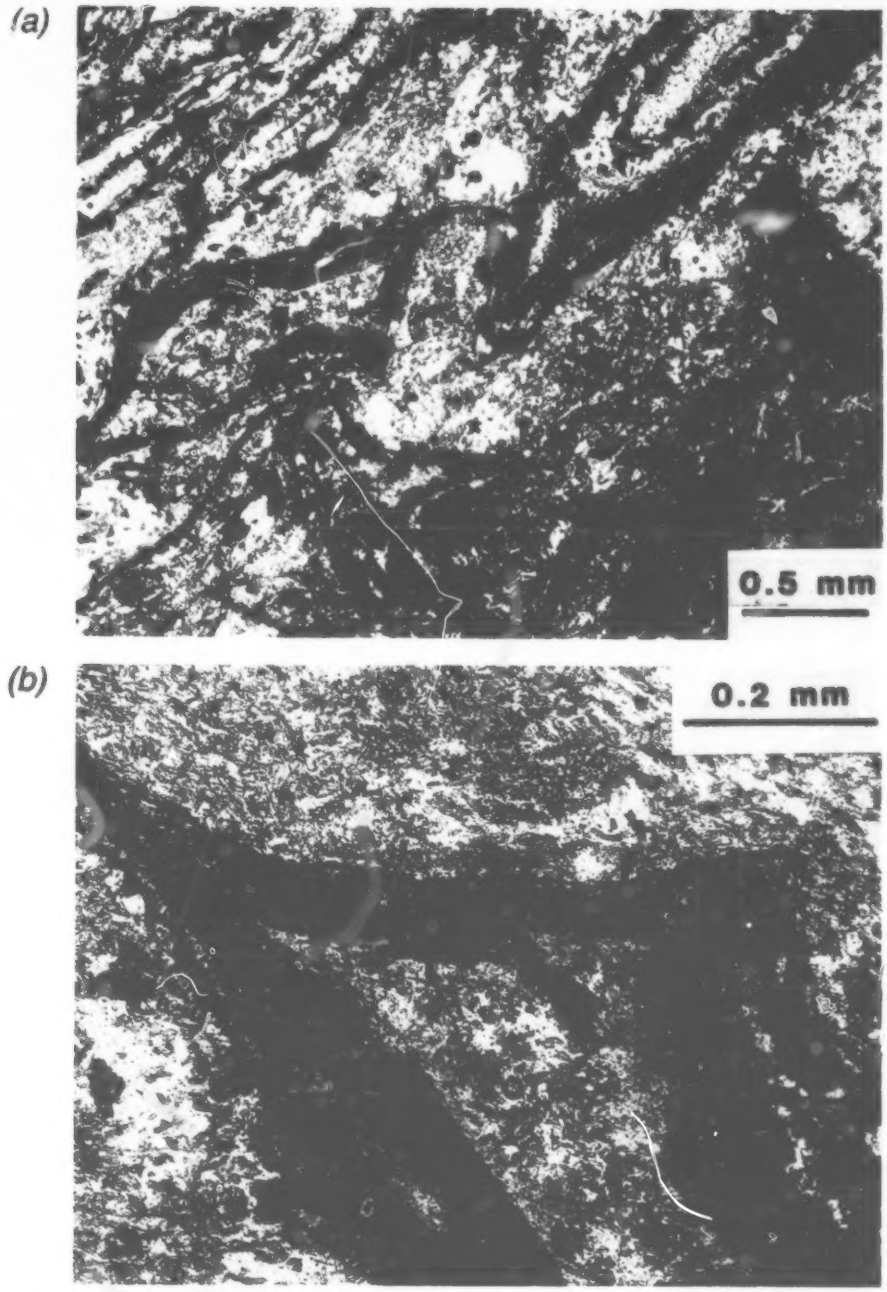

Figure 99: *Interpillow hyaloclastite, Scotty Lake basalt, sample 1126-1.*

a) *Granules in hyaloclastite are non-vesicular, slabby, bounded by conchoidal fracture surfaces with knife-sharp edges. They have well defined rims and zones with structures (see* ***(b)****) similar to those described by Dimroth and Lichtblau (1979), interpreted to represent original sideromelane glass with palagonite alteration rims. Intergranular pore spaces are filled with chlorite, albite, epidote and quartz. Plane polarized light.*

b) *Detail of granule in* ***(a)*** *showing* ***rims*** *with an outer crust (a) of Fe-Ti oxides (now leucoxene), an outer zone (b) of epidote + chlorite pseudomorphic after a fibro-radial mineral (probably zeolite which replaced fibro-palagonite), an inner zone (c) of very fine grained epidote clouded with leucoxene, and an inner crust (d) of oxides which is locally developed between the rim and core of the granule. Granule* ***cores*** *are structureless and composed dominantly of chlorite with subordinate albite and epidote; they are interpreted as chloritized sideromelane.*

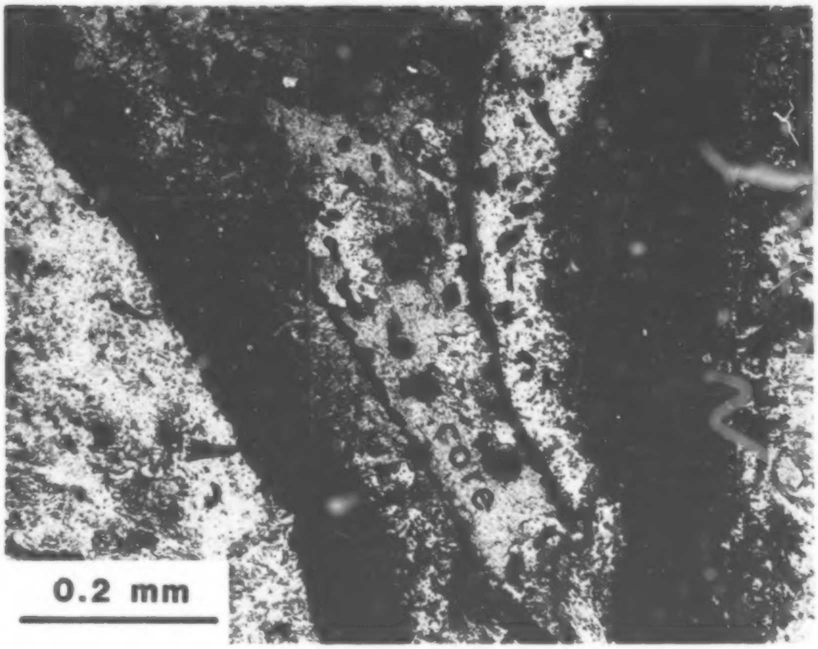

Figure 100: Detail of internal structure of an inter-pillow hyaloclastite granule, Scotty Lake basalt. Granule ***rim*** *has: a thin crust (a) of Fe-oxides (now leucoxene); an outer zone (b) composed of very fine grained epidote and lesser chlorite, with relict fibro-radial texture; an internal thin crust of leucoxene (c); a discontinuous inner zone (d) of structureless very fine grained epidote; a zone (e) of disseminated Fe-oxide granules, an inner zone (f) which is variably abiitized and chloritized; an inner crust (g) composed of epidote + leucoxene granules, which clearly separates the structured rim from the structureless core. The granule* ***core*** *is composed of chlorite, dark epidote + leucoxene granules, and feldspar spherulites (not shown). Equivalent structures in Archean and Cenozoic hyaloclastites have been interpreted by Dimroth and Lichtblau (1979) as former palagonite rim and sideromelane core. Sample 1126-1, plane polarized light.*

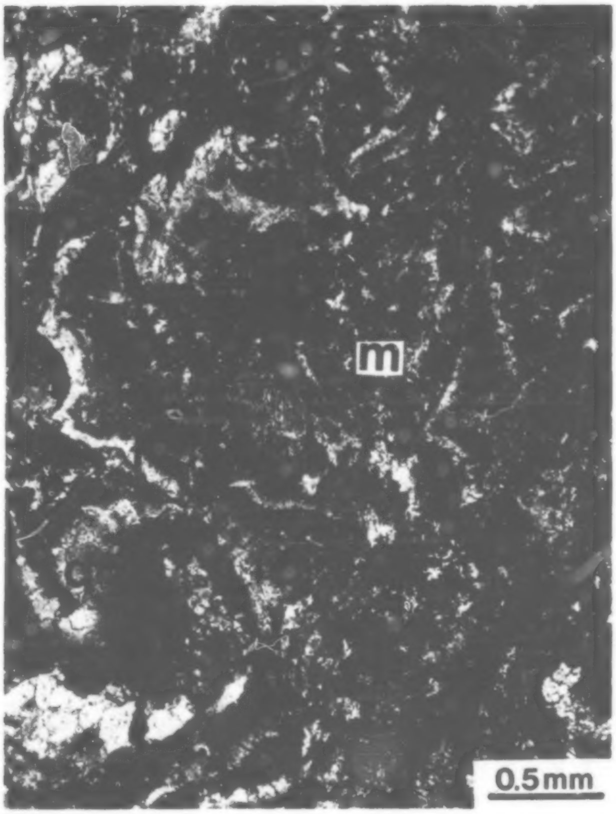

Figure 101: Partly silicified hyaloclastite granules with relict textures of former palagonite, Scotty Lake basalt. Equant to platy granules have conchoidal fracture-bounded margins (m), rims of pale orange-brown quartz (q) and cores of pale green chlorite (c) with local domains of fine grained epidote (e). The quartz, which exhibits remnant fibro-radial textures, is interpreted to be a replacement of fibro-palagonite. The chlorite-rich core, which is set sharply against the palagonite rim, is interpreted to be a replacement of sideromelane. As in Cenozoic palagonitized sideromelane hyaloclastite granules (Dimroth and Lichtblau, 1979) shown in Figure 85, these granules have finely divided Fe-Ti oxide coatings at the boundary between the palagonitized rim and the sideromelane core, along internal fractures (f) and on most exterior surfaces. Areas between granules are composed of a mixture of quartz, chlorite, sericite and semi-opaque fine grained epidote. Sample 136-3, plane polarized light.

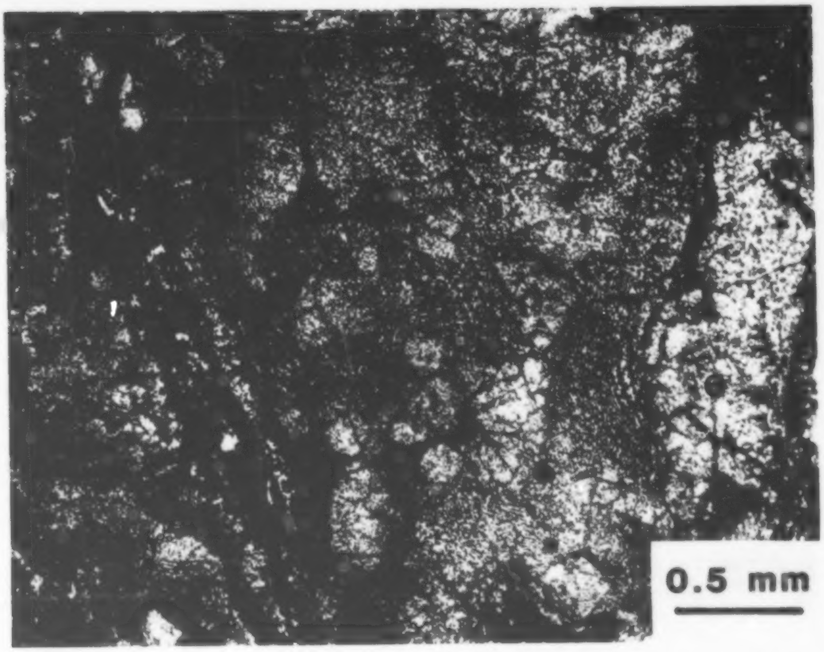

Figure 102: *Replacement of palagonitized hyaloclastite granules by botryoidal saponite (pseudomorphed by chlorite (c) and subsequent epidote (e)). Iron oxides (now leucoxene) are concentrated in growth rings of previous saponite. Sample 1115-1, plane polarized light.*

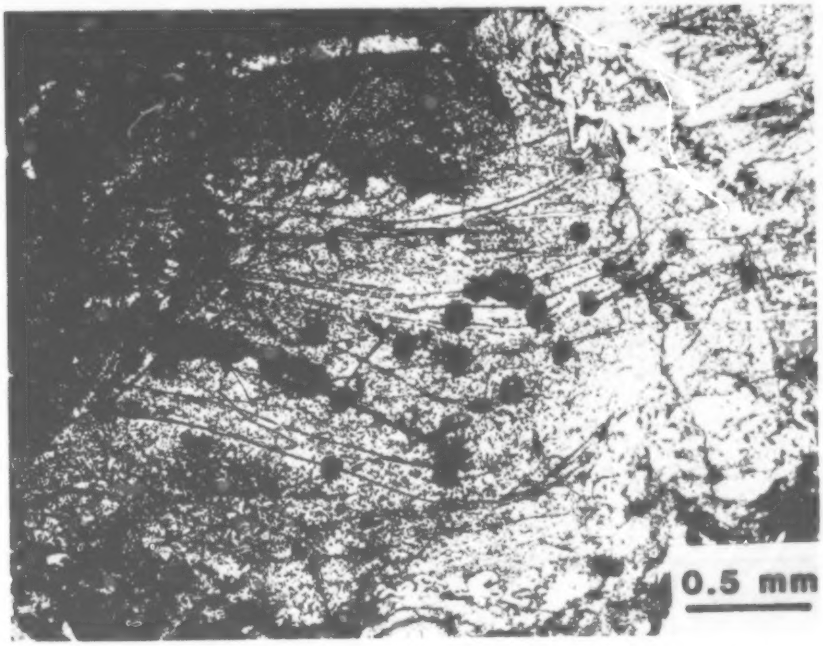

Figure 103: *Spherulites nucleated on perlitic cracks in a hyaloclastite granule. The entire granule, including spherulites, has been replaced by granoblastic epidote. Sample 1115-1, plane polarized light.*

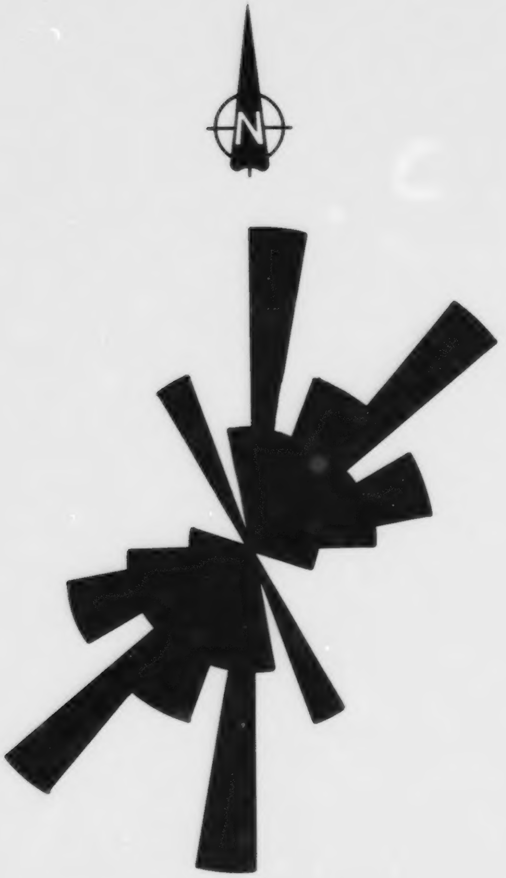

Figure 104: Rose diagram of orientation of 34 synvolcanic dykes, Scotty Lake basalt.

aphyric flow sequence (unit 4) to the north. The sediments comprise thinly bedded (5 — 50 cm) greywacke-siltstone with Bouma AB bed zonation and white mudstone laminae at or near bed tops. Some beds are pyritic.

Geochemistry

Scotty Lake basalt has the geochemical characteristics of high-Fe tholeiite. On Figures 105 to 107 the suite shows a broad range of FeO*/MgO, high FeO* (9 — 16%), and erratic increase in FeO* with stratigraphic elevation (Fig. 108).

The element variability observed between flows also occurs within individual flows (see analyses 1112-C1 to C8 and 117-C1 to C5, Appendix). SiO_2 shows a considerable variation, 50.55 — 58.10%, within a single flow which shows negligible metamorphic recrystallization (Fig. 89-93). This flow also has high and erratic LIL element contents, probably reflecting early, low temperature sea-floor alteration.

Interpretation

Scotty Lake basalt was deposited in a subaqueous environment: pillowed flows form about one-third of the sequence, massive flows have hyaloclastite breccia tops, granules of sideromelane in hyaloclastite were partially palagonitized, and flows commonly display low-temperature sea-floor alteration effects. The flows have a low overall vesicularity (generally less than 10%) which could be interpreted to indicate deposition in deep water. However, the presence of large amygdales (commonly to 4 mm, locally to 3 cm) and rare pipe vesicles throughout the sequence indicates relatively shallow water conditions (Table 5). Thus the low vesicularity must be due to a low volatile content in the magma. The absence of interflow basaltic pyroclastic rocks suggests deposition at depths greater than that at which eruption style changes to phreatomagmatic (about 300 m; Table 5).

Two features suggest that the exposed portion of the Scotty Lake basalt is proximal to source vents. First, the abundance of synvolcanic dykes is characteristic of proximal areas (Williams and McBirney, 1979). Second, the high proportion of massive flows is consistent with high effusion rates and proximity to source (Dimroth et al., 1978).

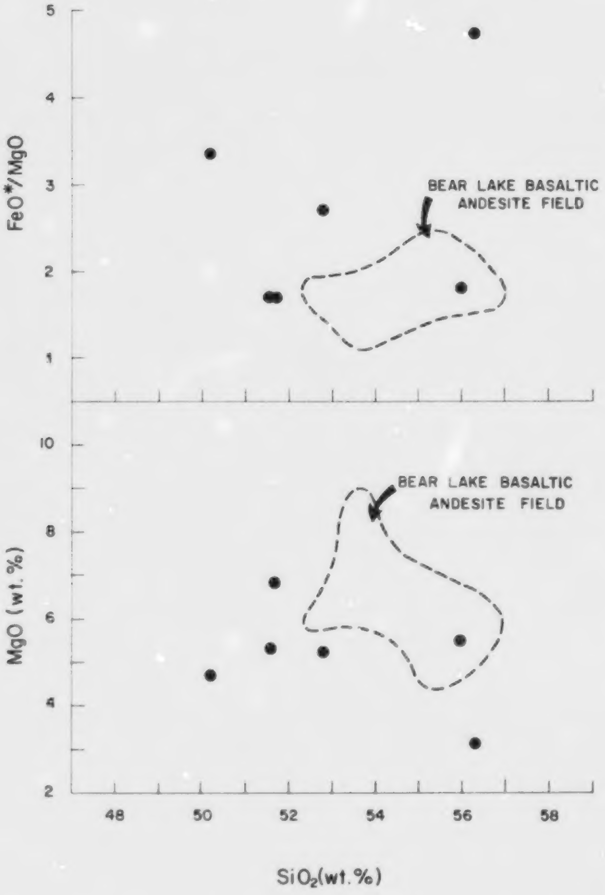

Figure 105: FeO/MgO vs. SiO_2 and MgO vs. SiO_2 (recalculated volatile-free), Scotty Lake basalt. Average compositions are shown for flows 117 and 1112. Bear Lake basaltic andesite compositional field for comparison.*

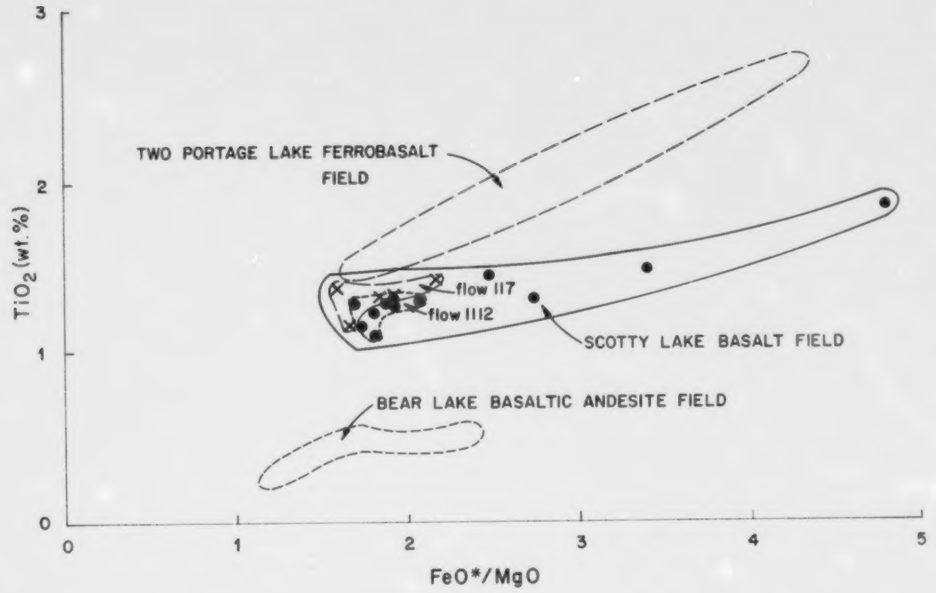

Figure 106: TiO_2 vs. FeO*/MgO, Scotty Lake basalt. Fields of Bear Lake basaltic andesite and Two Portage Lake ferrobasalt shown for comparison. Note strong Fe-enrichment trend expressed by wide range of FeO*/MgO in Scotty Lake basalt. Within-flow compositional variation shown by multiple samples taken through flows 117 and 1112.

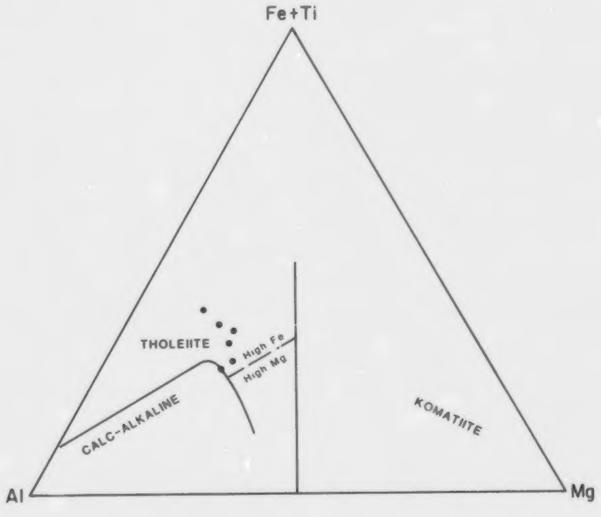

Figure 107: Jensen cation plot, Scotty Lake basalt. Average compositions are plotted for flows 117 and 1112. The analyses plot within the high Fe-tholeiite field and define a trend of Fe-enrichment.

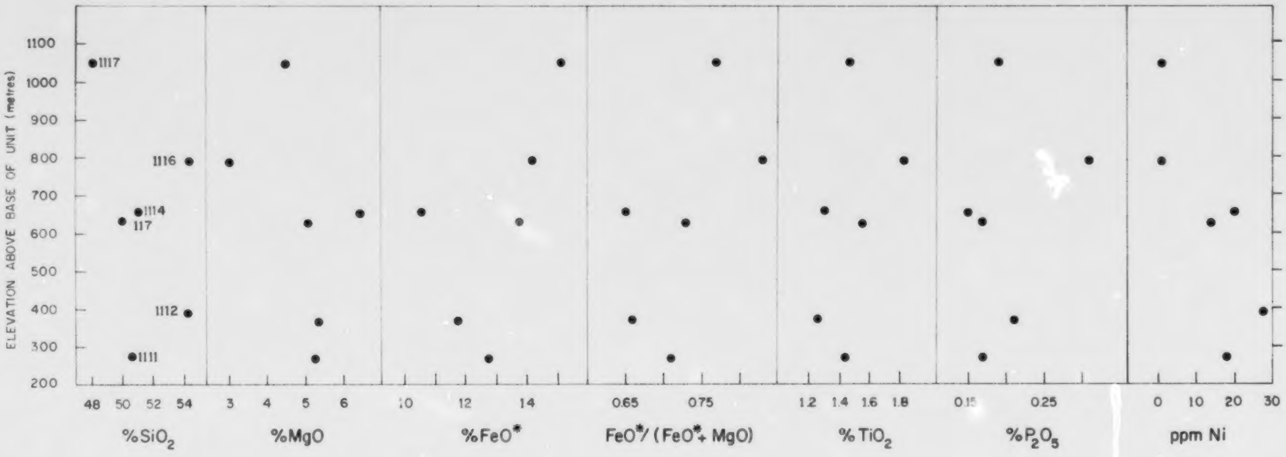

Figure 108: Element variation with stratigraphic elevation, Scotty Lake basalt. Average compositions are shown for flows 117 and 1112. Oxides in weight per cent, Ni in ppm. Analyses are plotted without removing volatiles (H_2O, CO_2). There is an erratic upward increase in FeO, FeO*/(FeO* + MgO), TiO_2 and upward decrease in MgO and Ni.*

NORTHEAST ARM MAFIC VOLCANICLASTIC ROCKS (UNIT 19)

The Northeast Arm volcaniclastics are composed of intermediate to mafic, redeposited, heterolithologic, coarse to fine breccias and tuffaceous, crystal-rich sandstone, siltstone and mudstone. Minor components include dacite, iron formation, and interlayered felsic tuff and mudstone. The unit is exposed for over 8 km, mostly along the east shore of the Northeast Arm of Schist Lake; its maximum exposed width at the north end of the Arm is 365 m. It "conformably" overlies Scotty Lake basalt and related intrusions, and the top of the unit is removed by the One Portage Lake Fault. At the north end of Schist Lake this unit is intruded by a layered ultramaficmafic body (unit 40) and quartz-megacrystic tonalite (unit 55). Notably, the volcaniclastics are not intruded by synvolcanic dykes (unit 4b) that characterize the underlying Scotty Lake basalts (unit 4a).

Approximately 90% of unit 19 is a well-bedded sequence of plagioclase-crystal bearing, coarse- to fine-grained volcaniclastic rocks (Fig. 109 and 110). These rocks contain 53.1 — 58.9% SiO_2 and 9.0 — 4.5% MgO, and thus are mafic to intermediate in bulk composition. They weather buff-brown to brown, are strongly foliated, and contain fragments that are strongly flattened (commonly 10:1 on outcrop surfaces). Beds are generally well defined, laterally continuous, and contain Bouma A and AB divisions. They range in thickness from 1 cm to 3.5 m, with coarse breccia beds being the thickest (pre-flattening thickness of beds must have been up to a maximum of about 16 m). Beds are defined by abrupt changes in clast size, and by interbeds of white mudstone, chert, and finer grained volcaniclastics (Fig. 109). Normal size and abundance grading of clasts is common, and reverse grading was noted in a few of the coarsest beds. Plagioclase crystals (contained within small fragments) also display normal grading.

Fragments in these volcaniclastic rocks are heterolithologic with respect to abundance, size and type of phenocrysts and abundance and size of vesicles. Despite their obvious heterogeneity they are approximately the same composition and are probably of common genesis. For the unit as a whole, about a dozen different fragment "types" have been identified; most are non-vesicular flow rocks with phenocrysts and glomerocrysts set in a pilotaxitic or felted groundmass. Variably vesicular, aphyric to porphyritic fragments are next in abundance, and a small percentage of scoriaceous fragments are ubiquitous in all beds. Phenocrysts in the fragments include plagioclase and, more rarely, pseudomorphs after pyroxene.

Lithic granules appear to exceed 50% of the volume of fine grained volcaniclastic rocks. Due to deformation and an imposed schistosity these granules are commonly indistinguishable from the matrix. Consequently only the plagioclase phenocrysts in the fragments are readily identifiable, and in the field the rock resembles crystal tuff. The granules are part of the same heterogeneous population as the larger fragments in breccias. As in the coarser fraction, some granules are scoriaceous.

Porphyritic fragments contain phenocrysts of plagioclase, pyroxene or both. Plagioclase phenocrysts (5 — 40%) are up to 5 mm; least deformed crystals are tablet shaped. In strongly deformed rocks they are oval or lens-shaped and largely replaced by brown fine grained epidote. Pyroxene phenocrysts (0 — 10%) are up to 2 mm across and are pseudomorphed by chlorite and overgrowths of tremolite-actinolite.

The volcaniclastic rocks are all matrix-supported. Where best preserved the matrix is composed of plagioclase crystal fragments and sand-sized lithic particles. More commonly the matrix is fine grained, foliated, and indistinguishable from recrystallized framework granules.

Interbedded mudstone and tuff (unit 35) occurs in two areas: along Highway 10 at the east shore of Schist Lake, and at the northern tip of Schist Lake. In a roadcut on Highway 10 the unit is 30 m thick and occurs within the volcaniclastic sequence. Well defined beds are characterized by sharp colour and composition contrasts: felsic layers weather white to light grey, are 0.3 — 30 cm thick, and are aphyric, whereas intermediate layers weather brown and green, are 0.5 — 35 cm thick, and contain sporadic 0.5 — 1 mm plagioclase crystals and lithic granules (Fig. 111). A single, 25 cm-thick, chalcopyrite-bearing sulphide formation occurs within the subunit. At the north end of Schist Lake unit 19 is 150 m thick and continues to the north of One Portage Lake; it is characterized by sharply interlayered white felsic tuff and green "chloritic mudstone". Felsic layers are 0.2 — 70 cm thick, very fine grained and aphyric to porphyritic (5%, 3 mm quartz; 10%, 2 mm plagioclase). Chloritic mudstone layers are 0.2 — 20 cm thick, fine grained, aphyric and strongly foliated. Adjacent to the Lavasseur Cu-Zn showing, which immediately underlies this

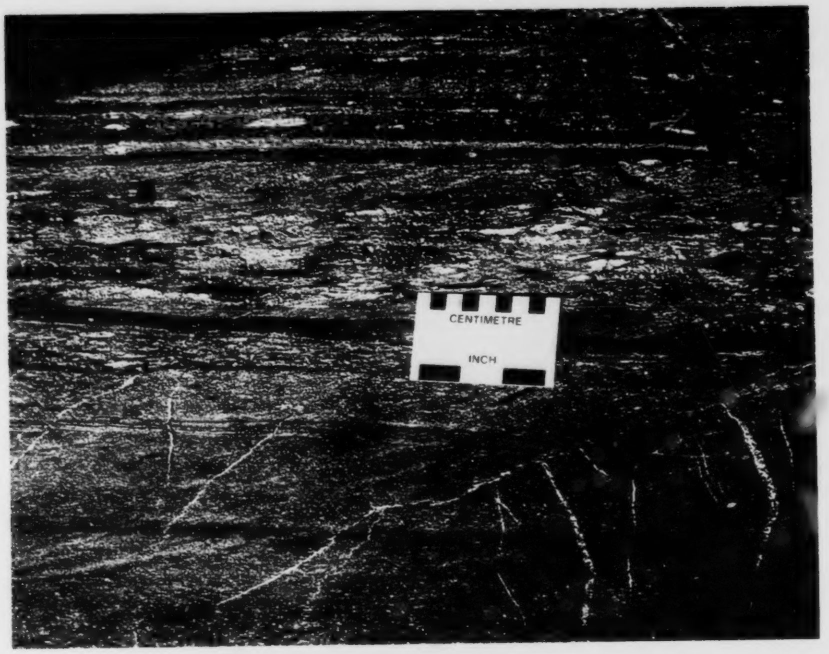

Figure 109: Northeast Arm mafic volcaniclastics (unit 19), Northeast Arm of Schist Lake. This example is relatively thin bedded, with graded crystal tuff layers, ash laminae, and thin lapilli-bearing beds. There has been significant flattening into the plane of foliation, parallel to bedding.

unit, there is an intermediate mudstone comprising alternating brown, red-brown and green laminae.

A 90 m thick banded iron formation (unit 38b) outcrops in tiny exposures for 100 m along strike at the northeast end of Schist Lake (Fig. 112). It consists of alternating: 0.2 to 2 cm thick, black, magnetite-rich layers; 1 to 4 cm thick, red-brown weathering, magnetite-bearing, grunerite-rich beds; and 1 — 2 cm thick, white, chert layers. The grunerite beds are partly altered to actinolite and are strongly overprinted by secondary stilpnomelane. The iron formation is tightly folded and chert beds are typically broken up into cigar-shaped tectonic lenses.

The iron formation is overlain by 10 m of dacite and dacite tuff (unit 18). This unit, which is only exposed in one small outcrop, contains a basal 3 m of tabular (up to 65 cm thick) bodies of massive white aphyric dacite in rusty brown weathering felsic material. The overlying 7 m consists of 5 to 10 cm thick layers of creamy buff and rusty brown weathering felsic tuff that grades upwards into thinner bedded tuff alternating with chert and pyritic tuff layers.

Interpretation

The volcaniclastic rocks of this unit vary in bulk composition; in addition contained clasts vary in composition and texture and include flow rocks and scoria. This heterogeneity indicates mixing of flow- and pyroclastic-derived detritus in the source area prior to deposition. Such mixing of detritus is most likely to have occurred in a subaerial environment. Since most fragments are broadly similar in composition the provenance was probably restricted to a single basaltic andesite source.

Sedimentary structures (graded bedding, Bouma zonation, lateral continuity of beds) indicate that the volcaniclastics were deposited in a subaqueous environment from high-concentration gravity flows. The presence of thick beds and overwhelming predominance of A and AB beds indicate that the deposits are proximal.

The presence of coarsening-upward and fining-upward sequences (Fig. 110 and 112) suggests that detritus supply was variable, possibly indicating fluctuations in volcanic activity in the source area. Chemical sediments (e.g. iron formation) are interpreted to have been deposited during periods of volcanic quiescence.

There was an abrupt break between Scotty Lake-type volcanism (basalt flows) and the deposition of unit 19 volcaniclastics, as indicated by a complete absence of Scotty Lake synvolcanic dykes in the volcaniclastic rocks, and by the abrupt change in rock type. Further, the local occurrence of subrounded quartz and rhyolite pebbles in a basal member of the sequence (Fig. 112) suggests that this break may in fact mark a disconformity in the Scotty Lake Block stratigraphy.

MAFIC MUDSTONE AND WACKE, BASALT, GABBRO (UNIT 34a)

This unit of thinly bedded to laminated mafic mudstone and wacke, subordinate thin basalt flows, and common narrow mafic sills is discontinuously exposed for 4.6 km between the north end of Schist Lake and the north end of Whitefish Lake. For most of its strike length it occurs as a slice bounded on the east by the One Portage Lake Fault and on the west by the Northeast Arm fault. At the north end of Schist Lake the separation between these faults increases, and the unit is overlain by ankerite-quartz-chlorite schist (unit 37a). In this area the unit is exposed over a width of 150 m. The unit structurally overlies unit 19 volcaniclastic rocks but is separated from it by the One Portage Lake Fault.

Mafic mudstone is layered on a scale of 0.1 — 20 cm, with individual beds defined by colour variation in shades of green and greenish brown and, locally, by grain size grading. In one locality A and AB beds were observed: the components of a coarser wacke bed include plagioclase-

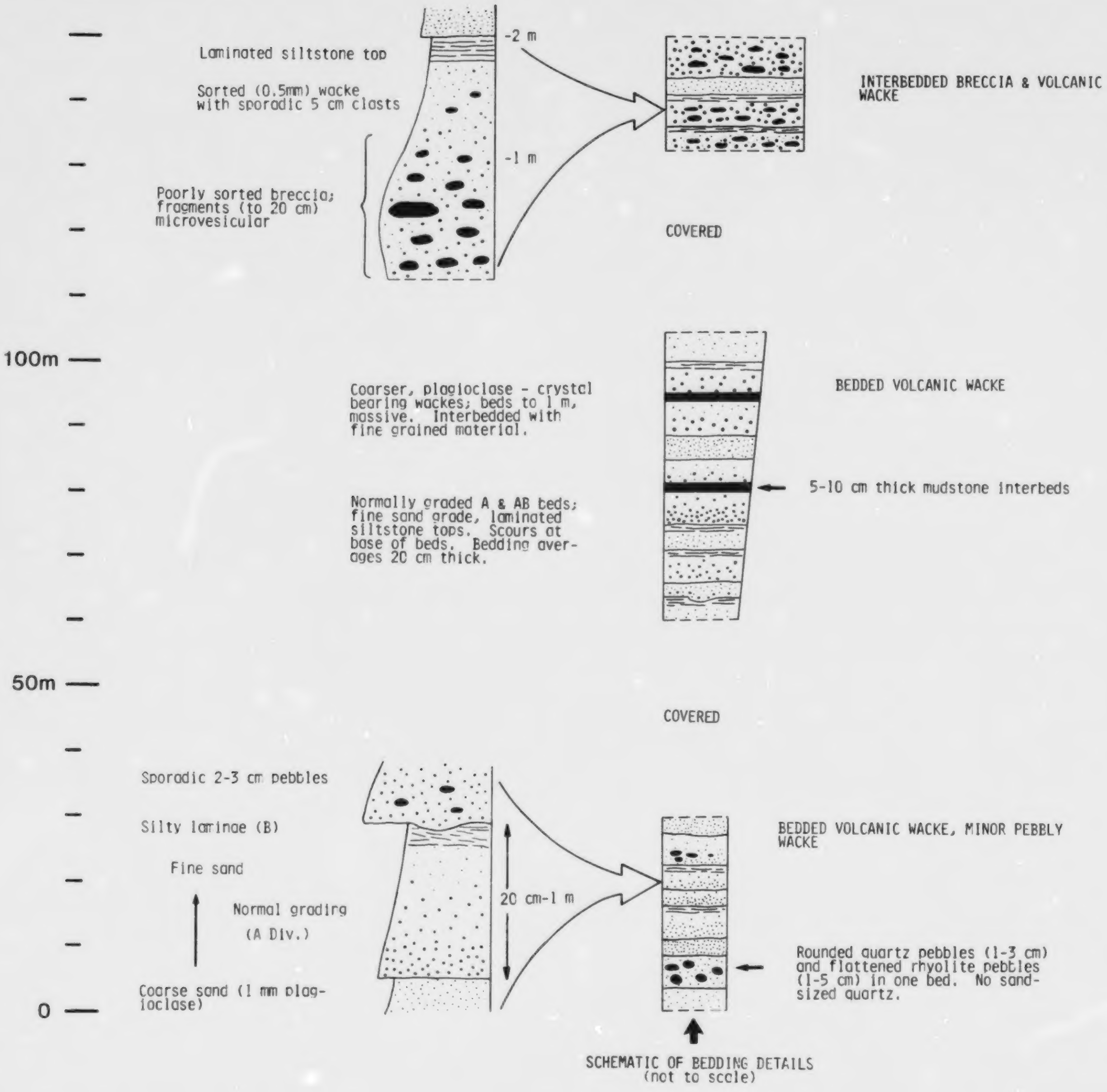
Laminated siltstone top
-2 m
Sorted (0.5mm) wacke with sporadic 5 cm clasts
-1 m
Poorly sorted breccia; fragments (to 20 cm) microvesicular
INTERBEDDED BRECCIA & VOLCANIC WACKE
COVERED
100m
Coarser, plagioclase - crystal bearing wackes; beds to 1 m, massive. Interbedded with fine grained material.
BEDDED VOLCANIC WACKE
Normally graded A & AB beds; fine sand grade, laminated siltstone tops. Scours at base of beds. Bedding averages 20 cm thick.
5-10 cm thick mudstone interbeds
50m
COVERED
Sporadic 2-3 cm pebbles
Silty laminae (B)
Fine sand
Normal grading (A Div.)
Coarse sand (1 mm plagioclase)
20 cm-1 m
BEDDED VOLCANIC WACKE, MINOR PEBBLY WACKE
Rounded quartz pebbles (1-3 cm) and flattened rhyolite pebbles (1-5 cm) in one bed. No sand-sized quartz.
0
SCHEMATIC OF BEDDING DETAILS
(not to scale)

Figure 110: Sequence in Northeast Arm volcaniclastic rocks (unit 19), east shore of Schist Lake. The sequence coarsens upward, from fine grained volcanic wackes near the base to thick bedded breccia and volcanic wacke approximately 150 m above the base.

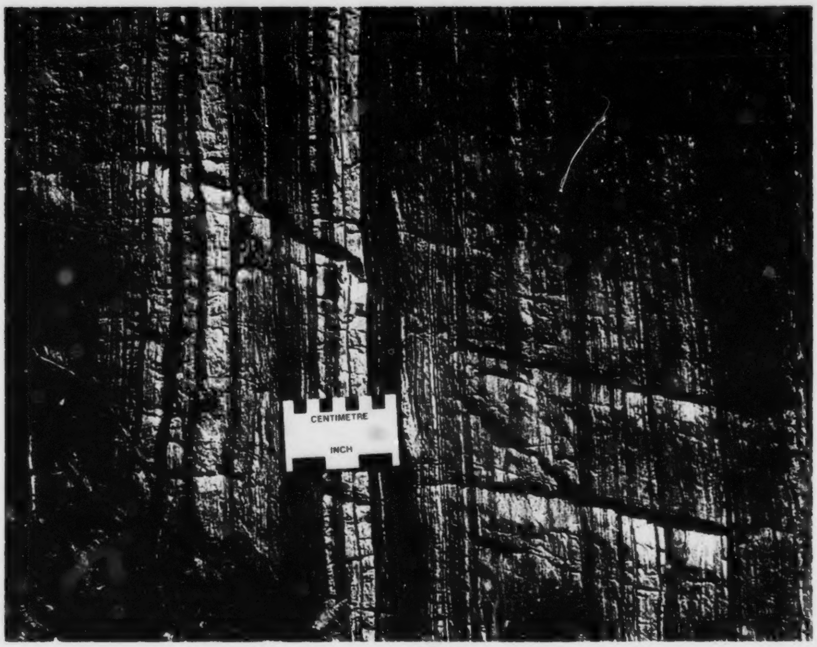

Figure 111: *Laminated felsic tuff (light) and mudstone (dark), unit 35, northeast end of Northeast Arm.*

phyric granules of basalt in a matrix of plagioclase crystals, chlorite, epidote and carbonate (locally a cement). More commonly the mudstones are strongly foliated and primary structures are obliterated. Irregular masses, stringers and pods of epidosite, elongate parallel to schistosity, are common. Thin interbeds of chert and ankeritic mudstone further define layering.

Mafic flows in the sequence are generally massive, non-amygdaloidal and aphyric; they are distinguished from the ubiquitous mafic sills by their finer grain size. One flow is clearly pillowed but primary structures are not preserved in other flows.

Mafic sills are 2 cm — 3 m thick, equigranular, and composed of blocky amphibole after pyroxene (0.5 — 2 mm) and lath-shaped plagioclase (0.5 — 2 mm). The sills are emplaced parallel to bedding and schistosity. They are abundant (up to 30% of some outcrops) and characterize this unit throughout its entire strike length.

ANKERITE-QUARTZ-CHLORITE-SERICITE SCHIST (UNIT 37a)

This minor unit is 30 m thick at the north end of Schist Lake. It is composed of red-brown to brownish green carbonate-rich layers with narrow siliceous partings. These rocks are strongly foliated and crenulated, with laminae composed of carbonate + quartz, chlorite + minor epidote + minor quartz, and sericite. Crosscutting veinlets of remobilized quartz-carbonate-pyrite are common.

MUDSTONE, SILTSTONE, GREYWACKE (UNIT 33)

Unit 33 is the topmost stratigraphic unit in the Scotty Lake Block. At the north end of Schist Lake it is 90 m thick, overlies unit 37a, and is truncated to the west by the Northeast Arm Fault. It is exposed sporadically in shoreline outcrops for 6 km on the west side of Schist Lake; other exposures are on Whitefish Lake and Mikanagan Lake.

On Schist Lake the lower portion of the unit consists of grey, green and brown chloritic mudstone. The upper portion is predominantly mudstone interlayered with greywacke, laminated reddish brown and light grey siltstone, and white to dark grey chert.

Chloritic mudstone is laminated to thinly bedded (0.1 — 15 cm) with layering defined by variation in colour. Individual laminae are characterized by variable chlorite and iron oxide content. Greywacke beds are up to 30 cm thick and display normal size grading in plagioclase (up to 2 mm; commonly less than 0.5 mm). Tops of some beds are parallel laminated mudstone. Detrital components of greywacke beds include subangular plagioclase crystal fragments, subrounded quartz (less than 5%), and rare, subhedral pyroxene crystal fragments replaced by tremolite-actinolite. Matrix consists of chlorite, epidote, feldspar, quartz, and opaque oxides.

Laminated, reddish and light grey weathering siltstone and mudstone are a distinctive and characteristic component of this unit. They are composed of very fine grained (0.01 — 0.05 mm) feldspar, quartz, stilpnomelane, epidote, magnetite and minor pyrite, hematite and carbonate. Lamination is defined by variation in the amount of stilpnomelane.

Adjacent to the Northeast Arm fault unit 33 is schistose, carbonate-bearing, tightly folded and transposed, with axial planar quartz-carbonate feldspar veins (some of which are boudinaged).

Greywacke and mudstone on Whitefish Lake occur in a mixed sedimentary and volcanic unit 150 m thick, overlying unit 9 pyroxene-phyric mafic flows. This sequence differs from that on Schist Lake only in that it contains pyroxene-phyric flows, and a greater proportion of greywacke. The sediments are generally tightly folded and intensely foliated.

SUMMARY

The Scotty Lake Block contains three main components: an aphyric Fe-tholeiite lava plain or shield volcano (Scotty Lake basalt), an overlying unit of porphyritic mafic to intermediate volcaniclastic rocks (Northeast Arm volcaniclastics), and a mixed dominantly volcanogenic sedimentary sequence (units 34a, 37a and 33). The relationship between the mixed sedimentary sequence and the underlying formations is uncertain

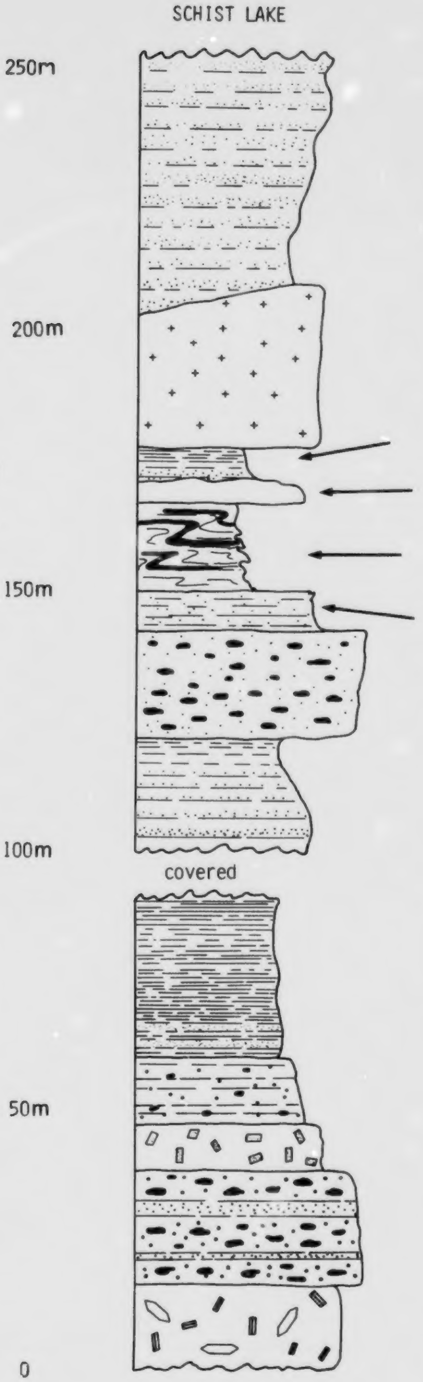

VOLCANICLASTIC GREYWACKE
Mafic to intermediate, abundant 1 to 2 mm (up to 1 cm) plagioclase crystal fragments, beds (up to 1 m thick) normally graded

TONALITE INTRUSION

FELSIC TUFF
Upward fining, thin bedded (5-10 cm) top, 2-3 dacite fragments at base

DACITE (?)
Aphyric, small tongues (< 60 cm) and blocks (up to 35 x 12 cm) in rusty brown matrix

IRON FORMATION
Alternating 0.2-4 cm layers of magnetite, grunerite (partly replaced by stilpnomelane) and chert. Tightly folded.

PLAGIOCLASE CRYSTAL-RICH VOLCANICLASTIC GREYWACKE
Mafic, 10% magnetite, more than 50% 0.1-0.2 mm lath-shaped plagioclase crystal fragments.

VOLCANICLASTIC BRECCIA
Mafic to intermediate, tectonically flattened fragments (up to 30 x 2 cm), matrix-supported, 5% 0.25-1.0 mm plagioclase crystal fragments in matrix.

VOLCANICLASTIC GREYWACKE
Mafic to intermediate, thin bedded (2-20 cm), normal size and abundant sorting of plagioclase crystal fragments (0.25-1 mm, 10-15%), rare quartz crystal fragments, bed thickness and grain size decrease upwards in this unit.

THINLY LAMINATED MUDSTONE, SILTSTONE AND TUFF
Mafic to intermediate, thin bedded (0.3 mm-15 cm), rare 0.25-0.5 mm plagioclase and quartz crystal fragments. Interlayered with volcanic wacke near base. Felsic tuff laminae weather white to buff.

VOLCANIC WACKE
Mafic to intermediate, medium bedded (50 cm-1 m). Wackes with 30% 1-2 mm plagioclase and sporadic 1-2 cm fragments predominate. Minor coarser volcaniclastic beds.

PYROXENE PORPHYRY SILL

PEBBLY VOLCANIC WACKE, VOLCANICLASTIC BRECCIA, VOLCANIC WACKE
Mafic to intermediate, thickly bedded. Fragments are tectonically flattened (up to 10's of cm long), matrix-supported, amygdaloidal. Matrix contains 0.5-1 mm plagioclase crystal fragments

QUARTZ-FELDSPAR PORPHYRY
Quartz 5%, 1 mm; Feldspar 15%, 1-2 mm. Massive

Figure 112: Stratigraphic section through Northeast Arm intermediate to mafic volcanclastic sequence (unit 19), north end of Schist Lake.

because the One Portage Lake Fault occurs between them.

Scotty Lake basalt comprises massive and pillowed aphyric flows and abundant synvolcanic dykes, emplaced in a shallow subaqueous environment. The absence of intercalated pyroclastic rocks, sediments or non-related flows, suggests that the Scotty Lake volcanic edifice is a lava plain or small shield volcano.

Northeast Arm volcaniclastic rocks lie with possible local disconformity upon the underlying Scotty Lake basalt flows. The volcaniclastics are basaltic andesite in bulk composition, porphyritic, heterolithologic and highly mixed. Fragment types include flow rocks and scoria, the latter probably derived from pyroclastic eruptions. The high degree of mixing and the presence of flow and pyroclastic fragments suggest provenance from a subaerial stratovolcano. Bedforms indicate that the material was transported from the margin of the stratovolcano to its site of deposition by subaqueous density flows. There is a possible correlation between these porphyritic volcaniclastic rocks and the porphyritic flows (units 8 and 9) that occur locally at the top of the aphyric Scotty Lake sequence. One possible interpretation is that the flows represent the subaqueous portion of the postulated subaerial stratovolcano source of the volcaniclastic rocks.

WHITEFISH LAKE-MIKANAGAN LAKE BLOCK

INTRODUCTION

The Whitefish Lake-Mikanagan Lake Block is bounded on the east by the Sourdough Bay Fault and on the west by a number of faults including the old Highway 10 Fault, the Scotty Lake Fault and the Northeast Arm Fault (Fig. 3; Map GR87-1-1).

The block does not contain a coherent stratigraphic succession because numerous strike faults tectonically interleave separate components of the sequence. What sets this particular block apart from other blocks is the porphyritic nature of the volcanic rocks and the high proportion of fragmental and conglomeratic units. This dominantly porphyritic sequence is interpreted to be part of a cogenetic series.

Missi Group rocks unconformably overlie the Amisk Group within a bundle of fault slivers on and south of Whitefish Lake. Apart from the main structural basin of Missi Group rocks in the Flin Flon Block, these fault-bounded slivers of Missi are the only occurrence of this group in the area.

BASALTS (UNITS 7 and 9)

At least 10 discrete basalt bodies occur in the Whitefish Lake-Mikanagan Lake Block (Fig. 113, Table 7). The flows are commonly porphyritic although the size and abundance of phenocrysts is highly variable and serves to distinguish the different bodies. Stratigraphic relationships between basalt bodies are generally unknown because they occur in different fault slivers.

Compared to other blocks in the Flin Flon area, these basalt units are poorly exposed in relatively small and lichen-covered outcrops. Consequently, data on flow thickness and organization is generally not available. Preservation of primary textures is moderate in areas away from schistose zones associated with faults. Primary clinopyroxene phenocrysts are preserved in the Sawmill Lake basalt and its possible equivalent, Body A (Fig. 113), at Athapapuskow Lake.

Two distinctive features of the basalt units in this block are: (1) they contain only a few synvolcanic dykes and (2) they are interlayered on a large scale with conglomerate, redeposited pyroclastic rocks and greywacke. These features contrast distinctly with those of the major basalt accumulations in the Bear Lake and Scotty Lake blocks, which are interpreted as the proximal or central facies of shield volcanoes. In this block the basalt units are more likely to be more removed from source.

All basalts in the Whitefish Lake-Mikanagan Lake Block were deposited in a subaqueous environment. Most units are moderately to strongly vesicular and thus were probably emplaced at depths of less than 1 km (Table 5).

MIKANAGAN LAKE MAFIC VOLCANICLASTIC ROCKS (UNIT 20)

A thick sequence of mafic volcaniclastic rocks is exposed between Mikanagan Lake and Whitefish Lake, bounded on the east and west by major faults. The true stratigraphic thickness of the unit is unknown because it is folded and broken into parallel fault-bounded slivers.

The mafic volcaniclastic rocks are well bedded and comprise porphyritic tuff, lapilli tuff and tuff breccia. Fragments are heterolithologic with respect to phenocryst population and vesicularity. Bedforms are dominantly Bouma A, AB and ABE types, indicating subaqueous deposition from density currents. Units 20a and 20b are mainly composed of tuff and are distinguished on the basis of weathering colour; unit 20a weathers dark grey-green to black whereas unit 20b weathers shades of brown. Unit 20c displays heterolithologic fragment populations similar to those of the tuff units, but differs in that it has greater bed thickness and fragment size.

Tuff (units 20a and 20b)

Mafic tuff is the dominant rock type in unit 20. Beds are well defined, laterally continuous, and commonly less than 1 m thick; exceptional beds are up to 2 m thick. They display Bouma A, AB and ABE zonation, with normal grading defined by size and abundance grading in pyroxene and plagioclase crystals. Pyroxene crystals (10-20%) are up to 2 mm across at the base of beds and less than 0.5 mm at the top; plagioclase crystals (0-20%) grade from 1 mm to less than 0.5 mm. Although not apparent in the field, these phenocrysts occur within small, closely packed fragments. Sedimentary structures observed in tuff beds include load structures, scours, graded bedding, flame structures and parallel lamination, all of which are typical turbidite-type structures.

Fragments in the tuff are angular to subrounded and generally less than 2 mm across. Margins are defined by fractures that cut across enclosed phenocrysts and vesicle trains. Fragments are heterolithologic and include, in decreasing order of abundance: coarsely pyroxene-phyric basalt with small plagioclase phenocrysts, plagioclase-phyric basalt with few or no pyroxene phenocrysts, plagioclase plus pyroxene-phyric basalt, scoriaceous aphyric to porphyritic basalt, and rare aphyric basalt. Individually these vary with respect to size and abundance of amygdales and texture of groundmass. Some are clearly derived from flows as they contain plagioclase microlites in felted to pilotaxitic texture. Beds are framework supported with few fines; in places the pore spaces between fragments are filled with quartz. The apparent grading in crystal size observed in these beds in fact reflects normal size grading in the enclosing granules: as granule size decreases the size of truncated crystals must also decrease.

Lapilli tuff and tuff breccia (unit 20c)

Coarse volcaniclastic rocks are locally interlayered with the dominant, finer grained tuff. They are matrix-supported, and occur in thick (to greater than 6 m), commonly massive, non-graded beds. Fragments are up to 20 by 60 cm but are commonly less than 10 cm long; they are flattened parallel to schistosity. Fragments are angular to subrounded; some are oval (Fig. 114). Phenocrysts in both matrix and fragments show the same size range, from 2 — 10 mm across. Most lapilli are densely vesicular. As in the tuff, the fragment population is heterolithologic. Some fragments are selectively epidotized.

Interpretation

Fracture bounded margins and truncation of phenocrysts and vesicles indicate that most fragments were broken in a brittle state. The relative absence of rounded detritus and fine grained matrix material suggests that these volcaniclastics are not epiclastic. Shallow subaqueous or subaerial phreatic explosions in a basaltic edifice, which incorporated lithic fragments from a variety of porphyritic flows and mixed these with juvenile scoria, is consistent with the restricted compositional range and morphology of fragments. Turbidite bedforms indicate that the products of these violent eruptions were transported by subaqueous density currents to their site of deposition. This model of eruption and deposition is similar to that proposed for the previously described Vick Lake tuff but differs in that eruptions responsible for the Mikanagan Lake mafic volcaniclastics are interpreted to have had a much lower juvenile magmatic component.

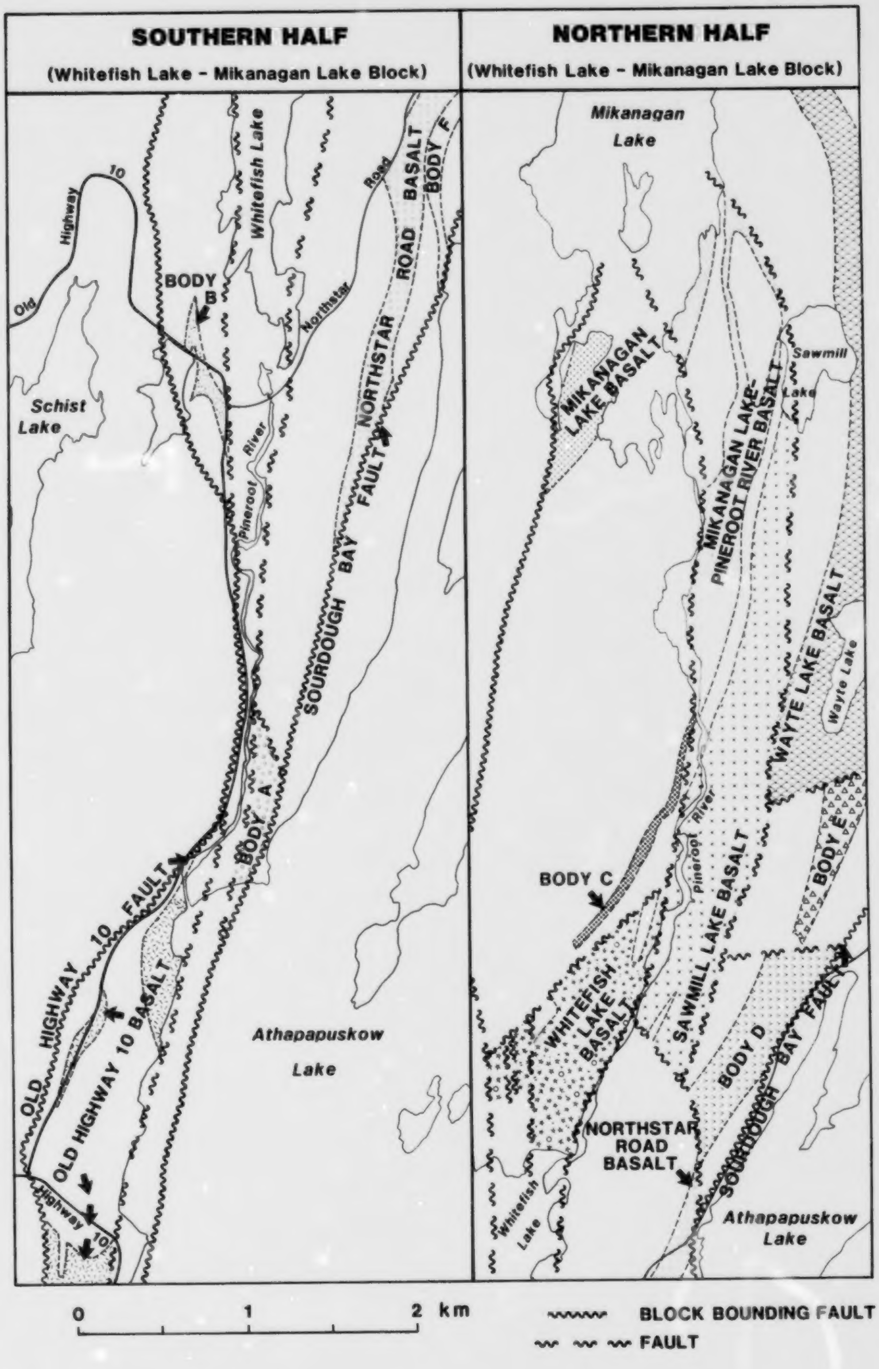
SOUTHERN HALF
(Whitefish Lake - Mikanagan Lake Block)
NORTHERN HALF
(Whitefish Lake - Mikanagan Lake Block)
Mikanagan Lake
Old Highway 10
Whitefish Lake
BODY B
Northstar Road
NORTHSTAR ROAD BASALT
BODY F
Schist Lake
Pineroot River
SOURDOUGH BAY FAULT
BODY A
OLD HIGHWAY 10 FAULT
OLD HIGHWAY 10 BASALT
Athapapuskow Lake
Highway 10
MIKANAGAN LAKE BASALT
MIKANAGAN LAKE-PINEROOT RIVER BASALT
Sawmill Lake
WAYTE LAKE BASALT
Wayte Lake
BODY C
BODY E
WHITEFISH LAKE BASALT
SAWMILL LAKE BASALT
BODY D
NORTHSTAR ROAD BASALT
SOURDOUGH BAY FAULT
Whitefish Lake
Athapapuskow Lake
0 1 2 km
BLOCK BOUNDING FAULT
FAULT

Figure 113: Location and distribution of major basalt bodies, Whitefish Lake-Mikanagan Lake Block. Characteristics of each basalt body are summarized in Table 7.

Table 7:
Basalt units in the Whitefish Lake-Mikanagan Lake Block

BODY	UNIT NUMBER	WEATHERING COLOUR	FRESH	PHENOCRYSTS			VESICLES		DISTINCTIVE FEATURES
				Type	Size (mm)	%	Size (mm)	%	
Wayte Lake	9	light brown	light grey-green	Px Pg	0.5-9 0.5-2	10-30 0-20	to 10	to 25	Massive and pillowed. Flow top breccias. Pillow selvages poorly defined. Size of px phenocrysts varies between and within flows.
N part	9, 7	brownish green	medium green	aphyric					Massive flows about 10 m thick, amoeboid pillow breccia tops.
Northstar Road	9b,7	creamy buff	pale to medium green	Px	1-3	10	1-2	10-15	Mainly flow breccia.
Sawmill Lake	7	light buff	pale greenish grey, light green	Px Pg	0.5-1 0.2-4	0-5 0-10	to 4	0-2	Pillowed and massive flows. Pillows bun to mattress shaped, up to 1.5 m in maximum dimension. Selvages thin (up to 3 mm), rusty weathering. Plagioclase glomerocrysts. Thick weathered rind, uniform colour. Locally interlayered with polymictic conglomerate (unit 31).
Mikanagan Lake Pineroot River									
S Part	7, 9, 21b	light tan	light green	Px Hb Pg	to 5 to 2 to 3	0-15 0-20 0-30	to 10 Gas cavities	 to 10 cm	Mixed unit of aphyric and porphyritic flows. Selvages variable: narrow, rusty brown to 3 cm, light tan.
N Part	7, 9	buff brown, rusty brown, dark grey, medium green	medium to dark green	Px Pg	to 3 to 2	0-20 0-15	to 2	2-8	Massive flows and flow breccia 1-3% leucoxene after Fe-Ti oxides.
Mikanagan Lake	7, 9	medium brown to medium brownish green	dark green	most are aphyric					Massive, structureless, homogeneous flows; equigranular, 0.5-1 mm, epidosite domains and veins common.
Whitefish Lake Base (150 m)	7, 9	grey-green, creamy buff, greenish brown, dark grey	dark grey, pale green	a) aphyric b) Px		 to 5	to 15	to 15	

BODY	UNIT NUMBER	WEATHERING COLOUR	FRESH	PHENOCRYSTS			VESICLES		DISTINCTIVE FEATURES
				Type	Size (mm)	%	Size (mm)	%	
Middle (150-570 m)	7	buff, rusty buff, brown	dark grey green				to 5		Dominantly aphyric to weakly porphyritic. Massive and pillowed. Local px-phyric flows.
Top (570-960 m)	9, 8	dark grey-green to buff		Px	1-3	10-15	to 5		Px-phyric and intercalated pg-phyric flows, distinguished by colour, selvage characteristics, px content, pillow size and shape.
				Pg	2	to 20			
Body C	9	creamy buff	medium green	Px	to 5	to 20	1-3, up to 20	5-30	Strongly quartz-amygdaloidal massive flows.
				Pg	0.5-1	0-10			
Body B	7	buff	light grey, medium green	Px	to 2	to 20	to 6	to 20	Aphyric, px-phyric and pg-phyric types. Pyrite locally in pillow interstices.
				Pg	to 1				
Body A	7	reddish buff	pale green	Px	to 1	1-2			Similar to Sawmill Lake except for weathering colour. Contains primary cpx phenocrysts.
Old Highway 10	7	buff brown, buff	medium to dark green	Px	to 1	1-2	1-5, up to 20	0-5	Mainly aphyric massive flows.
				Pg	0.5.-2	5			
Body D	9	buff brown, reddish green	pale green	Px	0.5-3	1-10	to 10	to 5	No information (very poorly exposed).
Body E	9	medium brown	grey-green	Px	4	5		1-3	Very poorly exposed.
				Pg	1-2	20			
Body F	7	creamy buff, buff brown	pale green	Px	1-3	0-15	up to 5	rare	Variable phenocryst populations, includes aphyric varieties. Pillowed and massive flows.
				Pg	1-3	0-15			

Abbreviations:
Px: pyroxene
Pg: plagioclase
Hb: hornblende

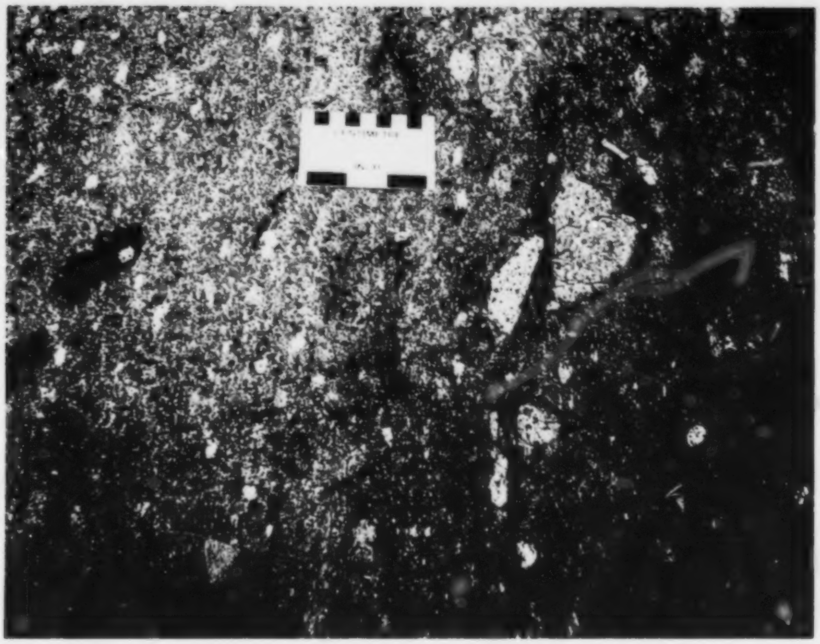

Figure 114: Plagioclase-pyroxene-phyric mafic lapilli tuff, Mikanagan Lake mafic volcaniclastics (unit 20c), south of Mikanagan Lake. Fragments are subrounded to subangular and vary with respect to phenocryst content, vesicularity, and colour. Abundant coarse pyroxene crystal fragments in the matrix.

INTERMEDIATE TO MAFIC TUFF, LAPILLI TUFF, TUFF BRECCIA (UNITS 21 and 22)

Intermediate to mafic volcaniclastic rocks occur in five discrete bodies in the White Lake-Mikanagan Lake Block. These rocks share many of the characteristics of unit 20 but are distinguished by light to medium brown weathering colours that probably reflect a more intermediate composition. They occur at a number of different stratigraphic levels, intercalated on a large scale with the various basalt flow units (Table 6) and volcanic conglomerate (unit 31).

Sawmill Lake

The largest body of intermediate volcaniclastic rocks occurs at Sawmill Lake. It is a minimum of 370 m thick at the north end of the map area. It overlies the Wayte Lake basalt and its top is truncated by a fault and a concordant quartz monzodiorite intrusion (unit 54). The body can be subdivided into a northern part composed of interlayered lapilli tuff and tuff breccia, and a southern part composed mainly of tuff.

The lapilli tuff and tuff breccia weather light-medium brown and rusty brown, and on fresh surface are light to medium green. Stratification is not prominent, partly due to small, lichen-covered outcrops. The volcaniclastic rocks are poorly sorted and matrix-supported, with fragments commonly up to 30 cm and having a maximum size of 60 cm. The fragments weather grey-white and are typically plagioclase-phyric and quartz amygdaloidal, set in a darker brown fine grained matrix. Most fragments are tectonically flattened and many are silicified and epidotized. Some are scoriaceous.

In the southern portion of the unit the sequence fines upward, with interlayered (1 — 7 m) tuff and tuff breccia at the base, overlain by relatively thick bedded tuff with a few beds containing fragments to 20 cm, in turn overlain by thin bedded (5 — 40 cm) lithic tuff which forms the upper half of the unit. The tuff weathers pale brown to rusty brown or light grey. Beds are laterally continuous, well graded, and have turbidite-type A, AB and ABE zonation. Reverse grading was observed but is rare; in one locality scoriaceous clasts were concentrated near bed tops. The normal grading is defined by an upward decrease in plagioclase crystal size (2 mm at base of beds) and lithic size (1 — 5 mm at base of beds). The lithic fragments comprise at least four different types corresponding to those found in unit 20; these include coarsely pyroxene-phyric basalt, plagioclase-phyric basalt, pyroxene-plagioclase phyric basalt and scoriaceous varieties. Some fragments have the microlitic textures of flow rocks.

The Sawmill Lake volcaniclastic sequence fines from north to south and from base to top, indicating that the source area lies to the north, outside the boundary of the map area. As in unit 20 these tuffs were probably produced by shallow subaqueous or subaerial phreatic eruptions and deposited by subaqueous density currents.

North Star Road

This 30 — 40 m thick unit of scoriaceous lapilli tuff occurs within the North Star Road volcanic conglomerate (unit 31), and has a lateral extent of about 2.7 km. It is massive, non-bedded, poorly sorted, matrix-supported and monolithologic. Fragments range in size from 0.2 to 35 cm but most are about 5 — 10 cm long. They are subangular to subrounded, densely vesicular, and contain a few phenocrysts of plagioclase and pyroxene. Some fragments contain felted to pilotaxitic plagioclase microlites. The matrix is relatively coarse and granular, with little fine grained material. The scoriaceous nature of the majority of fragments suggests a pyroclastic origin for this unit; it may represent a single eruptive event that punctuated the monotonous deposition of volcanic conglomerates.

Other occurrences

Intermediate tuff and tuff breccia occur in a 90 m thick unit that extends from the west shore of Sawmill Lake south to the Pineroot River. It lies stratigraphically between the overlying Sawmill Lake basalt and the underlying Mikanagan Lake-Pineroot River basalt (Fig. 113). This unit is poorly exposed but appears identical in components and bedforms to the thick unit exposed south and north of Sawmill Lake.

Intermediate tuff 600 m west of Sourdough Bay overlies the probable equivalent of the Wayte Lake basalt (Body D, Fig. 113) and is in fault contact with the Sawmill Lake basalt. It is identical in composition and bedforms to tuffs south of Sawmill Lake, and because they occupy the same stratigraphic position these two bodies are probably equivalent.

A similar tuff outcrops on and south of the power line, 820 m south of Wayte Lake. This body occurs between basalt sequences, and is truncated laterally to the north and south by faults. Where best exposed (on the power line) the tuff is well bedded (17 cm — 1.4 m) and comprises graded A, ABC and AB beds, some with E division tops, interlayered with pyritic siltstone. The beds contain plagioclase crystals to 1 mm, pyroxene crystals to 2 mm and porphyritic lithic fragments to 4 mm.

Intermediate breccia outcrops in small, poor exposures in a fault slice at the south end of Whitefish Lake. The breccias are poorly sorted, matrix-supported, and contain angular to subangular, pyroxene- and pyroxene-plagioclase-phyric, quartz amygdaloidal, mafic to intermediate, volcanic rock fragments. The breccias are commonly silicified and white weathering.

DACITE, RHYOLITE (UNIT 16a)

Felsic volcanic rocks are poorly exposed in a unit up to 180 m thick, at the southeast end of Whitefish Lake. They consist of white, buff to rusty brown weathering felsic tuff, breccia and massive rhyolite. Massive rhyolite is aphyric and forms small pods (to 1 m) within the fragmental material. In one locality massive rhyolite grades, through abrupt increase in vesicularity, to a medium brown weathering pumiceous felsic hyaloclastite. In general the unit contains a high proportion of breccia.

NORTH STAR ROAD VOLCANIC CONGLOMERATE (UNIT 31)

Coarse conglomerates composed dominantly of porphyritic basalt clasts occur in two major bodies, as well as in three small lenses within basaltic flow units. These conglomerates are interpreted to be proximal subaqueous debris flows on the basis of their bedforms, coarseness and limited rounding of largest clasts. They are intercalated with subaqueous porphyritic basalt flows and minor intermediate pyroclastic rocks. The large-scale stratigraphic relationships of these unique and distinctive conglomerates are not known because they occur in fault-bounded tectonic slices.

The conglomerates are thick bedded and are composed of boulders, cobbles and pebbles in a sandy matrix. In general bed contacts are either not observed or are subtle. Measured beds range from 2 to 33 m thick with bed contacts defined by abrupt changes in clast size, changes in clast population and roundness, and presence of minor sandy interbeds. Some beds are normally graded (base to top) whereas others display reverse grading at their base; upper portions of graded beds show the most rapid grading to pebbly tops. Approximately 60% of beds are clast-supported and 60% of beds are polymictic. The degree of heterogeneity varies widely from bed to bed; some contain a wide range of porphyritic basalt lithologies whereas others are restricted to one or two types. Basalt clast types are defined by size and abundance of phenocrysts, pyroxene:plagioclase phenocryst ratios, colour, and degree of vesicularity. Rare but significant clast types include fine grained hypabyssal mafic rocks, highly vesicular basalt, diabase, clasts with oxidized rims, and large clasts of pillowed basalt. Clasts vary in degree of rounding from subangular to rounded (Fig. 115, 116); very large clasts are typically angular, joint bounded, with somewhat rounded corners.

The matrix composition is similar to that of the clasts. It is composed of small basalt fragments, pyroxene and plagioclase crystals, and fine

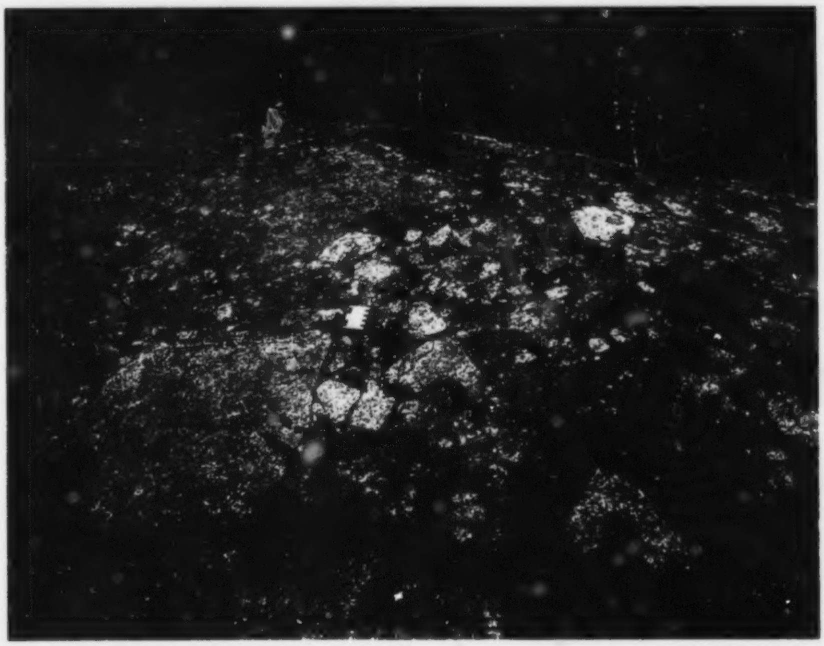

Figure 115: North Star Road volcanic conglomerate (unit 31), 150 m east of Whitefish Lake. Heterolithologic cobble and boulder conglomerate composed predominantly of porphyritic basalt clasts. Clast shape ranges from angular (largest boulder) to rounded (cobbles).

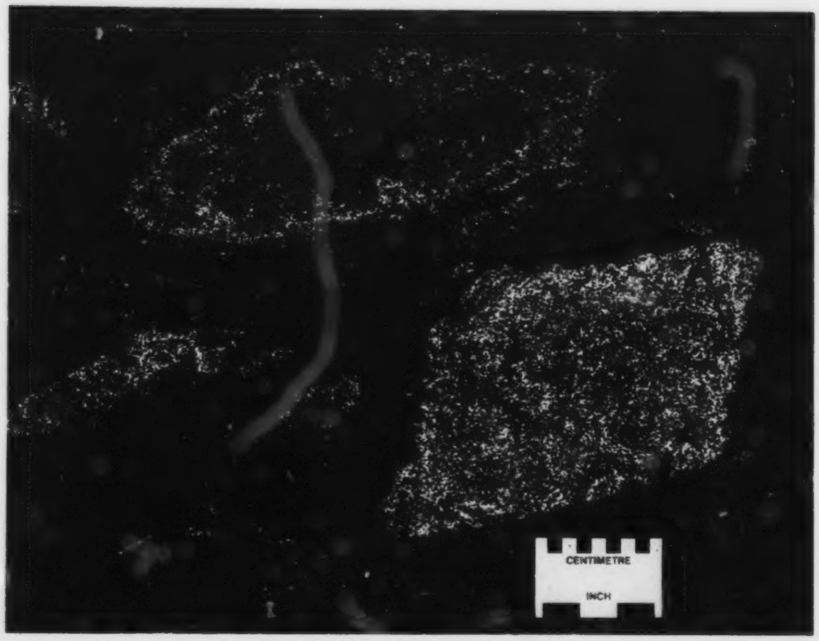

Figure 116: *Heterolithologic, framework-supported conglomerate (unit 31), 200 m east of Whitefish Lake. Fragments are subangular to subrounded and are intermediate to mafic in composition.*

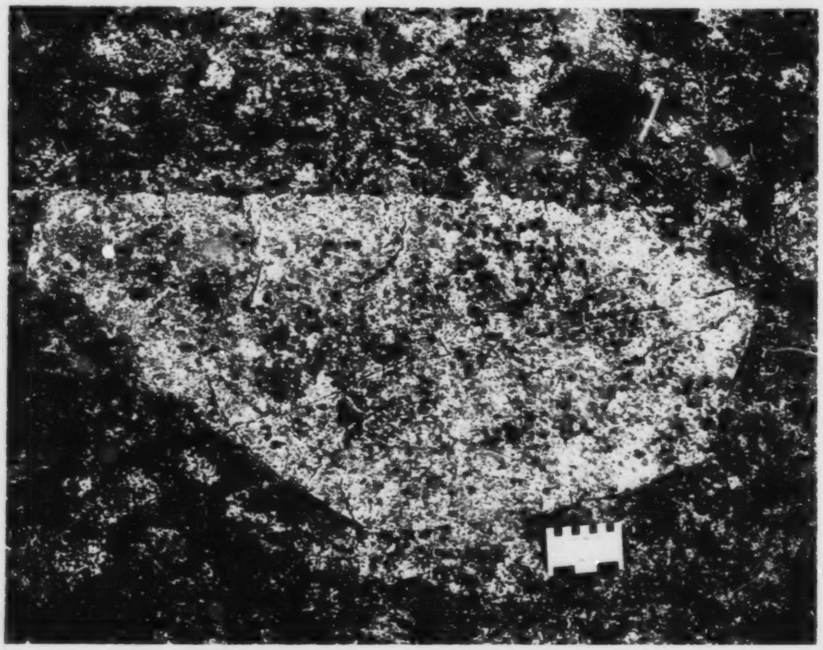

Figure 117: *Angular joint-bounded boulder of hypabyssal pyroxene-phyric intermediate intrusive rock in North Star Road volcanic conglomerate (unit 31), 600 m northeast of Whitefish Lake.*

grained foliated material. Matrix grain size corresponds approximately with clast size; coarser conglomerates have a coarse sandy to gritty matrix whereas finer conglomerates have a medium sand matrix. Conglomerates composed of well rounded clasts contain more matrix and are commonly matrix-supported. The largest clast observed is greater than 3 by 2 m, and clasts larger than 1 m are moderately common. These very large clasts are angular and joint bounded, with longest flat surfaces parallel to bed contacts (Fig. 117). The distribution of largest-clast-size (Fig. 118) shows two maxima.

Minor structures observed include clast imbrication (one locality) and a clastic dyke (one locality). The clastic dyke is emplaced in a 12 m thick sandy/gritty unit within the conglomerate section; it is exposed for 6 m along strike, cuts the sandstones at an angle of 60°, and is 15 — 20 cm wide. Pebbles are concentrated in the centre of the dyke.

Straight-walled porphyritic basalt dykes locally cut the volcanic conglomerate. They have chilled margins and compositions similar to the clasts in the conglomerate.

Interpretation

The volcanic conglomerates are interpreted to have been deposited by subaqueous debris flows derived from a sequence of porphyritic basalt lava flows. The conglomerate beds are organized in a manner similar to subaqueous debris flows described by Nemec et al. (1980), including presence of very large boulders, poor sorting (Fig. 119), thick bedding and absence of conspicuous grading. Features consistent with subaqueous deposition (Fisher, 1982) include intercalated pillowed porphyritic basalt flows, very thick bedding, relatively high proportion of matrix and presence of elongate clasts parallel to bed contacts.

The well rounded nature of cobbles and pebbles, high degree of mixing of different clast types, and oxidized rims on some clasts indicate that some of the debris originated and was mixed in a subaerial environment. However, the presence of pillowed basalt clasts and some beds with restricted compositional range suggest that some of the conglomerates may have originated by submarine slumping. The intermixing of beds derived from both subaerial and subaqueous sources is possible from the flanks of a single volcanic island.

GREYWACKE, SILTSTONE, MUDSTONE (UNITS 33 and 34)

Three small bodies of fine grained sedimentary rocks occur in the south Mikanagan Lake-Pineroot River area. On Mikanagan Lake mafic greywacke (unit 33) occurs on the southeast shoreline. These rocks weather buff-brown to grey-green and consist of A and AB beds with white siltstone-mudstone interbeds. They are composed of porphyritic basalt microclasts and locally abundant plagioclase and pyroxene crystal fragments in fine grained mafic groundmass.

South of Mikanagan Lake a unit of fine grained, laminated greywacke-siltstone (unit 34) forms a unit up to 120 m thick within unit 20b mafic tuff. The sediments weather shades of brown, green and grey and are delicately laminated to finely layered. Disseminated fine grained pyrite (up to 2%) occurs in some beds or sets of beds.

On Pineroot River the sedimentary unit (unit 33) is composed of buff and green weathering greywacke interlayered with siltstone and mudstone. Rock fragments to 5 mm occur in some beds, with detrital plagioclase and pyroxene. Beds are thin, disrupted, tightly folded and transposed into the plane of foliation. The transposition of layering is presumably related to one of the adjacent major faults that coincide with Pineroot River.

VOLCANIC ENVIRONMENT

Although the rocks exposed in the Whitefish Lake-Mikanagan Lake Block occur in a number of fault bounded slices with variable facing direction, some generalizations can be made about the volcanic environment in which they were deposited.

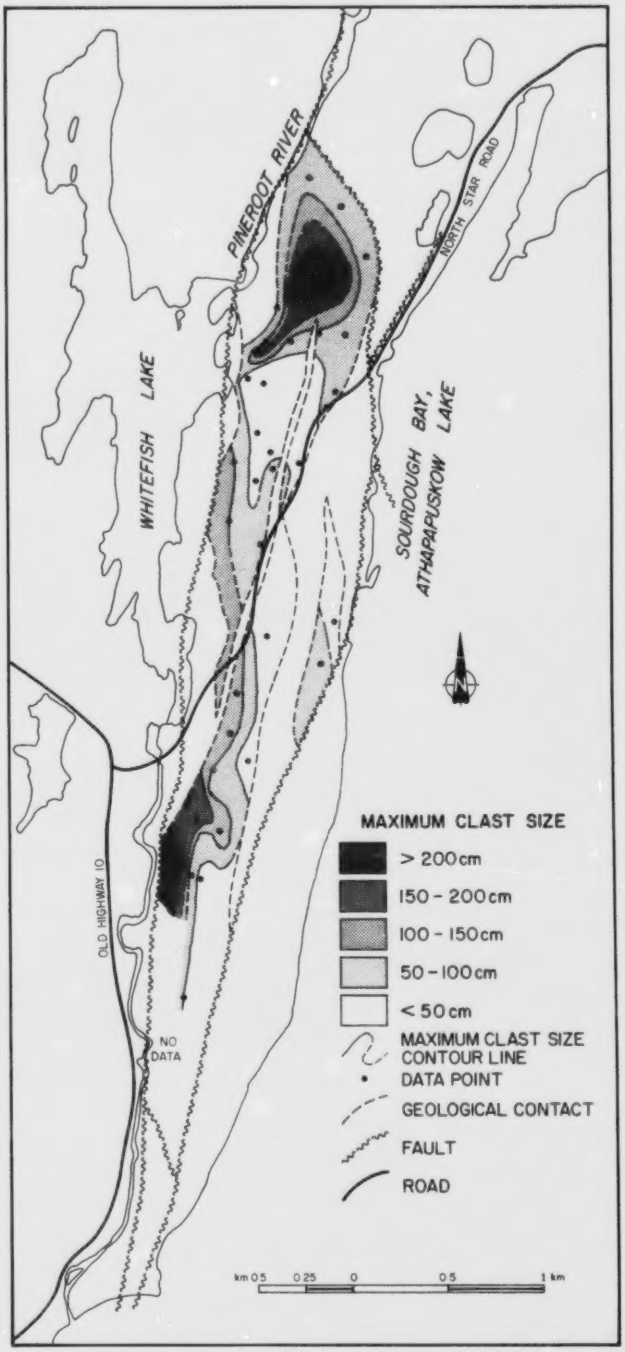

Figure 118: Maximum clast size distribution in the North Star Road volcanic conglomerate (unit 31). Contours at 50, 100, 150 and 200 cm. Two clast size maxima are indicated, possibly reflecting two distributory channels in the sequence. The conglomerate body tops to the west.

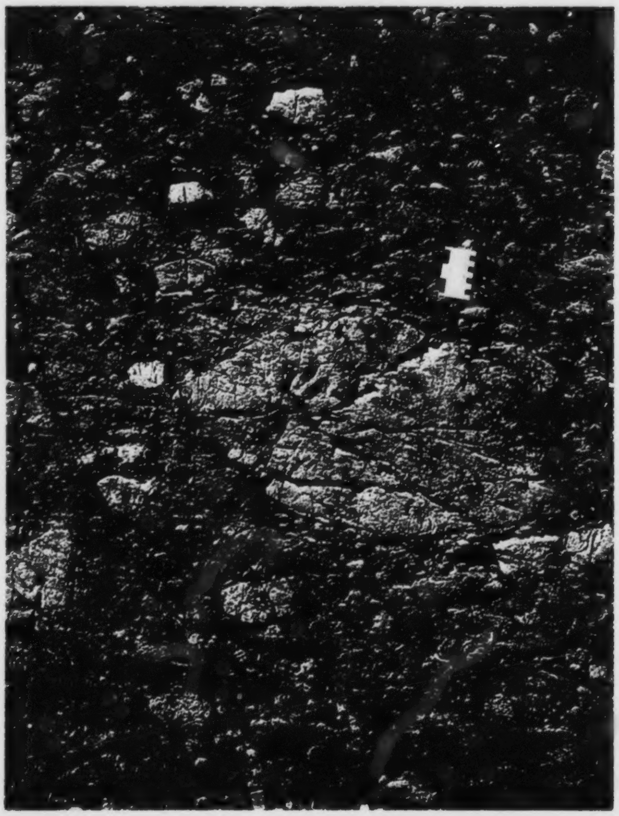

Figure 119: North Star Road volcanic conglomerate (unit 31). Clast-supported, very poorly sorted conglomerate composed of angular to subrounded clasts of porphyritic basalt. 490 m east of Whitefish Lake.

The dismembered sequence consists of a large-scale intercalation of porphyritic mafic rocks including pillowed basalt, pyroclastic rocks and volcanic conglomerate. The heterolithologic tuff and tuff breccia (unit 20) are interpreted as the products of shallow subaqueous or subaerial phreatic eruptions that were transported to their place of deposition by turbulent density currents. Coarse polymictic and oligomictic volcanic conglomerates are interpreted to be subaqueous debris flow deposits that were shed from both the subaqueous and subaerial portions of a volcanic island composed mainly of porphyritic basalt flows. By analogy to the subaerial facies variation described by Williams and McBirney (1979) this assemblage of flows, pyroclastic rocks and conglomerate characterizes the proximal zone of a central vent stratovolcano. This sequence is not part of the central zone of Williams and McBirney (1979), which is characterized by abundant dykes, coarse pyroclastic rocks, and hydrothermal alteration — none of which occur in the Whitefish-Mikanagan Block.

Although there are strong indications that some of the material in the sequence was derived from a subaerial source, all of the preserved rocks were deposited in a subaqueous environment.

BAKERS NARROWS BLOCK

INTRODUCTION

The Bakers Narrows Block consists of at least 3.8 km of homoclinal, southeast-facing lava flows truncated at a high angle to the west by the North Arm Fault (Fig. 3, Map GR87-1-1). The east- to northeast-trending flow contacts in the block are overprinted at a moderate to high angle by a north- northeast-trending schistosity.

The components of the Bakers Narrows Block include 5 units of subaqueous basalt and basaltic andesite flows (units 7—9) which alternate with 4 units of felsic flows (unit 18; Fig. 120 and 121). Good exposures of these rocks occur on the shorelines of Thompson, Wright and Sharpe bays on Athapapuskow Lake.

BASALT, BASALTIC ANDESITE (UNITS 7-9)

Five major basalt-basaltic andesite units, ranging from 120 m to more than 900 m thick, occur in the portion of the Bakers Narrows Block exposed in the map area. These major units (B_A to B_E) alternate with major units of felsic flows (F_A to F_D), resulting in a strongly bimodal stratigraphic sequence (Fig. 120 and 121). Major basalt units are distinguished on the basis of weathering colour, flow organization and phenocryst content. Similar distinctions serve to further subdivide them into members.

Unit B_A (Thompson Bay basalt)

More than 850 m of aphyric and porphyritic flows are poorly exposed on the peninsula between Thompson Bay and Wright Bay. The flows trend approximately east-west and face south, with a NNE-trending schistosity crossing flow contacts at a high angle (65° — 75°); pillows are commonly deformed into the plane of schistosity. This unit can be subdivided into 4 discrete members (Fig. 121) comprising, from base to top:

1) Aphyric, green to brownish green weathering massive flows with dispersed carbonate-filled amygdales to 2 cm in diameter. Many flows contain a flow-top amoeboid pillow breccia. Some flows contain plagioclase microphenocrysts (0.5 mm) in a groundmass of plagioclase microlites, plagioclase spherulites, tremolite-actinolite, chlorite, epidote, leucoxene and quartz.
2) Pyroxene-phyric, buff to buff-brown weathering pillowed flows containing 10% pyroxene phenocrysts (0.5 — 1 mm) and 5 — 10% quartz/carbonate amygdales (1 — 2 mm). Pillows in these flows are small, generally less than 1 m long, with selvages 2 — 4 mm thick and separated by 1 — 3 mm of epidotized interpillow material.
3) Plagioclase-phyric, buff to buff-brown weathering pillowed flows with 10 — 15% plagioclase phenocrysts (1 mm). Pillows are small (less than 60 cm long) with dark grey 3 — 4 mm thick selvages and no interpillow filling.
4) Aphyric, buff to buff-brown weathering pillowed flows greater than 10 m thick. Pillows are less than 1 m long, bun-shaped, with 1 — 4 mm thick rusty brown selvages and up to 10% carbonate amygdales to 5 mm diameter in or just above the pillow core.

Unit B_B (Wright Bay basalt)

A distinctive 120 m thick unit of dark green weathering massive basalt flows is exposed on the southern shore of Wright Bay. The basal 30 — 45 m of the unit consists of thin (1 — 2 m) pillowed flows alternating with thick layers of amoeboid pillow breccia and pillow fragment breccia. The remaining 75 to 90 m of the unit consists of massive, aphyric, fine

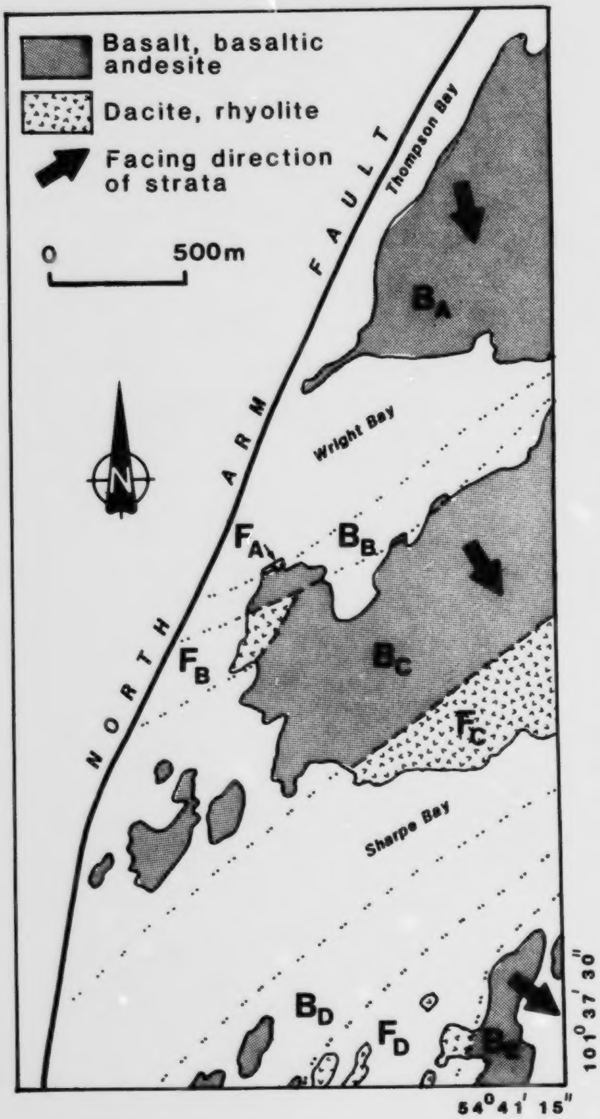

Figure 120: Distribution of major basalt-basaltic andesite and felsic units, Bakers Narrows Block. A stratigraphic section across these units is shown in Fig. 121.

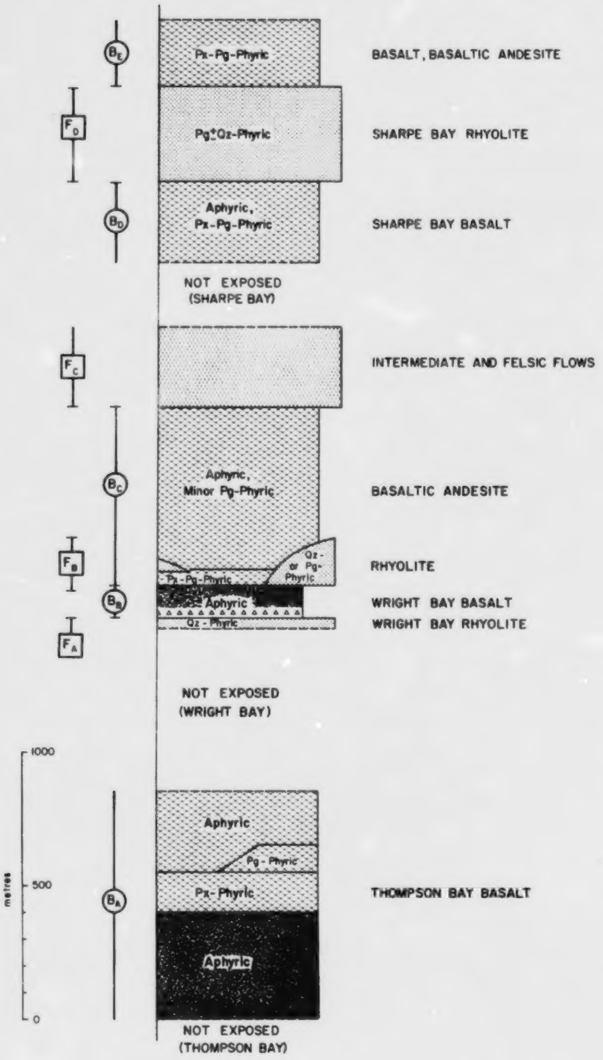
B_E
Px-Pg-Phyric
BASALT, BASALTIC ANDESITE
F_D
Pg±Qz-Phyric
SHARPE BAY RHYOLITE
B_D
Aphyric, Px-Pg-Phyric
SHARPE BAY BASALT
NOT EXPOSED (SHARPE BAY)
F_C
INTERMEDIATE AND FELSIC FLOWS
B_C
Aphyric, Minor Pg-Phyric
BASALTIC ANDESITE
F_B
Qz- or Pg-Phyric
RHYOLITE
Px-Pg-Phyric
B_B
Aphyric
WRIGHT BAY BASALT
Qz-Phyric
WRIGHT BAY RHYOLITE
F_A
NOT EXPOSED (WRIGHT BAY)
1000
500
0
metres
B_A
Aphyric
Pg-Phyric
Px-Phyric
THOMPSON BAY BASALT
Aphyric
NOT EXPOSED (THOMPSON BAY)

Figure 121: Stratigraphic sequence through Bakers Narrows Block. The exposed sequence, about 3.8 km thick within the map area, is composed of basalt and basaltic andesite (units B_A to B_E) intercalated on a large scale with felsic flows (unit F_A to F_D). Mafic units are subdivided according to phenocryst content (shown) and flow-type: massive flows (dark pattern), pillowed and massive flows (inverted pillow pattern), and interlayered breccia and thin pillowed flows (triangle pattern).

grained flows averaging 10 m thick, with interflow laminated chert, felsic tuff and mafic breccia (e.g. Fig. 122). There are probably only 6 — 8 massive basalt flows in this entire unit.

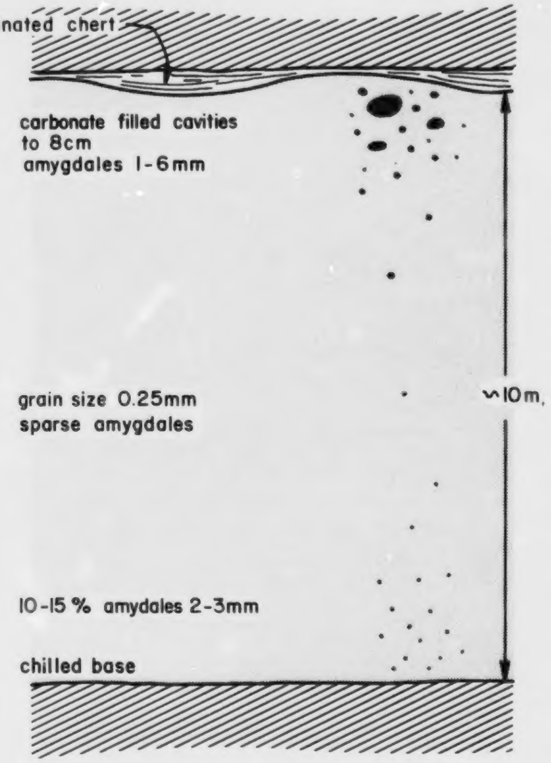
laminated chert
carbonate filled cavities to 8cm
amygdales 1-6mm
grain size 0.25mm
sparse amygdales
~10m
10-15 % amydales 2-3mm
chilled base

Figure 122: Sequence of structures through a typical Wright Bay basalt (B_B) flow. Flow top breccias are not developed. Inter-flow material includes laminated chert and bedded felsic tuff.

The contact of unit B_B basalts with the underlying felsic flow unit (F_A, Fig. 121) is exposed on the southwestern point in Wright Bay. The contact is sharp and slightly irregular; one felsic inclusion 75 cm long occurs in the basal 1 — 2 m thick pillowed flow.

The lower, 30 — 45 m thick unit of breccias and intercalated thin pillowed flows is somewhat chaotic in internal stratigraphy. Breccias are largely composed of angular to subrounded fragments up to 25 cm diameter in a black matrix; large amoeboid pillows are also present. One pillowed flow (1 m thick) is characterized by interpillow, strongly magnetic jasper.

Massive flows, which compose most of this unit, are aphyric and have chilled, non-vesicular bases. Interiors of flows are fine grained with sporadic carbonate-filled amygdales (to 6 mm, commonly 1 — 3 mm diameter). The top metre of the flows has a greater vesicularity (15%) with amygdales 1 — 6 mm and, in some flows, distinctive oval to round, carbonate-filled gas cavities 4 — 8 cm in diameter. Vesicularity decreases in the topmost 40 cm of one flow.

A thin section from near the top of one flow shows an aphyric, microlitic, spherulitic texture. About 60% of the rock consists of 0.4 mm plagioclase spherulites which overprint 0.1 mm long, randomly oriented plagioclase microlites. The remainder of the rock consists of chlorite (40%) between spherulites, leucoxene (1 — 2%) after primary disseminated Fe-Ti oxide grains (0.1 mm), epidote after plagioclase, and quartz (1%) as anhedral and equant grains.

Interflow laminated chert layers weather grey and black and are typically 10 cm thick. Interflow felsic tuff layers 0.6 — 7 m thick are thin bedded, locally graded, and are composed of quartz-plagioclase-phyric felsic fragments to 1.5 cm long in a matrix of chlorite, epidote and crystal fragments.

Unit B_C

This approximately 670 m thick sequence of pillowed and massive flows is exposed on the peninsula and islands between Wright Bay and Sharpe Bay. It overlies F_B felsic flows in the west but generally rests directly upon Wright Bay basalt in the east; it is overlain by F_C felsic and intermediate flows.

The lower 60 m of the unit is a distinct member characterized by pyroxene-plagioclase-phyric and pyroxene-phyric pillowed and massive flows. In this member phenocryst size and abundance varies between flows (pyroxene (0.5 — 2 mm, 5 to 20%) and plagioclase (0.5 — 1 mm, 5 to 10%)), epidote alteration is extensive, and pillows are commonly difficult to identify. Pyroxene phenocrysts are concentrated in the lower portion of one massive 4 m thick flow.

The overlying 610 m of the unit is mainly aphyric with minor, weakly plagioclase-phyric members. In this member, massive flows and pillowed flows are equally abundant. Most flows weather medium brown, brownish buff or rusty buff and are medium to dark green on fresh surfaces.

Pillowed flows in the upper 610 m are thick (greater than 10 m), but only a few flows could be measured from base to top. They commonly have amoeboid pillow breccia flow tops (up to 16 m thick) and contain poorly defined pillows characterized by epidote alteration, narrow selvages and little interpillow material. Amygdales vary widely in size and abundance. Flows range from non-amygdaloidal to coarsely amygdaloidal (1 cm) at the tops of some pillowed divisions.

Massive flows have measured thicknesses ranging between 2 and 16 m; most are greater than 14 m thick. Epidosite domains are common. Amoeboid pillow breccia flow tops occur on some flows; the best preserved example (Fig. 123) shows protruberances from the massive division into the overlying breccia. Bases of massive flows are non-amygdaloidal but sporadic quartz-carbonate amygdales to 5 mm and gas cavities to 10 cm long occur in the upper portions of some flows. Contacts between massive flows without amoeboid pillow breccia tops are marked by variation in weathering colour between flows and zones of *in situ* brecciation at flow tops and bases.

Unit Bc is notable for its complete absence of interflow tuff, pyroclastic breccia or sedimentary rocks. These flows presumably represent a depositional environment proximal to source vents.

Unit B_D (Sharpe Bay basalt)

This unit is approximately 300 m thick and is exposed only on three islands in the southwest part of Sharpe Bay. It is composed of strongly foliated aphyric and pyroxene-plagioclase-phyric pillowed flows which weather medium to dark green and are medium to light green on fresh surfaces. Intermediate to felsic intrusive rocks and intermediate tuff is poorly exposed on two of the islands.

Five pillowed flows ranging from 10 to 17 m thick occur in the best exposure. These flows are organized as shown in Fig. 9 and are charac-

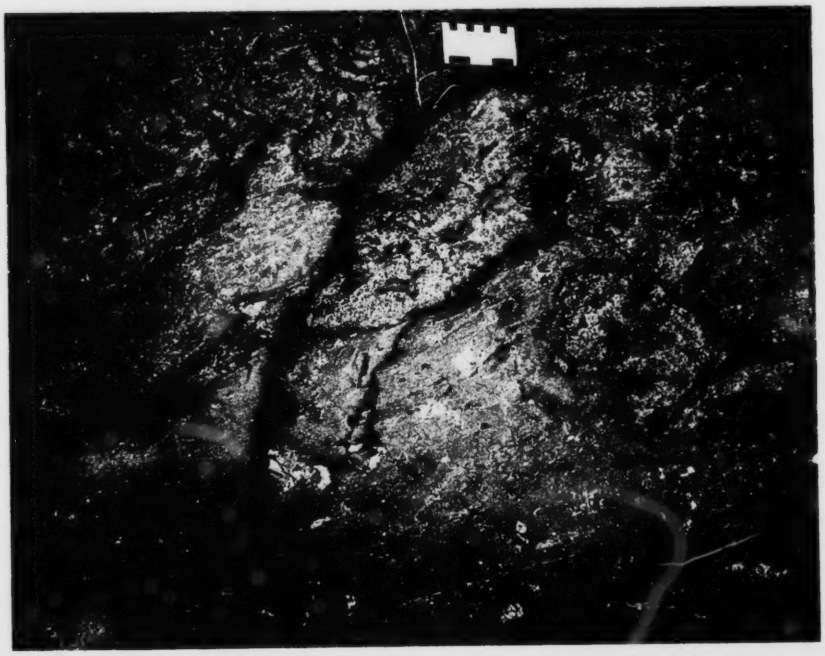

Figure 123: Contact between massive lava (bottom) and flow top amoeboid pillow breccia (top), unit 7, Bakers Narrows Block (unit B_C on Fig. 120). Note the irregular protrusions of massive lava into the breccia; the direction of overturn on the protrusions (to the right) gives the primary flow direction. Abundant quartz-carbonate amygdales occur in the top of the massive lava.

terized by thick amoeboid pillow breccia divisions: the breccias are subequal or greater in thickness (1.5 — 11 m) than the associated pillowed divisions (4 — 10 m). Amygdales (1 — 2 mm) are abundant in the uppermost parts of pillowed divisions and in amoeboid pillows. Gas cavities are up to 8 by 11 cm in some pillows.

Unit B_E

Porphyritic mafic flows overlying the unit F_D Sharpe Bay rhyolite are poorly exposed on a peninsula at the extreme southeast corner of the map area. There are too few outcrops to characterize the unit; flows appear to be plagioclase +/- pyroxene-phyric with locally abundant polymineralic amygdales to 5 mm.

Geochemistry

Four samples of mafic flows, from the better preserved lower half of the Bakers Narrows Block stratigraphic sequence, range in composition from basalt to basaltic andesite (52.7 — 57.0% SiO_2 calculated on an H_2O- and CO_2-free basis). On Jensen and TiO_2 vs. FeO*/MgO plots (Fig. 124 and 126) these rocks occupy virtually the same compositional field as the Bear Lake basaltic andesites. On plots of FeO*/MgO and MgO vs. SiO_2 (Fig. 125) the Bakers Narrows mafic flows similarly occupy a field close to that of the Bear Lake flows; both suites are characterized by relatively high MgO (5.8 — 9.1%) when compared to other mafic flow suites (e.g. Hidden Lake—Burley Lake sequence). The most important major and trace element characteristics of the Bakers Narrows suite are shared by the Bear Lake basaltic andesite, and are not equivalent to any other basaltic sequence in the Flin Flon area. The two suites differ only in the concentration of P_2O_5: 0.05 — 0.09% in Bakers Narrows flows versus 0.10 — 0.15% in Bear Lake flows. The overall similarities, however, strongly suggest that the two suites are comagmatic and correlative.

FELSIC FLOWS (UNIT 18)

Four major felsic (dacite-rhyolite) flow units (F_A to F_D), up to an estimated 460 m thick, are intercalated with the basalt flows that dominate the Bakers Narrows Block sequence (Fig. 121). Although individual felsic flows vary widely in thickness most conform to a single flow type comprising a massive base and breccia top.

Unit F_A (Wright Bay rhyolite)

The stratigraphically lowermost felsic unit is exposed for no more than 20 m at the southwest entrance to Wright Bay, where it is overlain by the Wright Bay basalt (B_B).

The felsic rock weathers light grey to light yellow and is medium grey on fresh surfaces. It contains 10 — 15% quartz phenocrysts (0.5 — 1 mm). In most places the rhyolite has a brecciated texture, ranging from *in situ* fracturing to discrete fragments within a matrix. Small, apparently massive zones are also present. The *in situ* brecciation is characterized by irregular, curving, anastomosing fractures whereas the more open breccias have discrete oval fragments in a granular matrix. These features are interpreted as the autobrecciated, thermally fractured top of a thick massive rhyolite flow.

Unit F_B

A sequence of "dacitic" flows is well exposed on the western shore of the peninsula between Wright Bay and Sharpe Bay. The unit overlies several metres of bedded felsic tuff and cherty tuff which in turn directly overlies the Wright Bay basalt. The felsic rocks are interpreted to form a relatively steep-sided structure because the entire felsic section pinches out to the east, within a lateral distance of 200 m. Weathering and fresh colour varies from flow to flow; weathering colours include white, light buff, buff, light green, light grey-green and medium green.

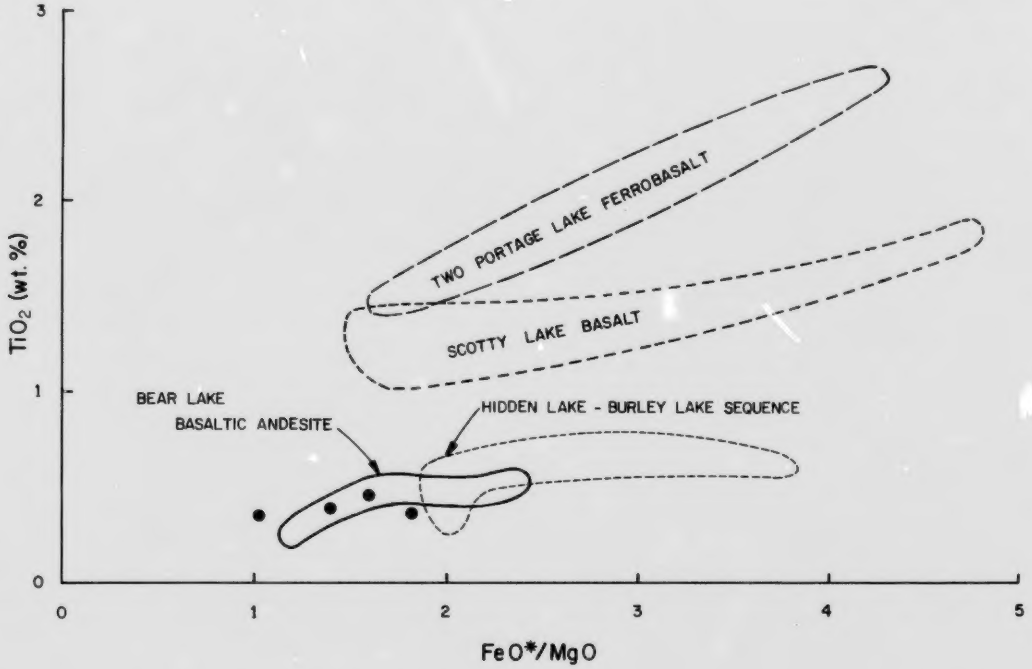

Figure 124: TiO_2 vs. FeO/MgO, Bakers Narrows Block basalt and basaltic andesite. Fields of other major mafic flow sequences in the Flin Flon area shown for comparison.*

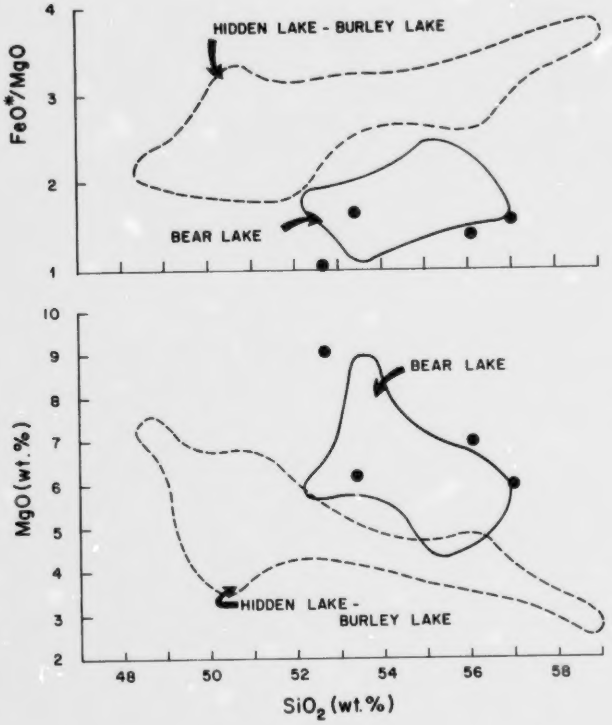

Figure 125: *FeO*/MgO vs. SiO_2 and MgO vs. SiO_2, Bakers Narrows Block basalt and basaltic andesite. Fields of Hidden Lake-Burley Lake basalt-basaltic andesite and Bear Lake basaltic andesite shown for comparison.*

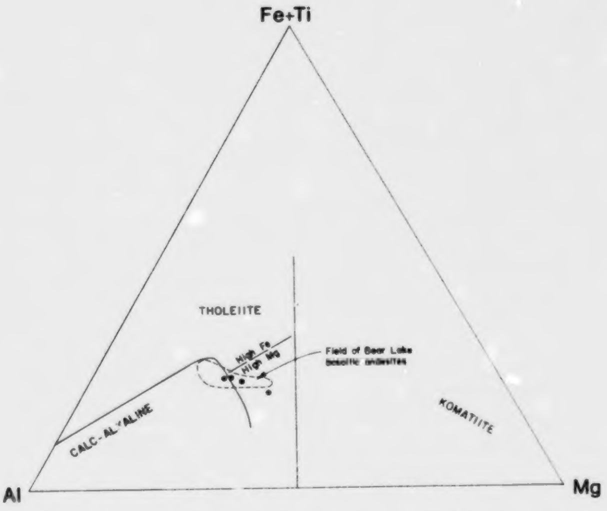

Figure 126: *Jensen cation plot of the Bakers Narrows Block basalts and basaltic andesites. Neither suite displays a significant Fe-enrichment trend.*

All or portions of 9 flows are exposed: one flow is greater than 30 m thick and 8 flows in a single sequence (Fig. 127) range from 1.6 to 3.8 m thick. All share the same flow morphology, comprising a lower massive zone (with chilled base) and an upper breccia zone. The proportion of massive to brecciated lava varies from flow to flow but in many the brecciated portion is thickest (Fig. 76).

Massive portions of flows are either non-vesicular or contain sporadic small carbonate-filled amygdales. Some massive flows have vesicular tops. The massive zone is abruptly gradational into overlying autobreccia.

Flow-top breccias (Fig. 128) are monolithologic and are fragment-supported to weakly matrix-supported. Fragments are angular to subangular, 1 — 30 cm (generally less than 5 cm in thin flows), and similar in phenocryst content to the massive portion of the flow. Matrix material commonly weathers a darker colour than fragments. In best preserved breccias matrix is composed of crystal fragments, lithic granules, and fine grained material. Significant carbonate occurs in both fragments and matrix of breccias in the thin-flow sequence (Fig. 127); in some flows the degree of carbonate replacement increases towards the flow top.

All flows are porphyritic. Some contain 3 — 5% embayed quartz phenocrysts (0.5 — 1 mm) whereas less siliceous members contain only plagioclase phenocrysts (3 — 15%, 1 mm). Groundmass is dominated by round feldspar spherulites (0.25 mm in diameter) and fine grained feldspar and quartz with subordinate chlorite, sericite, epidote and hematite.

Unit F_C

A heterogeneous sequence of intermediate and felsic flows, plus quartz-phyric felsic hypabyssal intrusions, is poorly exposed on the southeastern part of the peninsula between Wright Bay and Sharpe Bay. True stratigraphic thickness of this unit is not known because only the basal 200 m is exposed.

Flows weather cream to light buff to light blue and are medium green to pale grey on fresh surfaces. In one exposure portions of three massive flows are exposed, ranging in thickness from 1.8 m to more than 6 m. Most flows are strongly amygdaloidal, and proportion and size of amygdales increases upward from their chilled bases. Amygdales in the tops of flows are as large as 2 cm in diameter and gas cavities are up to 7 cm long.

Quartz-phyric felsic hypabyssal rocks in this unit contain up to 10% phenocrysts (0.5 — 1 mm) in a 0.2 — 0.5 mm groundmass. Some contain small angular mafic inclusions.

Unit F_D (Sharpe Bay rhyolite)

Massive felsic flows comprise a unit approximately 360 m thick, exposed on islands in the south central part of Sharpe Bay. These flows overlie Sharpe Bay basalt (B_D) and are in turn overlain by basalt unit B_E (Fig. 121). They weather light buff to white or pale grey and are light to dark grey on fresh surfaces. An analysis of one flow in the sequence (2421-C1, Appendix) is rhyolitic in composition.

Most flows have massive bases and brecciated tops (e.g. Fig. 129); flow thickness ranges from 6 m to more than 12 m. Massive portions of flows are non-vesicular. *In situ* brecciation, in which irregular fractures up to 3 cm wide separate sharply angular to slightly rounded fragments, characterizes the massive zone within 1 to 2 m of the overlying flow breccia top. The contact between this zone of *in situ* brecciation and the flow top breccia is abruptly gradational.

Flow top breccias are monolithologic and consist of angular to subrounded fragments 0.5 — 60 cm across, relatively close-packed in a dark grey fine grained matrix. One flow shows a decrease in fragment size from base to top of the breccia zone (Fig. 129).

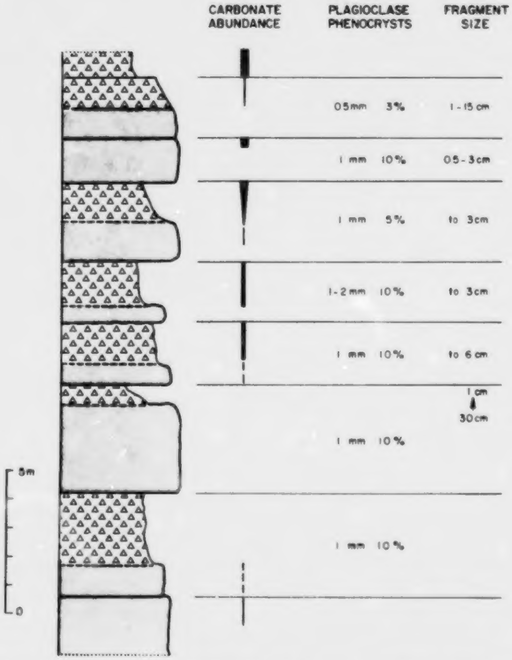
CARBONATE ABUNDANCE
PLAGIOCLASE PHENOCRYSTS
FRAGMENT SIZE
05mm 3%
1-15 cm
1 mm 10%
05-3cm
1 mm 5%
to 3cm
1-2mm 10%
to 3cm
1 mm 10%
to 6 cm
1 cm
30cm
1 mm 10%
1 mm 10%
5m
0

Figure 127: Measured sequence through a series of thin massive intermediate to felsic lava flows, unit F_B between Wright and Sharpe Bays. The base of each massive division is chilled against the underlying flow top breccia. The distribution of carbonate reflects primary porosity (abundance of vesicles, fragmental zones) in the flows.

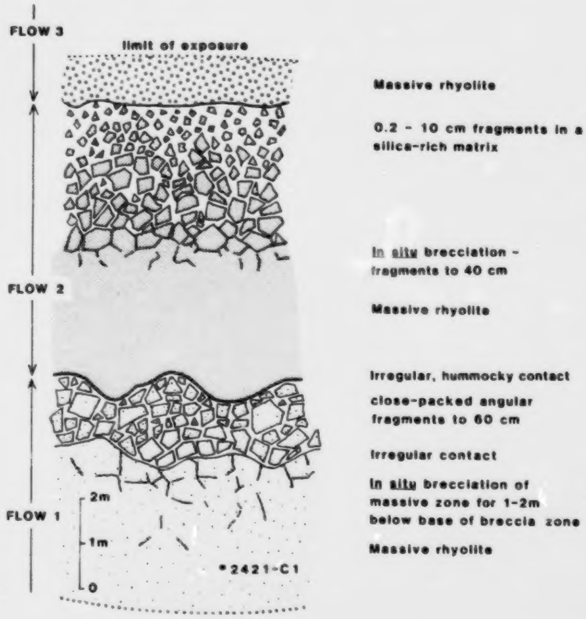
FLOW 3
limit of exposure
Massive rhyolite
0.2 - 10 cm fragments in a silica-rich matrix
FLOW 2
In situ brecciation - fragments to 40 cm
Massive rhyolite
Irregular, hummocky contact
close-packed angular fragments to 60 cm
Irregular contact
FLOW 1
In situ brecciation of massive zone for 1-2m below base of breccia zone
Massive rhyolite
2m
1m
0
•2421-C1

Figure 129: Schematic diagram of primary structures in three successive rhyolite flows, Sharpe Bay rhyolite (F_D, Fig. 121). Position of chemically analyzed sample 2421-C1 shown by dot.

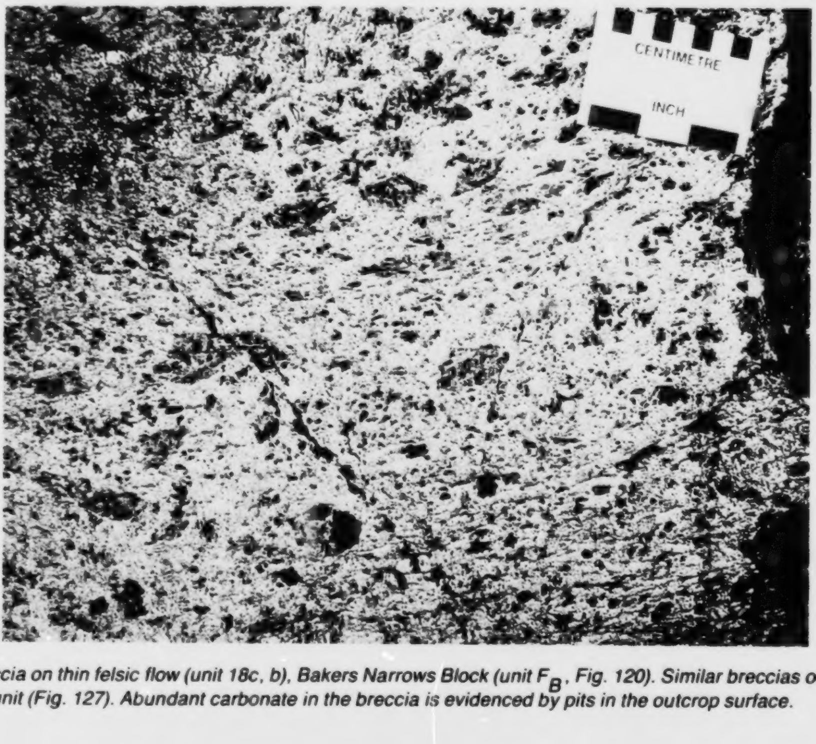
CENTIMETRE
INCH

Figure 128: Flow top breccia on thin felsic flow (unit 18c, b), Bakers Narrows Block (unit F_B, Fig. 120). Similar breccias occur at the tops of several flows in this unit (Fig. 127). Abundant carbonate in the breccia is evidenced by pits in the outcrop surface.

All flows are plagioclase +/- quartz-phyric. Plagioclase phenocrysts (1 — 10%) are euhedral stubby tablets that range from 0.2 to 1.4 mm long. Quartz phenocrysts (2%) are 0.1 — 0.8 mm in diameter and euhedral, with rims of spherulitic overgrowth. The phenocrysts are seté in a recrystallized groundmass of plagioclase microlites (0.02 — 0.1 mm, 50 — 65%) in part overprinted by chlorite, green or brown biotite, epidote and minor fibrous tremolite-actinolite. Very fine grained (0.01 — 0.2 mm) disseminated euhedral magnetite (1 — 5%) occurs in all rocks. Feldspar spherulites, up to 0.2 mm in diameter, compose between 15 and 25% of the groundmass.

Interpretation

Subaqueous rhyolite flows in the Bakers Narrows Block differ significantly in morphology from rhyolite flows in other blocks. Every exposed felsic flow in this sequence conforms to a general model comprising a massive lower portion, with a chilled base, grading upward through a zone of *in situ* brecciation to a flow-top breccia composed of close-packed angular fragments. Thickness of various components, and of entire flows, varies widely but the sequence of structures is constant. In contrast, the large Solodiuk Lake and Grassy Narrows rhyolite complexes exemplify a very different flow type and probably a different rhyolite eruption style. These rhyolite complexes, described elsewhere in this report, are composed of massive rhyolite lobes and pods emplaced in rhyolite microbreccia; the microbreccia has pumiceous components as well as granules and blocks derived from thermal disintegration of the massive lobes.

The differences in felsic flow morphology may reflect difference in depth of emplacement. Shallow depths (low hydrostatic pressures) are required for the formation of pumice and thus the Solodiuk Lake and Grassy Narrows rhyolites probably erupted in a relatively shallow marine regime. The absence of highly vesiculated material associated with the Bakers Narrows rhyolites suggests a somewhat greater depth of emplacement, where hydrostatic pressures would have been sufficient to inhibit a high degree of vesiculation.

INTERPRETATION

The 3.8 km thick Bakers Narrows stratigraphic sequence (Fig. 121) is notable in two important aspects: (1) pyroclastic and epiclastic units are absent, and (2) the sequence is strongly bimodal, comprising mafic flows and rhyolite. Large-scale intercalation of mafic and felsic flow units suggests proximity to source, especially for felsic flows as they presumably were highly viscous and would not have flowed far from their source vents. Large amygdales occur locally in mafic flows throughout the entire sequence, suggesting that most or all of the flows are emplaced at relatively shallow water depths (Table 5). However, the absence of mafic phreatomagmatic pyroclastic deposits and felsic pyroclastics suggests that water was sufficiently deep to inhibit large-scale exsolution of volatiles and resultant pyroclastic eruption styles. Subsidence must have kept pace with volcanic accumulation because deep-water features, such as negligible vesicularity and very small amygdales, are absent in the lower part of the sequence.

Geochemical characteristics of mafic flows in the Bakers Narrows Block are matched almost on a one-to-one basis with the Bear Lake basaltic andesite, suggesting a correlation between the two. The Bakers Narrows section differs lithologically from the Bear Lake basaltic andesite section in that synvolcanic dykes and pillow fragment breccias are not a conspicuous component of the Bakers Narrows sequence, and rhyolite flows are not intercalated in the Bear Lake section. Abundant synvolcanic mafic dykes and felsic lavas are both features of the proximal to central zones of volcanoes (Williams and McBirney, 1979) so these differences presumably reflect separate cross-sections through the proximal zone of a large composite subaqueous volcano.

SOURDOUGH BAY BLOCK

INTRODUCTION

The Sourdough Bay Block (Fig. 3) is bounded on the east by the Thompson Bay Fault and on the west by the Sourdough Bay Fault. The block comprises a homoclinal northwest-facing stratified assemblage composed of mafic to intermediate flows, felsic volcaniclastic rocks and associated felsic dykes, mafic volcaniclastic rocks and sedimentary rocks. The Centennial, Sourdough Bay and Pine Bay massive Cu-Zn sulphide deposits occur in this sequence. The block is cut internally by a north-northwest-trending fault west of McFee Bay that juxtaposes two differing stratigraphic sequences (Map GR87-1-1 and Fig. 130) here named the southern and northern sections. Stratigraphic correlations across this fault are restricted to a distinctive unit of plagioclase-quartz-phyric intermediate flows (unit 12) and a directly underlying unit of plagioclase crystal-rich mafic tuff and lapilli tuff (unit 22a, 21b). The only other possible correlation is the Centennial and Pine Bay Cu-Zn massive sulphide deposits which occur at approximately the same position in both sections (Fig. 130).

The Sourdough Bay Block contains a high proportion of volcaniclastic and sedimentary rocks, as well as the largest felsic complex in the map area. These rocks are mainly exposed in small shoreline outcrops. Six main components of the block are (in no stratigraphic order):

Unit	
7, 8, 9	Mafic to intermediate flows and pillow fragment breccia
12	Plagioclase-quartz phyric intermediate flows
22a, 21b	Plagioclase crystal-rich mafic tuff and lapilli tuff
17	Baker Patton felsic complex
18, 28	Felsic volcanic rocks
29, 30, 33, 36, 38	Volcaniclastic and sedimentary rocks

MAFIC TO INTERMEDIATE FLOWS AND PILLOW FRAGMENT BRECCIA (UNITS 7-9)

Mafic to intermediate aphyric and plagioclase-phyric flows occur in mappable units up to 120 m thick and in smaller unmappable bodies. They are intercalated with intermediate and felsic volcaniclastic rocks and sediments throughout the volcanic section exposed in the Sourdough Bay Block. A 180 m thick unit of pillow fragment breccia outcrops on the peninsula between Thompson Bay and Sourdough Bay.

Southern section

Mafic flows (unit 7) and pillow fragment breccia (unit 9a) form more than 75% of the exposed part of the southern section. The lowermost unit of flows (Fig. 130), exposed on the west shore of Thompson Bay, is 100 m thick, aphyric, and comprises epidotized greenish buff massive and pillowed flows. The succeeding unit, which overlies unit 28b felsic tuff, is 80 m thick, and dominantly aphyric with a porphyritic member near the top. These flows are pillowed, buff-brown to grey-green weathering, epidotized, and contain amygdales to 5 mm (rarely to 2 cm) in diameter. Pillow fragment breccia layers, 7 — 8 m thick, occur between flows.

The west side of the peninsula between Thompson Bay and Sourdough Bay comprises creamy buff weathering, indistinctly bedded pillow fragment breccia (unit 9b). Thin plagioclase-pyroxene-phyric flows are locally intercalated with the breccia, which include both matrix- and framework-supported types. Most breccias are monolithologic with strongly plagioclase and pyroxene-phyric pillow fragments 2 — 30 cm across, locally including complete pillows up to 1 by 3.5 m.

On the west shore of Sourdough Bay massive, buff to creamy buff weathering, aphyric to sparsely plagioclase-phyric flows (unit 7) are poorly exposed. They typically contain 2 — 3% disseminated euhedral pyrite.

Northern section

In the northern section (Fig. 130) more than 120 m of buff-brown weathering aphyric and plagioclase-phyric flows (unit 7, 10) underlie the Baker Patton felsic complex (unit 17). These flows are partly epidotized and contain rare quartz amygdales to 3 mm.

Mafic flows (unit 7), which form the southeast shore of the peninsula at the north end of Sourdough Bay, are not exposed in the map area, but to the northeast comprise aphyric to sparsely plagioclase-phyric pillowed types. Similar flows occur 260 m higher in the sequence, but in the latter locality are chloritized and pyritized. Both these flow units can be traced, to the northeast, into a much thicker monotonous sequence of flows and breccia.

Plagioclase and pyroxene-phyric pillowed flows (unit 8) outcrop west of central Sourdough Bay. They contain up to 20%, 1 — 3 mm plagioclase phenocrysts and in one locality have 20%, 1 — 3 mm pyroxene phenocrysts. They are intercalated with greywacke and siltstone (unit 33).

PLAGIOCLASE-QUARTZ-PHYRIC INTERMEDIATE FLOWS (UNIT 12)

This unit is important because it is a distinctive stratigraphic marker that is present in both the northern and southern sections (Fig. 130), and because it occurs approximately 500 m above both the Pine Bay and Centennial "mine horizons". The morphology of this unit is interesting as it was apparently extruded from a small dome (northeast of the map area) with flows preferentially moving down a paleoslope towards what is now the south-southwest. The dome, or perhaps another topographic feature off the present erosion surface, supplied detritus to the overlying volcaniclastic rocks (unit 33) as they contain an abundance of texturally similar coarsely plagioclase- and plagioclase-quartz-phyric intermediate volcanic fragments.

Flows are buff to buff-white weathering and are pale green to pale grey-green on fresh surfaces. They contain 3-10%, equant, euhedral, complexly twinned plagioclase phenocrysts (0.2 — 2.8 mm), 0-5%, embayed, monocrystalline quartz phenocrysts (0.8 — 4.4 mm) set in a microcrystalline groundmass composed of plagioclase, chlorite, epidote, carbonate and tremolite-actinolite. The typical groundmass texture consists of a felted mosaic of plagioclase microlites with interstitial mafic minerals altered to chlorite, epidote and tremolite-actinolite. Very fine grained and spherulitic groundmass textures are also present. The flows commonly contain 2-5%, flattened 0.5 — 3 mm chlorite-filled vesicles. Most flows contain 3-4%, 0.05 — 0.2 mm leucoxene and magnetite after primary Fe-Ti oxide grains.

PLAGIOCLASE CRYSTAL-RICH MAFIC TUFF AND LAPILLI TUFF (UNITS 22a and 21b)

This 50-100 m thick, poorly exposed unit of plagioclase crystal-rich mafic to intermediate tuff and lapilli tuff directly underlies unit 12 intermediate flows on the peninsula and small islands, at the north end of Sourdough Bay, and 1 km south, on the west shore of the bay. It is intercalated with thin greywacke, siltstone and mudstone beds in northern exposures and is underlain by plagioclase crystal-rich greywacke (unit 33) at its southern termination against the Sourdough Bay Fault. It thins to the northeast and

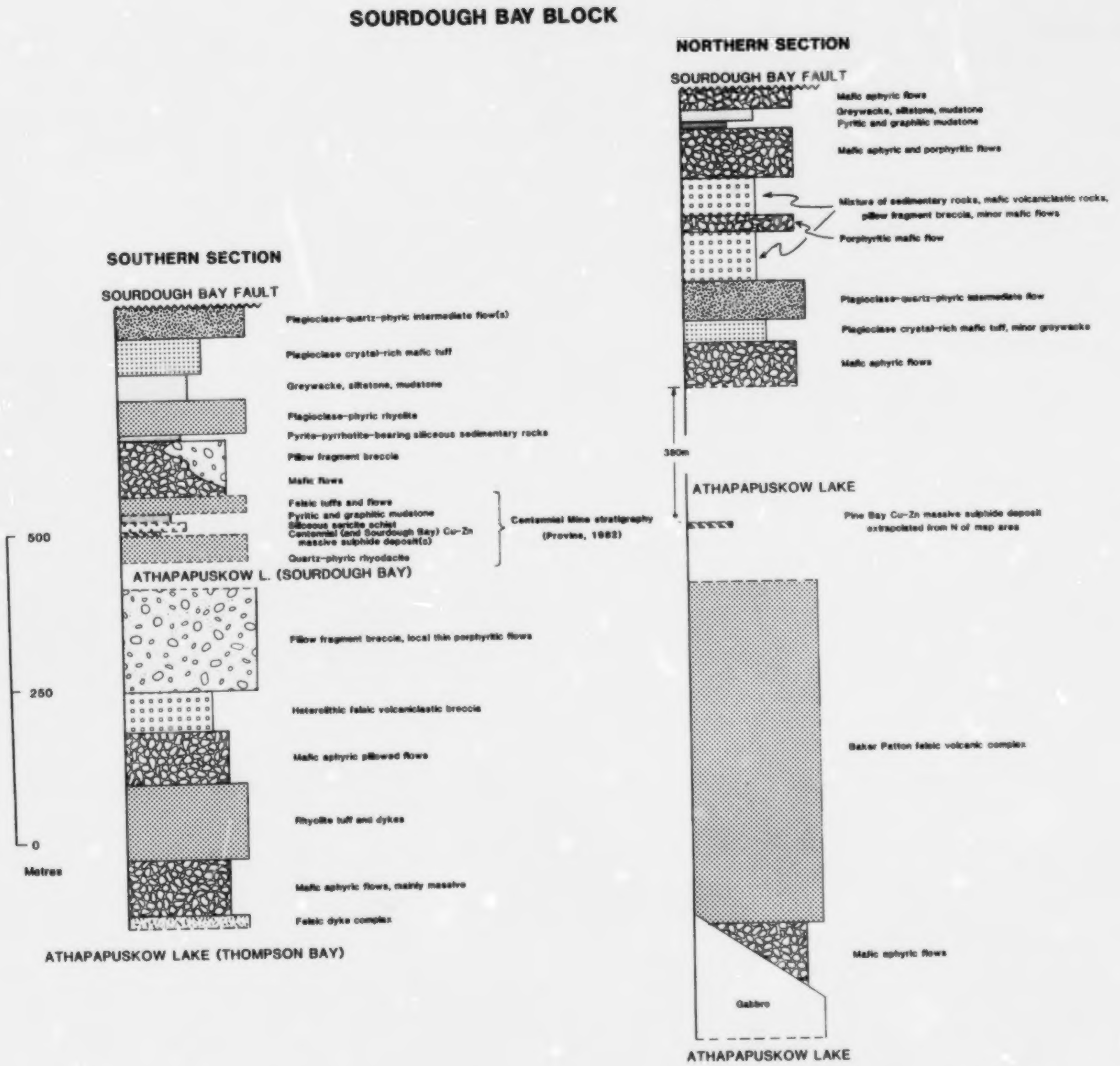
SOURDOUGH BAY BLOCK
NORTHERN SECTION
SOURDOUGH BAY FAULT
Mafic aphyric flows
Greywacke, siltstone, mudstone
Pyritic and graphitic mudstone
Mafic aphyric and porphyritic flows
Mixture of sedimentary rocks, mafic volcaniclastic rocks, pillow fragment breccia, minor mafic flows
Porphyritic mafic flow
Plagioclase-quartz-phyric intermediate flow
Plagioclase crystal-rich mafic tuff, minor greywacke
Mafic aphyric flows
380m
ATHAPAPUSKOW LAKE
Pine Bay Cu-Zn massive sulphide deposit extrapolated from N of map area
Baker Patton felsic volcanic complex
Mafic aphyric flows
Gabbro
ATHAPAPUSKOW LAKE
SOUTHERN SECTION
SOURDOUGH BAY FAULT
Plagioclase-quartz-phyric intermediate flow(s)
Plagioclase crystal-rich mafic tuff
Greywacke, siltstone, mudstone
Plagioclase-phyric rhyolite
Pyrite-pyrrhotite-bearing siliceous sedimentary rocks
Pillow fragment breccia
Mafic flows
Felsic tuffs and flows
Pyritic and graphitic mudstone
Siliceous sericite schist
Centennial (and Sourdough Bay) Cu-Zn massive sulphide deposit(s)
Quartz-phyric rhyodacite
Centennial Mine stratigraphy (Provins, 1982)
ATHAPAPUSKOW L. (SOURDOUGH BAY)
Pillow fragment breccia, local thin porphyritic flows
Heterolithic felsic volcaniclastic breccia
Mafic aphyric pillowed flows
Rhyolite tuff and dykes
Mafic aphyric flows, mainly massive
Felsic dyke complex
500
250
0
Metres
ATHAPAPUSKOW LAKE (THOMPSON BAY)

Figure 130: Representative stratigraphic sections, Sourdough Bay Block, with gabbro intrusions omitted. Northern section includes all rocks northeast of the fault that occur at the south end of McFee Bay. Southern section includes rocks southwest of fault.

dies out just outside the map boundary.

The tuff and lapilli tuff is massive to indistinctly bedded, buff weathering, and pale grey-green on fresh surfaces. Up to 30% subhedral plagioclase (0.5 — 1 mm) and 0-2% subhedral quartz (1 — 7 mm) are present. Fragments are typically indistinguishable from intervening matrix material due to recrystallization and imposition of a moderately strong foliation. Where observed they are tectonically flattened, partly silicified, and up to 17 cm in longest dimension. In best preserved fragments a primary microvesicularity is indistinctly retained. Some lithic fragments are present which texturally resemble unit 12 intermediate flows.

BAKER PATTON FELSIC COMPLEX (UNIT 17)

Felsic volcaniclastics and hypabyssal intrusions on the peninsula between Thompson Bay and Sourdough Bay are the western portion of a large felsic complex, here termed the Baker Patton complex after the mineralized property north of Murray Lake. The complete size of this felsic pile is not known but it can be traced to Thompson Lake, 4.8 km to the northeast. Within the map area the maximum thickness of this complex is 820 m. To the south the complex is in fault contact with the southern section (Map GR87-1-1). The unit is best exposed along the shoreline of

McFee Bay, where it is composed of tuff, lapilli tuff and abundant dacite/rhyolite dykes.

Tuff, lapilli tuff (unit 17a)

Felsic tuff and lapilli tuff occur as small screens between numerous dacite dykes. The unit is strongly foliated, and locally tectonically disrupted or tightly folded. The lapilli tuffs are monolithologic, matrix-supported and stratified, with various types (defined by fragment type and matrix colour and composition) interlayered with one another and with fine grained tuff. Stratification (rarely observed) is 0.5 — 6 m thick with some individual beds internally laminated on a 1 — 5 cm scale. Lapilli are lens-shaped, less than 5 cm long, and are quartz-phyric, plagioclase-phyric or aphyric. Matrix varies from green to buff; quartz and plagioclase crystals occur in some beds.

Undivided massive felsic rocks and possible flows (unit 17b)

White-weathering, plagioclase-phyric and plagioclase-quartz phyric, massive felsic rocks are exposed between McFee Bay and Sourdough Bay. They contain 2-5%, 0.5 — 1 mm vesicles, are locally strongly spherulitic, and rarely exhibit polygonal jointing. In one locality podiform bodies of massive rhyolite occur within buff-brown weathering felsic material, superficially resembling subaqueous rhyolite flows. The massive felsic rocks are cut by quartz-phyric dykes.

Felsic dykes (unit 17c)

Felsic dykes are the predominant lithology exposed in McFee Bay. They are 40 cm to at least 7 m thick, with chilled margins (10 — 50 cm thick) against felsic tuff and older dykes. Predominant dyke trends are 345° — 355° and 025° — 030°. Dykes are commonly quartz and plagioclase-phyric but phenocrysts are either small or absent in the chilled zones.

Many of the felsic dykes contain dark green to brown mafic inclusions in a zone up to 2 m thick adjacent to the chilled margins. The inclusions are strongly elongate parallel to regional schistosity and are 4 — 40 cm long (Fig. 131). The largest inclusions occur in the thickest dykes.

The dykes contain 2-25% quartz phenocrysts (0.2 — 1.6 mm) that are euhedral to strongly embayed single crystals. Plagioclase phenocrysts (0.2 — 3 mm) range in abundance from 5-25%; they are euhedral, tablet-shaped and polysynthetically twinned. Disseminated Fe-Ti oxide microphenocrysts (0.01 — 0.25 mm) form 0-2% of the rocks. The groundmass consists of feldspar, chlorite, biotite, epidote and minor hematite, carbonate, leucoxene, apatite and sericite.

Interpretation

The portion of the Baker Patton felsic complex exposed in the map area is interpreted to be proximal, because it is composed of fragmental (pyroclastic?) rocks intruded by very abundant porphyritic felsic dykes. The large number of felsic dykes precludes definition of internal stratigraphy.

FELSIC VOLCANIC ROCKS (UNITS 18 and 28)

Three separate felsic units occur in the southern section of the Sourdough Bay Block (Fig. 130). These include: a 150 m thick unit of felsic tuff (unit 28b, 18) on the peninsula between Thompson Bay and Sourdough Bay, approximately 100 m of felsic rocks associated with Centennial Mine, and a 60 m thick massive plagioclase-phyric rhyolite (unit 18b) on the west shore of Sourdough Bay.

The felsic tuff unit (28b, 18) is part of a stratified package of intermediate flows and pillow fragment breccias. It weathers medium brown, is crudely stratified, and is composed of variable amounts, sizes and proportions of quartz crystals (5—10%, 1 — 3 mm), plagioclase crystals (10—15%, 2 — 3 mm) and white rhyolite lithic fragments (2 mm — 25 cm). The tuff is intruded by white weathering rhyolite bodies up to 4 m across. These are irregular to straight in trend and contain fewer and smaller phenocrysts than the enclosing tuff.

Felsic breccias and tuff, not exposed at surface, are associated with the Centennial Cu-Zn massive sulphide deposit and have been described by Provins (1980). They include a unit of felsic breccia (greater than 60

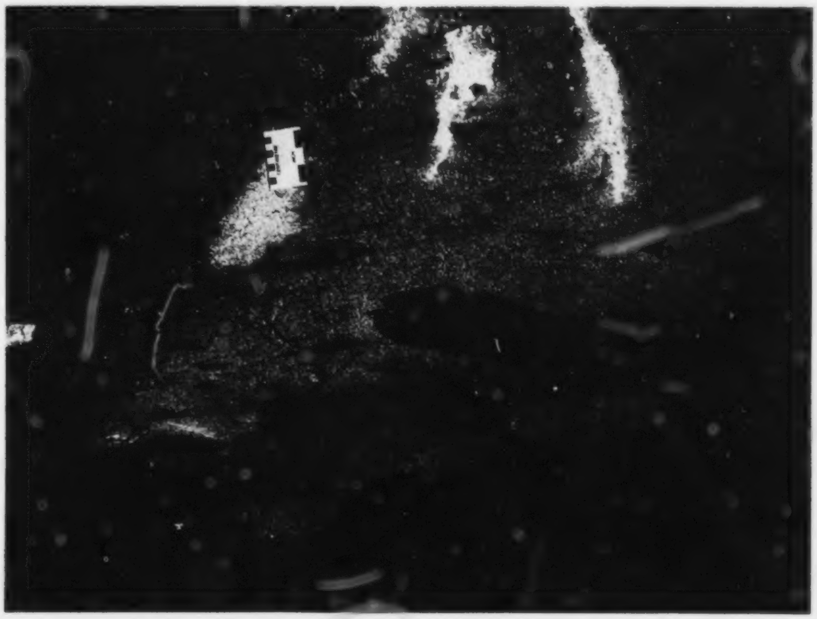

Figure 131: Inclusions in a quartz-plagioclase-phyric rhyolite dyke (unit 17c), north shore of Thompson Bay, Athapapuskow Lake. This dyke has a sharp, irregular intrusive contact with an older felsic dyke; inclusions occur within the rhyolite dyke but are absent in the 30 cm thick chilled margin of the dyke. Inclusions are flattened into the plane of schistosity.

m thick) that hosts the orebody. The breccia is composed of tectonically flattened quartz-phyric fragments and is crudely layered with bedding defined by variations in fragment size. A 50 m thick unit of carbonate-bearing felsic tuff and breccia also occurs 40 m above the Centennial orebody. It is separated from the breccias that host the orebody by a 30 m thick unit of pyritic mudstone.

The plagioclase-phyric rhyolite (unit 18b) on the west shore of Athapapuskow Lake is 60 m wide. It overlies pyrite-pyrrhotite-rich siliceous sediments (unit 38c) and its top is truncated to the northwest by the Sourdough Bay Fault. The rhyolite is white to rusty weathering and buff to pale grey on fresh surfaces. It contains 5—10%, euhedral, stubby plagioclase phenocrysts and glomerocrysts (0.5 — 2.0 mm). The rhyolite is massive to locally highly fractured; the fractures are filled with ankerite and lesser amounts of hematite, epidote, chlorite, silica and pyrite. Massive rhyolite contains abundant 0.25 mm spherulites, up to 20% carbonate and quartz-filled vesicles, and local poorly defined polygonal joints. It resembles the massive columnar jointed rhyolite and breccia body (unit 18b) that occurs north of Grassy Narrows on Manistikwan Lake.

VOLCANICLASTIC AND SEDIMENTARY ROCKS (UNITS 29, 30, 33, 36 and 38)

Volcaniclastic and sedimentary rocks form approximately 25% of the exposed portion of the Sourdough Bay Block. They are intercalated with mafic flows and mafic pillow fragment breccia at both outcrop scale and as mappable units. At one locality, on the peninsula at the north end of Sourdough Bay, the mixed volcaniclastic and sedimentary assemblage can be traced laterally (northeast of the map area) through an abrupt facies transition into a sequence dominated by mafic flows and associated breccias.

Northern section

The thickest unit of volcaniclastic and sedimentary rocks outcrops in the northern section (Fig. 130), on the peninsula at the north end of Sourdough Bay. At that locality mafic to intermediate volcaniclastic breccia, greywacke, siltstone, mudstone and graphitic-pyritic mudstone form a 200 m thick unit intercalated with thin mafic flows and mafic pillow fragment breccias. They directly overlie the distinctive mappable unit of intermediate plagioclase-quartz phyric flows (unit 12). Another unit of greywacke, siltstone and mudstone, topped by strongly pyritic mudstone, has been encountered in drill holes under the lake west of the peninsula. These sediments have been extrapolated to the northeast of the lake and are shown on the geological map (Map GR87-1-1) despite the fact they were not observed to outcrop.

Approximately 30-40% of the volcaniclastic/sedimentary sequence on the peninsula consists of thin bedded (1—40 cm), grey weathering turbiditic greywacke, siltstone and mudstone. Graded A and AB beds, scour channels, load structures and calcareous concretions are characteristic of these rocks. The greywacke beds are composed of plagioclase-phyric intermediate volcanic rock fragments (0.2 — 0.4 mm) and plagioclase crystal fragments set in a fine grained recrystallized matrix of plagioclase, chlorite, epidote and tremolite. Although the turbiditic greywacke, siltstone and mudstone occur throughout the sequence they are most abundant in the upper half of this unit, towards the west side of the peninsula.

Buff weathering, massive greywacke forms approximately 20% of the volcaniclastic/sedimentary assemblage. Bed contacts in this greywacke are nebulous and, where observed, are defined by rusty brown weathering siltstone bed tops and by local, well defined grading. Interbeds of siltstone and mudstone are negligible compared to the grey weathering turbiditic greywacke, siltstone and mudstones. The buff weathering greywackes are more typical of the east side of the peninsula and are commonly spatially associated with the plagioclase-quartz-phyric intermediate flows of unit 12. They are composed of plagioclase-phyric (and more rarely also quartz-phyric) intermediate volcanic rock fragments that are texturally identical to, and are clearly derived from, the flows of unit 12.

Heterolithologic and monolithologic mafic to intermediate breccias form 40 to 50% of the volcaniclastic sedimentary sequence in the northern section. Breccia beds are 1 m to over 6 m thick, poorly sorted, generally ungraded (rarely reverse graded), and contain subangular, matrix-supported fragments up to 30 cm across. Some monolithologic breccias are clearly pillow fragment breccias. The predominant heterolithologic breccias are composed of a mixture of plagioclase-phyric mafic volcanic fragments, aphyric mafic volcanic fragments and coarsely plagioclase-phyric (and rarely also quartz-phyric) intermediate volcanic fragments. The intermediate volcanic fragments are compositionally and texturally similar to the plagioclase- and plagioclase- and quartz-phyric flows of unit 12. These heterolithologic breccias are interpreted to have been deposited from subaqueous debris flows.

The greywacke and coarse volcaniclastics on the peninsula at the north end of Sourdough Bay contain clasts of mafic and intermediate volcanic flow rocks that appear to have been derived locally and were deposited in a subaqueous environment by sediment gravity flows, including turbulent density currents and debris flows. The lateral facies change to the northeast (outside the map area) into a thick sequence of basalt flows and breccia suggests that the latter were the source of detritus, with the sedimentary accumulations shed downslope towards what is now the south-southeast. The broad upward fining of the mixed volcaniclastic and sedimentary sequence suggests that positive relief in the source area decreased as this assemblage of volcaniclastic rocks accumulated.

Southern section

Volcaniclastic and sedimentary rocks are a relatively minor component of the southern section (Fig. 130). They include: a 60 m thick unit of heterolithologic intermediate breccia (unit 30) exposed on the peninsula between Thompson Bay and Sourdough Bay; a 30 m thick unit of graphitic and pyritic mudstone exposed only in the Centennial Mine; a single, small outcrop of finely laminated pyrrhotite- and pyrite-bearing siliceous sedimentary rocks (unit 38c) west of Sourdough Bay; and thin-bedded greywacke, siltstone and mudstone (unit 33) on the west shore of Sourdough Bay.

The heterolithologic breccia (unit 30) overlies aphyric and plagioclase-pyroxene-phyric mafic flows (unit 7) and is overlain by thick bedded mafic pillow fragment breccia (unit 9a). These breccias are poorly sorted, include both fragment- and matrix-supported types, and contain tectonically flattened angular to subrounded fragments. In approximate order of abundance contained fragments are: light grey weathering aphyric felsic volcanic rocks, buff weathering aphyric intermediate white weathering volcanic rocks, and white weathering chert. This 60 m thick unit has a strike length of 1.4 km, truncated to the north by a fault and covered to the south by Athapapuskow Lake.

The 30 m thick graphitic and pyritic mudstone unit in the Centennial Mine occurs 60 m stratigraphically above the massive Cu-Zn sulphide orebody. According to Provins (1980), this unit contains interbeds of chert, cherty carbonate and thin laminae of earthy pyrite.

The one small exposure of finely laminated pyrrhotite- and pyrite-bearing siliceous sedimentary rocks (unit 38c) on the west shore of Sourdough Bay occurs at the contact between an underlying unit of mafic aphyric flows (unit 7) and an overlying massive rhyolite flow (unit 18b). This unit is probably a sulphide-bearing chert or siliceous tuff and is only important because it occurs within the same general sequence of rocks that contains the Centennial and Sourdough Bay massive Cu-Zn sulphide deposits.

Greywacke, siltstone and mudstone (unit 33), exposed on the west shore of Sourdough Bay, are plagioclase-crystal-rich, are well bedded, and display turbidite bedforms. They are similar to, and probably belong to, the same general sequence as greywacke, siltstone and mudstone (unit 33) of the northern section. The only difference is that these sediments occupy a slightly lower stratigraphic position (below rather than above the distinctive unit 12 intermediate flows).

Interpretation

The volcaniclastic and sedimentary rocks in the Sourdough Bay Block are intercalated at all scales with pillowed mafic to intermediate flows and pillow fragment breccias indicating that they were deposited in a subaqueous environment contemporaneous with active volcanism. Bed forms and primary structures indicate that these rocks were deposited by subaqueous gravity flows, including turbulent density currents and debris flows. An abundance of clasts obviously derived from spatially associated volcanic units suggests they were probably derived by slumping of detritus from adjacent active volcanic structures. Periods of volcanic quiescence during which mudstones and chemical sediments accumulated are important as such rocks appear to be potential hosts for massive Cu-Zn sulphide deposits.

VOLCANIC ENVIRONMENT

The Sourdough Bay Block contains portions of two different volcanic environments. The Baker Patton felsic complex, dominated by high level felsic dykes, felsic pyroclastic rocks and possible felsic flows, is interpreted as the central (near vent) zone of a felsic edifice. In contrast, the stratified mafic sequence of subaqueous flows, volcaniclastic rocks and subordinate sedimentary rocks indicates a more distal environment. An increase to the northeast in proportion of flows to volcaniclastics suggests that the source area for more mafic components of the sequence is outside the map area, northeast of Sourdough Bay.

The Centennial, Sourdough Bay and Pine Bay (outside of the map area) massive Cu-Zn sulphide deposits all occur within the mafic flow and volcaniclastic sequence. The sulphide zones are associated with graphitic and pyritic mudstones, siliceous mudstone, and felsic volcaniclastics, indicating that deposition of the predominantly mafic sequence was punctuated by episodes of felsic volcanism and sedimentation of fine muds and chemical sediments. The Centennial and Pine Bay deposits have discordant footwall hydrothermal alteration zones and are therefore proximal by definition (Plimer, 1978).

GRASSY NARROWS ZONE

INTRODUCTION

The Grassy Narrows Zone consists of a number of fault slices containing a distinctive bimodal assemblage of basalt and rhyolite flows. The zone has a maximum width of 1340 m between Shore Lake and Rosenberg Lake. It is bounded on the east by the Inlet Arm Fault and on the west by the Rosenberg Lake Fault and associated intrusions (Fig. 3). The zone extends north out of the map area and south to the north end of Inlet Arm (Schist Lake). It is named after the narrow, grassy inlet to the northeast arm of Manistikwan Lake.

At least three separate north-trending fault slices are present within the zone (Fig. 132). They are bounded by faults that are either parallel to, or splay from, the Inlet Arm Fault, which is the dominant fault in the area. Within the westernmost fault slice there are two west-trending faults across which the facing direction of flows changes by 180°. In the easternmost fault slice there is a tight syncline-anticline pair with axial planar zoned gabbro sills (unit 41). Due to structural complexity of the zone the thickness of rock units and the total stratigraphic sequence is unknown.

There are only four volcanic/sedimentary units in the zone; they are:

Unit	
7, 8	Grassy Narrows basalt
18	Rhyolite
33	Siltstone, greywacke, pyritic mudstone
32	Felsic sandstone and pebble conglomerate

GRASSY NARROWS BASALT (UNITS 7 and 8)

Grassy Narrows basalt outcrops in three separate fault-bounded slices in the tectonically dismembered Grassy Narrows Zone (Fig. 132). A folded, but dominantly west-facing, series of flows east of Grassy Narrows has an estimated undeformed stratigraphic thickness of 500 m. West and north of Grassy Narrows approximately 300 m of basalt is exposed in a west-facing homoclinal sequence, and due west of Grassy Narrows a homoclinal, 350 m thick, east-facing section of flows is exposed. Grassy Narrows basalt is texturally and compositionally similar to Sawmill Lake basalt of the Whitefish-Mikanagan Lake Block and is clearly different from basalt flows of the adjacent Bear Lake and Manistikwan Lake blocks.

Basalt flows in the three fault slices share a number of distinctive characteristics. The flows have a uniform, smooth, pale buff-brown to orange-brown weathered surface with a 3 to 5 mm thick creamy buff weathering rind. They have very low vesicularity; only one exposure contains more than 2% amygdales. Pillows are typically uniform in size (30 — 80 cm), are bun- or sack-shaped, and do not have epidotized core or rim zones. Flows are further characterized by an absence of flow breccia tops and by negligible amounts of interpillow hyaloclastite. Flow contacts are difficult to identify due to the uniform character of flows and absence of marginal vesicular zones or flow breccia. Flows are aphyric to sparsely plagioclase-phyric, with the exception of prominent plagioclase-phyric varieties (unit 8) that outcrop in small shoreline exposures south of Grassy Narrows and on the islands farther south in the main part of Manistikwan Lake (Map GR87-1-1). The unit contains very few synvolcanic dykes.

The basalts are strongly recrystallized and composed of a mixture of colourless tremolite-actinolite, fine grained epidote and 5-10% semi-opaque grains of epidote, leucoxene and sphene after primary Fe-Ti oxide (0.01 — 0.02 mm). In well preserved samples tremolite-actinolite has overgrown the primary mafic mineral and is interstitial to stubby plagioclase laths (0.3 — 2 mm), the latter variably replaced by fine grained epidote. Plagioclase phenocrysts (0.5 — 1.5 mm) are rare (up to 1%).

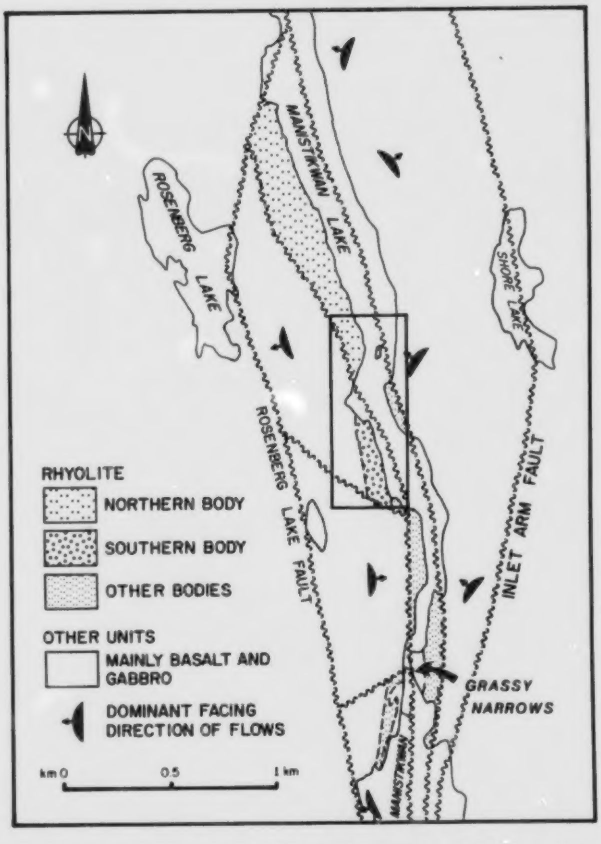

Figure 132: *Facing direction of Grassy Narrows basalt flows and location of major rhyolite bodies, Grassy Narrows Zone. See Figure 137 for detailed geology of area within rectangle.*

Major faults and, in the easternmost slice, tight isoclinal north trending folds have deformed the Grassy Narrows basalt. At an outcrop scale, pillows are tectonically flattened, with long axes oriented parallel to northerly trending schistosity. In fold hinges, where flow contacts are at a high angle to the direction of tectonic flattening, pillow elongation no longer reflects primary flattening, but facing directions can still be determined (Figs. 133, 134).

Geochemistry

Three analyses of relatively unaltered Grassy Narrows flows are listed in the Appendix. The flows are distinctly different in composition from the Bear Lake basaltic andesite of the adjacent Bear Lake Block (Fig. 135, 136). They range in SiO_2 content from 49.32 to 53.57% and in MgO from 8.73 to 5.56% (calculated H_2O- and CO_2-free). They are distinguished from other basalt flows in the map area by a combination of high TiO_2 (0.93 —

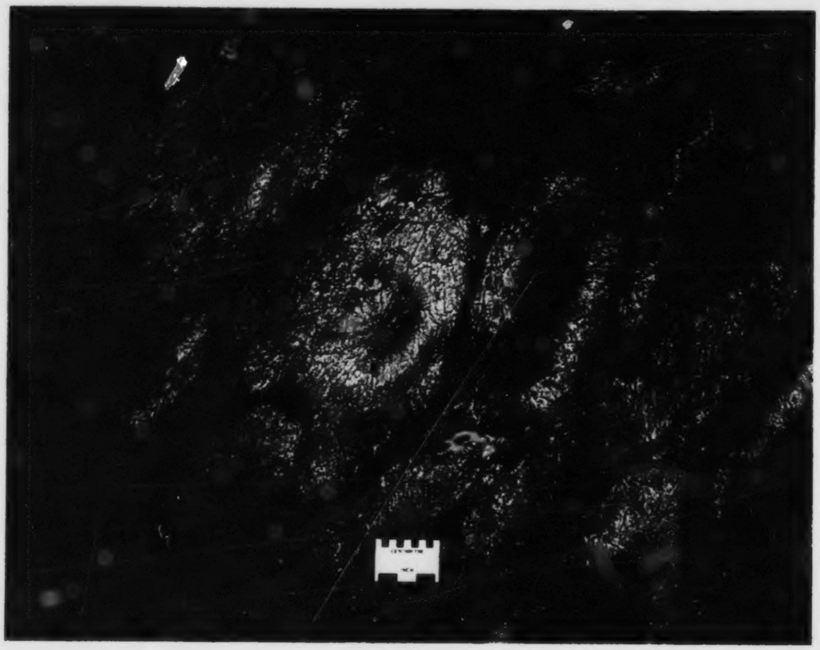

Figure 133: Tectonically flattened pillows from tightly folded Grassy Narrows basalt flow (unit 7), 500 m west southwest of Shore Lake. Crescent- and pear-shaped pillows (refer to Fig. 134) indicate flow tops to upper right of photograph with flattening direction of pillows at a high angle to primary stratification.

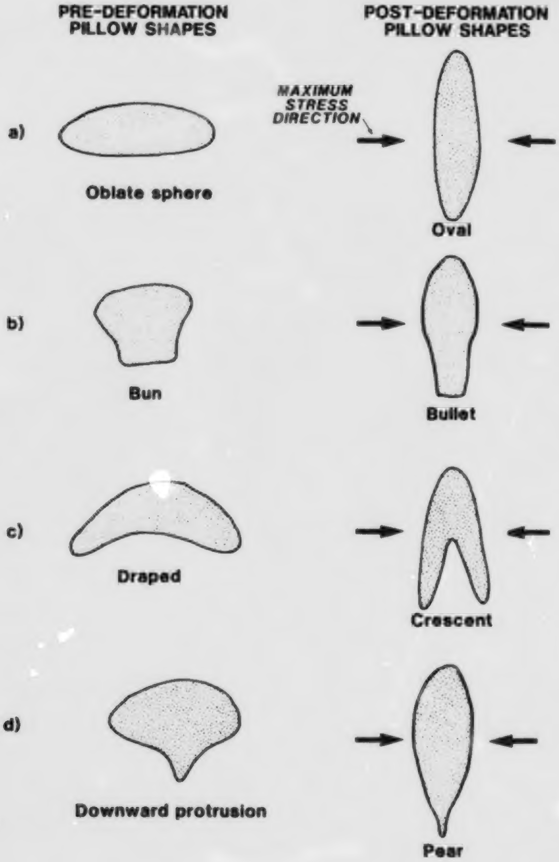
PRE-DEFORMATION PILLOW SHAPES
POST-DEFORMATION PILLOW SHAPES
MAXIMUM STRESS DIRECTION
a)
Oblate sphere
Oval
b)
Bun
Bullet
c)
Draped
Crescent
d)
Downward protrusion
Pear

Figure 134: Primary facing direction of mafic flows in deformed terrains can be ascertained from bullet-, crescent-, and pear-shaped pillows (b, c, and d), formed by tectonic flattening of bun, draped and downward protruding types at a high angle to their primary orientation. Oval pillows (a) in deformed flows are unreliable indicators of primary pillow and flow orientation.

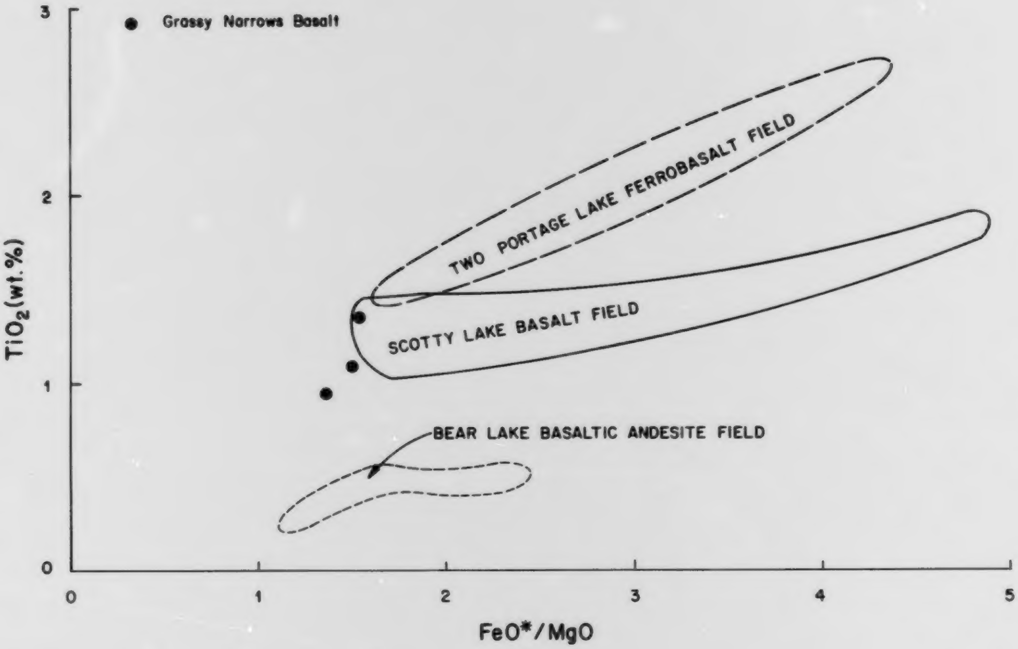

Figure 135: TiO$_2$ vs. FeO*/MgO, Grassy Narrows basalt-basaltic andesite, compared to Bear Lake basaltic andesite.

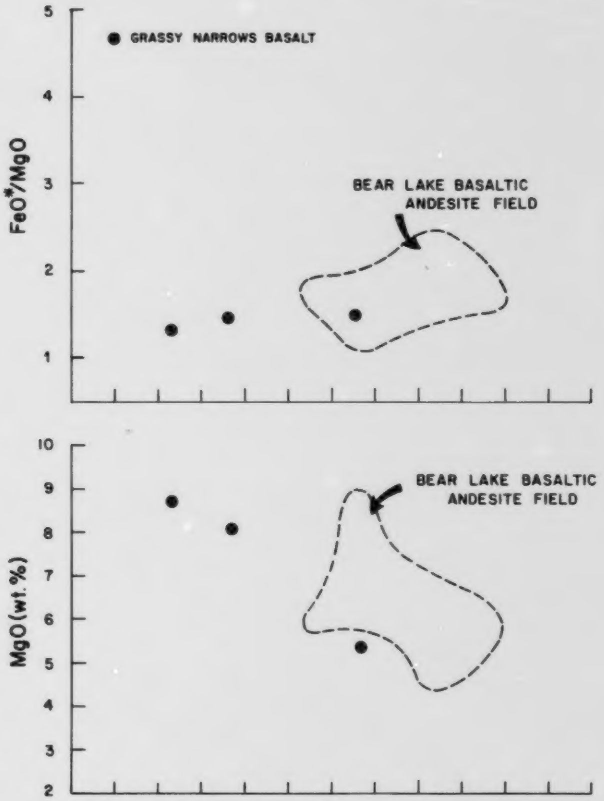

Figure 136: FeO*/MgO vs. SiO$_2$ and MgO vs. SiO$_2$, Grassy Narrows basalt-basaltic andesite, compared to Bear Lake basaltic andesite.

1.32%), high Ni and Cr (average 57 and 247 ppm, respectively), and high Zr/Y ratio (1.70 — 1.89). They have much lower P_2O_5 (0.10 — 0.11%) and total iron (FeO^* = 7.04 — 9.98%) than other TiO_2-rich units in the area (Scotty Lake basalt and the Two Portage Lake ferrobasalt).

Interpretation

Grassy Narrows basalt is composed entirely of subaqueous lava flows without intercalated pyroclastic or sedimentary rocks. The flows have a low overall vesicularity (generally less than 2%) which could be interpreted to indicate deposition in deep water. However, the presence of large gas cavities (to 15 cm) throughout the sequence east of Grassy Narrows indicates relatively shallow water conditions (Table 5). Thus, the low vesicularity may have been due to a low volatile content in the magma. The absence of large gas cavities in flows west and northwest of Grassy Narrows suggests they may have been deposited in deeper water. Absence of interflow basaltic pyroclastic rocks suggests deposition at depths greater than that at which eruption style changes to phreatomagmatic (about 300 m; Table 5). The paucity of synvolcanic dykes indicates the flows are not part of a central vent complex.

Grassy Narrows basalt and Sawmill Lake basalt are sufficiently similar in chemistry, texture and flow morphologies to be one of the few basalt units that can be correlated from one structural block to another. Their host blocks, the Grassy Narrows Zone and Whitefish Lake-Mikanagan Lake Block, respectively, are also similar in other respects. Both are characterized by numerous internal faults, juxtaposition of opposite-facing sequences across faults, internal isoclinal folds, a wide variety of mafic intrusions, and an absence of synvolcanic dykes.

RHYOLITE (UNIT 18)

Rhyolite flows comprise about 25% of the Grassy Narrows Zone. Two rhyolite bodies are described in detail: 1) a massive, sparsely plagioclase-phyric flow (northern body; Fig. 132, 137), and 2) a rhyolite complex comprising massive lobes in a microbreccia (southern body; Fig. 132, 137). Brief descriptions of various small units are also included.

Northern body

The northern rhyolite body (Fig. 132, 137) is interpreted to be a single west-facing massive flow that is exposed for a strike length of 1.2 km with a maximum width of 180 m. The complete length and thickness of this flow is not known because it is truncated to the north and west by faults and is covered by Manistikwan Lake to the east and south. Where best exposed (at the south end; Fig. 93) it is zoned from east to west (Peloquin et al., 1982) and contains a basal unit of massive, columnar-jointed rhyolite, a central unit of brecciated rhyolite in which columnar jointing is less distinct, and an upper unit of brecciated rhyolite in which columnar jointing is rarely preserved. The rhyolite is sparsely plagioclase-phyric (trace to 2%, 0.4 — 1.5 mm) and contains abundant spherulites (55 — 65%, 0.08 — 0.3 mm in diameter; Fig. 138).

In the basal massive rhyolite zone, joint-bounded columns are typically 10 to 20 cm in diameter, four-to-six-sided (Fig. 139), and variable in orientation from shallow east-plunging in the north to shallow southeast-plunging in the south (Fig. 137). Vesicles (less than 10%) range from pinhead-sized spheres to 3 cm by 2 mm flattened discs; the flattening is probably primary as it is perpendicular to column axes and is not parallel to the regional schistosity. The outer 1 — 4 cm of some joint columns are finely brecciated, with 0.1 to 3 cm angular fragments in an olive-green sericitic matrix. The degree of brecciation increases westward across the outcrop displaying a transition from massive rhyolite to brecciated rhyolite (Fig. 137).

The origin of the breccia in the upper zone, on the west side of the outcrop, can be explained by more than one mechanism. One origin, thermal fracturing of joint columns and accompanying alteration adjacent to

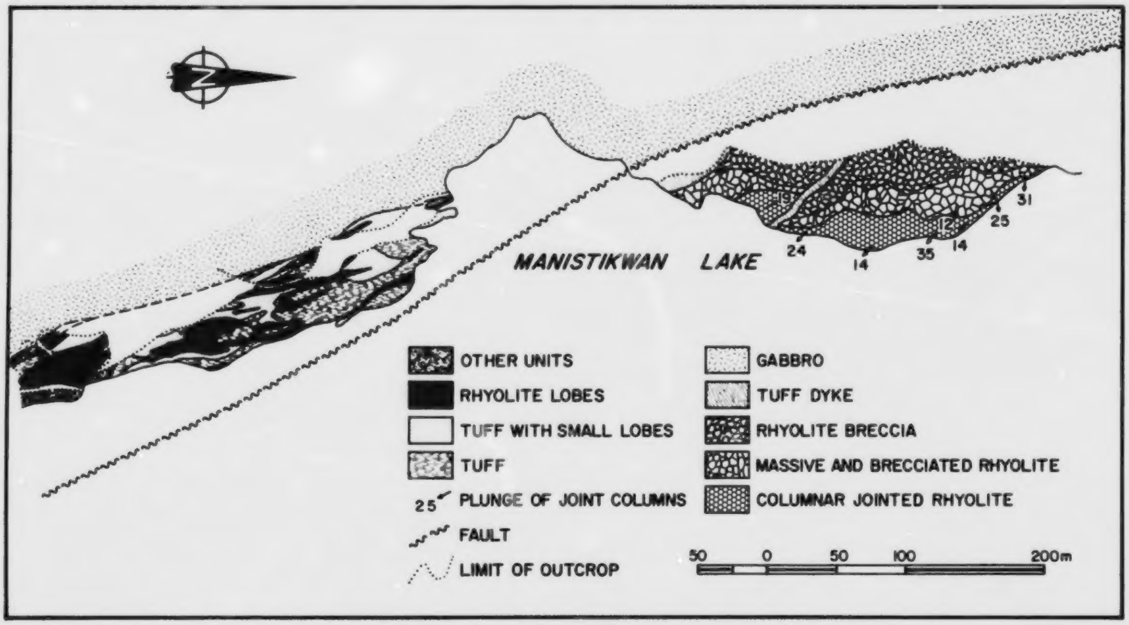

Figure 137: Distribution of rock types in the northern massive and brecciated rhyolite body and the southern rhyolite lobe-microbreccia body, Grassy Narrows, Manistikwan Lake. After Peloquin et al. (1982), Peloquin (1981) and Ayres (pers. com. 1981). Position of fault is from regional mapping (Fig. 132, Map GR87-1-1).

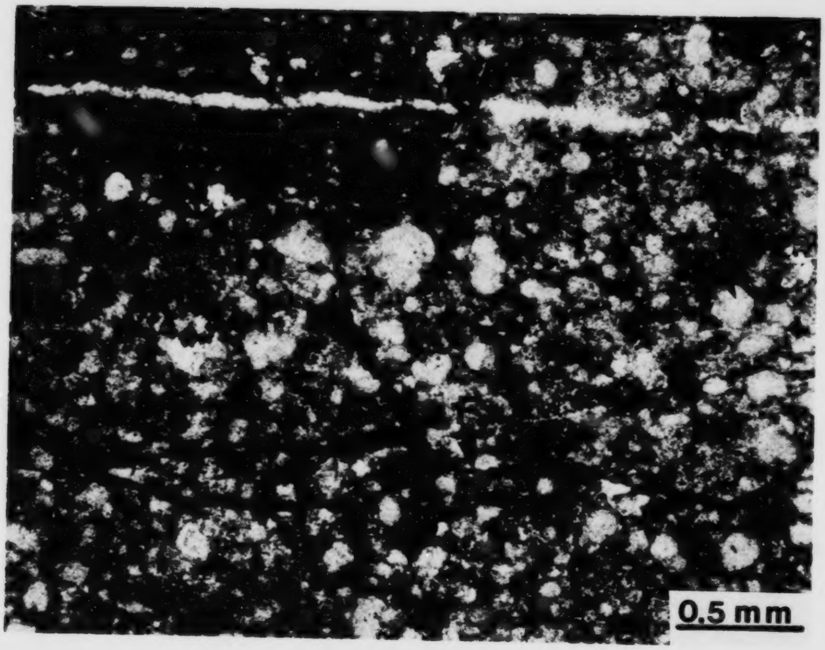

Figure 138: *Microfractured, massive spherulitic (sph) rhyolite (unit 18b), transition zone of northern flow (Fig. 137), Grassy Narrows zone. Fractures (F) are short, discontinuous and locally altered (A) to a mixture of sericite and minor chlorite. Altered rhyolite is dark grey in this photomicrograph. Sample 3441-2, plane polarized light.*

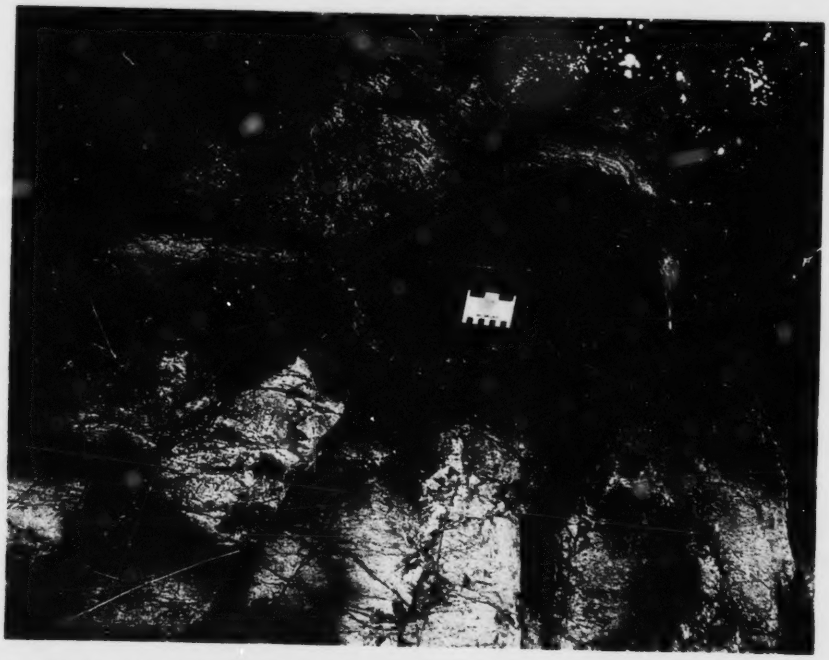

Figure 139: *Columnar joints in massive phase of Grassy Narrows rhyolite (unit 18b, northeast arm of Manistikwan Lake; see also Fig. 137). Columns are polygonal in cross-section and plunge into the lake at about 25°.*

fracture surfaces, is supported by the following observations:

1) local preservation of columnar joints in the breccia of the upper zone;
2) presence of small irregular bodies of massive columnar jointed rhyolite enclosed in breccia;
3) complete transition, visible in certain columns, from minor brecciation adjacent to joints to complete fracturing and brecciation of the entire column; and
4) nature of interfragment contacts which suggests *in situ* brecciation. Although the breccia appears to consist of light coloured fragments set in a light grey matrix, the "matrix" is a sericite-carbonate alteration that is developed to varying degrees along an anastomosing network of hairline fractures (Fig. 140).

The presence of columnar joints and the superimposed fine-scale fracture network in the western breccia unit indicates that in general there has been negligible interfragment movement. In this sense, the "breccia" is better termed a crackled, highly altered rhyolite. A flow-top or crumble breccia that displays significant interfragment movement, which would be anticipated at the top of a flow, is not exposed (possibly due to faulting; Fig. 132 and 137).

Southern body

The southern body (Fig. 132 and 137) consists of lensoid podiform bodies of massive, white-weathering rhyolite enclosed by light yellow-green weathering microbreccia (Fig. 141). The rhyolite complex is similar to rocks in the Archean Abitibi belt near Noranda, Quebec. These Archean rhyolites have been variously described as subaqueous flows (De Rosen-Spence et al., 1980) and subaqueous pyroclastics intruded by rhyolite (Gelinas et al., 1978).

The southern body has been mapped in detail (Peloquin et al., 1982; Ayres, pers. comm., 1981) and the following observations have been made:

1) Massive rhyolite lobes comprise 20% of the rhyolite complex; they range in thickness from 0.15 to 6 m and in length from 0.5 to 30 m. They are enclosed in a crudely layered tuff to tuff breccia matrix.
2) Lobes are partly to completely enclosed by tuff breccia envelopes several tens of centimetres wide and in many places best developed at the ends of lobes. The tuff breccia contains more than 50% rhyolite blocks up to 30 cm across.
3) Lobes range from aphyric to porphyritic with up to 10% quartz and 5% plagioclase phenocrysts; these are 0.2 — 0.8 mm long. Texturally similar lobes occur in discrete zones several tens of metres thick.
4) There is a direct correlation between the size and abundance of phenocrysts in the lobes with those in the enclosing tuff.
5) The tuff and lapilli tuff occur in crude beds that are generally lenticular and 50 cm to more than 2 m thick. Bedding is defined by variation in abundance and size of rhyolite clasts, crystals and accessory mafic clasts.
6) The uppermost 5 m of the rhyolite is pillowed; pillows vary in length from 0.5 to 6 m.

Peloquin et al. (1982) interpret the tuff and lapilli tuff to be a pyroclastic deposit. The lobes are interpreted by them to be minor flows on the surface of the pyroclastic deposit; their emplacement is considered to have been accompanied by quenching and downslope movement to produce the envelopes of tuff breccia. The presence of tuff breccia above the lobes suggests to the authors that the lobes were rapidly covered by contemporaneous tuff. They suggest that some of the brecciation of the lobes occurred after they were covered by the tuff.

The authors of this report concur with the observations noted above. Additional observations are that some of the lobes display well developed flow banding, flow folds and vesicular margins, all consistent with an extrusive origin. Brecciation of the lobes ranges from *in situ* disintegration to complete detachment of fragments from the massive rhyolite lobes (Fig. 142). Petrographic similarity of microbreccia and isolated rhyolite fragments to associated rhyolite lobes suggests that all coarser fragmental material was derived from massive rhyolite. Within the complex, sharp contacts exist between lobe — microbreccia units with different phenocryst contents. Individual units have distinctive phenocryst populations that are identical in lobes, fragments and enclosing microbreccia. These units are locally separated by thin intercalations of heterolithologic rhyolite breccia and local mudstone (Fig. 143).

All features in the southern rhyolite complex are interpreted to have formed in a manner similar to the Icelandic subaqueous rhyolite flows described by Furnes et al. (1980). In the Icelandic example two types of microbreccia are recognized: type 1 is a pumice-rich variety interpreted to have been produced by explosive magmatic eruptions, and type 2 consists of angular fragments of obsidian, flow banded pumiceous rhyolite and lithic rhyolite derived by quenching and thermal fragmentation of rhyolite lobes. In the highly recrystallized microbreccia of the southern body it is not possible to distinguish the original nature of fine grained material. Consequently it is impossible to determine how much of the microbreccia is pyroclastic in origin and how much originated by thermal fragmentation of associated lobes. In the Icelandic subaqueous rhyolite flows the lobes are interpreted as remnants of disintegrated subaqueous rhyolite flows or intrusions into water-saturated pumiceous tuff.

Other rhyolite bodies

Rhyolite is poorly exposed to the east and south of the northern and southern bodies, along the shore of Manistikwan Lake (Fig. 132). These rhyolites vary widely in phenocryst population, are commonly fault bounded, and southernmost bodies are carbonatized and strongly tectonized.

Sparsely quartz-phyric (1—3%, 0.2 — 1.0 mm) rhyolite occurs on the island and on the east shore of Manistikwan Lake opposite the northern and southern bodies. This rhyolite is strongly spherulitic (40—60%, 0.05 — 0.1 mm) and consists of angular white rhyolite blocks in a grey matrix. The rhyolite blocks locally contain up to 40% quartz amygdales.

Massive, strongly spherulitic, white weathering rhyolite similar to, and perhaps equivalent to, the northern body outcrops on the second peninsula south of the southern body. It differs only in that it contains more and larger vesicles and does not contain plagioclase phenocrysts.

Other occurrences of rhyolite are widely spaced, and are commonly altered and tectonized. They include prominent quartz- and plagioclase-phyric varieties (10%, 0.5 — 2 mm quartz and 5%, 0.5 — 1.5 mm plagioclase phenocrysts), strongly plagioclase-phyric types (20%, 0.5 — 1.0 mm) and aphyric varieties. Most occurrences are massive and one is a breccia. The breccia, which occurs west of Grassy Narrows, is monolithologic, aphyric and consists of angular, white rhyolite blocks in a pale green, locally rusty, strongly foliated matrix. Rhyolite south of Grassy Narrows is impregnated by iron carbonate, and is rusty weathering and deformed almost beyond recognition.

SILTSTONE, GREYWACKE (UNIT 33)

Delicately bedded, grey, grey-green and white weathering siltstone, greywacke and minor chert are exposed as screens between gabbro intrusions in the southern part of the Grassy Narrows Zone. The sediments overlie east-facing mafic pillowed flows (unit 8) on two of the small islands in Manistikwan Lake and also occur on a small outcrop on the east shore of Manistikwan Lake. Beds are continuous, narrow (5 mm — 12 cm) and commonly normally graded. A strong schistosity and later fracture cleavage intersect bedding at a high angle. Many beds are tectonically disrupted and transposed.

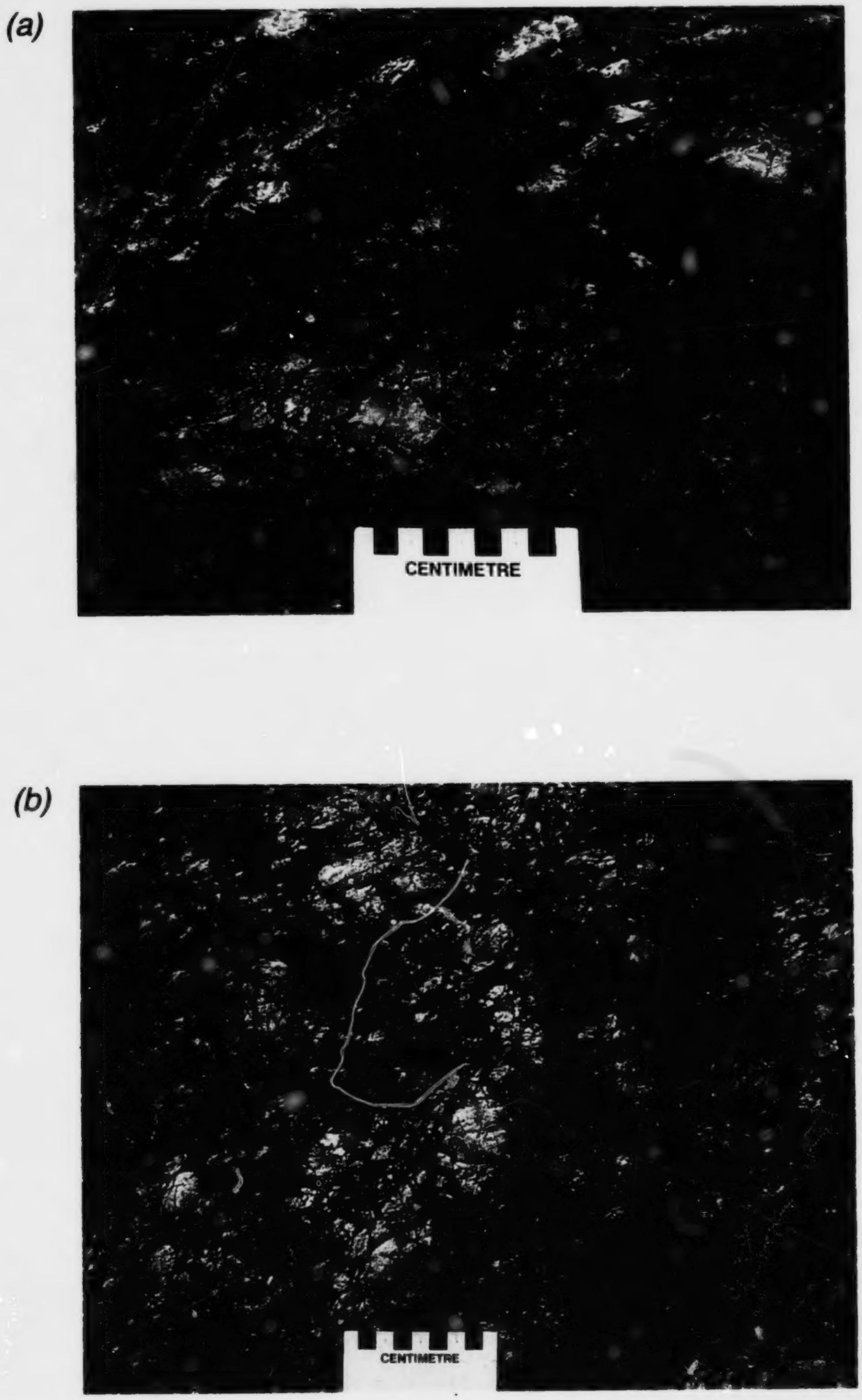

Figure 140: Breccia zone, Northern rhyolite body (Fig. 137), Grassy Narrows Zone, northeast arm of Manistikwan Lake: a) fine-scale fracturing in isolated pocket of massive rhyolite and b) sericite-carbonate alteration (dark) developed to varying degrees along fractures.

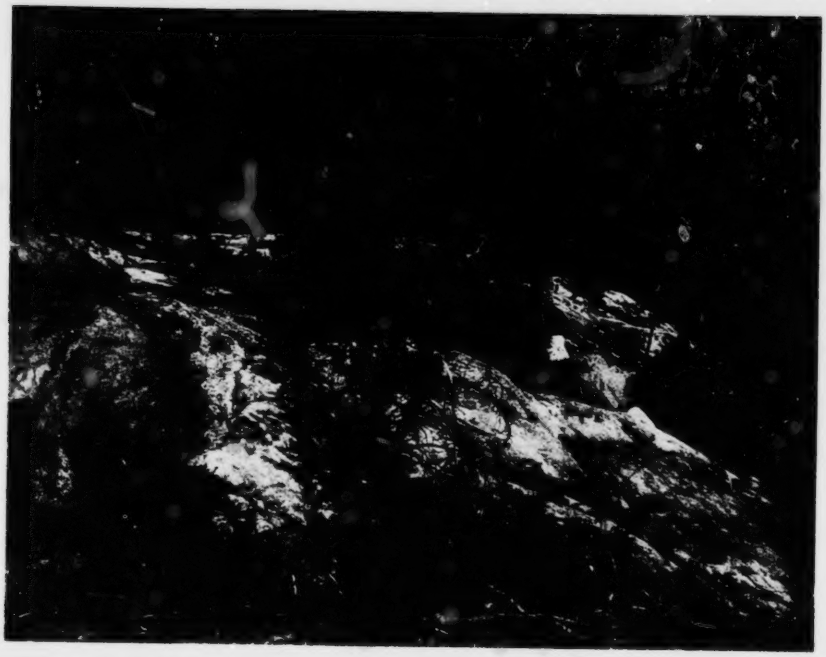

Figure 141: Large tongue of massive rhyolite (white) in microbreccia (dark), subaqueous Grassy Narrows rhyolite flow (unit 18a), northeast arm of Manistikwan Lake.

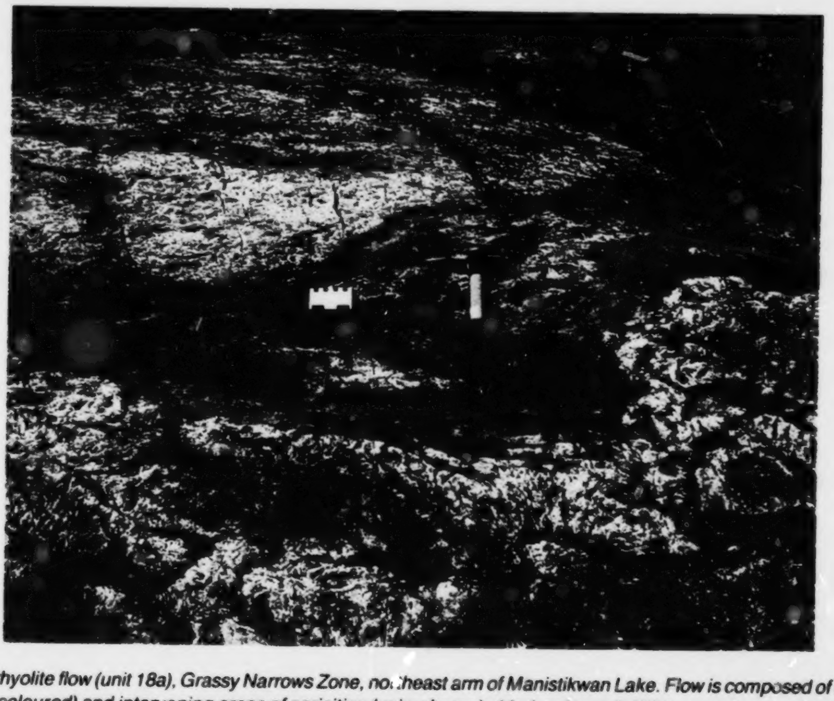

Figure 142: Subaqueous rhyolite flow (unit 18a), Grassy Narrows Zone, northeast arm of Manistikwan Lake. Flow is composed of lobate bodies of massive rhyolite (light coloured) and intervening areas of sericitized microbreccia (dark coloured). White massive rhyolite lobes below hammer are silicified.

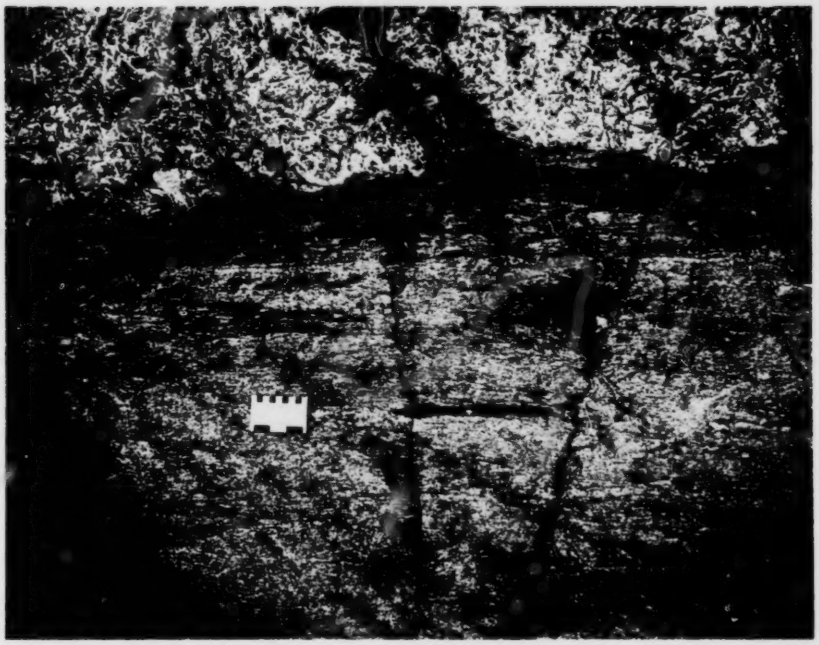

Figure 143: Contact between a massive rhyolite lobe (light, top) and intraflow unit of reworked rhyolite microbreccia and mudstone (bottom). A tabular intraclast of mudstone (dark, to the right of the scale card) occurs in the reworked microbreccia. This intraflow sedimentary unit is 3 m thick and separates two rhyolite flows with different phenocryst populations. Grassy Narrows rhyolite (unit 18a, d), Northeast Arm of Manistikwan Lake.

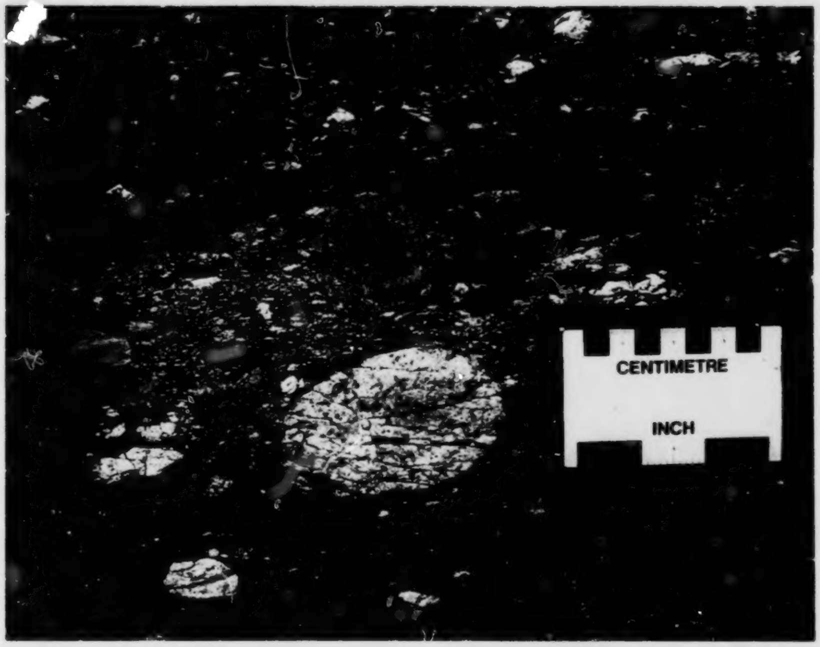

Figure 144: Rounded to well rounded pebble- and cobble-sized fragments in heterolithologic felsic pebble conglomerate (unit 32), Grassy Narrows Zone, west shore of northeast arm of Manistikwan Lake.

FELSIC SANDSTONE AND PEBBLE CONGLOMERATE (UNIT 32)

Sandstone and conglomerate of dominantly felsic volcanic provenance unconformably overlie east-facing Grassy Narrows basalt and contained gabbro intrusions in the western fault slice of the Grassy Narrows zone. This north-trending unit is only exposed across strike for 30 m and along strike for 750 m, with east, north and south boundaries marked by faults. In one of the two exposures of these sediments they display a knife-sharp unconformable contact which has up to 9 m of original relief on the underlying gabbro and basalt.

Conglomerate beds are clast-supported and composed of 50 to 70% subangular to rounded, white, aphryic to quartz-phyric rhyolite pebbles to 6 cm diameter. Most of the remaining fragments are intermediate to mafic volcanic clasts (Fig. 144). Other distinctive fragments include weakly pyritic, light grey chert and medium grey plagioclasite fragments with interlocking, euhedral, tabular, 1—2 mm plagioclase.

Similar, but better exposed and preserved felsic sandstone and conglomerate (unit 32) unconformably overlie hydrothermally altered basalt flows in the Manistikwan Lake Block. They contain devitrified (spherulitic) rhyolite and pumice, and are interpreted to be produced by redeposition of pyroclastic debris in a fluvial environment or by direct deposition by pyroclastic surges. Preservation in the Grassy Narrows zone is poorer, but high degree of rounding of some fragments, heterogeneity of contained clast-types, and topographic relief on the unconformably underlying basalt and gabbro is more consistent with a fluvial environment of deposition.

MANISTIKWAN LAKE BLOCK

INTRODUCTION

The Manistikwan Lake Block is bounded on the east by the Rosenberg Lake Fault and on the west by the Big Island Fault (Fig. 3). The block has a maximum width of 3 km but narrows to the north and south; its overall shape is lensoid. Flows within the block are homoclinal west-facing. The block contains a number of internal north-northwest-trending faults which prevent development of a coherent stratigraphy. Many faults appear to be high level brittle fractures with associated fault breccia, introduction of open-space carbonate fillings and local pervasive carbonatization.

The Manistikwan Lake Block contains abundant and diverse intrusions, as dykes, dyke swarms and larger, elongate plugs. Major rock types include rhyolite, various quartz- and quartz-plagioclase porphyries, diorite, magnetiferous quartz diorite, and quartz diorite. Age relationships and petrographic characteristics of these intrusions are described in a later section.

Mafic flows and related breccias (units 7 and 8) are dominant lithologies in the block. Minor rock types include pyritic mudstone (unit 36) and felsic sandstone and pebbly sandstone (unit 32). Flows in the Steeves Lake portion of the block are commonly aphyric whereas those on Big Island are porphyritic; for convenience these two areas are described separately.

STEEVES LAKE PORTION

Mafic flows and related rocks (unit 7)

Amoeboid pillow breccias, thin pillowed flows and pillow fragment breccia form a 600 m thick stratigraphic unit between the Rosenberg Lake Fault and the east shore of Steeves Lake. They weather buff to pale green and are medium grey to green on fresh surfaces. Amoeboid pillows are moderately to strongly epidotized and are commonly strongly deformed parallel to schistosity. They contain quartz and carbonate amygdales to 5 mm. Intercalated pillowed flows are thin (1 — 5 m) and typically discontinuous along strike. Massive flows are rare. Quartz amygdales to 8 mm and gas cavities to 6 cm long occur in some pillows; gas cavities were only observed in the upper portion of this subunit.

Aphyric to weakly plagioclase-phyric green to brownish green weathering mafic flows overlie the amoeboid pillow breccias and form the remainder of the Steeves Lake portion of the block. These flows are all pillowed and their thicknesses could rarely be determined due to generally poor exposure. Vesicularity in them is generally low, with carbonate-filled amygdales 1 — 5 mm commonly occurring only in outermost parts of pillows. Gas cavities (1 — 10 cm) occur in some pillows but are not abundant. Jasper and chert interpillow fillings, and local thin jasper layers, occur in some individual flows within the sequence. The flows are moderately to strongly foliated and, in general, pillow structures are poorly defined.

Pyritic mudstone (unit 36)

Pyritic mudstone occurs as a unit 140 m thick, west of Steeves Lake. It is truncated at its northern and southern extremities by north-northwest-trending faults. Outcrops of this mudstone are typically reduced to gossaned rubble due to the presence of 3% disseminated very fine grained pyrite. Where best preserved the mudstone is white to pale grey-green with pyrite- and quartz-filled fractures. The mudstone is laminated on a millimetre scale, with laminae defined by grain size variation. It is composed of small felsic fragments (to 0.4 mm in size and up to 10%), grains of quartz and plagioclase (less than 0.05 mm) and a fine grained groundmass mixture of chlorite and tremolite. The sediments are locally sericitic and rich in carbonate, particularly in association with the complex of rhyolite dykes at the south end of the unit.

Felsic sandstone, pebbly conglomerate, pyritic mudstone (units 32 and 36)

Epiclastic rocks of dominantly felsic volcanic provenance occur adjacent to the portage between Manistikwan Lake and Embury Lake. The unit has a maximum exposed thickness of about 350 m, of which 45 m comprises a basal unit of felsic sandstone and pebbly sandstone. The overlying pyritic mudstone is intruded by a gabbro sill and, consequently, the true thickness of this sedimentary sequence is unknown.

The contact of this unit with underlying, hydrothermally altered intermediate flows is knife sharp and non-foliated. At the south end of Embury Lake this contact truncates layering in the underlying hydrothermally altered intermediate volcanic rocks, suggesting that it is either an unconformity or a fault plane. The intense alteration which characterizes the intermediate volcanics is not present in the sediments. In the absence of any features that could be ascribed to faulting the felsic sediments are interpreted to unconformably overlie the hydrothermally altered volcanic rocks.

The felsic sandstone and pebbly conglomerate form cross-stratified (Fig. 145) and parallel-laminated beds of alternating pebble-sized and sand-sized material. The pebbly beds are clast-supported, with angular to subrounded white rhyolite pebbles up to 3 cm long. Approximately 5% of the conglomerate consists of densely microvesicular felsic pumice. In some exposures the sediments also contain minor mafic to intermediate volcanic pebbles, rounded quartz pebbles and rare angular laminated intermediate fragments (Fig. 146). Rhyolite pebbles are dominantly spherulitic and contain 1% embayed quartz phenocrysts and tabular plagioclase phenocrysts. The framework fraction of the sandy beds comprises quartz and rhyolite grains, generally less than 0.5 mm across.

The contact between the felsic sandstones and overlying pyritic siltstones and mudstones is not exposed. The mudstones are pale grey-green to rusty weathering, laminated to thin bedded (1 mm — 5 cm), with layers defined by colour contrast. Some exposures are reduced to highly gossaned rubble due to the oxidation of disseminated very fine grained pyrite. The mudstone is composed of very fine grained actinolite and subordinate epidote, chlorite and feldspar. Detrital plagioclase (to 0.1 mm) and felsic rock fragments (feldspar plus sericite) to 0.2 mm occur at the bases of some normally graded siltstone beds. Disseminated pyrite occurs in all laminae but is concentrated in the silt-sized middle to upper parts of beds.

Coarser grained sediments in this sequence have a very restricted provenance, indicated by the overwhelming abundance of rhyolite clasts and grains. The presence of devitrified (spherulitic) rhyolite and pumice indicates local derivation without significant reworking. Bedforms observed in these deposits could have been produced by redeposition of pyroclastic debris in a fluvial environment or by direct deposition from pyroclastic surges. There is insufficient exposure to distinguish between these contrasting modes of deposition. In either case, a subaerial provenance was probable.

BIG ISLAND PORTION

Pillow fragment breccia (unit 8a)

On the east side of Big Island approximately 500 m of stratified pillow fragment breccia underlies a unit of porphyritic pillowed flows. The

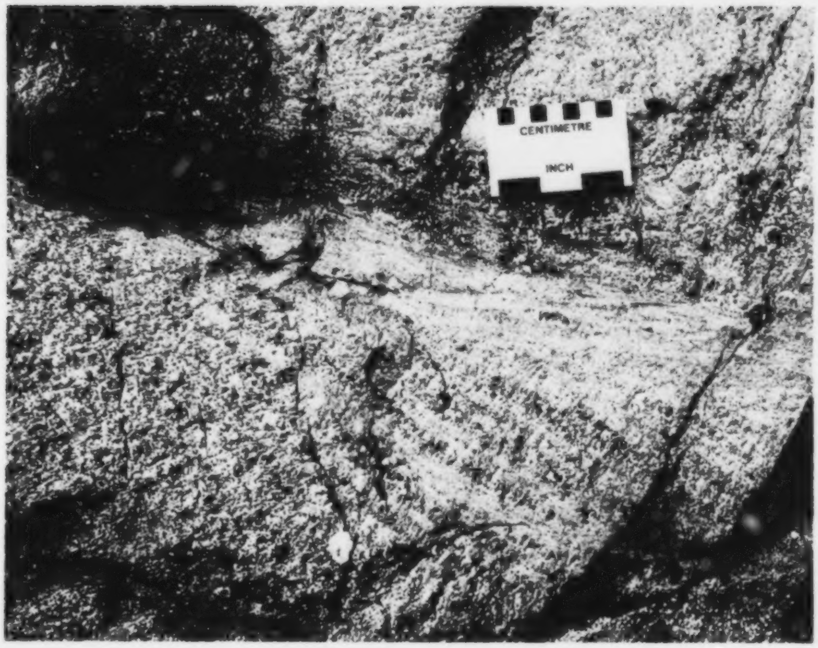

Figure 145: Crossbedding in felsic sandstone and pebble conglomerate (unit 32), south end of Embury Lake. Clasts (white) are rhyolite.

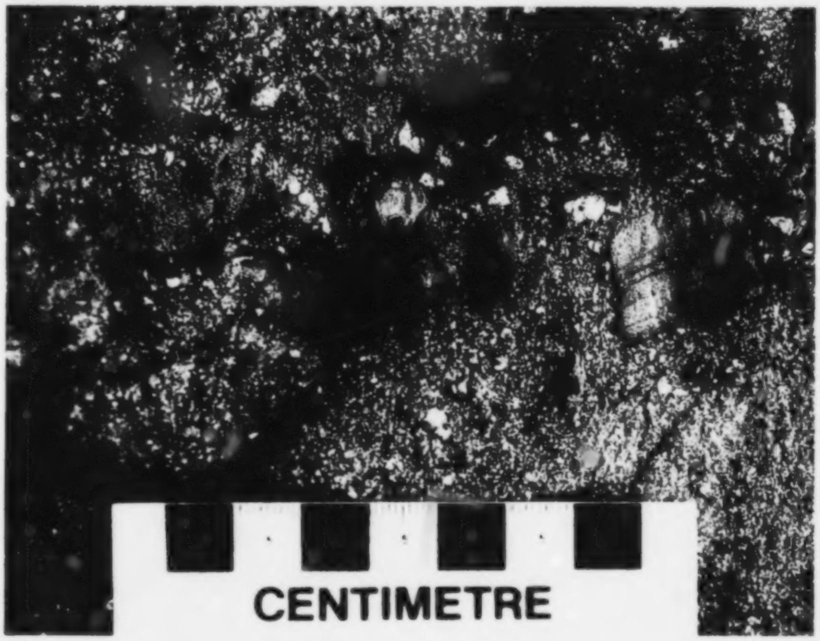

Figure 146: Heterolithologic felsic pebble conglomerate (unit 32) with angular, laminated intermediate fragments, adjacent to portage between Manistikwan and Embury Lakes.

breccia and flows are intruded by large bodies of quartz porphyry (units 48a and 48b), diorite (unit 42b), and magnetiferous quartz diorite (unit 42j). True stratigraphic thickness of the pillow fragment breccia, and its stratigraphic position relative to the Steeves Lake portion of the block, is not known due to presence of a major fault along the east shore of Big Island.

Pillow fragment breccias consist of pale green weathering clasts in a brown weathering matrix (Fig. 147). Fragments are pyroxene and plagioclase phyric, amygdaloidal and variably epidotized. They contain up to 10% pseudomorphs after pyroxene phenocrysts (1 — 3 mm) and 5 — 20% plagioclase phenocrysts (0.5 — 2 mm); amygdales (10 — 40%) range from 1 mm to 1 cm in diameter. Some fragments contain gas cavities and pipe amygdales. Shapes of fragments are diagnostic (angular to rounded, crescentic, wedge-shaped, and rare complete pillows), and all are considered to have been derived from pillowed flows. Most fragments are less than 30 cm across but may be up to 50 cm. The matrix consists of brown, plagioclase-phyric granules, plagioclase crystals and pale green epidotized granules.

Beds are 0.5 to 20 m thick, but most are less than 5 m. They are graded, as in the pillow fragment breccias in the Bear Lake basaltic andesite (see previous description), with massive basal to middle portions and graded tops with higher matrix:clast ratios (Fig. 148). Some beds have sandy tops that display normal size grading. Most beds are monolithologic, although a few beds have incorporated fragments with different phenocryst populations.

Pillow fragment breccias on Big Island, one of the thickest of such units in the Flin Flon area, are notable for complete absence of intercalated flows. This suggests that it was deposited away from the central (near vent) zone of the source volcano. Large gas cavities, pipe-shaped vesicles and abundant amygdales in pillow fragments indicate that the source flows were deposited in shallow water (300 — 700 m). Detritus was derived from only one source volcano, and deposited by subaqueous debris flows, as indicated by the restricted range of fragment types and characteristic bedforms in the breccia.

Porphyritic basalt and basaltic andesite (unit 8)

Approximately 600 m of strongly porphyritic basalt and basaltic andesite (unit 8) overlies the pillow fragment breccia (unit 8a). True stratigraphic thickness of this unit is unknown as its top is removed by the Big Island Fault. The flows are dominantly pillowed with a few massive flows and zones of amoeboid pillow breccia. Flow contacts were rarely observed and consequently flow thicknesses are unknown. The flows contain no synvolcanic mafic dykes and do not have intercalated beds of pyroclastic or sedimentary rocks.

The basal 430 m of this unit is well exposed on the southern part of Big Island. Pillowed flows at this locality are distinctive: they have a uniform buff-brown to pale buff-brown colour, a thick (0.5 — 3 cm) red-brown to dark red-brown selvage, and 1 — 3 cm of pale cream epidotized interpillow hyaloclastite (Fig. 149). Pillows are relatively large (0.5 — 2 m) and commonly interconnected. They are moderately vesicular, with 2 — 20% amygdales (1 — 5 mm), gas cavities to 4 cm and local radial pipe vesicles up to 1.5 cm long. Phenocrysts and glomerocrysts include 5 — 20% plagioclase (0.5 — 3 mm) and 0 — 5% pyroxene (0.2 — 1 mm).

On the southern tip of Big Island flows are more variable and include aphyric, sparsely plagioclase-phyric and strongly plagioclase-phyric types. Selvages and interpillow hyaloclastite are not as prominent as in flows to the north.

SUMMARY

The Manistikwan Lake Block is composed dominantly of basalt-basaltic andesite flows and related breccias. Sedimentary units include one intercalated formation of pyritic mudstone (west of Steeves Lake) and a sequence of felsic pebble conglomerate, sandstone and pyritic mudstone that unconformably overlies the mafic flows south of Embury Lake. The porphyritic sequence of pillow fragment breccia and pillowed flows on Big Island is in fault contact with the aphyric flows of the Steeves Lake portion of the Block.

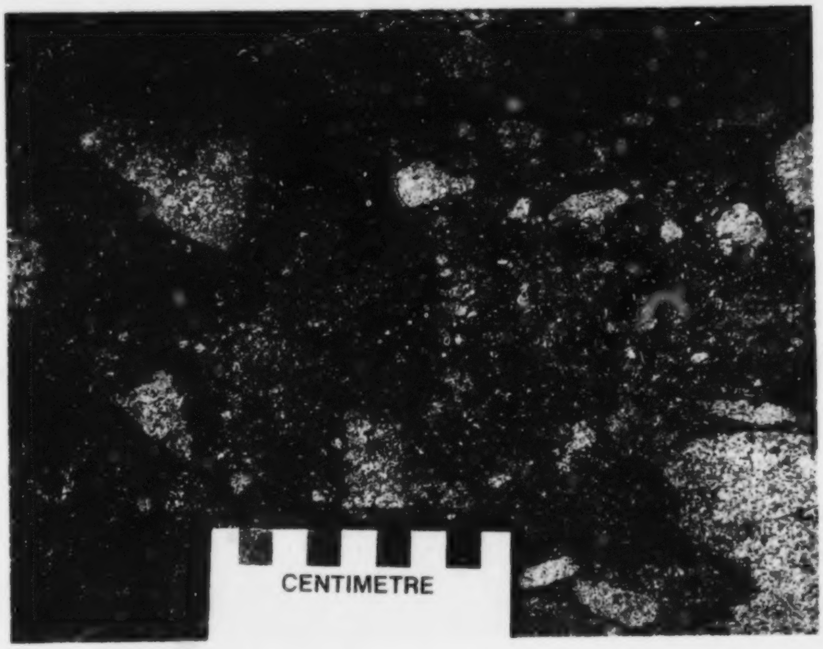

Figure 147: Pillow fragment breccia (unit 8a), Big Island, Manistikwan Lake. Pie-shaped, broken pillow fragment with part of dark pillow selvage (arrow) indicates origin of clast by "cold" fragmentation of a pillow along radial cooling joints (refer to Fig. 19).

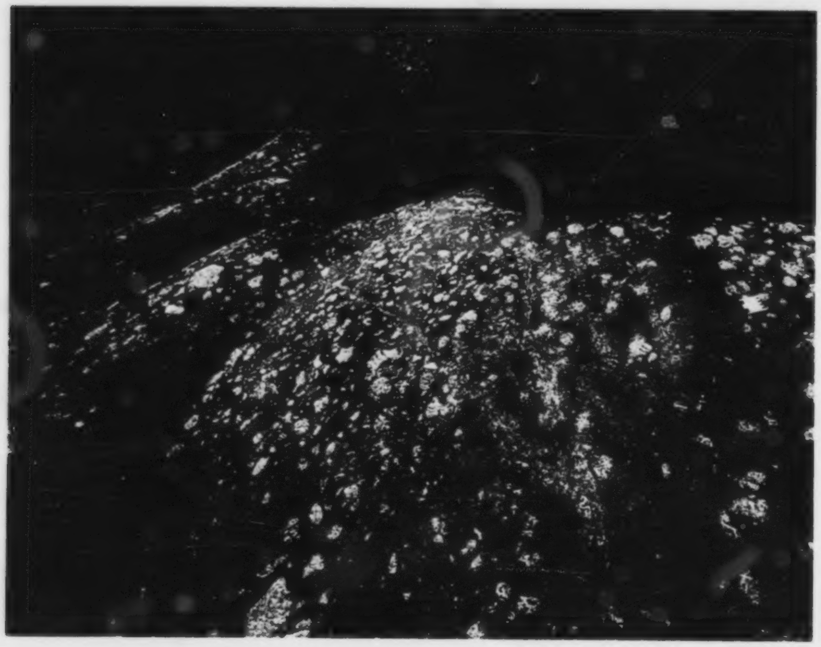

Figure 148: Stratified pillow fragment breccia (unit 8a), Big Island, Manistikwan Lake. The bed in the photograph is 2 m thick, with the base at the hammer (left) and top at the scale card (right). The lower 1.5 m of the bed is coarse, with abundant clasts; the top 0.5 m of the bed has a higher proportion of matrix. Abrupt contact with the coarse base of the overlying bed (right). This type of grading is typical for all pillow fragment breccia beds.

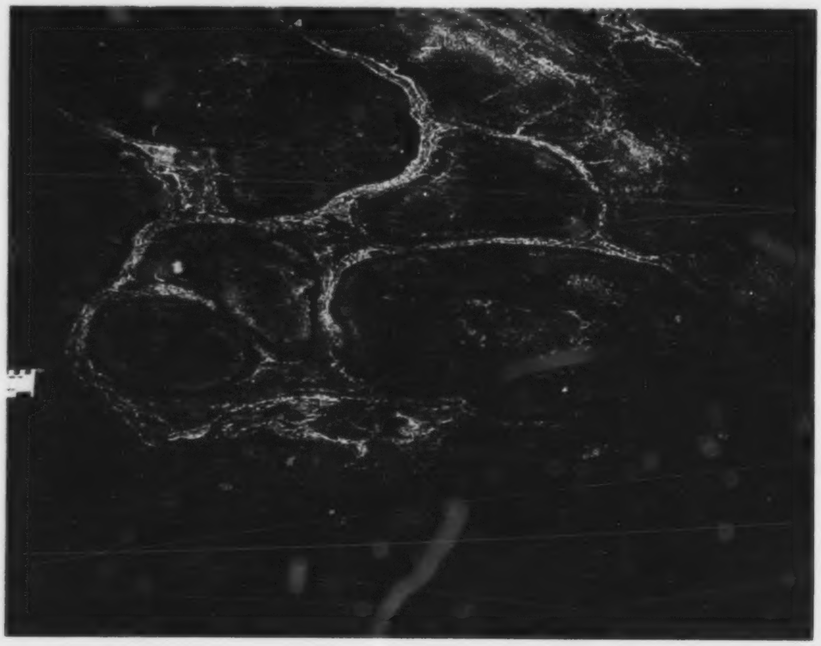

Figure 149: Pillowed mafic flow (unit 8), Big Island, Manistikwan Lake. Thick pillow selvages and wide interpillow domains characterize Big Island pillowed flows.

COPE LAKE BLOCK

INTRODUCTION

The Cope Lake Block is bounded on the east by the Big Island Fault and on the west by the Manistikwan Lake Fault (Fig. 3). The block is composed of a folded succession of aphyric to strongly porphyritic mafic flows, subordinate synvolcanic dykes, and minor pillow fragment breccia. The mafic flows can be subdivided into six stratigraphic members on the basis of their phenocryst content. They are listed below in stratigraphic order from top to base, accompanied by their approximate stratigraphic thicknesses.

Unit	
8	Porphyritic (300 m +)
7	Aphyric (140 m)
8, 9	Strongly porphyritic (700 m)
7, 9	Aphyric to sparsely porphyritic (550 m)
9	Strongly porphyritic (150 m)
7	Aphyric to sparsely porphyritic (170 m +)

MAFIC FLOWS

Basalt and basaltic andesite flows which dominate the stratigraphic sequence in the Cope Lake Block are divided on the geological map according to their phenocryst size and abundance. Contacts between members were not mapped in the field but are readily apparent from the areal distribution of flows with particular phenocryst assemblages, combined in some places with other distinguishing characteristics which serve to subdivide the sequence. Consequently, it is not known whether the contacts are abrupt or gradational through interlayering of flows with strongly contrasting phenocryst populations. The six members that compose the sequence are described below, in stratigraphic order from base to top.

Aphyric to sparsely porphyritic flows (unit 7)

This member is exposed in the bay at the northwest end of Manistikwan Lake, on the southwest limb of the Cope Lake Syncline. Minimum thickness of this unit is 170 m; it is terminated to the west against the Manistikwan Lake Fault and to the east against the Big Island Fault. Flows vary in weathering colour from light buff to light grey or grey, in part due to variable carbonatization. All are pillowed, and carry 0 — 10% plagioclase phenocrysts up to 2 mm. In some flows the plagioclase occurs as microphenocrysts.

Strongly porphyritic flows (unit 9)

Flows that contain abundant large phenocrysts of pyroxene and plagioclase constitute a unit approximately 150 m thick, between underlying and overlying units of sparsely porphyritic flows. Flows in the northern part of this member are distinctive light buff-brown weathering, with 15 — 25% plagioclase phenocrysts and glomerocrysts (0.3 — 5 mm) and 2 — 7% pyroxene phenocrysts (0.5 — 3 mm). The glomerocrysts contain up to 20 — 25 individual plagioclase and subordinate pyroxene crystals with anorthositic to gabbroic interlocking texture. These flows are pillowed, with 3 mm brown selvages and amygdales, up to 15 mm in diameter, concentrated either in pillow tops or in pillow cores. In one location pyroxene phenocrysts are concentrated at the base of pillows.

Flows in the southern part of this member weather light buff to green, are moderately to strongly foliated, and contain larger and more abundant pyroxene phenocrysts (10 — 30%, 1 — 10 mm) than those to the north. They contain 0 — 10%, 1 — 2 mm plagioclase phenocrysts.

Aphyric to sparsely porphyritic flows (units 7 and 9)

These flows weather shades of pale brown and green, and form the main part of the block south of Cope Lake. In the field the rocks appear aphyric but they contain 1 — 3%, small (0.3 — 0.7 mm) plagioclase and pyroxene phenocrysts in a groundmass of plagioclase microlites and mafic metamorphic minerals. Virtually all flows are pillowed. Pillows are distinguished by thick (1 cm) dark brown to dark green selvages and 1 — 3 cm of yellow epidotized interpillow hyaloclastite. Amygdales are up to 5 mm in diameter but are generally low in abundance, concentrated at the margins or tops of pillows. Equigranular, fine grained, synvolcanic dykes are locally abundant; some have colour banding parallel to margins.

Strongly porphyritic flows (units 8 and 9)

A 700 m thick unit of porphyritic flows occurs on both limbs of the syncline, north and west of Cope Lake. All flows in this member contain abundant phenocrysts of plagioclase and pyroxene, but size and quantity of phenocrysts varies between flows. Plagioclase phenocrysts are euhedral, blocky, 0.5 — 3 mm, and comprise 20 — 30% of the rock. Pseudomorphs after pyroxene phenocrysts are euhedral, equant, 1 — 10 mm and 0 — 10%. Flows in the lower half of the member are dominantly pillowed and weather buff to buff-brown. Pillows have thick selvages (to 1.5 cm) and up to 2 cm of epidotized interpillow hyaloclastite. Flows in the upper part of the member comprise both massive and pillowed varieties and weather pale creamy buff. Selvages are very thin and locally appear to be absent; interpillow hyaloclastite is not prominent. Amygdales throughout the member vary in abundance (5 — 20%) and size (up to 5 — 10 mm); radial pipe vesicles were noted locally. Gas cavities up to 10 cm long occur in the tops of some pillows.

Aphyric flows (unit 7)

A unit of aphyric flows approximately 140 m thick occurs on both limbs of the syncline, northwest of Cope Lake. Flows include both massive and pillowed varieties and weather creamy buff to buff-brown. As in the previous aphyric member some of the flows contain a small amount of plagioclase microphenocrysts. Amygdale content ranges from negligible to abundant; they are up to 1 cm in diameter in the cores of pillows. Much of this member is hydrothermally altered and locally weakly pyritized.

Porphyritic flows (unit 8)

Plagioclase- and plagioclase plus pyroxene-phyric flows occur in the core of the syncline, northwest of Cope Lake. Flows are both massive and pillowed, weather buff-brown, and are variably vesicular. Amygdales up to 1 cm, and gas cavities to 10 cm, occur in pillows of some flows whereas other flows are primarily non-vesicular. Phenocrysts similarly vary in size and abundance between flows, with plagioclase 5 — 10% (1 — 2 mm) and pyroxene 0 — 5% (1 — 2 mm).

SUMMARY

The stratigraphic sequence in the Cope Lake Block consists of alternating porphyritic and sparsely porphyritic members. The lower half is dominantly sparsely porphyritic and the upper half is more strongly porphyritic. Pillowed flows predominate throughout, indicating deposition in a subaqueous environment. Vesicularity varies considerably between flows, but the local presence of large (1 cm) amygdales, gas cavities and radial pipe vesicles suggests that the entire sequence was emplaced at moderately shallow water depths (Table 5). A single chemical analysis from the thick, sparsely porphyritic member south of Cope Lake is of a basaltic andesite, compositionally similar to the Bear Lake basaltic andesite and unlike the Hidden Lake suite. This member, where best preserved, also closely resembles the Bear Lake sequence in weathering colour, dyke content and flow morphology.

HOOK LAKE BLOCK

INTRODUCTION

The Hook Lake Block occurs between the Manistikwan Lake Fault on the east and the Cliff Lake Fault on the west (Fig. 3). The stratigraphic section contained in this block is folded about northwest-trending axial planes and is broken by several faults. Faults divide the Hook Lake Block into 5 major sub-blocks, each containing a portion of the complete stratigraphic section (Fig. 150, 151). Correlation between sub-blocks is based on repetition of distinctive sequences of units (Fig. 150). The composite stratigraphic section is approximately 7.5 km thick, and represents the thickest complete section recognized in the map area.

Basalt, basaltic andesite and rare andesite, in the form of subaqueous lava flows (79% of sequence), pillow fragment breccias (14%), and scoriaceous tuff and breccia (7%) compose the stratigraphic section. Thirteen stratigraphic units (A to M, Fig. 150) are defined in the Rennie Lake, Milliken Lake and Hartnett Lake sub-blocks. These are described

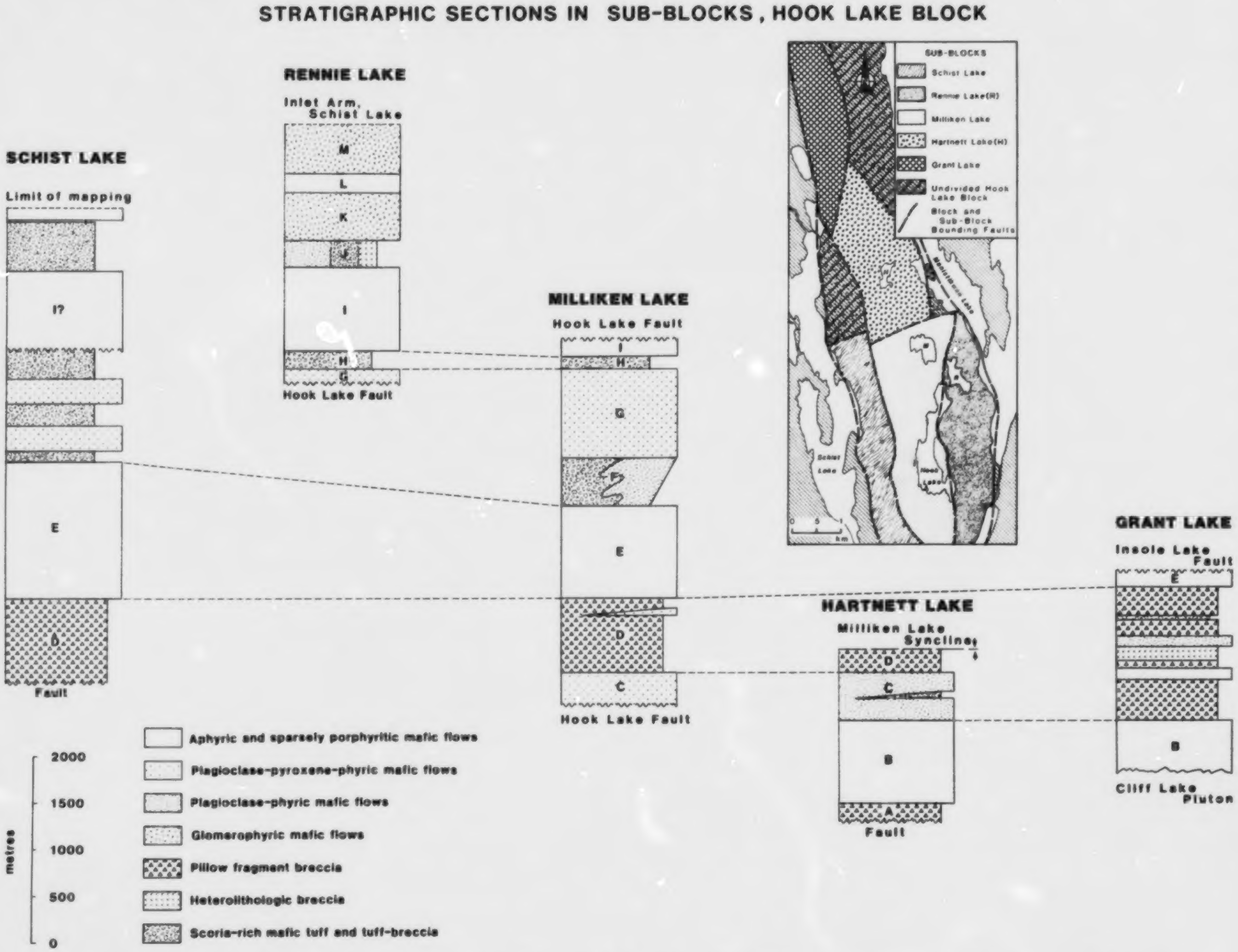
STRATIGRAPHIC SECTIONS IN SUB-BLOCKS, HOOK LAKE BLOCK
SCHIST LAKE
Limit of mapping
I?
E
D
Fault
RENNIE LAKE
Inlet Arm, Schist Lake
M
L
K
J
I
H
G
Hook Lake Fault
MILLIKEN LAKE
Hook Lake Fault
I
H
G
F
E
D
C
Hook Lake Fault
HARTNETT LAKE
Milliken Lake Syncline
D
C
B
A
Fault
GRANT LAKE
Insole Lake Fault
E
B
Cliff Lake Pluton
SUB-BLOCKS
Schist Lake
Rennie Lake(R)
Milliken Lake
Hartnett Lake(H)
Grant Lake
Undivided Hook Lake Block
Block and Sub-Block Bounding Faults
Schist Lake
Hook Lake
Manistikwan Lake
0 5 km
metres
2000
1500
1000
500
0
Aphyric and sparsely porphyritic mafic flows
Plagioclase-pyroxene-phyric mafic flows
Plagioclase-phyric mafic flows
Glomerophyric mafic flows
Pillow fragment breccia
Heterolithologic breccia
Scoria-rich mafic tuff and tuff-breccia

Figure 150: Stratigraphic sections contained in sub-blocks (inset map) of the Hook Lake Block. Correlations (dashed lines) are discussed in text. Stratigraphic subdivisions, indicated by letters, are described in text.

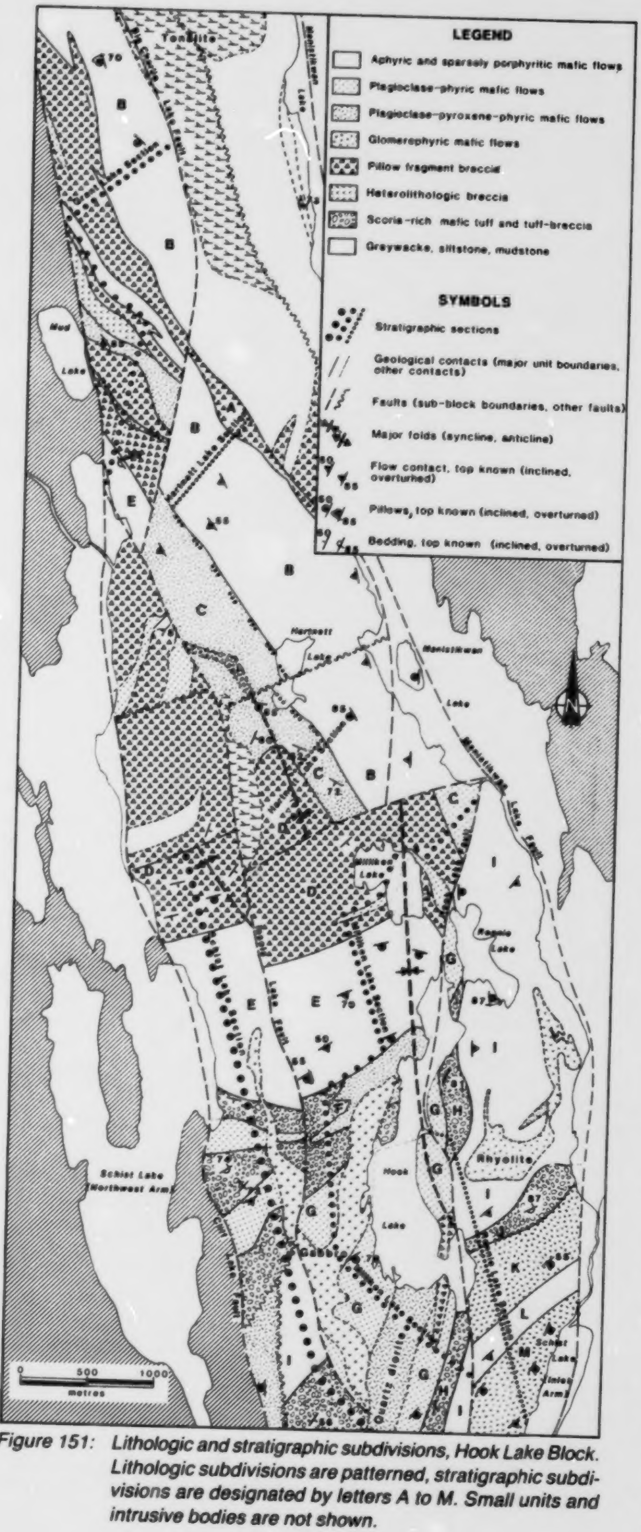
LEGEND
Aphyric and sparsely porphyritic mafic flows
Plagioclase-phyric mafic flows
Plagioclase-pyroxene-phyric mafic flows
Glomerophyric mafic flows
Pillow fragment breccia
Heterolithologic breccia
Scoria-rich mafic tuff and tuff-breccia
Greywacke, siltstone, mudstone
SYMBOLS
Stratigraphic sections
Geological contacts (major unit boundaries, other contacts)
Faults (sub-block boundaries, other faults)
Major folds (syncline, anticline)
Flow contact, top known (inclined, overturned)
Pillows, top known (inclined, overturned)
Bedding, top known (inclined, overturned)
Tonalite
Mud Lake
Hartnett Lake
Manistikwan Lake
Hook Lake
Rhyolite
Schist Lake Northwest Arm
Schist Lake Inlet Arm
Gabbro
Quartz diorite
A
B
C
D
E
G
H
I
K
L
M
0 500 1000
metres

Figure 151: *Lithologic and stratigraphic subdivisions, Hook Lake Block. Lithologic subdivisions are patterned, stratigraphic subdivisions are designated by letters A to M. Small units and intrusive bodies are not shown.*

in some detail in the following section. Shorter unit summaries are given for lithologies in the more diverse Schist Lake and Grant Lake sub-blocks. A summary of major observations and conclusions made from unit descriptions is given at the end of this chapter.

PLAGIOCLASE-PHYRIC PILLOW FRAGMENT BRECCIA (A)

The lowermost stratigraphic unit in the Hook Lake Block is a pillow fragment breccia which occurs at the bottom of the Hartnett Lake Section (Fig. 150). The unit is exposed for a maximum width of 180 m with its base removed by a fault. The breccia is buff-brown to buff-green, monolithologic, and contains clasts with 10 — 15% plagioclase phenocrysts (0.5 — 1 mm). Exposures at southern end of unit, adjacent to the fault, are strongly foliated; those farther north are strongly epidotized. Bedding is generally thick but poorly preserved. Most fragments are flattened and none of the characteristic pillow fragment shapes is preserved.

APHYRIC BASALTIC ANDESITE (B)

A 900 m thick unit of aphyric pillowed basaltic andesite flows occurs in both the Hartnett Lake and Grant Lake sections (Fig. 150). It is best exposed east and north of Hartnett Lake; in the Grant Lake section it is poorly exposed and intruded by the Cliff Lake Pluton. The basaltic andesite is characterized by ubiquitous epidotization that is not present in overlying unit "C" porphyritic flows. Tectonic flattening and intensity of foliation in rocks north of Hartnett Lake is greatest in the lower half of the unit and increases eastward. This deformation may be related to the fault which truncates the base of the Hartnett Lake section.

Basaltic andesite flows weather light buff to buff-brown and are medium grey to medium green on fresh surfaces. Most of the unit is composed of thick pillowed flows and associated amoeboid pillow breccia. Measured pillowed flow thickness ranges from 12.2 to 68.6 m and averages 37 m, whereas massive flows are only 5 — 10 m thick. Flows are organized in a manner similar to the flows that constitute the Bear Lake basaltic andesite (Fig. 9), including upward decrease in pillow size and increase in amygdale size and abundance. Although vesicularity varies between flows, quartz amygdales are generally 3 — 6 mm in diameter and amygdales to 1 cm are locally present. Total vesicularity of pillows varies with position in flow and is up to 40% in tops of some flows. Gas cavities to 4 cm long occur in uppermost parts of pillowed and massive flows. Radial pipe vesicles (in upper parts of some flows) and concentric thermal contraction fractures occur locally. Selvages are thin (2 — 10 mm) and range in colour from brown to greenish brown. Interpillow material is generally minor or absent. Interflow tuff is rare, but east of Grant Lake, for example, 1 m of tuff and 1 m of oxide facies iron formation occur between two pillowed flows.

Best preservation of primary textures occurs in the upper half of the unit, between Hartnett Lake and Provincial Road 291 to Channing. An aphyric pillowed flow from this area has randomly oriented plagioclase microlites (0.08 — 0.4 mm) set in a matrix of chlorite, epidote and subordinate actinolite. Thick massive flows at base of section east of Hartnett Lake are also locally well preserved. These flows are coarse grained with stubby plagioclase laths (up to 0.8 mm) in a groundmass of chlorite, tremolite-actinolite, and epidote. Some flows in the Hartnett Lake section are sparsely plagioclase-phyric. In the Grant Lake section porphyritic flows are more abundant, and they may contain up to 10% pyroxene phenocrysts (to 2 mm). Adjacent to the Cliff Lake Pluton flows are recrystallized and actinolite-rich, with subordinate epidote and sphene.

Chemical analyses of three basaltic andesite flows from the middle of unit, near Provincial Road 291, are similar to analyses of the Bear Lake basaltic andesite (Fig. 152-154). These flows contain about 55% SiO_2 (calculated volatile-free) and 3.7 — 5.9% MgO.

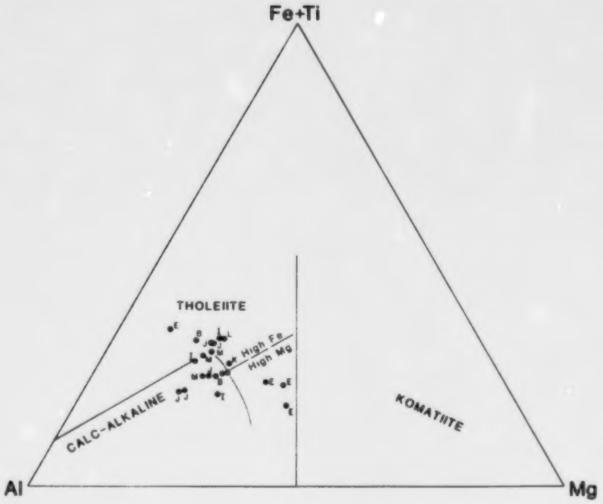

Figure 152: Jensen cation plot, Hook Lake Block mafic flows. Analyses are identified by unit alphamerics corresponding to those in Figures 150 and 151.

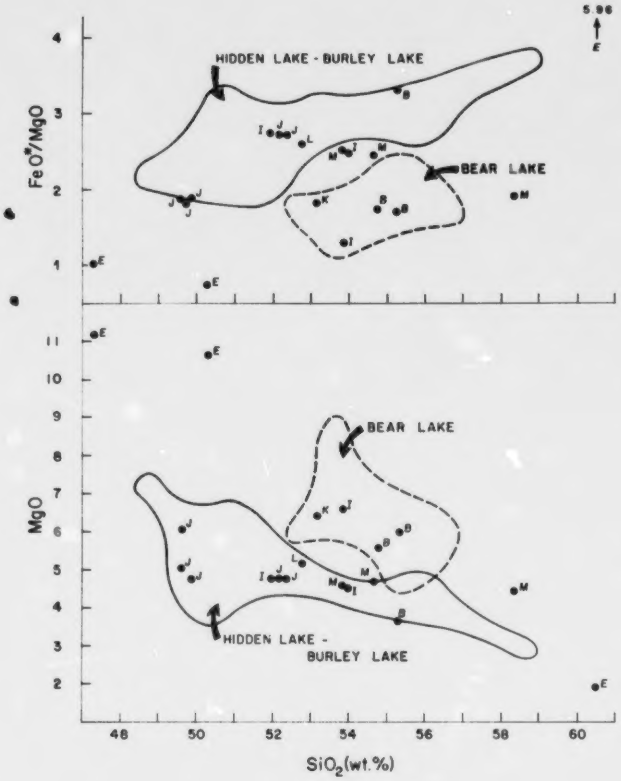

Figure 153: FeO/MgO and MgO vs. SiO₂, Hook Lake Block mafic flows. Analyses are identified by unit alphamerics corresponding to those in Figures 150 and 151. Fields of Bear Lake basaltic andesite and Hidden Lake-Burley Lake basalt-basaltic andesite are shown for comparison. Aphyric unit "B" flows are morphologically and chemically similar to Bear Lake basaltic andesites. Units "J", "K", "L" and "M" appear to compose a stratigraphic compositional sequence that evolves upwards from basalt through basaltic andesite and andesite. The diverse chemistry displayed by mafic flows of the Hook Lake Block suggests that the sequence is the product of more than one eruptive centre.*

PORPHYRITIC MAFIC FLOWS (C)

A distinctly porphyritic unit of pillowed mafic flows (C) sharply overlies unit "B" aphyric flows, in the Hartnett Lake section (Fig. 150). This unit is tentatively correlated with porphyritic flows at the base of the Milliken Lake section.

The unit occurs on the east limb and in the core of the Milliken Lake Syncline. It has a maximum stratigraphic thickness of at least 520 m, and includes a 60 m thick member of scoria tuff and pillow fragment breccia.

All observed flows are pillowed. They weather creamy buff to buff-brown and are grey on fresh surfaces. Phenocrysts vary in size and abundance between flows: plagioclase phenocrysts range in abundance from 10 to 20%, and pyroxene phenocrysts (pseudomorphed by tremolite-actinolite and chlorite) are 0.5 — 2 mm and 0 — 15%. Pillows have prominent brown to green selvages 0.5 — 3 cm thick, and many flows contain thick epidotized or laminated interpillow hyaloclastite. Vesicularity is variable; amygdales range in size from 0.3 — 1 cm and in abundance up to 25%. They occur in pillow margins, pillow cores or in concentric bands. Gas cavities up to 15 x 7 cm and radial pipe vesicles are present locally.

The scoria tuff and pillow fragment breccia member is well bedded. Scoria tuffs have normal grading defined by variation in plagioclase crystal size (0.5 — 2 mm). Scoria lapilli are plagioclase-phyric, epidotized, and contain abundant 0.5 mm vesicles. More complete documentation and interpretation of similar tuffs is provided in description of units "H" and "J". Pillow fragment breccia beds contain 3 — 10 cm blocks of broken pillows, and are dominated by either aphyric or plagioclase-phyric types.

At the base of the Milliken Lake section plagioclase-phyric flows with thick brown selvages and substantial interpillow filling are similar in appearance to the unit "C" flows of the Hartnett Lake section.

PORPHYRITIC PILLOW FRAGMENT BRECCIA (D)

An 820 m thick sequence of porphyritic pillow fragment breccias (D) and minor plagioclase-phyric flows and scoria tuffs occurs in the Milliken Lake section (Fig. 150); similar rocks are poorly exposed in the core of Milliken Lake Syncline in the Hartnett Lake section. Similarity in appearance and stratigraphic position of these breccias constitutes the basis for correlation between the Milliken Lake and Hartnett Lake sections.

As would be expected in a thick sequence of breccias derived from cold fragmentation of pillowed flows, individual beds or sets of beds have clast characteristics different from other beds in the sequence. West of Milliken Lake breccias include both plagioclase-phyric and plagioclase plus pyroxene-phyric fragments. Beds are thick but poorly defined due to a profusion of porphyritic mafic dykes (unit 43). Fragments are subangular (5 — 30 cm) and contain 5 — 15% plagioclase phenocrysts (1 — 3 mm), 0 — 10% pyroxene phenocrysts (1 — 2 mm) and 10 — 40% amygdales (1 — 2 mm). Northeast of Milliken Lake the unit includes plagioclase-phyric pillow fragment breccia and heterolithologic breccia containing clasts of varying phenocryst content and composition (Fig. 155). Rare round to bun-shaped pillows to 60 cm occur in all breccias; most clasts are less than 15 cm across.

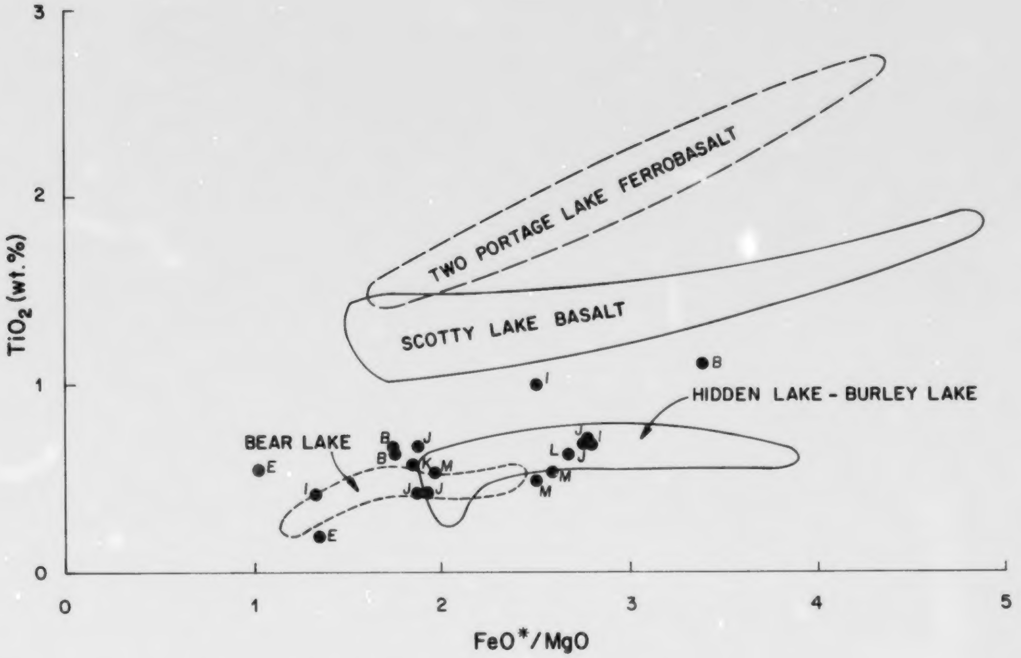

Figure 154: *TiO$_2$ vs. FeO*/MgO, Hook Lake Block mafic flows. Analyses are identified by unit alphamerics corresponding to those in Figures 150 and 151. Fields of Bear Lake basaltic andesite, Hidden Lake-Burley Lake basalt-basaltic andesite, Scotty Lake basalt and Two Portage Lake ferrobasalt are shown for comparison.*

Figure 155: *Pillow fragment breccia (unit 11), 180 m northeast of Milliken Lake. Matrix-supported, oligomictic (aphyric and plagioclase-phyric fragments). Fragments with remnant selvages and rare complete pillows identify this breccia as derived from the fragmentation of pillowed flows.*

Porphyritic flows within the pillow fragment breccia sequence, 600 m west of Milliken Lake, include both plagioclase-phyric and plagioclase plus pyroxene-phyric types.

Scoria tuff beds interlayered with pillow fragment breccia at Milliken Lake are crystal-rich, 2 cm to over 6 m thick, and include Bouma A, AB and ABC beds. Thin beds are normally size graded and thick beds display either normal or reverse grading. Large lithic blocks in some thick beds are porphyritic, contain 15%, 1 mm amygdales, and occur along discrete horizons within the beds.

Porphyritic pillow fragment breccia and associated flows (D) occur in the core of an anticline, at the base of the stratigraphic section east of Schist Lake (Fig. 150 and 151). These rocks are described separately, in the Schist Lake section.

APHYRIC AND SPARSELY PORPHYRITIC BASALT (E)

A 1 km thick unit of pillowed, aphyric, sparsely porphyritic and subordinate strongly porphyritic flows (E) is best exposed in the Milliken Lake section (Fig. 150), north and west of Hook Lake. Similar rocks are exposed in the Grant Lake section east of Schist Lake and south of Mud Lake. The flows weather light buff, light brown or light grey and are light to dark grey on fresh surfaces.

Virtually all flows are pillowed, and some have amoeboid pillow breccia tops (Fig. 156). Massive flows and pillow fragment breccias (Fig. 157) are rare. Selvages are thin (2 mm) and weather dark brown. Pillows are commonly small (20 — 100 cm) throughout the entire sequence. Although most flows are either aphyric or contain only a few small phenocrysts, some have abundant plagioclase and pyroxene phenocrysts up to 2 mm across; porphyritic flows are most abundant north of Hook Lake. Amygdale size and abundance varies between flows: they are commonly 1 — 4 mm in diameter but are up to 1 cm, and compose 5 — 40% of individual pillows (Fig. 158). Amygdale-filling assemblages in the lower 620 m of the unit comprise carbonate, epidote and lesser pyrite and chlorite; in the upper 380 m of the unit amygdales are filled with actinolite, chlorite or rarely clinopyroxene. A similar stratigraphic distribution of amygdale fillings occurs in equivalent unit "E" flows east of Schist Lake.

Unit "E" in the section east of Schist Lake is not particularly well exposed and appears to be more diverse in range of rock types present; they are described in the Schist Lake section.

Three whole rock geochemical analyses of unit "E" flows have been made of samples from the Milliken Lake section and one from the Grant Lake section. The number of analyses are not adequate to fully characterize such a thick pile of lava flows. Two analyses from the Milliken Lake Section and one from the Grant Lake section are of high-MgO basalts with 9.6 — 11.4% MgO (calculated volatile-free), and the remaining analysis is of an andesite with 61.0% SiO_2. The high-MgO basalts cannot be distinguished from the more intermediate compositions in the field. In the Milliken Lake section the two high-MgO basalt sample sites stratigraphically bracket the andesite sample site.

PORPHYRITIC SCORIA TUFF AND BRECCIA, PORPHYRITIC FLOWS (F)

A 520 m thick unit of variably porphyritic flows, scoria tuff and breccia (unit "F") overlies unit "E" aphyric and porphyritic flows west of Hook Lake, in the Milliken Lake section (Fig. 150 and 151). The northeastern portion of the unit is composed of flows whereas the southwest portion is predominantly breccia; based on the northeast trends of bedding these rock types are presumably facies equivalents.

Flows are poorly exposed and vary in weathering colour, phenocryst content and degree of alteration. Pyroxene phenocrysts (1 — 4 mm) compose nil — 15% and plagioclase phenocrysts (1 — 2 mm) form 15 — 20% of most flows.

Scoria-bearing tuff and breccia occur at the base of the unit on Hook

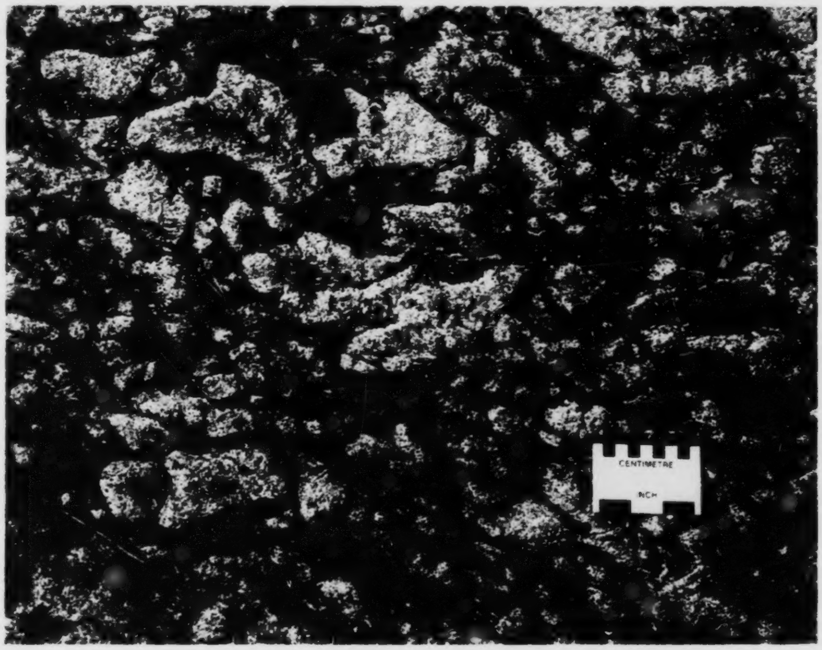

Figure 156: Amoeboid pillow breccia top of pillowed basalt flow (unit 7), 600 m south-southeast of Insole Lake. In this flow the weakly epidotized amoeboid pillows are small, close-packed and only rarely display well developed amoeboid shapes.

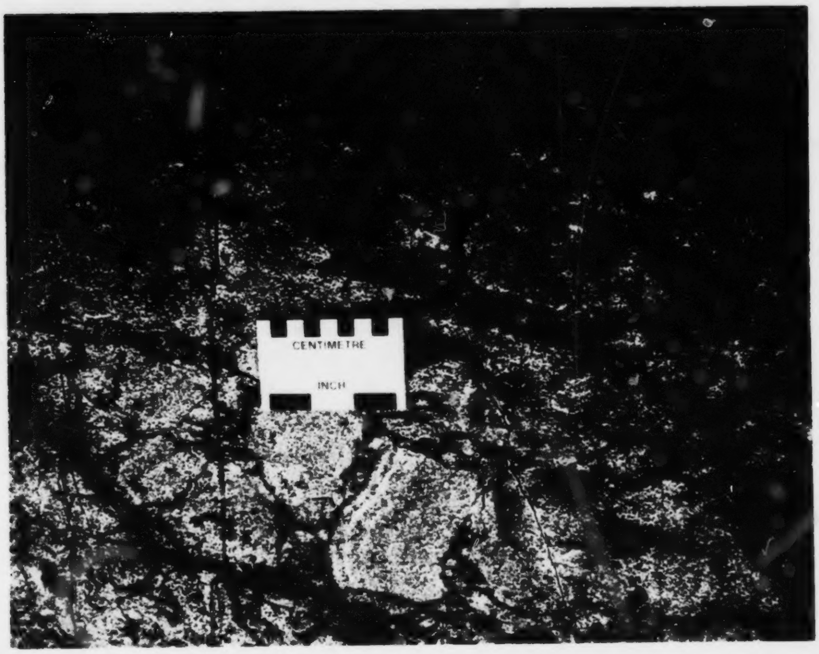

Figure 157: *Pillow fragment breccia (unit 7), 700 m southeast of Insole Lake, containing crescentic pillow fragment (below scale card) with bands of vesicles parallel to pillow selvage and truncated at fragment margin.*

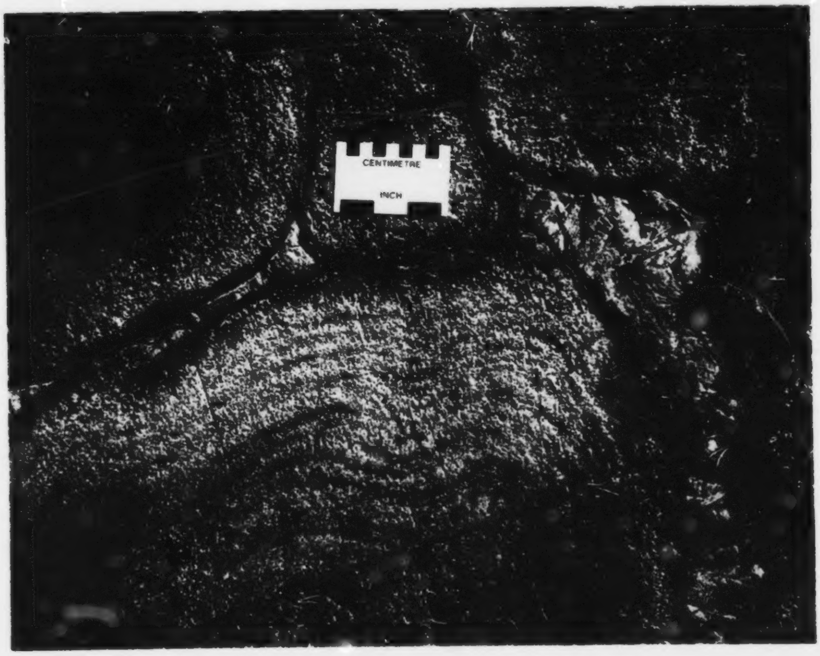

Figure 158: *Centimetre-scale amygdale banding in an aphyric pillow (unit 7), 640 m west of the north end of Hook Lake. In this flow, a 5-10 cm wide zone of banding occurs in the tops of pillows; bottoms are non-banded.*

Lake and predominate in the unit to the west. These rocks are bedded and layered: bedding is defined by fragment size and abundance, and crude layering is defined by "trains" of blocks *within* tuff beds. Individual breccia layers can be up to several metres thick. Many of these blocks, and larger blocks in the "trains", appear to be fragments of vesicular pillows. Phenocryst content varies between beds; some beds are strongly porphyritic with up to 50% plagioclase and pyroxene phenocrysts. In some areas densely microvesicular scoria granules and lapilli are preserved in the tuff matrix. In general these rock types are similar to those in units "H" and "J", where preservation is much better and the origin of the suite can be interpreted.

PLAGIOCLASE-PHYRIC MAFIC FLOWS (G)

A 910 m thick sequence of variably plagioclase-phyric pillowed flows (G) occurs in the Milliken Lake section (Fig. 150 and 151) west and south of Hook Lake. The unit is intruded by large bodies of gabbro (unit 41), diorite (unit 42) and rhyolite (unit 49) which disrupt stratigraphy. This unit is probably composed of 3 stratigraphic members.

The lowermost part of the unit, west of the gabbro intrusion, comprises coarsely plagioclase-phyric mafic lava. It weathers buff-brown to dark green and is grey on fresh surfaces. This distinctive rock is commonly massive and homogeneous, but zones occur in which pillow structure is clearly defined. Plagioclase phenocrysts (20%, 0.4 — 4 mm) and pyroxene phenocrysts (pseudomorphed by actinolite; 3%, 0.3 — 1 mm) occur in a matrix of plagioclase laths, tremolite-actinolite, feldspar and quartz.

East of the gabbro (unit 41) and west of the diorite (unit 42), at the southwest end of Hook Lake, the flows are variably plagioclase-phyric (2 — 15%, 1 — 2 mm), pillowed, with black, 5 — 10 mm thick selvages. Amygdale content is variable, with a maximum of 25% vesicles up to 1 cm.

The top of the unit at the south end of Hook Lake comprises sparsely (up to 10%) plagioclase-phyric pillowed flows; pillows have brown, 5 mm thick selvages and 10 — 25% amygdales up to 1 cm in diameter.

Variably plagioclase-phyric pillowed flows occur west of the Hook Lake Fault on the east side of Hook Lake. These are probably equivalent to similar flows southwest of Hook Lake. Pillow fragment breccia units up to at least 50 m thick are intercalated with the flows.

A thick (100 m) unit of pillow fragment breccia occurs near the top of the unit, at the south end of Hook Lake (Fig. 151). Fragments and matrix vary in phenocryst content from bed to bed and include aphyric, plagioclase-phyric, and plagioclase-pyroxene-phyric types. The breccias are typical of other pillow fragment breccia units in that they are monolithologic, matrix-supported, poorly sorted and composed of subangular to rounded pillow fragments.

Correlation between the Milliken Lake and Rennie Lake sections is based on repetition of parts of units "G", "H" and "I" on both sides of the Hook Lake Fault (Fig. 150). Unit "G" at the base of the Rennie Lake section comprises light buff pillowed flows that are variably plagioclase-phyric (2 — 25%, 1 — 2 mm), similar to the flows south of Hook Lake.

SCORIA TUFF AND BRECCIA (H)

A unit of scoria-rich mafic tuff and breccia (H), with subordinate intercalated strongly porphyritic pillowed mafic flows, occurs near the top of the Milliken Lake section (south of Hook Lake) and near the base of the Rennie Lake section (east of Hook Lake). This 140—210 m thick unit overlies plagioclase-phyric flows (unit "G") and is overlain by aphyric flows (unit "I").

The two most striking features of this unit are its very well bedded character and the abundance of porphyritic scoria granules and lapilli. Beds are continuous, 30 cm to more than 30 m thick, and contain sedimentary structures indicating that they were deposited from subaqueous density currents. Scoria fragments up to 3 cm are well preserved and their primary vesicularity is readily observed on outcrop surfaces. The vesicles are 0.05 — 1 mm in diameter, round to oval in section, and comprise up to 60% of the fragments. Thicker beds commonly contain angular to subrounded blocks of scoria and amygdaloidal basalt.

Internal structures of beds vary according to bed thickness. Thin beds (less than 2.5 m, average 70 cm) include A, AB and subordinate ABDE and ABCDE types. Sedimentary structures in thin beds are scours, load casts, rip-ups, and rare scoria-rich layers in the mid-upper parts of A divisions; some beds have white, fine grained E division tops. Thick beds (greater than 5 m, average 8 m) commonly contain blocks that are either non-graded or reverse-to-normally size-graded. In some beds blocks occur in discontinuous layers up to 50 cm thick. Blocks are typically 5 — 30 cm in size; the largest block observed was 82 x 63 cm. Tops of some thick beds contain few or no large blocks and display normal size-grading defined by plagioclase crystals and scoria granules.

Scoria granules and lapilli are equant to elongate. Plagioclase-phyric and plagioclase-pyroxene-phyric varieties occur together within individual beds. Plagioclase-phyric types contain 5 — 25% plagioclase phenocrysts (0.4 — 2 mm, rare glomerocrysts to 4 mm). Plagioclase-pyroxene-phyric types contain 5 — 10% plagioclase phenocrysts (0.5 — 2 mm) and 5 — 25% pyroxene phenocrysts (0.5 — 2 mm). Phenocrysts are set in a recrystallized groundmass composed of tremolite-actinolite, epidote and chlorite. Plagioclase phenocrysts are partly replaced by sericite and fine grained epidote, and colourless clinopyroxene phenocrysts are only partly replaced by tremolite-actinolite and chlorite.

These scoria-rich bedded deposits are interpreted to be resedimented pyroclastic rocks. The scoria lapilli, crystal-rich matrix, and some scoriaceous large blocks are juvenile magmatic material whereas the amygdaloidal basalt fragments are accessory. The scoria is interpreted to have been produced in subaerial or shallow marine (less than 200 m; Jones, 1970) magmatic eruptions and transported almost immediately by subaqueous density currents.

Scoria-rich tuff and breccia are distinguished from pillow fragment breccias by: (1) abundance of scoria, (2) better defined bedding, (3) abundance of A and AB beds, and (4) "trains" of blocks in a finer grained massive matrix. Where the scoria tuff and breccia are deformed or recrystallized they are virtually indistinguishable from pillow fragment breccias which have a different origin. The scoria-rich tuff is a pyroclastic rock produced in a shallow water or subaerial environment, whereas pillow fragment breccias are not pyroclastic and could occur in any depth of water.

APHYRIC BASALT (I)

Aphyric basalt (unit "I") is a prominent, 900 m thick unit in the Rennie Lake section, overlying porphyritic scoria-rich tuff and breccia (unit "H"). The base of a probably equivalent unit occurs at the top of the Milliken Lake section (Fig. 150).

The basal 240 m of the unit between Rennie Lake and Borne Lake consists of amoeboid pillow breccia (Fig. 159) and subordinate thin (1 — 5 m) pillowed flows, intercalated with thicker (4 — more than 21 m) pillowed flows with amoeboid pillow breccia tops. The flows weather light buff and pillows have 5 mm dark brown or green selvages. Amoeboid pillows have up to 40% amygdales as large as 7 mm in diameter.

The main part of the unit consists of light buff, aphyric to sparsely porphyritic pillowed flows with amoeboid pillow breccia tops. Vesicularity varies between flows, and amygdales (1 — 5 mm) are commonly concentrated in pillow cores; some pillows have radial pipe vesicles along their lower margins. Pillows are generally less than 50 cm across, with dark grey selvages 1 — 4 mm thick. Interpillow hyaloclastite is negligible. Topmost flows in the sequence, sharply overlain by unit "K" porphyritic scoria-rich tuff, are massive with large (to 3 cm) amygdales and gas cavities. Red-brown oxidation of these massive flows, either throughout the entire flow or restricted to the top 50 cm, suggests that they may have been erupted in a subaerial environment.

Primary textures of flows are locally well preserved. Plagioclase laths (0.08 — 0.4 mm) have felted to pilotaxitic texture (Fig. 160), and are

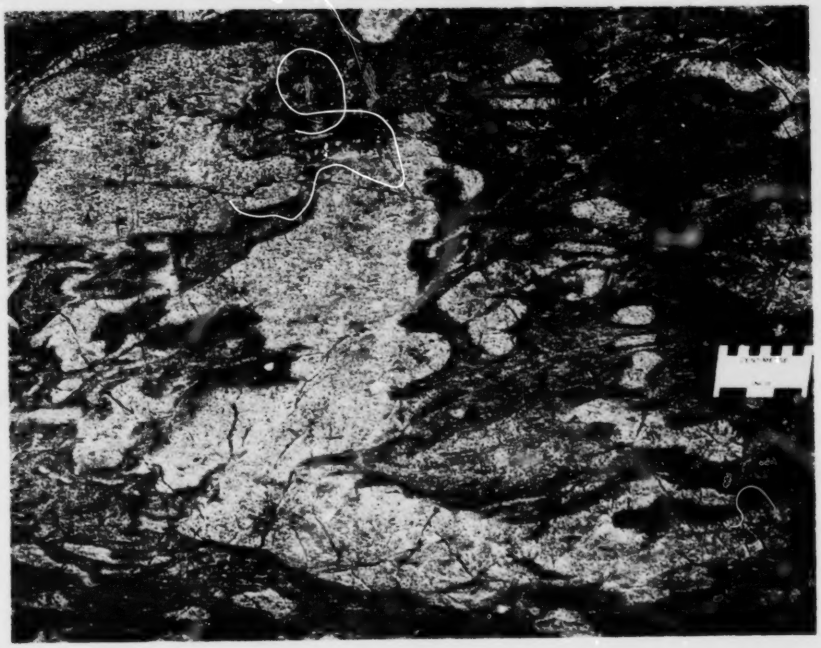

Figure 159: Amoeboid pillow breccia (unit 7b), between Borne and Rennie lakes, Hook Lake Block. Amoeboid pillows (light) have highly complex, involuted shapes, abundant amygdales, and narrow dark coloured selvages. They are supported by a matrix of recrystallized hyaloclastite. At this location amoeboid pillow breccia dominates; pillowed flows are minor and relatively thin (e.g. 3 m). "Breccias" such as these typically form the tops of flows (Fig. 8).

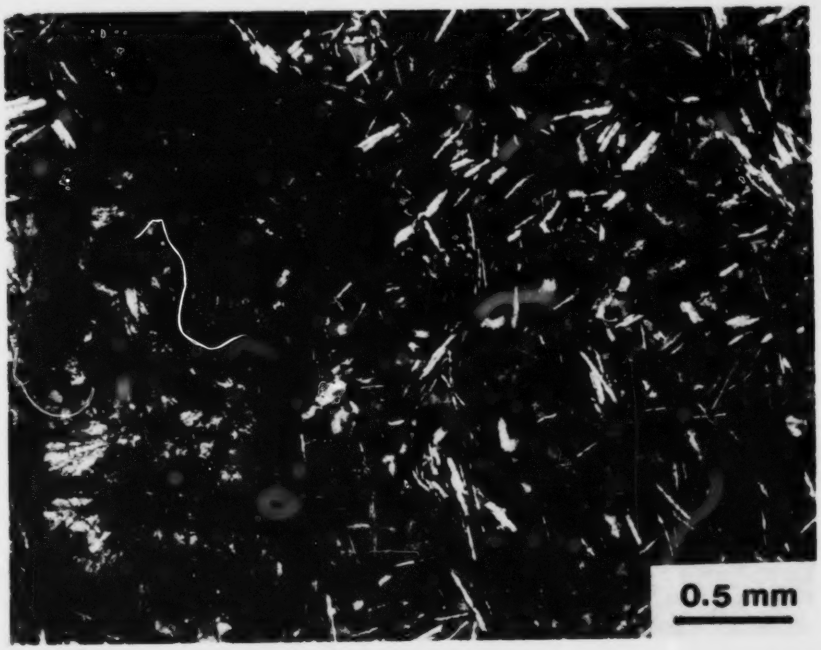

Figure 160: Aphyric mafic flow (unit 7), north of Borne Lake. Lath-shaped plagioclase microlites are well preserved. Amygdale has a dark rim and is filled with coarse epidote (ep). Sample 4028-1, crossed polarizers.

commonly oriented tangential to amygdale margins. Fine grained epidote, tremolite-actinolite and chlorite occur between plagioclase laths. Amygdales are commonly polymineralic and contain quartz, carbonate, epidote, pumpellyite, prehnite, chlorite and pyrite in various assemblages.

POPHYRITIC BASALT FLOWS, SCORIA TUFF, PILLOW FRAGMENT BRECCIA (J)

A distinctive porphyritic unit of intercalated pillowed basalt flows, scoriaceous tuff and pillow fragment breccia (J) sharply overlies massive, red-brown (oxidized?) aphyric flows of unit "I" (Fig. 150). The unit is up to 300 m thick, and is overlain by plagioclase-glomerophyric flows of unit K.

In the best preserved continuous section (Fig. 161), located adjacent to a quarry, 520 m west of the south end of Manistikwan Lake, this unit comprises 50% flows, 30% scoriaceous tuff and 20% pillow fragment breccia. The pillowed flows are 2 — 40 m thick, and contain 5 — 30% plagioclase phenocrysts and 1 — 5% pyroxene phenocrysts (Fig. 161). Some flows terminate abruptly in the exposed section. Pillow fragment breccia is directly associated with two of the flows; amoeboid pillow breccia is rare. Amygdales range in size up to 6 mm but vary in size and abundance between flows and between pillows in a single flow. Pillow fragment breccia beds are 3 — 5 m thick, contain fragments to 20 cm (Fig. 162), and include both monolithologic and heterolithologic types. Monolithologic breccias can in places be shown to contain fragments identical to the directly underlying basalt flow. Breccia beds have fragment-supported bases and matrix-rich tops but do not display normal size grading.

The distinctive component of unit "J" is scoria-rich tuff and lapilli tuff (Fig. 163, 164). Scoria tuff beds (15 cm — 13.4 m) are typically less than 5 m thick. Beds less than 1 m thick display normal grading with respect to size of plagioclase phenocrysts, are A and, less commonly, AB types, and have basal scours. Beds thicker than 1 m are commonly reverse to normally graded with respect to plagioclase crystal size (Fig. 165). They include A and AB types, and locally contain "trains" of accessory blocks (Fig. 165). The occurrence of scoria in Bouma-zoned beds intercalated with pillowed basalt indicates the pyroclastic material was transported and deposited by subaqueous density currents.

Scoria particles range in size from about 1 mm to 6 cm. Primary vesicularity and grain shapes of scoria are well preserved (Fig. 166) because this unit is within the prehnite-pumpellyite zone of regional metamorphism and does not have an imposed schistosity. In thin section two colour types can be distinguished: dark brown scoria particles are composed of a very fine grained semi-opaque mass of epidote and chlorite, and light brown particles are composed of fine grained anhedral feldspar overprinted by chlorite and epidote. The lighter coloured scoria particles are slightly flattened but are otherwise identical to the darker variety. Scoria grains are framework-supported with inter-particle voids and vesicles filled predominantly with carbonate.

The shapes of scoria particles are controlled by a combination of vesicle walls, fracture surfaces, and chilled droplet margins (Fig. 166). Vesicle-controlled margins are highly scalloped where vesicles are large, and less scalloped where vesicles are small. Fractures at particle margins are of two types: short fractures occur at points of weakness between adjacent vesicles and longer, planar fractures cut through several vesicles. Droplet margins are smooth or wrinkled and display no scalloping or fracture surfaces. Tiny vesicles (less than 0.1 mm) occur to outermost parts of droplet margins. The particles are interpreted to have been produced during explosive subaerial magmatic eruptions, probably on a small volcanic island. During eruptions, rapidly vesiculating magma droplets in the eruption column were probably fragmented first by internal gas pressure. Many of these hot vesiculated fragments were subsequently broken by thermal shock on contact with seawater.

The accessory blocks (Fig. 165) are interpreted to be ballistic fragments. Individual blocks are angular, up to 40 cm across, and are fragments of amygdaloidal pillowed basalt that can be matched to specific flows lower in the sequence (Fig. 161, 167). The blocks commonly occur in discontinuous "trains" (1 block thick) and as isolated fragments; both "trains" and isolated blocks can occur at any level within a tuff bed (e.g. Fig. 165). Blocks also occur in thin beds where, in places, they have depressed bedding contacts or laminae. The blocks are much larger and denser than the matrix scoria and were clearly not in hydraulic equilibrium with the density current that deposited the scoria. Evidence indicates that the ballistic fragments were incorporated into the scoria density flows as the density flows were in the process of being deposited. Accessory blocks may have been torn from vent walls by periodic phreatic explosions which punctuated the dominantly magmatic eruptions.

PLAGIOCLASE-GLOMEROPHYRIC MAFIC TO INTERMEDIATE FLOWS (K)

In the Rennie Lake section (Fig. 150) a 510 m thick unit of pillowed plagioclase-glomerophyric mafic to intermediate flows (unit "K") overlies the plagioclase-phyric basalt flows, scoriaceous tuffs and and pillow fragment breccias of unit "J". The flows are relatively undeformed and are within the prehnite-pumpellyite facies zone; primary textures and structures are generally well preserved.

Most flows are creamy buff to buff-brown weathering with pale to medium grey-green fresh surfaces. Adjacent to the Big Island Fault, flows are pervasively epidotized, medium to dark grey on weathered surfaces, and dark green on fresh surfaces.

Pillowed flows without associated amoeboid pillow breccias dominate this unit. Flow contacts were not identified and consequently flow thicknesses are not known. Pillows are typically bun-shaped, 0.5 — 2 m in size, and have white to rusty brown weathering selvages that range from 2 to 20 mm thick. Interpillow voids are filled with partly epidotized hyaloclastite and, more rarely, with vuggy quartz. Vesicles (0.5 — 3 mm, up to 10 mm) form 2 — 20% of pillows. Plagioclase phenocrysts and glomerocrysts (0.5 — 4 mm, 5 — 20%) are contained in a groundmass rich in randomly oriented plagioclase microlites.

Plagioclase glomerocrysts are commonly composed of over 25 individual, 0.2 — 1 mm, tabular to equant, euhedral plagioclase crystals. Many glomerocrysts include up to 15% subhedral, stubby 0.1 — 1 mm grains of clinopyroxene that, with the plagioclase, display a gabbroic intergranular texture. Individual 0.2 — 1 mm phenocrysts of plagioclase and clinopyroxene are also present in small amounts; they are the same size and shape as those in the glomerocrysts. The groundmass is composed of a felted mosaic of lath-shaped, euhedral, 0.1 — 0.3 mm plagioclase microlites enclosed in a fine grained secondary mixture of tremolite-actinolite, epidote and chlorite. Size and crystal morphology grade continuously between plagioclase microlites in the groundmass and plagioclase crystals that occur both as phenocrysts and glomerocrysts (seriate texture).

Gabbroic textured plagioclase glomerocrysts are present in glomerophyric basalts and basaltic andesites of unit "M" (higher in the Rennie Lake section; Fig. 150), and in glomerophyric mafic to intermediate flows between the Ross Lake Fault and Mitt Lake. Gabbroic textured glomerocrysts are sufficiently rare that their presence in the flows near Mitt Lake suggests these flows may correlate with units "K" and "M" of the Rennie Lake section.

APHYRIC TO SPARSELY PORPHYRITIC BASALT (L)

A 210 m thick sequence of creamy buff to buff-brown weathering aphyric and sparsely porphyritic pillowed basalt flows (unit "L") occurs between the glomerophyric basalt and andesite flows of units "K" and "M" in the Rennie Lake section (Fig. 150). The pillowed flows include zones of amoeboid pillow breccia (up to 45 m thick). Pillow selvages are 2 — 5 mm thick, red-brown to brown, and increase in thickness towards the top of some flows. Vesicles are 1 — 3 mm in diameter and form 5 — 15% of most flows. Measured flows are over 15 m thick.

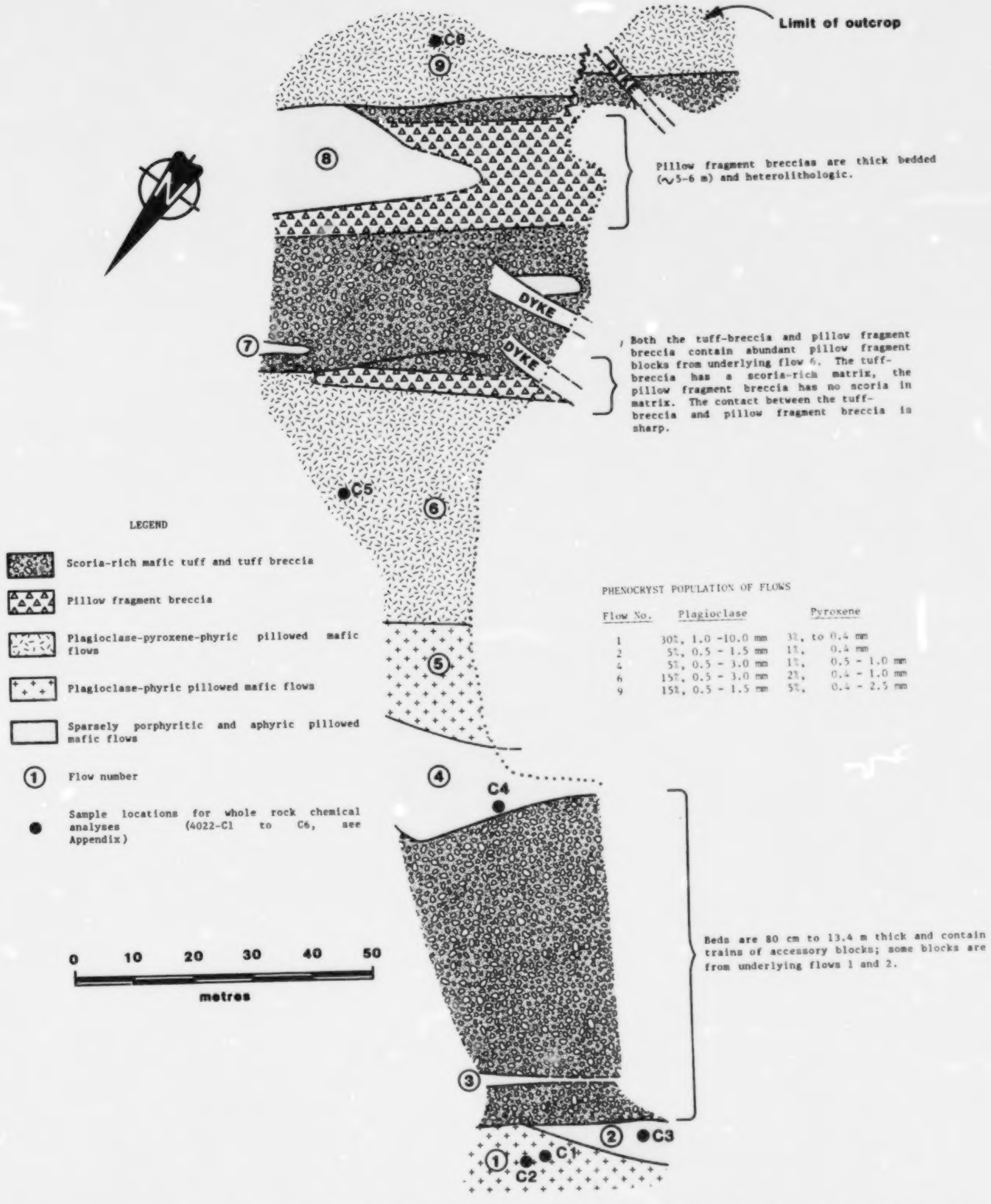
Limit of outcrop
C6
9
DYKE
8
DYKE
DYKE
7
C5
6
5
4
C4
3
2
C3
1
C1
C2
N
0 10 20 30 40 50
metres
LEGEND
Scoria-rich mafic tuff and tuff breccia
Pillow fragment breccia
Plagioclase-pyroxene-phyric pillowed mafic flows
Plagioclase-phyric pillowed mafic flows
Sparsely porphyritic and aphyric pillowed mafic flows
Flow number
Sample locations for whole rock chemical analyses (4022-C1 to C6, see Appendix)

Pillow fragment breccias are thick bedded (~5-6 m) and heterolithologic.

Both the tuff-breccia and pillow fragment breccia contain abundant pillow fragment blocks from underlying flow 6. The tuff-breccia has a scoria-rich matrix, the pillow fragment breccia has no scoria in matrix. The contact between the tuff-breccia and pillow fragment breccia is sharp.

Beds are 80 cm to 13.4 m thick and contain trains of accessory blocks; some blocks are from underlying flows 1 and 2.

PHENOCRYST POPULATION OF FLOWS

Flow No.	Plagioclase	Pyroxene
1	30%, 1.0 -10.0 mm	3%, to 0.4 mm
2	5%, 0.5 - 1.5 mm	1%, 0.4 mm
4	5%, 0.5 - 3.0 mm	1%, 0.5 - 1.0 mm
6	15%, 0.5 - 3.0 mm	2%, 0.4 - 1.0 mm
9	15%, 0.5 - 1.5 mm	5%, 0.4 - 2.5 mm

Figure 161: Stratigraphic sequence in a portion of unit "J", Hook Lake Block, modified from geology by T. Corkery (pers. comm., 1983). Well exposed scoria rich mafic tuffs and tuff breccia are present in this section located 520 m west of the south end of Manistikwan Lake. Flows at this location (4022) have been sampled for chemical analyses (bold dots mark sample locations, analyses in Appendix).

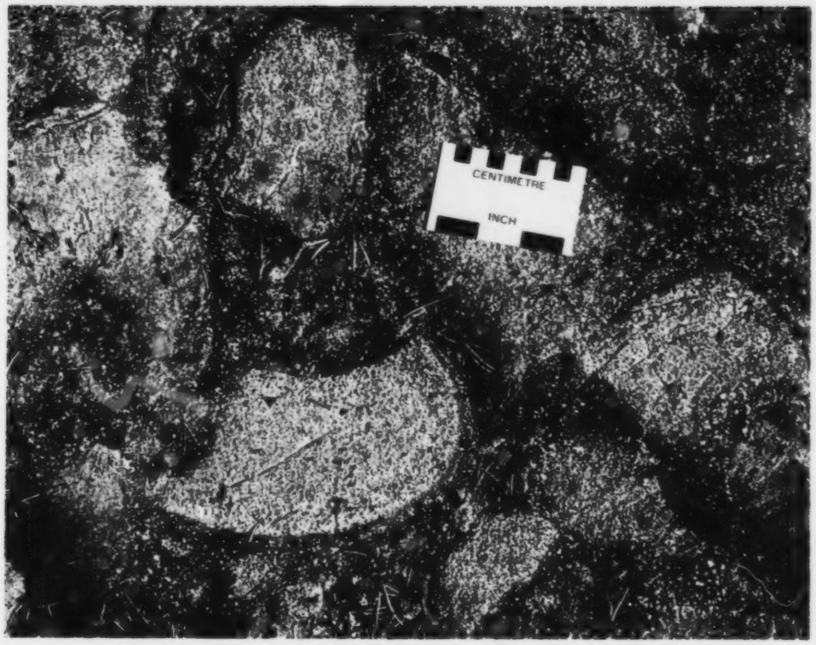

Figure 162: *Pillow fragment breccia (unit 9a) within stratigraphic unit J, Hook Lake Block (Fig. 150, 151), east of Kinsella Lake. Angular fragments of porphyritic pillows, some with the 5 mm thick selvage remaining, are in a fine grained clastic matrix. The deposit is monolithologic and clearly derived from fragmentation of a pillowed flow.*

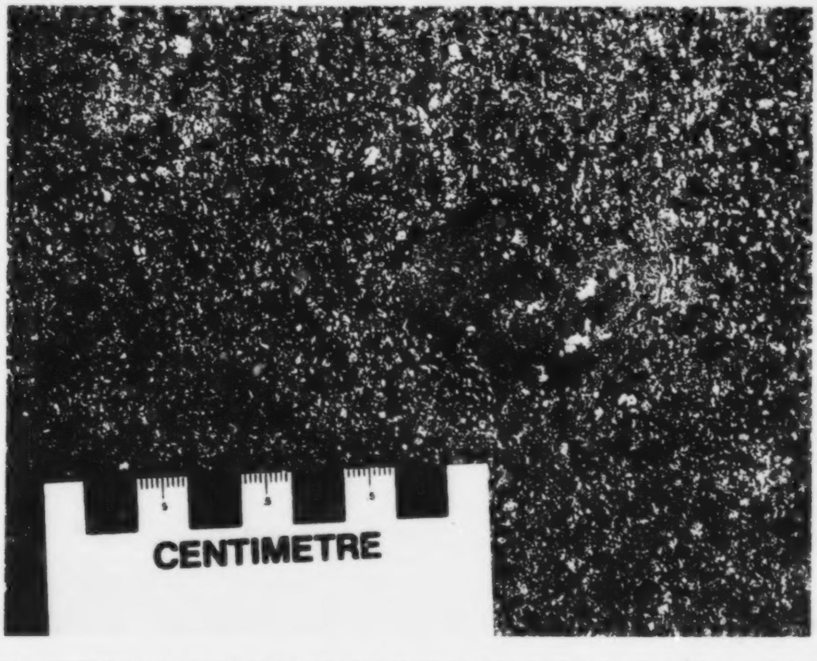

Figure 163: *Large, porphyritic scoria lapillus in scoria-rich plagioclase-phyric mafic tuff (unit 23b), adjacent to gravel pit at south end of Manistikwan Lake. Note dark oxidized rim of scoria fragment.*

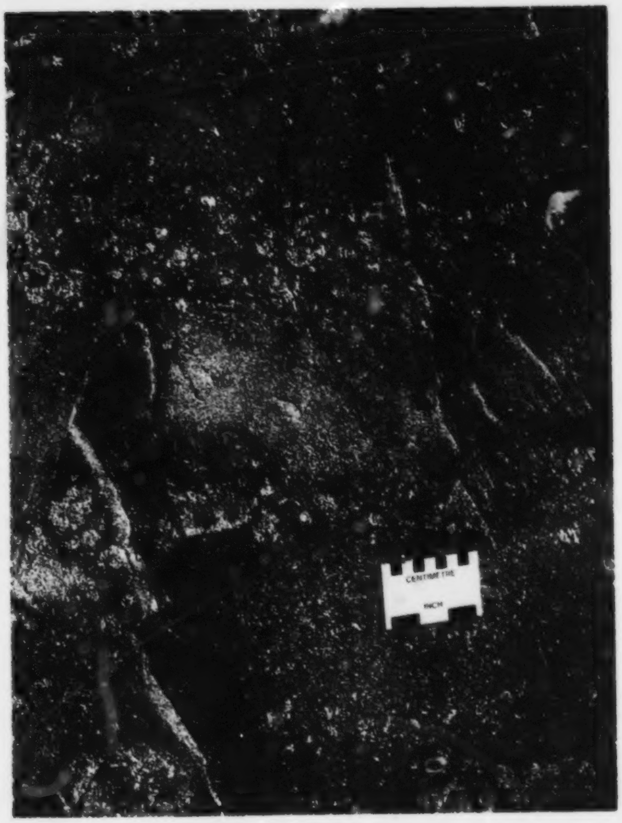
CENTIMETRE
INCH

Figure 164: *Layering in mafic, scoria-rich lapilli tuff (unit 23a), east of Borne Lake. Scoria fragments have about 60% vesicles and are subrounded to rounded in shape. Top is to the left.*

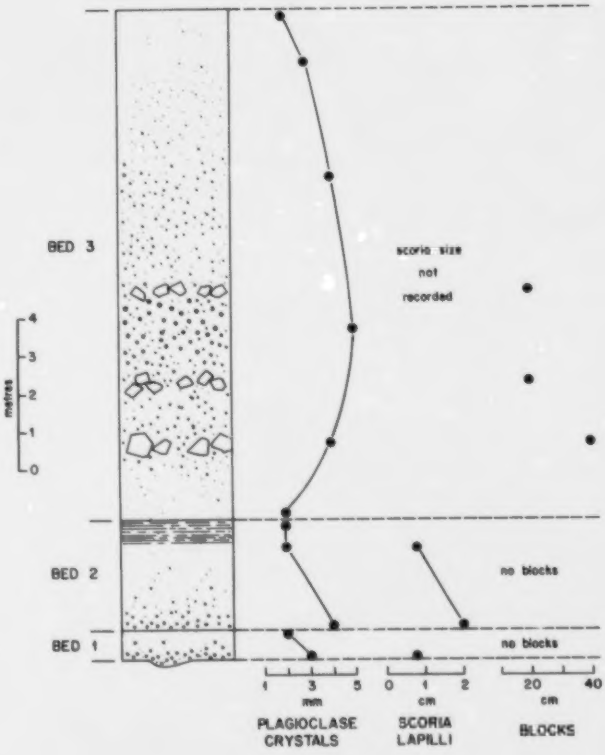
BED 3
BED 2
BED 1
metres
0
1
2
3
4
scoria size
not
recorded
no blocks
no blocks
1
3
5
mm
PLAGIOCLASE
CRYSTALS
0
1
2
cm
SCORIA
LAPILLI
20
40
cm
BLOCKS

Figure 165: *Grading displayed by three scoria-rich tuff beds, unit "J", Rennie Lake section (Fig. 150), Hook Lake Block. Maximum sizes of plagioclase crystals, scoria lapilli and accessory blocks are shown. Bed 1 is normally size-graded A type, bed 2 is normally graded AB type, and bed 3 is reverse to normally graded with three crude layers of blocks. The latter are accessory fragments derived from pillowed flows lower in sequence.*

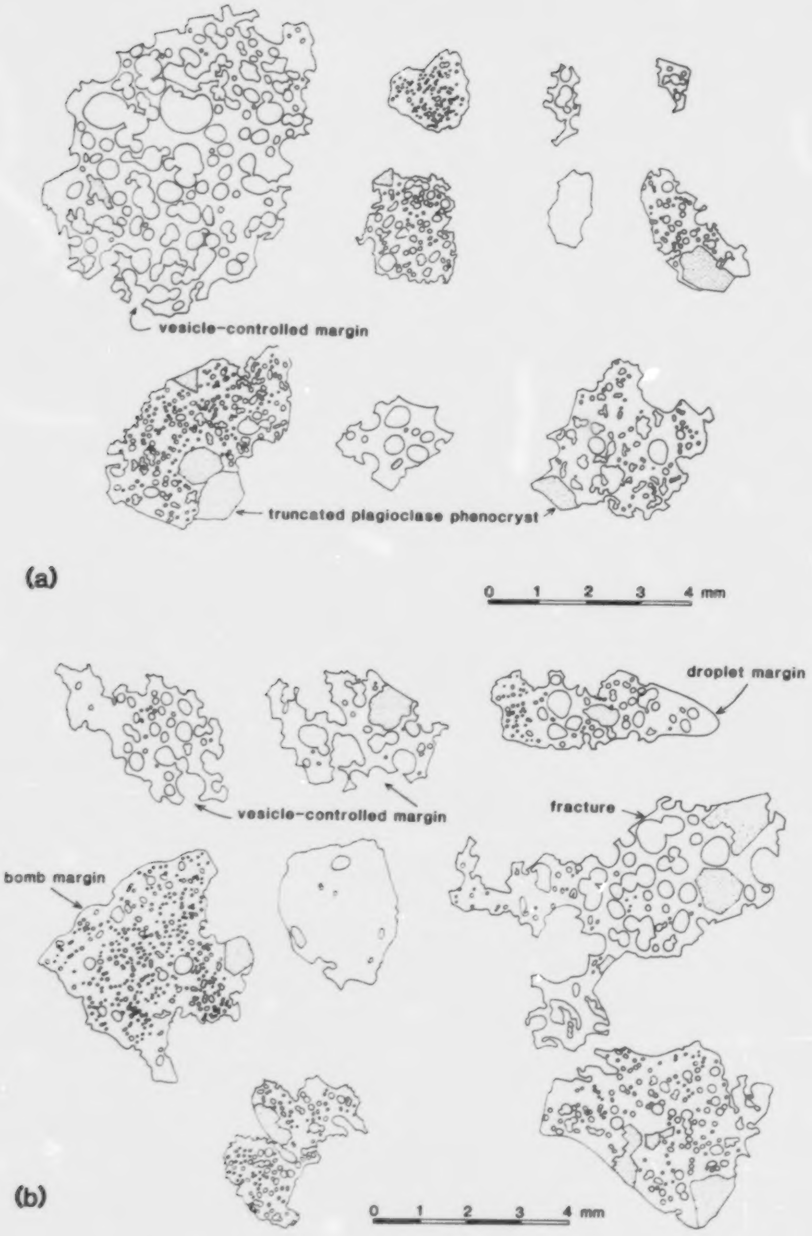
vesicle–controlled margin
truncated plagioclase phenocryst
(a)
0 1 2 3 4 mm
droplet margin
vesicle–controlled margin
fracture
bomb margin
(b)
0 1 2 3 4 mm

Figure 166: Tracings of scoria particles in scoria-rich mafic tuff, unit "J", Hook Lake Block. Scoria particles have predominantly vesicle-controlled margins; some are partly bounded by fractures or chilled droplet margins. (a) Sample from 6 m above base of bed 3 (Fig. 165). (b) Sample from 1.5 m above base of bed 2 (Fig. 165).

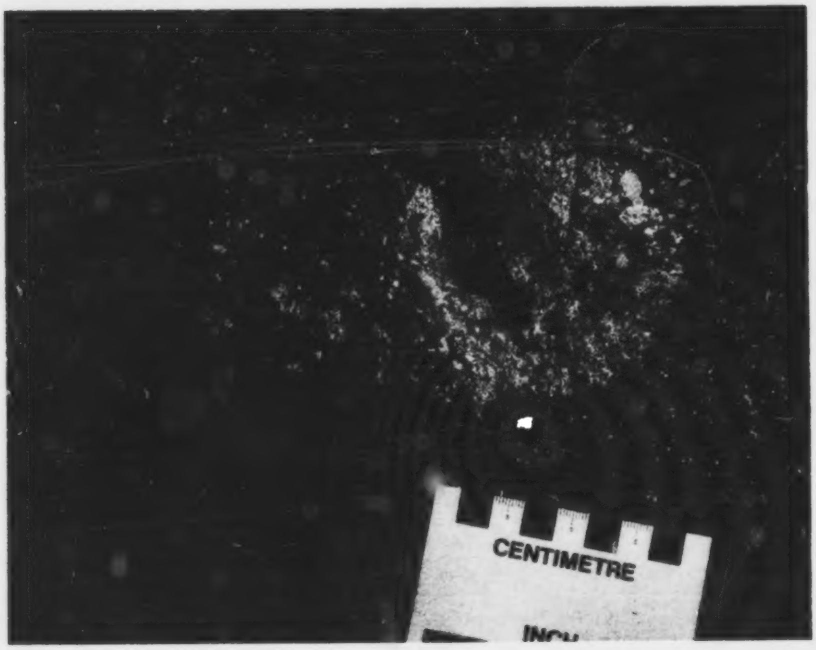

Figure 167: Accessory clasts of pillowed basalt in mafic scoria-rich tuff (unit 23b), east of Kinsella Lake. This photograph shows part of the basal tuff unit shown in Figure 161, and is part of bed 3 in Figure 165. The basalt fragments differ widely in colour and phenocryst content, and can be matched exactly to flows 1 and 3 in Figure 161.

The flows are mesoscopically aphyric to sparsely plagioclase-phyric. Microscopically all flows are plagioclase- and clinopyroxene-phyric, with 1 — 3% tabular to equant euhedral plagioclase (0.2 — 0.5 mm) and approximately 1% euhedral clinopyroxene (0.2 — 0.5 mm). Small plagioclase glomerocrysts (less than 1 mm) are present in most flows. The flows have an intergranular texture with stubby 0.1 — 0.2 mm plagioclase microlites and interstitial equant clinopyroxene grains (pseudomorphed by tremolite-actinolite, epidote and chlorite).

PLAGIOCLASE-GLOMEROPHYRIC BASALTIC ANDESITE AND ANDESITE (M)

More than 510 m of pillowed, predominantly glomerophyric, basaltic andesite and andesite (unit "M") forms the uppermost member of the Rennie Lake section (Fig. 150), and are the youngest flows exposed in the Hook Lake Block. The Big Island Fault truncates the top of this unit. The flows are characterized by plagioclase-rich, gabbroic-textured glomerocrysts identical to those previously described in the glomerophyric flows of unit "K". Minor aphyric and sparsely plagioclase- and pyroxene-phyric flows are also present in unit "M".

The flows are creamy buff to buff-brown weathering and are pillowed throughout. Flow contacts, rarely observed, are marked by narrow amoeboid pillow breccia zones at flow tops, and large mattress-shaped pillows at flow bases. A 2 m wide tube was followed for over 10 m along a dip surface in one exposure. Pillows are bun-shaped to turnip-shaped (where tectonically flattened) and have approximately 1 cm thick chocolate brown selvages. Tops of pillows contain up to 15% vesicles (1 to 5 mm).

Glomerocrysts (0.4 — 3 mm) are composed of up to 25 individual plagioclase and pyroxene crystals. They include monomineralic and gabbroic types, the latter typically containing less than 20% clinopyroxene. Plagioclase crystals are either stubby laths or equant grains; they display abundant albite, pericline and carlsbad twins. The groundmass is strongly plagioclase microlitic with intergranular textures predominant. Plagioclase microlites have skeletal morphologies in some flows. Both plagioclase and clinopyroxene crystals display all gradations in size and shape between grains in the groundmass and those contained in glomerocrysts. Groundmass clinopyroxene grains are partly altered to brown hornblende or to tremolite-actinolite, epidote and chlorite; clinopyroxene phenocrysts are commonly unaltered. Flows that appear aphyric in hand specimen typically contain a few microphenocrysts of plagioclase and clinopyroxene, and some contain small gabbroic-textured glomerocrysts.

Unit "M" contains a 30 m thick unit of mafic to intermediate tuff and lapilli tuff 200 m above its base, near the northwest end of the Inlet Arm of Schist Lake. The tuff and lapilli tuff are monolithologic and are composed of juvenile plagioclase- and pyroxene-phyric scoria and broken plagioclase and pyroxene phenocrysts. The scoria are finely vesicular with up to 50%, 0.1 — 0.2 mm round to elliptical vesicles. They contain phenocrysts of clinopyroxene (0.2 — 3 mm, 5 — 10%) and plagioclase (0.2 — 3 mm; 5 — 10%) and 10% glomerocrysts (0.4 — 2 mm) similar to those in flows.

Three analyses of unit "M" flows indicate an upward change in composition from basaltic andesite to andesite. Silica (calculated volatile-free) increases from 53.92% to 58.40% and FeO decreases from 11.59% to 8.46%; other elements remain relatively constant (e.g. MgO — 4.38 to 4.65%, TiO_2 — 0.49 to 0.55%, P_2O_5 — 0.14 to 0.15%, Zr — 23 to 28 ppm, Y — 18 ppm).

SCHIST LAKE SECTION

The Schist Lake section is approximately 5 km thick (Fig. 150), exposed between the Insole Lake Fault and Cliff Lake Fault (Fig. 151). The section is folded about a northeast-trending anticline located west of Insole Lake (Fig. 151); best preservation is in south-facing rocks on the southwest limb of the fold.

The lowermost unit in the section comprises porphyritic pillow fragment breccias and subordinate thin (1 — 4 m) flows, which are correlated with unit "D" in the Milliken Lake section (Fig. 151). The breccias are generally monolithologic and composed of 2 — 30 cm angular to subrounded pillow fragments in a poorly sorted coarse sandy matrix of granules and crystals. Beds are 30 cm to more than 4 m thick and display the typical organization for similar breccias elsewhere (Fig. 10), including a massive non-graded lower portion and a more matrix-rich, graded top. Fragments are moderately to strongly porphyritic, with plagioclase (0.5 — 4 mm, 10 — 20%) and pyroxene (0.5 — 4 mm, 0 — 15%) phenocrysts. Some fragments retain partial pillow selvages; others have bands of vesicles that are truncated at fragment margins. Amygdales in fragments vary in size and abundance, up to 20% and 4 mm diameter. Fragments are up to 30 cm across but are generally less than 10 cm; shapes include crescentic, wedge-shaped and rare complete pillow types characteristic of this type of deposit. On the northeast limb of the fold breccias are variably epidotized and weather dark grey to green. Epidotization includes a number of forms:

1) selective grey to black alteration along close-spaced fractures,
2) anastomosing, commonly folded yellow-green epidote veins and stockworks,
3) complete epidotization of interiors of most fragments, leaving a few millimetres of dark grey to black (unepidotized?) material in sharply defined fragment rims,
4) pervasive, complete epidotization which obliterates primary structures. This type of alteration is associated with breccias in proximity to a porphyritic granodiorite (unit 57) intrusion, where there is also an apparent superimposed K-metasomatism.

A 1460 m thick sequence of aphyric and porphyritic mafic flows overlies the pillow fragment breccias. This sequence of flows can be directly correlated across the Insole Lake Fault with similar flows of unit "E" in the Milliken Lake section (Fig. 150). The sequence displays the same upward zonation in amygdale fillings as in unit "E" (carbonate in the lower two-thirds of the unit and mafic minerals in the upper portion). Displacement of amygdale-filling zonation indicates 300 m of apparent left lateral offset across the fault. Flows in this sequence are identical to those in unit "E", but are not as well exposed. In addition there are intercalated units of bedded heterolithologic tuff and tuff breccia, porphyritic pillow fragment breccia and an amphibole-plagioclase-quartz-phyric intermediate flow.

A 120 m thick unit of plagioclase-phyric scoria tuff and lapilli tuff overlies unit "E"-type flows. Beds in this unit display excellent normal size grading of plagioclase crystals and scoria. Bed types are AB and ABC; bed thickness ranges from 0.3 to 10 m. Plagioclase crystals are up to 3 mm across and form 10 — 25% of most beds.

Plagioclase-phyric and aphyric flows form a 270 m thick unit overlying the scoria tuff. Composite flows (cf. Fig. 9) predominate. Plagioclase phenocrysts are 1 — 2 mm in size and constitute 5 — 15% of the porphyritic flows.

The succeeding unit in the sequence is 240 m of scoria tuff and pillow fragment breccia. Scoria tuff beds are 0.1 — 2 m thick and display a classic Bouma turbidite zonation with A, AB and ABDE bed types. Sedimentary structures displayed by the tuff are normal size grading of plagioclase crystals, load structures, and rare current laminations (Fig. 168).

The scoria tuff is overlain by 270 m of thick flows with highly variable phenocryst contents. Massive, composite and pillowed flows, up to 55 m thick, are present. Porphyritic flows contain up to 10% plagioclase phenocrysts (0.2 — 3 mm) and up to 3% pyroxene phenocrysts (0.2 — 2.4 mm). Massive flows and massive divisions of flows contain 5 — 10% amygdales (0.2 — 2 mm); upper portions of flows contain 20% amygdales to 10 mm in diameter. Some pillows have radial pipe vesicles. Pillowed flows show an upward increase in amygdale content and decrease in pillow size.

Three hundred and thirty metres of scoria tuff, lapilli tuff and tuff

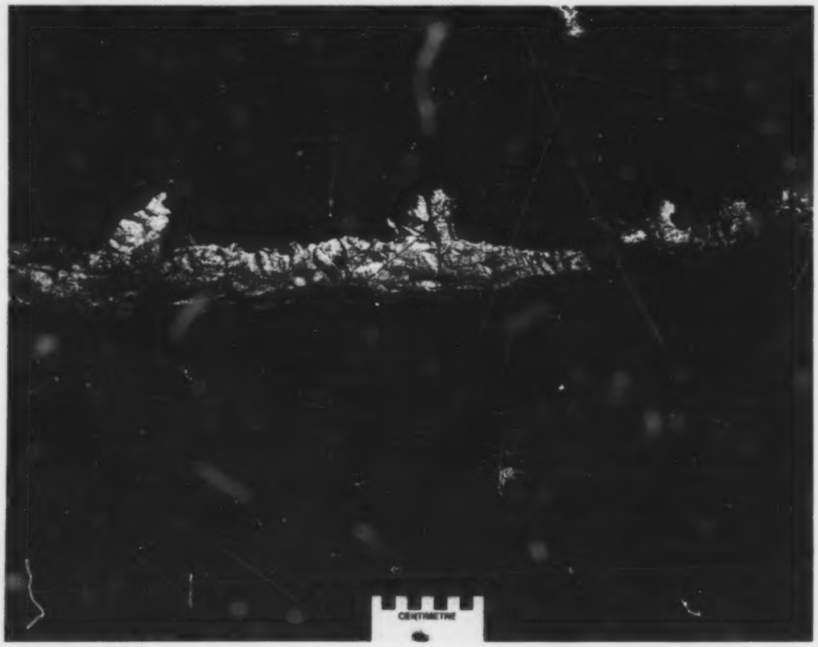

Figure 168: Well bedded mafic scoria-rich tuff (unit 23), 900 m west of Hook Lake. Primary structures include indistinct ripple laminations (R) near top of lower bed, size-grading (G) in overlying bed and load casts on top of white tuff.

breccia overlie the flows described above. The top of the unit is truncated by a fault (Fig. 151). The tuffs are strongly porphyritic with up to 30% plagioclase (0.5 — 3 mm) and 0 — 10% pyroxene (1 — 4 mm). Beds range from 0.3 to over 6 m thick and are typically A and AB types. They are composed of porphyritic scoria to 6 cm, non-vesicular granules and lapilli, and 5 — 20 cm accessory amygdaloidal mafic blocks and rare rhyolite blocks. Some beds have reverse size-grading at their base but most display normal size-grading from base to top. The mafic accessory blocks form discontinuous "trains" (cf. Fig. 165) and are interpreted to be ballistic fragments.

Poorly exposed aphyric and porphyritic mafic flows form an approximately 820 m thick unit southwest of Hook Lake, the base of which has been removed by a fault that also truncates the top of the underlying scoria tuff. These flows include both massive and pillowed types, contain amygdales to 10 mm in size, and closely resemble the west-facing flows in a small adjacent fault-bounded panel (Fig. 151).

A thick (520 m) unit of scoria tuff, breccia, and rare pillow fragment breccia overlies the flows. Scoria tuff beds are 15 cm — 9 m thick and include A, AB and massive types. Many have white weathering fine grained tops. The tuffs display normal size-grading, scours, and "trains" of accessory ballistic blocks similar to other units of this type. Phenocryst content varies between beds. Beds are composed of both scoriaceous and non-vesicular material. Scoria breccia beds are distinctive in that they contain large (2 — 20 cm), rounded, porphyritic scoria clasts honeycombed with large vesicles. Rims of scoria clasts contain smaller and fewer vesicles than their interiors. Scoria breccia beds range from 3 to 13 m thick, display reverse to normal size-grading and commonly have fine grained tops. Rare pillow fragment blocks are present in some beds.

A thin (15 m) unit of pyritic mudstone overlies the scoriaceous tuff. The unit is composed of pyritic mafic tuff with intergranular carbonate, topped by 1 m of graphitic argillite. The fine grained sediments are overlain by massive, sparsely plagioclase-phyric flows which top the stratigraphic sequence.

GRANT LAKE SECTION

The Grant Lake section (Fig. 150) is bounded on the east and south by the Big Charlie Lake Fault and on the west by the Cliff Lake Fault. Volcanic rocks in this section are intruded by the Cliff Lake Pluton. Stratigraphic correlation with other sections in the Hook Lake Block is based on:

1) a lithologic similarity between the aphyric mafic flows at the base of the section with aphyric basaltic andesite flows of unit "B" in the Hartnett Lake section.
2) a chemical similarity of aphyric flows at the top of the section with high-MgO aphyric basalts of unit "E" in the Milliken Lake section,
3) a general similarity between the sequence of aphyric and porphyritic flows and pillow fragment breccia (described below) and units "C" and "D" in the Hartnett Lake and Milliken Lake section (Fig. 150).

The lowermost unit in the Grant Lake section comprises aphyric to sparsely porphyritic pillowed flows. These weather buff to grey and are moderately to strongly deformed and epidotized. As in the equivalent unit "B" in the Hartnett Lake section, intercalated breccias or tuffs are absent, apart from amoeboid pillow breccia flow tops. Amygdales are common and up to 10 mm in diameter; radial pipe vesicles occur locally. Adjacent to the Cliff Lake Pluton the flows are epidotized or strongly recrystallized (hornfelsed?) although primary structures are well preserved in the contact zone. Local stratiform zones of disseminated pyritic alteration also characterize the contact zone.

The aphyric flows are overlain by up to 430 m of aphyric and porphyritic pillow fragment breccia and minor intercalated pillowed flows. Beds are thicker than 10 m, reverse to normally graded, and display an upward increase in the proportion of matrix to fragments. Individual beds are monolithologic; however, fragment types vary with respect to phenocryst populations between beds. Some units containing a particular fragment type are of mappable dimensions. Pillow fragment breccia beds are internally organized as elsewhere (cf. Fig. 10) and contain all the characteristic fragment shapes.

The remainder of the Grant Lake section consists of 8 stratigraphic units, the topmost being equivalent to unit "E" in the Milliken Lake section (Fig. 150). These 8 units are described briefly below, in ascending stratigraphic order:

1) Strongly deformed and foliated aphyric and porphyritic pillowed mafic flows (120 m).
2) Massive, monolithologic, pyroxene-phyric pillow fragment breccia (80 m). Fragments in breccia contain 5 — 15% pyroxene phenocrysts (up to 4 mm) and are angular to subrounded, 3 — 10 cm in size, and amygdaloidal (5 — 40%, up to 5 mm). Many fragments have portions of pillow selvages and radial pipe vesicles. The matrix is fine grained, sandy, and contains 20% pyroxene crystals.
3) Light grey, plagioclase-phyric heterolithologic breccia (150 m). Fragments in the breccia are angular to subrounded and up to 25 cm long.
4) Porphyritic and minor aphyric pillowed mafic flows (100 m). These flows contain abundant large (to 1 cm) amygdales and quartz-filled gas cavities to 3 cm.
5) Plagioclase-phyric and pyroxene-phyric mafic pillow fragment breccia (200 m). Bedding is thick, fragments and matrix are similar in composition, and most fragments are non-vesicular. Minor heterolithologic mafic breccia and lapilli tuff are present in the unit adjacent to Cliff Lake Fault.
6) Mafic to intermediate tuff (30 m). Beds are A and AB types and range from 0.5 to 2 m thick. The tuff is fine grained and contains plagioclase and pyroxene crystals.
7) Monolithologic porphyritic pillow fragment breccia, heterolithologic breccia, scoria-bearing lapilli tuff, and minor pillowed plagioclase-phyric mafic flows (300 m). This diverse sequence is well bedded (0.4 — 10 m). The scoriaceous lapilli tuff is similar to that in unit "K", and contains sporadic angular accessory blocks.
8) Aphyric pillowed basalt (180 m). These basalts have a high MgO content, similar to high-MgO flows that occur in unit "E" in the Milliken Lake section. The lower part of this unit has intercalated tuff and pyritic tuff units up to 2 m thick.

SUMMARY AND INTERPRETATION

The Hook Lake Block contains approximately 7.5 km of basalt and basaltic andesite, and rare andesite. The sequence is composed of thick pillowed flows and subordinate intercalated units of pillow fragment breccia and scoriaceous tuff and breccia. Mafic flows occur in mappable units 120 — 1000 m thick, with each unit defined by phenocryst type and abundance. Contacts between these major units are sharp. Pillow fragment breccia units up to 820 m thick are composed of thick breccia beds; as in the flows, these units can be distinguished on the basis of their phenocryst content. Scoriaceous tuff and breccia form a small proportion (7%) of the entire sequence but have important environmental implications, discussed below.

There are major differences between the Hook Lake volcanic sequence and the 3.3 km-thick Bear Lake sequence, suggesting the two had significantly different evolutionary paths. The Bear Lake basaltic andesite displays systematic stratigraphic variations which are interpreted to have been produced during the growth of a single subaqueous mafic volcano into progressively shallower water. These stratigraphic variations include a well defined upward increase in vesicle content and size, an upward decrease in average flow thickness, and an upward decrease in the proportion of pillowed to massive flows. The mafic flows in the Hook Lake sequence do *not* display a well defined upward increase in vesicularity. Rather, strongly amygdaloidal members, some with large (1 cm) amygdales, gas cavities and radial pipe vesicles, are present *throughout* the succession. These relatively shallow-water features (Table 5) suggest that subsidence must have kept pace with volcanic accumulation, maintaining a roughly constant water depth. The Hook Lake sequence also does not display any large-scale systematic stratigraphic variations in flow thickness or organization; virtually all of the flows are thick and pillowed. The sharp intercalation of thick units which vary significantly in phenocryst content and whole-rock composition suggest that the sequence may be the product of more than one eruptive centre.

Pillow fragment breccias were formed through the cold fragmentation of pillowed flows, and were transported to their site of deposition by subaqueous density currents. They can form at any water depth, although in the Bear Lake basaltic andesite volcano they occur associated with strongly vesicular flows near the top of the volcano. In the Hook Lake sequence the largest accumulation of pillow fragment breccia (unit "D") occurs in the lower third of the section and smaller bodies occur throughout the section. A thick unit of transported breccias such as unit "D" is most likely to have accumulated on the flanks and base of a major subaqueous volcano.

Scoria-rich tuffs and breccias provide the most information regarding eruption style and environment. The scoria in these pyroclastic rocks was formed during very shallow water or subaerial magmatic eruptions, possibly punctuated by phreatic or phreatomagmatic eruptions. The pyroclastic components have turbidite bedforms indicating that they were transported and deposited by subaqueous density currents. Many beds contain accessory ballistic pillow fragment blocks, the size of which indicates proximity to vent. The location of dense, ballistic flow fragments in the centre or upper parts of graded scoria-rich beds indicates that the fragments must have been incorporated into the density currents before deposition was completed. These deposits constitute a small but ubiquitous component of the entire sequence, indicating that very shallow water or subaerial sources were present during subaqueous accumulation of this 7.5 km thick section.

FLIN FLON BLOCK

INTRODUCTION

The Flin Flon Block is bounded on the east by the Cliff Lake Fault, unconformably overlain by Missi Group rocks to the north, and extends beyond the boundaries of the map area to the south and west (Fig. 3). As in the Hook Lake Block, the stratigraphic sequence is broken by numerous faults into several distinct sub-blocks (Fig. 169). However, in the Flin Flon Block, stratigraphic correlation between sub-blocks is much more limited than in the Hook Lake Block. Maximum exposed thickness in the Flin Flon Block is in the Hapnot Lake sub-block, where approximately 4 km of section is exposed.

A wide range of rock types occur in the Flin Flon Block. Pillowed basalt and basaltic andesite flows are the predominant rock type. Pillow fragment breccia, scoria-bearing tuff and breccia, and mafic volcanogenic sediments are less abundant, but form a significant proportion of the sequences west of Schist Lake. Rhyolite flows and heterolithologic breccia are minor components. Major lithologies are set forth below, in descriptions of individual sub-blocks, and a summary of conclusions is given at the end of this chapter.

The Flin Flon Cu-Zn massive sulphide deposit occurs in the Hapnot Lake sub-block (Fig. 169 and 170). This 62 million tonne deposit, now largely mined out, contained more ore than the combined tonnage in all other mines in the Flin Flon-Snow Lake mining district.

HAPNOT LAKE SUB-BLOCK

The Hapnot Lake sub-block is bounded to the east by the Ross Lake Fault and to the south by the Phantom Lake Fault (Fig. 169). To the north it is unconformably overlain by Missi Group rocks and to the west extends beyond the map area. The sequence is folded about the Burley Lake Syncline and refolded around the Hidden Lake Synform (Fig. 171), as well as being broken by a number of internal faults.

An east- and southeast-facing stratigraphic section, approximately 4 km thick, is exposed in the Hapnot Lake sub-block between Flin Flon Lake and the top of the exposed section, in the core of the Burley Lake Syncline (Fig. 170 and 171). The base of the section begins approximately 700 m stratigraphically below (i.e. west of) the Flin Flon Cu-Zn sulphide ore deposit. This stratigraphic section comprises the seven units described below in ascending order.

South Main basalt (unit 6)

This basalt underlies the Flin Flon ore deposit. It is at least 700 m thick, extending an unknown distance west, into Saskatchewan. Much of the mapped portion of this basalt lies within the hydrothermal alteration zone associated with the Flin Flon deposit (Fig. 170). It is best preserved and least altered in the large outcrops at South Main shaft. The unit displays a lateral facies change from pillowed flows (unit 6a), at South Main shaft, northwards into pillow fragment breccias (unit 6b).

Flows (unit 6a)

South Main basalt flows weather dark green to brownish green, but are dark rusty brown to dull green where altered. They are dark green on fresh surfaces and typically contain yellow epidosite domains. Flows are pillowed, commonly with a substantial proportion of amoeboid pillow breccia. "Normal" flow organization (Fig. 9), displayed by most of the flows in the map area, is not prominent in South Main basalts. It is common for pillowed flows, or even individual megapillows, to change laterally into units of amoeboid pillow breccia. Flow thicknesses are generally unknown in this unit as complete flows were rarely recorded. At one locality, where complete flows could be measured, they are 8 — 15 m thick and include pillowed and massive types with amoeboid pillow breccia tops. To the north, where flows are intercalated with pillow fragment breccia, flows are thin, typically less than 3 m thick.

Primary structures are locally well preserved in South Main basalt. Pillows vary in size from less than 1 m to megapillows up to 3 m across; they have rusty brown weathering selvages 5 mm thick. Amygdales are abundant throughout the entire mapped portion of the unit. They are filled with quartz or quartz plus epidote, and are commonly 1 — 5 mm in diameter (up to a maximum of 1 — 2 cm). In some flows there is a bimodal amygdale size distribution, with abundant small 0.5 — 1 mm amygdales and sporadic larger 3 — 7 mm amygdales. Radial pipe vesicles up to 8 cm long by 8 mm in diameter are characteristic of flows in the upper 370 m of the unit. Pipe vesicles occur either along the top or completely around entire margin of pillows (Fig. 172).

South Main basalt in hand specimen appears aphyric but in fact contains 2 — 3% pyroxene microphenocrysts (0.2 — 0.8 mm) pseudomorphed by actinolite. Pyroxene microphenocrysts commonly occur in clumps (glomerocrysts) up to 1 mm across. Groundmass is composed of elongate plagioclase laths (up to 0.4 mm long) and abundant dark green actinolite, chlorite, epidote and local leucoxene or magnetite. Rare, sparsely plagioclase-phyric flows were also observed.

Alteration of basalt in surface exposures takes a variety of forms, but most commonly comprises intense epidotization, accompanied by local zones of chloritization and sericitization. Epidotized pillows have yellow epidosite domains in pillow cores and dark green chloritic margins. Some pillows are thoroughly epidotized. Local zones of "bleaching" due to introduction of silica, and gossaned zones characterized by anastomosing chlorite-pyrite-filled fractures, are also present. Within mine workings the alteration zone is characterized by abundant dark green chlorite, which occurs in the stratigraphically overlying Mine rhyolite as well as the South Main basalt. This intense chloritization is not exposed at surface.

The top of the South Main basalt is exposed 250 m northeast of South Main shaft. There, a 10 — 20 m wide zone of gossaned, foliated, chloritic basalt with disseminated and fracture-filling pyrite is directly overlain by unaltered, unmineralized, plagioclase-phyric basalt belonging to the Hidden Lake basalt sequence. This gossan zone is interpreted to be laterally equivalent to the Flon Flon ore zone (Fig. 170).

Pillow fragment breccia (unit 6b)

South Main pillow fragment breccia forms a 400 m thick unit directly underlying the Flin Flon orebody (Fig. 170). North of the orebody this breccia underlies Mine rhyolite. South of the orebody the breccia is laterally gradational into South Main pillowed basalt flows through a transition zone of intercalated amoeboid pillow breccia, pillow fragment breccia, and subordinate thin pillowed flows. Petrographically, fragments in the pillow fragment breccia are pyroxene microporphyritic, identical to South Main basalt flows, clearly indicating that these units are facies equivalents.

Pillow fragment breccias are dark green weathering, monolithologic, poorly sorted, clast-supported and massive, without recognizable bedding contacts. Where best preserved (northwest of the smelter complex) fragments (1 mm — 40 cm) are subangular to rounded, equant, and variably amygdaloidal (Fig. 173). Range in amygdale size and abundance is identical to those in the South Main basalt flows. Matrix of the breccia is a mosaic of epidote, actinolite, chlorite and feldspar which has overprinted small basalt granules.

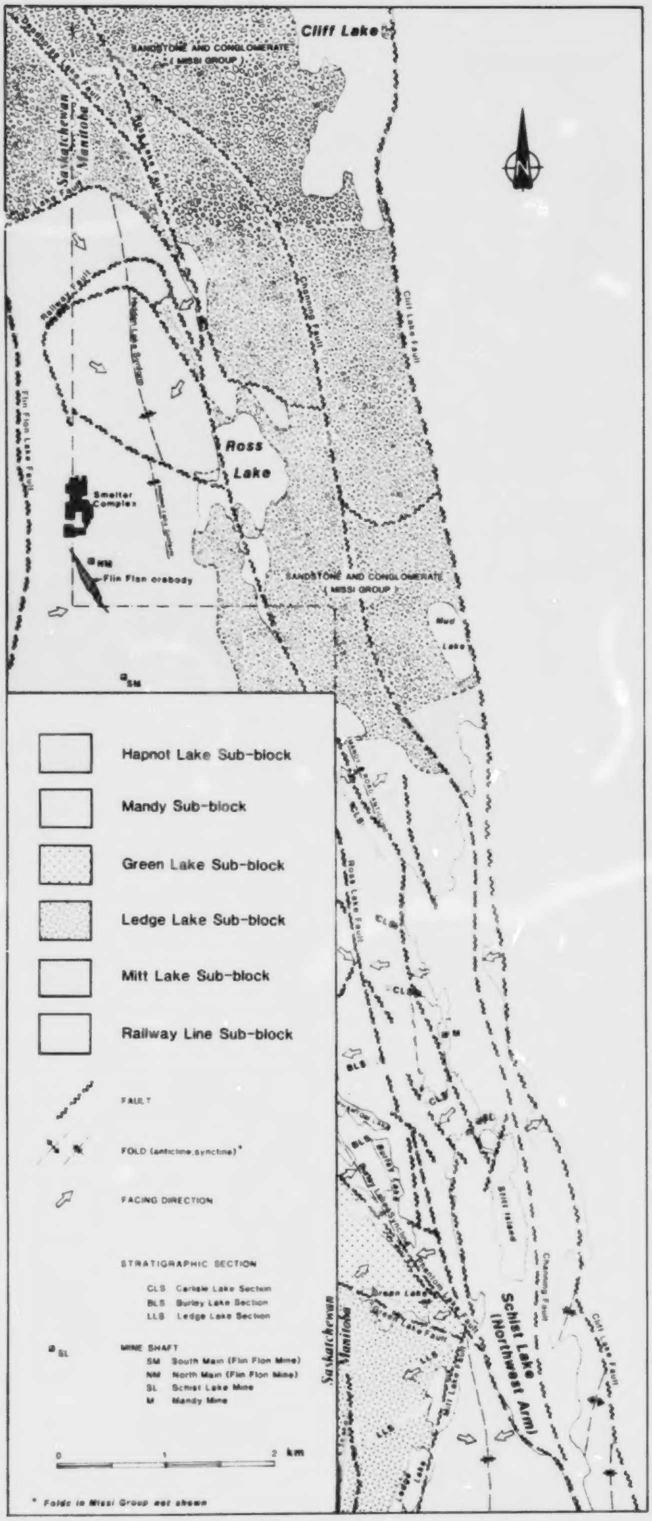
Cliff Lake
SANDSTONE AND CONGLOMERATE (MISSI GROUP)
Saskatchewan
Manitoba
Railway Fault
Ross Lake
Channing Fault
Cliff Lake Fault
Flin Flon Lake Fault
Smelter Complex
NM
Flin Flon orebody
SANDSTONE AND CONGLOMERATE (MISSI GROUP)
Mud Lake
SM
Ross Lake Fault
CLS
BLS
M
Birch Island
Channing Fault
Green Lake
Schist Lake (Northwest Arm)
LLS
Cliff Lake Fault
Hapnot Lake Sub-block
Mandy Sub-block
Green Lake Sub-block
Ledge Lake Sub-block
Mitt Lake Sub-block
Railway Line Sub-block
FAULT
FOLD (anticline, syncline)*
FACING DIRECTION
STRATIGRAPHIC SECTION
CLS Carlisle Lake Section
BLS Burley Lake Section
LLS Ledge Lake Section
SL
MINE SHAFT
SM South Main (Flin Flon Mine)
NM North Main (Flin Flon Mine)
SL Schist Lake Mine
M Mandy Mine
0
1
2 km
* Folds in Missi Group not shown

Figure 169: Structural sub-blocks, major faults and folds and location of Ledge Lake and Mandy stratigraphic sections (see also Fig. 191, 200), Flin Flon Block. Structure in the Missi Group is from Stockwell (1960).

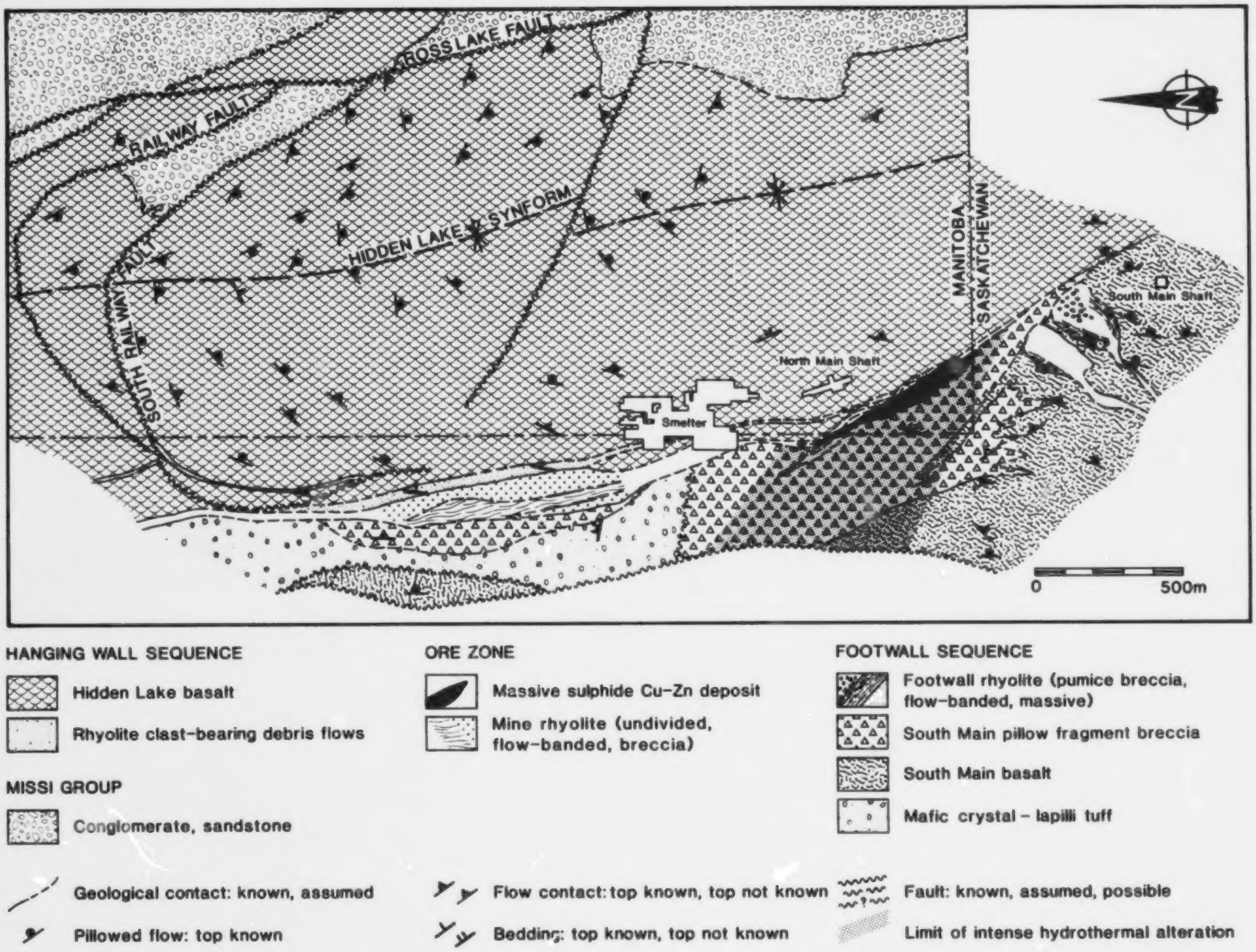
ROSS LAKE FAULT
RAILWAY FAULT
HIDDEN LAKE SYNFORM
SOUTH RAILWAY FAULT
MANITOBA
SASKATCHEWAN
South Main Shaft
North Main Shaft
Smelter
N
0
500m
HANGING WALL SEQUENCE
Hidden Lake basalt
Rhyolite clast-bearing debris flows
MISSI GROUP
Conglomerate, sandstone
ORE ZONE
Massive sulphide Cu-Zn deposit
Mine rhyolite (undivided, flow-banded, breccia)
FOOTWALL SEQUENCE
Footwall rhyolite (pumice breccia, flow-banded, massive)
South Main pillow fragment breccia
South Main basalt
Mafic crystal – lapilli tuff
Geological contact: known, assumed
Pillowed flow: top known
Flow contact: top known, top not known
Bedding: top known, top not known
Fault: known, assumed, possible
Limit of intense hydrothermal alteration

Figure 170: Simplified geology of the Flin Flon Mine area. Minor faults and all intrusions have been omitted to clarify relationships between volcanic units.

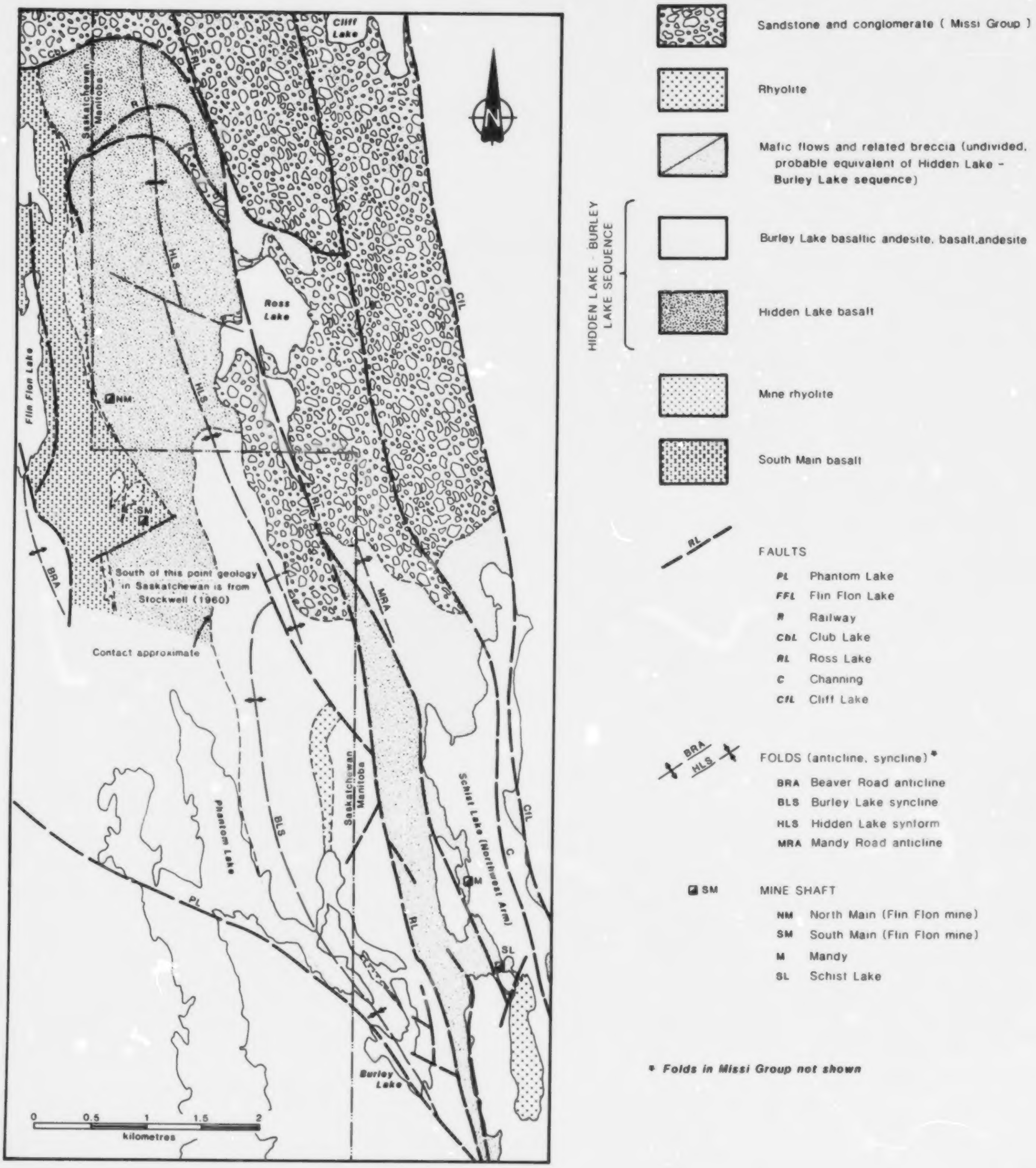
Cliff Lake
Saskatchewan
Manitoba
Ross Lake
Flin Flon Lake
NM
SM
HLS
RL
MRA
BRA
BLS
CfL
C
PL
R
South of this point geology in Saskatchewan is from Stockwell (1960)
Contact approximate
Phantom Lake
Schist Lake (Northwest Arm)
Burley Lake
M
SL
N
0
0.5
1
1.5
2
kilometres
Sandstone and conglomerate (Missi Group)
Rhyolite
Mafic flows and related breccia (undivided, probable equivalent of Hidden Lake - Burley Lake sequence)
HIDDEN LAKE - BURLEY LAKE SEQUENCE
Burley Lake basaltic andesite, basalt,andesite
Hidden Lake basalt
Mine rhyolite
South Main basalt
FAULTS
PL Phantom Lake
FFL Flin Flon Lake
R Railway
CbL Club Lake
RL Ross Lake
C Channing
CfL Cliff Lake
FOLDS (anticline, syncline)*
BRA Beaver Road anticline
BLS Burley Lake syncline
HLS Hidden Lake synform
MRA Mandy Road anticline
SM MINE SHAFT
NM North Main (Flin Flon mine)
SM South Main (Flin Flon mine)
M Mandy
SL Schist Lake
* Folds in Missi Group not shown

Figure 171: Distribution of major mafic flow units in the Hapnot Lake and Mandy sub-blocks. Intrusions, volcaniclastic rocks and sedimentary rocks are not shown (except Missi Group).

Figure 172: *Pillowed South Main basalt (unit 6a), South Main shaft. The pillows have strongly epidotized cores and well developed radial pipe amygdales in margins, typical of the upper part of this unit.*

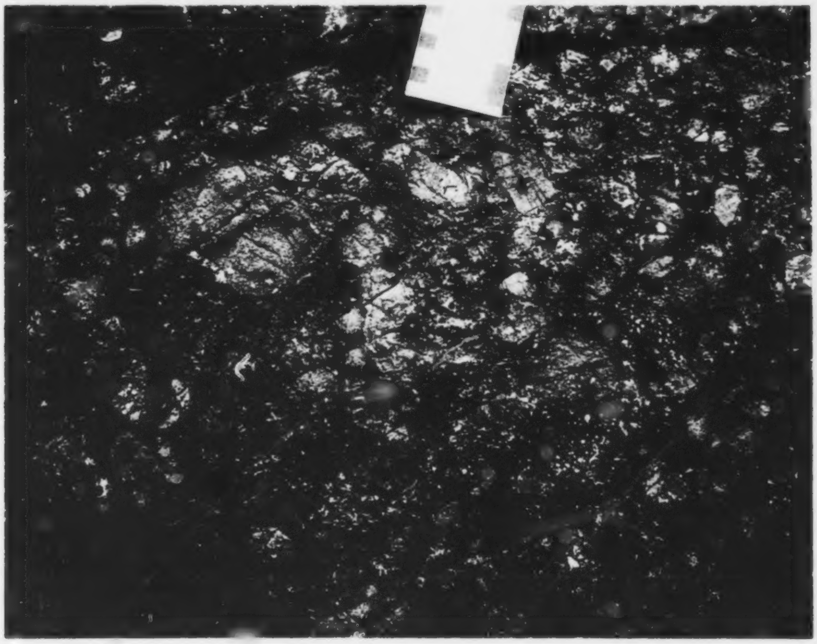

Figure 173: *South Main pillow fragment breccia (unit 6b), 300 m northwest of HBMS smelter. Fragments are relatively small, subrounded to subangular, amygdaloidal, and petrographically identical to South Main basalt (unit 6a).*

Stratigraphically beneath the Flin Flon orebody the breccias are variably altered. In "least altered" varieties the matrix is chlorite-rich and fragments vary from relatively unaltered to partially silicified or epidotized. With increasing intensity of alteration fragments also are strongly chloritized. Other forms of alteration include epidotization and local strong sericitization accompanied by 5 — 20% disseminated pyrite.

Plagioclase-phyric mafic volcaniclastic rocks (unit 22)

A bedded sequence of yellow-buff weathering, altered, plagioclase-phyric mafic volcaniclastic rocks unconformably underlies pillow fragment breccia, 850 m north-northwest of North Main shaft (Fig. 170). The volcaniclastic rocks comprise interbedded plagioclase-rich tuff and heterolithologic breccia.

The tuff contains up to 50% plagioclase crystals (1 — 10 mm), contained in mafic fragments up to 3 cm across; outlines of fragments are poorly defined due to recrystallization. Plagioclase crystals are equant to stubby tabular and are altered to fine grained epidote and chlorite; some are glomerocrystic.

Heterolithologic breccia is composed of variably amygdaloidal fragments 2 mm — 10 cm long. Beds are thick, poorly sorted, fragment-supported, and vary in abundance of plagioclase phenocrysts and size of fragments. Fragments include coarsely plagioclase-phyric types (identical to those in the tuff), sparsely plagioclase-phyric types with plagioclase microlitic groundmass, and white, silicified, densely quartz-amygdaloidal clasts with few, if any, crystals. Contacts with tuff beds are abruptly gradational over a few centimetres.

An angular unconformity, between mafic crystal lapilli tuff and overlying pillow fragment breccias, is exposed in two outcrops three hundred metres west of the north end of the Flin Flon smelter complex. The unconformity is sharp, and truncates bedding in the tuff at a high angle (Fig. 174, 175, 176). Thin (1 m) mafic dykes in the bedded tuff and breccia are also clearly truncated at the unconformity (Fig. 174); the dykes have chilled margins and amygdaloidal cores.

One kilometre north-northwest of the unconformity outcrop similar plagioclase crystal-rich tuff units, interlayered with pillowed basalt, are demonstrably pyroclastic in origin. There, the crystal-rich units are lenticular, up to 11 m thick, and appear to fill topographic lows within the pillow basalt sequence. Individual units are internally bedded; some beds display excellent plagioclase size and abundance grading (Fig. 177). Evidence of pyroclastic origin includes presence of plagioclase-phyric scoria at tops of some beds (Fig. 178), bomb sags beneath plagioclase-phyric lithic blocks, and monolithologic character.

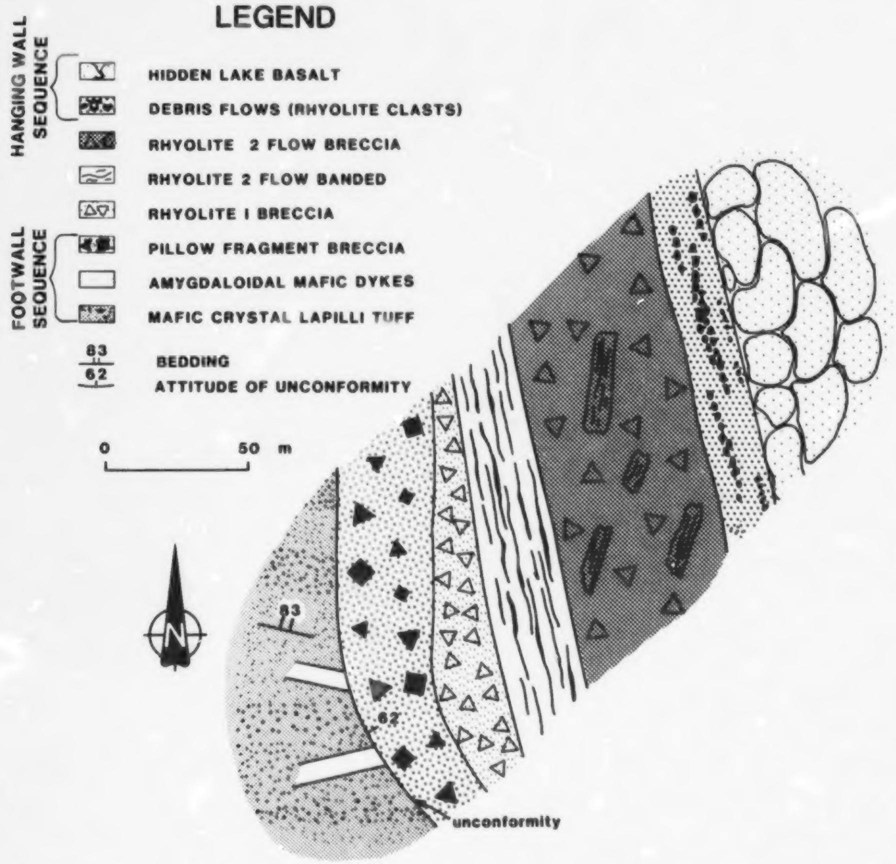

Figure 174: Schematic illustration depicting the stratigraphic sequence northwest of HBMS smelter (Fig. 170), through the stratigraphic footwall and hanging wall of the Flin Flon Cu-Zn sulphide orebody (section tops to the east). Unconformity at base of the pillow fragment breccia truncates bedding and mafic dykes in underlying mafic crystal lapilli tuff.

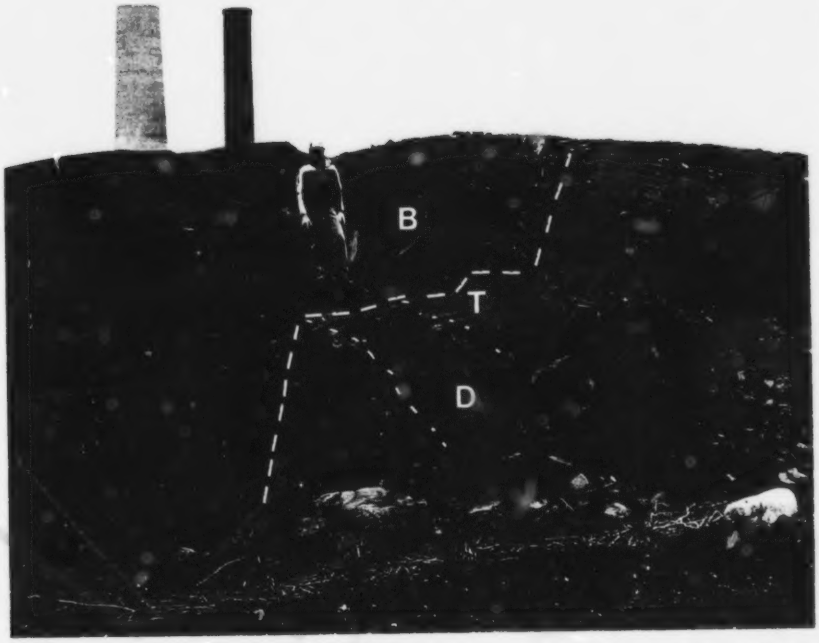

Figure 175: Overview of the unconformity contact between plagioclase-phyric mafic tuff (unit 22b, "T") and overlying South Main pillow fragment breccia (unit 6b, "B"), 300 m northwest of HBMS smelter. The contact is shown by long white dashes; it trends parallel to formation contacts above the unconformity. Short white dashes mark the contact of an amygdaloidal mafic dyke ("D") emplaced in the mafic tuff and truncated at the unconformity; layering in the tuff is approximately parallel to the trend of the dyke. The contact relationships are shown schematically in Figure 174.

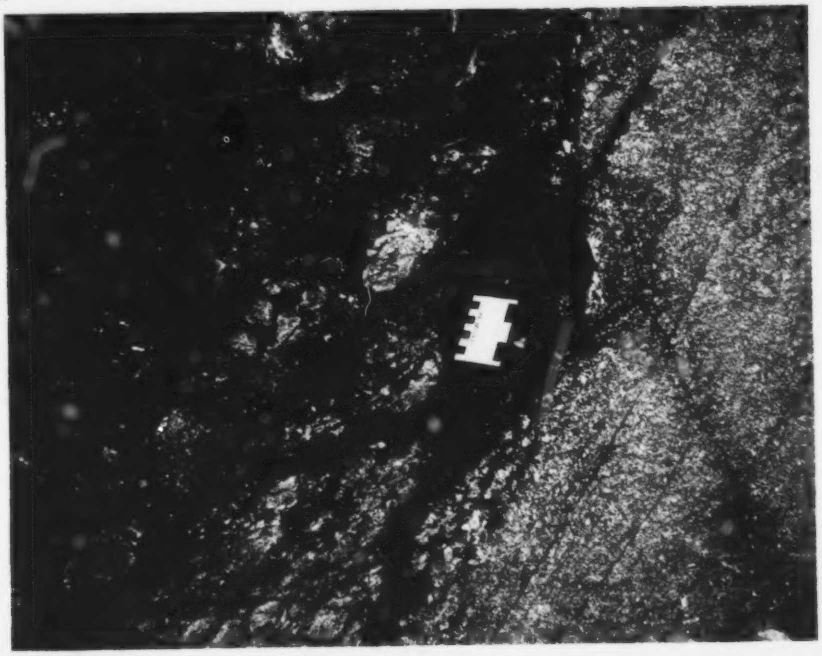

Figure 176: Unconformable contact between plagioclase-phyric mafic tuff (unit 22b, right) and overlying South Main pillow fragment breccia (unit 6b, left), 300 m northwest of HBMS smelter. Contact is not faulted, and is interpreted to be depositional as evidenced by a small degree of mixing at the base of the pillow fragment breccia. Layering in the mafic tuff trends at a high angle to unconformity (Fig. 174 and 175).

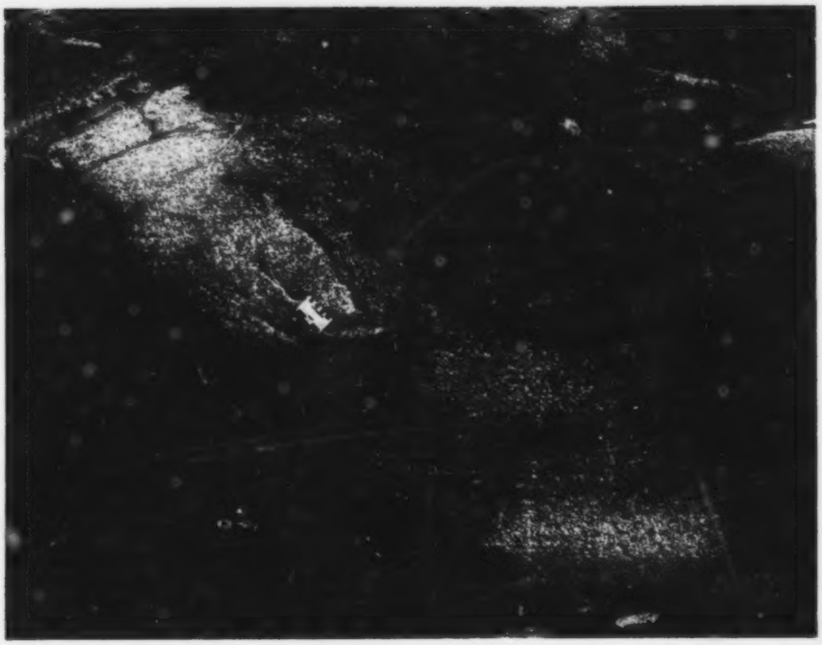

Figure 177: Graded beds of plagioclase crystal tuff (unit 22b), 1160 m northwest of HBMS smelter, by Flin Flon Lake. Stratigraphic tops to top right of photograph.

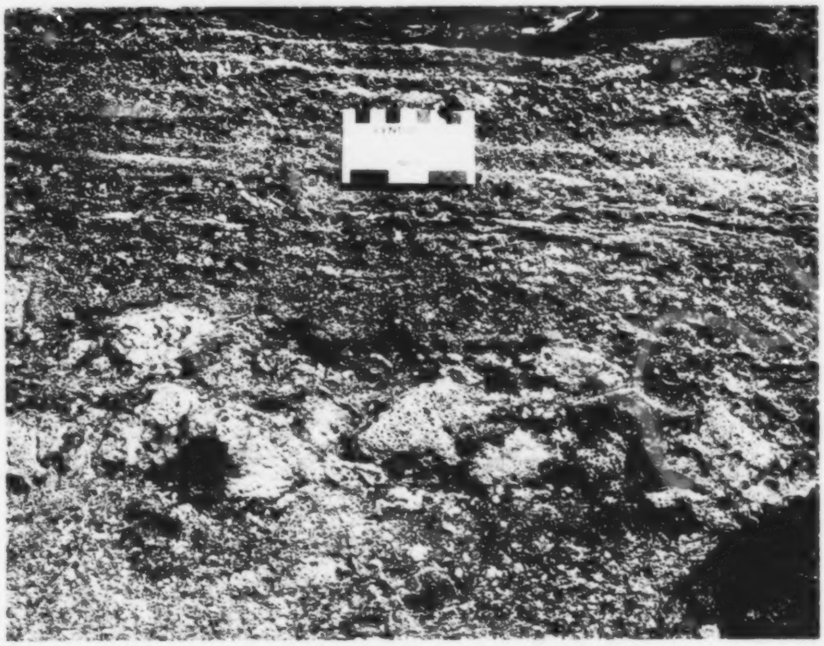

Figure 178: Plagioclase-phyric mafic crystal-lapilli tuff (unit 22b), same locality as Figure 177. Stratigraphic top at top of photograph. Scoriaceous lapilli at the top of one bed are overlain by vaguely laminated crytal-rich tuff.

South Main rhyolite domes (unit 16)

Two rhyolite bodies, which cut across flow contacts in the South Mine basalt, are interpreted as small rhyolite domes. They have bulbous upper portions, up to 150 m across, connected to feeder dykes less than 45 m across. Feeder dykes contain xenoliths of South Main basalt.

Bulbous portions of the domes have a number of primary structures including well defined flow banding (parallel to margins of the domes), clasts of long-tube pumice, pumice breccia in the top of one dome, and rhyolite breccia alternating with flow banded rhyolite. These structures are all consistent with interpretation of the rhyolite bodies as high-level intrusive domes (Fink and Pollard, 1983).

Rhyolite domes are composed of at least four separate phases, indicated by variation in phenocryst population:

1) Quartz-phyric rhyolite with 3 — 5% quartz phenocrysts (0.2 — 2.2 mm) — the most abundant phase;
2) Virtually aphyric rhyolite with less than 1% plagioclase phenocrysts (0.2 — 0.8 mm);
3) Coarsely porphyritic rhyolite with 5% quartz phenocrysts (0.3 — 10 mm) and 10% plagioclase phenocrysts (0.5 — 2.5 mm); and
4) Porphyritic rhyolite with 5% quartz phenocrysts (0.3 — 1.8 mm) and 5% plagioclase phenocrysts (0.3 — 1 mm).

Quartz phenocrysts in the four phases are commonly euhedral but are embayed or corroded in some phases. Plagioclase phenocrysts vary from euhedral elongate tablets to stubby crystals and glomerocrysts. The groundmass comprises a fine grained recrystallized mosaic of quartz and feldspar, sericite, carbonate and less than 5% chlorite and epidote. Zircon is an accessory mineral in some samples.

Mine rhyolite (unit 15)

A porphyritic light yellow weathering rhyolite flow, composed of two distinct phases, overlies the pillow fragment breccia (Fig. 170 and 174) and hosts the Flin Flon orebody (Price, 1978; Koo and Mossman, 1975). The rhyolite has been traced on surface, in underground workings, and in exploration drilling (Price, pers. comm., 1983) for approximately 3 km. It is a maximum of 150 m thick northwest of the smelter complex and thins to both north and south (Fig. 170).

The basal phase in the rhyolite is 30 m thick and contains 1 — 2% euhedral quartz phenocrysts (0.4 — 1.2 mm) and 4% euhedral tabular plagioclase phenocrysts (0.4 — 2 mm). This phase of the flow is a breccia composed of angular to subrounded rhyolite fragments (1 mm — 20 cm) closely packed in a lighter yellow, more chloritic rhyolite matrix. Quartz and plagioclase phenocrysts are locally glomerocrystic and there are rare oval phenocrysts of a micrographic quartz-feldspar intergrowth.

The main phase of the Mine rhyolite contains 3 — 4% lavender, euhedral quartz phenocrysts (0.2 — 2.5 mm) and 7% euhedral tabular plagioclase phenocrysts (0.2 — 1.2 mm). It is readily distinguished on outcrop from the basal phase by presence of quartz phenocrysts 2 mm or more in diameter. The main phase has two components; a lower zone of massive rhyolite and an upper unit of rhyolite flow breccia (Fig. 174).

The massive rhyolite is up to 40 m thick. It is flow banded, with alternating dark greyish yellow and yellow bands 1 mm — 1 m wide. In addition to quartz and plagioclase phenocrysts it contains rare oval phenocrysts of micrographic quartz-plagioclase intergrowth (to 2.5 mm). The groundmass is a recrystallized mosaic of quartz, feldspar, chlorite, magnetite, biotite and carbonate; mafic minerals comprise only 3% of the rock. Variation in groundmass grain size occurs between adjacent flow bands.

The upper rhyolite flow breccia (Fig. 174) contains exactly the same phenocryst population as the underlying massive rhyolite. It contains tabular slabs of flow-banded rhyolite ranging up to 1.9 m long by 20 cm wide. These flow-banded slabs compose 5 — 20% of the breccia and have a more or less consistent attitude, striking 190° and dipping 55° to 60° west. The slabs are in a rhyolite breccia "matrix" composed of angular to subangular rhyolite fragments (to l0 cm) in a dark grey rhyolite groundmass (Fig. 179).

The top of the Mine rhyolite is a gossaned, foliated breccia in which fragments are less abundant than in the main portion of the flow. This sug-

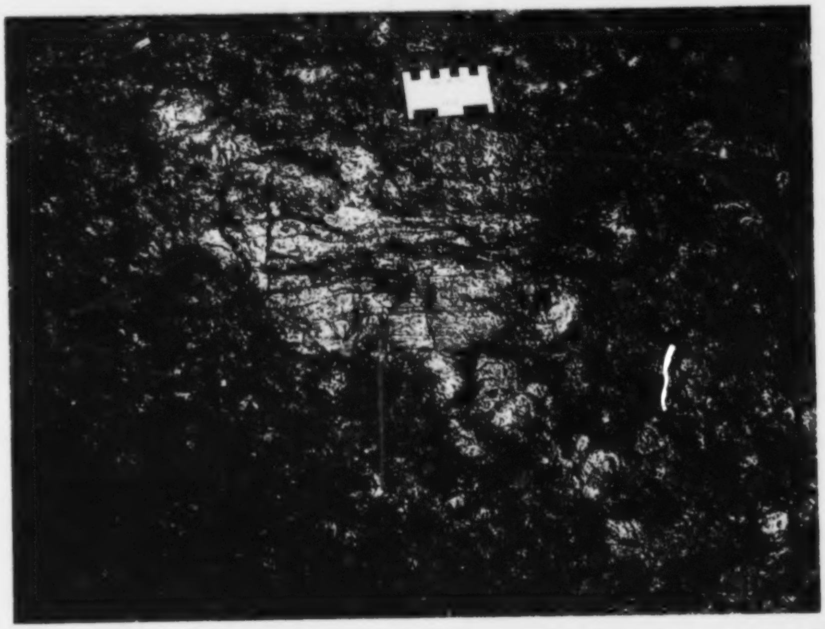

Figure 179: Mine rhyolite, upper breccia (unit 15c), 330 m northwest of HBMS smelter. The large fragment is flow banded and rests in a framework-supported "matrix" composed of smaller, angular rhyolite fragments.

gests that the contact with the overlying rhyolite clast-bearing Railway volcaniclastic rocks (unit 30a) is gradational.

Koo and Mossman (1975) have observed that orebodies of the Flin Flon massive Cu-Zn sulphide deposit occur within, as well as directly above or below, the rhyolite designated here as the second (upper) phase of the Mine rhyolite. Within the mine a chloritic alteration zone has been outlined 2000 x 1000 x 200 m which transects the underlying pillow fragment breccia and Mine rhyolite, and terminates against the hanging wall Hidden Lake basalt.

Railway volcaniclastic rocks (unit 30a)

Bedded volcaniclastic rocks with abundant felsic fragments make up a 35 m thick unit which overlies the Mine rhyolite north of the smelter complex (Fig. 170 and 174). These rocks also directly overlie the Flin Flon orebody, according to Stockwell (1960).

Beds are well defined, 0.1 — 1 m thick, parallel-sided to lenticular, and defined by grain size differences in sandy beds and by variable fragment abundance in coarser beds (Fig. 180). Some lenticular beds clearly fill scours that cut underlying beds. Size-grading, either normal or reverse to normal type, occurs in some beds.

In coarse beds the predominant fragment type is a yellow weathering porphyritic rhyolite corresponding to the upper phase of the Mine rhyolite. These rhyolite fragments are 1 mm — 18 cm long and are crudely lenticular in shape, with long axes parallel to bedding. A subsidiary fragment type is sparsely plagioclase-phyric, amygdaloidal basalt containing 1% stubby euhedral plagioclase phenocrysts (0.2 — 0.6 mm). The rhyolite and basalt fragments are contained in, and supported by, a matrix composed of poorly defined rock fragments, plagioclase, quartz and pyroxene crystals and crystal fragments, and a fine grained mixture of epidote, chlorite, actinolite, biotite and pyrite.

Fine grained, recrystallized sandy interbeds are similar in composition to matrix of breccia beds; detrital quartz and plagioclase (to 0.25 mm) are present but fine grained mafic minerals predominate.

Hidden Lake — Burley Lake mafic flows (units 2 and 3)

Mafic flows that constitute the Hidden Lake-Burley Lake sequence are exposed at two localities in the map area (GR87-1-1): west of Ross Lake and north and northeast of Burley Lake. Flows west of Ross Lake are basaltic, form the base of the sequence, and are here referred to as the Hidden Lake basalt (unit 2). Flows north and northeast of Burley Lake are basalts, basaltic andesites and andesites, form the uppermost exposures in the sequence, and are referred to as the Burley Lake basaltic andesite (unit 3). Much of this Hidden Lake-Burley Lake sequence (south of Hapnot Lake) is in Saskatchewan and was not mapped. Thus, the exact relationship between the Hidden Lake basalt and the Burley Lake basaltic andesite is uncertain, as is the total thickness of the unit. Whole rock chemical analyses from the Hidden Lake basalt and Burley Lake basaltic andesite form a continuous magmatic trend (Fig. 181) with a wide range in SiO_2, FeO^*/MgO and MgO, consistent with the Burley Lake flows being the more differentiated, upper part of the sequence. The approximate distribution of Hidden Lake basalt and Burley Lake basaltic andesite, including unmapped portions of the sequence in Saskatchewan, is displayed in Figure 171. Basalt and basaltic andesite, with chemical composition intermediate between the Hidden Lake basalt and Burley Lake basaltic andesite, are exposed in the Mandy sub-block between the Ross Lake and Mandy Road faults (Fig. 171). Because of their chemical similarity to the Hidden Lake-Burley Lake sequence these flows have been placed within unit 3 on the geological map (GR87-1-1).

The total thickness of the combined Hidden Lake-Burley Lake basalt-basaltic andesite sequence is difficult to determine due to folding about the Burley Lake Syncline, refolding about the Hidden Lake Synform, movement on various faults (e.g. Club Lake, Railway, South Railway), and absence of mapping of the central part of the sequence south of Hapnot Lake. Measured from the northern extension of the Mine rhyolite along the axis of the Hidden Lake Synform to the core of the Burley Lake Syncline, the sequence is a minimum of 3.3 km thick (Fig. 171; the top is not

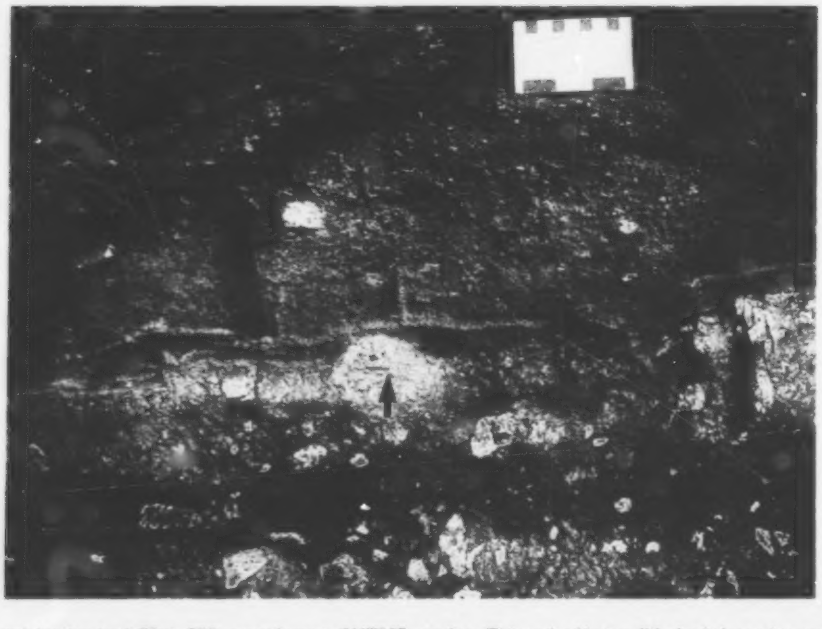

Figure 180. *Railway volcaniclastics (unit 30a), 330 m northwest of HBMS smelter. This unit of heterolithologic breccia composed dominantly of rhyolite fragments overlies the mine rhyolite (unit 15) and the Flin Flon Cu-Zn massive sulphide deposit. Bedding is defined by variation in clast size and abundance. Note that the large (8 cm) clast (arrow) protrudes from a bed top, and the overlying laminated sediment is draped over this clast.*

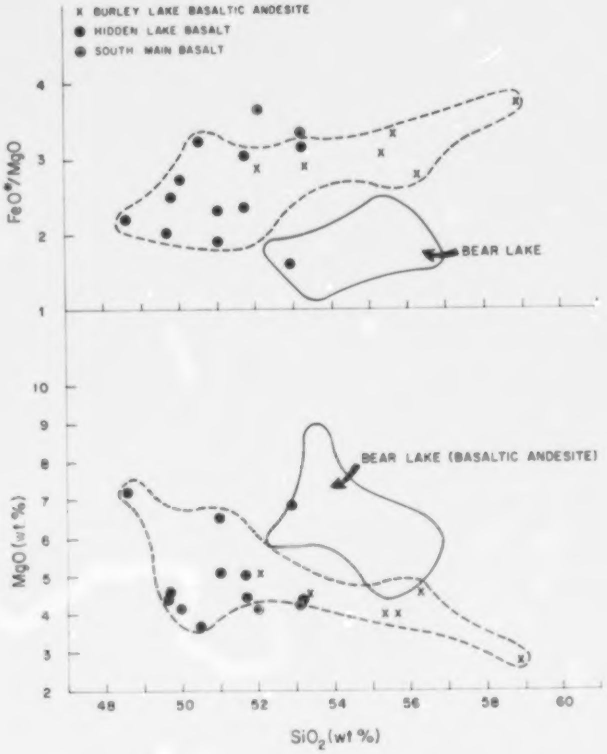

Figure 181: FeO/MgO and MgO vs. SiO_2, South Main basalt, Hidden Lake basalt and Burley Lake basaltic andesite. Field of Bear Lake basaltic andesite for comparison.*

exposed). Measured from the exposed base of the sequence at South Main shaft across the west limb of the Hidden Lake Synform to the core of the Burley Lake Syncline the sequence is a minimum of 1.3 km thick (Fig. 171). The difference (2 km) is interpreted to be due to removal of part of the section by the southern, unmapped extension of the Railway Fault.

The Hidden Lake basalt (unit 2) and Burley Lake basaltic andesite (unit 3) are described separately below, despite the fact that they represent part of one continuous sequence. The basalt and basaltic andesite (unit 3) that occurs between the Ross Lake and Mandy Road faults is described within the section on the Mandy sub-block.

Hidden Lake basalt (unit 2)

Hidden Lake basalt conformably overlies South Main basalt at South Main shaft (Fig. 170). It is distinguished from South Main basalt by distinctive buff weathering colour, absence of pipe vesicles, absence of hydrothermal alteration, abundance of plagioclase phenocrysts, and lower specific gravity. To the north, Hidden Lake basalt overlies the Railway volcaniclastic rocks; the contact is not exposed.

Over 90% of flows comprising the Hidden Lake basalt are pillowed, commonly with associated amoeboid pillow breccia. Pillow fragment breccia, interflow tuff, interflow sediments and pyroclastic rocks are virtually absent. A distinctive feature of the sequence is the relative abundance of concentrically zoned lava tubes, which vary from a few metres to several tens of metres in long dimension (Fig. 182). Synvolcanic dykes with banded margins are also common.

Figure 182: Cross-section of tube-shaped, banded, concentrically zoned structure interpreted to be a lava tube. Hidden Lake basalt (unit 2), 100 m north of Hidden Lake. Banding is considered to result from chilling of successive pulses of magma passing through tube.

All rocks in the Hidden Lake area display deformation features associated with the Hidden Lake Synform, such as constriction and rodding of pillows that form a distinct lineation plunging about 30° to the southeast. Pillows viewed down plunge most closely approximate their primary morphology. Other deformation features observed include development of minor folds in pillow selvages and inter-pillow laminated tuff, and larger scale tight folds in flow contacts.

The "typical" Bear Lake basaltic andesite pillowed flow zonation (Fig. 9) is only rarely displayed by Hidden Lake basalt; consequently it is difficult to determine flow contacts and measure flow thicknesses. Hidden Lake pillowed flows show irregular lateral transitions from pillowed lava to amoeboid pillow breccia. Flow contacts are in some localities identified by changes in phenocryst content or significant changes in colour. Folding of flow contacts and repetition or omission of section through faulting also introduce complications that serve to obscure flow contacts. Flows that could be measured are thick (approximately 6 — 140 m), but in view of difficulties experienced there is insufficient data to completely characterize flow thickness and morphology.

Pillows range in size from less than 1 m to megapillows several metres in long dimension. Selvages range in thickness from 2 — 10 mm and weather rusty brown. A common inter-pillow filling is epidotized, laminated fine grained tuff. This laminated material generally has a constant orientation in adjacent voids and is interpreted to have been deposited subhorizontally; consequently least deformed inter-pillow fillings can be used to approximate flow attitudes. Another common inter-pillow filling comprises small angular basalt fragments set in a matrix of quartz. Type and abundance of inter-pillow material varies between flows but is constant within an individual flow. Amygdales vary in size and abundance between and within flows; they are commonly 1 — 5 mm in diameter but are up to 2 cm across. They form 5 — 35% of pillows and may be concentrated either in pillow cores or pillow margins. There is no systematic stratigraphic change in amygdale abundance. Gas cavities were noted locally; the largest recorded is 40 x 8 cm. Radial pipe vesicles in pillows are rare, as are concentric thermal contraction cracks.

Amoeboid pillow breccia is relatively common in Hidden Lake basalt. Contacts between the breccia and associated pillowed flows are invariably marked by small to large protruberances from the topmost pillows into the breccia (Fig. 183, 184, 185). This relationship and previously discussed details of the matrix material (Fig. 80 and 81), demonstrate that these breccias are integral parts of flows and are distinctly different from pyroclastic breccias.

The great majority of Hidden Lake basalt is plagioclase-phyric and glomerophyric, although the abundance and size of the plagioclase crystals in flows varies considerably. Aphyric and sparsely plagioclase-phyric flows form thin members in the Hidden Lake and Ross Lake areas. In the lowermost 350 m of the unit there are rare pyroxene-phyric flows. Within a single flow plagioclase phenocrysts show a large range in size (e.g. 0.4 — 6 mm); maximum phenocryst size ranges throughout the sequence from 1.5 to 8 mm. Phenocryst abundance ranges from 5 to 25% between flows. About half of the phenocrysts in any given flow occur in glomerocrysts comprising 2 — 8 mm crystals. Individual plagioclase phenocrysts are euhedral, stubby tabular to equant in shape. Groundmass (in best preserved samples) consists of plagioclase microlites (0.1 — 0.4 mm) with interstitial chlorite, actinolite, epidote and minor biotite. In rocks that are more intensely deformed, especially those between the Railway and Club Lake faults, the groundmass textures are completely obliterated and locally even plagioclase phenocrysts are totally overprinted by mafic minerals and their form destroyed.

Burley Lake basaltic andesite (unit 3) and related rocks

Although the precise relationship of Burley Lake basaltic andesite (unit 3) to Hidden Lake basalt (unit 2) is not known, extrapolation of approximate boundaries of these units through Saskatchewan (Fig. 171), using geology from Stockwell (1960), suggests that Burley Lake basaltic andesite is the more differentiated, upper part of the Hidden Lake-Burley Lake basalt sequence. This is supported by the fact that the sequence forms a continuous magmatic trend (Fig. 181).

In contrast to thick poorly defined flows in Hidden Lake basalt, flows at Burley Lake are thinner, well defined and similar in zonation to flows shown in Figure 9, possibly reflecting a less proximal depositional environment. Consistent with this less proximal environment is the fact that the Burley Lake portion of the sequence is more variable, with intercalated units of pillow fragment breccia, mafic scoria tuff and breccia, and minor rhyolite. Burley Lake mafic flows display a broad two-fold subdivision: 1) a lower section of aphyric to sparsely plagioclase-phyric flows and pillow fragment breccia (units 3b and 3c) exposed north of Burley Lake; and 2) an upper section of porphyritic flows exposed about the Burley Lake Syncline at Burley Lake. A brief descrption of the two sections of mafic flows, as well as intercalated units of pillow fragment breccia and rhyolite, is given in following paragraphs. Scoria-bearing mafic tuff and lapilli tuff (unit 23b) are identical to those occurring in the Mandy sub-block and are described with the latter rocks.

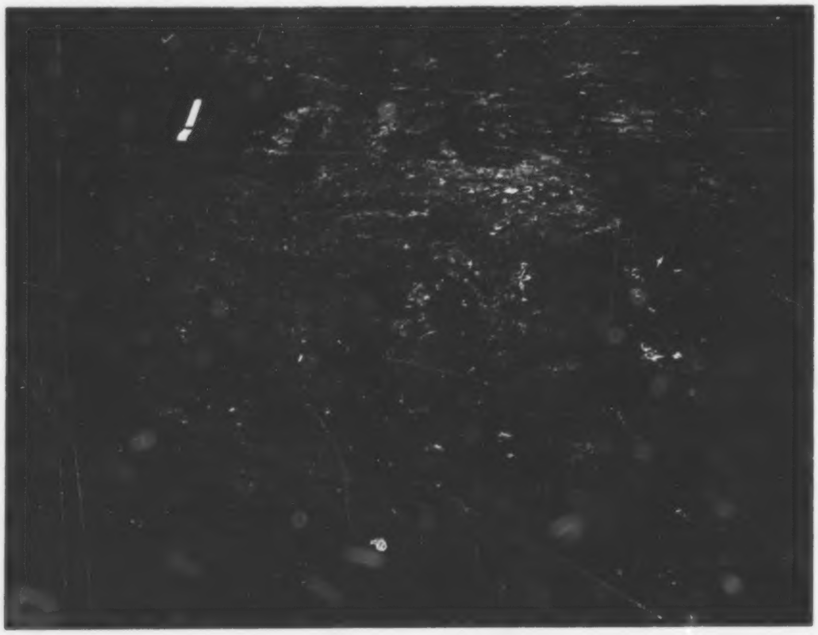

Figure 183: Large protrusion from the top of the pillowed portion of a flow (lower left) into amoeboid pillow breccia flow top. Hammer handle indicates stratigraphic tops. Note the highly irregular nature of the protrusion, and amoeboid pillow buds from the margin of the protrusion. Hidden Lake basalt (unit 2a), 580 m west southwest from the south end of Little Cliff Lake.

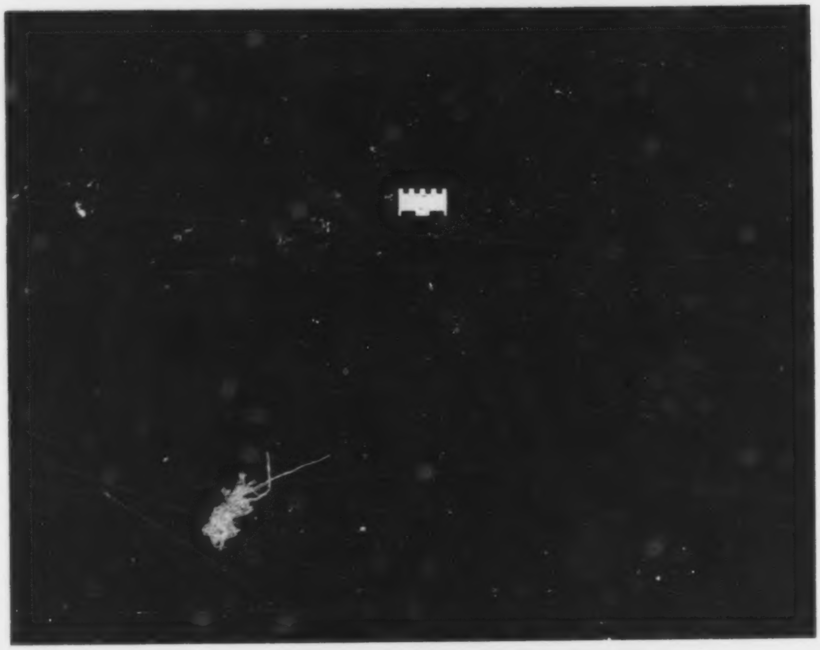

Figure 184: Contact between the pillowed portion of a basalt flow (bottom) and amoeboid pillow breccia flow top (top). Hidden Lake basalt (unit 2a), 370 m west of the south end of Little Cliff Lake. Irregular protrusions occur in the top of this topmost pillow in the flow; the relationship to flow top breccia is the same as in massive flows.

Figure 185: Flow top breccia, same locality as Fig. 184. Small irregularly shaped amoeboid pillows (with dark selvages) emplaced in a matrix of recrystallized hyaloclastite.

Aphyric to sparsely plagioclase phyric flows (unit 3b) north and northeast of Burley Lake, and west of the Ross Lake Fault, are intercalated with substantial units of pillow fragment breccia (unit 3c) and scoria tuff (unit 23b). The flows are buff-brown weathering, and commonly display well defined flow contacts. Thirteen complete flows documented are 3 — 40 m thick and average 13 m. Two-thirds of the examined flows are massive. Primary features of two particularily well exposed flows are shown in Figure 186. Oval lava tubes up to 7 m in diameter occur in one locality north of Potter Bay on Phantom Lake.

Pillow fragment breccias (unit 3c) intercalated with the aphyric to sparsely plagioclase-phyric flows north of Burley Lake vary considerably: some are monolithologic and aphyric, whereas others are heterolithologic, aphyric and plagioclase-phyric. Beds are 0.5 — 10 m thick, normally size-graded with sandy, clast-free tops. They are characterized by rare complete oval pillows, crescentic and wedge-shaped pillow fragments, and fragments containing bands of amygdales truncated at clast margins (Fig. 187).

Porphyritic flows (unit 3a), northwest of Burley Lake and on its east and south shores, constitute the uppermost part of the exposed Hidden Lake-Burley Lake sequence. They are tightly folded by the Burley Lake Syncline, weather light buff to buff-brown, and display a wide variation in phenocryst content between flows. Plagioclase phenocrysts form 1 — 30% of flow rocks, and range in size up to 3 mm; pyroxene phenocrysts are sparse or absent. Multi-crystal, dominantly plagioclase glomerocrysts occur in coarsely porphyritic flows. Large amygdales (up to 1 cm) and gas cavities (up to 5 by 15 cm) occur in uppermost parts of some flows. Massive, composite and pillowed flows (organization as in Fig. 9) range in thickness from 10 to 45 m.

A 240 m thick, east-facing assemblage of heterolithologic pillow fragment breccia (unit 11) overlies a very thick, massive, polygonally jointed flow south of Carlisle Lake. The top of this breccia unit is interpreted to be truncated by a fault, inasmuch as the sequence faces opposite to other rocks west of the Ross Lake Fault. Breccias in this unit are stratified (0.3 — 4 m) and contain thin (3 — 20 cm, up to 2.5 m) normally graded, fine to medium sandy interbeds. Fragments of pillows in the breccias vary with respect to phenocryst content (aphyric to plagioclase-phyric), amygdale content (0 — 40%), colour (green to brown) and degree of rounding (angular to rounded). Matrix consists of plagioclase crystals, chocolate brown granules and fragments to 1 cm, and fine grained buff material. Sandy interbeds locally contain accessory pillow fragments up to 15 cm across.

The thin (maximum 30 m) northwest-trending rhyolite flow between

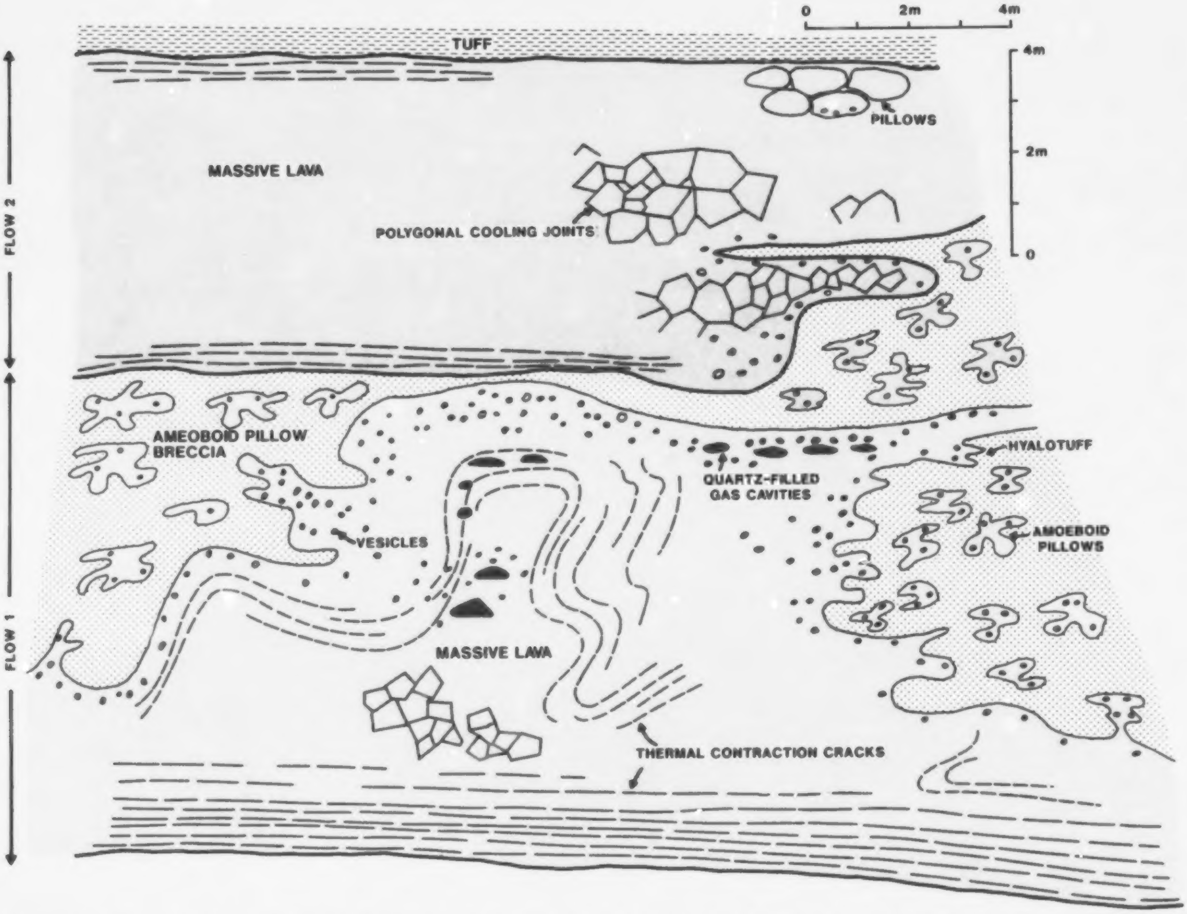

Figure 186: Sketch showing primary features and internal organization in two massive mafic flows (unit 3b) northeast of Potter Bay on Phantom Lake, Hapnot Lake sub-block.

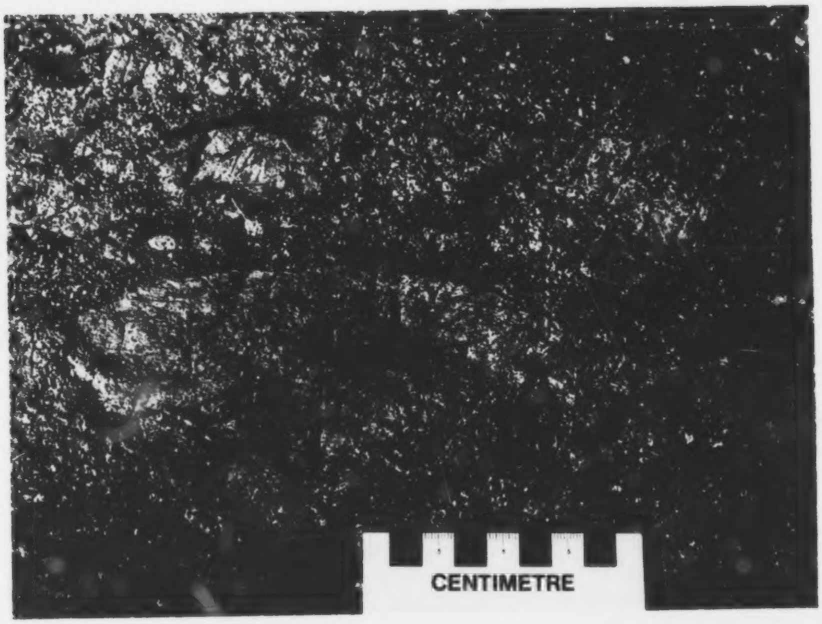

Figure 187: Pie-shaped and crescentic pillow fragments, pillow fragment breccia (unit 3c), 750 m west of Mandy Mine. Note curving broken pillow margins (m) characteristic of many clasts in pillow fragment breccias. Oxidized pillow selvage (dark) is present at margin of one fragment.

Burley Lake and Phantom Lake displays lateral variation in structures and thickness which suggest that its source is to the northwest (Fig. 188). A southeasterly transport/flow direction is consistent with structures in underlying sediments and overlying andesite flow (Fig. 188). The thickest portion of the rhyolite flow displays excellent flow banding and flow folds (Fig. 189), with flow bands 5 mm — 1 m alternating white and very light buff in colour. Some of the buff bands have been stretched and fragmented in place. As the flow thins to the southeast the basal portion of the flow becomes distinctly brecciated, and the top contact has a flow banding produced by stretching of fragments. Fragments of rhyolite ("rip-ups") up to 40 cm across, occur in the basal pillowed zone of the overlying andesite flow. Near the shore of Burley Lake the rhyolite flow is absent, but rhyolite fragments occur in inter-pillow positions in the basal 2 — 3 m of the overlying flow. The rhyolite contains 1% rounded quartz phenocrysts (0.2 — 1 mm) and 3% stubby tabular plagioclase phenocrysts and glomerocrysts (0.4 — 2 mm). Flow bands consist of alternating dense, spherulitic (0.04 — 0.4 mm) rhyolite, more chloritic rhyolite with fewer spherulites (the buff bands), and some lithoidal bands containing 0.05 — 0.1 mm lath-shaped feldspars. Spherulites are oval, recrystallized (quartz or quartz plus feldspar) and are separated by wisps of sericite, dark green chlorite and minor oxides.

Geochemistry

Eighteen analyses have been made of mafic flow rocks from the Hapnot Lake sub-block. Twelve are from exposures of Hidden Lake basalt (unit 2) located between South Main shaft and Hapnot Lake; all are basaltic in composition (SiO_2 between 48.6 — 53.2%, H_2O and CO_2 free). Six analyses are from the Burley Lake basaltic andesite (unit 3) and are basaltic to andesitic in composition (SiO_2 between 52.0 — 58.8%). Together the Hidden Lake-Burley Lake mafic flows form a continuous magmatic trend (Fig. 181), with a wide range in FeO^*/MgO and MgO. Their field is distinct from that of the Bear Lake basaltic andesite (Fig. 181), which is characterized by higher MgO and a narrower range of FeO^*/MgO. Two analyses are from flows at the top of the South Main basalt (unit 6). They are broadly similar to analyses of the overlying Hidden Lake basalt (Fig. 181, Appendix) but are different in two aspects:

1) they have higher FeO^*/MgO ratios than Hidden Lake basalts (reflecting higher FeO^* content consistent with higher specific gravity of South Main basalts),
2) they have higher bulk REE contents than Hidden Lake basalts, even though the REE pattern is very similar (Fig. 190).

Two analyses of the Mine rhyolite (one of each phase) and one analysis of the South Main rhyolite dome (southern body) yielded a wide range in SiO_2, K_2O, Na_2O, K_2O/Na_2O, Rb, Ba and Sr (Appendix) reflecting mobility in silica and alkalies. The least mobile trace elements (Ti, Zr and Y) show the Mine rhyolite and South Main domes to have significantly different trace element "fingerprints". This is consistent with field and petrographic observations which suggested that they are distinctly different and not part of a single large rhyolite body.

Summary and Interpretation

Rocks in the Hapnot Lake sub-block are of particular importance because they host the largest Cu-Zn massive sulphide deposit in the Flin Flon belt. Although the rocks have been complexly deformed, faulted and cut by dioritic intrusions, well preserved primary structures and map-scale facies relationships permit interpretation of physical environment of deposition of the various rock units.

South Main basalt pillowed flows and pillow fragment breccias form the immediate footwall to the Flin Flon deposit (Fig. 170). A lateral facies change from pillowed flows, at South Main shaft, northwards into a thick sequence of now altered pillow fragment breccias, underlying the orebody, indicates that source area for this mafic pile lay south of South Main shaft. Breccias presumably accumulated on the flank of a subaqueous basalt volcano or in a basin adjacent to the volcano. The uppermost part of the South Main basalt shows evidence of relatively shallow water emplacement, including abundance and large size of amydales and local profusion of radial pipe vesicles (Table 5). Water depth was probably greater than 200 m as there are no associated pyroclastic rocks.

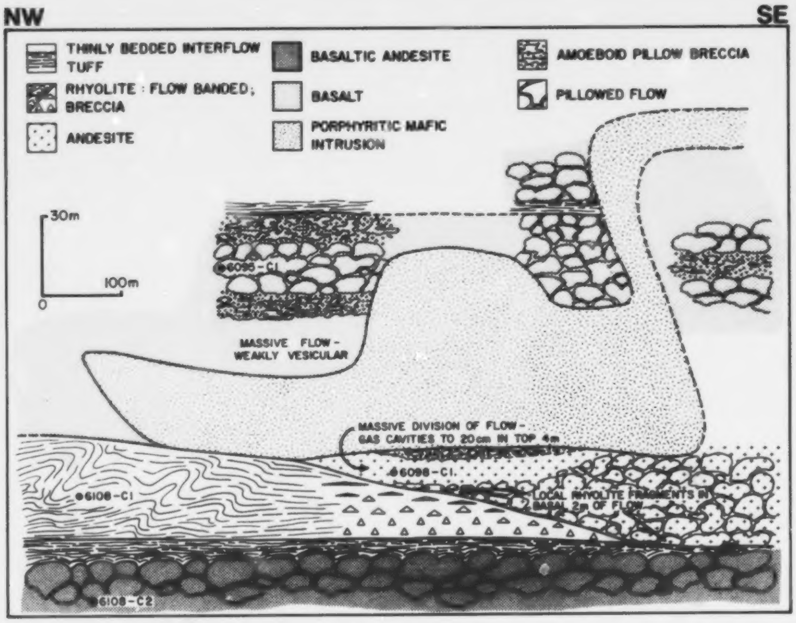
NW
SE
THINLY BEDDED INTERFLOW TUFF
RHYOLITE : FLOW BANDED; BRECCIA
ANDESITE
BASALTIC ANDESITE
BASALT
PORPHYRITIC MAFIC INTRUSION
AMOEBOID PILLOW BRECCIA
PILLOWED FLOW
30m
100m
0
6095-C1
MASSIVE FLOW - WEAKLY VESICULAR
MASSIVE DIVISION OF FLOW - GAS CAVITIES TO 20cm IN TOP 4m
6098-C1.
6108-C1
LOCAL RHYOLITE FRAGMENTS IN BASAL 2m OF FLOW
6108-C2

Figure 188: Sketch showing lateral and vertical variation in flow morphology and thickness, Burley Lake, Hapnot Lake sub-block. Southeast paleoslope is indicated by thinning and brecciation of rhyolite flow, lateral transition from massive to pillowed andesite, and thinning of interflow tuff. Sample numbers refer to chemical analyses (Appendix).

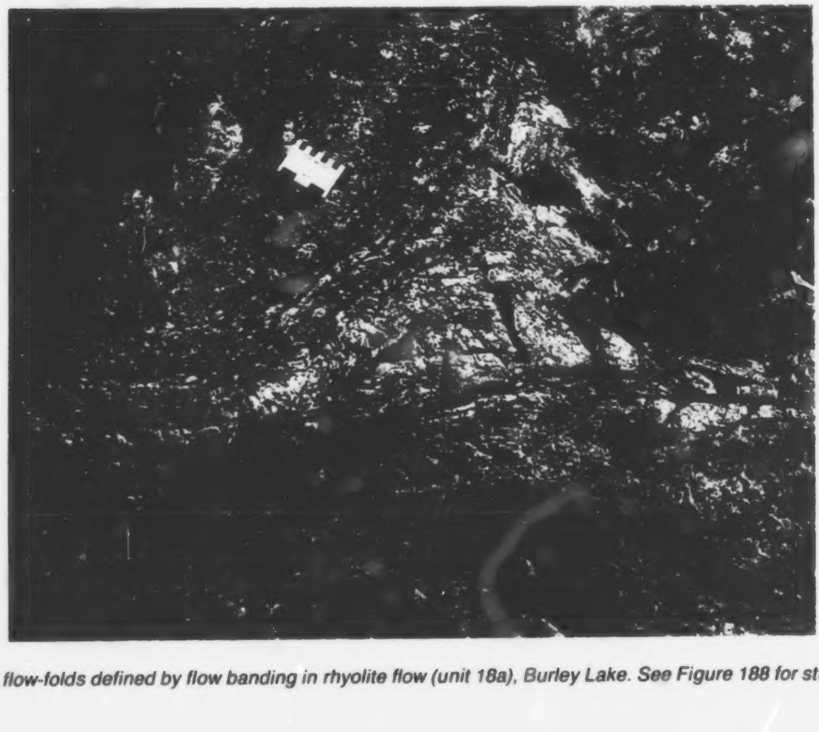

Figure 189: Contorted flow-folds defined by flow banding in rhyolite flow (unit 18a), Burley Lake. See Figure 188 for stratigraphic relationships.

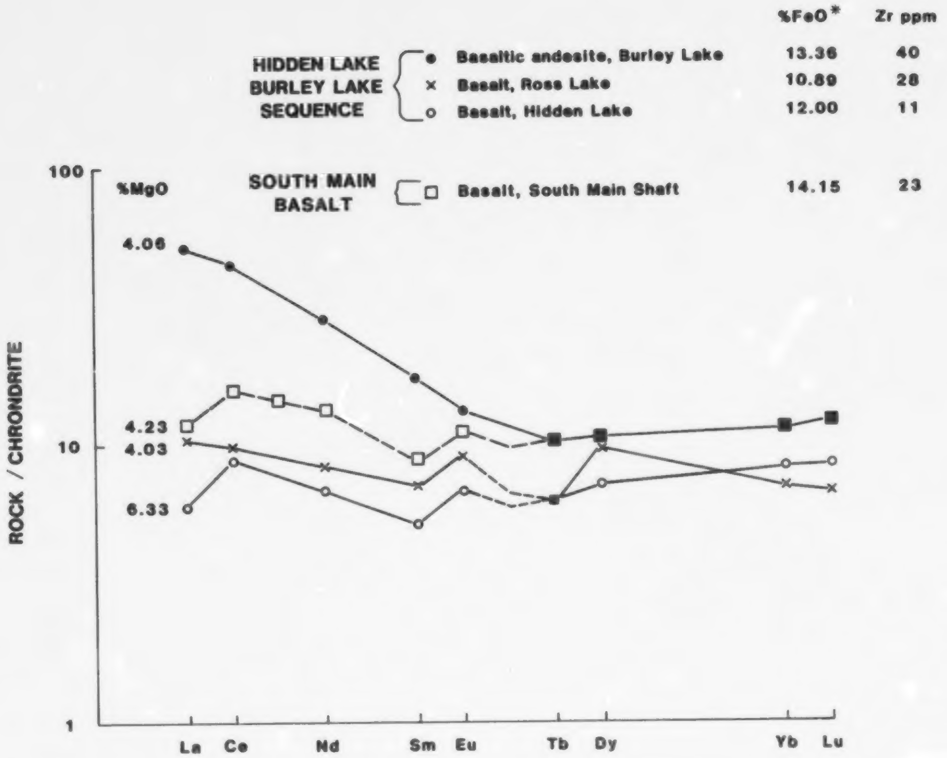

Figure 190: Chondrite-normalized REE plot, South Main basalt, Hidden Lake basalt and Burley Lake basaltic andesite.

The Flin Flon massive sulphide orebody was deposited during a hiatus in basaltic volcanism. During this hiatus volcanic activity shifted to intrusion of high-level rhyolite domes, extrusion of the Mine rhyolite flow, and development of a large-scale hydrothermal convection system which altered the footwall basaltic sequence and led to the deposition of the stratiform volcanogenic Flin Flon orebody comptemporaneous with the Mine rhyolite. An unconformity exposed in footwall rocks may be one expression of a synvolcanic fault which may have acted as a focus for the discharge of hydrothermal solutions. Bedded volcaniclastic rocks that overlie the Mine rhyolite and Cu-Zn orebody represent the final depositional unit accumulated during the hiatus in basaltic volcanism.

The Hidden Lake-Burley Lake sequence (more than 3.3 km thick) represents resumption of basaltic volcanism following deposition of the Flin Flon orebody. These rocks are chemically and petrographically distinct from underlying South Main basalts, and do not show evidence of hydrothermal alteration. At South Main shaft they directly overlie South Main basalt whereas to the north of the smelter there are 180 m of rhyolite and volcaniclastic rocks between the two basalt units.

The Hidden Lake portion of the Hidden Lake-Burley Lake sequence was probably extruded in relatively shallow water, evidenced by abundant amygdales up to 1 cm in diameter. Flow morphology (dominated by thick amalgamated flow units) and scarcity of intercalated sedimentary rocks suggest rapid accumulation of the Hidden Lake portion of the mafic pile. It contains few tuffaceous intercalations and no subaerial flows, indicating that subsidence kept pace with volcanic accumulation. Sparse data on flow direction at South Main shaft suggest paleoslope was to the north.

The Burley Lake portion of the Hidden Lake-Burley Lake sequence comprises large-scale interlayering of pillowed mafic flows, mafic pillow fragment breccia, heterolithologic breccia and mafic scoria-rich tuff. This part of the sequence differs from the lower part (at Hidden Lake) in the following respects:

1) it is composed of basalt and basaltic andesite, compared to basalt in the Hidden Lake area;
2) flows are thinner and better organized than those in the Hidden Lake area;
3) flows are intercalated with a variety of volcaniclastic rocks that are not present in the lower part of the sequence at Hidden Lake.

These differences are interpreted to reflect a somewhat less proximal depositional environment for rocks in the Burley Lake Lake area than that for lower parts of the section at Hidden Lake. Flows throughout the Burley Lake area contain large (commonly to 1 cm) amygdales, local radial pipe vesicles and local large gas cavities, consistent with a relatively shallow subaqueous environment (Table 5). Scoria tuff units, although deposited in this shallow water environment, contain features which suggest they were erupted subaerially.

MANDY SUB-BLOCK

The Mandy sub-block is bounded on the west by the Ross Lake Fault, on the south by the Phantom Lake Fault, on the east by the Channing Fault and on the north by Missi Group rocks (Fig. 169). Within this sub-block several north-northwest-trending faults offset units and do not permit construction of a simple stratigraphic sequence. For this reason these rocks are described according to lithology rather than stratigraphic position. The largest structurally intact stratigraphic section, between the Mandy Road and Ross Lake faults, is 1.7 km thick, faces west to northwest, and is shown in Fig. 191.

The Schist Lake and Mandy Cu-Zn massive sulphide deposits occur within the Mandy sub-block. However, due to faulting, their stratigraphic position relative to major rock units exposed west of Schist Lake is not known.

Basalt, basaltic andesite (units 3 and 7)

Mafic flows are the dominant rock type in the Mandy sub-block. They include aphyric to sparsely porphyritic unit 3 flows, west of the Mandy Road Fault, and aphyric unit 7 flows, east of this Fault. Placement of flows west of the Mandy Road Fault into unit 3 is based on lithological and chemical similarity to flows in the Hidden Lake-Burley Lake sequence. Flows east of the Mandy Road Fault are placed in undivided unit 7 aphyric flows because there are no analysed samples and these flows are thus of unknown affinity.

Unit 3 flows, east and southeast of Carlisle Lake, are predominantly aphyric but include some porphyritic and sparsely porphyritic members. They weather buff-brown, top to the west and northwest, and include pillows and amoeboid pillow breccia (Fig. 192, 193). Best preservation of primary structures occurs in exposures along the abandoned power line southeast of Carlisle Lake. Detailed descriptions of these outcrops are given in field trip guidebooks (Syme et al., 1982; Bailes et al., 1987). Primary features observed include amoeboid pillows which bud from lava tongues, radial pipe vesicles up to 8 cm long by 8 mm in diameter at margins of pillows, upward decrease in pillow size and increase in vesicle abundance towards tops of pillowed flows, bedded interflow tuffs, and pillows apparently without selvages with shapes defined by quartz filled concentric thermal contraction cracks (Fig. 194).

Unit 3 flows, 550 m west of the Schist Lake Mine, form a 60 — 120 m thick unit underlain and overlain by scoria-bearing tuff (unit 23b). Flow types there include massive and pillowed types, ranging in thickness from 10 — 30 m. Primary features include quartz-filled thermal contraction cracks at the base of massive flows and 10 — 25% amygdales ranging in size from 1 — 20 mm.

Unit 7 aphyric flows east of the Mandy Road Fault weather shades of green and, rarely, brown. They are strongly deformed and flow contacts are rarely preserved. Most flows consist of pillows and associated amoeboid pillow breccia. Amygdales typically comprise 5 — 20% of pillows and are 1 — 10 mm in size.

Pillow fragment breccia (units 3c and 11)

Between the Mandy Road and Ross Lake faults several mappable units of pillow fragment breccia (unit 3c), up to 200 m thick, are intercalated with unit 3b mafic flows (Map GR87-1-1). A 120 m thick unit east

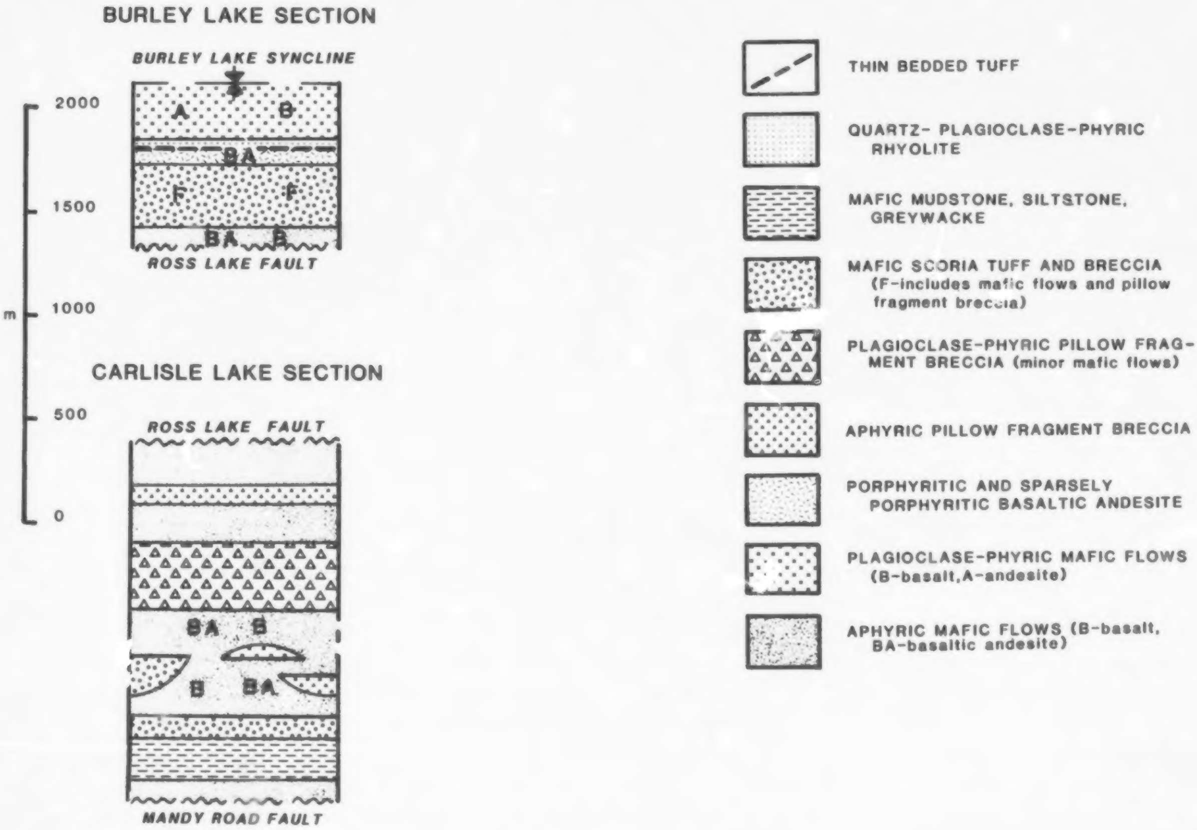
BURLEY LAKE SECTION
BURLEY LAKE SYNCLINE
2000
1500
1000
500
0
m
A
B
BA
F
F
BA
B
ROSS LAKE FAULT
CARLISLE LAKE SECTION
ROSS LAKE FAULT
BA
B
B
BA
MANDY ROAD FAULT
THIN BEDDED TUFF
QUARTZ- PLAGIOCLASE-PHYRIC RHYOLITE
MAFIC MUDSTONE, SILTSTONE, GREYWACKE
MAFIC SCORIA TUFF AND BRECCIA (F-includes mafic flows and pillow fragment breccia)
PLAGIOCLASE-PHYRIC PILLOW FRAGMENT BRECCIA (minor mafic flows)
APHYRIC PILLOW FRAGMENT BRECCIA
PORPHYRITIC AND SPARSELY PORPHYRITIC BASALTIC ANDESITE
PLAGIOCLASE-PHYRIC MAFIC FLOWS (B-basalt, A-andesite)
APHYRIC MAFIC FLOWS (B-basalt, BA-basaltic andesite)

Figure 191: Burley Lake section, Hapnot Lake sub-block, and Carlisle Lake section, Mandy sub-block. Section lines shown on Figure 169.

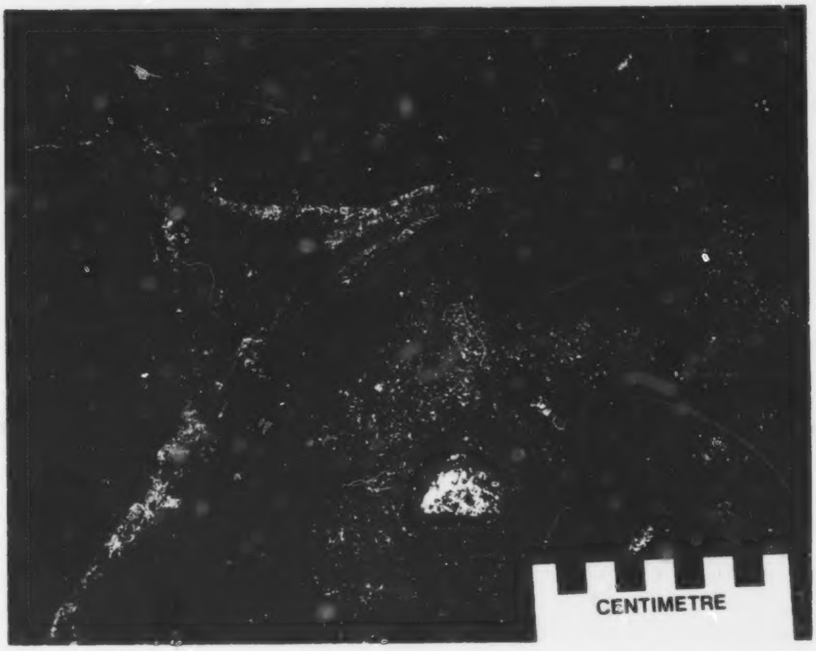

Figure 192: Basalt pillows (unit 3b) with dark oxidized selvages, 300 m southeast of Carlisle Lake. Note slabby pillow margin fragments (F) in epidotized interpillow hyaloclastite.

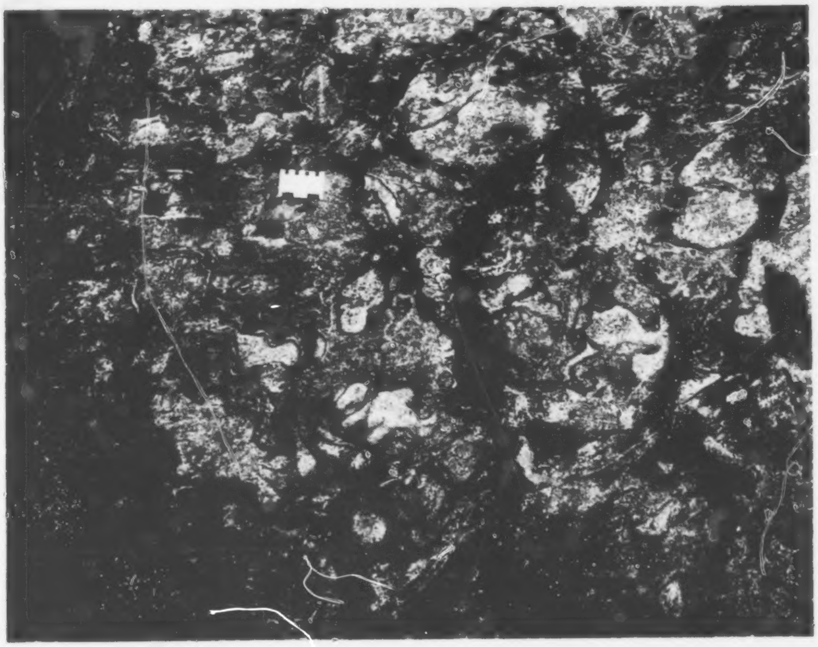

Figure 193: Amoeboid pillow breccia, Burley Lake basaltic andesite (unit 3b); on power line, 360 m southeast of Carlisle Lake. Individual amoeboid pillows have dark selvages and are highly irregular in shape. They are supported by a matrix of recrystallized hyaloclastite.

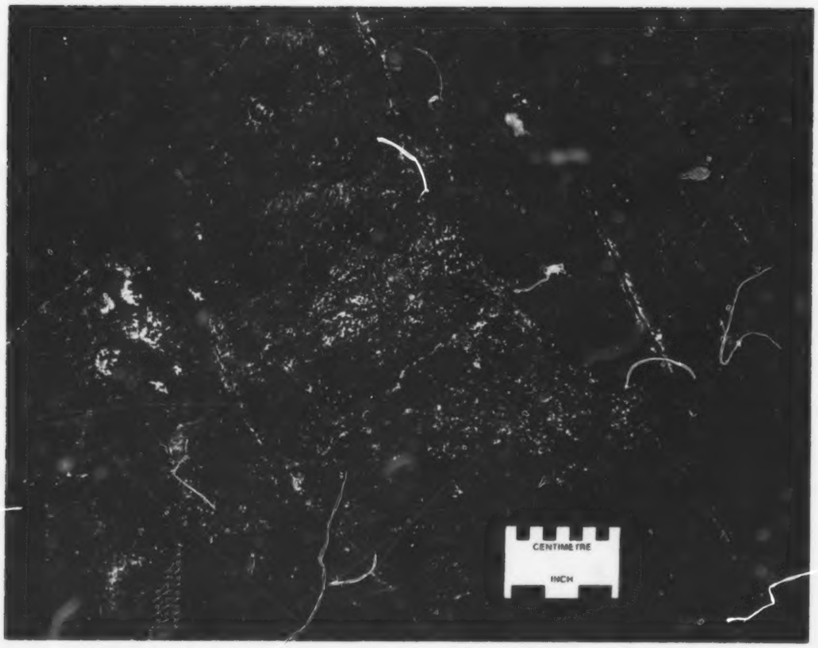

Figure 194: Pillowed basaltic andesite (unit 3b). 200 m southeast of Carlisle Lake. Pillows have no selvages and shapes are defined by quartz-filled thermal contraction cracks (TCC) that are parallel to pillow margins (M). Interpillow domain is composed of epidotized hyaloclastite. Note partly spalled pillow rim (R) that has separated along a TCC. Spacing between TCC's increases with distance from the pillow margin.

of Carlisle Lake is composed of dominantly aphyric amygdaloidal pillow fragments. This breccia becomes increasingly schistose and deformed towards its eastern (faulted) margin. The series of pillow breccia units north of Carlisle Lake are bedded and composed of plagioclase-phyric pillow fragments. Beds in these units are well defined, 1 — 7 m thick, monolithologic, and normally size-graded. Most fragments contain 5 — 10% plagioclase phenocrysts (0.5 — 2 mm). Fragments are typically less than 6 cm across but large blocks occur at the base of some beds.

A thick unit of west-facing pillow fragment breccia and intercalated heterolithologic mafic breccia (unit 11, 29) outcrops northwest of the Mandy Mine and east of the Mandy Road Fault. It overlies the Mandy massive Cu-Zn sulphide zone and reaches 200 m in thickness before its top is truncated by the Mandy Road Fault. The breccias weather buff-green and include monolithologic matrix-supported types and heterolithologic framework-supported types. Monolitholgic breccias are composed of pillow fragments, with bedding defined by "trains" of large blocks and by variation in phenocryst population (some beds contain plagioclase-pyroxene-phyric and others plagioclase-phyric fragments). Heterolithologic breccias are composed of angular to rounded fragments typically 2 — 50 cm across. Fragment types include plagioclase-pyroxene-phyric, plagioclase-phyric and aphyric mafic volcanic rocks. Many are pillow fragments and some are complete oval pillows up to 2.5 by 1.9 m in size. The monolithologic and heterolithologic breccias are interbedded, in beds up to 20 m thick. Individual beds vary in degree of rounding of clasts and in number of different clast types present. Patchy alteration is locally present and takes the form of carbonate blastesis, pervasive chloritization of matrix and selective chloritization of the margin and/or core of some clasts.

Heterolithologic breccia (units 29 and 30)

Heterolithologic breccias occur in several distinct, lithologically unique bodies in the Mandy sub-block. They include dominantly mafic breccias (unit 29) at the north end of Northwest Arm and northwest of Stitt Island, and dominantly felsic breccias (unit 30) in bodies hosting the Schist Lake Cu-Zn sulphide deposit and exposed on a small island west of Stitt Island (Map GR87-1-1).

Northeast of Parsons Airways float plane base, at the north end of Schist Lake, the unit of heterolithologic breccia (unit 29) is up to 210 m thick and overlies pillowed aphyric flows. In southeastern exposures, the breccia is poorly sorted, matrix-supported and composed of a heterolithologic mixture of mafic flow fragments 1 mm to 2.8 m across. Fragments include greenish aphyric, buff plagioclase-phyric, and pyroxene-plagioclase-phyric types. They vary in shape from well rounded to distinctly angular, suggesting there may have been previous rounding of part of the clast population. Fragments are amygdaloidal (0 — 40%, up to 5 mm diameter) and some display typical pillow fragment morphologies. Northwest portions of the unit differ in that there is a greater proportion (90%) of aphyric fragments, plagioclase phenocrysts to 8 mm occur in the matrix, and breccias are in general matrix-supported. Beds are thick, massive or reverse to normally size graded.

Northwest of Stitt Island approximately 100 m of poorly sorted, heterolithologic mafic breccias (unit 29) occur east of and stratigraphically underlie the Schist Lake and Mandy Cu-Zn orebodies. These breccias are moderately to intensely altered and are not obviously bedded. They contain angular to rounded clasts of mafic, intermediate and felsic volcanic lithologies. Plagioclase-phyric intermediate clasts predominate, and plagioclase crystals are abundant in matrix material between fragments. East of the Schist Lake Mine headframe these breccias contain 20% disseminated 0.5 — 2 mm carbonate blasts which locally mask fragmental texture. Patchy carbonate blastesis, local chloritization of matrix and selected chloritization of the margin and/or core of some fragments characterizes this breccia north of the Mandy Mine open pit.

Heterolithologic, dominantly felsic volcanic breccia (unit 30) hosts the Schist Lake Cu-Zn orebody. These hydrothermally altered breccias weather light grey to buff but also commonly have rusty weathering due to oxidation of small amounts of disseminated sulphides. Despite their leucocratic appearance they contain plagioclase-phyric mafic to intermediate volcanic fragments in addition to the dominant felsic volcanic types. Less common fragments include aphyric mafic volcanics, amygdaloidal mafic volcanics, and rare laminated sediment or tuff. Fragments are angular to rounded, up to 30 cm across, framework-supported and set in a dark rusty brown matrix of plagioclase crystals (1 — 3 mm) and chlorite. Stratification, defined by fragment size, shape and composition, is 0.5 — 3 m thick. The rocks are strongly foliated and are variably chloritized, silicified and pyritized; malachite staining is also common. Although most primary features have been obliterated in this sequence, they locally display the characteristics of debris flow deposits.

Heterolithologic felsic breccia (unit 30) also occurs on a small island west of Stitt Island. This breccia is composed of white aphyric rhyolite clasts, cream-coloured chert clasts and light brown aphyric intermediate volcanic clasts supported by a granular matrix. In this breccia, rhyolite fragments are up to 1 m, angular to rounded, and some display re-entrant angles. Chert slabs are massive to laminated and are up to 1 m long.

Mafic scoria-rich tuff and tuff breccia (unit 23b)

Plagioclase-phyric, scoria-bearing mafic tuff and tuff breccia (unit 23b) occur in units up to at least 110 m thick, between Schist Lake and Phantom Lake, in the Mandy and adjacent Hapnot Lake sub-blocks. The Ross Lake and related faults cut through the volcanic sequence in this area, consequently the number and precise stratigraphic positions of the tuff and tuff-breccia units are not known. Tuff units are intercalated on a map scale and outcrop scale with pillowed, dominantly aphyric mafic flows and pillow fragment breccias.

Components of the tuff are plagioclase-phyric scoria granules and lapilli, and 10 — 40% accessory granule to block-sized flow fragments. Scoria and accessory fragments are close-packed with very little intergranular matrix. Plagioclase phenocrysts range in size from 1 — 7 mm, rarely up to 2 cm, and in abundance from 20 — 40% (Fig. 195). They are euhedral, equant, oscillatory zoned and commonly comprise multi-crystal glomerocrysts (some with pyroxene), wholly or partially contained within scoria fragments. Vesicles in the scoria are spherical, 0.05 — 0.4 mm in diameter and vary in abundance, to a maximum of 70%. Accessory clasts are plagioclase-microlitic, aphyric to plagioclase-phyric, and dense to moderately amygdaloidal. Large accessory blocks, derived from pillowed flows, occur as isolated fragments or in "trains" within beds.

Beds are well defined, continuous, 5 cm — 10 m thick, and include massive, A and AB types. Normally size-graded beds are defined on outcrops by systematic upward decrease in plagioclase crystal size; plagioclase crystals occur in fragments so this must reflect an upward decrease in scoria fragment size. Reverse size-grading occurs at the base of some thick, coarse beds. Sandy tops of some beds result from abrupt grain size decrease in the uppermost few centimetres of beds. Load structures occur at the bases of some beds.

The presence of intercalated pillowed flows and Bouma zonation of the beds indicate that scoria-rich tuffs were deposited in a subaqueous environment, by turbulent density currents. Large accessory blocks and block "trains" are not in hydraulic equilibrium with the material in which they are found; consequently they are interpreted as ballistic fragments. These redeposited pyroclastic rocks are virtually identical to those in unit "J" in the Hook Lake Block, and are similarly interpreted to have shallow subaqueous to subaerial origin.

Stitt Island dacite (unit 14)

Stitt Island is underlain by a large body of variably carbonatized dacite. The dacite is interpreted to be fault bounded, on the basis of its oblique trend with respect to adjacent units to the northwest, and the presence of extremely schistose zones on the southwest, southeast and northeast shorelines. Its precise stratigraphic relationship to heterolithologic breccias which host the Schist Lake and Mandy mines is therefore unknown. The dacite weathers white to light buff and is light olive to pinkish buff on fresh surface. It is commonly massive or weakly brecciated; polygonal columnar joints are exposed along 240 m of the central east shore of Stitt Island. Joint columns are 5 — 25 cm in diameter, plunge 40 degrees to the southeast, and range from straight (Fig. 196) to slightly curved, as in the entablature of polygonally jointed basalt. Mauve quartz phenocrysts (0 — 1%, 0.5 — 1 mm) in the dacite are rounded and some are deeply embayed; they are set in a spherulitic groundmass comprising 0.1 — 0.15 mm recrystallized quartz-feldspar spherulites separated by sericite, pale green chlorite and disseminated fine grained leucoxene. Virtually all of the dacite on Stitt Island has suffered some form of carbonatization, ranging from relatively weakly developed carbonate blastesis and quartz-carbonate-hematite open space filling, to intense brecciation and veining by a high proportion of purple to orange-weathering Fe-carbonate (as in the quarry at the north end of Stitt Island). Rusty-weathering carbonate pods and veins up to 3 m wide occur in the centre of the island. These veins are commonly internally traversed by stockwork quartz veinlets.

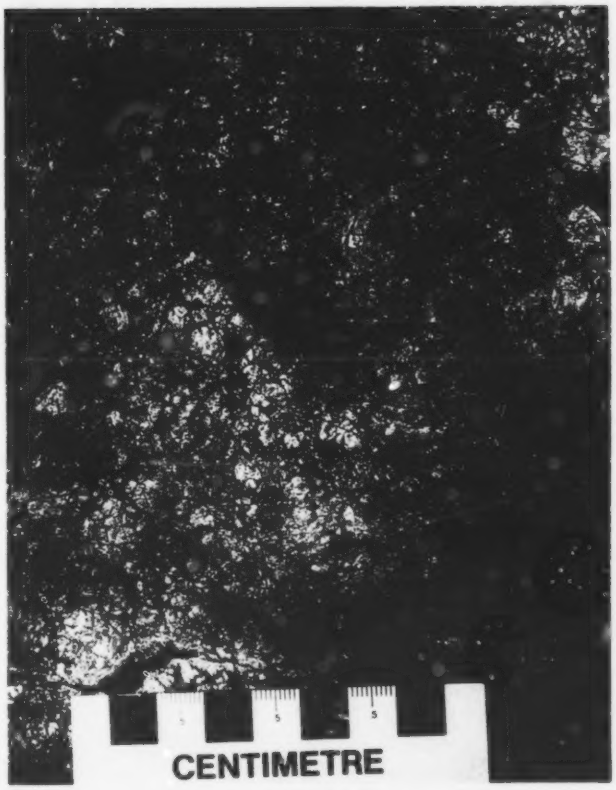

Figure 195: Large oscillatory zoned plagioclase phenocrysts characteristic of mafic scoria tuffs (unit 23b) exposed 570 m west of Mandy Mine.

Volcaniclastic sedimentary rocks (units 33 and 34)

Volcaniclastic sedimentary rocks outcrop 200 m west of the Mandy Cu-Zn orebody and 300 m southwest of Stitt Island. West of the Mandy deposit they comprise mafic greywacke, siltstone and mudstone (unit 34). Southwest of Stitt Island they consist of feldspathic greywacke, siltstone and mudstone (unit 33), with local beds of polymictic rhyolite-pebble-bearing conglomerate.

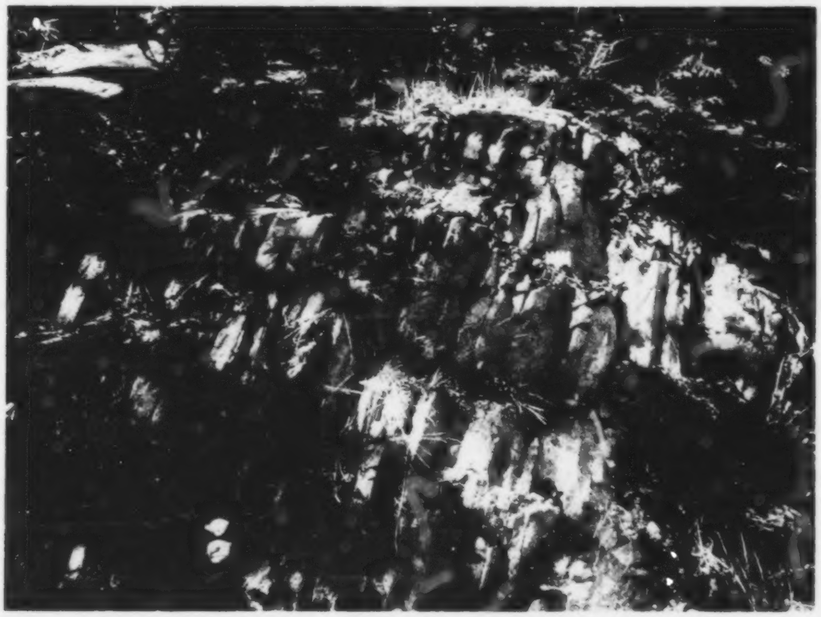

Figure 196: Well defined primary columnar joints in Stitt Island dacite (unit 14), east shore of Stitt Island. Columns (10-12 cm wide) plunge steeply towards the camera.

Mafic greywacke, siltstone and mudstone (unit 34) west of the Mandy deposit is 150 m thick. These sediments overlie pillowed basalt flows (unit 3b) and are overlain by, and locally intercalated with, plagioclase-phyric mafic tuff (unit 22b). The unit has a strike length of 2.4 km, terminated by faults at both ends. Beds are a few centimetres to 1.5 m thick, continuous, parallel-sided and normally size-graded, with bedding defined by variation in grain size and colour. Typical weathering colours are dull buff-green and various hues of greenish grey. Beds are generally well defined, but on some outcrops bed contacts are virtually unrecognizable due to absence of significant variations in grain size and colour. Detrital components of these rocks are rarely recognizable due to fine grain size, an imposed schistosity and strong recrystallization. Plagioclose crystals to 1.5 mm, pyroxene pseudomorphs to 2 mm, epidote-replaced granules (1 — 3 mm) and mixtures of plagioclose-phyric, pyroxene-phyric and plagioclase-pyroxene-phyric mafic volcanic granules and cobbles are preserved in some coarse greywacke beds. Fine grained rocks are composed of a recrystallized mixture of tremolite-actinolite, chlorite, epidote and minor carbonate. Epidosite masses up to 30 cm across are present in outcrops west of the Schist Lake Cu-Zn deposit. The sequence shows a crude upward and southward coarsening in grain size and increase in bed thickness. The presence in the sequence of a narrow plagioclose-phyric mafic flow with quartz amygdales up to 10 mm in size suggests that these rocks were deposited in relatively shallow water.

Well bedded sedimentary rocks (unit 33) on the small peninsula southwest of Stitt Island include intercalated 6 — 36 cm thick beds of grey to greyish green greywacke and siltstone, 1 — 10 mm thick interbeds of green to buff mudstone, 2 — 5 cm thick beds of pale buff to white felsic tuff or chert, and rare, up to 1 m thick beds of polymictic pebble conglomerate. Beds are laterally continuous and parallel sided, with scours at the base of some greywacke beds. Normal size-grading and Bouma ABC(DE) internal zonation is typical for greywacke and siltstone beds (Fig. 197). Thick greywacke beds contain small pebbles up to 1 cm across at their base; thin beds contain 0.5 — 1 mm plagioclase crystals set in a fine grained matrix at their base. White felsic tuff or chert beds are very fine grained, internally laminated and locally compose up to 30% of this unit. Polymictic pebble conglomerate beds are normally size-graded, vary from framework- to matrix-supported and contain well rounded pebbles, including numerous aphyric rhyolite clasts up to 12 cm across. Presence of well rounded rhyolite pebbles indicates a subaerial source for at least part of the detritus in this unit. Bouma zonation in greywacke beds and normal size-grading in pebble conglomerate beds indicate deposition by subaqueous density currents. Preservation of delicate sedimentary structures suggests deposition was in water over 200 m deep.

Geochemistry and summary

Three samples obtained from aphyric mafic flows (unit 3b) southeast of Carlisle Lake range in SiO_2 from 51.2 — 55.1% (H_2O and CO_2 free) and in MgO from 4.4 — 6.2% (Fig. 198). Two of the analyses fall within the Hidden Lake-Burley Lake basalt-basaltic andesite field and one falls in the Bear Lake field on FeO^*/MgO vs. SiO_2 plots; on a TiO_2 vs FeO^*/MgO plot the Carlisle Lake, Bear Lake and Hidden Lake compositional fields overlap (Fig. 199). The average Zr/Y ratio for the Carlisle Lake flows is 1.2, indistinguishable from either the Hidden Lake basalt (1.2) or Bear Lake basaltic andesite (1.3). Ni contents average 5 ppm, similar to the Hidden Lake basalt (average 5 ppm) and lower than the Bear Lake basaltic andesite (average 28 ppm). Therefore, the mafic flows east of Carlisle Lake are considered to be broadly similar to the basaltic lower half of the Hidden Lake-Burley Lake sequence.

Unit 3b Carlisle Lake flows are interlayered with pillow fragment breccia, heterolithologic breccia, mafic volcaniclastic sediments and mafic scoria-rich tuff. They are also thin, well organized flows, different than the thick amalgamated flow units, with scarce intercalated volcaniclastic rocks, that dominate the Hidden Lake basalt. In this respect they are similar to Burley Lake basaltic andesite. It is therefore suggested that the Carlisle Lake flows represent a fault slice containing the middle portion of the Hidden Lake-Burley Lake sequence. The Carlisle Lake flows contain primary structures analogous to flows in the Burley Lake section, and for this reason are similarily interpreted to have been deposited in a relatively shal-

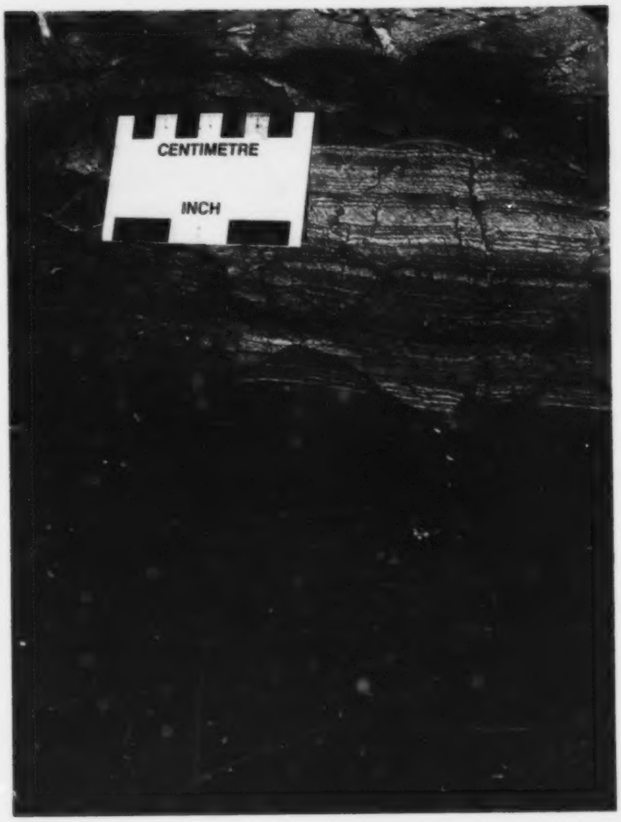

Figure 197: *Thin-bedded greywacke, mudstone and felsic mudstone (reworked tuff?), unit 33, west shore of Northwest Arm, southwest of Stitt Island. The 6 cm thick greywacke bed (centre) has scours at the base and comprises Bouma zones A, B, C and D.*

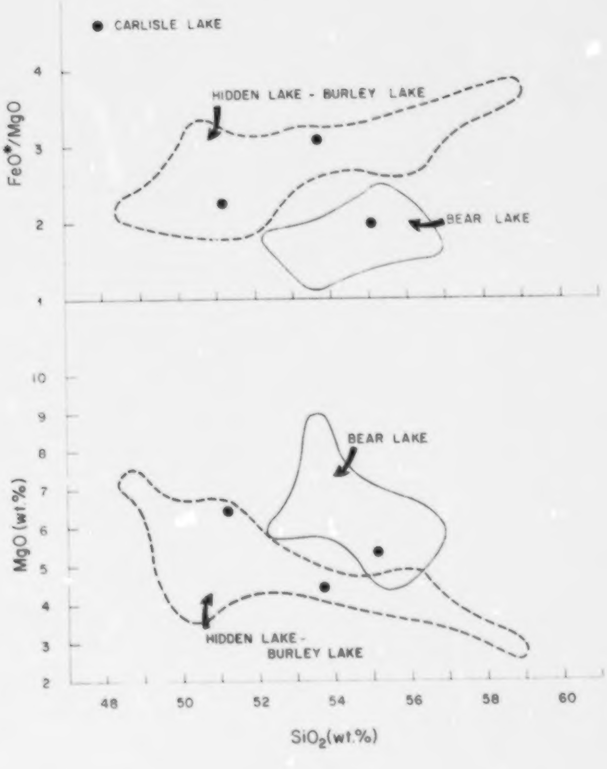

Figure 198: *FeO*/MgO and MgO vs. SiO_2, Carlisle Lake basalts, Mandy sub-block. Fields of Hidden Lake-Burley Lake basalt-basaltic andesite and Bear Lake basaltic andesite for comparison. Carlisle Lake flows are compostionally closest to the Hidden Lake-Burley Lake sequence.*

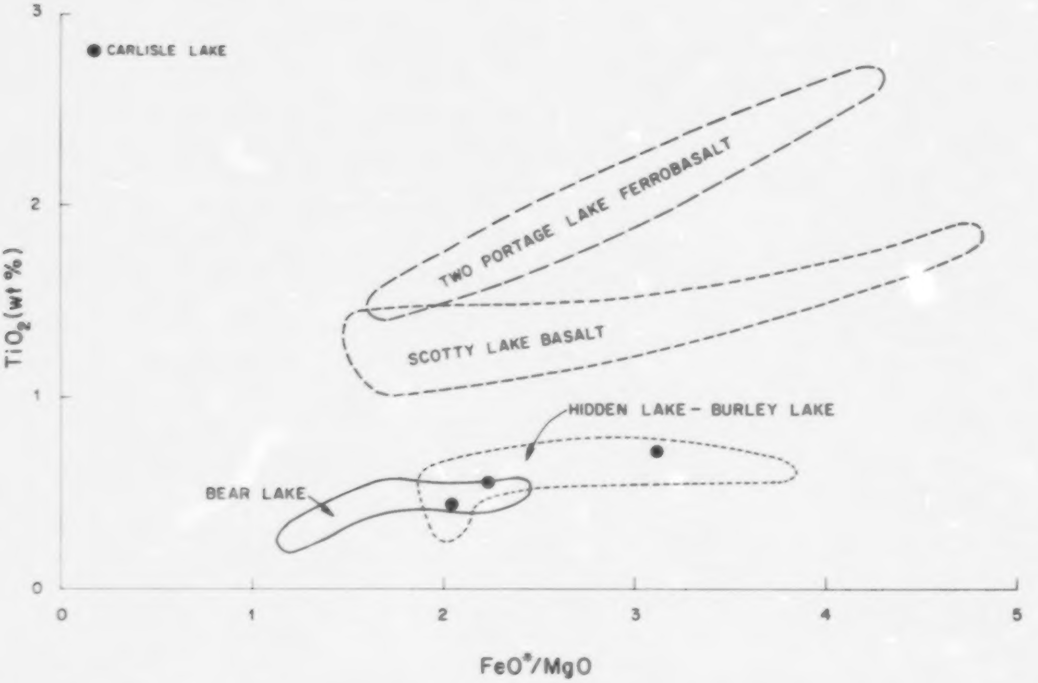

Figure 199: TiO_2 vs. FeO/MgO, Carlisle Lake basalts, Mandy sub-block. Fields of other major mafic flow units for comparison. Like most non-ferroan basalts in the Flin Flon area, Carlisle Lake basalts are characterized by low TiO_2 contents.*

low subaqueous environment with intercalated scoria-rich mafic tuffs having possibly been erupted subaerially.

LEDGE LAKE SUB-BLOCK

Rocks of the Ledge Lake sub-block are bounded on the north by the Green Lake Fault, on the east by the Mitt Lake Fault, and extend beyond the map area to the west and south (Fig. 169). The portion of the sequence in the map area is homoclinal, west-southwest-facing and over 1810 m thick (Fig. 200). It comprises plagioclase-glomerophyric and aphyric mafic pillowed flows, and a single, 500 m thick unit of aphyric and plagioclase-quartz-phyric rhyolite.

Plagioclase-glomerophyric mafic flows (unit 10)

Plagioclase-glomerophyric mafic flows (unit 10) form two 300 m thick units in the Ledge Lake sequence (Fig. 200). The lowermost unit, truncated to the east by the Mitt Lake Fault, contains minor plagioclase-pyroxene-rich mafic tuff near its west margin. Flows in both units are pillowed, contain 10 — 20% plagioclase glomerocrysts (1 — 2 mm) and have groundmass plagioclase microlites. They are sparsely quartz amygdaloidal, with up to 10% amygdales (up to 4 mm) concentrated in pillow margins. Pillows have narrow rusty brown selvages up to 3 mm thick. Flow contacts were rarely observed and consequently flow thicknesses are not known.

Many flows in the northeast portion of the Ledge Lake area, in particular the two plagioclase-glomerophyric units, are weakly to strongly epidotized. This epidotization is generally uniform and converts flows to hard, dark grey to black weathering rocks. In intensely epidotized areas alteration is concentrated adjacent to anastomosing fractures, and includes up to 5% disseminated pyrite.

Aphyric mafic flows (unit 7)

Well preserved mafic pillowed aphyric flows (unit 7) occur in a 300 m thick unit northwest of Mitt Lake and in a more than 900 m thick unit west of Ledge Lake. These flows include approximately equal proportions of massive, pillowed and composite types, and have well defined contacts (Fig. 201). Nine complete flows were measured, displaying a range in thickness from 3 to 28 m, and an average thickness of 12 m. Pillowed flows are thickest. Except for minor interflow mafic tuff other rocks are not intercalated with these two sequences of mafic flows.

Primary structures are well preserved in unit 7 flows. Pillows have narrow selvages, and are locally defined only by curving fracture-bounded outlines or by quartz-filled thermal contraction cracks. Largest pillows (up to 10 m x 1.5 m) occur at the base of pillowed divisions and decrease in size toward tops of flows. Vesicle content varies from flow to flow (5 — 35%) and shows a slight upward increase in the sequence. Most vesicles are quartz-filled and 1 — 5 mm in size. Largest amygdales (up to 15 cm across) occur at topmost portions of massive divisions of flows. Large vesicles and local cupola-shaped gas cavities (up to 20 cm) are present in many of the aphyric flows.

Intergranular textures characterize aphyric flows. Equant to tabular clinopyroxene grains in the flows are replaced by tremolite-actinolite, epidote and chlorite. Plagioclase microlites are 0.1 to 0.3 mm in length.

Rhyolite (unit 18)

A 500 m thick unit of white to pale buff weathering rhyolite outcrops in the Ledge Lake sub-block near the west boundary of the map area. This flow unit has been traced over 5 km to the northwest by Heywood (1966) and Stockwell (1960). It is abruptly terminated by a north-trending fault 130 m east of the interprovincial boundary, and is not present east of the

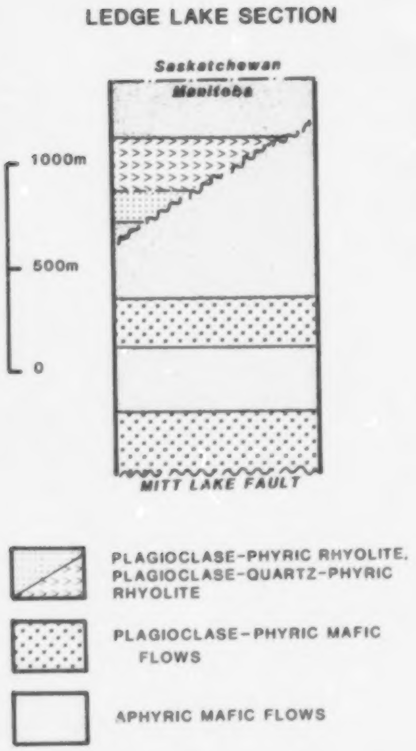
LEDGE LAKE SECTION
Saskatchewan
Manitoba
1000m
500m
0
MITT LAKE FAULT
PLAGIOCLASE-PHYRIC RHYOLITE, PLAGIOCLASE-QUARTZ-PHYRIC RHYOLITE
PLAGIOCLASE-PHYRIC MAFIC FLOWS
APHYRIC MAFIC FLOWS

Figure 200: Ledge Lake section, Ledge Lake sub-block. Section line shown on Figure 169.

fault, either within or south of the map area (Heywood, 1966).

The northeastern, lower 170 m of this unit comprises quartz-plagioclase-phyric massive rhyolite (unit 18d) and the upper 330 m is plagioclase-phyric rhyolite (unit 18b). Several metres of angular rhyolite breccia are present in pockets along the flow top. Massive quartz-plagioclase-phyric rhyolite contains 5% euhedral quartz phenocrysts (1 — 3 mm) and 10% tablet-shaped plagioclase phenocrysts (1 — 2 mm). Plagioclase-phyric rhyolite contains 10% plagioclase glomerocrysts and tablet-shaped phenocrysts, up to 2% carbonate-filled vesicles (up to 2 cm across), locally abundant spherulites, local trachytic textures, and rare flow banding. Vesicles, spherulites, flow banding and stratiform character of the unit are consistent with an extrusive origin.

GREEN LAKE SUB-BLOCK

Rocks of the Green Lake sub-block are bounded on the north by the Phantom Lake fault, on the east by the Mitt Lake fault, on the south by the Green Lake fault, and extend west into Saskatchewan (Fig. 169). Approximately 730 m of northeast- and east-facing section are exposed between the southwest boundary of this sub-block and a north-trending synform east of Green Lake. A wide variety of mafic aphyric, porphyritic and plagioclase-phyric pillowed flows, plagioclase and pyroxene-bearing tuff and lapilli tuff, and minor mafic sedimentary rocks occur in this section. These lithologies are intercalated at both a map and outcrop scale. Mafic flows are typically separated by units of mafic tuff and lapilli tuff.

Mafic flows

Mafic flows form over 60% of rocks exposed in the Green Lake sub-block. Porphyritic and aphyric flows occur throughout the lower 610 m of the sequence and plagioclase porphyritic flows form the upper 120 m (Map GR87-1-1).

Aphyric flows are rare in the Green Lake sub-block. They contain less than 5% vesicles, are pillowed, and are buff-brown to dark grey. Two complete flows were measured, one 9 m thick and the other 45 m thick. The 45 m flow is pillowed throughout and characterized by pockets of

Figure 201: Contact (FC) between two massive mafic flows, 200 m west of Ledge Lake. Vesicles (V) occur selectively in basal 10 cm of upper flow and spacing between quartz-filled thermal contraction cracks (TCC) increases upward in flow.

angular, carbonate-cemented breccia at its base; it overlies mafic tuff, and the breccia is interpreted to have been formed by phreatic explosions generated from water trapped in the underlying tuff.

Porphyritic flows range from 0.6 to 15 m thick, include massive, composite and pillowed types, and exhibit variable vesicle content (less than 5 to 30%, 1 — 5 mm). They contain 7 — 20% plagioclase phenocrysts (0.5 — 3 mm) and 0 — 5% tremolite-actinolite pseudomorphs after pyroxene phenocrysts (1 — 4 mm).

Plagioclase-phyric flows are buff to buff-brown, include massive and pillowed types, and contain up to 20% quartz amygdales. Plagioclase phenocrysts (15 — 30%) are equant, euhedral, 1 — 4 mm in size, and locally glomerocrystic.

Mafic tuff and lapilli tuff

Buff-brown, brown and dark grey weathering mafic tuff and lapilli tuff form approximately one third of the sequence exposed in the Green Lake sub-block. Tuff and lapilli tuff beds are parallel-sided, laterally continuous, and 5 — 30 cm thick (rarely up to several metres thick), normally size graded (including A and AB types), and locally have pale buff to white very fine grained E tops. Basal scours, removal of E tops of underlying beds (Fig. 202) and slabby rip-ups of white tuff attest to erosion by the subaqueous density currents which deposited the tuff and lapilli tuff.

CENTIMETRE

Figure 202: Bedded mafic volcanic wacke or tuff (unit 22), 300 m southwest of Burley Lake. Middle bed has an erosional basal contact, a normally size graded A division and an upper indistinctly laminated B division. Size grading is defined by both lithic clasts (dark) and plagioclase crystals (light coloured).

Individual tuff beds are monolithologic, but vary in phenocryst abundance and type from bed to bed . Beds contain up to 40% pyroxene and plagioclase phenocrysts (up to 3 mm) within blocky, angular, 0.3 — 3 mm, fracture-bounded fragments. Phenocrysts are commonly broken and truncated at clast margins. Fragments are rarely visible in hand specimen; consequently in outcrop tuffs appear to be rich in crystals. Most beds contain pyroxene-plagioclase-phyric fragments, but some beds are composed of plagioclase-phyric clasts and rare beds comprise aphyric types. Vesicle content of fragments is variable, but generally low.

Normal size-grading, Bouma zonation of beds, rip-ups and scours indicate the tuff and lapilli tuff were deposited by subaqueous density currents. Blocky shape and low vesicle content of fragments suggest clasts were produced by phreatic or phreatomagmatic eruptions. Presence of ballistic blocks (not in hydraulic equilibrium with the enclosing tuff and lapilli tuff), local occurrence of bomb sags, and rare accretionary lapilli suggest that the tuff and lapilli tuff formed in shallow water or subaerial eruptions. Preservation of delicate primary structures in tuff and lapilli tuff indicates deposition in water over 200 m deep (storm wave base). Breccia at the base of one mafic volcanic flow, which appears to have formed by steam explosions from water trapped in tuff underlying the flow, indicates water depth could not have been significantly deeper than 200 m.

Tuff and lapilli tuff in the Green Lake sub-block are similar in composition, texture, colour, clast morphologies and bed forms to the Mikanagan Lake mafic volcaniclastic rocks (unit 20). The latter deposits are also interpreted to have been produced by phreatomagmatic eruptions.

Sedimentary rocks

Sedimentary rocks occur only in minor amounts in the Green Lake sub-block, mainly in shoreline outcrops on Burley Lake. Sedimentary rocks are mafic, very fine grained, dark green to buff-brown, and typically well bedded. Beds are parallel-sided, continuous, 5 cm to 1 m thick and A, AE and massive types. White chert beds, up to 1.5 m thick, are locally interbedded with the mafic beds.

MITT LAKE SUB-BLOCK

The Mitt Lake sub-block is bounded on the west by the Mitt Lake Fault, on the northeast by the Ross Lake and Phantom Lake faults, and extends beyond the map area to the south (Fig. 169). The volcanic section comprises three members: a lower glomerophyric mafic flow unit (at least 370 m), a middle aphyric mafic flow unit (120 m maximum) and an upper glomerophyric mafic flow unit (at least 180 m). The flows are tightly folded about a southerly plunging upright syncline; the axial trace of this syncline is truncated in the north by the Phantom Lake Fault. The fold may be equivalent to the Burley Lake Syncline; thus there would be 900 m of left lateral offset on the Phantom Lake Fault and the volcanic flows in the Mitt Lake area are approximately equivalent to those northwest of Burley Lake; i.e. the Mitt Lake flows belong to the upper part of the Hidden Lake - Burley Lake sequence. Rocks in the Mitt Lake sub-block are at or just above the prehnite-pumpellyite isograd (Map GR87-1-1) and, consequently, primary structure and textures are well preserved.

The lower glomerophyric mafic flows weather light buff to light brown and are medium green on fresh surfaces. Virtually all flows are pillowed. Pillow selvages are thick (5 — 10 mm) and weather rusty brown; polymineralic amygdales to 6 mm are concentrated either at pillow margins or pillow cores, but degree of vesicularity is generally low. Flows are strongly porphyritic, containing 10 — 25% plagioclase phenocrysts (0.4 — 3 mm) and 0 — 3% pyroxene phenocrysts (0.4 — 1.5 mm). These phenocrysts are commonly aggregated in multicrystal (up to 22 individual crystals) glomerocrysts up to 5 mm in diameter. The glomerocrysts have a hypidiomorphic texture similar to medium grained anorthositic gabbro and are not simple aggregates of plagioclase tablets (Fig. 203). The pyroxene phenocrysts range from fresh clinopyroxene to pseudomorphs composed of chlorite and tremolite-actinolite. Groundmass consists of

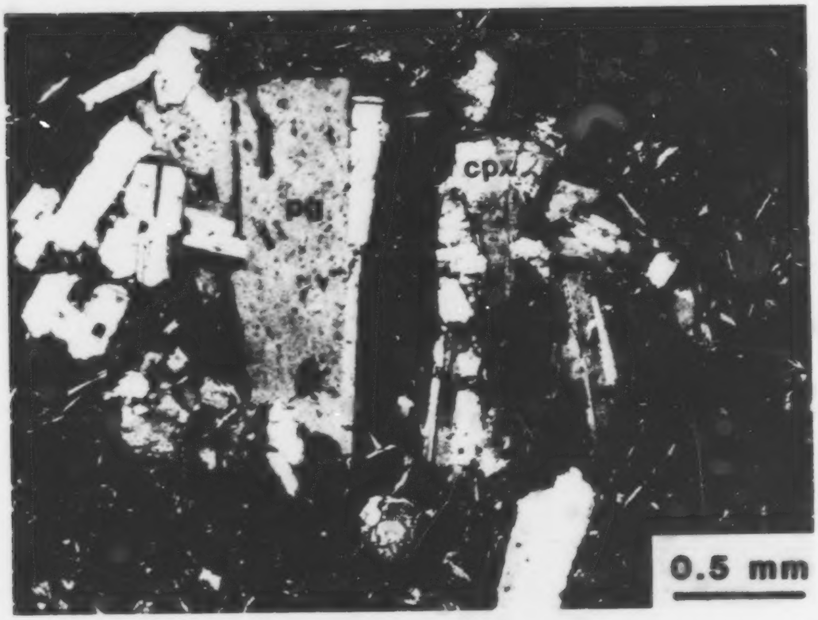

Figure 203: Glomerophyric mafic flow (unit 10), Mitt Lake area. The large glomerocryst is composed of a great many subhedral plagioclase crystals (pg; twinned) with interstitial anhedral fresh clinopyroxene (cpx). The interlocking texture of these glomerocrysts suggests that they may be cognate xenocrysts. Sample 4518-1, crossed polarizers.

plagioclase laths (0.1 — 0.4 mm), fibrous sheaves of actinolite, pale green chlorite, epidote, pyrite and sphene.

The middle, aphyric mafic flow member of the sequence is poorly exposed, and outcrops only in the hinge zone of the fold, east of Mitt Lake. Buff-brown weathering composite and pillowed flows are both represented, locally separated by thin interflow mafic tuff units. One composite flow is 20 m thick and contains a massive lower portion (13 m) grading upward into a pillowed upper portion (7 m thick); vesicles (up to 5%) occur in the massive base and in the pillowed division of this flow. Pillowed flows in this member locally contain radial pipe vesicles. Interflow tuffs display south-plunging minor folds presumably related to the large synclinal structure.

The upper glomerophyric member, in the core of the syncline east of Ledge Lake, is similar to the lower glomerophyric member but pillowed flows typically weather red-brown and contain fewer pyroxene phenocrysts (0 — 1%). In some flows the glomerocrysts are the multicrystal hypidiomorphic type described above (but composed entirely of plagioclase), whereas in other, more sparsely porphyritic flows the glomerocrysts are simple clumps of tabular plagioclase crystals. Groundmass texture and mineralogy is similar to that described for the lower member. Small amounts of stilpnomelane locally occur in chlorite-filled amygdales and along late fractures, overprinting actinolite. At one locality the pillowed sequence contains a concentrically banded, vesicular lava tube 13 m in long dimension.

RAILWAY LINE SUB-BLOCK

This sub-block is bounded to the east by the Cliff Lake Fault, to the west by the Channing Fault, to the north by Missi Group rocks, and extends beyond the map area to the south (Fig. 169). The rocks comprise a generally south-younging sequence which is closely folded about south-plunging folds with north-northeast-trending axial planes. From oldest to youngest (north to south, Map GR87-1-1) the sequence comprises thinly bedded mafic volcaniclastic rocks and sediments (thickness unknown), aphyric mafic flows (minimum 240 m), pillow fragment breccia and subordinate flows (approximately 1060 m), and mafic scoria-rich tuff, subordinate debris flows and rare pillowed flows (minimum 600 m). The sequence, from the aphyric mafic flows upwards, is at prehnite-pumpellyite grade (Map GR87-1-1); consequently primary structures and textures are well preserved.

Mafic volcaniclastic rocks and sediments (units 22b, 23b and 33)

Bedded mafic valcaniclastic rocks and sediments outcrop on the east shore of Schist Lake on two peninsulas north and northeast of Stitt Island. They weather buff to grey-green and include plagioclase-crystal-rich greywacke or reworked tuff, siltstone and mudstone (units 22b and 33). Beds are 2 — 100 cm thick, parallel-sided, continuous, and display Bouma A, AE and ABE zones. Plagioclase crystals range in size from 0.2 — 4 mm and are abundant in some beds. Lithic fragments up to 4 cm across occur at bases of some beds. Interbeds and bed-tops of mudstone are mafic (chloritic), laminated and contain disseminated 1 — 2 mm Fe-carbonate blasts.

Scoria tuff and tuff breccia (unit 23b), intercalated with the rocks described above, occur on the north side of the peninsula northeast of Stitt Island. They weather buff-grey to grey-green and occur in beds ranging in thickness from 0.5 m to several metres. Thinner beds are A and AB types; thick beds contain scoria blocks to 5 cm and epidotized accessory blocks to 50 cm. These scoria tuffs (unit 23b) are similar to others described later in this section.

Aphyric mafic flows (unit 7)

Aphyric to sparsely plagioclase-phyric, buff-brown weathering mafic flows (unit 7) are pillowed with amoeboid pillow breccia tops. Flows contain amygdales to 3 mm and pillow selvages are brown to medium green, up to 5 mm thick.

Pillow fragment breccia, pillowed flows (units 7a and 8b)

The lower part of this unit is poorly exposed and consists of scoria-rich tuff and lapilli tuff, and aphyric pillow fragment breccia. The middle part of the unit consists of plagioclase-phyric amoeboid pillow fragment breccia with local irregular areas of pillowed flow.

The upper part of the unit is better exposed, and comprises aphyric pillow fragment breccia and aphyric mafic flows. Pillow fragment breccias are bedded (1 — 5 m thick at one locality) and normally graded to matrix-rich tops. Fragments are light brown, angular to rounded or crescentic, amygdaloidal and microlitic (Fig. 204). They vary chiefly in the content and size of polymineralic amygdales.

Aphyric pillowed flows weather light brown. Flows include composite and pillowed types; vesicularity is up to 20% (1 — 3mm) in the pillowed division.

Mafic scoria-rich tuff and tuff breccia (unit 23b)

Scoria-rich mafic tuff and tuff breccia, along with subordinate heterolithologic debris flows and pillow fragment breccia, and rare pillowed flows, comprise the topmost portion of the Railway Line sub-block in the map area. The scoria tuffs are identical to tuffs previously described in unit "J" of the Hook Lake Block, and are products of a similar eruptive and depositional process. Bedding in tuffs ranges from 4 cm to more than 10 m thick and includes Bouma AB (Fig. 205), A, AE, and ABDE types. Normal size-grading is defined by plagioclase crystal size and abundance (Fig. 206) and in places by size of scoria lapilli. Beds display many other features typical of subaqueous density current deposits, including rip-ups, load casts, flame structures, and scours. These pyroclastic beds differ from epiclastic turbidite deposits as they contain abundant fine grained scoria (Fig. 207), scoria blocks, internal layers or laminae composed of scoria particles, accessory pillow fragment blocks (Fig. 208), and bomb sags below some accessory blocks (Fig. 209).

Scoria particles in the tuff commonly contain plagioclase phenocrysts, which are truncated at fragment margins (Fig. 207). Tuff is framework-supported by scoria grains and granules; there are virtually no plagioclase crystal fragments. Observed size-grading of plagioclase (Fig. 206), therefore, reflects the size of scoria particles (i.e. only large particles contain complete, large crystals). Margins of scoria particles are largely vesicle-controlled, although fracture-controlled margins are present in some particles (Fig. 207). Contained plagioclase phenocrysts (Fig. 210) are 0.2 — 4 mm, euhedral, tablet-shaped, oscillatory-zoned and variably replaced by epidote, sericite, carbonate and prehnite. Their abundance ranges up to 40% at base of beds. Fresh pale green clinopyroxene phenocrysts (to 2%, 0.2 — 1 mm) occur in some scoria.

Heterolithologic debris flows, which occur locally, are thick bedded (up to 15 m), and reverse to normally size-graded with largest clasts approximately in bed centres. They contain a variety of subangular boulders supported in a poorly sorted gravelly matrix. Clast types include aphyric mafic volcanic rocks, plagioclase-phyric mafic volcanic rocks, equigranular coarse grained gabbro, banded synvolcanic mafic dyke rocks (Fig. 211), equigranular medium grained quartz diorite, and aphyric scoria. At one locality these debris flows are intercalated with aphyric, densely amygdaloidal pillowed flows.

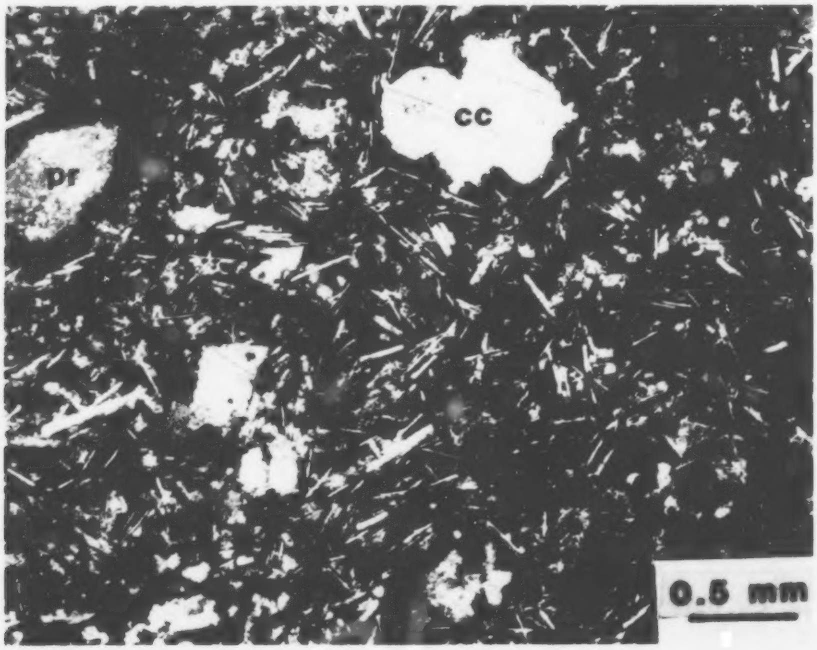

Figure 204: Clast in pillow fragment breccia (unit 7a), west of Hook Lake. The clast has a well preserved plagioclase microlitic texture identical to that in mafic flows, providing support to the interpretation of these breccias as composed of pillow fragments rather than pyroclasts (which would have a predominantly glassy groundmass). Plagioclase microlites are lath-shaped, up to about 0.4 mm long. Amygdales are filled with carbonate (cc) and prehnite (pr). Sample 4166-1, crossed polarizers.

Figure 205: *Scoria tuff (unit 23b) bed 1.2 m thick. Base of bed (arrows) is marked by scours and large flame structures. "A" division is normally graded with respect to plagioclase crystal size. "B" division is parallel laminated and contains scoria granules. Top of bed is marked by a narrow interlayer of white mudstone.*

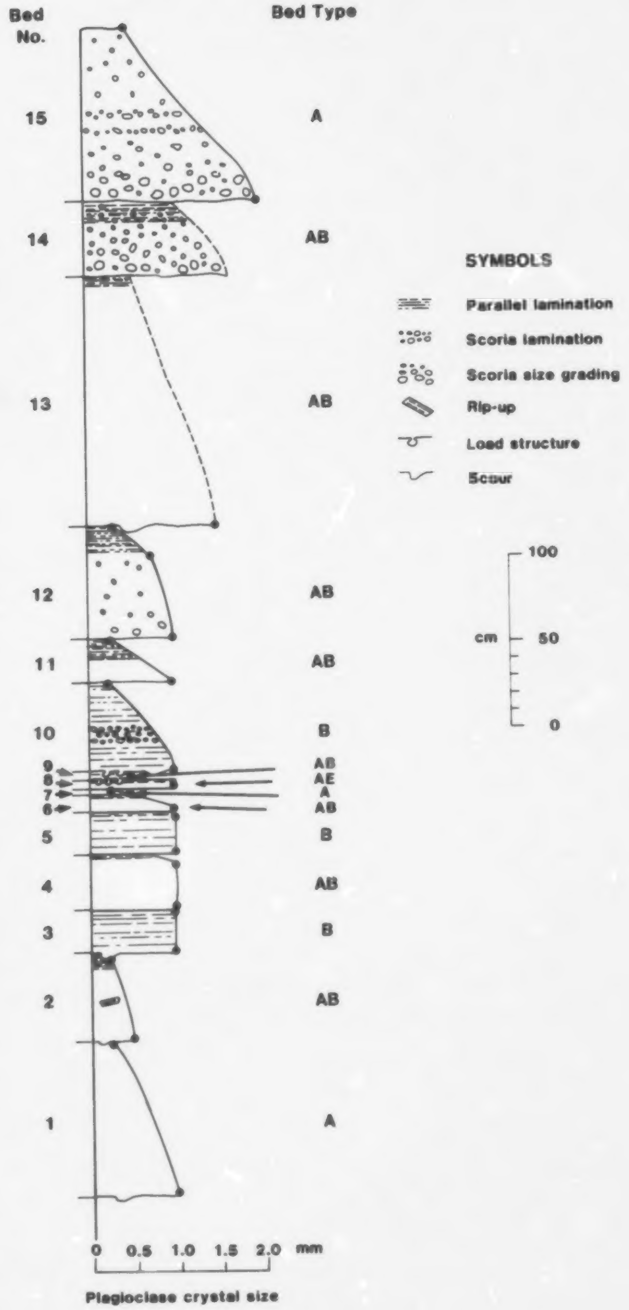
Bed No.
Bed Type
15
A
14
AB
13
AB
12
AB
11
AB
10
B
9
AB
8
AE
7
A
6
AB
5
B
4
AB
3
B
2
AB
1
A
SYMBOLS
Parallel lamination
Scoria lamination
Scoria size grading
Rip-up
Load structure
Scour
100
cm
50
0
0
0.5
1.0
1.5
2.0
mm
Plagioclase crystal size

Figure 206: *Measured section through thinly bedded mafic, scoria-rich tuff (unit 23b), Railway Line sub-block, about 1900 m southeast of Stitt Island. Maximum plagioclase crystal size (dots) measured in field. Scoria fragments shown are up to 1 cm across. Morphology of small scoria fragments from base of bed number 12 is shown in Figure 207.*

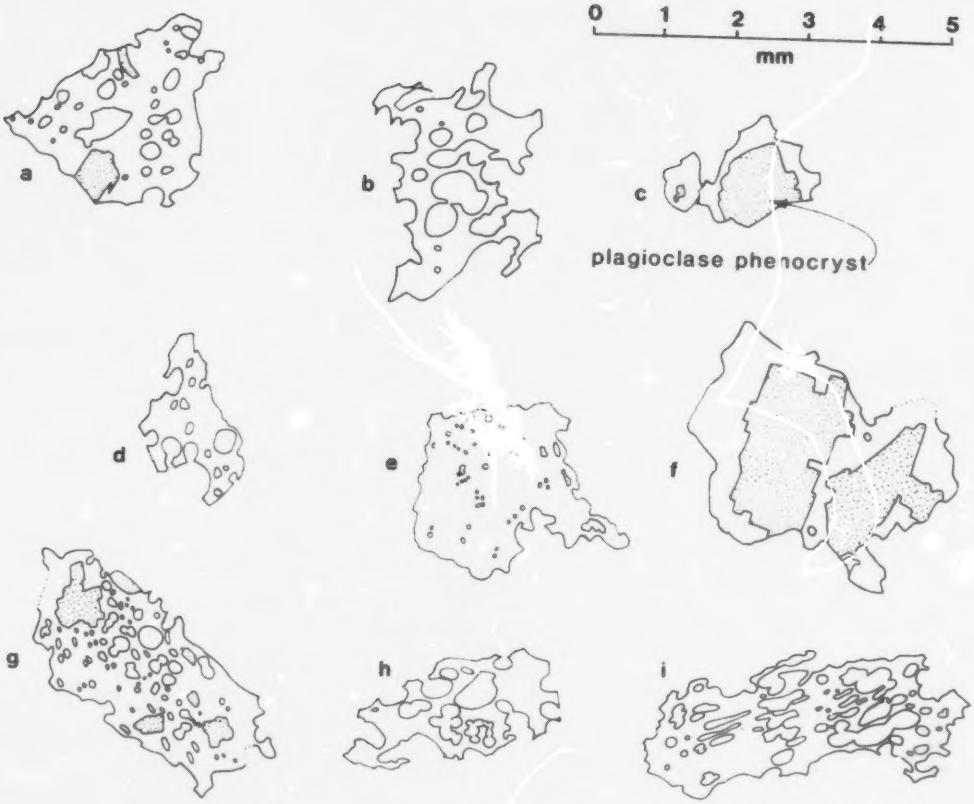

Figure 207. Scoria particles in bedded, mafic, scoria-rich tuff (unit 23b), Railway Line sub-block, about 1900 m southeast of Stitt Island. Particles were traced from projections of thin sections. (a) to (g) from base of bed 12 (65 cm thick, Fig. 206); (h) and (i) from base of 1 m thick bed in nearby locality. Compare with Figure 166. Note truncation of plagioclase phenocrysts (dot pattern) at particle margins, variation in vesicle size and abundance, and combination of vesicle-controlled and fracture-controlled margins.

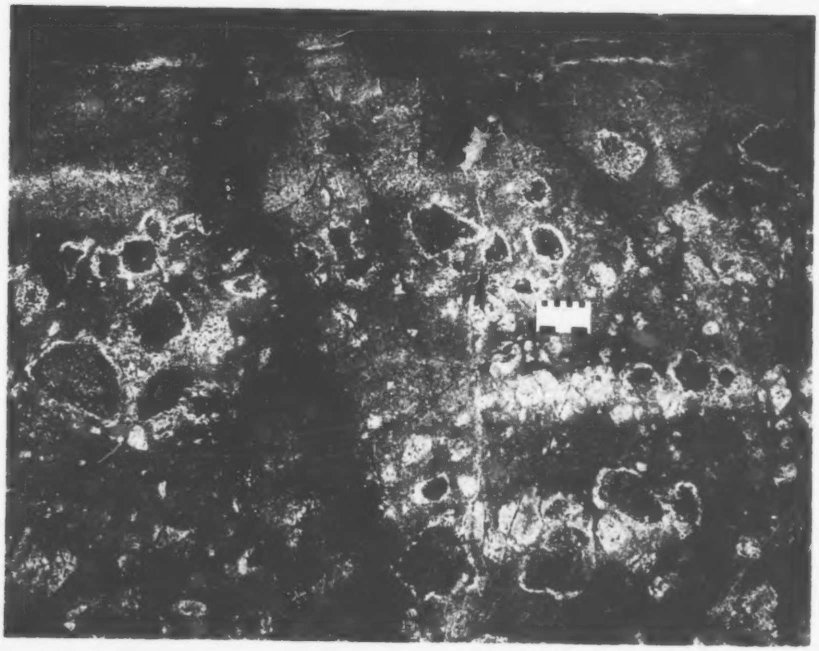

Figure 208: Trains of accessory fragments defining crude layers in mafic scoria-rich tuff (unit 23b), 100 m east of northwest arm of Schist Lake. Accessory fragments have bleached margins interpreted to have formed during post-depositional, possibly diagenetic, alteration.

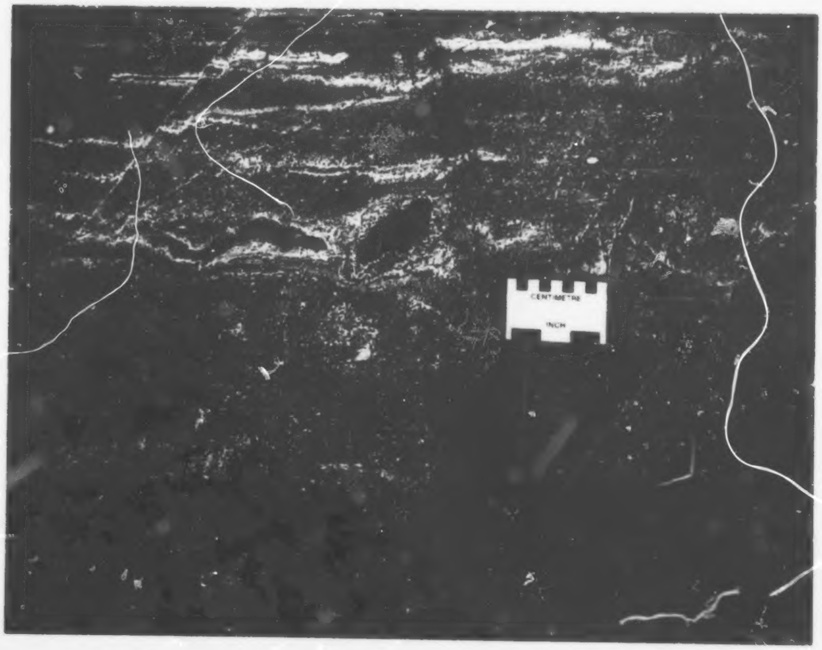

Figure 209: Bedded mafic scoria-rich tuff (unit 23b), 100 m east of northwest arm of Schist Lake. Distorted bedding beneath fragment (to upper left of scale card) is a possible bomb sag.

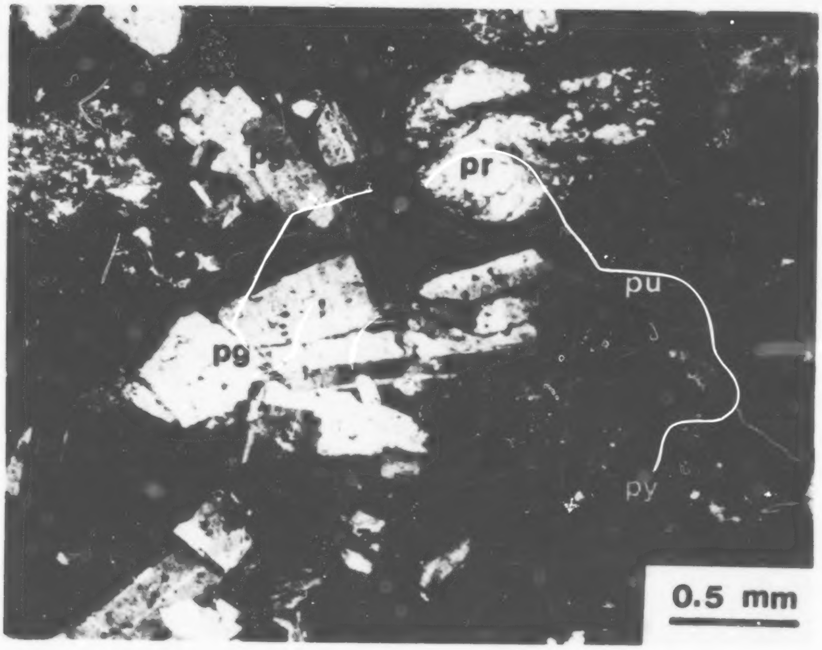

Figure 210: Plagioclase-glomerophyric fragment in mafic tuff breccia (unit 23b), west of Hook Lake. Plagioclase (pg, twinned) occurs as single-crystal phenocrysts and large, multi-crystal glomerocrysts. Groundmass consists of very fine grained plagioclase microlites in a matrix of fine epidote (dark). Amygdales are filled with prehnite (pr), pumpellyite (pu), carbonate (cc), quartz (qz) and pyrite (py). Sample 4157-2, crossed polarizers.

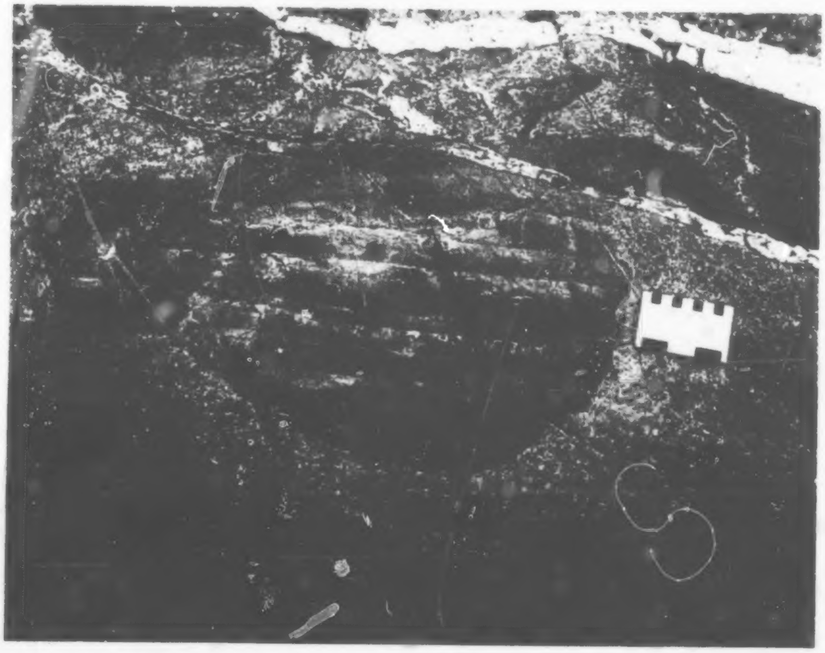

Figure 211: Heterolithologic breccia (unit 29), west of Cliff Lake fault near the south border of the map area. The large boulder is of a banded, synvolcanic mafic dyke.

FLIN FLIN BLOCK: SUMMARY AND COMPARISON TO OTHER BLOCKS

The Flin Flon Block contains several fault-bounded sub-blocks (Fig. 169) which make precise stratigraphic correlations difficult. A major part of the volcanic section in the Flin Flon Block appears to belong to a single magmatic series ranging from basalt to basaltic andesite defined in this report as the Hidden Lake-Burley Lake sequence. This sequence is underlain by another basaltic sequence (South Main basalt), only the top of which has been mapped. The two major mafic sequences appear to be locally separated by felsic volcanic rocks, as at Flin Flon Mine, where rhyolite domes, rhyolite flows, widespread footwall hydrothermal alteration and a major body of massive Cu-Zn sulphides occur at the contact. South Main basalts are only exposed in Saskatchewan and therefore details of larger-scale contact relationships between the South Main and Hidden Lake-Burley Lake sequences remain undefined.

The Hidden Lake-Burley Lake sequence is a minimum of 3.3 km thick. The lower part of the sequence (Hidden Lake basalt) comprises thick, poorly organized, plagioclase-phyric and subordinate aphyric basalt flows. The upper part of the sequence (Burley Lake basaltic andesite) comprises thinner, well defined aphyric, plagioclase-phyric and glomerophyric basalt and basaltic andesite flows intercalated with units of pillow fragment breccia, heterolithologic breccia, and scoria-rich mafic tuff.

All volcanic rocks exposed in the mapped portion of the Flin Flon Block were deposited in a subaqueous environment. Some units, in particular scoria-rich mafic tuff, must have been erupted in a very shallow subaqueous or subaerial environment. Radial pipe vesicles, abundant and large amygdales, and large gas cavities in flows throughout the block suggest that in general the pillowed flows were emplaced in relatively shallow water (Table 5). Given the minimum 4 km thickness of the volcanic section this implies that subsidence kept pace with volcanic accumulation.

The Hidden Lake-Burley Lake basalt-basaltic andesite sequence shares a number of characteristics with the sequence exposed in the Hook Lake Block. Both contain a large-scale intercalation of porphyritic and aphyric flows, pillow fragment breccia and scoria-rich mafic tuff. Glomerophyric flows southeast of Hook Lake are virtually identical to flows in both the Burley Lake and Mitt Lake areas. Scoria tuff units in both blocks have similar components and bedforms. Chemical compositions of flows in the two sequences share a number of similarities, summarized elsewhere in this report. These shared characteristics suggest that the volcanic rocks in the Flin Flon and Hook Lake blocks are both parts of the same general sequence. In addition, the two blocks have many structural elements in common, including north-northwest-trending folds, and abundant small fault-bounded sub-blocks with variable facing.

AMISK GROUP GEOCHEMISTRY

In this chapter the general features of Amisk Group geochemistry are discussed, with a view to interpreting the tectonic environment in which the Amisk Group was emplaced. In previous chapters each distinct lithostratigraphic component of the Amisk Group was shown to be identifiable on a variety of major element variation diagrams (see also Tables 8 and 9). The compositional characteristics correlate with lithologic properties of the various units (colour, flow type, flow thickness, vesicularity), so that virtually every major mafic unit in the area can be mapped as a formation.

In spite of the uniqueness of each major mafic unit, Amisk Group basalts and basaltic andesites in the Flin Flon-White Lake area can be subdivided into three main types:

1) those with high Rb, Ba, K and low Hf, Zr, Y, Ni and Cr contents (e.g. Bear Lake basaltic andesite (unit 1), Hidden Lake basalt (unit 2), Burley Lake basaltic andesite (unit 3); see also Table 8).
2) basalts characterized by high REE, P, Hf, Zr, Y and low Ni and Cr contents (e.g. Scotty Lake basalt (unit 4) and Two Portage Lake ferrobasalt (unit 5)).
3) basalts similar in major element chemistry to those in group 1 above, but with significantly higher Hf, Zr, Ti, Y and Ni and lower Rb, Ba, and K (basalts in the Grassy Narrows Zone (unit 7)).

Rare earth element (REE) contents of the majority of Amisk Group mafic flows fall within a relatively narrow range at approximately 10 times chondritic abundances (Fig. 212). REE patterns are flat, unfractionated, and display negligible Eu anomalies. The REE abundances of group 2 (above), including Scotty Lake and Two Portage Lake basalts, are higher than all other mafic units and chondrite-normalized patterns are slightly light rare earth element (LREE) enriched (Fig. 212). High REE abundances, high incompatible trace element contents, low Ni and Cr and generally high Fe contents suggest these rocks are the products of significant fractionation.

REE patterns of rhyolites (Fig. 213) range from flat (with slight middle REE depletion) to strongly LREE enriched; most (but not all) have negative Eu anomalies. Recent work in the Superior Province (e.g. Campbell et al., 1983) has demonstrated that REE geochemistry can be used to distinguish felsic volcanic rocks associated with Cu-Zn massive sulphide deposits from those not associated with sulphide deposits; rhyolites associated with deposits have flat REE patterns and strong negative Eu anomalies. It is noteable that in Flin Flon the only rhyolite body *directly* associated with a major sulphide deposit (3 in Fig. 213; Mine rhyolite, unit 15) has a flat pattern with *no* Eu anomaly. Therefore it appears that the

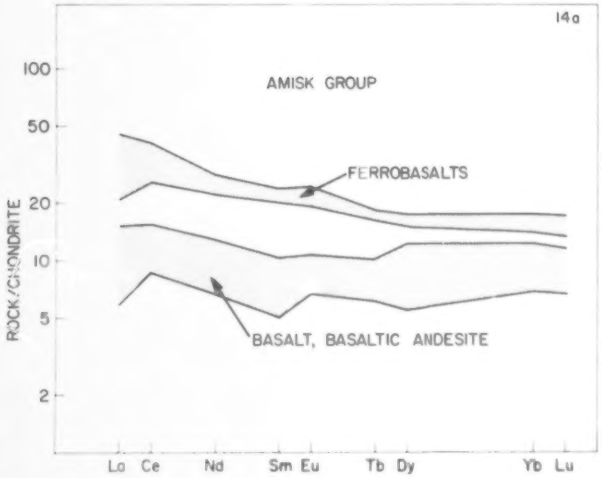

Figure 212: Chondrite normalized REE plots of Amisk Group mafic rocks, showing ranges for basalt, basaltic andesite and ferrobasalt (n = 10).

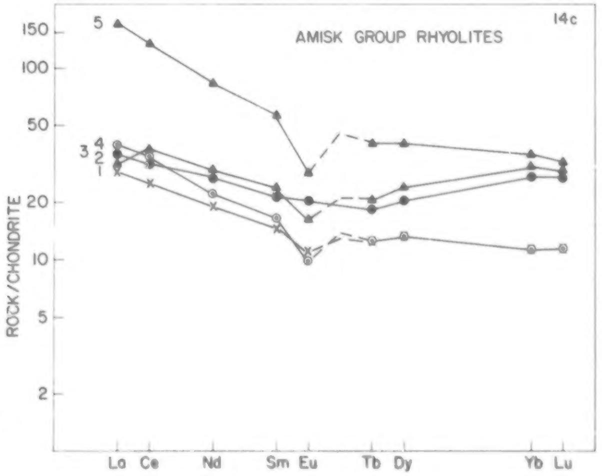

Figure 213: Chondrite normalized REE plots of Amisk Group rhyolites: 1 — flow in Bakers Narrows block (unit 18b, sample 2421-C1); 2 — Borne Lake rhyolite (unit 49c, sample 4015-C1); 3 — Mine rhyolite (unit 15b, sample 6141-C1); 4 — Solodiuk Lake rhyolite (unit 13, sample 429-C1); 5 — Grassy Narrows rhyolite (unit 18b, sample 3340-C1).

Table 8:
Average compositions of some major mafic flow units, Flin Flon-White Lake area

1	BEAR 2	HIDDEN 3	BURLEY 4	BAKERS 5	BIG ISLAND 6	CARLISLE 7	SOUTH MAIN 8	GRASSY 9	SCOTTY 10	TWO PORTAGE
SiO_2	53.08	49.98	53.67	52.70	52.65	52.02	51.60	49.84	51.43	47.43
TiO_2	0.47	0.61	0.62	0.39	0.41	0.58	0.83	1.07	1.48	2.12
Al_2O_3	15.43	16.32	14.72	15.32	14.80	15.14	14.09	14.74	14.21	13.08
Fe_2O_3	2.46	2.89	2.90	2.33	2.77	2.80	3.53	1.73	2.76	2.67
FeO	7.74	9.37	9.18	7.78	9.64	9.43	11.21	8.90	9.84	13.36
MnO	0.18	0.25	0.20	0.14	0.20	0.20	0.24	0.17	0.22	0.22
MgO	5.99	5.02	4.07	7.09	4.60	4.93	4.12	7.24	4.85	5.44
CaO	7.53	8.58	7.32	5.95	6.08	8.02	7.26	9.69	7.80	8.72
Na_2O	2.99	3.21	2.89	3.55	4.54	3.11	3.41	3.04	2.80	2.70
K_2O	0.90	0.42	0.45	0.76	0.49	0.50	0.56	0.15	0.69	0.52
P_2O_5	0.14	0.10	0.13	0.07	0.08	0.08	0.12	0.11	0.20	0.28
H_2O	3.15	2.97	3.05	3.56	2.70	3.02	2.85	2.90	3.39	3.04
S	0.03	0.01	0.01	0.01	0.01	0.01	0.02	0.01	0.06	0.18
CO_2	0.23	0.48	0.30	0.16	0.55	0.17	0.48	0.24	0.26	0.55
Other	0.10			0.11		0.03		0.03	0.08	0.08
Rb	10	3	3	8	1	5	10	0	9	3
Ba	336	219	221	353	164	227	329	30	232	192
Sr	184	177	161	159	145	141	107	136	205	171
Th	0.34	0.23	2.6				0.61	0.2	2.9	0.2
Nb	2	4	1	0	1	0	0	0	9	16
Hf	1.4	1.0	1.9				1.9	2.0	4.0	3.7
Zr	22	19	29	11	24	19	23	44	89	82
Y	17	15	17	7	12	17	20	25	36	33
Ni	28	5	5	33	9	5	13	57	12	55
Cr	94	74	56	176	57	47	57	247	37	70
n	9	12	6	4	2	3	2	3	6	5

1 Bear Lake basaltic andesite (unit 1) (analyses 1-9, Appendix)
2 Hidden Lake basalt (unit 2) (analyses 14-25, Appendix)
3 Burley Lake basaltic andesite (unit 3) (analyses 26-30, Appendix)
4 Basalts, Bakers Narrows block (analyses 78-81, Appendix)
5 Basalts, Big Island (analyses 85, 86, Appendix)
6 Basalts, Carlisle Lake (analyses 32-34, Appendix)
7 South Main basalt (unit 6) (analyses 57, 58, Appendix)
8 Basalts, Grassy Narrows zone (analyses 82-84, Appendix)
9 Scotty Lake basalt (unit 4) (analyses 35, 38, 44-46, 48, Appendix)
10 Two Portage Lake ferrobasalt (unit 5) (analyses 52-56, Appendix)

Table 9:
Average compositions of some major volcaniclastic and rhyolite units, Flin Flon-White Lake area

	LITTLE SPRUCE 1	VICK 2	WHITE 3	SOLODIUK 4	MINE 5	GRASSY 6
SiO_2	56.09	55.13	67.48	75.65	77.48	78.87
TiO_2	0.42	0.67	0.30	0.26	0.14	0.13
Al_2O_3	14.64	17.70	12.78	11.86	11.70	10.90
Fe_2O_3	2.93	2.70	2.59	0.27	0.08	0.19
FeO	8.31	5.24	5.43	1.24	0.66	1.03
MnO	0.19	0.15	0.11	0.02	0.03	0.02
MgO	4.23	2.78	1.52	0.53	0.01	0.44
CaO	5.82	6.14	2.86	0.55	1.01	0.43
Na_2O	1.58	3.66	2.44	2.76	5.80	4.49
K_2O	1.52	3.09	2.32	5.03	0.39	1.99
P_2O_5	0.29	0.36	0.16	0.10	0.01	0.03
H_2O	3.54	2.44	1.94	0.52	0.28	0.46
S	0.03	0.05	0	0.04	0.01	0.01
CO_2	0.69	0.12	0.41	0.44	0.70	0.47
Other	0.12	0.24	0.13	0.26		0.07
Rb	27	72	43	57	6	22
Ba	395	1054	610	1830	105	403
Sr	395	618	317	65	30	90
Th						
Nb						
Hf						
Zr	12	55	30	45	75	289
Y	14	26	21	14	39	74
Ni	2	15	<2	2	4	< 2
Cr	15	53	<4	3	26	< 4
n	4	8	3	1	1	3

1 Little Spruce Lake andesitic lapilli tuff (unit 24) (analyses 107-110, Appendix)
2 Vick Lake andesitic tuff (unit 25) (analyses 113, 114, 116-121, Appendix)
3 White Lake dacite tuff (unit 26) (analyses 122-124, Appendix)
4 Solodiuk Lake rhyolite (unit 13) (analysis 89, Appendix)
5 Mine rhyolite (unit 15) (analysis 91, Appendix)
6 Grassy Narrows rhyolite (unit 18) (analyses 95-97, Appendix)

classification developed to distinguish Archean ore-associated rhyolites cannot be extended to these Proterozoic rocks (see Syme, 1985 for similar results in the Proterozoic Lynn Lake belt).

TECTONIC SETTING

Volcanic rocks from different tectonic settings have distinct MORB-normalized trace element characteristics (e.g. Pearce, 1982; Ewart and Hawkesworth, 1987); these can be used to interpret the tectonic setting of volcanic rocks from regions where the original tectonic environment has been obscured by subsequent deformation (e.g. Weaver et al., 1982; Pharaoh and Pearce, 1984; Condie, 1986). These MORB-normalized trace element plots display in a different manner the same information as conventional "tectonic discriminant" diagrams (e.g. Pearce and Cann, 1973; Fig. 214); however, many more elements can be represented than is possible on binary or ternary "discriminant" diagrams and relationships between different groups of elements are readily determined.

Mid ocean ridge basalt (MORB)-normalized trace element data for representative Amisk Group basalts (Syme, 1988) reflect the three-fold subdivision established for these rocks (Fig. 215). Bear Lake and Hidden Lake basalts (typifying group 1 above) are enriched in large ion lithophile (LIL) elements (Rb, Ba, K, Th, Sr) and moderately to strongly depleted in high field strength (HFS) elements (P, Hf, Zr, Ti, Y), resulting in patterns very similar to an average island arc tholeiite (Fig. 215a). Decoupling of LIL and HFS elements is a common feature of subduction related magmas (Saunders et al., 1980; Gill, 1981; Tarney et al., 1981). LIL element enrichment is commonly attributed to transport of these elements to the fore-arc mantle wedge from the subducting slab during dehydration (eg. Saunders et al., 1980). HFS-element depletion is interpreted to result from either (a) derivation of arc magmas from a depleted lherzolite source (Ewart and Hawkesworth, 1987), or (b) partial melting under high $P_{(H_2O)}$ conditions in subduction zones, stabilizing HFS-element-bearing minor phases (such as sphene, ilmenite or rutile) in the source residuum and thereby depleting derived melts in these elements (Saunders et al., 1980). Relative abun-

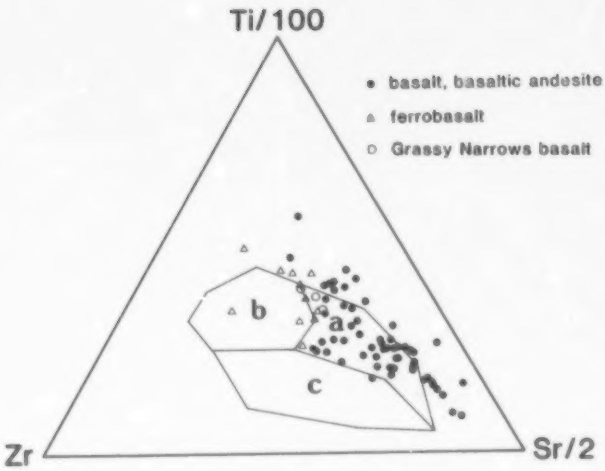

Figure 214: *Tectonic discrimination diagram using Ti, Zr and Sr (Pearce and Cann, 1973). Low — K tholeiites (island arc tholeiites) plot in field "a", ocean-floor basalts plot in field "b" and calc-alkali basalts plot in field "c". The Amisk Group clearly comprises a suite of arc tholeiites. Subdivision of Amisk Group basalts is discussed in text.*

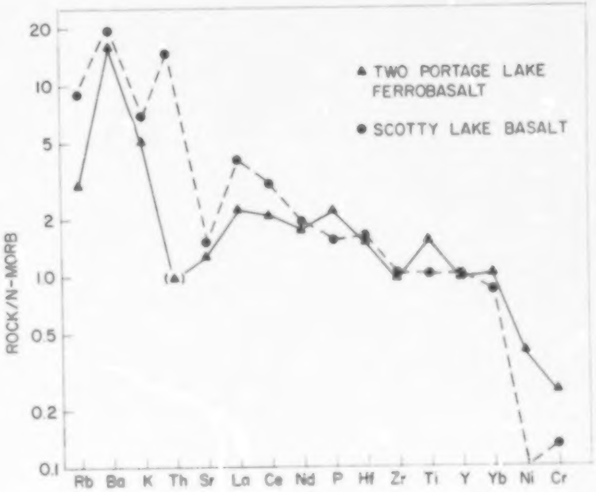

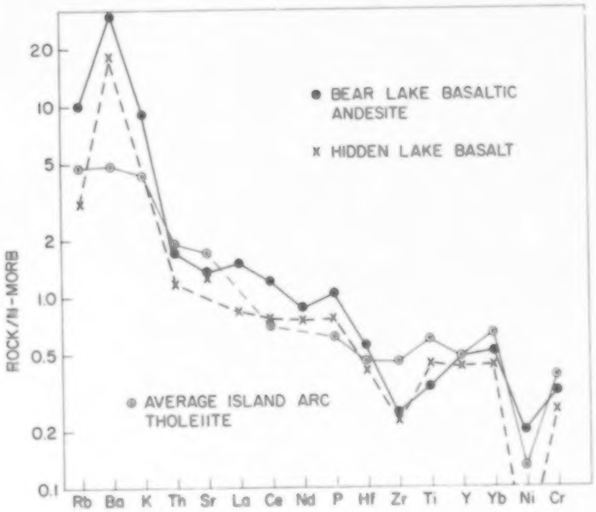

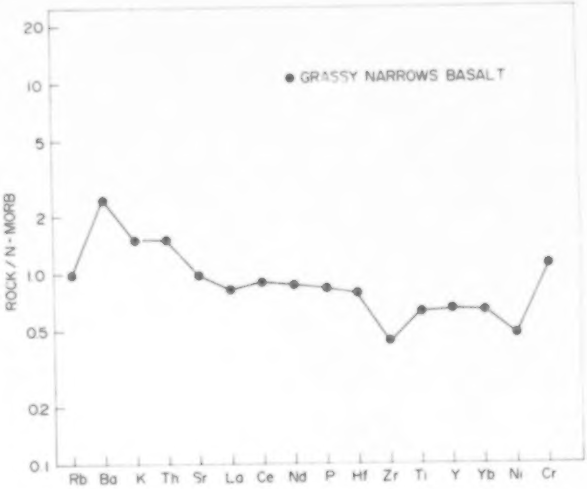

Figure 215: *MORB-normalized trace element patterns for representative Amisk Group rocks (Syme, 1989): (a) average Bear Lake basaltic andesite (unit 1) and Hidden Lake basalt (unit 2) with average island arc tholeiite (Pearce, 1982) for comparison, (b) average Scotty Lake basalt (unit 4) and Two Portage Lake ferrobasalt (unit 5), (c) average Grassy Narrows basalt (unit 7). N-MORB normalizing values are those of Saunders and Tarney (1984).*

dances of LIL and HFS elements in most Amisk Group basalts, typified by the Bear Lake and Hidden lake suites, constitute strong evidence that these Proterozoic volcanic rocks were generated by subduction-related processes similar to those that were operative in Cenozoic island arcs.

Two Portage Lake and Scotty Lake basalts (typifying group 2 above) have high incompatible element and REE abundances, and low Ni and Cr (Fig. 215b), identifying these rocks as fractionated basalts. Intercalation of the Two Portage ferrobasalts with rhyolite crystal tuff also suggests this bimodal suite was derived from a chemically zoned, fractionated magma chamber.

Grassy Narrows basalt (representing group 3 above) has a much flatter MORB-normalized pattern than the arc-type basalts (group 1), and is characterized by low Rb, Ba, K and Th contents and less depletion in HFS elements. They are intermediate between group 1 basalts and another group of rocks in the Flin Flon area (Athapapuskow basalt; Syme, 1989) interpreted to have been emplaced in a backarc basin environment.

The two major Proterozoic greenstone belts in Manitoba are the Flin Flon and Lynn Lake belts (Fig. 3). The Flin Flon belt appears to represent a less evolved arc compared to that at Lynn Lake (Syme, 1989). Both the Amisk Group (at Flin Flon) and Wasekwan Group (at Lynn Lake) plot within the field of arc lavas on a Ti-Zr plot (Fig. 216) but there is very little overlap between the two: Amisk Group rocks generally contain slightly less Ti and much less Zr than Wasekwan Group counterparts. Most Amisk Group basalts (apart from obviously fractionated units) contain very low HFS-element and REE abundances. These basalts are similar to the "low HFS-element" group of island arc tholeiites which erupt at an early stage in modern arc development, occur only in arcs associated with rapid subduction of old lithosphere, and are often accompanied by the formation of backarc basins (Gill, 1987).

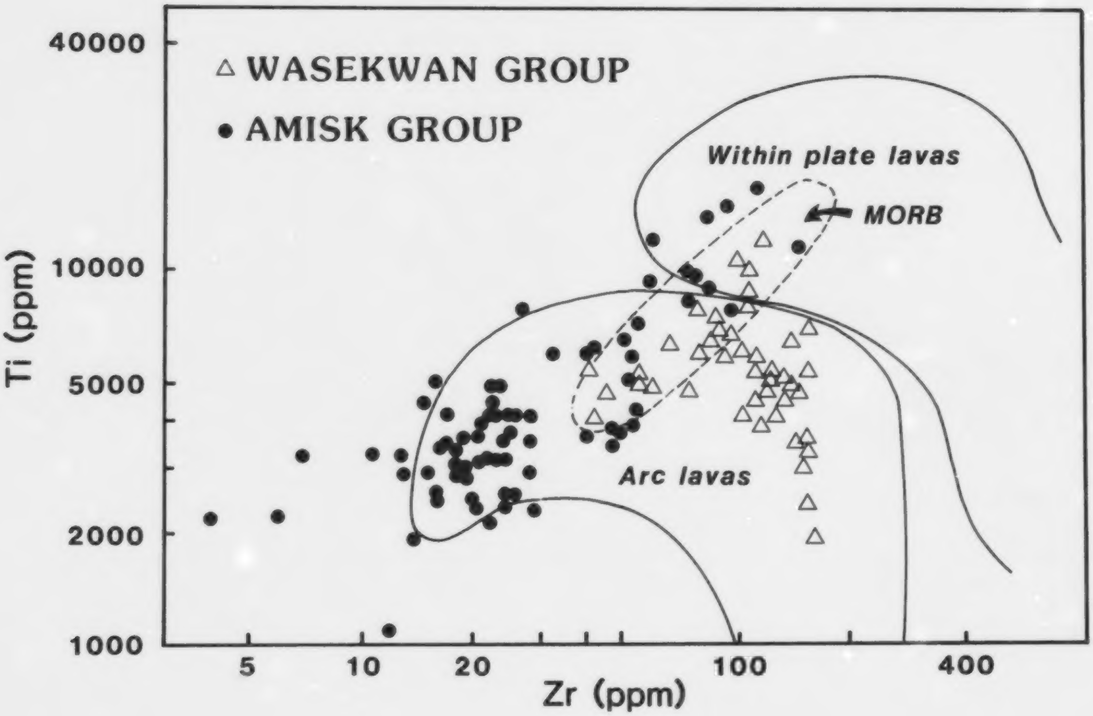

Figure 216: Ti vs. Zr, Amisk Group (Flin Flon metavolcanic belt) and Wasekwan Group (Lynn Lake metavolcanic belt) (Syme, 1989). Fields of arc lavas, within-plate lavas and MORB from Pearce et al. (1981). Amisk Group rocks contain significantly less Zr than Wasekwan Group.

PRE-MISSI INTRUSIVE ROCKS, INTRUSIONS OF UNKNOWN AGE

INTRODUCTION

Amisk Group rocks in the Flin Flon-White Lake area are cut by a wide variety of intrusive rocks that are not present in the unconformably overlying Missi Group. Some intrusions are syn-Amisk Group (e.g. White Lake Sill, synvolcanic mafic dykes associated with Bear Lake basaltic andesite and Scotty Lake basalt), some were emplaced in folded Amisk rocks and thus postdate volcanism (e.g. Hook Lake gabbronorite), and others occur as isolated intrusions whose relative age to Amisk volcanism and the Missi Group are unknown. Crosscutting relationships are not common; consequently it is not possible to determine the chronological order of all intrusions. Detailed descriptions of major intrusive units follow. Relative age relationships are discussed at the end of the chapter.

WHITE LAKE SILL AND RELATED INTRUSIONS (UNIT 39)

A suite of distinctive gabbro sills (unit 39) occupies a 760 m thick stratigraphic interval in the Bear Lake Block, east of White Lake (Map GR87-1-1). These sills are iron-rich and display a sequence of readily mappable zones related to iron enrichment during fractionation. Portions of the sills are petrographically similar to the directly overlying Two Portage Lake ferrobasalt (unit 5), and the sills and basalt flows are geochemically indistinguishable (Appendix; Fig. 217, 218 and 219). Accordingly this intrusive suite is considered to be synvolcanic. Some undifferentiated gabbro sills in the same 760 m thick stratigraphic interval also have petrographic similarities with the differentiated sills; these are included with unit 42 gabbro and diorite. Only zoned, differentiated intrusions are included in unit 39.

Five bodies of White Lake-type gabbro have been mapped east and northeast of White Lake. The largest sill (White Lake Sill, Fig. 220), for which the suite has been named, is exposed for 8.8 km between the southern boundary of the map area and Solodiuk Lake. It has a maximum thickness of 410 m in the south, tapering to 60 m at Solodiuk Lake. The second largest sill (Johnson Lake Sill, Fig. 220) outcrops adjacent to the road between White Lake Mine and old Highway 10. It is approximately 5 km long, with a maximum thickness of 170 m. The remaining three sills in the suite are small and poorly exposed.

White Lake Sill

The White Lake Sill contains 4 zones; in ascending order they are:

1) brown weathering basal gabbro;
2) dark green weathering ferrogabbro;
3) ferrodiorite, quartz ferrodiorite, minor granophyric tonalite;
4) brown weathering, pyroxene-phyric gabbro top.

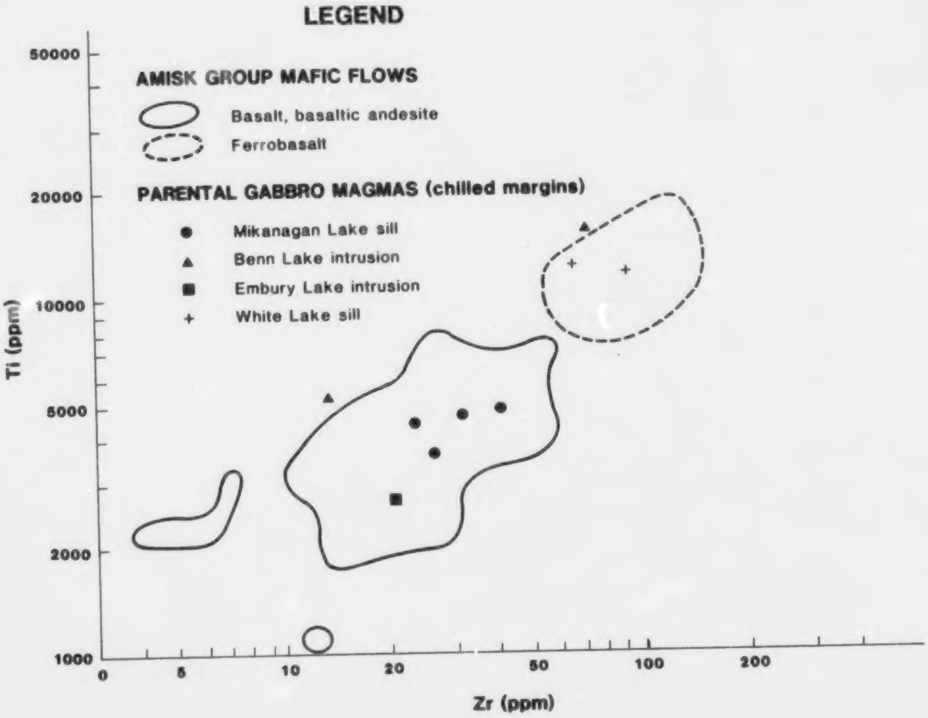

Figure 217: Ti vs. Zr comparing parental magmas of major gabbro intrusions with fields of Amisk Group basalt/basaltic andesite and ferrobasalt.

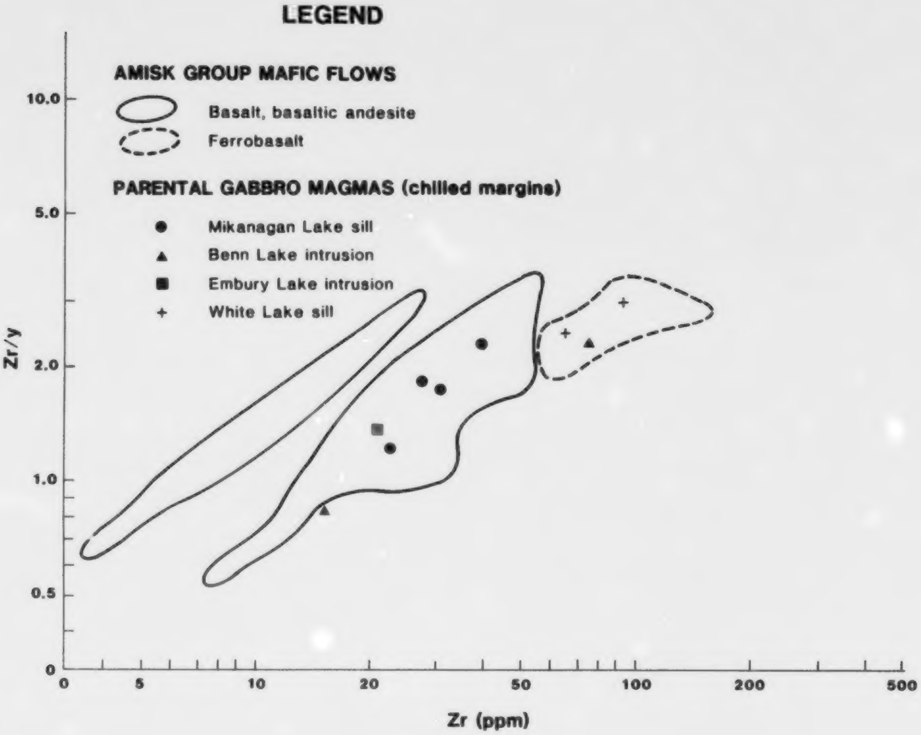

Figure 218: Zr/Y vs. Zr comparing parental magmas of major gabbro intrusions with fields of Amisk Group basalt/basaltic andesite and ferrobasalt.

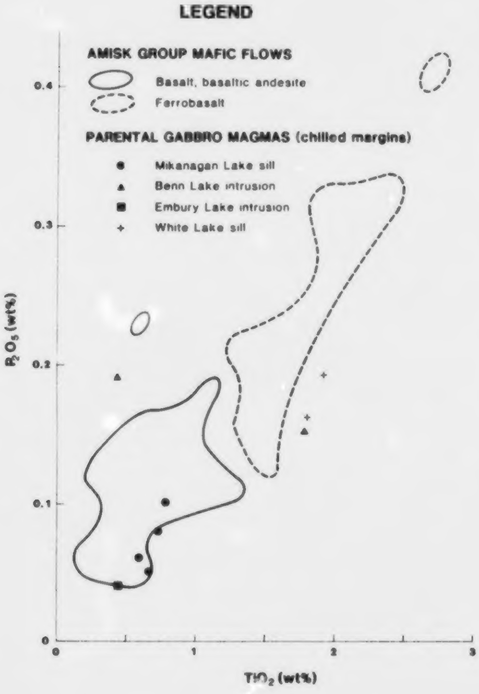

Figure 219: P_2O_5 vs TiO_2 comparing parental magmas of major gabbro intrusions with fields of Amisk Group basalt/basaltic andesite and ferrobasalt.

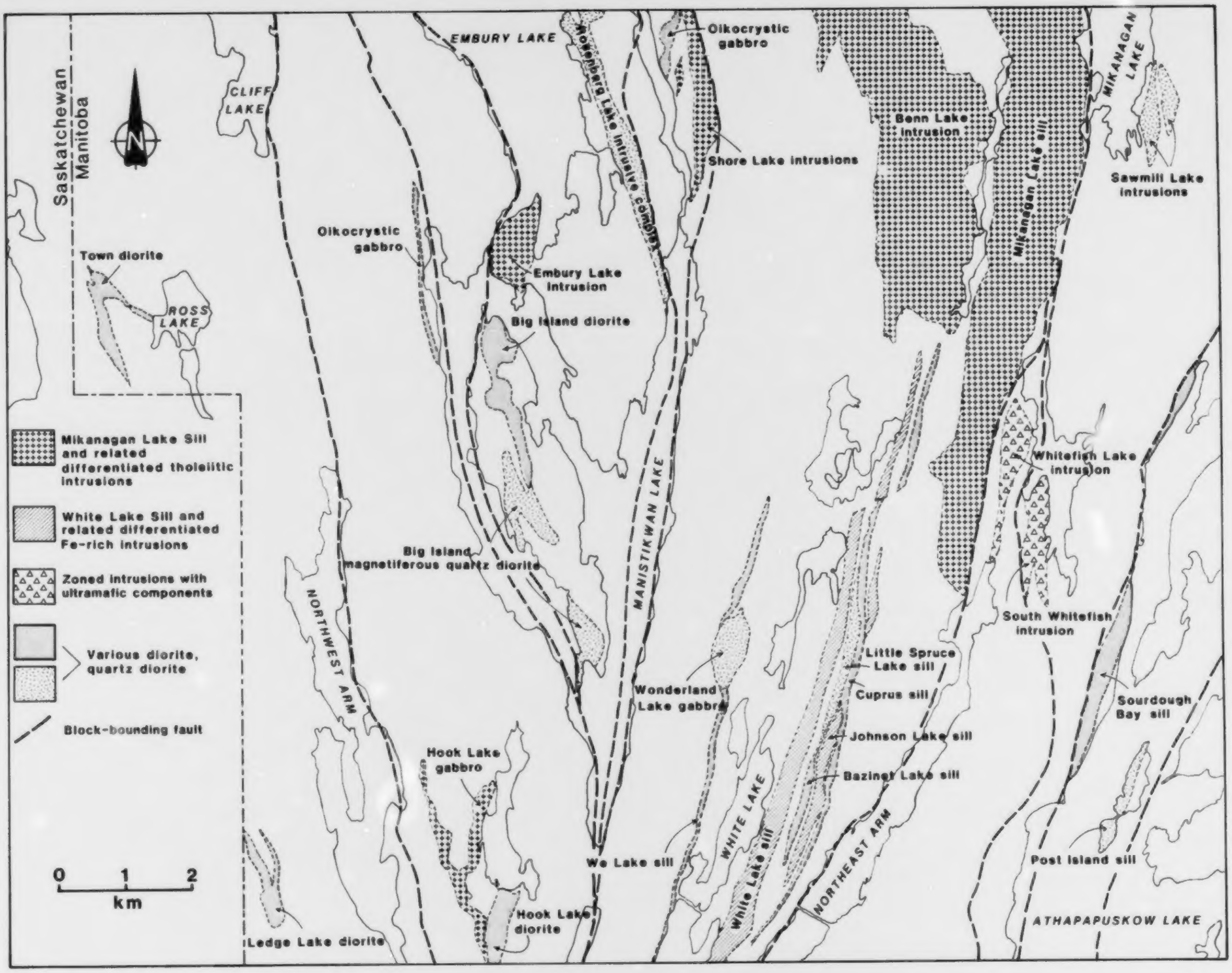
EMBURY LAKE
Rosenberg Lake intrusive complex
Oikocrystic gabbro
Saskatchewan
Manitoba
N
CLIFF LAKE
Benn Lake intrusion
Mikanagan Lake sill
MIKANAGAN LAKE
Sawmill Lake intrusions
Shore Lake intrusions
Oikocrystic gabbro
Embury Lake intrusion
Town diorite
ROSS LAKE
Big Island diorite
Mikanagan Lake Sill and related differentiated tholeiitic intrusions
White Lake Sill and related differentiated Fe-rich intrusions
Zoned intrusions with ultramafic components
Various diorite, quartz diorite
Block-bounding fault
Whitefish Lake intrusion
MANISTIKWAN LAKE
Big Island magnetiferous quartz diorite
NORTHWEST ARM
South Whitefish intrusion
Little Spruce Lake sill
Cuprus sill
Wonderland Lake gabbro
Sourdough Bay sill
Johnson Lake sill
Hook Lake gabbro
Bazinet Lake sill
WHITE LAKE
NORTHEAST ARM
0 1 2
km
We Lake sill
White Lake sill
Post Island sill
Hook Lake diorite
Ledge Lake diorite
ATHAPAPUSKOW LAKE

Figure 220: Location of major mafic intrusive bodies, Flin Flon area.

Brown gabbro (unit 39a)

The brown gabbro zone of the White Lake Sill ranges in thickness from 12 and 122 m. Variation in thickness appears to be independent of total sill thickness. The base of the brown gabbro contains a narrow chilled zone, and a fine grained zone up to 4 m thick. The main part of the unit is a massive, relatively homogeneous, medium grained (1 — 2 mm) gabbro with hypidiomorphic granular to subophitic texture. The top of the brown gabbro zone characteristically exhibits moderately developed igneous layering in a zone up to 25 m thick. The contact with overlying green gabbro is sharp, but locally gradational over 2 m.

The gabbro is composed of epidote and chlorite after plagioclase; pale green actinolite, chlorite and rare brown hornblende after pyroxene; magnetite and leucoxene after Fe-Ti oxides; and accessory quartz and apatite. Primary plagioclase (up to 1 mm) forms lath-shaped crystals interstitial to, or partially enclosed by, the original anhedral to euhedral pyroxene. Fe-Ti oxides (up to 2.5 mm) form euhedral, equant, commonly skeletal crystals. Primary modes of gabbro in this zone are estimated to have been 35 — 50% plagioclase, 40 — 60% pyroxene, 2 — 5% Fe-Ti oxides, and trace quartz.

Igneous layering at the top of the brown gabbro zone is wispy, discontinuous to semi-continuous, with individual layers 5 — 20 cm thick. Bases of layers are brown or mottled brown and green, and grade upward to green weathering gabbro (Fig. 221). In general layering is parallel to the contact with overlying green gabbro but varies somewhat in attitude and dip even within single exposures. Trough-like layering was noted at one locality.

Green ferrogabbro (unit 39b)

Dark green to dark greenish black and rusty red-brown, Fe-rich gabbro forms a zone 30—180 m thick in the centre of the White Lake Sill. As in the brown gabbro, the thickness of this zone is not related to total thickness of the sill. This zone does, however, pinch out south of Solodiuk Lake. At the base, green ferrogabbro is commonly massive but locally displays igneous layering similar to the top of the brown gabbro. At one locality xenoliths of brown gabbro occur within 5 m of the contact; the xenoliths are thin wisps or partially digested blocks up to about 3 m in length, with long axes parallel to the brown gabbro-green ferrogabbro contact.

Green ferrogabbro is composed of pseudomorphs after pyroxene (40 — 50%), plagioclase (40 — 50%), Fe-Ti oxides (10%), and less than 1% each of quartz and apatite. Pyroxenes are replaced by light green and dark green actinolitic amphibole and minor chlorite. They are anhedral to euhedral, equant, 0.5 — 1.5 mm across, and in some instances partially enclose plagioclase laths. Plagioclase laths and stubby tablets (to 1.5 mm) are recrystallized and largely replaced by fine grained chlorite and epidote. Fe-Ti oxides (to 3 mm) are anhedral to euhedral, equant, commonly skeletal, and replaced by various proportions of magnetite, leucoxene and sphene. In least-deformed crystals the leucoxene alteration products occur along octahedral parting planes in the primary crystal. Golden brown, strongly pleochroic stilpnomelane overprints plagioclase and amphibole and is selectively concentrated near fractures; its abundance ranges from 2 — 25%. Green ferrogabbros with abundant stilpnomelane have a characteristic dark brown almost resinous fresh surface colour.

Ferrodiorite, quartz ferrodiorite, tonalite (unit 39c)

The upper zone (0 — 150 m thick) in the White Lake Sill varies considerably in colour, texture and composition. Rocks weather dark green, brown, and buff to light grey, reflecting varying quartz and plagioclase content and degree of stilpnomelane overprint. This zone appears to be a product of virtually contemporaneous crystallization, upward from the green ferrogabbro and downward from the roof of the intrusion, such that the most siliceous differentiates occur in a discontinuous layer in its upper central portion.

The contact with the underlying green ferrogabbro is not exposed and may be gradational. The zone is recognized in the field by an abrupt increase in quartz and plagioclase content. From the base to the upper central part of the zone there is a general increase in plagioclase, quartz, micrographic quartz-plagioclase intergrowth, and a parallel decrease in total mafics and apatite. Modal abundance of apatite peaks in the lower part of the zone at about 8%. The upper part of the zone is a condensed, inverted version of the lower portion. The top of the ferrodiorite zone is in contact with either a narrow (1 m) chilled margin or a thin unit of pyroxene-phyric brown gabbro (unit 39d).

Ferrodiorite and quartz ferrodiorite contain quartz (5 — 25%), micrographic quartz-plagioclase intergrowths (2 — 40%), pseudomorphs after plagioclase (30 — 60%), primary mafic minerals (5 — 40%) and Fe-Ti oxides (5 — 10%), and apatite (1 — 8%). Plagioclase laths and tablets (to 3 mm) are randomly oriented, locally interlocking, and extensively replaced by chlorite and epidote. Quartz grains are anhedral, equant, interstitial to plagioclase and commonly surrounded by micrographic quartz-plagioclase intergrowths. Primary mafic minerals are replaced by chlorite, amphibole and stilpnomelane; they vary from interstitial to elongate prismatic pseudomorphs.

Pyroxene-phyric gabbro (unit 39d)

Brown weathering, pyroxene-phyric gabbro locally forms the topmost unit in the White Lake Sill. It is in abrupt contact with the ferrodiorite zone and has a chilled contact against host volcanic rocks. The zone is up to 15 m thick and is present as a mappable unit in the southern half of the sill.

Johnson Lake Sill

The zoned gabbro-ferrogabbro sill exposed for 5 km between Johnson Lake and Highway 10 is the only other major zoned mafic sill in this suite. It has a maximum thickness of 170 m, and has a brown gabbro base (maximum 76 m) and top (maximum 60 m), and a green ferrogabbro-ferrodiorite core (maximum 30 m).

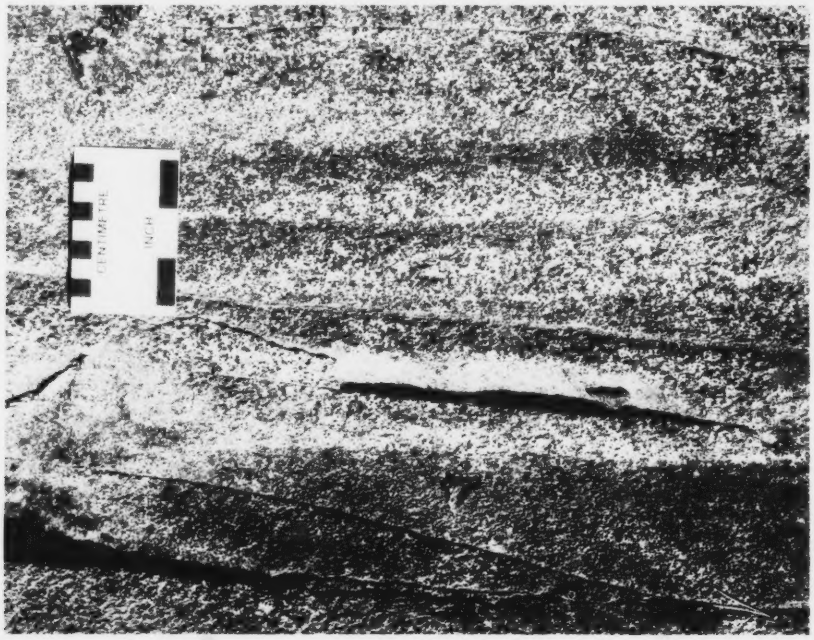

Figure 221: Igneous layering in gabbro (unit 39a), White Lake Sill at White Lake. At this locality approximately 21 m of thinly layered gabbro occurs at the top of the gabbro zone, overlain by ferrogabbro (unit 39b). Note that individual layers have a polarity opposite to "normal" modally graded layers: the mafic portions (dark) occur at the tops. Chemical zonation clearly indicates that the sill tops to the east (top in this photograph).

Brown gabbro (unit 39a)

The basal and upper brown weathering gabbros are identical, massive, homogeneous and fine grained (0.5 — 1 mm). The lower gabbro has a pyroxene-phyric zone 10 m thick adjacent to the green ferrogabbro. Unlike the White Lake Sill, this intrusion does not exhibit layering in the brown gabbro at its contact with green ferrogabbro.

The brown gabbro is weakly foliated and composed of 50 — 55% pale green amphibole after pyroxene, 40 — 45% albite, chlorite and epidote or zoisite after plagioclase, 5 — 7% leucoxene and magnetite after Fe-Ti oxides and up to 2% interstitial quartz. Primary crystal shapes are not well preserved due to recrystallization and imposition of a foliation. Where best preserved the texture is hypidiomorphic equigranular with stubby subhedral twinned plagioclase and equant pyroxene. Fe-Ti oxides are irregular, equant grains.

The pyroxene-phyric top of the lower gabbro zone is characterized by 25 — 35% 1 — 3 mm clinopyroxene phenocrysts that are almost completely replaced by green amphibole. The area between pyroxenes is a fine grained mixture of albite, epidote and chlorite, presumably after plagioclase. It contains 3% magnetite and leucoxene after Fe-Ti oxides.

Green ferrogabbro, ferrodiorite (unit 39b)

This unit weathers dark brown to black and is dull brown-green on fresh surface. It is foliated, thus primary texture is not preserved. The gabbro is massive, fine grained (1 mm), unlayered and has sharp upper and lower contacts. It is composed of 35 — 45% plagioclase, 45 — 55% pyroxene, and 10 — 12% Fe-Ti oxides. These primary minerals are replaced by a suite of metamorphic minerals identical to those in the White Lake Sill. Stilpnomelane is present, locally forming up to 20% of the rock; it generally increases in abundance to the east (top) across this unit.

Geochemistry

The White Lake Sill is a tholeiitic intrusion which fractionated to extremely iron-rich compositions. Analyses of chilled samples from the base of the intrusion contain approximately 14% FeO^*, indicating that the initial magma was iron-rich. These chilled samples have major-element concentrations similar to the Two Portage ferrobasalt (Table 10).

Table 10:
Comparison of compositions in the White Lake Sill (unit 39) and an average of 5 analyses of Two Portage Lake ferrobasalt (unit 5)

	WHITE LAKE SILL						
	GABBRO		FERRO-GABBRO	FERRO-DIORITE	CHILLED MARGIN		AVERAGE TWO PORTAGE LAKE FERROBASALT
	1229-C1	1241-C1	1230-C1	1232-C1	254-8	1312-1	
SiO_2	45.94	46.38	46.92	47.10	47.3	47.7	47.43
Al_2O_3	14.42	15.19	12.03	11.10	13.4	13.2	13.08
Fe_2O_3	3.83	2.72	8.90	5.58	2.9	4.3	2.67
FeO	10.11	11.08	11.06	12.59	11.4	10.1	13.36
CaO	10.74	8.14	7.26	6.78	8.8	8.6	8.72
MgO	6.63	7.17	4.76	3.41	6.6	6.9	5.44
Na_2O	2.39	3.03	4.05	2.81	1.9	2.3	2.70
K_2O	0.16	0.32	0.42	0.33	0.4	0.8	0.52
TiO_2	1.86	1.55	2.91	2.64	1.80	1.92	2.12
P_2O_5	0.17	0.14	0.22	0.30	0.16	0.19	0.28
MnO	0.18	0.21	0.25	0.25	0.19	0.15	0.22
H_2O	3.42	4.08	3.18	3.18	3.22	3.06	3.04
S	0.05	0.00	0.00	0.01	0.1	0.01	0.18
CO_2	0.09	0.67	0.09	4.67	0.9	0.22	0.55
Other	0.07	0.07	0.08	0.06	0.13	0.12	0.08
Less 0 = S	0.02				0.04		0.09
Total	100.04	100.75	102.13	100.81	99.16	99.64	100.30
Cu	90	82	90	15			85
Ni	35	37	13	0			85
Pb							<3
Zn	40	85	151	100			90
Cr	108	55	73	36			70
Rb	0	0	0	0			7
Sr	198	161	191	165			171
Ba	0	36	0	0			192
Zr	70	81	123	143	66	91	82
Y	25	25	32	31	27	31	33
Nb	0	5	10	0			
FeO^*	13.56	13.52	19.07	17.61	14.01	13.97	15.76
FeO^*/MgO	2.05	1.89	4.01	5.16	2.12	2.02	2.90
Zr/Y	2.80	3.24	3.84	4.61	2.44	2.94	2.48

During fractionation of the sill, SiO_2 remained relatively unchanged (note however that the most siliceous rocks were not analyzed), whereas FeO*, TiO_2, P_2O_5, Zr, Y and Zn increased and Al_2O_3, MgO, Ca and Ni decreased. Most of the Two Portage ferrobasalts analyzed are very similar to the White Lake Sill ferrogabbro zone (Fig. 47, Table 10).

Three lines of evidence suggest that the Two Portage Lake ferrobasalts and the White Lake Sill are comagmatic:

1) the close compositional similarity outlined above;
2) this type of fractionated, iron-rich sill is present only in proximity to the base of the Two Portage ferrobasalt;
3) these intrusions never occur stratigraphically above the Two Portage Lake ferrobasalt.

WHITEFISH LAKE MAFIC INTRUSIONS (UNIT 40)

Two mafic intrusions south and west of Whitefish Lake are characterized by an ultramafic component. Rock types in these intrusions (Fig. 220, Map GR87-1-1) include peridotite (wehrlite), pyroxenite, gabbro, and quartz diorite/tonalite. The intrusions are dissected and truncated by faults and are intruded by unrelated gabbro and pyroxenite dykes related to the faulting. Inasmuch as rock types in the two intrusions are slightly different, they are described separately below.

One Portage Lake Intrusion

The One Portage Lake Intrusion is exposed for 2400 m north of Northeast Arm (Schist Lake). It is a maximum of 400 m thick and includes a comagmatic differentiated sequence of wehrlite, pyroxenite, gabbro and quartz diorite (Fig. 222). The intrusion lies within a structurally complex zone and is cut by faults subparallel to lithologic contacts; consequently a complete, intact stratigraphic section through the intrusion is not present. Well exposed contacts in one fault slice, east of One Portage Lake, display gradational relationships between wehrlite (in the west), pyroxenite, and gabbro (in the east), indicating that the intrusion tops to the east. Just north of Schist Lake, however, the pyroxenite is underlain by gabbro, which suggests that the ultramafic components do not lie at the base of the intrusion.

Wehrlite (unit 40a)

A 70 m thick unit of wehrlite occurs at the faulted(?) base of the intrusion east of One Portage Lake. This massive, unfoliated rock weathers rusty brown and is greenish black on fresh surface. Local cross-fibre asbestos veinlets up to 1 cm wide trend 305° and dip 80° northeast. Equant, oval olivine (1—4 mm), pseudomorphed by serpentine, composes 50% of the rock. The serpentine pseudomorphs are crossed by abundant irregular to rectilinear, magnetite-filled fractures, and contain euhedral magnetite inclusions (0.2 mm) probably after primary Fe-Ti oxides. Clinopyroxene crystals (1 — 4 mm) composing 47% of the rock are anhedral, interlocking, and partially enclose serpentinized olivines. Clinopyroxene is irregularly altered to tremolite + magnetite; this recrystallization is associated with closely spaced intersecting fractures. Pale green, anhedral hornblende (to 1 mm, 2%) is a late magmatic phase that occurs interstitial to olivine, and as epitaxic overgrowths on clinopyroxene.

Pyroxenite (unit 40b)

Pyroxenite forms a unit up to 120 m thick that overlies wehrlite east of One Portage Lake, and apparently overlies gabbro at the north end of Northeast Arm. It is unfoliated, coarse grained (4 — 10 mm, locally 20 mm), weathers reddish brown and is medium grey to dark green on fresh surfaces. The contact with wehrlite is gradational over several metres, through decrease in olivine content. At the north end of Northeast Arm, pyroxenite and olivine pyroxenite are interlayered, with layering defined by grain size and olivine content (up to about 20% serpentine in some pyroxenites). The contact with overlying gabbro east of One Portage Lake is gradational over about 6 m. This gradational contact zone is marked by (1) intrusive relationships, with unchilled gabbro dykes in pyroxenite and pyroxenite xenoliths in gabbro, and (2) an eastward increase in plagioclase content.

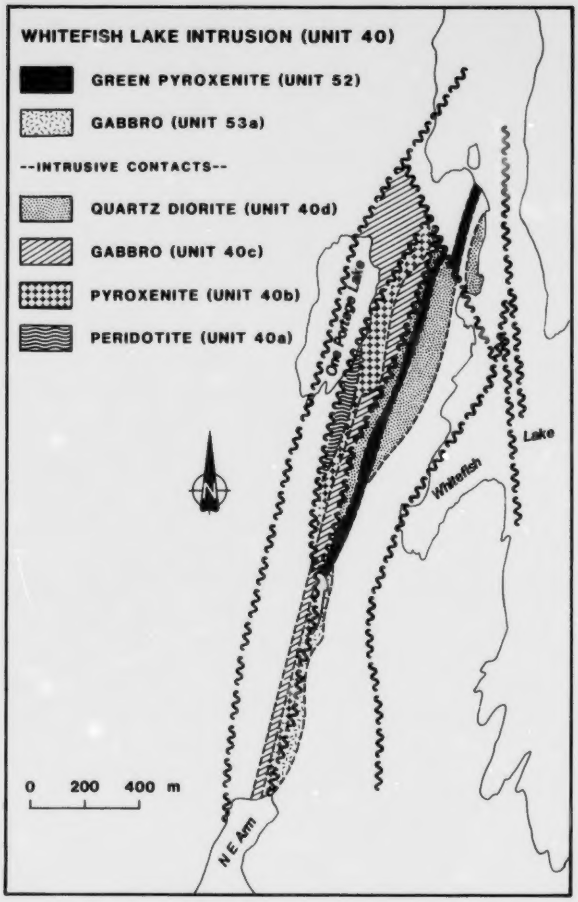

Figure 222: Disposition of lithologic units in the Whitefish Lake Intrusion (unit 40). Note the west to east ultramafic to mafic zonation in the portion of the intrusion contained in the central fault slice.

North of Northeast Arm, pyroxenite is in fault contact with gabbro (unit 53a). The fault is marked by a 1 — 7 m wide zone in which the pyroxenite contains a strong shear foliation that is locally chevron folded. The gabbro adjacent to sheared pyroxenite is undeformed, and is texturally different from gabbros in the main One Portage Lake Intrusion. This fault is probably an extension of the one east of One Portage Lake that separates gabbro and quartz diorite.

Least-altered pyroxenites comprise an interlocking mosaic of anhedral-subhedral clinopyroxene crystals. Late magmatic or deuteric alteration of clinopyroxene produced pleochroic green to greenish brown hornblende (1) in patches throughout clinopyroxene crystals, (2) as extensive replacement and overgrowth of clinopyroxene crystal margins, resulting in relicts of pyroxene lying within large plates of amphibole, and (3) as anhedral grains interstitial to clinopyroxene. Both the primary clinopyroxene and the late magmatic amphibole are partially replaced by colourless tremolite, which occurs as patches, single-crystal pseudomorphs, bladed multi-crystal pseudomorphs and epitaxic overgrowths. More completely altered pyroxenites are composed entirely of single crystal tremolite or multi-crystal bladed tremolite-chlorite pseudomorphs after pyroxene.

Gabbro (unit 40c)

Gabbro occurs both east and west of the ultramafic portion of the intrusion, suggesting that the ultramafic rocks form a subunit in a larger, dominantly gabbroic sequence. The gabbro is medium grained (2 — 5 mm), equigranular, and weathers white and green to rusty brown and green. Fresh surfaces are mottled light grey and dark green.

East of One Portage Lake the contact with pyroxenite is gradational over about 6 m, with increase in plagioclase content and decrease in mafic content. The gabbro contains abundant partly assimilated xenoliths of reddish brown pyroxenite; xenoliths (up to 2 m) are sharply angular to nebulous, and range down to 1 — 5 cm pyroxenitic clots. Similar contact relationships also occur north of Northeast Arm, where gabbro occurs to the *west* of pyroxenite.

The contact between gabbro and quartz diorite is a 0.5 — 2 m wide shear zone that locally contains quartz veins. This fault is probably an extension of that separating pyroxenite from unit 53a gabbro at the north end of Northeast Arm.

Gabbro is intruded by a 10 m wide green pyroxenite dyke (unit 52), and locally contains gabbro pegmatite veins (a few centimetres wide) and pods (to 0.5 x 1 m).

Textures in the gabbro are hypidiomorphic equigranular, similar to those in unit 41 Mikanagan Lake sill and Hook Lake Gabbro. The texture is considerably coarser than most other unit 42 gabbro/diorite bodies in the map area. Plagioclase (2 — 4 mm) occurs as stubby laths and equant subhedral crystals; it is pseudomorphed by semi-opaque masses of brown fine grained epidote with minor chlorite-filled fractures. Clinopyroxene (1 — 6 mm) is subhedral, equant, twinned and commonly contains a prominent malacolite parting. Late magmatic, pleochroic green to brown hornblende replaces clinopyroxene rims and occurs as patches within some clinopyroxene crystals. It also occurs as interstitial anhedral grains and large (to 4 mm) subophitic crystals. Both clinopyroxene and hornblende are variably replaced by bladed tremolite and colourless chlorite. Locally leucoxene, after primary opaque oxides (to 0.4 mm), occurs enclosed in hornblende.

Quartz diorite (unit 40d)

Quartz diorite occurs as a lensoid body up to 135 m thick, on the east side of the One Portage Lake Intrusion. As previously indicated, quartz diorite is in fault contact with the gabbroic phase of the intrusion. This suggests that either the quartz diorite is unrelated to the mafic portion of the intrusion or an unknown thickness of a transitional lithology is missing.

Quartz diorite weathers light buff to buff-white or rusty buff and is medium grey and white on fresh surfaces. It locally contains coarse grained reddish brown pyroxenite xenoliths (unit 40b) to 30 cm across, and is intruded by a large dyke of green pyroxenite (unit 52), with which it has a sharp, irregular contact.

Quartz (1 — 4 mm) composes 30% of the rock; it is anhedral, equant, strongly strained, and interstitial to plagioclase and the mafic phase. Plagioclase (1 — 2 mm, 40%) occurs as stubby lath-shaped crystals almost completely replaced by fine grained brown epidote, sericite, and chlorite. Primary pyroxene or amphibole (to 2 mm, 30%) is completely replaced by pale green chlorite and epidote. Least-deformed pseudomorphs have a prismatic form.

South Whitefish Lake Intrusion

The South Whitefish Lake Intrusion is a north-trending pyroxenite-gabbro body 2 km long and 90 — 120 m wide. It outcrops in a small, fault-bounded tectonic slice, and is truncated to the north, south and east by faults. It is crosscut by a younger, unrelated, 180 m wide north-northwest-trending dyke of tonalite and leucotonalite (unit 42h).

Pyroxenite occurs on the east side of the intrusion, and ranges from zero to 40 m thick. The pyroxenite is foliated, dull green to brown weathering, medium green on fresh surfaces, and medium to coarse grained (1 — 5 mm). It is composed of a mixture of secondary green amphibole, pale green tremolite and colourless chlorite after primary pyroxene, with scattered rare plagioclase crystals and up to 2%, 0.2 — 0.4 mm crystals of Fe-Ti oxide. Although the pyroxene is almost completely altered to secondary mineral assemblages, two different grain morphologies with slightly different secondary assemblages are present. One comprises large grains selectively replaced by tremolite and pale green chlorite and the other occurs as smaller, twinned, euhedral crystals generally replaced by green amphibole. The large grains locally contain relict orthopyroxene cores and the smaller grains have the twinning and morphology of clinopyroxene.

A subophitic gabbro and quartz diorite forms the western 30 — 40 m of the intrusion. It is younger than the pyroxenite phase as it locally contains small xenoliths of the pyroxenite. The gabbro weathers buff-green to buff-brown and is a mottled green and white on fresh surfaces. It is composed of 30 — 40% stubby plagioclase laths (0.5 — 2 mm) replaced by epidote, 50 — 70% pyroxene (0.5 — 2 mm) replaced by actinolite, trace to 10% quartz and 2 — 3% Fe-Ti oxide (0.2 — 0.5 mm).

The South Whitefish Lake Intrusion is different from, and not necessarily related to, the One Portage Lake Intrusion. Both have similar ultramafic phases but the less mafic components are dissimilar. The South Whitefish intrusion contains no tonalite and its gabbro and quartz diorite phase is finer grained and texturally different than the gabbro of the One Portage Lake body.

MIKANAGAN LAKE SILL AND RELATED INTRUSIONS (UNIT 41)

The Flin Flon-White Lake area contains several major differentiated gabbroic intrusions which, despite differences in detail, share a number of important characteristics. These intrusions (Fig. 220) are all medium- to coarse-grained and have prominent compositional zoning. They display strong Fe-enrichment and are clearly tholeiitic. The intrusions are the largest mafic bodies in the area, with the largest, the Mikanagan Lake Sill, 1.2 km thick and over 15 km long. Similar large, compositionally zoned tholeiitic sills are prominent throughout the entire Flin Flon metavolcanic belt (e.g. Josland Lake Gabbro at File Lake [Bailes, 1980]). This suite of intrusions, assuming they are of similar age, collectively represents a major magmatic episode in the development of the belt.

The precise age of the intrusions is not known. In the Flin Flon area none of the intrusions cut the Missi Group and for this reason they are interpreted to be pre-Missi; however, no clasts of Mikanagan-type gabbroic rocks were observed in Missi Group conglomerates. Several features indicate that the intrusions could be synchronous with Amisk volcanism: (1) the parental magmas (represented by chilled margins) are virtually identical in composition to Amisk basalts and basaltic andesites (see below), (2) high level apparently synvolcanic dykes cut the Hook Lake Intrusion, and (3) some coarse grained gabbroic clasts occur in an Amisk debris flow east of Schist Lake.

Individually, the intrusions differ in form (sills to plug-like bodies), zoning (e.g. not all contain a siliceous differentiate), and parental magma composition.

Layered mafic intrusions are commonly hosts for Ni, Cr and Pt-group metal deposits. However, none of the sills in the Flin Flon area have an ultramafic component, nor are they rhythmically layered. Consequently the intrusions are not likely to contain these types of deposits. Minor disseminated chalcopyrite is associated with the base of the ferrogabbro zone in both the Mikanagan and Hook Lake intrusions. Weak pyritic mineralization was observed within the contact alteration zone in host rocks at the south end of the Benn Lake Intrusion.

Primary textures and some primary minerals are retained in most of the intrusions, despite metamorphism up to lower or middle greenschist grade. The alteration of primary minerals occurred during a series of events ranging in age from late magmatic to regional metamorphic. Table 10 details mineralogical changes observed in the Mikanagan Lake Sill and an interpretation of their relative ages. Similar alteration styles occur in all other intrusions. Typical alteration assemblages for the various primary minerals are summarized below and in Table 11.

Table 11:
Alteration sequence in the Mikangan Lake Sill (unit 41)

ZONE	LATE MAGMATIC	DEUTERIC-METAMORPHIC	METAMORPHIC
Gabbronorite	1. cpx → brown amph (replacement of cpx margins; interstitial amph) 2. cpx → green amph brown amph → green amph (patches overprinting earlier phases)	1. cpx → trem/act (bladed epitaxic overgrowths) 2. cpx → trem/act + chl (along fractures and parting planes) 3. cpx, brown amph, green amph → trem/act + chl + Fe-oxide (large oval patches 1-1.5 mm overprinting cpx mosaic, or sited within older amphibole, or between plag and cpx)	1. plag → ep + chl + sph(?) (very fine grained semi-opaque alteration) 2. opx → chl (single crystal) 3. opx → trem + chl (fibrous trem with simultaneous extinction) 4. opx → chl + qz + trem 5. Fe-Ti oxides → leucox, mt, hmt All of the above involve complete replacement of the primary mineral
Gabbro	As above; brown amph not as abundant	As above; alteration patches have scalloped margins against cpx and are commonly sited within late magmatic amph. Some alteration patches are fracture controlled. Alteration assemblage is overprinted by colourless ep overgrowths on the fine grained ep pseudomorphs after plag.	1. plag → ep + chl (very fine grained semi-opaque alteration) 2. cpx → trem/act + chl (pseudomorphs) 3. Fe-Ti oxide → leucox, mt, hmt, jade-green chl
Oikocrystic Gabbronorite	1. cpx → green amph (patches)	As above	1. plag → ep (fine grained dark brown) 2. cpx → trem/act + chl + Fe oxides (patches 3. Fe-Ti oxides → leucox, hmt, py 4. opx → trem + chl + py (fibrous trem with near simultaneous extinction)
Transition Gabbro	As above	1. cpx → trem/act + chl + ep + py (pseudomorphs: single crystals, crystal mosaics, bladed crystal aggregates; chl patches) 2. green amph → trem + chl (patches)	1. plag → ep, qz (fine grained grey-brown transluscent ep - group minerals; seamed by qz) 2. Fe-Ti oxides → leucox, hmt, py, jade-green chl
Gabbro Pegmatite	Interstitial green amph	1. cpx → trem/act + chl + ep (extensive patches) 2. green amph → trem/act (patches)	1. plag → ep group 2. Fe-Ti oxide → leucox + mt

ZONE	LATE MAGMATIC	DEUTERIC-METAMORPHIC	METAMORPHIC
Ferrogabbro	1. cpx → green amph + ep + py (partial to complete)	1. cpx → trem/act, chl (pseudomorphs) 2. green amph → trem/act + chl (patches)	1. plag → ep (weak to complete) 2. plag → srct, ep, chl 3. Fe-Ti oxide → mt, leucox, chl 4. cpx → stilp (along fractures, cleavage, partings, patches) 5. green amph → stilp (scaly masses) 6. plag → stilp (overprint generally at margins, adjacent to other mafic phases)
Ferrotonalite	1. cpx → amph (patches)		1. cpx → ferroact + ep, Fe-oxides, py (single crystal pseudomorphs) 2. magmatic amph → ferroact (fibrous aggregates) 3. plag → ep + srct (commonly in cores or calcic zones in plag) 4. Fe-Ti oxide → mt, hmt, leucox 5. cpx → stilp (along fractures, partings, margins and in small irregular patches) 6. ferroact → stilp (round to irregular patches) 7. plag → stilp (along twin planes, cleavage planes and fractures) 8. Fe-Ti oxides → stilp (rims)
Leucotonalite			1. prismatic px or amph → chl, carb, mt (pseudomorphs) 2. primary anhedral amph → act, ep, sph 3. primary anhedral amph → chl 4. plag → ep, carb (patches) 5. Fe-Ti oxides → leucox, sph, hmt 6. stilp (along late fractures) 7. tour (along intersecting fractures or associated with amph)

Abbreviations:
cpx: clinopyroxene
opx: orthopyroxene
amph: amphibole
plag: plagioclase
leucox: leucoxene
trem/act: tremolite/actinolite
ferroact: ferroactinolite
chl: chlorite
ep: epidote
mt: magnetite
hmt: hematite
py: pyrite
stilp: stilpnomelane
carb: carbonate
qz: quartz
tour: tourmaline

1) Plagioclase in gabbronorite, gabbro and ferrogabbro is completely replaced by a very fine grained semi-opaque mass of epidote-group minerals and chlorite. In more siliceous zones plagioclase is replaced by albite and disseminated epidote.
2) Clinopyroxene is partially replaced by late magmatic brown and green amphibole. Subsequent alteration to tremolite-actinolite, chlorite and epidote occurred during deuteric and regional metamorphism. Clinopyroxene relicts are common in gabbronorite, gabbro, and ferrotonalite but are rare in ferrogabbro and leucotonalite.
3) Orthopyroxene is completely replaced by a characteristic fibrous tremolite-actinolite + chlorite assemblage with simultaneous extinction.
4) Brown to green amphibole is a late magmatic phase that occurs both as a partial replacement of pyroxene and as an interstitial mineral. This amphibole is commonly the site of subsequent alteration to tremolite-actinolite, chlorite, minor epidote and Fe-oxides. These alteration domains spread into adjacent pyroxene.
5) Fe-Ti oxides are replaced by a mixture of leucoxene, magnetite, hematite and local sphene that commonly preserve the primary octahedral partings of the original oxide.
6) Stilpnomelane is present and locally abundant in Fe-rich rocks of the ferrogabbro, quartz ferrodiorite/ferrotonalite and leucotonalite zones, where it overprints all other minerals, both primary and metamorphic. The presence of stilpnomelane results in a characteristic resinous brown tint on fresh surfaces.

In the descriptions of the intrusions which follow, petrography is discussed with reference to interpreted primary mineralogy. Alteration mineralogy and texture is not included in the descriptions.

Mikanagan Lake Sill

The Mikanagan Lake Sill is a large differentiated tholeiitic intrusion emplaced in rocks of the Bear Lake Block. The sill is estimated to be approximately 15 km long, only 8 km of which are exposed in the map area. It ranges in thickness from 520 m, east of One Portage Lake, to 1250 m west of Mikanagan Lake. The intrusion is emplaced in east-facing Vick Lake andesitic tuff, and compositional zoning within the sill indicates that it also tops to the east.

The Northeast Arm Fault locally removes part of the top of the sill and truncates the intrusion at its south end. At least three northeast-trending faults produce minor right-lateral and left-lateral displacements of up to 500 m. More northerly-trending minor faults (not shown on the geological map) produce local repetition of sill stratigraphy. The relationship of the Mikanagan Lake Sill to the Northeast Arm Syncline is not certain. At the north end of Schist Lake (Northeast Arm) the sill has a strong north-northeast foliation but it is not known whether the foliation is due to folding or proximity to the Northeast Arm Fault.

The Mikanagan Lake sill contains 8 major compositional zones that are readily defined on the basis of interpreted primary mineralogy (Table 12 and Fig. 107). These zones are described below in ascending stratigraphic order.

Table 12:
Estimated primary mineral modes, Mikanagan Lake Sill and related intrusions

<table>
<tr><th></th><th>Orthopyroxene</th><th>Clinopyroxene</th><th>Amphibole</th><th>Plagioclase</th><th>Quartz</th><th>Micrographic Intergrowths</th><th>Fe-Ti Oxides</th><th>Apatite</th></tr>
<tr><td>MIKANAGAN LAKE SILL</td><td></td><td></td><td></td><td></td><td></td><td></td><td></td><td></td></tr>
<tr><td>Upper margin ferrodiorite</td><td>0</td><td>40-50</td><td>10</td><td>25-35</td><td>5</td><td>0</td><td>5-10</td><td>0.5-1</td></tr>
<tr><td>Micrographic leucotonalite</td><td>0</td><td>0-10</td><td>5-10</td><td>20-40</td><td>10-50</td><td>15-60</td><td>0.5-7</td><td>tr-1</td></tr>
<tr><td>Ferrotonalite</td><td>0</td><td>5-20</td><td>5-25</td><td>30-60</td><td>15-40</td><td>0-25</td><td>1-5</td><td>tr-1</td></tr>
<tr><td>Ferrogabbro</td><td>0</td><td>25-35</td><td>5-15</td><td>40-50</td><td>0-2</td><td>0</td><td>5-15</td><td>tr-3</td></tr>
<tr><td>Gabbro pegmatite</td><td>0</td><td>40</td><td>7</td><td>47</td><td>0-1</td><td>0</td><td>5</td><td>tr</td></tr>
<tr><td>Transition gabbro</td><td>0</td><td>20-50</td><td>5-25</td><td>40-50</td><td>0-2</td><td>0</td><td>1-4</td><td>0</td></tr>
<tr><td>Oikocrystic gabbronorite</td><td>10-30</td><td>30-45</td><td>2-5</td><td>30-50</td><td>tr-2</td><td>0</td><td>tr-3</td><td>0</td></tr>
<tr><td>Gabbro</td><td>0</td><td>40-55</td><td>1-3</td><td>40-60</td><td>0</td><td>0</td><td>tr</td><td>0</td></tr>
<tr><td>Gabbronorite</td><td>5-15</td><td>40-70</td><td>2-5</td><td>20-50</td><td>0-tr</td><td>0</td><td>0-tr</td><td>0</td></tr>
<tr><td>Chill</td><td>0</td><td>65</td><td>tr</td><td>30-35</td><td>0</td><td>0</td><td>2-3</td><td>0</td></tr>
<tr><td>BENN LAKE INTRUSION</td><td></td><td></td><td></td><td></td><td></td><td></td><td></td><td></td></tr>
<tr><td>Oikocrystic gabbronorite</td><td>20</td><td>45-50</td><td>1-2</td><td>30</td><td>0</td><td>0</td><td>tr</td><td>0</td></tr>
<tr><td>Gabbro</td><td>0</td><td>75-80</td><td>tr-2</td><td>20-25</td><td>0</td><td>0</td><td>0-tr</td><td>0</td></tr>
<tr><td>Gabbronorite</td><td>5-15</td><td>50-65</td><td>1-5</td><td>20-30</td><td>0-tr</td><td>0</td><td>0-1</td><td>0</td></tr>
<tr><td>Chill</td><td colspan="3">50-65</td><td>35-45</td><td>0</td><td>0</td><td>1-5</td><td>tr</td></tr>
<tr><td>HOOK LAKE INTRUSION</td><td></td><td></td><td></td><td></td><td></td><td></td><td></td><td></td></tr>
<tr><td>Ferrogabbro</td><td>0</td><td colspan="2">40-45</td><td>50</td><td>0-1</td><td>0</td><td>1-3</td><td>0</td></tr>
<tr><td>Gabbronorite</td><td>5-30</td><td>10-30</td><td>0-5</td><td>50-60</td><td>0-1</td><td>0</td><td>1-3</td><td>0</td></tr>
<tr><td>SHORE LAKE INTRUSIONS</td><td></td><td></td><td></td><td></td><td></td><td></td><td></td><td></td></tr>
<tr><td>Ferrotonalite</td><td>0</td><td>20-30</td><td></td><td>55-65</td><td>10-20</td><td>0</td><td>tr</td><td>0</td></tr>
<tr><td>Ferrogabbro</td><td>0</td><td colspan="2">55-60</td><td>35-40</td><td>2</td><td>0</td><td>7-8</td><td>0</td></tr>
<tr><td>Gabbronorite</td><td>5</td><td>40-45</td><td>10-15</td><td>30-40</td><td>tr</td><td>0</td><td>2</td><td>0</td></tr>
<tr><td>EMBURY LAKE INTRUSION</td><td></td><td></td><td></td><td></td><td></td><td></td><td></td><td></td></tr>
<tr><td>Quartz diorite</td><td>0</td><td>50</td><td>0</td><td>40</td><td>5-8</td><td>0</td><td>5</td><td>tr</td></tr>
<tr><td>Gabbro</td><td>0</td><td>65</td><td>3</td><td>30</td><td>0</td><td>0</td><td>1</td><td>0</td></tr>
</table>

Gabbronorite zone (unit 41a)

The lowermost 100 — 300 m thick part of the sill comprises massive, homogeneous gabbronorite. The basal contact zone is chilled for almost 50 cm and passes into 5 m of subophitic to ophitic fine grained gabbro. The gabbronorite zone is virtually indistinguishable from the overlying gabbro zone in the field; however, the gabbronorite has a slightly darker weathering colour and finer grain size. The contact shown on the geological map is constrained by petrographic examination of numerous samples.

Gabbronorite weathers shades of buff and buff-brown and is mottled white and grey-green on fresh surfaces; typical grain size is 1 — 2 mm. It is composed of 65 — 75% mafic minerals and 25 — 35% plagioclase.

Clinopyroxene (0.2 — 0.5 mm) occurs as anhedral to subhedral crystals in an interlocking mosaic (Fig. 223). Many have prominent malacolite and diallage partings, a feature characteristic of clinopyroxene throughout the sill. Plagioclase (0.2 — 1 mm) forms euhedral lath-shaped crystals comprising an open mesh network; some are partly or completely enclosed by clinopyroxene. Large, anhedral orthopyroxenes (1 — 10 mm) poikilitically enclose numerous clinopyroxene and plagioclase crystals. Anhedral pleochroic brown and green late magmatic amphibole (up to 2.5 mm) is interstitial and has a reaction relationship to clinopyroxene. Fe-Ti oxides (0.2 — 0.6 mm) are subhedral and interstitial.

Gabbro zone (unit 41b)

The gabbro zone is 140 — 300 m thick. It contains massive, homogeneous, gabbro which weathers light buff to buff-brown and is mottled white and grey-green on fresh surfaces. Gabbro has a typical grain size of about 2 mm, and comprises 45 — 60% mafic minerals and 40 — 55% plagioclase. Vague layering was observed in only one locality.

Epidotization occurs along some joints and veinlets, and is more widespread in association with closely spaced fracture systems. Epidotized gabbro is white weathering.

Plagioclase (0.2 — 1.5 mm) occurs as stubby laths in interconnected clumps forming a crude mesh network (Fig. 224). Larger anhedral to subhedral clinopyroxene crystals (0.2 — 3 mm) occur either as single crystals or as mosaics of several crystals in the spaces between plagioclase clumps. Some clinopyroxene crystals partially enclose plagioclase laths. Trace orthopyroxene was noted at one locality. Late magmatic green amphibole (to 1.5 mm) partially replaces clinopyroxene and also occurs as anhedral interstitial grains. Fe-Ti oxides (to 0.5 mm) are anhedral and interstitial.

Oikocrystic gabbronorite zone (unit 41c)

A 90 — 180 m thick gabbronorite zone is distinguished by its content of large orthopyroxene oikocrysts. The rock is massive, relatively homogeneous, weathers shades of light buff, and is white and light green on fresh surfaces. Large, pale green, poikilitic orthopyroxene pseudomorphs composing 20 — 30% of the rock are commonly 1 cm in diameter (up to 3 cm locally), set in a "matrix" of 2 mm clinopyroxene and plagioclase.

The contact with the underlying gabbro zone is not exposed; however, closely spaced outcrops of gabbro and gabbronorite suggest an abrupt transition. The contact with the overlying transition zone gabbro is gradational over 1 — 2 m, with gradual disappearance of orthopyroxene oikocrysts.

Plagioclase laths (1 — 1.5 mm) are slightly larger than in the gabbro zone, and have larger length:width ratios (approximately 2 — 3 in gabbro, 4 in oikocrystic gabbronorite; Fig. 225). Clinopyroxene (0.4 — 3 mm) is anhedral, equant and partially encloses adjacent plagioclase laths. Poikilitic orthopyroxene (to 20 mm) forms large, anhedral to prismatic isolated

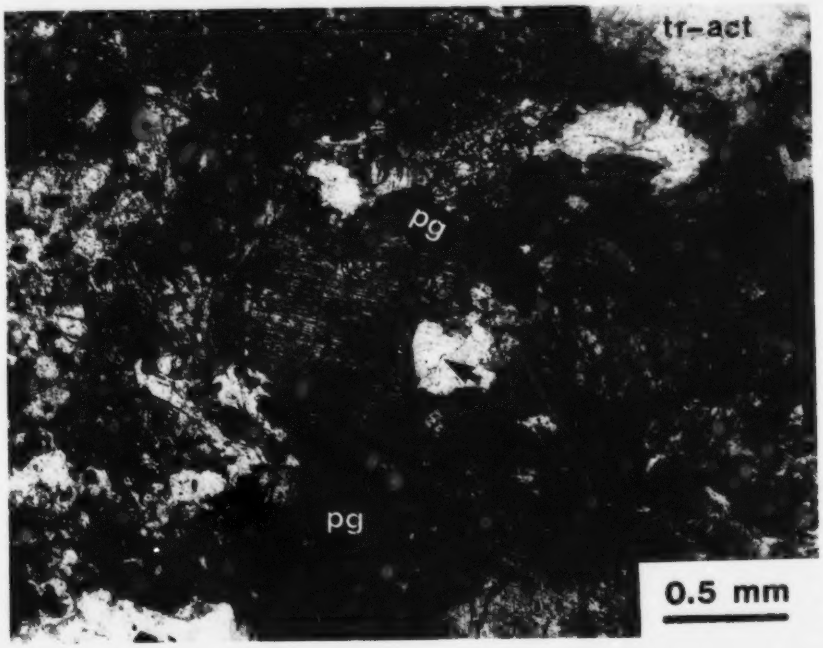

Figure 223: Gabbronorite (unit 41a), Mikanagan Lake Sill. Interlocking mosaic of small, lath-shaped plagioclase (pg; pseudomorphed by dark, fine grained epidote), clinopyroxene (cpx), and orthopyroxene (not shown). Clinopyroxene is variably altered to tremolite-actinolite (tr-act) and chlorite; two spots of alteration shown by arrows. Note the smaller plagioclase content, compared to gabbro (unit 41b). Sample 2083-1, plane polarized light.

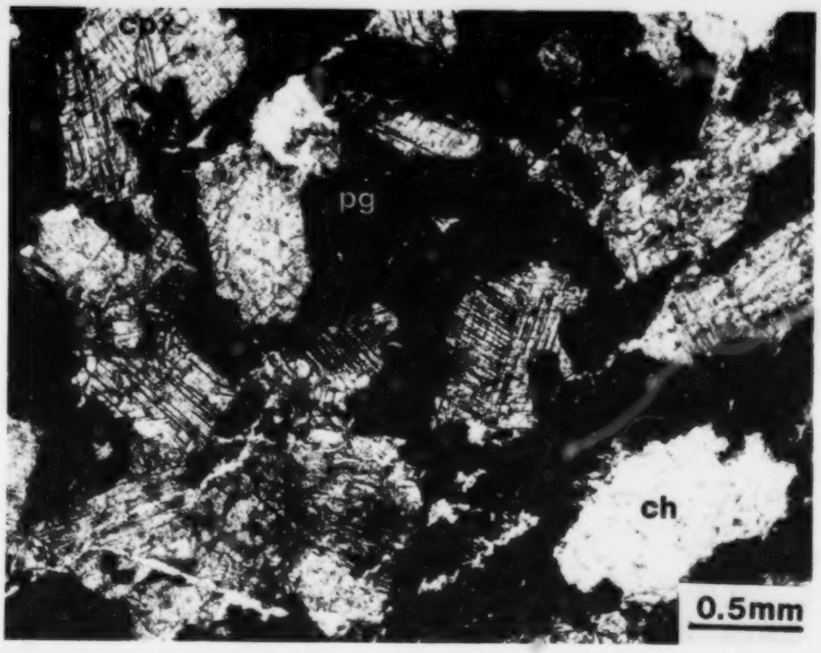

Figure 224: *Gabbro (unit 41b), Mikanagan Lake Sill, composed of primary clinopyroxene (cpx) and epidote-replaced plagioclase (pg). Clinopyroxene displays strong cleavage and diallage parting. Colourless, secondary chlorite (ch), is a minor constituent here, but in other gabbro samples is a prominent alteration phase. Sample 06-1, plane polarized light.*

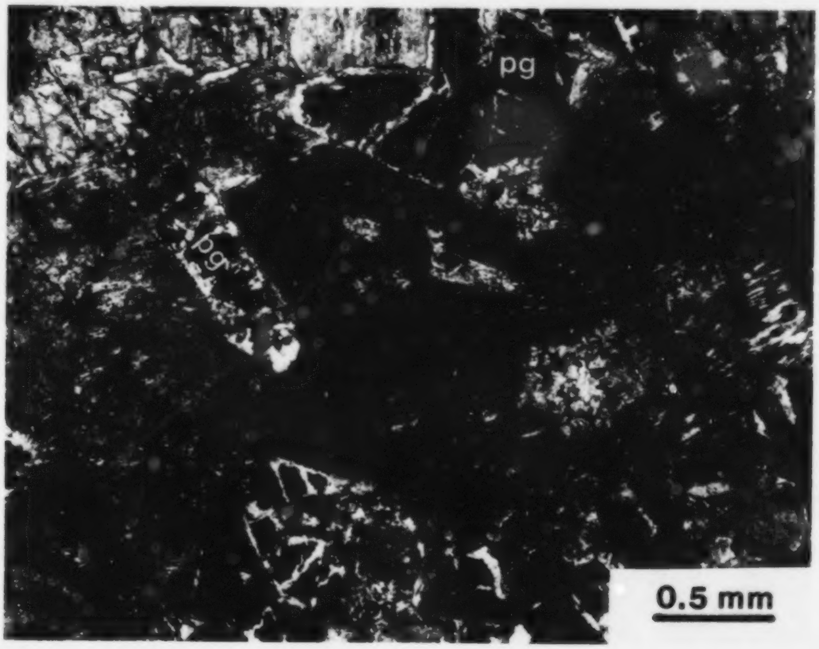

Figure 225: *Oikocrystic gabbronorite (unit 41c), Mikanagan Lake Sill. Plagioclase (pg) is pseudomorphed by very fine grained epidote (dark) and chlorite (light). Clinopyroxene (cpx) is subhedral and relatively fresh in this slide. Orthopyroxene (opx) is pseudomorphed by fibrous tremolite and forms large poikilitic crystals that partially enclose plagioclase and clinopyroxene. Sample 1076-1, plane polarized light.*

crystals that enclose abundant small plagioclase laths and clinopyroxene crystals. Green amphibole occurs both as an anhedral interstitial phase and as a late magmatic replacement of clinopyroxene. Fe-Ti oxides (0.5 mm, locally up to 7 mm) are interstitial and commonly associated with the late magmatic amphibole. Quartz (to 0.8 mm) is anhedral and interstitial to plagioclase and pyroxenes.

Transition gabbro (unit 41d), gabbro pegmatite (unit 41e) zone

A 20 m thick unit of gabbro and gabbro pegmatite (Fig. 226) occurs stratigraphically between the oikocrystic gabbronorite and overlying ferrogabbro. This "transition gabbro":

1) has a gradational contact with the underlying gabbronorite,
2) contains one to five percent Fe-Ti oxides (intermediate between the gabbronorite, less than 1%, and the ferrogabbro, 5 — 15%), and
3) shares an aligned tabular plagioclase texture with the ferrogabbro.

The transition gabbro zone has a lower massive section and an upper modally layered section containing bodies of gabbro pegmatite.

The contact between oikocrystic gabbronorite and massive transition gabbro is gradational over 1 — 2 m, through disappearance of poikilitic orthopyroxene and appearance of a crude alignment of plagioclase laths. The contact between layered transition gabbro and overlying ferrogabbro is abrupt and defined by the appearance of abundant Fe-Ti oxides (Fig. 227 and 228).

Plagioclase (0.5 — 2 mm) occurs as euhedral laths commonly with a moderate preferred orientation imparting a distinctive igneous lamination. In some gabbros the plagioclase is randomly oriented. Clinopyroxene (0.5 — 3 mm) is anhedral to subhedral and partially encloses adjacent plagioclase laths. Green amphibole is an interstitial, late magmatic phase in reaction relationship with clinopyroxene. Fe-Ti oxides (0.3 — 5 mm) are anhedral; large grains poikilitically enclose plagioclase and small clinopyroxene crystals. The oxides are euhedral where enclosed by late magmatic amphibole. Quartz is a minor, interstitial phase.

Layering in the upper part of the zone (Fig. 108) is 1 — 30 cm thick and defined by modal variation in the pyroxene:plagioclase ratio from 65:35 in mafic layers to 45:55 in more leucocratic layers. The mafic layers

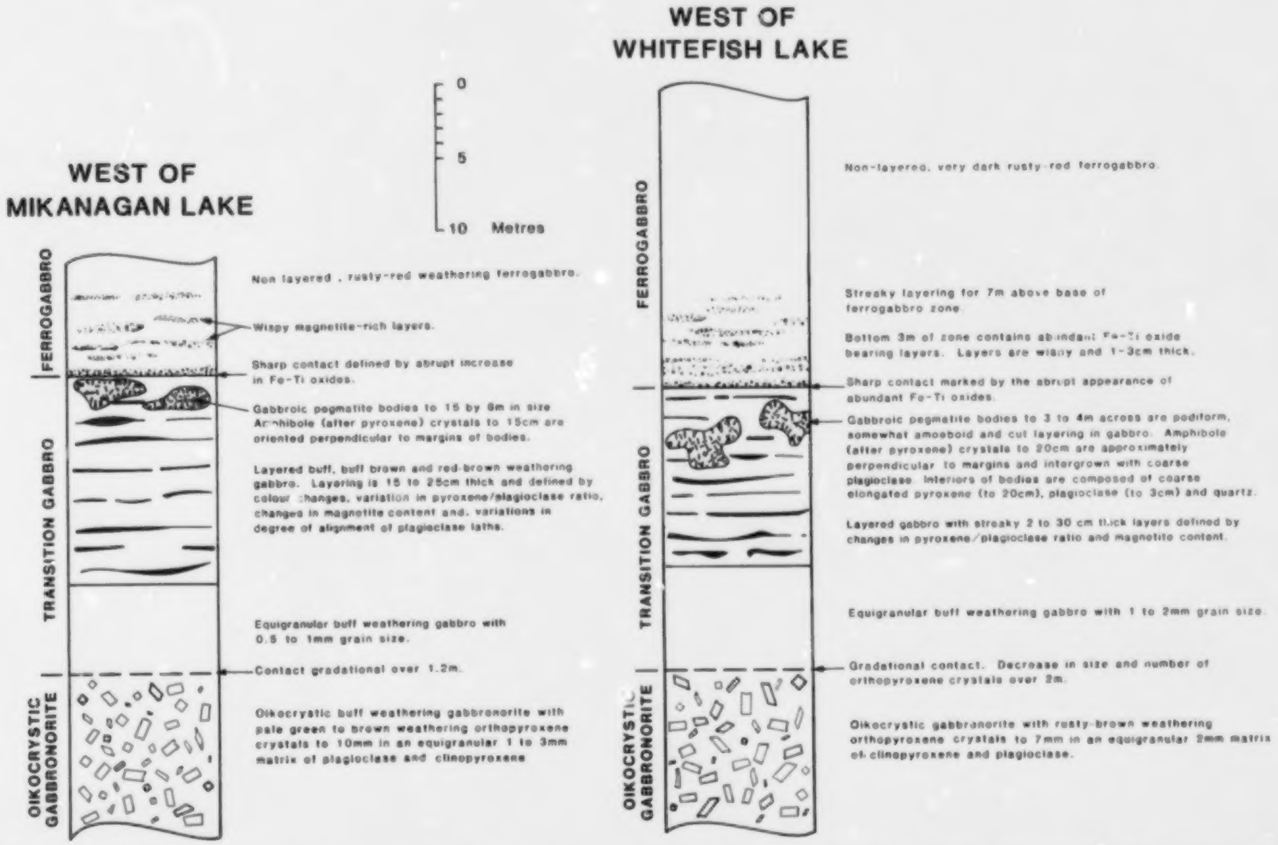
WEST OF MIKANAGAN LAKE
0
5
10 Metres
FERROGABBRO
TRANSITION GABBRO
OIKOCRYSTIC GABBRONORITE
Non layered , rusty-red weathering ferrogabbro.
Wispy magnetite-rich layers.
Sharp contact defined by abrupt increase in Fe-Ti oxides.
Gabbroic pegmatite bodies to 15 by 8m in size Amphibole (after pyroxene) crystals to 15cm are oriented perpendicular to margins of bodies.
Layered buff, buff brown and red-brown weathering gabbro. Layering is 15 to 25cm thick and defined by colour changes, variation in pyroxene/plagioclase ratio, changes in magnetite content and, variations in degree of alignment of plagioclase laths.
Equigranular buff weathering gabbro with 0.5 to 1mm grain size.
Contact gradational over 1.2m.
Oikocrystic buff weathering gabbronorite with pale green to brown weathering orthopyroxene crystals to 10mm in an equigranular 1 to 3mm matrix of plagioclase and clinopyroxene
WEST OF WHITEFISH LAKE
FERROGABBRO
TRANSITION GABBRO
OIKOCRYSTIC GABBRONORITE
Non-layered, very dark rusty-red ferrogabbro.
Streaky layering for 7m above base of ferrogabbro zone.
Bottom 3m of zone contains abundant Fe-Ti oxide bearing layers. Layers are wispy and 1-3cm thick.
Sharp contact marked by the abrupt appearance of abundant Fe-Ti oxides.
Gabbroic pegmatite bodies to 3 to 4m across are podiform, somewhat amoeboid and cut layering in gabbro. Amphibole (after pyroxene) crystals to 20cm are approximately perpendicular to margins and intergrown with coarse plagioclase. Interiors of bodies are composed of coarse elongated pyroxene (to 20cm), plagioclase (to 3cm) and quartz.
Layered gabbro with streaky 2 to 30 cm thick layers defined by changes in pyroxene/plagioclase ratio and magnetite content.
Equigranular buff weathering gabbro with 1 to 2mm grain size.
Gradational contact. Decrease in size and number of orthopyroxene crystals over 2m.
Oikocrystic gabbronorite with rusty-brown weathering orthopyroxene crystals to 7mm in an equigranular 2mm matrix of clinopyroxene and plagioclase.

Figure 226: Schematic diagram showing characteristic features of the transition gabbro zone (unit 41d) as exposed at two widely separated localities in the Mikanagan Lake Sill. Well defined layering (modal and textural) and gabbroic pegmatite bodies (unit 41e) are typical of this zone.

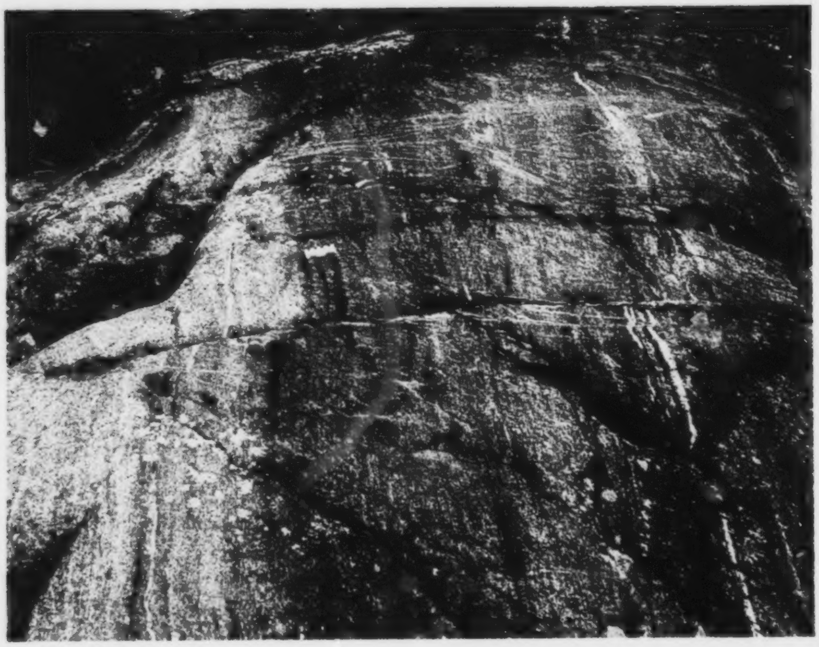

Figure 227: *Contact between transition gabbro (unit 41d), on the left, and ferrogabbro (unit 41f), on the right. Contact is sharp, conformable, and marked by abrupt appearance of wispy oxide layers (dark). See Figure 226 for stratigraphic relationships. Same locality as Figure 228.*

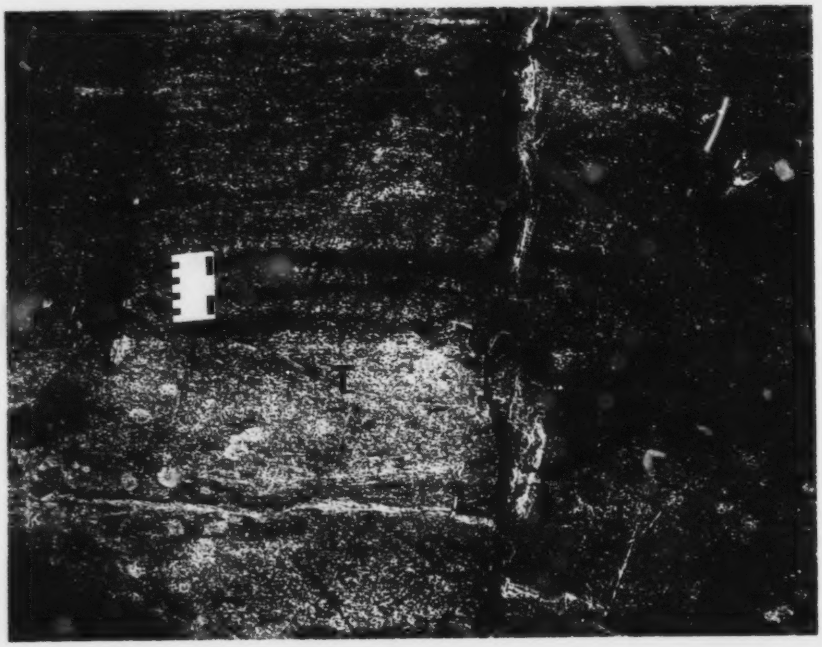

Figure 228: *Detail of transition gabbro (T) — ferrogabbro (F) contact shown in Figure 227. Scale card rests on ferrogabbro at the contact. Note oxide layers in ferrogabbro to the right of scale card. Contact is offset along minor east-trending dextral fault.*

weather rusty brown, and more leucocratic layers buff-brown. In some layered sequences the degree of plagioclase preferred orientation varies between layers.

Gabbroic pegmatite pods occur in the upper layered part of the transition gabbro (Fig. 229). These pods range in size from 3 m across to 6 x 15 m; they are tabular, irregular to ovoid in shape. Amphibole crystals (replacing clinopyroxene), are up to 20 cm long and oriented approximately perpendicular to the pod margins. They are typically intergrown with coarse plagioclase. The pegmatites contain a coarse grained intergrowth of amphibole after pyroxene, plagioclase, and up to 10% interstitial quartz. Fe-Ti oxides (to 10 mm) are concentrated in clusters, or occur as anhedral crystals interstitial to plagioclase. Apatite (to 1.2 mm) is stubby and prismatic.

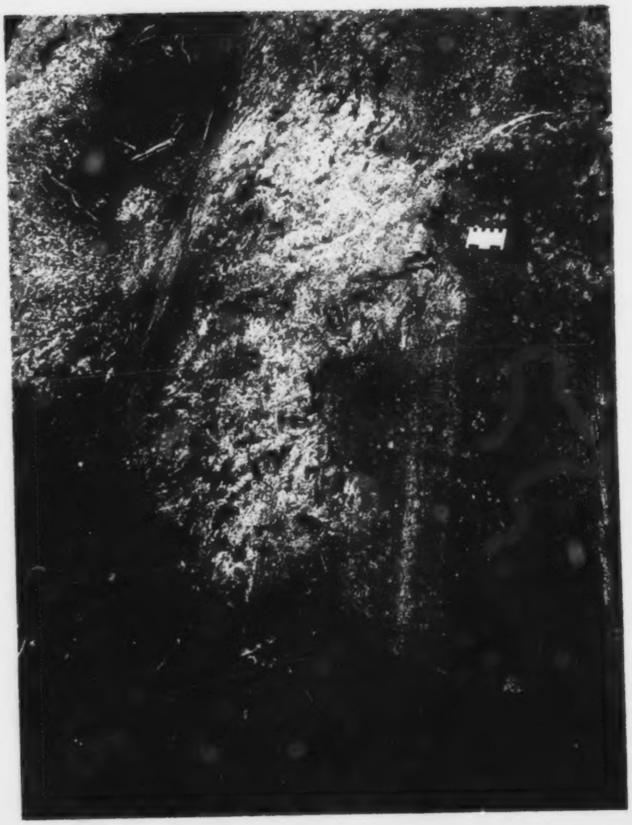

Figure 229: Irregular pod of gabbroic pegmatite (unit 41e) emplaced in layered transition gabbro (unit 41d), Mikanagan Lake Sill. The pegmatite is composed of coarse prismatic amphibole (after clinopyroxene), plagioclase and minor quartz. Contacts (arrows) cut across layering in the gabbro. See Figure 226 for stratigraphic relationships exposed at this locality 370 m west of the south end of One Portage Lake.

Ferrogabbro zone (unit 41f)

The ferrogabbro zone, 60 — 240 m thick, abruptly overlies transition gabbro (Fig. 108) and is in turn overlain abruptly by quartz ferrodiorite of the succeeding zone. Ferrogabbro is massive, homogeneous, weathers reddish brown and is medium to dark green on fresh surfaces. Adjacent to veins and fractures ferrogabbro is variably epidotized and altered, weathering greenish white, green or red.

The basal contact of the ferrogabbro zone is defined by an abrupt appearance of abundant Fe-Ti oxides, concentrated in 1 — 3 cm thick (locally to 15 cm) wispy laminae. These oxide-rich layers occur only within the lowermost few metres of the zone (Fig. 226). The remainder of the ferrogabbro is massive and characterized by abundant disseminated oxides, reaching a maximum of about 15% approximately midway through the zone. Trace apatite occurs throughout the zone but increases significantly (to 3%) in the uppermost part.

Plagioclase (0.2 — 3 mm) is lath- to tablet-shaped with a moderate preferred orientation (Fig. 230). Clinopyroxene (0.5 — 3 mm) is anhedral to crudely prismatic (Fig. 231), with euhedral crystal faces against late magmatic amphibole and Fe-Ti oxides. In places clinopyroxene partially encloses plagioclase. Green amphibole is a late magmatic phase that occurs both as a partial replacement of clinopyroxene and as interstitial grains. Fe-Ti oxides (0.2 — 1 mm) are anhedral and interstitial to plagioclase and clinopyroxene; they are euhedral where enclosed by late magmatic green amphibole. Apatite (0.2 — 2.5 mm) occurs as (1) large stubby subhedral crystals interstitial to clinopyroxene and plagioclase and locally partially encloses small clinopyroxene crystals, (2) euhedral prisms commonly enclosed by amphibole and less commonly by clinopyroxene, or (3) small interstitial enhedral grains (in the lower part of the zone). Quartz (up to 0.5 mm) is anhedral and interstitial to plagioclase.

Quartz ferrodiorite, ferrotonalite zone (unit 41g)

The quartz ferrodiorite and ferrotonalite zone is 60 — 300 m thick. It abruptly overlies ferrogabbro and grades over 3 m to overlying micrographic leucotonalite. In places the micrographic leucotonalite zone is absent and the ferrotonalite grades abruptly into the upper marginal zone.

Ferrotonalite and quartz ferrodiorite weather rusty buff, red-brown or buff, and on fresh surfaces is dull greenish brown (at the base of the zone) to orange-brown and white (at the top of the zone). Outcrops in this zone are recessive, small and rubbly. At any given locality, ferrotonalite grain size and texture vary considerably. Typically, plagioclase occurs as 1 — 6 mm tablet-shaped crystals and pyroxene forms elongate prismatic crystals, up to about 5 cm long in coarse grained varieties. Quartz content ranges between 5 — 30%.

The base of the ferrotonalite zone was observed at only one locality, where the contact with ferrogabbro is abrupt. The basal 15 — 25 m comprises quartz ferrodiorite with a weathering colour, fresh colour, and plagioclase morphology similar to ferrotonalite (see below) but with only 5% quartz and up to 45% mafic minerals. This basal quartz ferrodiorite grades to typical ferrotonalite, 30 m above the contact with ferrogabbro.

Most ferrotonalite displays little variation in modal composition. There is a crude upward decrease in mafic, Fe-Ti oxide and apatite content and an increase in quartz. The top of the ferrotonalite zone displays an abrupt increase in quartz and micrographic quartz-plagioclase intergrowth (Fig. 232). The contact with the overlying micrographic leucotonalite zone is gradational through further decrease in mafic contact.

In "typical" ferrotonalite plagioclase (1 — 6 mm) occurs as tabular, randomly oriented crystals in an interlocking texture, commonly with irregular boundaries against quartz (Fig. 233). Quartz (0.5 — 5 mm) is anhedral and commonly coarsely intergrown with plagioclase. Clinopyroxene (0.5 — 4 mm, locally up to 5 cm) is subhedral, elongate prismatic, interstitial to plagioclase and euhedral against magmatic amphibole. Late magmatic amphibole (to 2 mm) partially replaces some clinopyroxene but in many places occurs as large grains interstitial to plagioclase and

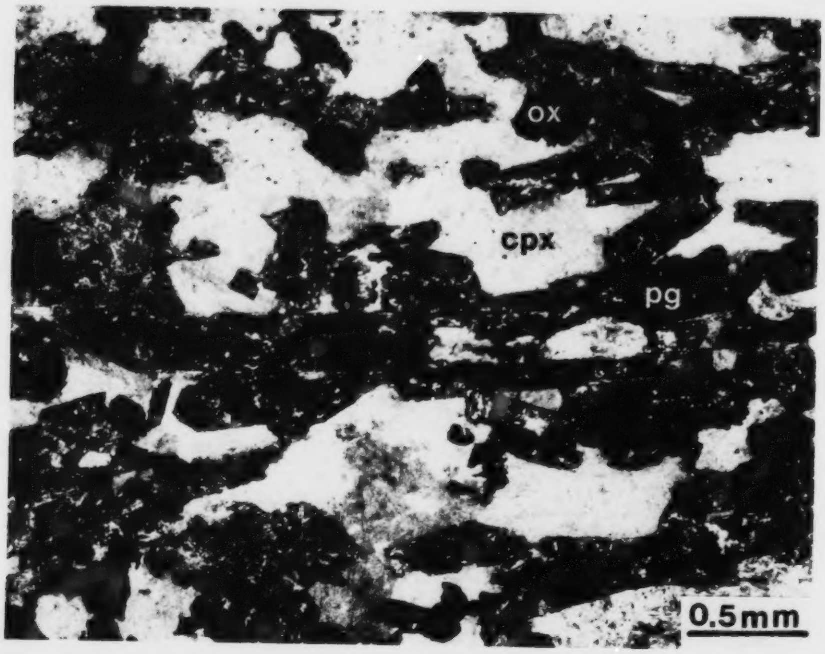

Figure 230: Igneous lamination of plagioclase (pg) in ferrogabbro (unit 41f), Mikanagan Lake Sill. Tabular, subhedral to euhedral plagioclase crystals are replaced by epidote; clinopyroxene (cpx) is replaced by tremolite. Abundant Fe-Ti oxide (ox) is typical of ferrogabbro. Sample 04-1, plane polarized light.

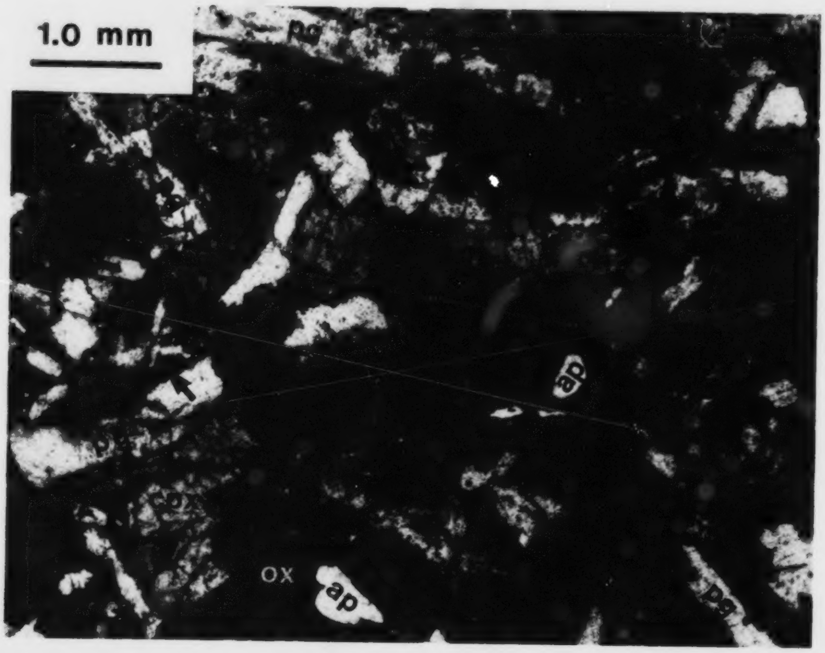

Figure 231: Ferrogabbro (unit 41f), Mikanagan Lake Sill. This sample (2292-1) represents some of the freshest material from the ferrogabbro zone. Fresh subhedral clinopyroxene (cpx) is only slightly altered to chlorite and stilpnomelane. Plagioclase laths (pg) are not particularly well oriented in this sample, compared to the common igneous lamination observed elsewhere. Chlorite (chl; arrows, grey) after amphibole is interstitial to clinopyroxene and plagioclase crystals. Note abundant oxides (ox, black) and apatite (ap). Plane polarized light.

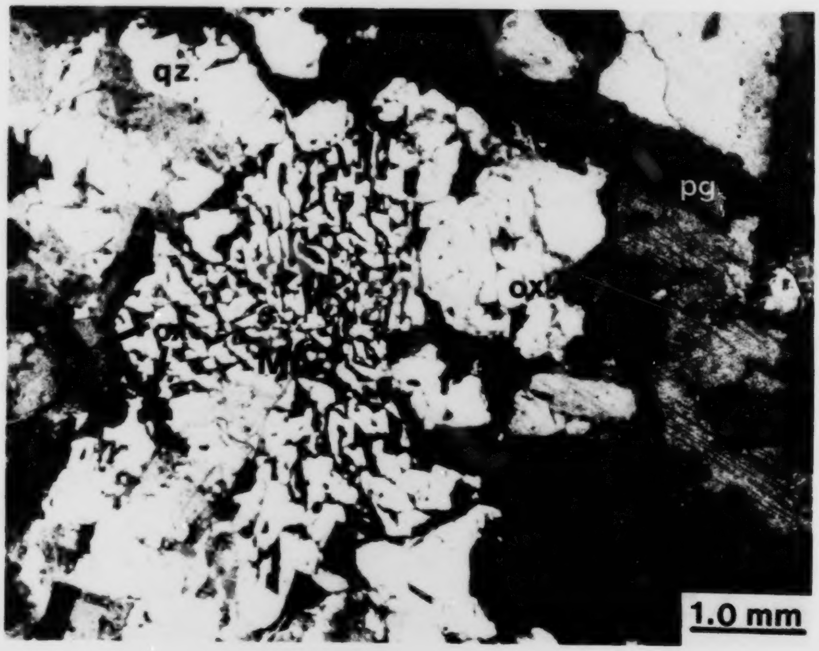

Figure 232: *Ferrotonalite (unit 41g), Mikanagan Lake Sill, composed of subhedral, elongate plagioclase (pg), anhedral quartz (qz), Fe-Ti oxide (ox) and micrographic intergrowths (M) of quartz and plagioclase. Sample 3108-1, crossed polarizers.*

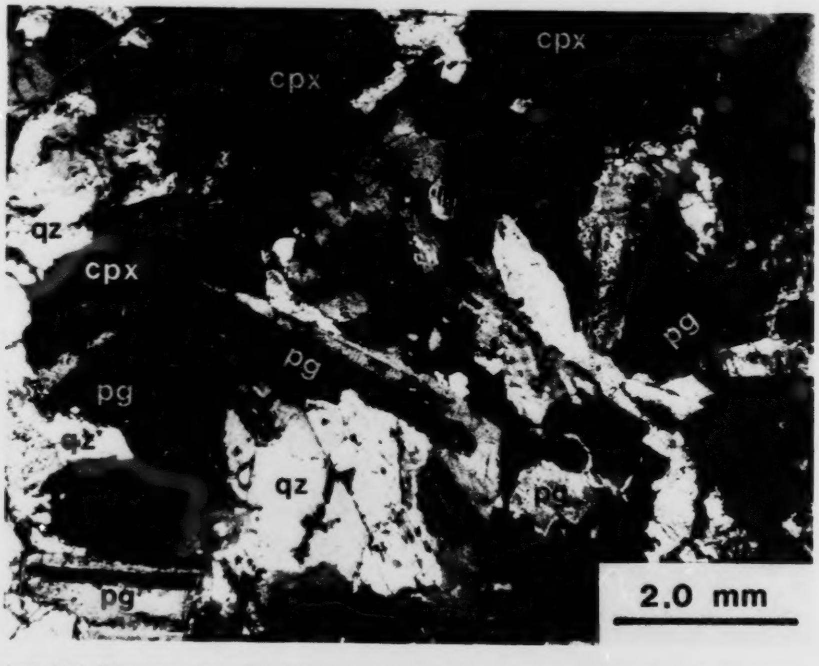

Figure 233: *Ferrotonalite (unit 41g), Mikanagan Lake Sill. Clinopyroxene (cpx) forms large, subhedral prismatic crystals, patchily altered to amphibole and stilpnomelane. Plagioclase (pg) is twinned, lath-shaped, and corroded against blebby quartz (qz). Sample 2092-2, crossed polarizers.*

clinopyroxene. Fe-Ti oxides (0.2 — 2 mm) occur in subhedral, euhedral and skeletal forms, generally amphibole. Apatite prisms up to 3 mm long occur as inclusions in all minerals and commonly cross crystal boundaries.

Micrographic leucotonalite zone (unit 41h)

Micrographic leucotonalite forms a zero to 180 m thick zone at or near the top of the Mikanagan Lake Sill. It weathers white to pink and is light to dark grey on fresh surfaces. In contrast to the ferrotonalite, outcrops in this zone are relatively large and resistant. The basal contact with ferrotonalite is gradational; the contact with the overlying marginal zone is not exposed.

Plagioclase (0.5 — 3 mm) occurs as tabular elongate crystals, commonly with albitic overgrowths; phenocrysts up to 6 mm long occur in some leucotonalites. Plagioclase generally has scalloped boundaries against quartz; both plagioclase and albitic overgrowths are partially to completely enclosed by, and graphically intergrown with, quartz. Quartz (0.5 — 2 mm, phenocrysts to 5 mm) occurs as equant blebs, commonly in optical continuity with adjacent micrographic intergrowths. Micrographic quartz-plagioclase intergrowths form (1) equant to oval blebs (1 — 6 mm) which are fine-scale intergrowths in the core and become coarser towards the margins, and (2) interstitial intergrowths, commonly between larger quartz and plagioclase. Phenocrysts commonly occur at the cores of micrographic blebs (Fig. 234). Mafic minerals form irregular masses or pseudomorphs after a prismatic mafic phase up to 4 mm long. Apatite forms acicular crystals up to 0.7 mm long. Disseminated Fe-Ti oxides (0.2 — 0.8 mm) are subhedral to euhedral.

Upper margin zone (unit 41i)

The upper part of the Mikanagan Lake Sill comprises mainly quartz ferrodiorite, and a very narrow (about 50 cm) chilled gabbro contact with Vick Lake andesitic tuff. The maximum observed width of the marginal zone is 6 — 10 m. The top of the sill is in many places removed by the Northeast Arm fault; in other places the marginal zone is not exposed. Consequently information on the upper margin of the sill is limited.

The quartz ferrodiorite weathers red-brown and is medium to dark green on fresh surfaces; grain size is 1 — 5 mm. It locally contains subrounded xenoliths and stoped blocks (up to 2 m long) of recrystallized Vick Lake tuff. In some localities the quartz ferrodiorite is cut by narrow dykes of ferrotonalite and leucotonalite.

Plagioclase (0.5 — 3 mm) occurs as lath- to tablet-shaped crystals. Quartz (up to 6 mm) is blebby, anhedral, and interstitital to all other minerals. Clinopyroxene (0.5 — 5 mm) occurs as subhedral elongate prisms and as euhedral grains interstitial to plagioclase. Late magmatic brownish green amphibole replaces clinopyroxene, and occurs as large interstitial grains. Fe-Ti oxides (to 2.5 mm) are subhedral to euhedral, partially enclosing plagioclase. Apatite (to 2 mm) is euhedral and occurs as inclusions in quartz, late magmatic amphibole, and plagioclase.

Recrystallized country rocks

Vick Lake andesitic tuff (unit 25) is the host formation for much of the Mikanagan Lake Sill. The sill is not absolutely concordant, in that its lower contact cuts up through stratigraphy from Two Portage Lake fer-

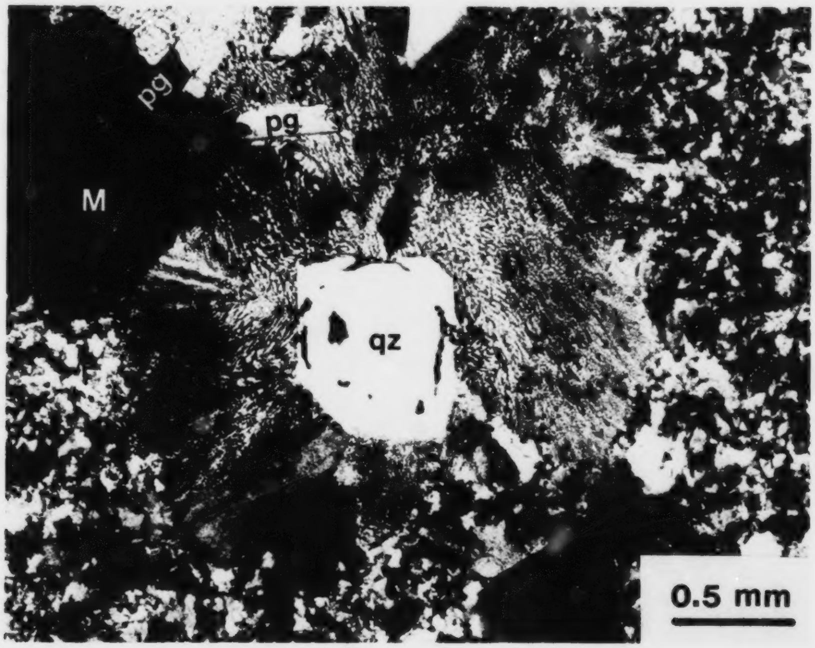

Figure 234: Micrographic leucotonalite (unit 41h), Mikanagan Lake Sill. This sample has quartz (qz) and plagioclase (pg) phenocrysts in a fine grained matrix of quartz and feldspar. Many of the phenocrysts have served as nuclei for envelopes of micrographic intergrowth (M) of quartz and albite. Note that the quartz phenocryst in the centre of the photomicrograph is skeletal in its outer portions, possibly due to corrosion by a late stage vapour phase. The micrographic texture may indicate quenching by rapid decrease in temperature and/or pressure (P. Lenton, pers. comm. 1988). Sample 2076-1, crossed polarizers.

robasalt (unit 5) at the north end of the map area to dacite (unit 18) at the north end of Schist Lake.

The andesitic tuff for several metres below the sill appears bleached, recrystallized (hornfelsed), contains abundant close-spaced fractures, and contains numerous narrow epidote-filled veinlets. A similar but somewhat wider zone of recrystallized altered tuff occurs above the sill. In one locality on Mikanagan Lake the tuff contains up to 20% retrograded pseudomorphs after subhedral to euhedral garnet (to 0.7 mm). Bedding in the tuff adjacent to the sill is commonly obliterated, but pumice fragments are still recognizable in xenoliths in the marginal zone, and within the hornfels aureole of the sill.

Geochemistry

The Mikanagan Lake Sill is a major tholeiitic intrusion displaying extreme iron enrichment (Fig. 235, 236 and 237). Distribution of major, minor and trace elements through the sill follows the pattern typical of many other major differentiated tholeiitic sills. These include:

1) SiO_2 decreases slightly from the base of the sill to about the middle of the ferrogabbro zone, and increases steadily thereafter.
2) FeO^*, TiO_2 and MnO contents are constant through the gabbronorite and gabbro zones, peak in the upper part of the ferrogabbro zone and decrease from that point to the top of the sill, reflecting the abrupt crystallization of abundant Fe-Ti oxides in the ferrogabbro zone.
3) P_2O_5 is constant throughout the lower part of the sill and peaks in the upper part of the ferrogabbro zone, coincident with the crystallization of abundant apatite.
4) MgO displays a steady decrease from the base to the top of the sill, probably reflecting decreasing Mg/Fe ratio in crystallizing pyroxenes.
5) Al_2O_3 shows an abrupt, significant increase at the base of the gabbro zone, reflecting the higher modal plagioclase content in this zone relative to the underlying gabbronorite zone. It then decreases steadily to the top of the ferrogabbro zone and is constant thereafter, reflecting upward change to more sodic plagioclase compositions.
6) Na_2O increases, and CaO decreases, steadily from base to top of the sill, indicating progressive upward increase in Na/Ca ratio in crystallizing plagioclase. High CaO in the upper part of the ferrogabbro zone is due to high modal apatite contents (see (3) above). K_2O is constant and very low (except for one altered sample) to the base of the ferrogabbro zone, peaks in the lower part of the ferrotonalite zone and decreases steadily thereafter, presumably in response to changing plagioclase composition.
7) Ni and Cr are high in the gabbronorite zone, decrease steadily to the top of the ferrogabbro zone and are negligible in the overlying zones. These elements are probably concentrated in orthopyroxene in the gabbronorite; Cr content in clinopyroxene must decrease upwards.
8) Rb and Ba follow K_2O contents, and are highest in the lower part of the ferrotonalite.
9) Sr follows Al_2O_3 in that it increases abruptly at the base of the gabbro zone, reflecting higher plagioclase content in gabbro relative to gabbronorite. It then decreases to the top of the ferrogabbro zone, indicating progressively higher Na/Ca ratio in crystallizing plagioclase. Sr peaks at the top of the ferrogabbro and decreases irregularly thereafter, reflecting crystallization of Sr-bearing apatite.
10) Cu and Zn peak in the ferrogabbro zone and are low in overlying zones. The Cu peak in the lower part of the ferrogabbro is expressed by local disseminated chalcopyrite.
11) Zr and Y are low and approximately constant through to the base of the ferrotonalite zone, where they abruptly increase by an order of magnitude and then increase irregularly to the top of the leucotonalite.

Element distribution trends, and absence of intrusive zone contacts, are consistent with an interpretation that the sill was emplaced as a single pulse of basaltic magma which differentiated to a siliceous end member. Furthermore the regular, uninterrupted increase in the $FeO^*/(FeO^* + MgO)$ ratio from the base to the upper part of the sill, does not suggest the existence of more than one batch of magma.

The best estimate for the parental magma composition is an average of four analyses of chilled gabbro from the base and top of the sill (Table 13). The four analyses are similar but display some variation in MgO, FeO^*, K_2O, Rb, Ba, Ni and Cr concentrations. Assimilation of small amounts of the Vick Lake andesitic tuff host rocks may account for the variation in alkali content. A sample from the top chill has the lowest MgO, Ni and Cr, and a sample from the basal chill has the highest concentrations of these elements. The average analysis is that of a basalt distinctive only in its slightly elevated MgO content. A weighted average composition of the sill (Table 13) is virtually identical to the average chill composition, giving further support to the interpretation that the observed zones in the sill developed by closed-system fractionation of a single batch of basaltic magma. The slightly higher SiO_2 and lower MgO in the calculated bulk composition may indicate the presence of a small amount of ultramafic rocks in the non-exposed portion of the sill. Alternatively, the weighting factor chosen for the ferrotonalite may be too large (as suggested also by high Zr and Y in the calculated bulk composition).

The Mikanagan Lake Sill is emplaced in Amisk Group rocks, but the age of the intrusion with respect to the volcanism is presently unknown. The concentrations of immobile trace and minor elements in chilled gabbros from the sill are, however, very similar to those in Amisk Group mafic lavas (Fig. 217, 218, 219 and 238), raising the possibility that the magmas may be cogenetic. The analyses of both Amisk lavas and chilled gabbros tend to plot within the fields of island arc lavas (Fig. 217 and 218). The chilled gabbros exhibit higher Ni and Cr contents than typical Amisk lavas (Fig. 239), but nevertheless fall on trend and within the general range shown by the Amisk Group.

The Mikanagan Lake Sill is more strongly differentiated than any other intrusion in the area (Fig. 240 and 241). The quartz ferrodiorites have FeO^*/MgO ratios an order of magnitude higher than quartz diorites from other intrusions (Fig. 241, Appendix). All major mafic intrusions share, with the Mikanagan Lake Sill, the characteristic of strong iron enrichment. The differences in presumed parental magma composition (Fig. 217, 218, 219, 240 and 241) preclude these intrusions having an identical magma source.

Benn Lake Intrusion

The Benn Lake Intrusion (Fig. 220) is a large teardrop-shaped body with an abrupt southern termination at Soloduik Lake and tapered shape north of the map area. It is a maximum of 1.7 km across east of Benn lake and over 10 km long. The intrusion is emplaced predominantly within east-facing Bear Lake basaltic andesite (unit 1). Three rock types occur within the body: massive gabbronorite (unit 41a), massive gabbro (unit 41b), and scattered small areas of oikocrystic gabbronorite. These rock types are superficially similar to equivalent rock types in the Mikanagan Lake Sill; however, significant compositional differences exist between the two intrusions. The Benn Lake Intrusion does not contain ferrogabbro, ferrotonalite nor leucotonalite as in the Mikanagan Lake Sill.

Contact relationships

The western and eastern contacts of the intrusion are distinctly different. The western contact, which *may* be the floor of the intrusion, is planar, steeply dipping, and concordant with host Bear Lake flows. The eastern contacts are much more irregular, and display abrupt variations in trend that are locally highly discordant.

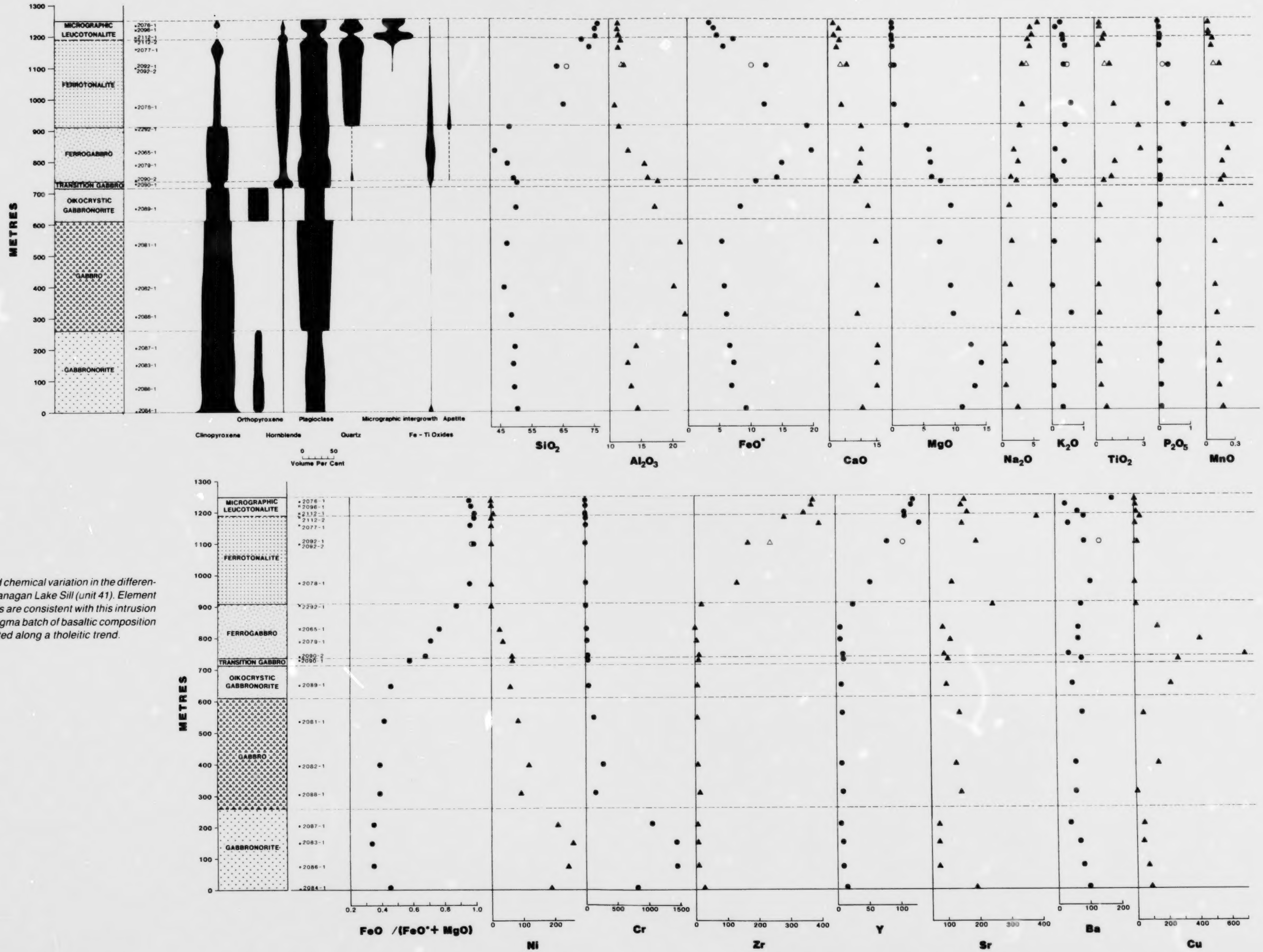

Figure 235: *Mineralogical and chemical variation in the differentiated, zoned Mikanagan Lake Sill (unit 41). Element distribution trends are consistent with this intrusion being a single magma batch of basaltic composition which differentiated along a tholeitic trend.*

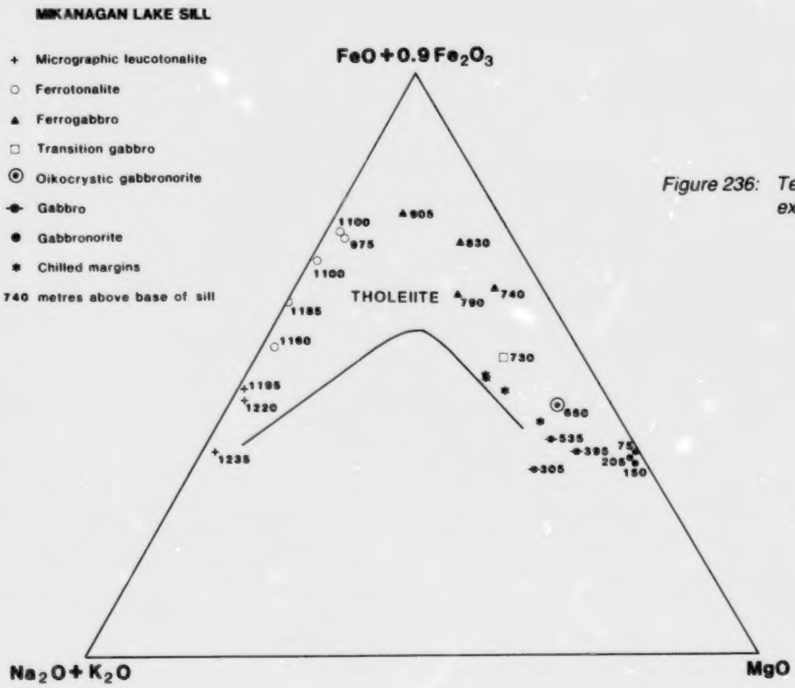

Figure 236: *Ternary AFM diagram showing tholeiitic character and extreme Fe-enrichment trend of the Mikanagan Lake Sill.*

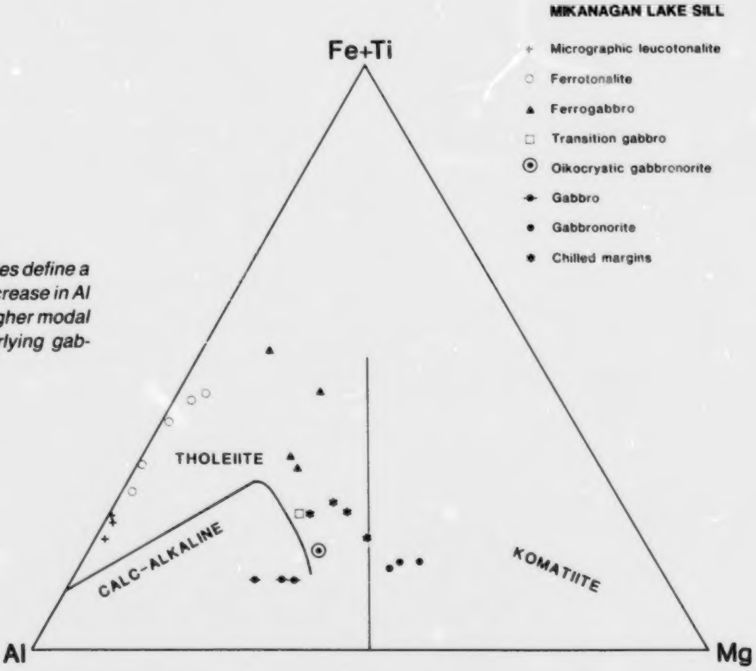

Figure 237: *Jensen cation plot, Mikanagan Lake Sill. Samples define a trend of extreme Fe-enrichment. The abrupt increase in Al at the base of the gabbro zone reflects much higher modal plagioclase in this zone relative to the underlying gabbronorite zone.*

Table 13:
Average compositions of zones and chilled margins in the Mikanagan Lake Sill, calculated bulk composition of the Mikanagan Lake Sill, and comparative data from the Josland Lake Sill (Bailes, 1980)

	MIKANAGAN LAKE SILL									JOSLAND L. SILL	
	Average of 4 Chilled Margins	Calculated Bulk Composition	Gabbronorite	Gabbro	Oikocrystic Gabbronorite	Transition Gabbro	Ferrogabbro	Ferrotonalite	Micrographic Leucotonalite	Chilled Base	Calculated Bulk Composition
Thickness (m)		1250	260	350	105	20	180	275	60		750
SiO_2	49.33	52.45	47.62	46.10	48.60	48.10	45.80	66.52	74.22	46.4	49.69
Al_2O_3	14.17	15.22	13.09	20.62	16.87	16.90	13.77	11.51	11.28	14.2	14.5
FeO^*	9.81	8.54	6.77	5.68	7.88	10.53	16.86	9.48	4.04	14.48	12.30
CaO	9.84	10.30	14.70	12.88	12.27	9.13	10.02	4.08	2.29	9.75	10.93
MgO	8.77	6.81	12.83	8.66	9.16	7.61	5.21	0.28	0.11	8.30	6.77
Na_2O	2.57	2.25	0.54	1.89	1.28	2.44	2.30	4.00	5.18	2.05	1.96
K_2O	0.64	0.30	0.03	0.25	0.11	0.13	0.27	0.48	0.28	0.72	0.32
TiO_2	0.70	0.63	0.28	0.24	0.28	0.55	1.98	0.73	0.33	0.80	0.98
P_2O_5	0.07	0.10	0.03	0.01	0.03	0.06	0.25	0.20	0.04	0.06	0.10
MnO	0.18	0.16	0.14	0.11	0.16	0.17	0.22	0.13	0.05	0.26	0.21
H_2O	2.95	2.85	3.29	3.63	3.44	3.71	2.92	1.53	0.78	2.10	1.33
S	0.01	0.03	0.03	-	0.03	0.03	0.09	0.02	0.03	0.04	0.04
CO_2	0.71	0.34	0.15	0.11	0.10	0.19	0.20	0.79	1.24	tr.	0.79
Other	0.15	0.11	0.25	0.08	0.07	0.08	0.08	0.05	0.03		
Less 0 = S	-	0.01	0.01	-	0.01	0.01	0.04	0.01	0.01		
Total	99.90	100.08	99.74	100.26	100.27	99.62	99.93	99.79	99.89	99.4	100.2
Ni	99	87	235	98	58	68	32	<2	2	196	63
Cr	399	328	1310	179	27	38	9	3	5	411	171
Rb	12	2	<2	<2	<2	<2	<2	2	2		
Sr	227	139	75	138	100	105	138	212	160		
Ba	166	72	63	67	50	80	65	92	93		
Cu	105	104	56	70	230	277	317	12	7		
Zn	74	55	56	49	64	72	82	45	21		
Zr	30	78	7	9	7	12	11	244	366		
Y	17	33	8	8	9	12	13	96	117		

Table 14:
Chemical analyses of chilled margins of major gabbro intrusions in the Flin Flon area

	WHITE LAKE SILL		MIKANAGAN LAKE SILL				BENN LAKE INTR.		EMBURY LAKE INTR.
Sample No.	(Base) 254-8	(Base) 1312-1	(Base) 2084-1	(Base) 3401-C1	(Base) 3419-C1	(Top) 3146-C1	(East) 2312-2	(West) 2317-2	(Base) 4384-2
SiO_2	47.3	47.7	48.70	48.89	49.77	49.96	48.3	54.2	47.96
Al_2O_3	13.4	13.2	14.02	13.40	13.46	14.78	13.6	14.7	14.82
Fe_2O_3	2.9	4.3	1.54	1.40	1.55	2.54	3.0	2.7	1.88
FeO	11.4	10.1	7.55	8.83	9.05	7.47	11.15	9.83	6.70
CaO	8.8	8.6	10.35	9.40	9.39	10.23	8.9	6.6	13.01
MgO	6.6	6.9	10.91	8.86	8.00	7.31	6.3	4.5	9.58
Na_2O	1.9	2.3	2.41	2.79	2.64	2.43	2.0	1.8	1.41
K_2O	0.4	0.8	0.31	0.47	0.92	0.86	0.6	0.3	0.11
TiO_2	1.8	1.92	0.58	0.73	0.78	0.72	1.78	0.43	0.44
P_2O_5	0.16	0.19	0.06	0.08	0.10	0.05	0.15	0.19	0.04
MnO	0.19	0.15	0.17	0.18	0.21	0.16	0.22	0.15	0.15
H_2O	3.22	3.06	3.23	3.23	2.46	2.88	2.88	3.36	2.90
S	0.1	0.01	0.01	0.00	0.01	0.01	0.01	0.01	0.03
CO_2	0.09	0.22	0.17	1.48	0.70	0.48	0.06	0.17	0.36
Other	0.13	0.12	0.20	0.13	0.16	0.09	0.11	0.1	0.11
Less 0 = S	(0.04)								(0.01)
Total	99.16	99.57	100.21	99.87	99.20	99.97	99.06	99.04	99.49
Ni			186	83	80	45	54	12	116
Cr			820	111	316	88	79	20	348
Rb			2	11	22	11	14	8	0
Sr			190	203	288	228	206	276	140
Ba			100	131	263	249	380	240	31
Cu			86	111	178	44	94	184	50
Zn			100	64	93	39	120	137	66
Zr	66	91	27	31	40	22	73	12	21
Y	27	31	15	18	17	18	29	15	16

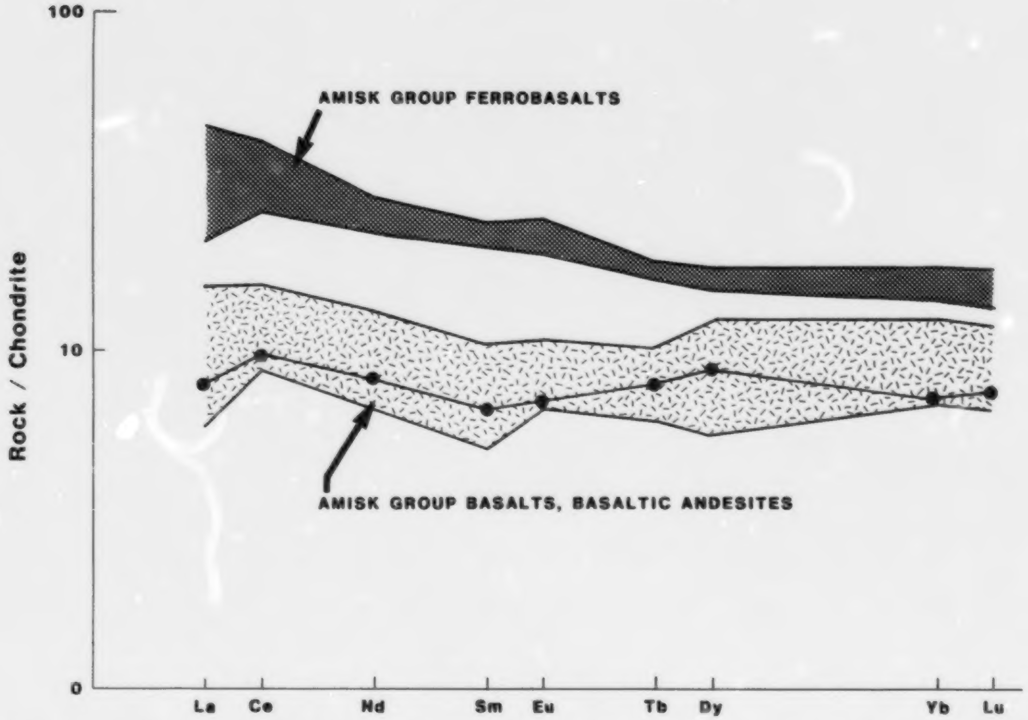

Figure 238: *Chondrite normalized REE plot of sample from chilled margin of Mikanagan Lake Sill, with range for Amisk Group basalts/basaltic andesites and ferrobasalts for comparison.*

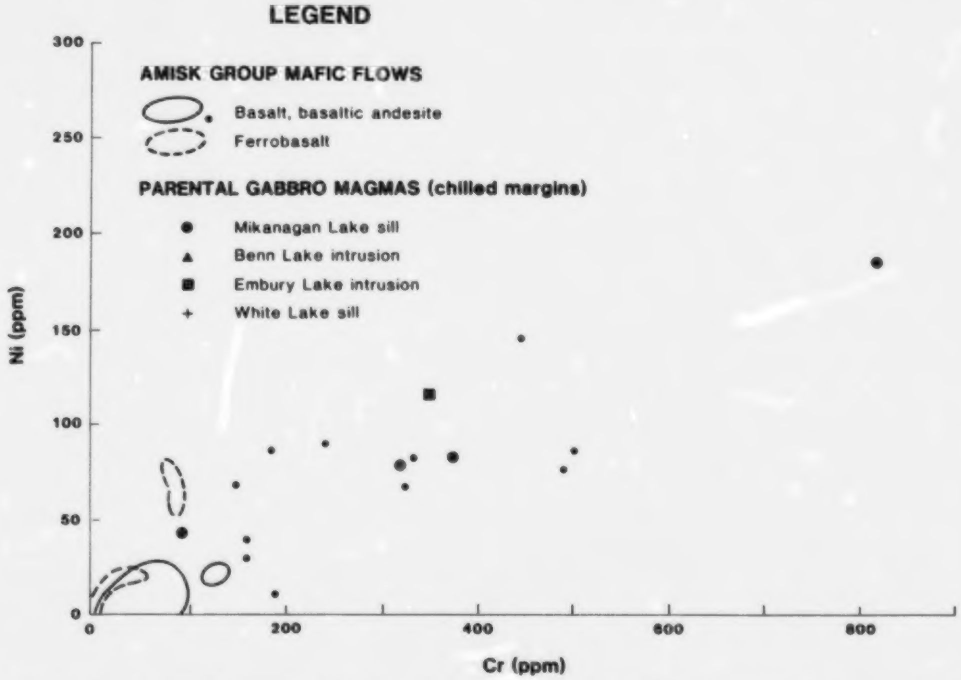

Figure 239: *Ni vs. Cr comparing parental magmas of major gabbro intrusions with fields of Amisk Group basalt/basaltic andesite and ferrobasalt.*

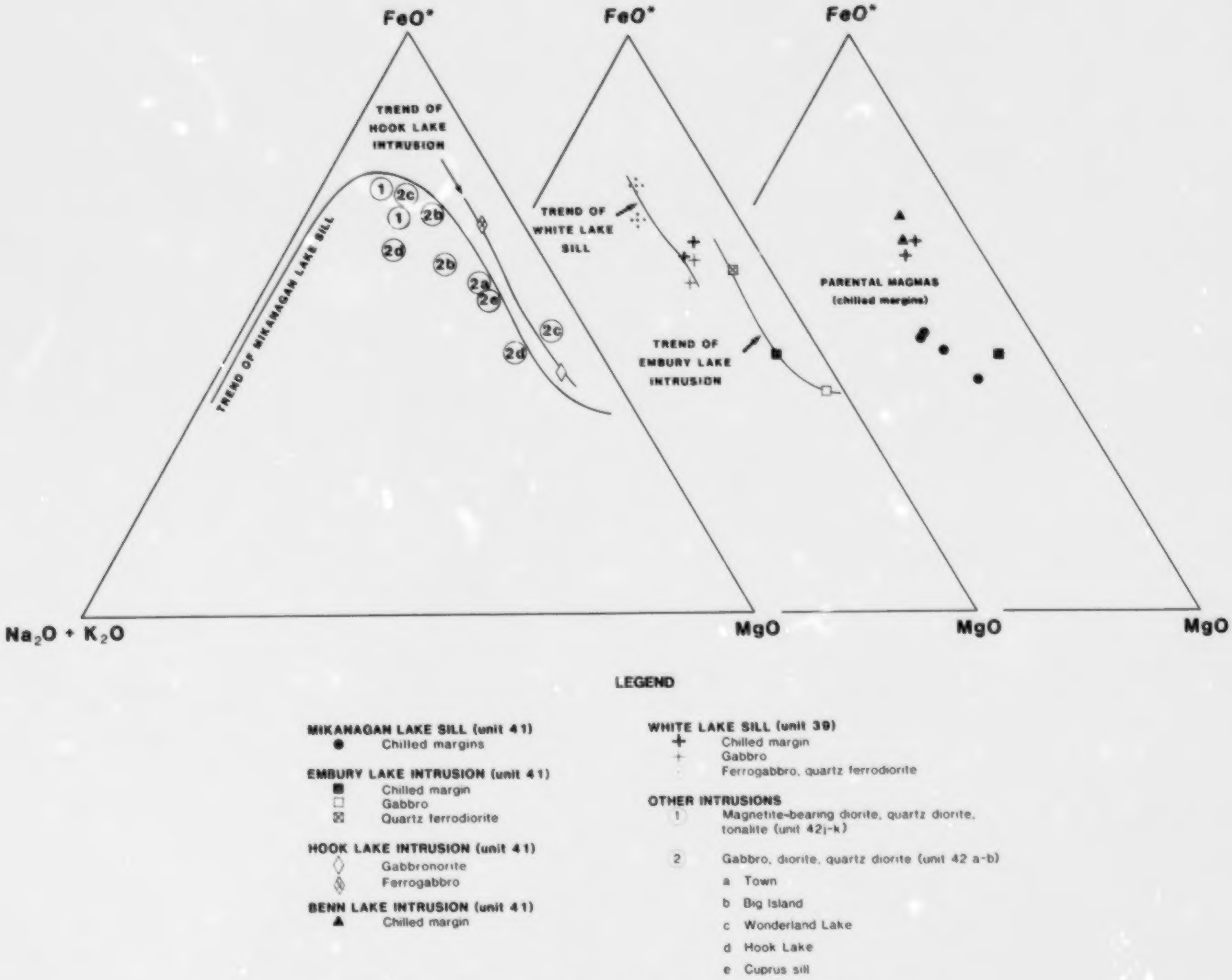

Figure 240: Ternary AFM diagram, mafic intrusions, Flin Flon area.

At the southern termination of the intrusion (Solodiuk Lake) the host volcanic rocks are strongly epidotized and pyritized for up to 300 m from the intrusion. Western and eastern contact zones are up to 150 m wide, in which the host flows are characterized by recrystallization, pervasive weak epidotization and grey-green weathering colour (cf. buff weathering outside the contact zone). Basaltic andesite flows within the contact metamorphic zone are not deformed to any greater degree than those outside.

The contact between the Benn Lake Intrusion and Bear Lake flows is knife-sharp. Fine grained (less than 1 mm) chilled gabbro extends from 2 — 15 m from the contact. Texturally the chilled zone is distinguished by poikilitic amphibole (after pyroxene) that encloses randomly oriented, evenly distributed elongate plagioclase laths (less than 1 mm; 30%). The poikilitic amphibole increases in size from less than 1 mm near the contact to 4 mm within metres of the contact. Fe-Ti oxides vary in abundance (1 — 6%) in the chilled zone, and increase in size (up to 2 mm) in the coarser material.

Gabbronorite (unit 41a)

Gabbronorite dominates the Benn Lake Intrusion. It is massive, relatively homogeneous, weathers shades of brown and is mottled pale green and white on fresh surface. In hand specimen it appears equigranular with a grain size of 2 — 3 mm.

In thin section, orthopyroxene (up to 10 mm across) occurs as medium- to large-sized, anhedral, poikilitic crystals enclosing many smaller clinopyroxene and plagioclase crystals. Clinopyroxene (up to 3 mm) forms a mosaic of anhedral, equant, colourless to pale brown crystals, some of which partially enclose plagioclase. Commonly clinopyroxene, and local orthopyroxene, is partially replaced by late magmatic amphibole. This amphibole also occurs as interstitial grains which appear to have crystallized directly from a fluid phase. Plagioclase (0.2 — 1 mm) occurs as clusters of stubby lath-shaped crystals. Fe-Ti oxides (0.2 — 2 mm) are anhedral and interstitial to plagioclase and both pyroxenes. They commonly occur, in subhedral forms, within late magmatic amphibole.

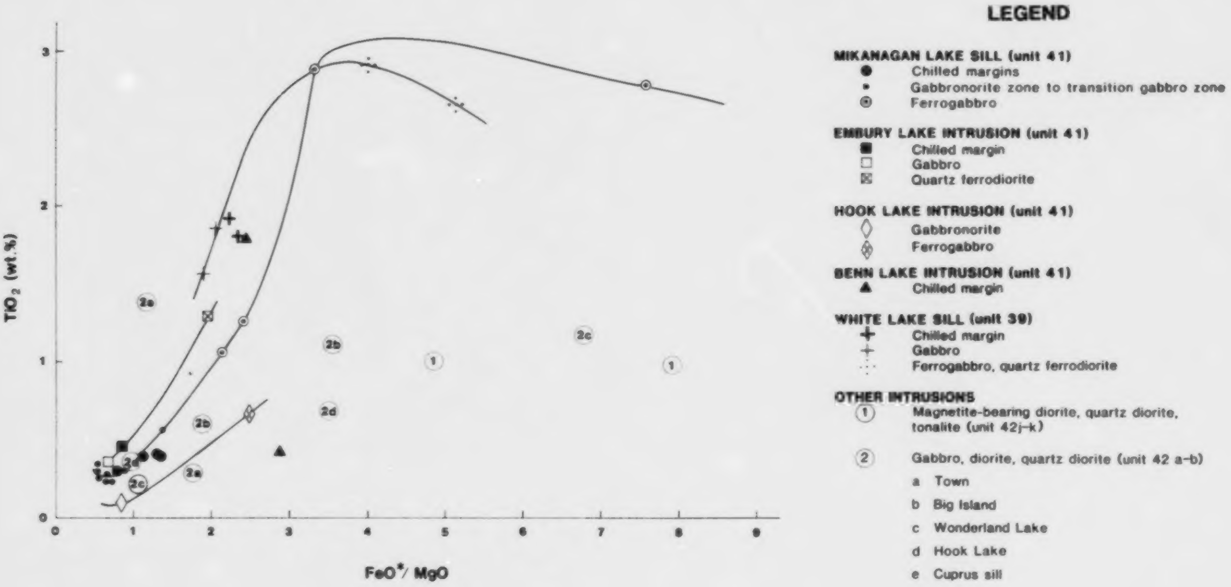

Figure 241: TiO_2 vs. FeO/MgO, mafic intrusions, Flin Flon area.*

Gabbro (unit 41b)

Gabbro forms the core of the intrusion east of Benn Lake and the east margin of the intrusion at Alleyn Lake. It is medium grained (2 mm), massive, homogeneous, weathers identical to gabbronorite and is pale green and white on fresh surface. In places gabbro can be distinguished from gabbronorite in hand specimen by the presence of large orthopyroxene oikocrysts (pseudomorphed by pale green amphibole) in the latter.

Clinopyroxene (0.5 — 2.5 mm) occurs as equant, anhedral to subhedral crystals forming an interlocking mosaic; some clinopyroxene partially encloses stubby plagioclase (0.5 — 1.5 mm) laths. Minor late magmatic brown to greenish amphibole occurs as patches within clinopyroxene. Fe-Ti oxides are present in trace amounts.

Gabbro in the Benn Lake Intrusion differs from gabbro in the Mikanagan Lake Sill in plagioclase and clinopyroxene content (Table 12). The Benn Lake gabbro is considerably more mafic.

Oikocrystic gabbronorite

A distinctive gabbronorite characterized by large (to 10 mm), rusty weathering pseudomorphs after orthopyroxene occurs in scattered outcrops south of Alleyn Lake. This rock type is identical to oikocrystic gabbronorite in the Mikanagan Lake Sill (Table 12). The orthopyroxene crystals are anhedral to subhedral and enclose abundant small clinopyroxene and plagioclase crystals.

In the Benn Lake Intrusion, oikocrystic gabbronorite does not form a mappable entity, as it does in the Mikanagan Lake Sill.

Geochemistry

Analyses of chilled gabbro from the eastern (2312) and western (2317) contacts are significantly different (particularly in SiO_2, FeO*, CaO, MgO, TiO_2, Zr and Y), raising the possibility that the intrusion is a composite body with two slightly different parental magma compositions (Table 13). However, no internal intrusive relationships were observed. Neither chilled gabbro is similar to the chilled phases of the Mikanagan Lake Sill (Fig. 218, 219, 240 and 241). The eastern chilled zone has a composition very similar to the chilled phase of the synvolcanic White Lake Sill (Table 14, Fig. 217, 218, 219 and 241), despite the fact that associated gabbros are completely different.

Hook Lake Intrusion

The Hook Lake differentiated gabbro intrusion (Fig. 220) is a Y-shaped body exposed between Hook Lake and Schist Lake. The western portion of the body, offset by faults, measures almost 3 km in length. Maximum thickness of the intrusion is 240 m.

The intrusion cuts across southeast-facing host volcanic rocks. Ferrogabbro and minor tonalite occur on the northern side of the "Y", indicating that the intrusion tops to the north, opposite to the enclosing volcanic flows. The intrusion, interpreted as a tabular body plus feeder dyke, has been deformed during regional flattening parallel to the north-northeast-trending schistosity.

Unlike the Mikanagan Lake Sill and Benn Lake Intrusion, the Hook Lake Intrusion is cut by numerous porphyritic mafic dykes, some of which are amygdaloidal and presumably high level (Fig. 242).

On the basis of limited petrography the intrusion appears to be composed of gabbronorite (unit 41a), ferrogabbro (unit 41f) and minor micrographic leucotonalite (unit 41h). The gabbronorite is medium- to coarse-grained (2 — 8 mm), massive, weathers white, green and buff, and is mottled green and white on fresh surfaces. It commonly contains coarse grained gabbro pegmatite pods (generally less than 1 m long) and veins up to 30 cm wide (Fig. 243); the veins generally trend between 215° and 260°. Contacts between pegmatite and gabbronorite are sharp to locally gradational. The ferrogabbro and micrographic leucotonalite are similar to their counterparts in the Mikanagan Lake Sill; the ferrograbbro is medium grained, weathers reddish brown and is dark green on fresh surfaces.

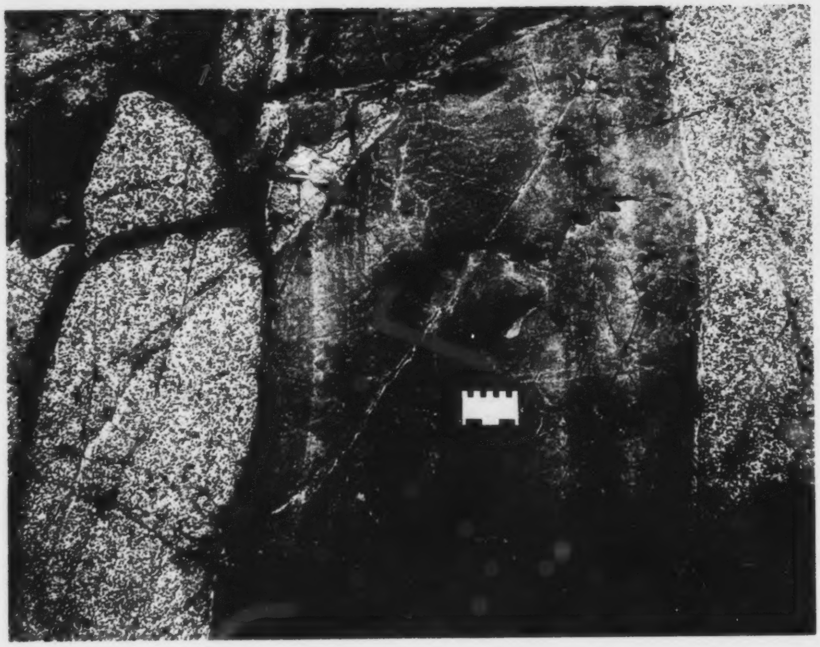

Figure 242: Scale card rests on a banded, fine grained mafic dyke emplaced in Hook Lake gabbronorite (unit 41a), 550 m southwest of Hook Lake. Morphologically similar dykes cutting Amisk Group flows are interpreted to be synvolcanic.

Figure 243: Gabbro pegmatite vein emplaced in Hook Lake gabbronorite (unit 41a), 430 m west of the south end of Hook Lake. Prismatic amphibole (after pyroxene) crystals locally form fan-like arrays nucleated on the vein walls.

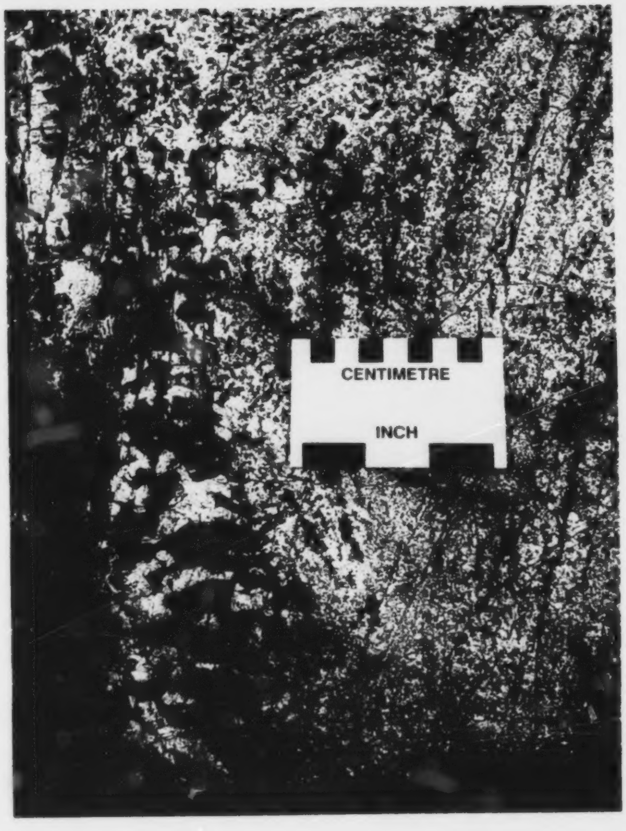

In thin section the gabbronorite is characterized by large, stubby equant plagioclase (1 — 8 mm) and anhedral interstitial pseudomorphs after orthopyroxene (1 — 5 mm). Clinopyroxene (1 — 2 mm) is anhedral and interstitial to plagioclase. Brown to pale green amphibole partially replaces clinopyroxene and is also an interstitial phase. Fe-Ti oxides and quartz are minor, interstitial phases. The Hook Lake gabbronorite differs from Benn Lake gabbronorite in its higher plagioclase content (Table 12) and larger and more equant plagioclase morphology. The large, equant plagioclase crystals also serve to distinguish it from gabbronorite in the Mikanagan Lake Sill.

Ferrogabbro contains euhedral plagioclase laths (0.2 — 1 mm) with a moderate preferred orientation partially enclosed by green amphibole after pyroxene. Fe-Ti oxides (0.1 — 0.4 cm) are euhedral. As in the Mikanagan Lake Sill, the Hook Lake ferrogabbro locally contains trace amounts of chalcopyrite.

On the basis of a single analysis from each of the two zones the Hook Lake Intrusion can be characterized as tholeitic with a strong iron enrichment trend, similar to the Mikanagan Lake Sill (Fig. 240 and 241).

Shore Lake Intrusions

Two differentiated, west-facing mafic intrusions, near Shore Lake, occur in dominantly west-facing basalt flows of the Grassy Narrows Zone (Fig. 220). Basalt flows (not in direct contact with the intrusions) locally face east and north raising the possibility that the gabbro intrusions were emplaced into previously folded rocks. An alternate explanation is that the variable facing direction of host rocks is due to post-intrusion faulting and deformation. Although no post-intrusion faults have been identified between Manistikwan Lake and Shore Lake, unmapped faults are distinctly possible as the Grassy Narrows Zone is characterized by numerous late faults.

The intrusions are zoned from east to west from gabbronorite (unit 41a) to ferrogabbro (unit 41f) to ferrotonalite (unit 41g); zoning that is broadly similar to that displayed by the Mikanagan Lake Sill. The Shore Lake Intrusions are, however, poorly exposed and there are no complete sections across individual zones or zone contacts. Contacts with host volcanic rocks are not exposed.

The larger intrusion is tapered to the north and south, with a maximum width of 380 m at the south end of Shore Lake. It is exposed for 2.75 km in the map area and extends an undetermined distance north of the map area. To the south, the intrusion is truncated against a younger gabbro body (unit 42) and a fault. The smaller intrusion, located 400 m west of Shore Lake, is approximately 120 m wide and 600 m long. A brief description of the individual zones in the larger gabbro body is given below.

Gabbronorite forms the basal 230 m of the intrusion at the south end of Shore Lake. It is massive, homogeneous, equigranular (1 — 2 mm), weathers buff to buff-brown, and is medium green on fresh surface. In the one thin section examined, plagioclase (0.5 — 2 mm) is lath-shaped, euhedral, randomly oriented and clustered in clumps surrounding small, multi-crystal domains of anhedral to subhedral clinopyroxene (0.5 — 2 mm). Clinopyroxene, which partially encloses some plagioclase laths, is locally pseudomorphed by pale green to brown late magmatic amphibole; the amphibole also occurs as an interstitial phase. Orthopyroxene (2 — 4 mm) is anhedral, and encloses crystals of plagioclase and clinopyroxene. Minor Fe-Ti oxide and quartz are present as interstitial grains.

Up to 80 m of ferrogabbro overlies the gabbronorite. The ferrogabbro is massive, homogeneous, weathers reddish brown and is dull medium green to dark green on fresh surface. In one thin section, plagioclase (0.5 — 2 mm) is euhedral, lath-shaped and moderately aligned. Pyroxene (0.5 — 1 mm) is subhedral, equant, and completely replaced by secondary green amphibole. Fe-Ti oxide (0.2 — 0.5 mm) is present as equant subhedral grains, and minor quartz occurs as an interstitial phase.

Buff-brown weathering ferrotonalite forms a discontinuous zone (up to 70 m wide) on the west margin of the intrusion. Where best exposed, southwest of Shore Lake, this zone displays a westerly increase in quartz content and grain size. Typically quartz and plagioclase grains are equant and 1 — 2 mm in size. Amphibole pseudomorphs of elongate pyroxene prisms are generally 5 — 10 mm but locally are up to 5 cm in size. The ferrotonalite contains minor Fe-Ti oxide and on fresh surfaces is dull green to brownish green.

Embury Lake Intrusion

The Embury Lake Intrusion occupies the isthmus between Embury Lake and Manistikwan Lake. Only a portion of what presumably is a much larger intrusion is exposed: the western (top) and northern parts of the body are terminated against major faults. The eastern and southern contacts are intrusive into pyritic siltstone and mudstone. Maximum thickness of the presently exposed portion of the intrusion is 670 m.

The Embury Lake Intrusion (Fig. 118) is predominantly composed of medium grained (1 — 2 mm) gabbro (unit 41b) that weathers light buff to medium brown and is a medium grey on fresh surfaces. About 60 m of light buff quartz diorite (unit 41g) occurs on the western side of the intrusion, indicating that it is a fractionated body that tops to the west.

Gabbro is massive, relatively homogeneous, and distinguished in hand specimen by lath-shaped plagioclase (1 mm, 40%) and interstitial green mafics (1 — 2 mm). Other features noted in the gabbroic portion of the intrusion include:

1) screens of weakly pyritized, foliated felsic volcanic rocks, with dimensions up to 10 m by more than 15 m, occur locally in the western part of the gabbro;
2) rare gabbroic pegmatite pods to over 1 m across are internally zoned and contain pyroxene crystals up to 5 cm long oriented perpendicular to pod margins;
3) a set of irregular, anastomosing, oxidized fractures 1 — 10 mm wide are best developed in the northern half of the body; they are subvertical, generally trend about 025° and are locally folded about axial planes trending 010°.

In thin section, gabbro contains clinopyroxene (0.5 — 3 mm) as anhedral to subhedral grains, some of which enclose small plagioclase crystals. Plagioclase (0.3 — 0.7 mm) occurs as stubby laths which form an open-mesh network between the larger clinopyroxenes. Brown and green late magmatic amphibole occurs interstitial to clinopyroxene and plagioclase, and shows reaction with clinopyroxene. Fe-Ti oxides are a minor phase.

Quartz diorite (unit 41g) is characterized by pseudomorphs after pyroxene up to 15 mm long, occurring as feather-shaped crystals and crystal rosettes. Plagioclase (0.2 — 1 mm) laths occur between pyroxene crystals, and quartz is interstitial to plagioclase. Fe-Ti oxides (up to 1 mm) are anhedral, interstitial to plagioclase and pyroxene. Quartz diorite grades eastward into Fe-oxide rich diorite (poorly exposed) through decrease in quartz content.

The Embury Lake Intrusion has a fine grained, chilled contact 50 — 100 cm wide against pyritic mudstone. An analysis of this chilled gabbro is similar in composition to the chills from the Mikanagan Lake Sill (Table 14, Fig. 240 and 241). A single analysis each of Embury Lake gabbro and quartz diorite outline a trend of extreme iron enrichment which parallels that of the Mikanagan Lake Sill (Fig. 240 and 241). These data, although few in number, suggest that the Embury Lake Intrusion and Mikanagan Lake Sill had similar parental magmas and evolved along similar fractionation paths.

GABBRO, DIORITE, QUARTZ DIORITE (UNIT 42)

Mafic intrusions of unit 42 range in age from syn- to post-volcanic, and vary widely in size, shape, texture and composition. Virtually no two intrusions are identical in all aspects. The intrusions in this unit are subdivided on the geological map on the basis of primary texture and composition; they do not represent a comagmatic suite.

Larger or important intrusions of unit 42 are named and described in Table 14 and located on Fig. 220. Smaller intrusions (shown on the geological map) are not individually described but are generally similar to the corresponding larger intrusions.

Mafic intrusions of unit 42 are abundant west of the Inlet Arm Fault but are relatively minor components of rocks east of the fault. This fact, among other features of the Inlet Arm Fault, indicates that it is one of the most important structures in the area.

The largest intrusions of unit 42, in terms of both size and abundance, occurs on Big Island in Manistikwan Lake (Fig. 220). Here the contrast between two distinct types of mafic intrusion (Big Island diorite and quartz diorite (unit 42a) and Big Island magnetiferous quartz diorite (unit 42j) are particularly pronounced (Table 15). The diorite (unit 42a) is nonmagnetic, hypidiomorphic equigranular, does not contain micrographic intergrowths of quartz and plagioclase, and is somewhat more mafic than unit 42j. The magnetiferous quartz diorite (unit 42j) is strongly magnetic, equigranular with interstitial mafics, and generally contains abundant micrographic quartz-plagioclase intergrowth (Fig. 244). These two intrusion types can also be identified and readily distinguished in the Steeves Lake area to the east (Map GR87-1-1). Unit 42j-type magnetiferous quartz diorite is rare outside the Manistikwan Lake Block.

In most occurrences the intrusions of unit 42 are distinctly different from the major mafic sills previously described. Exceptions to this general rule are the Little Spruce Lake and Cuprus sills (Fig. 220, Table 15), which are stratigraphically associated with, and petrographically similar to, the White Lake Gabbro. However, in contrast to the White Lake Gabbro, the Little Spruce Lake and Cuprus sills are not compositionally zoned.

ROSENBERG LAKE INTRUSIVE COMPLEX (UNIT 43)

The Rosenberg Lake Intrusive Complex (unit 43a) occurs on the west side of Rosenberg Lake Fault and west of Rosenberg Lake. It is bounded by faults on both east and west sides, south of Rosenberg Lake. The complex is a maximum of 390 m wide and is at least 3 km in length. North of Rosenberg Lake the intrusive complex is cut by a genetically related breccia (unit 43b).

The intrusive complex is composed of aphyric and porphyritic intermediate-mafic dykes, equigranular gabbro, and tonalite. South of Rosenberg Lake, gabbro is generally the oldest rock type whereas, north of the lake, intermediate-mafic dykes are oldest. With few exceptions tonalite is the youngest phase.

Intermediate-mafic dykes weather buff to brown and are grey-green on fresh surface. They include a variety of aphyric, plagioclase-phyric and plagioclase-pyroxene-phyric types, all of which are texturally similar to syn-Amisk dykes of the same composition. At Rosenberg Lake a distinctive plagioclase-phyric type with 2 — 6 mm long phenocrysts is intrusive into the aphyric fine- to medium-grained dykes. Plagioclase-pyroxene-phyric dykes south of Rosenberg Lake are 0.5 — 4 m thick and strike 310° — 350°.

Gabbro in the intrusive complex weathers white and dark green to pale buff or brown. Grain size is 1 — 3 mm, comprising lath-shaped crystals of plagioclase and interstitial mafics. Gabbro dykes form a stockwork pattern, similar to the tonalite dykes.

Tonalite weathers white and is grey on fresh surface. It contains 20 — 50% quartz megacrysts up to 6 mm in a 1 — 2 mm groundmass of plagioclase, chlorite and quartz. Tonalite dykes 0.3 — 10 m wide occur as anastomosing stockworks or as boudinaged, disrupted dykes trending 140°. They locally contain xenoliths of mafic volcanic rocks, gabbro, and fine grained intermediate-mafic intrusive rocks.

Breccia (unit 43b) composed largely of intrusive rock fragments occurs north and northwest of Rosenberg Lake. The breccia cuts across

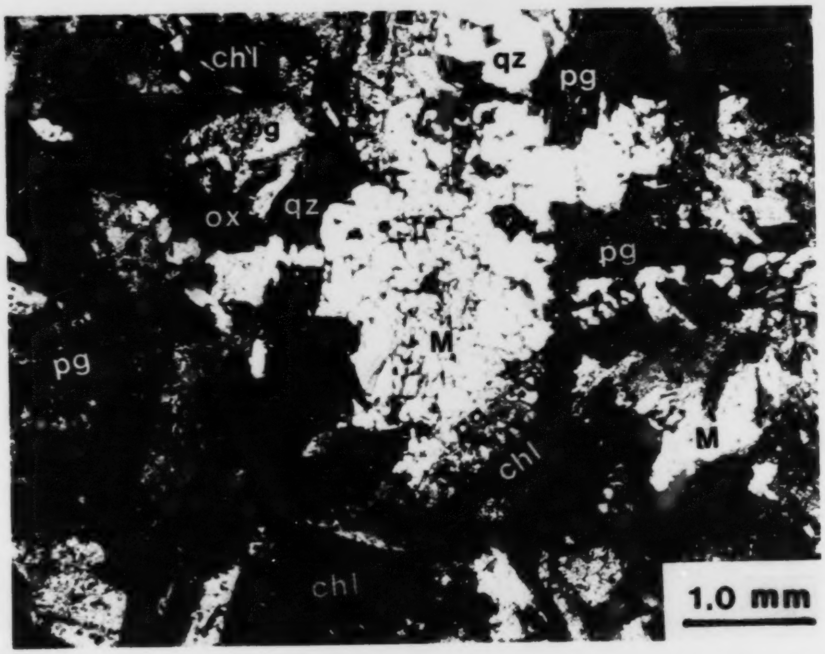

Figure 244: Magnetiferous quartz diorite (unit 42j), Manistikwan Lake. Plagioclase laths (pg; twinned) are partly altered to epidote and chlorite. Large blebs of quartz-feldspar micrographic intergrowth (M) and small blebs of quartz (qz) occur in interstices in plagioclase mosaic. Chlorite (chl) after primary mafic mineral is interstitial. Abundant disseminated magnetite (ox). Sample 4368-1, crossed polarizers.

Table 15:
Colour, mineralogy, texture and general characteristics of various gabbro, diorite and quartz diorite intrusions (unit 42). Location of intrusions on Fig. 220

Intrusion Name	Unit No.	Weathering Colour	Fresh Colour	Grain Size (mm)	Homogeneity	Plagioclase
Town diorite	42b	brown	med-dk green	0.5-3	variable qz content; locally consists of at least 2 phases	40%, 0.5-1 mm, subhedral to euhedral laths, tablets and blocky crystals. Rarely as phenocrysts
Big Island diorite, quartz diorite	42b	reddish brown, buff-brown	med-dk green, grey-green, med grey	1-2	variable qz content; multi-phase with intrusive contacts between phases	45-55%, 0.2-2 mm, lath, tabular and blocky crystals
Big Island magnetiferous quartz diorite	42j	reddish brown, brown, grey-green	dark green	1-1.5	variable qz content	35-55%, 0.2-1.6 mm, subhedral stubby laths
Hook Lake diorite, quartz diorite	42a	reddish brown to light brown	med green	0.3-1	complex of dykes and small irregular intrusions. Local intrusion breccia. Wide variation in qz and micrographic intergrowth	35-60%, 0.5-1.5 mm, laths, stubby laths, replaced by ep and pump
Ledge Lake diorite, quartz diorite	42a, e, f	brown, reddish brown	med green	0.3-0.5	grain size and texture variable. Complex of intrusions	50%, 0.3-1mm, interlocking mosaic of euhedral to subhedral laths and stubby laths
Diorite, quartz diorite commonly associated with rhyolite (unit 49)	42b	medium brown, buff-brown, reddish brown	green, dk green	0.5-2	homogeneous	50%, 0.3-1 mm, euhedral, lath-shaped, weak to mod srct + ep alteration
Oikocrystic gabbro (NW end of Manistikwan Lake)	42e	light buff, buff-brown	light grey, med green	1, with 5-15 mm px oik.	homogeneous	50%, 0.2-2 mm, euhedral to subhedral laths, tablets; replaced by ep, chl, ab
Oikocrystic gabbro (Grassy Narrows Manistikwan Lake)	42e	buff, buff-brown	med green	1, with px to 3 mm	Ophitic to px-phyric	50%, 0.5-1.5 mm, subhedral to euhedral stubby laths

Quartz	Micrographic Intergrowth	Mafics	Fe-Ti Oxides	Accessory	Texture	Other
0-10%, 0.3-0.5 mm, anhedral, interstitial to plag	0-5%, 0.3-1 mm, equant, radiating from a central core. Interstitial to plag	45-55%, 0.5-2 mm, anhedral-subhedral px replaced by green amph. Interstitial to plag; rarely as phenocrysts	2-3%, 0.2-0.5 mm, disseminated, subhedral equant. Replaced by leuxoc		Ophitic, subophitic hypidiomorphic equigranular	
0-20%, 0.5-1.5, anhedral, interstitial to plag; blebby intergrowth with plag	0%	30-50%, 0.5-2 mm, subhedral, blocky to prismatic px replaced by trem-act	2-5%, 0.2-6 mm, disseminated, anhedral to subhedral, some poikilitically enclose plag and px	Apatite: tr.	Hypidiomorphic equigranular	1. Sporadic small (< 50 cm) pegmatitic patches 2. Local oikocrysts to 10 mm diameter 3. Non-magnetic 4. Intrudes units 48a and 48b quartz porphyry
0-20%, 0.1-0.7 mm, anhedral, interstitial to plag	0-12%, 0.1-1 mm, interstitial to plag; some with qz or plag core; radiate from point source; margins of clear qz	25-40%, anhedral, interstitial; larger patches enclose plag. Primary mafic replaced by trem-act, chl, stilp	5%, 0.1-0.4 mm, disseminated, equant; replaced by leucox + mt	Apatite: 1%, 0.1-0.7 mm	Equigranular mosaic of stubby plag laths, interstitial mafic, equant qz, interstitial micrographic qz + plag	1. Weakly epidotized along irregular fractures 2. Strongly magnetic 3. Intrudes units 48a and 48b quartz porphyry 4. Rare amygdales
0-20%, 0.3-1 mm, anhedral equant, interstitial to plag and px, blebby intergrowths with plag	0-15%, 0.3-1 mm, interstitial to plag and px; commonly cored by plag; margins of clear qz	20-40%, 0.2-1.5 mm, subhedral to euhedral cpx; partially replaced by trem-act, ep, chl	2-5%, 0.2-0.4 mm, disseminated, equant, replaced by leucox		Hypidiomorphic equigranular mosaic of plag and cpx; interstitial qz and micrographic intergrowth (when present)	1. Intruded by white aphyric rhyolite (unit 49) 2. Locally contains polymineralic amygdales (0.5-3 mm, 2-3%). 3. Intrudes Hook Lake gabbro (unit 41)
3-5%, 0.3-0.7 mm, anhedral, interstitial to plag	0%	45%, 0.3-1 mm, subhedral mafic replaced by trem-act	3-4%, 0.5 mm, disseminated anhedral to euhedral, equant		Hypidiomorphic equigranular to ophitic	
2-5%, 0.5-1 mm, anhedral, interstitial to plag	0%	45%, 0.2-1 mm, anhedral interstitial to plag; partially encloses some plag. Trem-act	3%, 0.2-1 mm, disseminated anhedral to subhedral, interstitial; pseudomorphed by leucox, mt, hmt, chl	Apatite: tr.	Subophitic	1. Intrudes rhyolite (unit 49): chilled contacts, rhyolite xenoliths; irregular dyke-like bodies
0%	0%	40-45% total, up to 25% oikocrysts. Oikocryts are anhedral, enclose plag, Fe-Ti ox, replaced by single crystals of trem-act. Remainder of mafics are interstitial to plag	3-8%, 0.2-1 mm, anhedral to subhedral, some skeletal; interstitial		Ophitic, with large, distinct px oikocrysts	
0%	0%	40%, 0.5- 3 mm, anhedral to subhedral interstitial px replaced by trem-act and chl; partly to completely enclose plag	4-7%, 0.3-1 mm, subhedral, equant, rarely skeletal; interstitial to plag, enclosed by px		Subophitic to ophitic	

Table 15 (continued)

Intrusion Name	Unit No.	Weathering Colour	Fresh Colour	Grain Size (mm)	Homogeneity	Plagioclase
Wonderland Lake	42b					
a) gabbro (west half of intrusion)		light brown, rarely light green	mottled white and medium green	0.5-2	qz present, in small amounts, only adjacent to gradational "contact" with quartz diorite	25-30%, 0.5-1 mm, equant to tabular, subhedral, commonly replaced by ep and ab
b) quartz diorite (east half of intrusion)		buff-brown to reddish brown	dk green or mottled white and dk green	0.5-2	variable qz and Fe-Ti oxide content	40%, 0.5-1 mm, subhedral to euhedral stubby laths; replaced by ep
Little Spruce Lake sill (diorite, quartz diorite)	42a, g	lt to med brown	lt-med grey, grey-green	1	relatively homogeneous. Quartz diorite occurs in core of sill west of Cuprus Mine	45%, 0.2-1 mm, lath shaped to stubby tabular, some anhedral; partial alteration to ep + chl
Cuprus sill (diorite)	42a	lt brown, brown, reddish brown	med-dk grey, med-dk green	0.25-1	relatively homogeneous. Multiple intrusions in Cuprus Mine area. Quartz diorite west margin, west of Two Portage Lake	30-40%, 0.2-1 mm, laths, stubby laths and equant grains; replaced by ep + chl
We Lake sill (diorite, quartz diorite)	42a	dk grey, med brown, reddish brown	med grey, dk green	0.3-1	qz content variable, probably more than one phase	30-45%, 0.3-1 mm, subhedral to euhedral stubby laths replaced by ep + chl
Sourdough Bay sill						
a) ophitic gabbro	42f	brown, reddish brown	med-dk green	0.5-1	abrupt variations in grain size and texture	30-40%, 0.2-1 mm, euhedral narrow laths
b) gabbro, quartz diorite	42b, d	buff to reddish brown	mottled white and green	1-2.5	as above	35-45%, 0.5-2.5 mm, equant to tabular subhedral

Quartz	Micrographic Intergrowth	Mafics	Fe-Ti Oxides	Accessory	Texture	Other
0-2%, 0.2, anhedral, interstitial	0%	65-70%, 0.5-2.5 mm, subhedral, px replaced by trem-act + chl. Minor late magmatic amph	0-tr., 0.2-0.3 mm, equant, replaced by leucox		Hypidiomorphic equigranular	1. Gabbro contains up to 5% white mica 2. Gabbro occurs on west side of intrusion and has a gradational contact with quartz diorite which forms most of east side of intrusion 3. Wonderland Lake intrusion truncates We Lake sill
5-20%, 0.5-2 mm, anhedral, interstitial to subhedral. Coarse blebby intergrowths with plag	0-15%, 0.5-2 mm, cored by plag, coarsens to margin	35-45%, 0.5-2 mm, subhedral to euhedral, equant to prismatic px, replaced by green trem-act	2-5%, 0.2-1 mm, small equant grains to larger skeletal grains	Apatite: tr.	Hypidiomorphic equigranular	
0-tr. in diorite 5% in quartz diorite, 0.2-0.5 mm	0%	50%, 0.4-1 mm, subhedral prismatic px replaced by trem-act + chl	3%, 0.2-1.5 mm, anhedral interstitial, pseudomorphed by leucox and hmt	Apatite: tr., commonly assoc. with Fe-Ti ox	Hypidiomorphic equigranular	1. Minor epidote veining parallel to foliation
0-tr.	0%	55-65%, 0.3-1 mm, subhedral px replaced by trem-act, anhedral interstitial amph. Anhedral mafic partially encloses plag	3-7%, 0.2-1mm, anhedral interstitial to plag and px; replaced by leucox		Hypidiomorphic granular. Moderately to strongly foliated	1. Chilled margins 2. Chilled against Johnson Lake Sill ferrogabbro (unit 39b) 3. Local sharp, intrusive contacts between different phases 4. At Cuprus Mine, multiple intrusions 5-200 m thick are separated by screens of amygdaloidal mafic flows 5. Locally contains regularly-spaced epidote-alteration veins 2-20 cm wide spaced 20-40 cm apart, imparting pseudo-layering 6. Local shear zones parallel schistosity. Local fault contact with volcanic rocks 7. West of Two Portage Lake: 15 m of quartz diorite on west margin of sill. Rhyolite xenoliths
0-10%, 0.2-1 mm, anhedral equant to subhedral, interstitial	0-5%, irregular patches marginal to qz	45-55%, 0.5-1 mm, subhedral prismatic px replaced by trem-act + chl. Stilp overprint	3-7%, 0.2-0.5 mm, disseminated anhedral equant	Apatite: 0-tr.	Hypidiomorphic equigranular	1. Commonly foliated, with poor preservation of texture
0%	0%	50-60%, 0.5-1.5 mm, anhedral-subhedral px replaced by trem-act; partly to completely enclose plag	5%, 0.2-0.5 mm, disseminated subhedral equant		Ophitic	1. Ophitic gabbro forms marginal 30-60 m of sill 2. Chilled margin several metres thick, characterized by plag microlites and spherulites
0-10%, 0.2-0.5 mm, anhedral, interstitial to plag and px	0%	40-50%, 0.5-2.5 mm, anhedral to subhedral px replaced by trem-act; partly encloses plag. Minor late magmatic amph	5%, 0.5-1.5 mm, skeletal, assoc. with late magmatic amph	Apatite: 0-tr.	Subophitic to hypidiomorphic equigranular	3. Gabbro-quartz diorite forms central 90-120 m of sill; gradational contacts with ophitic gabbro

Table 15 (continued)

Intrusion Name	Unit No.	Weathering Colour	Fresh Colour	Grain Size (mm)	Homogeneity	Plagioclase
Post Island sill						
a) quartz diorite	42g	buff to buff-brown	med green	0.5-1	homogeneous	35-40%, 0.3-1 mm, tablets, laths
b) tonalite	42h	white or pale buff	pale to med green	0.5-1 (up to 3)	texture, grain size and composition variable	40-45%, 0.5-2 mm, euhedral laths
Bazinet Lake sill (gabbro, px-phyric gabbro)	42f, d	buff-brown, brown	med to dk green	1-2, px to 10	non-porphyritic to porphyritic	40-45%, 0.5-2 mm, euhedral to subhedral stubby laths and tablets
Sawmill Lake intrusions (meladiorite, diorite, quartz diorite)	42i	buff, buff-brown, shades of green, grey	med-dk green	0.5-1, phenocrysts to 7 mm	Multiphase; wide variations in composition and texture	30-35%, 0.3-1.5 mm, blocky phenocrysts to 5 mm. Subhedral to euhedral stubby laths

Abbreviations

ab	albite	chl	chlorite	leucox	leucoxene	px:	pyroxene	stilp:	stilpnomelane
act	actinolite	ep	epidote	mt	magnetite	qz:	quartz	trem:	tremolite
amph	amphibole	hmt	hematite	plag	plagioclase	srct:	sericite	cpx	clinopyroxene

volcanic stratigraphy and across pyroxene-phyric gabbro (unit 42e), and, according to R. MacQuarrie (pers. comm., 1983) dyke-like bodies of breccia locally cut across the Rosenberg Lake Intrusive Complex (unit 42a). In general, contacts with the intrusive complex are sharp. The breccias are characterized by a high proportion of angular rock fragments in a matrix of gabbro granules, plagioclase and quartz grains and, locally, carbonate. Fragments are typically granule-size to 50 cm; largest blocks are 2.5 m across. Fragment lithologies include pyroxene-phyric gabbro, fine grained intermediate-mafic dyke rocks, plagioclase-phyric mafic dyke rocks, tonalite, and rare mafic and felsic volcanic types. Tonalite and intermediate dykes locally cut the breccia; in some localities these dykes are tectonically disrupted resulting in highly irregular forms in a schistose matrix. The origin of the breccia is uncertain but it is likely genetically related to the Rosenberg Lake Intrusive Complex and is probably an intrusion breccia.

CHANNING TONALITE (UNIT 44)

A small body of strongly deformed tonalite, exposed at and south of Channing, intrudes Amisk Group volcanic rocks and unit 42f ophitic gabbro; it is nonconformably overlain by Missi Group conglomerate. It is one of the few unequivocably pre-Missi felsic plutons in the Flin Flon area.

The tonalite weathers rusty buff to buff and is rusty buff, grey-green or grey on fresh surfaces. It has a hypidiomorphic equigranular texture and 1 — 3 mm grain size, but the rock is typically strongly foliated so that primary textures are not well preserved. Foliation ranges in type and intensity, from closely spaced (5 — 10 mm) discrete cleavage planes to felsic schist. In least-deformed examples, plagioclase (1 — 4 mm, 60%) is subhedral interlocking, with a moderate sericite-chlorite-epidote alteration. Quartz (0.5 — 3 mm, 25%) is rose to lavender, anhedral, equant, interstitial to plagioclase, and commonly finely intergrown with plagioclase in interstices between plagioclase crystals. Chlorite (10%) is interstitial to plagioclase, and local, partially oxidized pyrite (3%) occurs with chlorite and along fractures. Apatite (0.1 mm, trace) forms euhedral crystals associated with chlorite.

On a map scale, Channing tonalite is clearly nonconformably overlain by Missi Group sedimentary rocks, although the actual contact is not exposed. Contrary to Stockwell (1960) this tonalite is not likely to be a schistose equivalent to the Cliff Lake Pluton (unit 45), mainly because it lacks the characteristic quartz-megacrystic character of the Cliff Lake tonalite.

CLIFF LAKE PLUTON (UNIT 45)

The Cliff Lake Pluton is a multiphase, quartz-megacrystic tonalite stock that occurs in the Hook Lake Block, east of Cliff Lake. Approximately 70 — 80% of the intrusion is exposed in lichen-free outcrops, permitting several similar but discrete phases to be mapped. The pluton is 6.2 km long and a maximum of 1.8 km wide; the elongate shape is partly due to displacement of up to 1.2 km along north- and northwest-trending faults. A number of features in the intrusion, including magmatic stoping of wall rocks, mineralized breccia pipes (Baldwin, 1980), and abundant Amisk xenoliths, suggest that the Cliff Lake tonalite is a high-level intrusion.

The age of the Cliff Lake Pluton relative to the Missi Group has been a source of controversy for many years (Baldwin, 1980; MacQuarrie, 1980; Stauffer, 1974). The intrusion is emplaced entirely within Amisk Group volcanic rocks and therefore its age relative to the younger Missi Group is based solely on indirect evidence from geological relationships and isotope dating procedures. Geological evidence for age of the intrusion relative to the Missi Group is inconclusive. For example, although no similar

Quartz	Micrographic Intergrowth	Mafics	Fe-Ti Oxides	Accessory	Texture	Other
5-15%, 0.2-1.5 mm, anhedral to subhedral, interstitial to plag	0-5%, irregular patches intergrown with qz, interstitial to plag	35-45%, 0.5-1 mm, completely recrystallized replaced by tremact + chl	5%, 0.3-3 mm, subhedral irregular	Apatite: tr.	Hypidiomorphic equigranular	1. Tonalite intrudes quartz diorite; no chilled margins
15-20%, 0.5-2 mm, subhedral	15-20%, irregular patches grading into qz grains; interstitial to plag and Fe-Ti ox	20-35%, replaced by trem-act + chl Locally forms radiating xls up to 20 mm long	5-8%, 0.2-0.4 mm, euhedral to subhedral	Apatite: tr.	Hypidiomorphic equigranular	
0%	0%	55-60%, 0.5-10 mm, euhedral to subhedral px replaced by trem-act; contain inclusions of plag and Fe-Ti ox	2-3%, 0.5-1 mm, skeletal; interstitial to plag. Replaced by leucox		Ophitic to porphyritic	1. Px-phyric type is typical of the west side of the sill
0-20%, 0.3-0.5 mm, anhedral, interstitial to plag and px	0%	45-50%, 0.3-1 mm, phenocrysts up to 7 mm. Subhedral to euhedral px replaced by trem-act. Phenocrysts partly enclose plag	1-3%, 0.2-0.4 mm, subhedral; replaced by leucox	Apatite: 0-2%	Hypidiomorphic granular to subophitic with phenocrysts of px and plag	1. Chilled margins 2. Different phases chilled against older phases 3. Locally forms matrix of intrusion breccia, with volcanic xenoliths 4. Similar to Boundary intrusions (unit 51)

Abbreviations:

ox:	oxides	assoc:	associated	dk:	dark	mod:	moderate
pump:	pumpellyite	oik:	oikocrysts	med:	medium	tr:	trace
		xls:	crystals	lt:	light		

intrusive rocks cut the Missi Group, clasts of Cliff Lake tonalite were not observed in Missi conglomerates. Isotopic dating suggests a pre-Missi age for the Cliff Lake Pluton. Missi Group volcanic rocks from the east end of the Flin Flon volcanic belt, at Wekusko Lake, yielded a U/Pb zircon age of 1832 +/-2 Ma, whereas the Cliff Lake Pluton is older, with a U/Pb zircon age of 1871 + 34/-24 Ma (Gordon et al., 1987 and 1989). Although the age for the pluton overlaps the age of Amisk Group volcanic rocks at Flin Flon (1886 +/- 1.3 Ma, Syme et al., 1987) the pluton is not necessarily syn-Amisk as it clearly cuts late rhyolite dykes (unit 49); this is discussed further in the section on Age Relationships at the end of this chapter.

The Cliff Lake Pluton is composed of six discrete mappable units (45a to 45f) and minor associated aplite dykes. The oldest unit (45a) is a non-megacrystic quartz diorite that occurs only as large xenoliths in unit 45b tonalite. The remaining tonalite units are distinguished by the amount and degree of assimilation of contained recrystallized volcanic xenoliths.

Quartz diorite (unit 45a)

The oldest phase in the Cliff Lake Pluton is a quartz diorite that occurs only as large xenoliths in unit 45b tonalite. The xenoliths are angular and up to 500 m long; several of the larger xenoliths are shown on the geological map. The quartz diorite xenoliths themselves locally contain small, recrystallized mafic volcanic xenoliths up to 30 cm across.

Quartz diorite weathers buff-brown to brown and is dark grey-green on fresh surfaces. It has a hypidiomorphic to subophitic equigranular texture with a grain size of 1 — 4 mm. Plagioclase (0.2 — 4 mm, 25 — 45%) occurs as subhedral-euhedral stubby tablet-shaped crystals extensively replaced by fine grained epidote and sericite. Mafic minerals include green amphibole, and secondary tremolite-actinolite and chlorite; these form anhedral to subhedral prismatic crystals (0.4 — 6 mm, 45 — 60%) that locally enclose plagioclase. Quartz (0.2 — 3 mm, 5 — 15%) occurs as anhedral grains interstitial to plagioclase and amphibole. Fe-Ti oxides, pseudomorphed by sphene, chlorite and leucoxene, are equant to subhedral or skeletal grains (0.1 — 0.7 mm, 0.5 — 3%). Apatite (0 — trace) occurs as euhedral prisms in quartz.

Quartz-phyric tonalite with abundant large xenoliths (unit 45b)

This distinctive phase of the intrusion occurs at the southwest margin of the pluton and in a fault-bounded slice at its south end. It is characterized by abundant, slabby, relatively unassimilated xenoliths of recrystallized mafic volcanic rocks and unit 45a quartz diorite. The tonalite has a sharp, irregular contact with host volcanic rocks (Fig. 245). Locally the tonalite intrudes pillowed basalt along pillow selvages and fractures (Fig. 246 and 247). A particularly well exposed example of this contact relationship is located 580 m east of the north end of Grant Lake. At that locality the contact is gradational, and displays an increase in tonalite component over about 70 m, from minor veins along pillow selvages to abundant tonalite with stoped pillows, pillow fragments and selvage fragments. Farther from the contact the basalt xenoliths become more recrystallized and contain plagioclase, amphibole and quartz blasts.

An intrusive contact between this phase of the tonalite and unit 45c tonalite (Fig. 248) is superbly exposed along virtually its entire length. The contact is sharp, nearly vertical, irregular/serated, with unit 45c tonalite chilled against unit 45b. A wide (16 m) zone of moderately rusty weathering gossan in the older, unit 45b tonalite locally occurs adjacent to the contact. The contact has 1.2 km of right-lateral offset across the Big Charlie Lake Fault.

Tonalite weathers white and is pale grey on fresh surfaces. Plagioclase (0.5 — 4 mm, 50 — 60%) occurs as subhedral, equant crystals with moderate alteration to epidote and sericite. Quartz (1 — 8 mm, 30 — 40%) occurs as equant megacrysts and smaller interstitial grains.

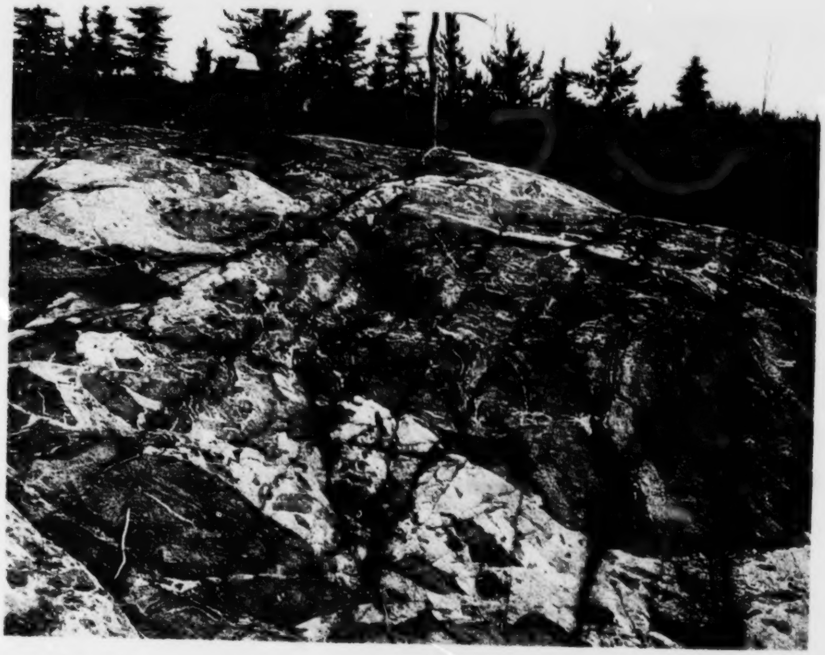

Figure 245: Western contact of Cliff Lake Pluton (unit 45b) with host pillowed basalt (unit 7). Large xenoliths of basalt and numerous irregular tonalite dykes characterize pluton margin. 600 m east of Grant Lake.

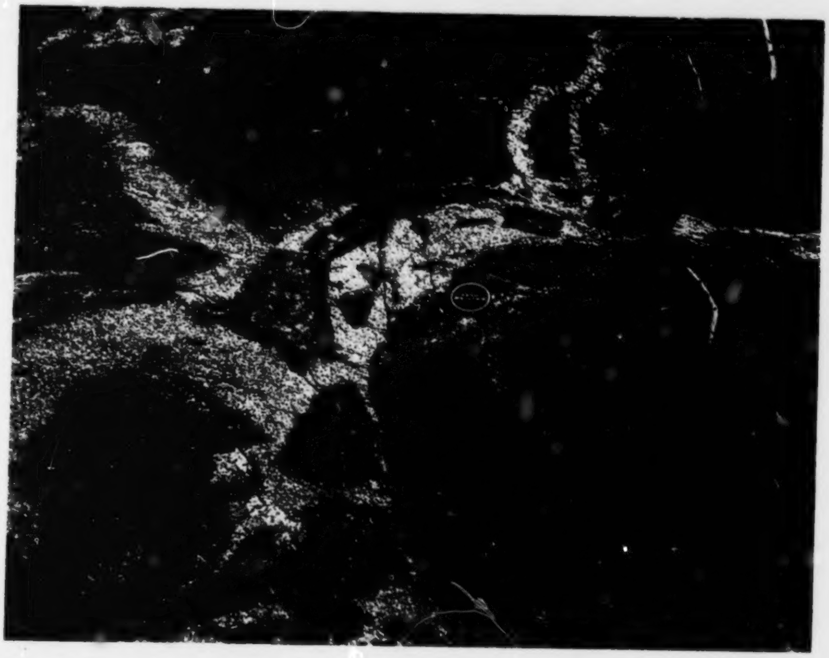

Figure 246: Contact zone of the Cliff Lake Pluton (unit 49), 600 m east of Grant Lake. Apophyses of tonalite (light) have intruded a pillowed mafic flow along the contacts between pillow selvages and pillow margins, resulting in xenoliths composed of selvage (dark) and interpillow epidosite (lighter).

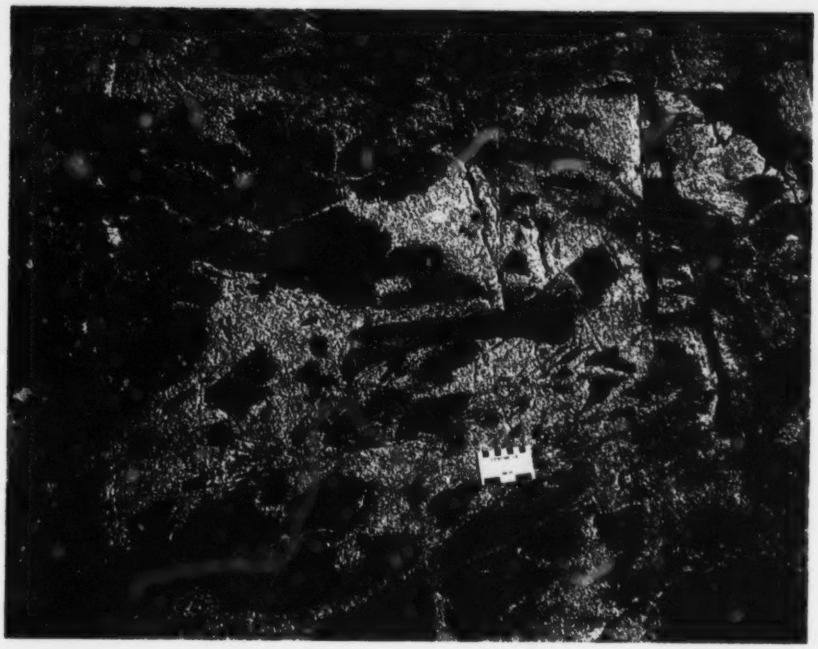

Figure 247: Xenoliths of basalt in unit 45b, Cliff Lake Pluton. Many xenoliths display remnants of dark pillow selvages (arrows). 600 m east of Grant Lake.

Figure 248: Intrusive contact (arrows) between tonalite with abundant large mafic xenoliths (unit 45b) and younger tonalite with fewer and smaller xenoliths (unit 45c). Cliff Lake Pluton, 850 m east of Grant Lake.

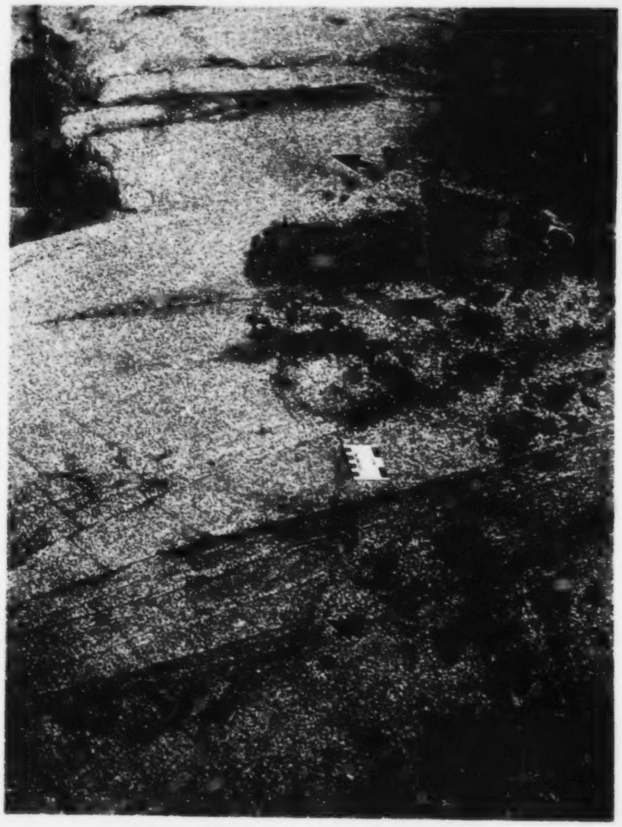

The megacrysts are single strongly strained crystals with slightly irregular, interstitial boundaries with plagioclase; some have crudely hexagonal outlines. Mafic minerals (0 — 15%) include local amphibole, chlorite, epidote and biotite, interstitial to plagioclase. Fe-Ti oxides (to 0.5 mm, trace — 1%) are subhedral and pseudomorphed by leucoxene, magnetite and hematite. Apatite (to 0.2 mm, trace — 0.5%) occurs as small euhedral prisms enclosed by chlorite and Fe-Ti oxides. Other accessory minerals include tourmaline (overprinting chlorite), allanite and zircon.

Mafic xenoliths are the most conspicuous components of this phase of the pluton. The xenoliths are angular or slabby to nebulous and lensoid, and are generally about 10 — 200 cm long. The xenoliths vary widely in abundance, and commonly are concentrated in linear, inclusion-rich zones in which xenoliths are aligned (Fig. 249).

Xenoliths of basalt display a range in recrystallization textures as a result of elevated temperature and metasomatism, from fine grained with relict volcanic structures, to coarse grained pseudo-quartz diorite with large plagioclase, amphibole and quartz blasts. Quartz amygdales in host pillowed basalt are obliterated by even moderate recrystallization. Zones of recrystallization in xenoliths locally follow fractures or form irregular patches within finer grained basalt. Quartz blasts similar to the megacrysts in the tonalite occur sporadically in some recrystallized xenoliths. Tourmaline (associated with chlorite) occurs in small amounts in the moderately to strongly recrystallized rocks.

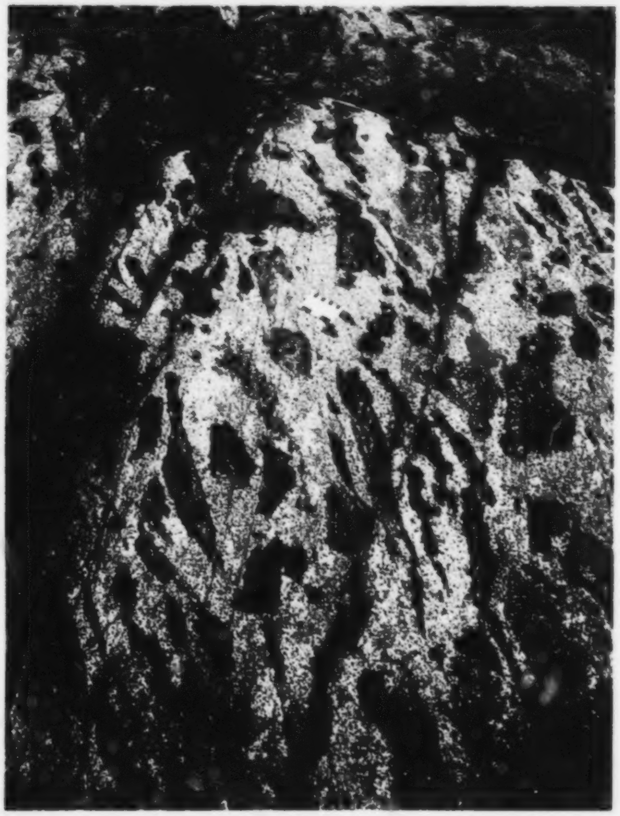

Figure 249: Aligned, partially assimilated mafic xenoliths in Cliff Lake tonalite (unit 45b), 1430 m southeast of Grant Lake. Typical of the inclusion-rich phase of this pluton.

Quartz-phyric tonalite with abundant small, highly digested xenoliths (unit 45c)

This phase of the Cliff Lake Pluton is characterized by abundant (commonly 25 — 40%) small (2 — 5 cm), highly assimilated, rounded, recrystallized mafic xenoliths. It contains *none* of the large, conspicuous xenoliths so characteristic of unit 45b tonalite. As discussed previously, the contact between units 45b and 45c is sharp and intrusive, with unit 45c chilled against unit 45b. The contact with unit 45d is faulted and relative ages are not known.

This phase of the intrusion appears to be relatively homogeneous. However, 300 m west of Big Charlie Lake the tonalite is characterized by repeated dyke-like intrusions with chilled, inclusion-free margins and xenolith-bearing cores. Thus unit 45c may be a composite of several related small intrusions.

Unit 45c tonalite weathers white to creamy buff and is pale grey on fresh surfaces. Texturally and mineralogically it is similar to unit 45b tonalite discussed previously. The abundance of mafic minerals ranges from 2% (in a chilled margin) to 35%, depending upon the abundance of assimilated mafic xenoliths (Fig. 250).

Quartz-phyric leucotonalite and micrographic leucotonalite with few, small, highly assimilated xenoliths (unit 45d)

This unit forms an elongate, lensoid body separated from unit 45c tonalite by two major faults. It differs from unit 45c in that it is generally more leucocratic, contains very few, small, highly assimilated mafic xenoliths, and in its central portion contains abundant plagioclase-quartz micrographic intergrowth. This is the only phase of the Cliff Lake Pluton that also occurs in a separate body, at Cope Lake, outside the main pluton.

Tonalite (unit 45d) in the main pluton weathers white, pale buff to light pink and is white to light pink on fresh surfaces. It contains rare, small (up to 5 cm), rounded, almost completely assimilated xenoliths; in most exposures xenoliths cannot be identified. A systematic compositional and textural variation is present in this phase of the intrusion. At the east and south margin the tonalite has a hypidiomorphic inequigranular texture with quartz (40 — 50%) as small interstitial grains and subhedral, up to 6 mm megacrysts. Plagioclase (0.5 — 6 mm, 45 — 50%) occurs as subhedral equant crystals; mafic minerals (3 — 6%) include chlorite, epidote, rare biotite, magnetite and sphene. Towards the centre of the plug quartz megacrysts become more euhedral and the tonalite contains up to 25% micrographic intergrowth of quartz and plagioclase. In addition, the modal abundance of mafic minerals decreases in the core area.

The core of unit 45d tonalite southeast of Big Charlie Lake is also the locus for abundant alteration features, including:

1) pervasive epidotization, most intense adjacent to fractures (Fig. 251)
2) sericitization of plagioclase
3) chlorite and magnetite coatings on fractures
4) silicification along and adjacent to fractures
5) anastomosing chlorite networks (Fig. 252)
6) local disseminated pyrite, rare chalcopyrite
7) carbonate-filled fractures
8) hematization of plagioclase adjacent to joints and fractures.

The unit 45d tonalite plug east of Cope Lake is a multiphase intrusion with locally abundant screens of host volcanic rocks. Quartz-phyric tonalite and micrographic leucotonalite (unit 45d) are the major lithologies in this small complex body. Dyke complexes composed of a number of texturally and compositionally different tonalite phases are common. Portions of this plug-like body are crosscut by zones of chloritic alteration.

Fine grained, quartz-phyric micrographic tonalite (unit 45e)

Two small, poorly defined plug-like bodies of fine grained porphyritic tonalite (unit 45e) occur east and west of Big Charlie Lake, in units 45d and 45c, respectively. This tonalite has sharp contacts with enclos-

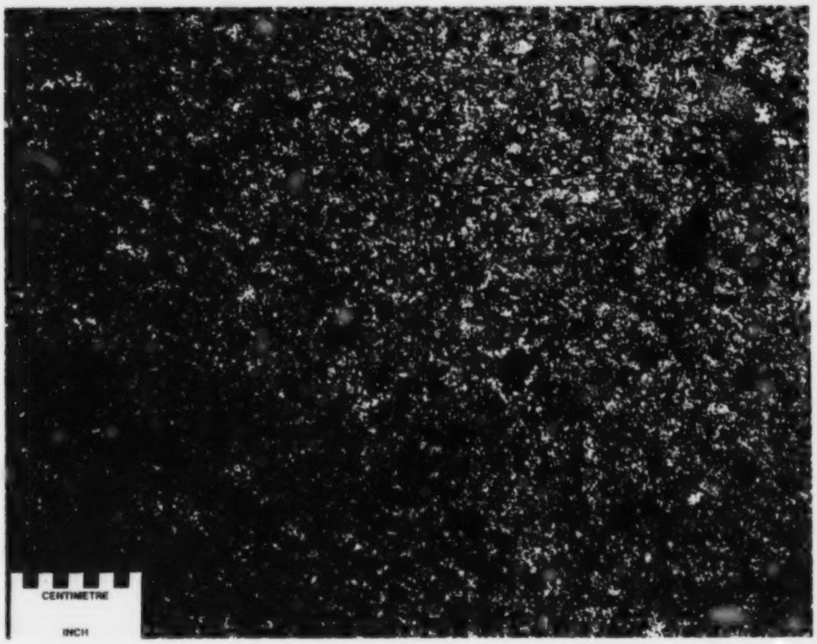

Figure 250: *Small mafic xenoliths (arrows) in quartz-phyric tonalite (unit 45c), Cliff Lake Pluton, 850 m east northeast of Grant Lake.*

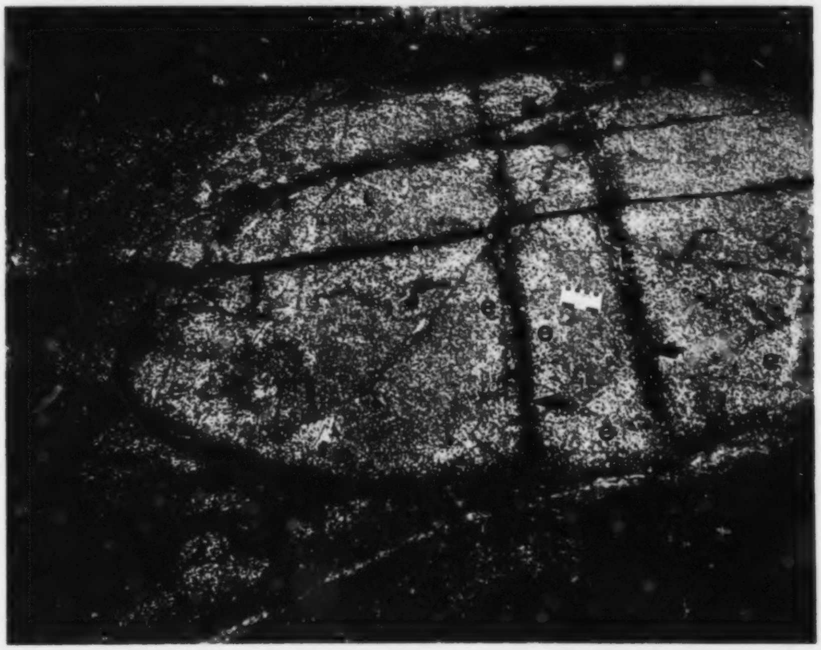

Figure 251: *Cliff Lake tonalite (unit 45c) displaying envelopes of epidotization (e, lighter shade) around rusty chloritic fractures (arrows). 580 m south-southwest of Big Charlie Lake.*

ing coarser, quartz-megacrystic tonalite, weathers white to cream and is pale buff on fresh surfaces. The porphyritic tonalite is characterized by oval quartz phenocrysts (1 — 6 mm) and plagioclase phenocrysts (2 — 3 mm) in a fine grained (0.2 — 0.6 mm) aplitic groundmass of plagioclase, quartz, minor micrographic quartz-plagioclase intergrowth, chlorite and epidote.

Leucotonalite marginal phase (unit 45f)

The northern end of the plug-like unit 45d tonalite has a marginal phase of leucotonalite. East of Big Charlie Lake this white-weathering marginal phase is 10 m wide and is intruded by unit 45d tonalite. To the north the leucotonalite widens, to form the irregular termination of the intrusion; to the south the marginal phase disappears.

The leucotonalite contains rare small tabular xenoliths, is not conspicuously quartz-megacrystic, and contains only about 5% mafic minerals, mainly chlorite. The texture is a 1 — 3 mm mosaic of subhedral plagioclase, anhedral quartz and interstitial mafics.

Micrographic aplite dykes

Light pink micrographic aplite dykes occur in all phases of the Cliff Lake Pluton but are rarely observed outside the intrusion; they are the youngest intrusive phase of the pluton. The dykes are generally only a few centimetres wide (up to 50 cm), straight-walled and continuous, and have no preferred orientation. They are characterized in thin section by a fine grain size (less than 1 mm), abundance (60% or more) of fine quartz-plagioclase intergrowth commonly radiating from a point source or crystal, negligible mafics, a small amount of white mica and accessory sphene and allanite. Thicker dykes are weakly porphyritic.

Post-Cliff Lake Pluton mafic intrusive rocks

The Cliff Lake tonalite is cut by a wide variety of texturally and compositionally distinct mafic dykes and small mafic plugs.

The largest mafic intrusion in the Cliff Lake Pluton is a red-brown weathering gabbro (unit 42b). It is equigranular, with a 1 — 2 mm grain size. The gabbro has a chilled contact against unit 45d tonalite and locally contains tonalite xenoliths.

North of the gabbro plug is a small intrusion of massive, fine grained, equigranular, magnetiferous quartz diorite (unit 42j). The contact between the quartz diorite and gabbro body to the south was not observed but dykes of the former occur in the gabbro. The gabbro is also cut by pyroxene-plagioclase-phyric intermediate dykes.

The most widespread group of mafic intrusions in the Cliff Lake Pluton are fine grained (0.5 — 1 mm) equigranular diorite dykes (unit 42a). These dykes are generally 1 — 3 m wide (maximum 7 m), straight-walled, continuous to *en echelon*, chilled, and are characterized by lath-shaped plagioclase. The dykes commonly trend northwest to north-northeast and are steeply east-dipping; a more easterly trending group dips moderately south.

Geochemistry

Tonalite samples from units 45b, c, e, and f containing the least inclusions are all very similar in major, minor and trace element abundances (Appendix). The compositions of other samples can be explained in terms of varying amount of assimilation of mafic volcanic xenoliths (Fig. 253 and 254). The compositional uniformity of the different phases is somewhat surprising in view of the fact that intrusive relationships exist between all of the phases (except between 45d and 45c, where the contact is faulted).

The mafic volcanic xenoliths also display compositional similarity despite varying degrees of recrystallization (Appendix). They are all high-Al_2O_3 basalt and differ from the magmatic quartz diorite xenoliths in Al_2O_3, CaO, MgO, Na_2O, K_2O, Rb and Ba. Thus although some coarsely recrystallized basalt xenoliths texturally resemble quartz diorite, clearly they are not the same rock type. The quartz diorite (Appendix), represented by the large xenoliths in unit 45a, are the earliest intrusive phase of the Cliff Lake Pluton.

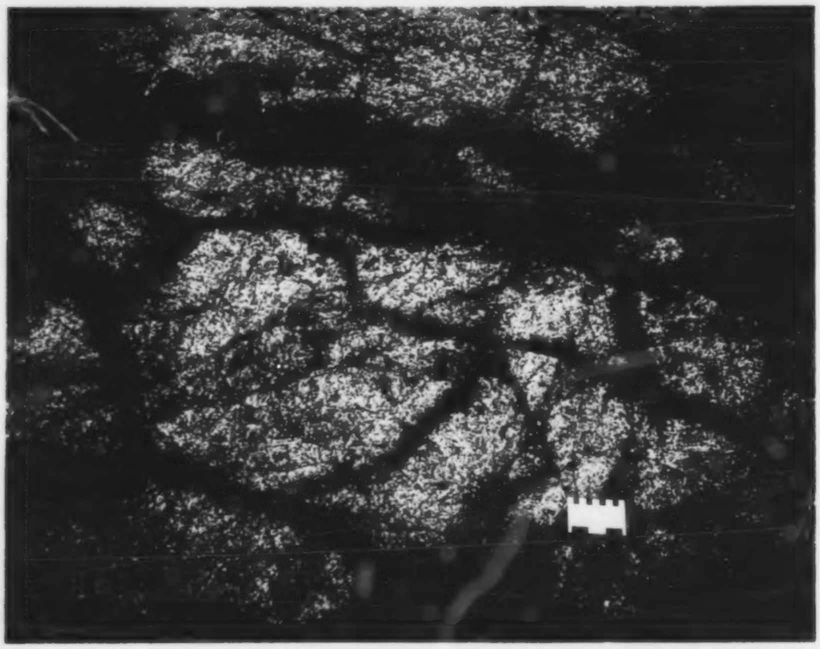

Figure 252: Chlorite-rich alteration (dark) along fractures in quartz-phyric leucotonalite (unit 45d), Cliff Lake Pluton, 700 m north of McWater Lake.

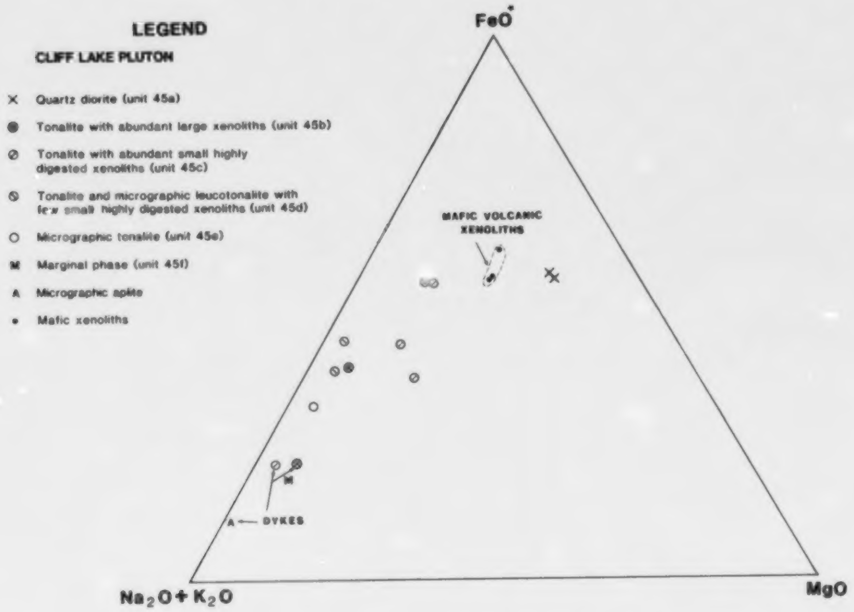

Figure 253: Ternary AFM diagram showing various phases of the Cliff Lake Pluton and samples of contained mafic volcanic xenoliths.

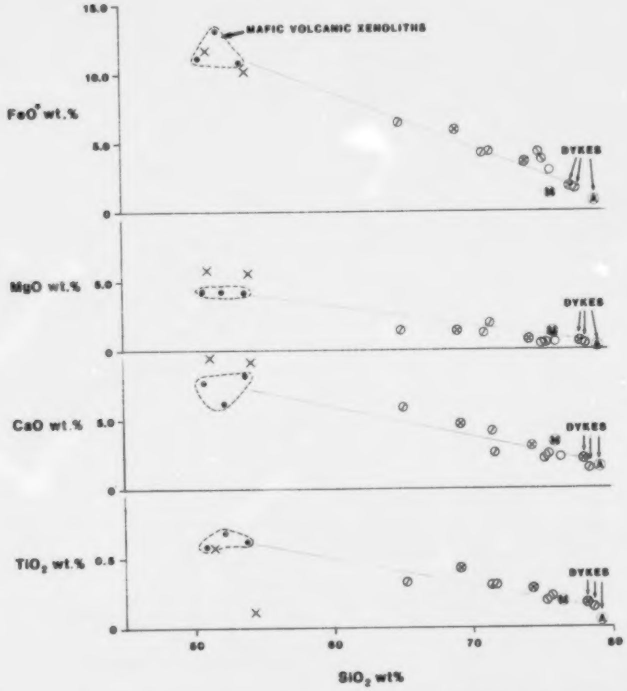

Figure 254: FeO, MgO, CaO, TiO$_2$ plotted against SiO$_2$ showing various phases of the Cliff Lake Pluton and samples of contained mafic xenoliths. Line joins samples of Cliff Lake Pluton, with little or no contamination by mafic xenoliths, to field encompassing samples of mafic xenoliths. Other samples of the Cliff Lake Pluton plot close to this line suggesting that their compositions reflect varying amounts of assimilation of mafic volcanic xenoliths. Legend as in Figure 253; dykes contain only rare xenoliths and represent least-contaminated magma samples.*

TONALITE, LEUCOTONALITE (UNIT 46)

Several unrelated small bodies of tonalite and leucotonalite occur throughout the map area (Map GR87-1-1). Two of these bodies, one at Insole Lake and the other 600 m west of Steeves Lake, are briefly described in this section.

The Insole Lake tonalite (unit 46a) is truncated on the west by the Cliff Lake Fault and intruded by magnetite-bearing equigranular quartz diorite (unit 42f). Two phases of tonalite are recognized in this intrusion. The older, and most prominent phase, is buff weathering, homogeneous, equigranular to weakly quartz-phyric, and medium green on fresh surfaces. It is composed of stubby euhedral laths of plagioclase (25 — 35%, 0.5 — 1 mm), anhedral quartz (25 — 35%, 0.3 — 2 mm) interstitial to and coarsely intergrown with plagioclase, micrographic quartz-plagioclase intergrowths (5%), green chlorite (35%) after an unknown mafic mineral, and leucoxene (1%, 0.1 — 0.2 mm) after primary Fe-Ti oxides. The second phase is more leucocratic, intrudes the earlier phase, and locally forms an intrusion breccia with abundant angular xenoliths of the earlier tonalite phase. It is white weathering, equigranular to weakly quartz-phyric, and pale grey on fresh surfaces. It is mineralogically and texturally similar to the early phase with the exception that it contains up to 30% micrographic quartz-plagioclase intergrowths (up to 2 mm) and correspondingly less chlorite.

The Steeves Lake Intrusion (unit 46b) is a small, homogeneous, plug-like body truncated by a fault to the southwest, with southern portions cut by numerous narrow dykes of quartz-phyric rhyolite (unit 49a). It is equigranular to quartz-phyric, buff-white on weathered surfaces, pale grey on fresh surfaces, and a tonalite to leucotonalite in composition. It is composed of euhedral stubby plagioclase laths (50 — 60%, 0.3 — 1.0 mm), anhedral quartz (0.3 — 4 mm) interstitial to and intergrown with plagiclase, colourless chlorite (10%), leucoxene (2%, 0.2 — 1.0 mm) after Fe-Ti oxide minerals, and apatite (0 — trace).

CENTENNIAL MINE LEUCOGRANITE/LEUCOGRANODIORITE (UNIT 47)

An elongate, irregular body of leucogranite and leucogranodiorite (unit 47) occurs on the west shore of Athapapuskow Lake near the Centennial Mine. Major north-trending faults, part of the zone of faults that extends from Athapapuskow Lake to Mikanagan Lake, truncate the east and west margin of the intrusion. The body intrudes and locally contains xenoliths of mafic pillowed lavas.

The intrusion is composed of two texturally different but related phases. The main component is hypidiomorphic equigranular with a 1 to 2 mm grain size. The other contains 3 to 10 mm quartz megacrysts in a 2 to 4 mm groundmass. Contacts between the two phases are abruptly gradational with the quartz-megacrystic variety forming irregular bodies up to several tens of metres across within the equigranular phase.

Both phases of the intrusion weather pale buff, white or pale pink and are pale grey on fresh surfaces. Both are composed of an equal proportion of plagioclase, microcline and quartz. Plagioclase is subhedral interlocking with a weak to moderate sericite-epidote-chlorite alteration. Microcline is also subhedral interlocking, with a slight tendency to form larger grains in some localities. Quartz is anhedral (interstitial) to subhedral interlocking and is strained and crushed. In quartz-megacrystic varieties the large quartz grains are typically flattened, crushed and lenticular in shape.

The intrusion has a weak pervasive cataclastic foliation, and contains anastomosing narrow cataclastic shears (a few millimetres wide) and quartz-filled fractures. These brittle deformation structures are likely related to the same tectonic forces that faulted and truncated the east and west margins of the intrusion. The narrow cataclastic shears vary widely in orientation, but are typically north-trending with a steep dip. North-trending, several metre wide, chlorite-rich shear zones, with associated rusty gossan, are present in a few localities at the south central margin of the intrusion. The large fault that truncates the east margin of the intrusion was not observed in surface exposures but is exposed in the decline of the Centennial Mine where it is only a centimetre wide (Syme et al., 1982). Rocks adjacent to the western fault are schistose and strongly crushed. The crushed rocks consist of broken recrystallized quartz grains in a completely sericitized fine grained groundmass.

The intrusion is cut by dykes of equigranular gabbro and pyroxene-gabbro, which may form up to 30% of some exposures. These intrusions are both pre- and post-foliation. Both ages of intrusions are chilled against the leucogranite/leucogranodiorite.

QUARTZ PORPHYRY, QUARTZ-PLAGIOCLASE PORPHYRY (UNIT 48)

Two distinct porphyritic felsic rock types occur on Big Island in Manistikwan Lake. They differ from one another in size and type of phenocrysts: the older (unit 48a) contains abundant 1 — 3 mm quartz phenocrysts and the younger (unit 48b) contains large quartz phenocrysts (2 — 10 mm) and abundant plagioclase phenocrysts (1 — 6 mm). Both are intruded by unit 42h diorite and unit 42j magnetiferous quartz diorite.

Quartz porphyry (unit 48a)

The quartz porphyry unit on Big Island includes predominant massive rhyolite, rare lapilli tuff and tuff breccia, rare heterolithologic felsic breccia, and sporadic well defined dykes. The unit is thus clearly syn-Amisk Group; the massive rhyolite could be either a high-level intrusion (or group of intrusions), or an extrusive dome.

Massive rhyolite weathers white, pale buff, to light grey and is light grey to medium green on fresh surfaces. Local rusty patches result from oxidation of minor disseminated pyrite. An intrusive nature of the massive material is indicated by local well defined dykes, variations in weathering colour and phenocryst populations, rare mafic volcanic xenoliths, and rare intrusive contacts with mafic flows. The high-level environment of emplacement is indicated by local vesicles and ubiquitous spherulites (Fig. 255) in the groundmass (spherulites are devitrification structures which indicate that the groundmass was originally glass). Quartz phenocrysts (10 — 20%, up to 3 mm) are euhedral and embayed. They are set in a densely spherulitic matrix comprising individual round to oval spherulites (0.05 — 0.2 mm) composed of quartz or feldspar and chlorite. Most quartz phenocrysts have narrow spherulitic rims (Fig. 255). Spherulites are separated by sericite, feldspar, quartz and chlorite.

Lapilli tuff and tuff breccia consist of quartz-phyric rhyolite clasts supported in a matrix of similar composition. Fragmental units are small, and lack lateral continuity; sharp contacts occur between some lapilli tuff and massive rhyolite. Heterolithologic breccias contain quartz-phyric, plagioclase-phyric, and aphyric rhyolite clasts and local mafic volcanic clasts. Fragments are angular, and range in size from 2 — 30 cm. Bedding was observed in a locality north of the lake in the centre of Big Island; at this locality the breccia unconformably overlies pillowed flows and massive quartz porphyry.

Quartz-plagioclase porphyry (unit 48b)

Coarse quartz-plagioclase porphyry occurs on the west wide of Big Island. In general the contact between this unit and quartz porphyry (unit 48a) is not exposed; where it was observed (north of the lake) coarse porphyry intrudes both heterolithologic breccia and massive rhyolite. Locally this unit contains large xenoliths of mafic volcanic rocks. Thus unit 48b is considered intrusive; it contains spherulites and was probably emplaced in a high-level environment.

The porphyry weathers white to light buff and is light grey on fresh surface. It is predominantly massive but locally displays a fragmental texture in which subangular to subrounded clasts (2 mm — 1 m) are dispersed in a slightly darker coloured matrix. Quartz phenocrysts (5 — 10%, up to 10 mm) are euhedral with somewhat rounded outlines; some are deeply embayed. Larger quartz phenocrysts contain rounded inclusions (to 0.3

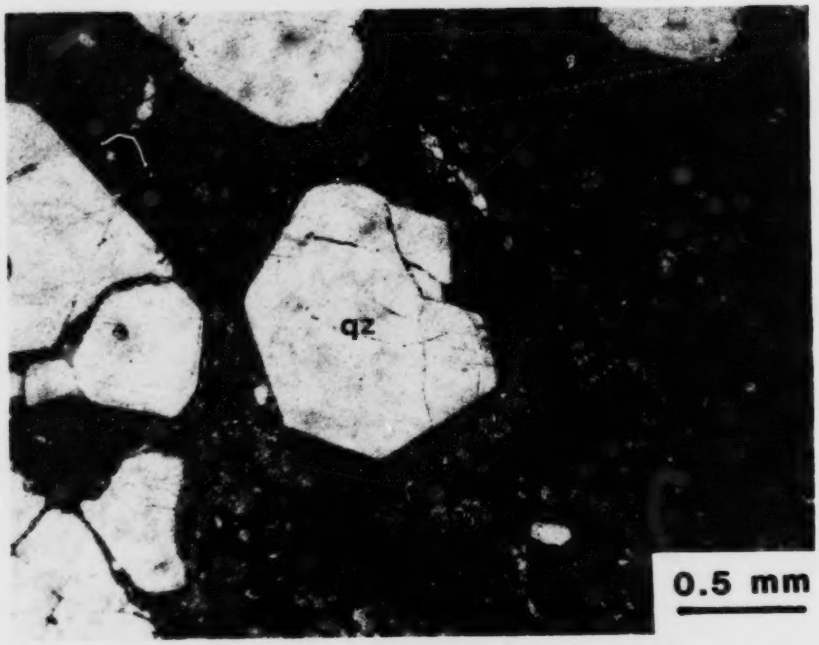

Figure 255: Quartz porphyry (unit 48a), Manistikwan Lake. Subhedral to euhedral, embayed quartz phenocrysts (qz) are rimmed by coalesced feldspar spherulites. Round spherulites (sph) with a radiate structure dominate the groundmass. Sample 4343-1, plane polarized light.

mm) composed of chlorite, feldspar, epidote and carbonate. Plagioclase phenocrysts (10 — 20%, to 5.5 mm) are euhedral, equant and strongly altered to carbonate and sericite. Mafic minerals (chlorite, leucoxene, pyrite) compose 5%. Feldspar spherulites (0.1 — 0.2 mm in diameter) occur in the groundmass and as rims on quartz phenocrysts.

RHYOLITE (UNIT 49)

High-level rhyolite intrusions (unit 49) occur between the Cliff Lake Fault and Inlet Arm Fault, in the Hook Lake, Manistikwan Lake and Cope Lake blocks (Fig. 3; geological map). They are not present in other fault blocks in the map area.

Rhyolite intrusions range widely in shape and size, from dykes a few metres wide to irregular bodies a few hundred metres wide and over a kilometre long. Most can be readily demonstrated to be intrusive, in that they cut across stratigraphy and/or contain xenoliths of host volcanic rocks. They are considered to be high level because almost all have spherulitic textures (indicating a primary glassy nature) and some contain vesicles, flow banding and perlitic fractures. Individual rhyolite bodies, groups of geographically related bodies and some rhyolite swarms are described below.

Borne Lake rhyolite

A large irregular body of rhyolite (unit 49c) occurs south and east of Borne Lake (south end of Manistikwan Lake). This intrusion has a lateral extent of about 1.7 km and a maximum thickness of about 300 m. It cuts across 1 km of basalt stratigraphy east of Borne Lake but is broadly conformable south of Borne Lake. The rhyolite is relatively homogeneous but locally contains rhyolite dykes with different phenocryst populations.

The rhyolite weathers white and is light grey on fresh surface. It is commonly massive with local zones of flow banding (on a scale of 1 — 20 cm) and patchy zones of "breccia", the latter consisting of white unaltered fragments in a pale olive green sericitic matrix. The breccias do not form continuous units, are not layered, and are gradational with massive rhyolite. The "breccia" texture is considered to be hydrothermal in origin, possibly the result of chloritization and sericitization along various types of fractures including fine-scale perlitic cracks (Fig. 256).

In thin section, Borne Lake rhyolite is characterized by euhedral, embayed quartz phenocrysts (3 — 10%, 0.3 — 3 mm) and euhedral, tablet-shaped plagioclase phenocrysts (2 — 10%, 0.3 — 2.5 mm). Groundmass is dominated by feldspar spherulites (up to 0.3 mm in diameter; Fig. 257) in a "matrix" of fine grained sericite, feldspar, quartz, chlorite and epidote.

A small (100 m) oval body of heterolithologic breccia (unit 30) occurs within the rhyolite intrusion, 300 m east of Borne Lake. This breccia contains a variety of angular to rounded rhyolite clasts (up to 50 cm), scoriaceous aphyric basaltic andesite clasts and rare laminated mudstone clasts. It has a gradational contact over 6 m with massive rhyolite and is intruded by the same suite of gabbro dykes that cuts the main rhyolite body.

Gabbro dykes that cut the rhyolite (described in Table 14) are irregular in orientation, appear to be fracture-controlled, and contain xenoliths/rafts of rhyolite. They are most abundant on the east side of the Borne Lake rhyolite.

Hook Lake area

A suite of numerous, north-trending rhyolite dykes intrudes the volcanic sequence in the Hook Lake area. They range in size from small, unmappable bodies to dykes tens of metres across. With the exception of some small intermediate dykes they form the youngest intrusive suite in the area.

Rhyolite dykes vary in phenocryst content from aphyric to quartz-phyric to quartz-plagioclase-phyric. As in the Borne Lake body, most are massive, but flow-banded, vesicular and "brecciated" textures occur locally. Spherulites to 0.4 mm in diameter are abundant in virtually every intrusion.

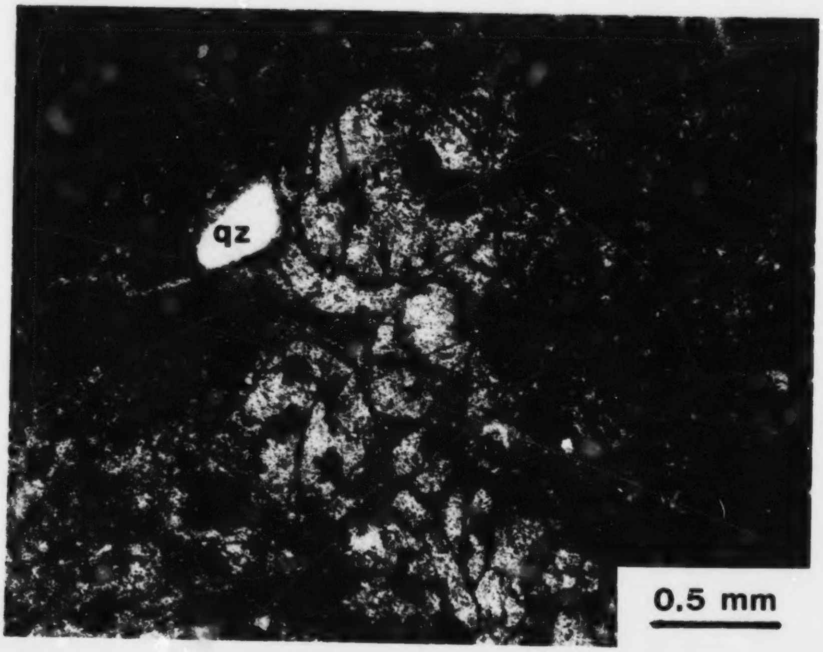

Figure 256: *Curvilinear perlitic cracks (arrows) in Borne Lake rhyolite (unit 49c). The presence of these structures and spherulites in unit 49 rhyolite intrusions indicates that the groundmass was originally glass. Sample 4016-1, plane polarized light.*

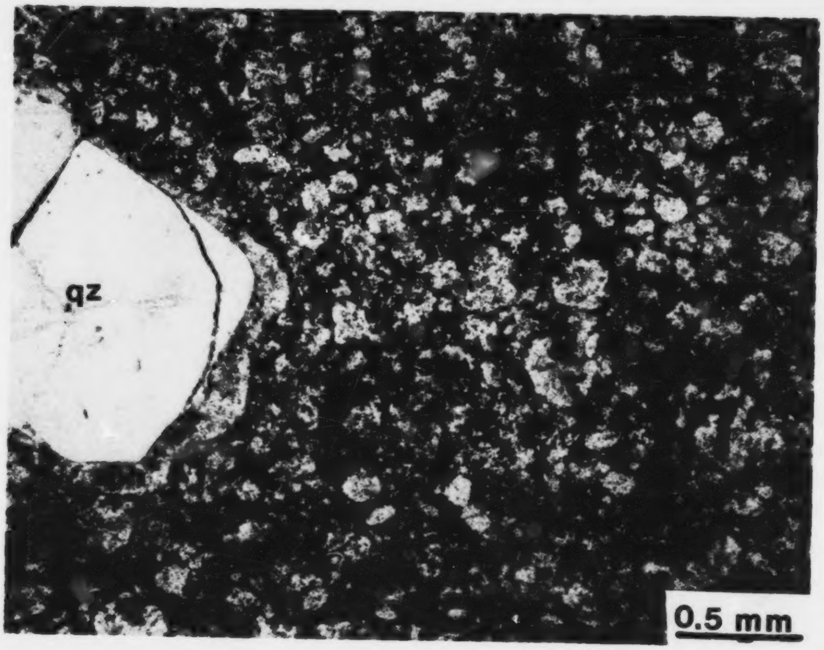

Figure 257: *Spherulites (sph) in Borne Lake rhyolite intrusion (unit 49c) attest to original vitric nature of this plug-like body. Note spherulites nucleated on partly resorbed quartz (qz) phenocryst. Sample 5030-1, plane polarized light.*

South of Cliff Lake Pluton

Several large sill-like to irregular bodies of rhyolite occur south of the main mass of the Cliff Lake Pluton. Most are poorly exposed, and the exact sizes and shapes of some bodies are poorly defined. All are massive, and contain a moderate foliation and/or fracture cleavage. Phenocryst content ranges from zero to 10% but is generally low.

The age relationship with the Cliff Lake Pluton is well constrained. One body of rhyolite is clearly truncated at its contact with unit 45d tonalite. In addition, one xenolith observed in unit 45b tonalite consists of rhyolite and the fine grained gabbro characteristic of the mafic suite that commonly intrudes rhyolite. Thus all phases of the Cliff Lake Pluton are likely to be younger than unit 49 rhyolite.

Steeves Lake area

In the Steeves Lake portion of the Manistikwan Lake Block rhyolite dyke swarms, mappable rhyolite dykes, and one large (150 x 1100 m) sill-like body of rhyolite comprise a major concentration of unit 49-type intrusions.

The large sill-like body west of Steeves Lake weathers white and is pale grey on fresh surface. It is massive and aphyric. An adjacent rhyolite dyke swarm to the west of the main body comprises aphyric and sparsely quartz-phyric types. These dykes form up to 40% of exposures and cut the southern part of unit 46b tonalite. The rhyolite sill, dyke swarm, and tonalite are all truncated by a fault to the southwest.

The rhyolite dyke swarm east of the portage between Embury Lake and Manistikwan Lake comprises individual, white-weathering dykes 3 — 5 m wide with planar to irregular contacts with host volcanic rocks. The dykes range in trend between 170° and 220° and all dip steeply to the west. They contain sporadic vesicles, local hydrothermal brecciation, and are characterized by varying contents of plagioclase and quartz phenocrysts (to 2 mm) in a very fine grained quartzofeldspathic groundmass. Some contain diorite/quartz diorite microxenoliths.

Another major porphyritic rhyolite dyke swarm occurs at the southeast end of Embury Lake. Individual dykes up to 5 m wide commonly trend 345-350° and compose up to 40% of exposures. The dykes weather buff to cream; they contain quartz phenocrysts (5 — 10%, 0.5 — 3 mm) and plagioclase phenocrysts (0 — 5%, 0.3 — 3 mm) in a densely spherulitic groundmass similar to other rhyolites in unit 49 (Fig. 258). Chlorite, epidote and Fe-oxides form less than 10% of the rhyolite.

AGE RELATIONSHIPS

The abundance and variety of intrusive rocks is not uniform across the map area. Major faults divide the area into 10 fault-bounded blocks (Fig. 3), and some of the major faults separate blocks with significantly different intrusive suites. Thus, relative age relationships among intrusions are most reliably established in individual blocks or restricted areas within blocks. Relative age relationships of intrusions in some of these areas are given in Tables 16 to 22 and are discussed briefly below.

Manistikwan Lake, Hook Lake and Cope Lake Blocks

These three blocks, bounded by the Inlet Arm Fault and Cliff Lake Fault, contain the greatest abundance and variety of intrusions in the area. Many intrusions are not present outside this fault-bounded domain. For example, the Inlet Arm Fault is very clearly the eastern limit of occurrence of rhyolite intrusions (unit 49), magnetiferous quartz diorite (unit 42j), quartz porphyry and quartz-plagioclase porphyry (units 48a and b), and quartz-megacrystic tonalite of Cliff Lake type (unit 45). This fault is post-metamorphism in age, so the juxtaposition of widely different intrusive suites across the fault is evidence of major displacement (further discussed under Structure). However, some major groups of intrusions occur

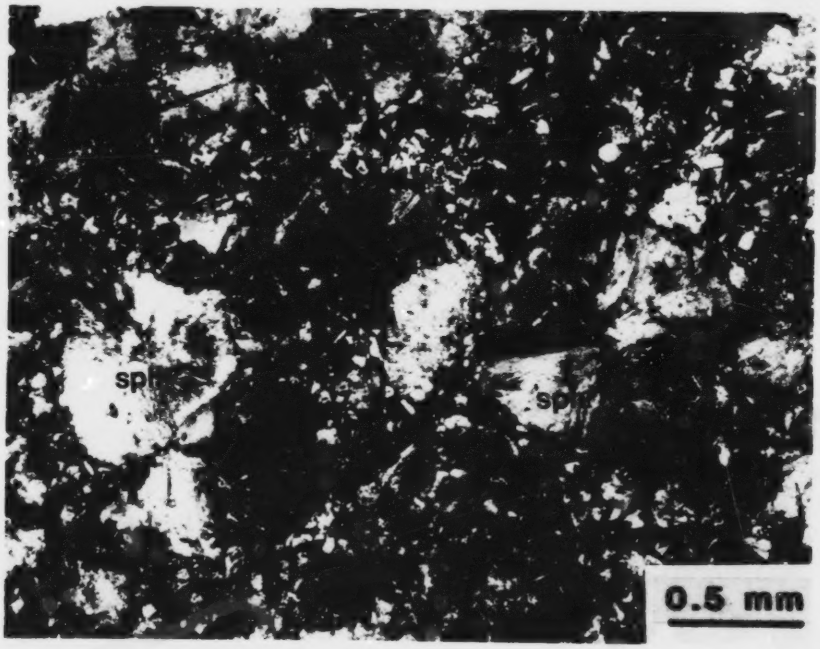

Figure 258: Spherulitic rhyolite dyke (unit 49d), Manistikwan Lake. Round spherulites (sph) up to 1 mm in diameter dominate the groundmass. Spherulites have a radiating structure composed of feldspar and minor quartz. Sample 4324-1, crossed polarizers.

Table 16: Age relationships of intrusive rocks in the Hook Lake area, in order from oldest (bottom) to youngest (top)

INTRUSION		ROCK TYPE	CUT BY
Gabbro associated with rhyolite (unit 42)	P	Plagioclase-phyric gabbro	
	O	Equigranular gabbro	
Rhyolite (unit 49)	N	Aphyric rhyolite	M
	M	Porphyritic rhyolite	N, O, P
	L	Plagioclase-phyric mafic dykes	
	K	Pyroxene-plagioclase-phyric mafic dykes	
Hook Lake Diorite (unit 42a)	J	Diorite, quartz diorite	K, L, N
Hook Lake Gabbro (unit 41)	I	Pyroxenite veins	
	H	Gabbro pegmatite veins	
	G	Ferrogabbro	H
	F	Gabbronorite	H, I, J, K, N
	E	Quartz diorite, diorite dykes	F, N, O
Synvolcanic Intrusions (unit 42)	D	Diabase	
	C	Pyroxene-plagioclase-phyric mafic dykes	F
	B	Aphyric intermediate intrusions	D
	A	Plagioclase-phyric mafic intrusions	E, F, N

on both sides of the Inlet Arm Fault. The Hook Lake gabbronorite-ferrogabbro (unit 41) in the Hook Lake block is megascopically, petrographically, and chemically similar to the Mikanagan Lake Sill in the Bear Lake Block. Both intrusions belong to a very widespread group of major differentiated gabbroic intrusions in the Flin Flon belt, which have been identified as far east as the File Lake area (Josland Lake Sill; Bailes, 1980). Hook Lake gabbro possibly postdates Amisk volcanism because it faces opposite to the host mafic flows. Rhyolite dykes of unit 49 have features indicative of a very high level environment of intrusion (e.g. spherulitic devitrification structures, vesicles and flow banding) yet they must postdate Amisk volcanism because they cut gabbro similar to the Hook Lake gabbro.

The age of the Cliff Lake tonalite pluton (unit 45) has been a subject of speculation for many years (e.g. Baldwin, 1980; MacQuarrie, 1980; Stauffer, 1974). The Cliff Lake tonalite is a high level pluton emplaced in Amisk Group volcanic rocks: it displays sharp crosscutting contacts with host volcanic rocks, stoping, assimilation of xenoliths and breccia pipes (Baldwin, 1980). It has been considered to be pre-Missi Group because clasts of this distinctive tonalite have been reported in Missi Group conglomerate (Bruce, 1918; Stockwell, 1960; Baldwin, 1980). However, despite specific search for these clasts by the present authors, Cliff Lake type tonalite pebbles were not observed in the Missi conglomerate. The fact that this pluton clearly cuts late rhyolite dykes (unit 49; Table 16) indicates that it postdates Amisk volcanism and most of the post-Amisk intrusions. Recent U/Pb zircon dates (Table 1) clearly indicate it to be pre-Missi in age.

Bear Lake Block

Intrusions in the Bear Lake Block range in age from those that are syn-Amisk volcanism to those that postdate folding and faulting.

Syn-Amisk intrusions include the many dykes and sills that are part of the Bear Lake basaltic andesite (unit 1f) and the White Lake gabbro-ferrogabbro sills (unit 39). Unit 1f mafic sills and dykes are not present in units stratigraphically overlying the Bear Lake basaltic andesite; they display all of the structures and textures expected in synvolcanic feeder dykes. The White Lake differentiated sills occur in a stratigraphically restricted zone beneath chemically similar Two Portage Lake ferrobasalt (unit 5). The unique combination of spatial association and chemical similarity between the intrusive and extrusive rocks strongly indicates that they are part of the same magmatic event.

Intrusions that appear to postdate Amisk volcanism include the Mikanagan Lake Sill and the compositionally similar Benn Lake gabbro. The Mikanagan Lake Sill cuts across at least 1.6 km of volcanic stratigraphy, including the uppermost volcanic unit in the Bear Lake Block. Assuming that the sill was originally emplaced in a near-horizontal attitude this implies that the host volcanic rocks were at least strongly tilted, and may have been folded, prior to intrusion. Similar differentiated intrusions (Hook Lake and Shore Lake bodies) also are emplaced in Amisk rocks that must have been folded prior to intrusion. However, there is a striking compositional similarity between the chilled margins of the sills and Amisk basalts (Fig. 217, 218, 219 and 238), raising the possibility that the intrusions and Amisk Group are cogenetic. If the observed pre-intrusion deformation accompanied volcanism, then the intrusions are syn-

Table 17:
Age relationships of intrusive rocks in the northern Hook Lake Block, in order from oldest (bottom) to youngest (top)

INTRUSION		ROCK TYPE	CUT BY
	P	Feldspar porphyry dyke	
	O	Fine grained diorite, quartz diorite	
	N	Pyroxene-plagioclase-phyric mafic dykes	
	M	Magnetiferous quartz diorite	
	L	Diorite, quartz diorite	M, J
Cliff Lake Pluton (unit 45)	K	Micrographic aplite dykes	O
	J	Fine grained quartz-phyric micrographic tonalite	
	I	Quartz-phyric leuctonalite and micrographic leucotonalite with few, small, highly assimilated xenoliths	P
	H	Quartz-phyric tonalite with abundant, small, highly assimilated xenoliths	J, K, L, N, O
	G	Quartz-phyric tonalite with abundant large xenoliths	H, J, K, O
	F	Leucocratic tonalite marginal phase	I
	E	Quartz diorite	G
	D	Equigranular gabbro	
	C	Pyroxene-plagioclase-phyric mafic dykes	G
Rhyolite	B	Aphyric and porphyritic rhyolite	C,D,G,I
	A	Oikocrystic gabbro	

Table 18:
Age relationships of intrusive rocks in the Southern Manistikwan Lake Block, in order from oldest (bottom) to youngest (top)

INTRUSION		ROCK TYPE	CUT BY
	K	Mafic dykes	
	J	Quartz-phyric tonalite	
Big Island Mafic Intrusive Suite	I	Magnetiferous quartz diorite (unit 42j)	
	H	Quartz diorite, diorite (unit 42b)	J
	G	Aphyric rhyolite (unit 49a)	
Big Island Felsic Intrusive Suite	F	Quartz-plagioclase porphyry (unit 48b)	H, I, K
	E	Quartz porphyry (unit 48a)	F, H, I
Embury Lake Gabbro	D	Quartz diorite (unit 41g)	
	C	Gabbro (unit 41b)	G
	B	Equigranular tonalite (unit 46b)	G
Synvolcanic Intrusions	A	Intermediate intrusions	G

Table 19:
Age relationships of intrusive rocks in the Hook Lake and Manistikwan Lake Blocks, compiled from Tables 16, 17 and 18; in order from oldest (bottom) to youngest (top).

Feldspar porphyry dyke

Fine grained diorite, quartz diorite dykes (unit 42b)

Quartz-phyric tonalite dykes

Pyroxene-plagioclase-phyric mafic dykes (unit 42d)

Big Island magnetiferous quartz diorite, diorite (unit 42j)

Big Island diorite, quartz diorite (unit 42b)

Cliff Lake tonalite pluton (unit 45)
  Micrographic aplite dykes
  Fine grained, quartz-phyric micrographic tonalite (unit 45e)
  Quartz-phyric tonalite with abundant, small, highly assimilated xenoliths (unit 45c)
  Quartz-phyric tonalite with abundant large xenoliths (unit 45b)
  Leucocratic tonalite marginal phase (unit 45f)
  Quartz diorite (unit 45a)

Plagioclase-phyric gabbro (unit 42c)

Equigranular gabbro (unit 42a, b)

Pyroxene-plagioclase-phyric mafic dykes (unit 42d)

Aphyric and porphyritic rhyolite (unit 49)

Plagioclase-phyric mafic dykes (unit 42c)

Pyroxene-plagioclase-phyric mafic dykes (unit 42d)

Big Island quartz-plagioclase porphyry (unit 48b)

Hook Lake diorite, quartz diorite (unit 42a)

Hook Lake gabbronorite, ferrogabbro (unit 41)

Embury Lake gabbro, quartz diorite (unit 41)

Equigranular tonalite (unit 46b)

Quartz diorite, diorite dykes (unit 42)

Diabase
Pyroxene-plagioclase-phyric mafic dykes
Aphyric intermediate intrusions
Plagioclase-phyric intrusions
Synvolcanic

Table 20:
Age relationships of intrusive rocks in the Bear Lake Block, in order from oldest (bottom) to youngest (top)

Intrusions that postdate the Northeast Syncline	Quartz-plagioclase-phyric felsic dykes (unit 56), parallel to axial plane of Northeast Arm syncline and cutting across Northeast Arm fault
	Unfoliated gabbro (unit 53a), along faults
	Equigranular gabbro (unit 42a, b) and plagioclase-phyric gabbro (unit 42c), parallel to axial plane of Northeast Arm Syncline (eg. Cuprus sill)
	Benn Lake gabbro, gabbronorite (unit 41)
	Mikanagan Lake sill (unit 41)
	Wonderland Lake gabbro, quartz diorite (unit 42b)
	Equigranular diorite, quartz diorite (unit 42a; eg. We Lake sill, Little Spruce Lake sill)
Amisk Group synvolcanic intrusions	Plagioclase-phyric diorite (unit 42c) in Vick Lake tuff
	White Lake Gabbro (unit 39)
	Bear Lake quartz diorite (unit 1f)

Table 21:
Age relationships of intrusive rocks in the Scotty Lake Block, in order from oldest (bottom) to youngest (top)

Intrusions that postdate the One Portage Lake fault	Unfoliated gabbro (unit 53a), along faults
	Pyroxenite (unit 52)
	Foliated quartz-megacrystic tonalite (unit 55), along faults
	Tonalite (unit 46)
	Melatonalite (unit 42h)
	Whitefish Lake wehrlite, pyroxenite, gabbro, quartz diorite (unit 40)
Amisk Group synvolcanic intrusions	Scotty Lake quartz diorite (unit 4b)
	Equigranular mafic dykes
	Pyroxene-phyric, plagioclase-phyric and pyroxene-plagioclase-phyric mafic to intermediate dykes (unit 4b)

Table 22:
Age relationships of intrusive rocks in the Whitefish-Mikanagan Lakes Block and the Sourdough Bay Block, in order from oldest (bottom) to youngest (top)

Postdate Missi Group	Unfoliated gabbro (unit 53), along faults
	Whitefish Lake pluton (quartz monzodiorite, unit 54)
	Plagioclase porphyry
Age relationships within this group unknown	Centennial granite, granodiorite (unit 54)
	Quartz diorite, tonalite (unit 42)
	Whitefish Lake pyroxenite, gabbro, quartz diorite (unit 40)
	Sawmill Lake porphyritic meladiorite, diorite, quartz diorite (unit 42i)
	Sourdough Bay ophitic gabbro (unit 42f)
	Post Island quartz diorite, tonalite (unit 42g, h)
	Equigranular gabbro (unit 42b)
	Equigranular diorite, quartz diorite (unit 42a)
Amisk Group synvolcanic intrusion	Baker Patton felsic complex, intrusions (unit 17)

volcanic. If the deformation postdated volcanism then the intrusions are post-Amisk despite their chemical similarity to Amisk basalts.

Intrusions that postdate the Northeast Arm fold include unit 42a gabbro (in the stratigraphic hanging wall of Cuprus Mine) and unit 42c gabbro (a narrow sill in the Vick Lake tuff). The gabbro in the Vick Lake tuff is compositionally and texturally zoned (Table 15) and tops to the west, opposite to the facing direction in the host rocks.

Two groups of intrusions are younger than the Northeast Arm Fault. These are (1) the quartz-plagioclase porphyry dykes (unit 56) which can be traced across the fault without offset, and (2) undeformed gabbro (unit 53a) that is intrusive into strongly deformed rocks associated with the fault.

Scotty Lake Block

Intrusive rocks in the Scotty Lake Block span the same time period as those in the adjacent Bear Lake Block. The oldest intrusions comprise the suite of synvolcanic dykes and sills (unit 45b) that are common in Scotty Lake basalt (Fig. 78) but are absent in the overlying volcaniclastic formation (unit 19).

The Whitefish Lake ultramafic and mafic intrusive suite (unit 40) includes a differentiated intrusion exposed at the north end of Schist Lake. The relative age of these rocks is not known, but gabbroic members have similar compositions and textures to the Mikanagan Lake Sill and may belong to the same magmatic episode.

Felsic plutonic rocks in the Scotty Lake block (tonalite, melatonalite; units 46 and 42b) are exposed south of Highway 10 at the southern margin of the map area. They are the northern portions of larger stocks; they are older than old Highway 10 fault but the age of the tonalites relative to the Missi Group and other intrusive rocks is not known.

At least three different intrusive rock types intrude the One Portage Lake Fault (Map GR87-1-1). They are undeformed gabbro (unit 53a; Table 21), strongly foliated quartz-megacrystic tonalite (unit 55), and green pyroxenite (unit 52).

Whitefish-Mikanagan Lakes Block, Sourdough Bay Block

Synvolcanic dykes and sills are a significant component only of the Baker Patton felsic complex (unit 17). They are rare in the stratified mafic sequences of subaqueous flows, volcaniclastic rocks and subordinate sedimentary rocks that compose the greater portion of these blocks.

Gabbroic rocks diverse in composition, texture and age are present throughout both blocks. These gabbros are relatively coarse grained, some are zoned, and most form relatively large, mappable bodies. Some intrusions may be syn-Amisk but most are unlike the small, fine grained, clearly synvolcanic mafic dykes in the Scotty Lake and Bear Lake blocks. Relative ages among the various gabbros have not been established.

The intrusive complex southwest of Whitefish Lake includes gabbro and pyroxenite similar to the differentiated Whitefish Lake intrusion. These rocks are intruded by quartz diorite and tonalite (units 42b and 42h).

The Centennial granite-granodiorite forms a plug-like body truncated on the east and west sides by major faults. Field relationships do not indicate whether this body is pre- or post-Missi.

MISSI GROUP

INTRODUCTION

The Missi Group (unit 50) is composed of metamorphosed sandstone, pebbly sandstone and conglomerate that lies with profound angular unconformity on the Amisk Group, and nonconformably overlies a wide variety of intrusions that cut the Amisk Group. Missi sediments are in turn cut by a limited number of ultramafic to felsic intrusions. The Missi Group in the Flin Flon area is at least 1900 m thick; the top is not observed. Missi Group volcanic rocks at Wekusko Lake, 130 km east of Flin Flon, have a U/Pb zircon age of 1832 +/- 2 Ma (Gordon et al., 1987, 1989).

Previous work on the Missi Group began with Bruce (1918) who defined the Lower and Upper Missi Series; the Lower Missi is now known to be greywacke and conglomerate units within the Amisk Group. Ambrose (1936a and b) described the metamorphism and deformation in the Missi, and estimated its thickness to be up to 2.3 km at Flin Flon. Buckham (1944) recognized a marked angular unconformity at the base of the Missi, north of Athapapuskow Lake, and described a zone of hematized and spheroidally weathered Amisk volcanic rocks at the unconformity surface. Stockwell (1946, 1960) mapped the Missi Group at Flin Flon in detail. He subdivided the Missi into 3 rock types and also recognized that it lies with marked angular unconformity on the Amisk Group. Byers (1953) described the Missi at Amisk Lake and concluded that the sediments were deposited "in a rapidly subsiding basin, mainly by torrential fluvial action carrying coarse clastic material from uplifted adjacent source areas." According to Byers (op. cit.) the relationship between the Amisk and Missi is one of regional structural conformity, with only local structural discordance. He concluded that although minor folding affected the Amisk prior to deposition of the Missi, a major time break is not represented at the contact between the two groups. Byers and Dahlstrom (1954) and Byers et al. (1965) maintained these conclusions and considered that the Amisk and Missi rocks underwent the same history of folding, faulting and metamorphism. Mukherjee (1971) and Stauffer and Mukherjee (1971) described the stratigraphy and structure of the Missi Group, and subdivided the Missi into four units based largely on abundance of pebbles; the subdivision is partly after that of Stockwell (1960). Mukherjee et al. (1971) described the environment of deposition of the Missi as fluviatile; Stauffer (1974) described it as an alluvial fan to alluvial plain deposit. Stauffer (op. cit.) noted that a pre-Missi weathered zone is present on Amisk rocks but agreed with previous interpretations that no major angular unconformity appears to exist between the Amisk and Missi Groups.

On the geological map (Map GR87-1-1) contacts and structural symbols within the Missi Group are from Stockwell (1960) with minor revisions along the Amisk-Missi contact. Locations of fold axial traces are from Stauffer and Mukherjee (1971). Only a small portion of the Missi Group was remapped during this project. A composite stratigraphic section through the Missi Group, in the vicinity of Ross Lake, was measured (Fig. 259; Table 23) to provide detailed information on the upward variation in sandstone type, pebble abundance and size, and sedimentary structures.

RELATIONSHIP TO AMISK GROUP AND CONTAINED INTRUSIONS

It is readily apparent from current mapping and Stockwell's (1960) detailed mapping that the Missi Group lies with profound angular unconformity on previously folded Amisk Group rocks. Stockwell (1960) shows the Burley Lake Syncline to be truncated at the unconformity, with over 2.5 km of Amisk section removed on the north limb of the fold (Fig. 171). Further evidence of pre-Missi folding is observed at the unconformity east of Scotty Lake, where Amisk units face in opposite direction from overlying Missi Group.

All Amisk Group rocks at exposed, unfaulted contacts with the Missi Group display a hematiferous weathered zone (regolith) up to several metres thick. The regolith is particularly well exposed and undeformed in Missi structural outliers west of Channing, at the base of the Missi 780 m north of Carlisle Lake (Stockwell, 1960), and south of the old Highway 10 — North Star Road intersection.

Regolith developed on Amisk Group volcanic rocks shows distinctive spheroidal weathering defined by concentric bands of reddish-purple to black hematite (Fig. 260). The spheroidal weathering pattern is largely controlled by concentric and planar hairline fractures. Adjacent to the unconformity the Amisk rocks are commonly intensely hematized over a width of up to 1 m (Fig. 261). Degree of hematization and spheroidal weathering decreases away from the unconformity surface. A series of samples collected across the regolith west of Channing (Appendix) shows an increase in Fe_2O_3/FeO ratio, Al_2O_3 and K_2O, and decrease in CaO and MgO as the unconformity surface is approached. At the unconformity 780 m north of Carlisle Lake (in Saskatchewan; Stockwell, 1960) similar but larger scale spheroidal weathering is developed on pre-Missi quartz diorite. There, joints strongly controlled development of the weathering pattern.

Abundant weathered Amisk regolith detritus is incorporated into lowermost Missi sediments; many pebbles display spheroidal weathering identical to that developed in underlying Amisk rocks (Fig. 262). Basal Missi conglomerates and sandstones that are particularly rich in hematiferous regolith detritus have a distinctive mauve weathering colour relative to the normally grey weathering Missi (Table 23).

The Missi Group nonconformably overlies a number of intrusions such as strongly foliated equigranular granodiorite (unit 44) at Channing, various textural varieties of diorite/gabbro (unit 42), and a granodiorite west of Beaverdam Lake (Stockwell, 1960; MacQuarrie, pers. comm.). U/Pb zircon dating (previously discussed) has clearly demonstrated that the Missi Group is younger than the Cliff Lake Pluton (unit 45).

STRATIGRAPHY OF THE MISSI GROUP

Approximately 1900 m of Missi Group stratigraphic section is represented in Figure 259. The section consists of three parts: one part south and east of Ross Lake is semi-continuous and 1260 m thick, another west of Grant Lake is 310 m thick and a third east of Little Cliff Lake is 310 m thick (Fig. 259). A unit of conglomerate (GE, Fig. 121) can be correlated between the Grant Lake and Little Cliff Lake sections. Correlation cannot be made between these sections and the Ross Lake section because they are separated by the Birch View and Little Cliff Lake faults (Stauffer and Mukherjee, 1971). However, it is probable that the Ross Lake section underlies the sequence at Grant and Little Cliff lakes, with an unknown amount of section repeated or, more likely, removed.

The various units in the Ross Lake section can be combined into four major members. The lowermost member, 58 m thick, consists of purplish weathering, intercalated conglomerate and subordinate coarse to very coarse sandstone. Conglomerate occurs as massive to normally size-graded beds composed of well rounded pebbles and cobbles. Clasts are mainly Amisk Group mafic volcanic and fine grained mafic intrusive rocks (Table 24), many of which were derived from the underlying regolith. Most of the conglomerate and sandstone beds appear to be lensoid scours with erosive bases (Table 23).

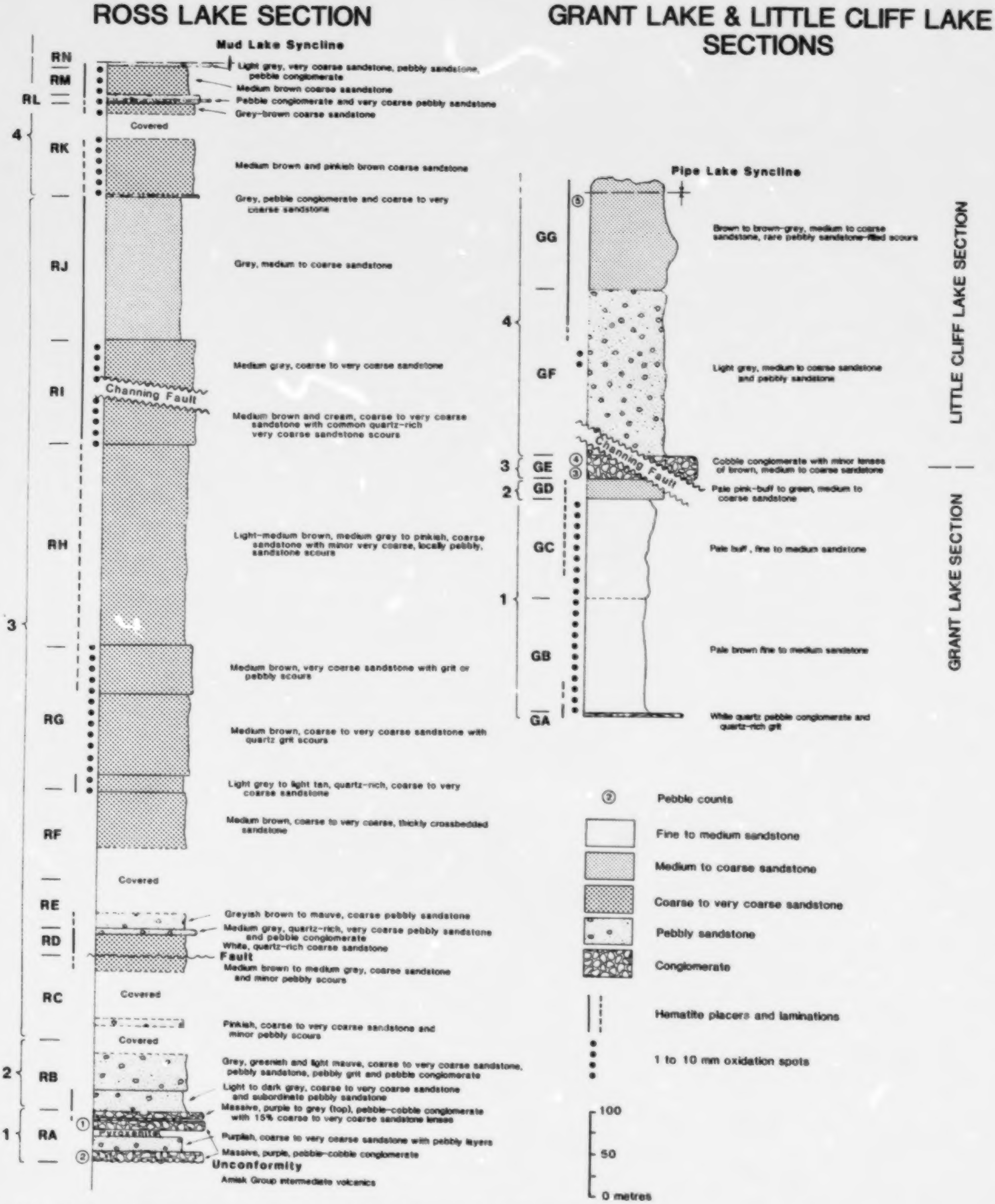
ROSS LAKE SECTION
Mud Lake Syncline
RN
RM
RL
4
RK
RJ
RI
RH
3
RG
RF
RE
RD
RC
2
RB
1
RA
Light grey, very coarse sandstone, pebbly sandstone, pebble conglomerate
Medium brown coarse saandstone
Pebble conglomerate and very coarse pebbly sandstone
Grey-brown coarse sandstone
Covered
Medium brown and pinkish brown coarse sandstone
Grey, pebble conglomerate and coarse to very coarse sandstone
Grey, medium to coarse sandstone
Medium grey, coarse to very coarse sandstone
Channing Fault
Medium brown and cream, coarse to very coarse sandstone with common quartz-rich very coarse sandstone scours
Light-medium brown, medium grey to pinkish, coarse sandstone with minor very coarse, locally pebbly, sandstone scours
Medium brown, very coarse sandstone with grit or pebbly scours
Medium brown, coarse to very coarse sandstone with quartz grit scours
Light grey to light tan, quartz-rich, coarse to very coarse sandstone
Medium brown, coarse to very coarse, thickly crossbedded sandstone
Covered
Greyish brown to mauve, coarse pebbly sandstone
Medium grey, quartz-rich, very coarse pebbly sandstone and pebble conglomerate
White, quartz-rich coarse sandstone
Fault
Medium brown to medium grey, coarse sandstone and minor pebbly scours
Covered
Pinkish, coarse to very coarse sandstone and minor pebbly scours
Covered
Grey, greenish and light mauve, coarse to very coarse sandstone, pebbly sandstone, pebbly grit and pebble conglomerate
Light to dark grey, coarse to very coarse sandstone and subordinate pebbly sandstone
Massive, purple to grey (top), pebble-cobble conglomerate with 15% coarse to very coarse sandstone lenses
①
Pyroxenite
Purplish, coarse to very coarse sandstone with pebbly layers
②
Massive, purple, pebble-cobble conglomerate
Unconformity
Amisk Group intermediate volcanics
GRANT LAKE & LITTLE CLIFF LAKE SECTIONS
Pipe Lake Syncline
⑤
GG
4
GF
3
GE
④
③
2
GD
GC
1
GB
GA
Brown to brown-grey, medium to coarse sandstone, rare pebbly sandstone-filled scours
Light grey, medium to coarse sandstone and pebbly sandstone
Channing Fault
Cobble conglomerate with minor lenses of brown, medium to coarse sandstone
Pale pink-buff to green, medium to coarse sandstone
Pale buff, fine to medium sandstone
Pale brown fine to medium sandstone
White quartz pebble conglomerate and quartz-rich grit
LITTLE CLIFF LAKE SECTION
GRANT LAKE SECTION
② Pebble counts
Fine to medium sandstone
Medium to coarse sandstone
Coarse to very coarse sandstone
Pebbly sandstone
Conglomerate
Hematite placers and laminations
1 to 10 mm oxidation spots
100
50
0 metres

Figure 259: Measured section through Missi Group in vicinity of the town of Flin Flon. All sandstones are trough cross-bedded; individual units shown are characterized by different crossbed set thickness, sand size, colour, quartz content, and number, distribution and size of contained pebbles (see Table 23).

Table 23:
Measured stratigraphic section through the Missi Group at Flin Flon

Member	Unit	Interval*(m)	Rock Type(s)**	Colour	Pebble Abundance	Pebble Size (cm)***	Bedforms	Comments
					ROSS LAKE SECTION			
1	RA	0-11.5	Conglomerate	Purple	60%	D_5 at 2.1 m = 21 4.9 m = 17 7.1 m = 16 10.6 m = 16 Max qz pebble = 11	Massive. Rare thin sandstone layers/ lenses	Base normally graded. Matrix (<5 mm) dark purple, dominated by regolith. Approx. 20% quartz. Most clasts well rounded. Well foliated.
1	RA	11.5-12.6	Coarse sandstone	Purplish		D_5 at 12.1 m = 4.8 Max qz pebble = 6	Crossbeds, 3-5 cm thick	Pebbly layers are sharply bedded, lens-shaped scours. Pebbles rounded.
1	RA	12.6-16.8	Coarse to very coarse sandstone with pebbly layers	Purplish		D_5 in basal, 60 cm thick conglomerate D_5 = 7.8 (pebbly layer) at 16.3 m = 5.4	Crossbeds, up to 7 cm thick	Pebbly layers are a few pebbles to 60 cm thick. Isolated pebbles in sandstone. Beds are lens-shaped scours. Contacts between sandstone and pebbly layers are sharp and erosive.
		16.8-23.8	Covered					
		23.8-36.6	Pyroxenite intrusion (sill)					
1	RA	36.6-47.7	Conglomerate	Purple	60%	D_5 at 38.0 m = 29 40.1 m = 18 42.9 m = 15 46.5 m = 16 47.0 m = 14 Max qz pebble = 15	Massive	Normally graded in lower half of unit. Matrix is coarse pebbly sandstone. Clasts well rounded to rounded, dominantly regolith. Elongate 2-3:1 in the plane of schistosity. Pebble count (Table 24, Column 1) at 41.7 m.
1	RA	47.7-50.0	Coarse to very coarse sandstone	Purplish	Rare in sandstone	D_5 (pebbly scour) at 49.8 m = 6.4 Max qz pebble = 4	Crossbeds, up to 30 cm thick	Two 30 cm thick pebbly scours in top 1 m. Pebbly units occur in trough crossbeds. Unit is laterally continuous across large outcrop with only minor variation in thickness. Sharp contact with underlying conglomerate.

Member	Unit	Interval (m)	Rock Type(s)	Colour	Pebble Abundance	Pebble Size (cm)	Bedforms	Comments
1	RA	50.0-56.2	Conglomerate, with about 15% sandstone lenses 5-40 cm thick	Purplish		D_5 at 50.3 m = 13 52.1 m = 13 54.2 m = 15 56.0 m = 11 Max qz pebble = 13	Crossbeds to 9 cm thick in sandstone	Conglomerate beds 30 cm — 3.8 m thick. Sandstone beds 5-40 cm thick. Topmost conglomerate (3.8 m thick) is sharply overlain by grey conglomerate (see below). Intensity of purplish colour increases to top of interval, due to increase in amount of pebble- to small cobble-sized volcanic regolith clasts. Fuchsite pebbles <1%. Matrix — very coarse pebbly sandstone with abundant regolith grains. Clasts — round to oval, deformed 2-3:1 into plane of schistosity.
1	RA	56.2-57.7	Conglomerate, with 20% sandstone lenses	Grey		D_5 at 57.1 m = 10 Max qz pebble = 12		Clasts as in underlying conglomerate. More fuchsite pebbles than underlying conglomerate. Matrix — coarse-very coarse — pebbly sandstone with much fewer regolith grains; clean sandy appearance.
2	RB	57.7-62.0	Coarse to very coarse sandstone, pebbly sandstone	Grey		D_5 at 59.2 m (in coarsest pebbly bed in unit) = 2	Crossbeds, to 10 cm thick	Crossbed orientation indicates sediment transport from west to east (in outcrop plane).
2	RB	62.0-83.8	Coarse to very coarse sandstone and subordinate pebbly sandstone	Light to dark grey	Isolated pebbles (to 1 cm) common	D_5 in pebbly layers: at 65.1 m = 2.2 69.4 m = 2.0 69.4 m (pebble train) = 4.4 77.6 m (1 m thick crossbedded pebbly sandstone = 3.7	Crossbeds, commonly 3-5 cm thick (max. 15 cm). In top 3 m crossbeds become thicker, up to 25 cm thick. Pebbly crossbeds generally ≤20 cm.	West to east sediment transport. Pebbles dominantly quartz, rhyolite, epidosite, mauve quartzite. Some volcanic clasts with hematiferous rinds. Abrupt contact with overlying unit.
2	RB	83.8-126.2	Coarse to very coarse sandstone, pebbly sandstone, pebbly grit and pebble conglomerate	Grey, greenish, light grey to white, light mauve unit	Isolated pebbles in sandstone. Pebbly scours are 10% of	D_5 in pebbly layers: at 93 m = 5.3 99.3 m = 3.1 105 m = 2.8 106.4 m = 6.6 115.6 m = 1.5	Trough crossbeds, 10-70 cm thick (average 30 cm)	Unit is composed entirely of scour deposits. Differs dramatically from underlying unit in thickness and nature of crossbeds, and variability in sandstone lithology.

Member	Unit	Interval (m)	Rock Type(s)	Colour	Pebble Abundance	Pebble Size (cm)	Bedforms	Comments
								Lightest coloured sandstone is generally quartz rich very coarse sandstone or grit. Crossbeds defined by sandstone lithology, colour, grain size. Pebbles dominantly quartz, mauve quartzite, white rhyolite, less common mafic volcanics (commonly with hematite rinds or veinlets).
		126.2-164	Covered					
3	RC	164-180	Coarse to very coarse sandstone	Pinkish		Max pebble size in pebbly sandstone scour = 2	Thick crossbeds, similar to underlying unit	Pebbly scours 5-10% of unit.
		180-219	Covered					
3	RC	219-237.5	Coarse sandstone	Medium brown to medium grey to slightly pinkish	Rare isolated pebbles	D_5 (in a pebbly scour) at 228.3 m = 1.8	Crossbeds, 5-10 cm thick	Almost complete absence of clearly defined bedding structure. Pebbly scours to 50 cm thick.
		237.5	Fault					Strike 278°, dip 90°, occupied by a 3 cm thick quartz vein.
3	RD	237.5-262.5	Coarse quartz-rich sandstone	White to light grey		D_5 at 258 m = 2.1	Crossbeds, 1.5-20 cm thick (average 7 cm)	80-85% quartz, <5% mafics. Trough crossbeds indicate west to east sediment transport. Dominant pebble type is quartz.
3	RD	262.5-268.8	Very coarse quartz-rich pebbly sandstone and conglomerate	Medium grey	50% of the unit is pebbly	D_5 at 262.8 m = 4.8 261.5 m = 6.5	Crossbeds throughout	Basal 1.8 m consists of conglomerate with quartz, mauve quartzite, chert, jasper and rhyolite pebbles, some with hematite rinds. Matrix supported by very coarse pebbly sandstone. Remainder of unit is pebbly scours into coarse pebbly sandstone. Becomes less pebbly upwards. Abrupt contact with overlying unit.

Member	Unit	Interval (m)	Rock Type(s)	Colour	Pebble Abundance	Pebble Size (cm)	Bedforms	Comments
3	RE	268.8-287.0	Coarse pebbly sandstone	Greyish brown to mauve	10% isolated pebbles	D_5 (isolated pebbles) at 277.9 m = 1.5 Max pebble size (in a pebbly layer) = 6	Crossbeds (≤ 70 cm thick) are not common	Pebbles include angular to subrounded quartz, chert, mauve quartzite and jasper.
		287-362	Covered					
3	RF	362-430.9	Coarse to very coarse sandstone	Medium brown	Rare (3%)	D_5 (in pebbly grit scour) at 307.8 m = 2.5 Max qz pebble (isolated pebbles in crossbeds) at 321.5 m = 5	Crossbeds, 10-60 cm (average 37 cm)	Thickly trough crossbedded sandstone with individual crossbeds varying in grain size and quartz content. Pebble-filled scours not abundant; pebbles include subrounded to angular quartz, mafic and felsic volcanics. Shallow scours filled with quartz grit and small pebbles; quartz pebbles generally ≤ 1.5 cm. Very coarse sandstone scours tend to be quartz-rich (70% quartz), more poorly sorted, and contain abundant quartz granules.
3	RG	430.9-450.9	Coarse to very coarse quartz-rich sandstone	Light grey, light tan to off-white	1%	Isolated pebbles ≤ 1 cm, generally quartz	Crossbeds, 9-20 cm (average 13 cm)	More quartz than underlying unit.
3	RG	450.9-542.9	Coarse to very coarse sandstone	Medium brown	3%	D_5 at 416.6 m = 2.5 464 m = 2.6 Max qz pebble = 5 Mudstone rip-ups = 4-8	Crossbeds, 12-30 cm thick (average 19 cm)	Thickly crossbedded. Small round to subround quartz pebbles (≤ 1.5 cm) in very coarse sandstone scours. Crossbeds defined by grain size and quartz content. Conspicuous very coarse to grit-sized, whitish, quartz-rich (70-80%) scours with 5% magnetite up to 1 mm. Pebble types include quartz, rhyolite, chert.
3	RG	542.9-596.4	Very coarse sandstone		3%	D_5 for entire unit = 7.1 Mudstone rip-ups = 6-8, Max qz pebble = 8.0	Crossbeds, 20-45 cm thick.	Differs from underlying interval in greater abundance of coarse detritus and poorer sorting. Mudstone ripups occur in coarse grit-pebble scours.

Member	Unit	Interval (m)	Rock Type(s)	Colour	Pebble Abundance	Pebble Size (cm)	Bedforms	Comments
3	RH	596.4-825.4	Coarse sandstone	Light to medium brown, medium grey, local pinkish tones	1-2%	D_5 at 558 m = 3.9 Mudstone = 6-11 630 m = 3.3 Mudstone = 2-10 750 m = 5.5	Crossbeds, 20-70 cm thick	Differs from underlying interval in finer grain size and slightly better sorting. Very coarse sandstone scours, locally pebbly are locally present. Crossbeds subtle — defined by grain size and quartz content. Pebbles include quartz, chert (common), rhyolite. Slabby mudstone ripups throughout.
3	RI	825.4-876.4	Coarse to very coarse sandstone with common quartz-rich very coarse sandstone scours	Medium brown, cream	2-3%	D_5 at 765 m = 4.5	Crossbeds, 15-50 cm thick for very coarse material	Overall this unit is coarser and more quartz-rich than underlying unit, but some pinkish coarse sandstone is present. Pebble types include quartz, chert, rhyolite and sericite schist.
		876.4	Channing fault					
		876.4-946	Coarse to very coarse sandstone	Medium grey	3-5%	D_5 = 4.2	Crossbeds, 5-50 cm thick	Individual scours defined by grain size, quartz content, and in places by hematite. Sediment transport direction south to north (within outcrop plane).
3	RJ	946-1109	Medium to coarse sandstone	Grey	<1%	D_5 at 885 m = 1.5 1035 m = 1.8	Crossbeds, 50-60 cm thick in coarse material	Finer grained than underlying sandstone. Few bedforms observed. Finer sandstone has about 40% quartz. Becomes somewhat coarser upwards; the top few metres contains increasing amounts of much coarser sandstone scours.
4	RK	1109-1111	Pebble conglomerate and pebbly sandstone			D_5 = 3.5	Sandstone is crossbedded	Dominant pebble type is white, grey to purplish quartz, angular to subrounded in shape. Other pebble types include angular, laminated chert, rhyolite. Matrix supported conglomerate poorly sorted, with hematite laminations.

Member	Unit	Interval (m)	Rock Type(s)	Colour	Pebble Abundance	Pebble Size (cm)	Bedforms	Comments
4	RK	1111-1176	Coarse sandstone	Medium brown, pinkish brown	Very rare	D_5 at 1100 m = 2.0 Mudstone to 8 cm	Crossbeds, 3-30 cm thick, average 15 cm	Crossbeds defined by grain size; very coarse sandstone on foresets of some beds. Commonly quartz-rich. Pebble types include rhyolite and chert; there is virtually no quartz.
		1176-1207	Covered					
4	RK	1207-1217	Coarse sandstone	Grey-brown	1%	D_5 = 1.8	Large trough crossbeds	
4	RL	1217-1219.5	Very coarse to gritty, quartz rich sandstone and grit	Light grey to white			Crossbeds, 12-44 cm thick	80% quartz. Pebbly scours, poorly sorted. Trough crossbeds.
4	RL	1219.5-1222.5	Pebble conglomerate and very coarse pebbly sandstone			D_5 (for coarsest conglomerate) = 8.2	Trough crossbeds	Pebbles dominantly quartz; also chert-hematite iron formation, grey chert, epidosite, rhyolite. Pebble shapes dominantly subangular but range from angular to rounded. Matrix of the conglomerate is quartz-rich very coarse to gritty pebbly sandstone. Conglomerate composed of several overlapping conglomerate — sandstone scours, commonly with conglomerate at the base.
4	RL	1222.5-1227.5	Very coarse, quartz-rich sandstone and pebbly sandstone	Light grey			Trough crossbeds	Sediment transport from south to north in outcrop plane.
4	RM	1227.5-1261.5	Coarse sandstone	Medium brown	2% Mainly quartz	D_5 = 2.7	Small-scale crossbeds	Quartz content (50-60%) is lower than in underlying unit. Abrupt contact with underlying unit.
4	RN	1261.5-1264.5	Very coarse sandstone, pebble conglomerate	Light grey		D_5 = 7.9	Crossbeds, 5-70 cm thick	Quartz-rich, trough crossbedded. Thicker crossbeds are poorly sorted, pebble conglomerates. Pebble types include quartz, chert, rhyolite, rare jasper. Pebble shapes vary from angular to rounded.

Member	Unit	Interval (m)	Rock Type(s)	Colour	Pebble Abundance	Pebble Size (cm)	Bedforms	Comments
					GRANT LAKE SECTION			
1	GA	0-4	Quartz pebble conglomerate (2 narrow beds)	Light grey	NA	D_5 = 6.5, 6.2	Lensoid beds, 38.6 cm and 37.1 thick	Conglomerate beds are framework supported; largest pebbles are in centre of beds; weakly to moderately rounded quartz pebbles form over 60% of beds. Conglomerate beds fill scour channels in sandstone. Quartz grains in sandstone are polycrystalline with sutured grain contacts.
			Medium to very coarse quartz-rich sandstone	Light grey to white	1-2%	NA	Trough crossbedded, sets average 17.3 cm thick and range from 5.2 to 52.7 cm	
	GB	4-136	Fine to medium sandstone	Pale brown	<0.5%	Pebbles over 5 mm are virtually absent	Massive, virtually no bedforms except for rare, nebulous crossbeds	Magnetite placers and layers are present in bottom 10 m, but are absent higher in this section. 0.5-1 m thick, shallow angle cross-beds (defined by red oxidation spots) occur rarely.
	GC	136-250	Fine to medium sandstone	Pale buff	<0.5%	Pebbles over 5 mm are virtually absent	Massive, rare nebulous crossbeds, very similar to GB	Similar to GB with the following differences: a) slightly higher quartz content; b) rare, well defined, up to 2.5 m deep scours; c) sporadic well defined heavy mineral placers; and d) more red oxidation spots (which increase in abundance up-section). Crossbed geometry suggests northerly component of sediment transport.
2	GD	250-270	Medium to coarse sandstone and pebbly sandstone	Pale pink-buff to green	up to 10%	D_5 (isolated pebbles in basal sandstone bed) = 5.2 D_5 (pebbly sandstone fill in scour) = 10.4	Lensoid beds, 0.2 to 4.5 m thick Trough crossbeds common (in one bed they average 19 cm in depth and range from 8.8 to 31.3 cm)	Bed contacts are erosional surfaces that are well defined. Isolated pebbles and pebble lags are common. Heterolithologic pebble population. Oxidation spots (characteristic of member 1) are not present.

Member	Unit	Interval (m)	Rock Type(s)	Colour	Pebble Abundance	Pebble Size (cm)	Bedforms	Comments
3	GE	270-297	Small cobble conglomerate	Pale brown	NA	D_5 (series of beds in order up section) = 20, 19.2, 14.2, 16.5, 16.3, 18.8, 16.6	Ten planar (?) beds, average 2.95 m thick and range from 1.25 m to 6.65 m	Section consists of intercalated units of conglomerate and sandstone. Conglomerate beds are heterolithologic, framework supported and ungraded to weakly upward coarsening. Sandstone beds are discontinuous along strike. Cobbles of Missi sandstone form 10% of framework clasts in conglomerate beds.
			Medium to coarse sandstone	Brown	5%	D_5 (pebble lag deposit) = 6.6	Eight lensoid beds, average 0.6 m thick and range from 0.12 to 1.96 m	
4	GF	297-313	Medium to coarse sandstone and pebbly sandstone		0-20%	D_5 (pebble lag deposit) = 10.8	Lensoid beds, average 1.3 m thick and range from 0.38 to 3.2 m. Bed contacts are erosional surfaces.	Pebble population is heterolithologic. Pebble lag deposits are common with rarer thick pebble deposits infilling scour channels.
LITTLE CLIFF LAKE SECTION								
3	GE	0-10	Medium to large cobble conglomerate		NA	D_5 = 26.8	None	Pebbles tectonically flattened, rock foliated. Pebble population heterolithogic, framework supported and moderately rounded to well rounded. Pink equigranular granitoid cobbles and boulders are common.
4	GF	10-184	Medium to coarse sandstone and pebbly sandstone	Light grey	10-15%	D_5 (pebble lag deposits) = 9.7, 8.4, 3.1 D_5 (isolated pebbles) = 6.8, 4.1, 4.3	Well defined trough crossbeds (0.25 to 1 m deep) are ubiquitous	Pebbles occur mainly in pebble lag deposits one to two pebbles thick. Pebbles are well rounded and include a high proportion of "resistant" lithologies (e.g. rhyolite, quartz, felsic intrusive rocks).

Member	Unit	Interval	Rock Type(s)	Colour	Pebble Abundance	Pebble Size (cm)	Bedforms	Comments
	GG	184-310	Medium to coarse sandstone	Brown to brown grey	2%	Isolated pebbles are generally less than 3 cm in diameter	Lenticular beds, generally 1 m thick. Trough crossbedding is common (15 to 25 cm thick)	Pebbles are rare and occur mainly in small isolated scour channels; isolated pebbles are present throughout section. The sandstone contains dispersed iron oxide grains and magnetite-rich placers. The section contains one lenticular, up to 13 m thick conglomerate unit that is characterized by angular to rounded, heterolithologic, matrix-supported pebbles.
			Small cobble conglomerate		50%	D_5 = 11.8		

* Measured intervals represent true thickness (i.e. corrected for dip).
Base of Ross Lake section is taken at the unconformable contact with Amisk Group rocks.

** Sandstones named according to Wentworth size classification: 0.0625-0.125 mm very fine sand, 0.125-0.25 mm fine sand, 0.25-0.50 mm medium sand, 0.50-1.00 mm coarse sand, 1.00-2.00 mm very coarse sand, 2-4 mm grit, 4-24 mm pebbles, 24-256 mm cobbles, >256 mm boulders.

***D_5 is the average diameter of the 5 largest pebbles at the stratigraphic height or interval indicated.
Max. qz pebble is the diameter of the largest quartz clast in the stratigraphic interval.

Table 24:
Framework clast percentages in Missi Group conglomerates
(Location of counts shown on Fig. 259)

	1	2	3	4	5
Intermediate to mafic volcanic	63.2	54.4	46.6	48.4	47.5
Intermediate to mafic intrusive	4.5	29.2	20.9	7.7	17.7
Epidosite	5.8	3.5	5.1	2.3	1.3
Felsic volcanic	21.0	3.5	2.4	12.7	7.6
Felsic hypabyssal	—	—	9.9	10.9	8.2
Granitoid	—	4.3	tr.	1.8	1.9
Quartz	3.6	4.3	3.6	4.5	tr.
Quartzite	0.5	0.4	—	0.9	0.9
Chert	—	0.4	—	—	
Sandstone	1.3	tr.	11.5	10.9	13.9
Iron formation	tr.	—	—	tr.	0.6
Fuchsite	0.5	—	—	—	—
Detrital matrix	39.4	27.8	30.3	26.6	57.5
Total counts	371	356	363	301	372

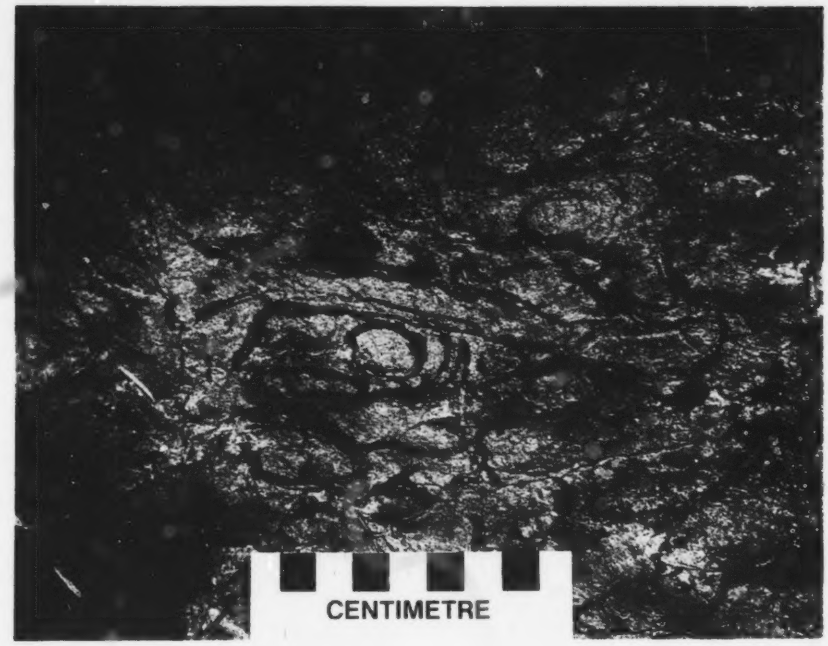

Figure 260: *Hematiferous, "onionskin" weathering in unit 7 Amisk Group pillowed flows within the sub-Missi regolith; old Highway 10 at Northstar Road.*

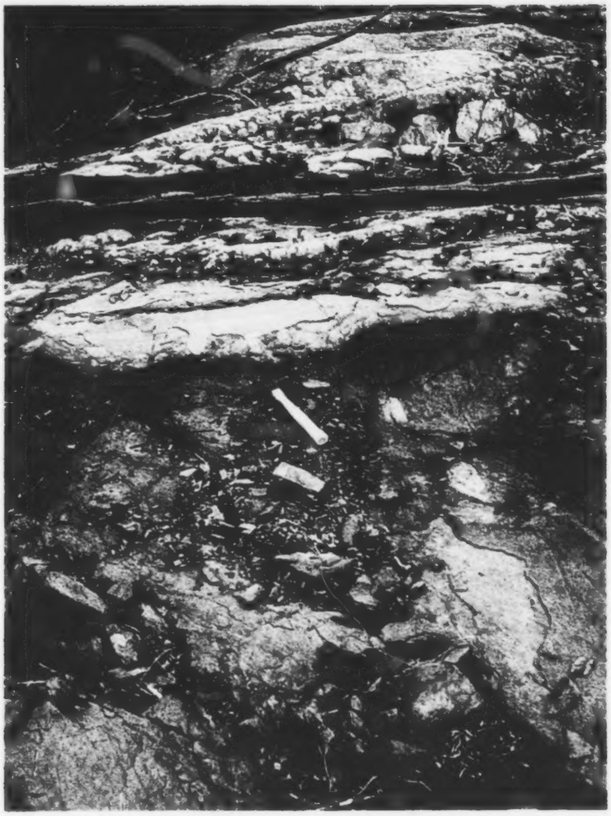

Figure 261: *Hematiferous regolith (dark) developed on Amisk Group basalt (unit 7) beneath unconformably overlying Missi Group fluviatile pebble and cobble conglomerate (unit 52c, b). Structural outlier of Missi, 1 km west of Channing.*

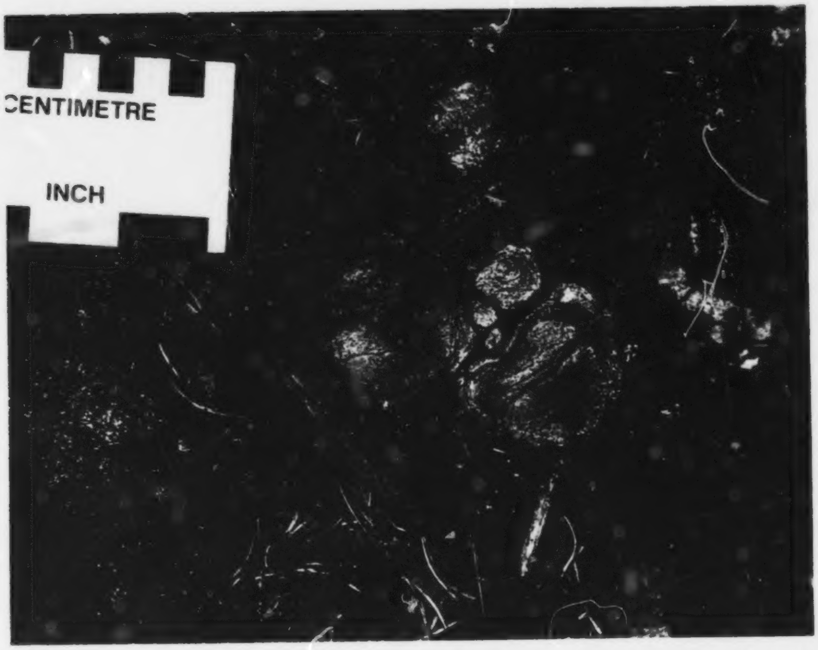

Figure 262: Missi Group conglomerate (unit 50b), 600 m southeast of Ross Lake (unit RA on Fig. 259). Featured is a clast of Amisk Group volcanic rock displaying hematiferous, onionskin weathering characteristic of the Amisk regolith (see Fig. 260).

The basal conglomerate member is overlain by about 87 m of grey, trough crossbedded coarse to very coarse sandstone and pebbly sandstone. Pebbles in this second member occur in discrete beds, crossbeds, and scours. The form of crossbeds indicates a horizontal component of transport towards the east (Fig. 263).

The third and thickest member in the Ross Lake section comprises thirteen sandstone units (RC to RJ) with a total thickness of 964 m (Fig. 259). The various sandstone units are defined by colour, grain size, composition and contained sedimentary structures (Table 23). Most units are dominated by coarse to very coarse detritus, with only the topmost unit somewhat finer grained. Crossbedded sandstones (Fig. 264) predominate, and pebbles occur as rare isolated clasts generally composing less than 3% of the rock.

The fourth (topmost) member in the Ross Lake section comprises of 156 m of coarse to very coarse sandstone with three thin pebble conglomerate units. The conglomerates are trough crossbedded and are dominated by pebbles of quartz, chert, oxide-facies iron formation and felsic volcanics. The thicker, associated sandy units are crossbedded and contain few pebbles.

The combined Grant Lake-Little Cliff Lake section (Fig. 259) contains four major members. The first member is 250 m thick and consists almost entirely of fine- to medium-grained massive sandstone that is virtually free of pebbles. A 4 m thick unit of quartz pebble conglomerate and medium to very coarse quartz-rich sandstone occurs at the base of this member. This unit is similar to the pebble conglomerates in the fourth (topmost) member of the Ross Lake section.

The second member in the section comprises 20 m of trough crossbedded medium to coarse sandstone and pebbly sandstone. Bed contacts are well defined erosional surfaces.

The third member comprises of 27 m of cobble conglomerate organized into ungraded to weakly upward coarsening beds. This conglomerate differs from the basal Missi conglomerate in that it contains a significant proportion of intraformational sandstone clasts and very few regolith clasts (Table 24). Conglomerate beds are intercalated with discontinuous lensoid sandstone beds.

The uppermost member in the Grant Lake-Little Cliff Lake section comprises 300 m of trough crossbedded medium to coarse sandstone and pebbly sandstone. Pebbles are common in the lower 174 m, as lag deposits and isolated clasts, but are not common in the upper 126 m.

PROVENANCE

Rock types that were present in the source area of Missi Group sediments are represented by clasts in the conglomerates and by sand-sized grains in the finer grained fraction.

Two significant conglomeratic units occur in the Missi section, one at the base and another halfway through the Grant Lake-Little Cliff Lake section (Fig. 259). These conglomerates contain similar clast types except that the upper conglomerate contains 11 — 14% intraformational sandstone clasts (Table 23). With the exception of jasper, chert and iron formation, which are rare in the presently exposed Amisk Group, the great majority of clasts are similar to rock types that occur in the underlying volcanic sequence. Granitoid clasts, although present in both conglomerates, are not a common component of the coarse fraction. Notably, pebbles of "metamorphic" rocks (i.e. higher grade than the regional greenschist facies) and gneissic rocks are absent. All clasts are moderately to well rounded, but resistant clasts (e.g. quartz, chert) are not selectively concentrated in the two main conglomerates.

The various thin conglomerate units that occur throughout the Missi section differ from the two main conglomerate units in that they are characterized by an abundance of resistant lithologies: quartz, chert, iron formation and felsic volcanics. These rock types occur also as isolated pebbles throughout the sandstones. The thin conglomeratic units simply represent concentrations of coarse detritus winnowed in stream channels, and are not representative of the source terrane to the same extent as are the two main conglomerate units.

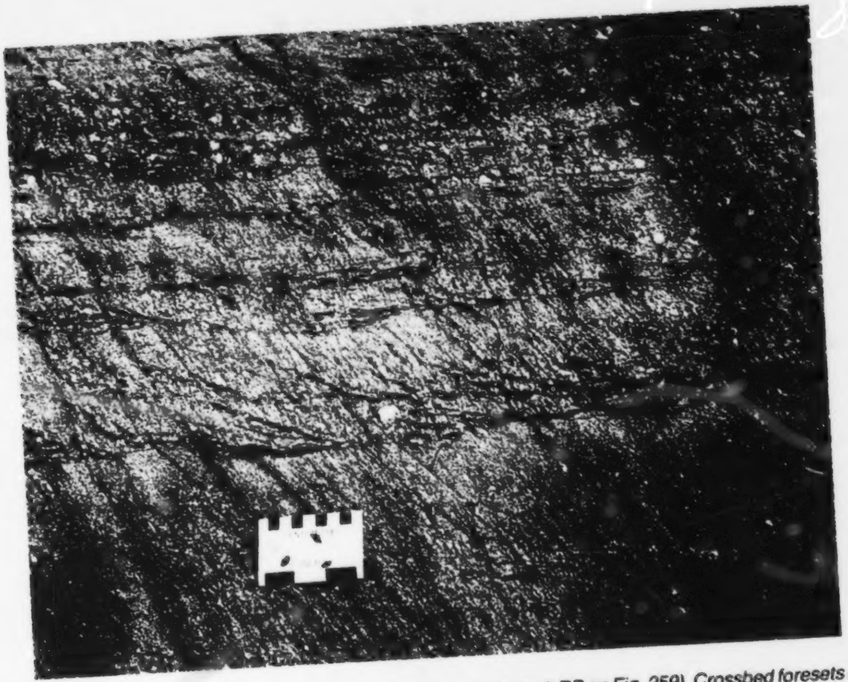

Figure 263: Missi Group pebbly sandstone (unit 50b), 600 m southeast of Ross Lake (unit RB on Fig. 259). Crossbed foresets and bottomsets are defined by blacksand laminae (Fig. 266). Schistosity crosses bedding at a high angle.

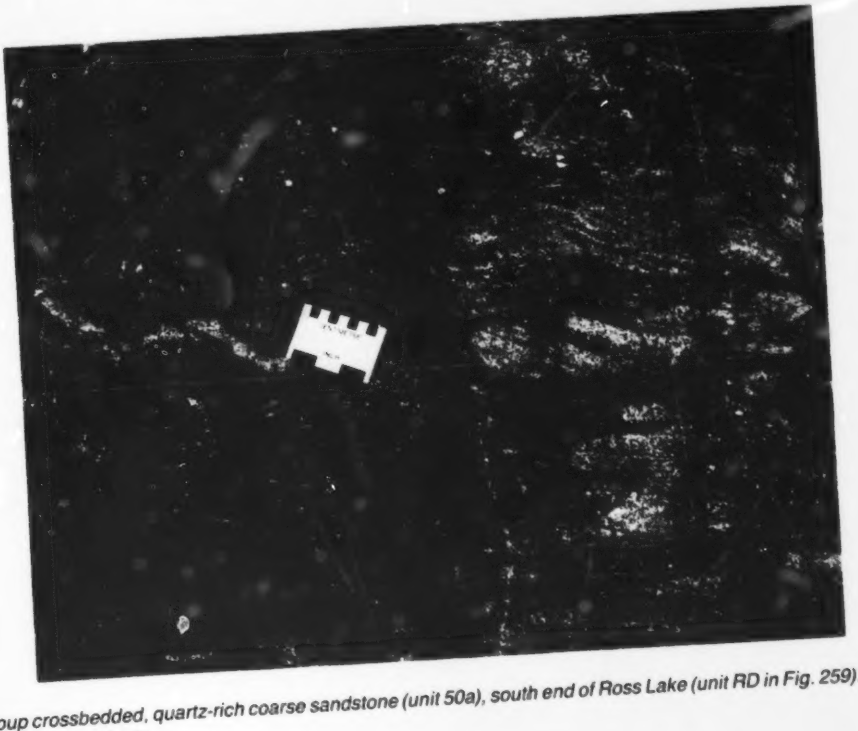

Figure 264: Missi Group crossbedded, quartz-rich coarse sandstone (unit 50a), south end of Ross Lake (unit RD in Fig. 259). Blacksand heavy mineral laminae define crossbeds.

Sand-sized grains in Missi rocks include quartz, plagioclase and rock fragments (Fig. 265). Quartz grains occur as polycrystalline and monocrystalline varieties, in highly varying proportions. The polycrystalline types are interpreted to be mainly vein quartz. Like vein quartz they display sutured internal grain boundaries, rare acicular inclusions of tremolite-actinolite and tourmaline, vermiform inclusions of actinolite, and, in some grains, coarse intergrowths with carbonate or epidote. Monocrystalline types are interpreted to be largely plutonic quartz because they contain rare inclusions of apatite, plagioclase, and zircon. Some monocrystalline grains occur in sand-sized quartz-plagioclase mosaics or in micrographic intergrowths with plagioclase. Quartz clearly derived from volcanic rocks (e.g. embayed crystals) is very low in abundance. Plagioclase grains are mainly altered to sericite; least altered plagioclase is subangular, albite-twinned, and commonly contains abundant exolved iron (as Fe-oxide). Most plagioclase grains are considered to be of plutonic derivation. Sand-sized rock fragments are generally poorly preserved and include common felsic volcanics, mafic volcanics, chert and minor granitoid types. In the upper part of the Grant Lake-Little Cliff Lake section sandstone rock fragments are present in the sand-sized fraction.

Accessory heavy minerals in Missi Group sandstones include specular hematite, zircon, epidote, allanite and tourmaline. The specular hematite is particularly abundant, and occurs as subrounded sand-sized grains in laminae, placers, and crossbed forsets (Fig. 266). Detrital zircon and epidote crystals are commonly associated with the specular hematite placers. Tourmaline forms only a small part of the heavy mineral assemblage, but occurs in most sandstones in the upper 440 m of the Ross Lake section.

In summary, an interpreted source area for the clastic detritus in the Missi Group must be consistent with:

1) high proportion of mafic volcanic and high-level intrusive rocks in conglomerates,
2) granitoid pebbles, abundant sand-sized plutonic quartz and plagioclase, and trace zircon and allanite,
3) vein quartz pebbles, abundant sand-sized vein quartz, detrital epidote and tourmaline,
4) intraformational sandstone clasts in the upper 320 m of the Grant Lake-Little Cliff Lake section,
5) chert, jasper, chert-hematite iron formation and sand-sized specular hematite,
6) absence of clasts derived from a higher grade metamorphic terrane.

Mapped geological relationships clearly indicate that prior to deposition of the Missi Group, Amisk Group volcanic rocks were folded and intruded by granitoid plutons. A source area composed of these rock types is consistent with the provenance of the clastic material in the Missi. Selective concentration of mechanically and chemically stable components such as vein quartz, chert, iron formation and jasper explains their abundance out of proportion to their abundance in the exposed Amisk group.

Intraformational sandstone clasts in the upper part of the Missi Group indicates that lithified Missi Group sedimentary rocks were uplifted, eroded and incorporated into later members of the group.

INTERPRETATION

The Missi Group is interpreted to have been deposited by fluvial processes in an alluvial system, adjacent to a highland source (Byers, 1953; Mukherjee et al., 1971; Stauffer, 1974). Sedimentary structures observed in the Missi at Flin Flon (Fig. 267, 268, 269; Table 23) are consistent with this interpretation. Provenance data (above) indicate that the source area was composed of folded Amisk Group volcanic rocks and contained quartz veins and granitoid intrusions.

A speculative model showing four stages leading up to and including deposition of the Missi Group is depicted in Figure 270. In this model,

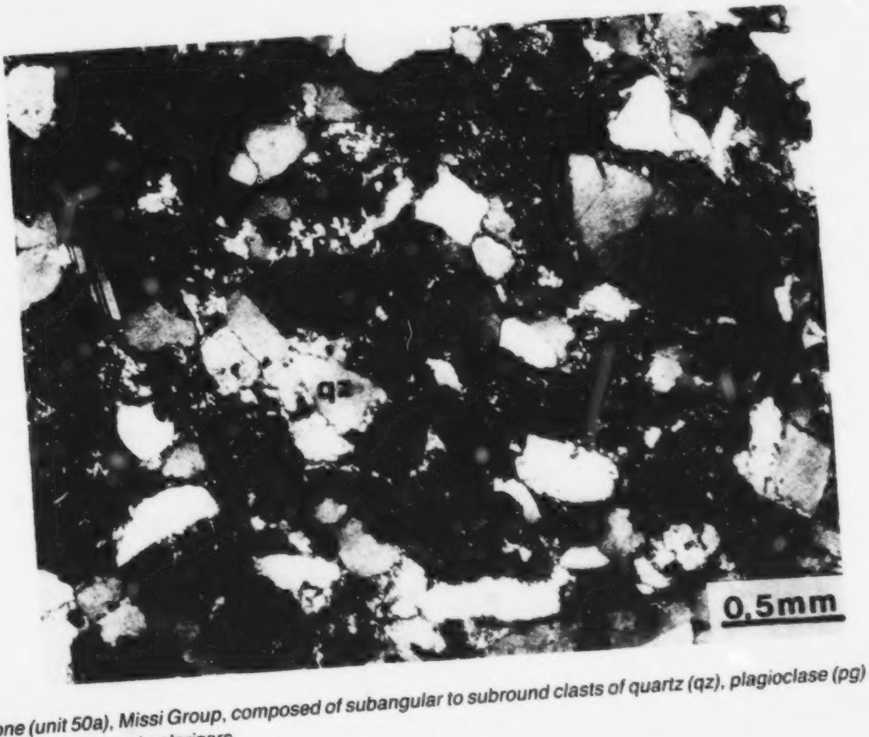

Figure 265: Sandstone (unit 50a), Missi Group, composed of subangular to subround clasts of quartz (qz), plagioclase (pg) and lithic fragments (lth). Sample 3634-1, crossed polarizers.

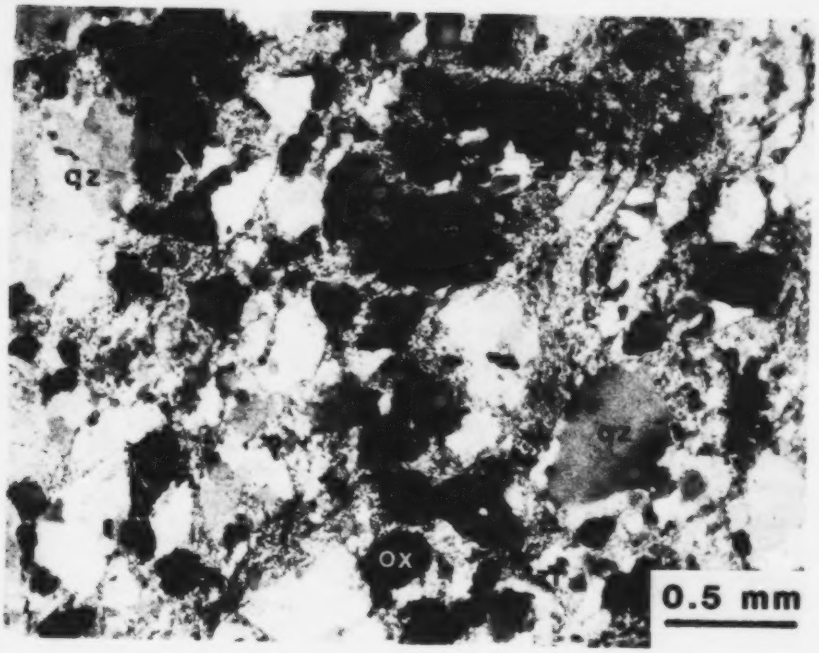

Figure 266: Heavy mineral placers/lamellae, Missi Group sandstone (unit 50a) 400 m northwest of Mud Lake. The lamellae are composed predominantly of subrounded grains of specular hematite (ox; black) and sporadic subhedral zircon (zr). The sandstone is composed mainly of quartz (qz), fine grained recrystallized feldspar, and sericite. Sample 6167-1, crossed polarizers.

Figure 267: Trough crossbedding in structural outlier of Missi Group sandstone (unit 50c), 1 km west of Channing. Note pebble lag deposits at base of crossbed sets and heavy mineral placers (dark) on foreset beds.

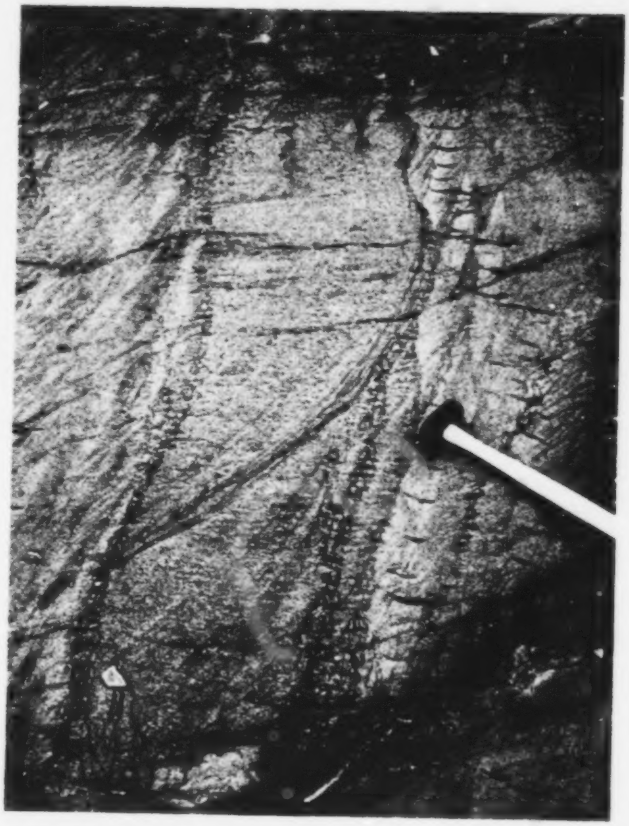

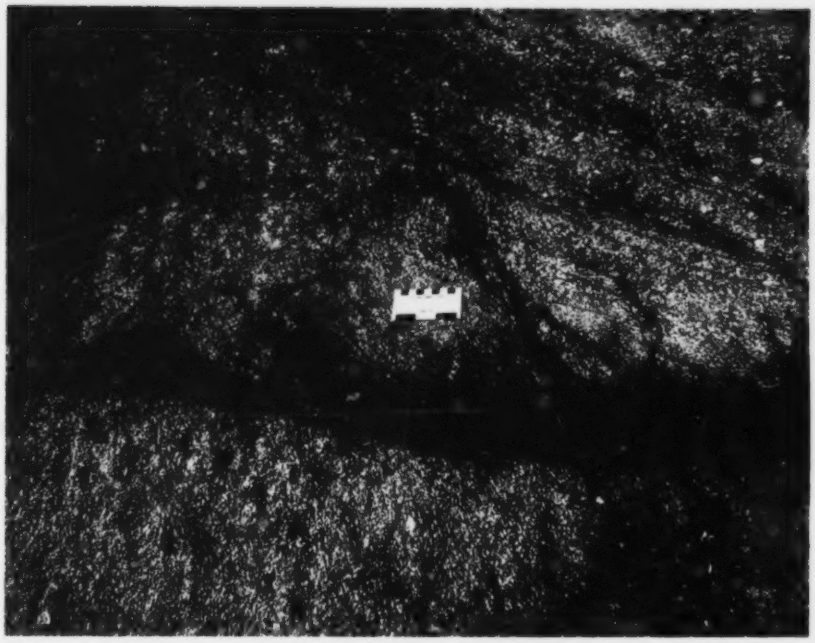

Figure 268: Missi Group trough crossbedded pebbly sandstone (unit 50b, c), 100 m east of Scotty Lake. Unusually thick heavy mineral placers (black) on foresets and bottomsets of crossbed.

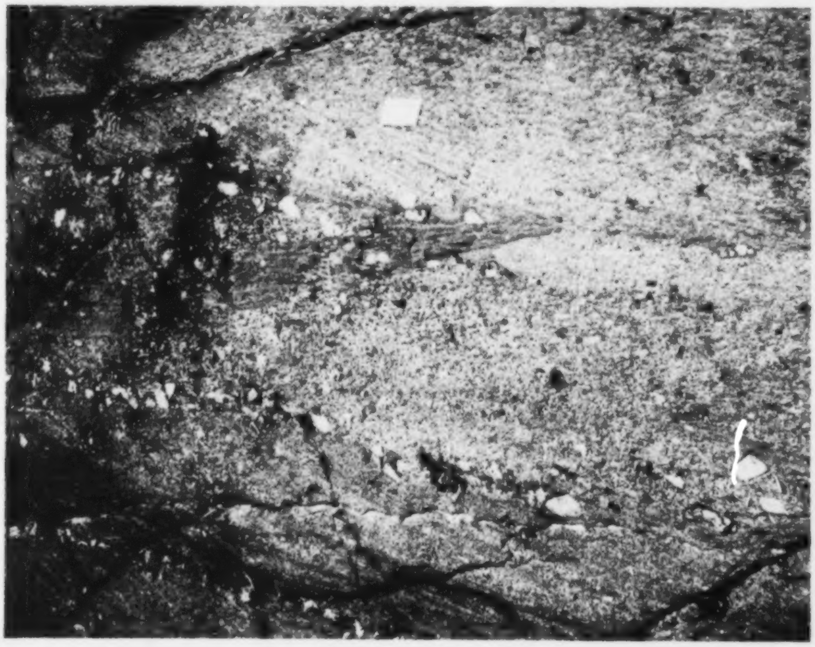

Figure 269: Missi Group trough crossbedded coarse pebbly sandstone (unit 50b, c), old Highway 10 at Northstar Road.

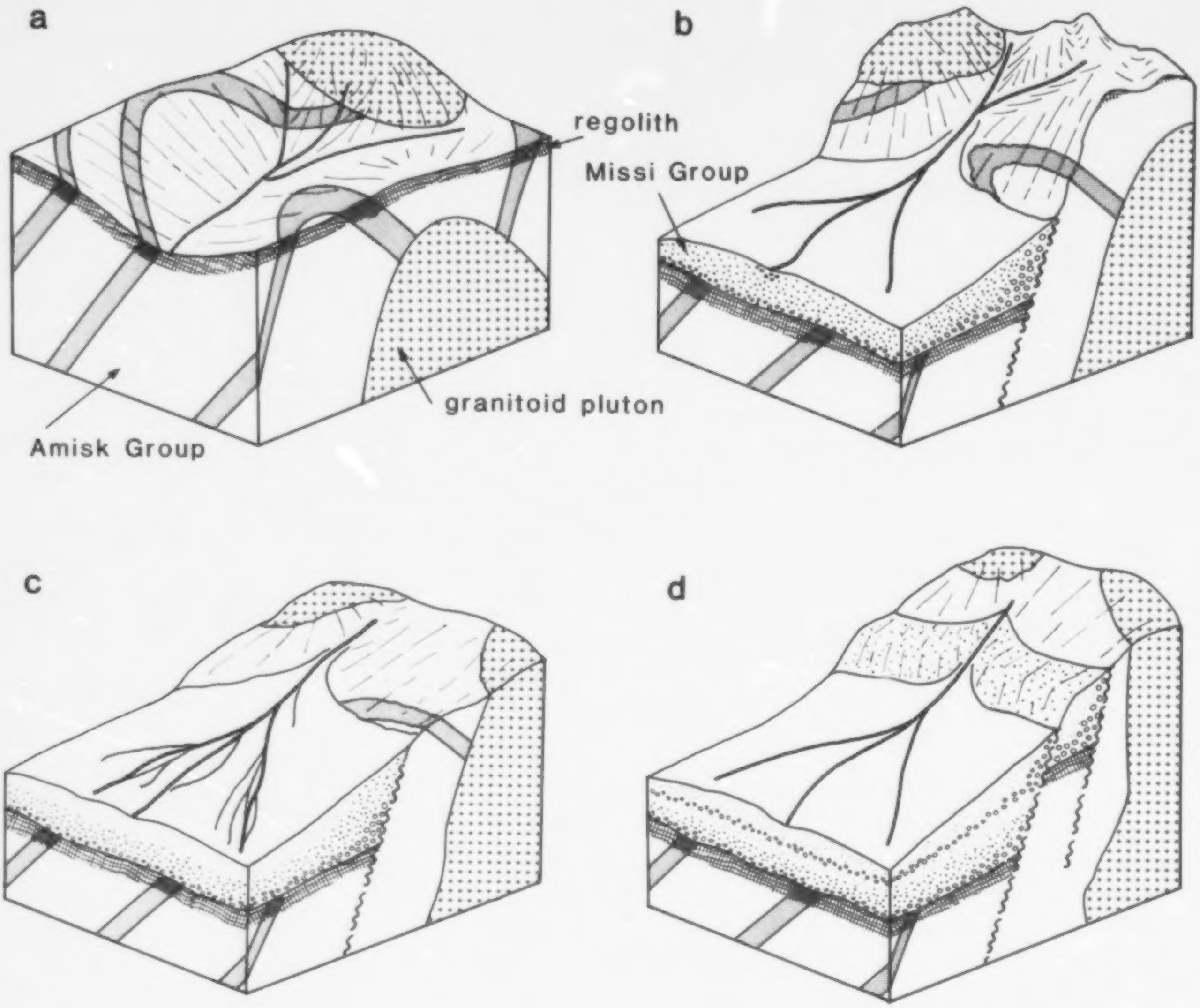

Figure 270: Schematic diagram depicting four stages leading up to and including deposition of the Missi Group. See text for discussion.

cessation of Amisk volcanism was followed by tight folding of the volcanic rocks and intrusion of granitoid plutons. This deformed, volcanic-plutonic terrane was subsequently peneplaned, and a thick hematiferous regolith developed in a subaerial environment (Fig. 270). Changing tectonic conditions resulted in vertical movement and the development of highlands and basins. Regolith and granitoid detritus stripped from the highland areas were deposited as a conglomerate in adjacent basinal areas floored by weathered Amisk rocks (Fig. 270). In the Ross Lake section this stage is represented by the 58 m thick basal conglomerate-sandstone unit rich in Amisk regolith detritus. Overlying sandstones in the Ross Lake section contain less regolith material, representing deeper erosion of less-weathered Amisk rocks in the highland source area. Continued erosion and retreat of the bordering highland resulted in finer detritus being supplied to the basin (Fig. 270). This sand and gravel was deposited from braided streams and sheetfloods which formed thick alluvial fans and plains now represented by the broadly upward-fining lower two-thirds of the Missi Group. Coarse conglomerates at the base of the Little Cliff Lake section indicate an abrupt change in sedimentary pattern, probably in response to renewed vertical movements. Intraformational sandstone clasts in the Little Cliff Lake section indicate that lithified portions of the lower Missi, along with Amisk rocks, were elevated in the rejuvenated highlands (Fig. 270). Upward fining in the Little Cliff Lake section represents a second cycle of highland erosion and retreat.

POST-MISSI INTRUSIVE ROCKS

INTRODUCTION

Post-Missi intrusions (units 51-57) are strictly defined as those that either are observed to cut the Missi Group (eg. units 51, 52, 53, 57) or are emplaced within or across post-Missi faults (eg. units 52, 53, 54, 55, 56). Intrusions of this age constitute only a minor component of the magmatic rocks in the area.

MELADIORITE AND PYROXENITE (BOUNDARY INTRUSIONS) (UNIT 51)

Plug and dyke-like bodies of the Boundary intrusion suite occur only in the Flin Flon block, in the extreme western portion of the map area. Field relationships, petrography and chemical characteristics of the Boundary intrusions indicate that they are composed of three compositionally distinct, sequentially emplaced groups (Syme and Forester, 1977). From oldest to youngest, these are: (1) a mafic, augite- and biotite-bearing meladioritic group, (2) a felsic group ranging from leucodiorite to granodiorite, and (3) an olivine-bearing group comprising wehrlite and olivine gabbro. The felsic group is chemically similar to post-Missi granodioritic plutons and is not genetically related to the mafic and ultramafic members of the Boundary suite.

Boundary intrusions are emplaced in folded Amisk and Missi Group rocks, and contain structures related to P5 shear zones. The zone of intrusion for these rocks trends parallel to the P3 Hidden Lake Synform. On Phantom Lake in Saskatchewan, mafic members of the suite are cut by the 1.82 Ga Phantom Lake granite (MacQuarrie, pers. comm. 1981).

Within the map area the Boundary intrusion types include pyroxenite (replaced by an assemblage of tremolite-actinolite, chlorite, biotite and carbonate) and meladiorite. Meladiorite, the predominant lithology, contains 40 — 50% pseudomorphs after clinopyroxene (2 — 4 mm), primary brown biotite (10 — 15%) and subhedral plagioclase (35 — 45%).

Emplacement of the mafic intrusions was accompanied by significant dyking and brecciation of both country rocks and earlier crystallized phases of the Boundary suite. An example of intrusion breccia (unit 51a) directly north of South Main shaft contains large inclusions of pillowed flows and rhyolite, and is cored by Boundary meladiorite.

PYROXENITE DYKES (UNIT 52)

A dyke-like body of coarse grained pyroxenite, 45 m wide and exposed for 1200 m, occurs 200 m east of One Portage Lake. It cuts both Amisk Group rocks and the Whitefish Lake Intrusion (unit 40).

The pyroxenite is dark green on both weathered and fresh surfaces, and has a grain size up to 6 mm. It is composed of an interlocking mosaic of equant, anhedral to subhedral amphibole with minor (2%) interstitial quartz. The amphibole crystals have cores of colourless tremolite-actinolite and epidote, pseudomorphic after subhedral-euhedral prismatic pyroxene.

Locally, the eastern portion of the dyke is intensely veined by white to pink leucotonalite; the veins increase in size and abundance towards the eastern contact of the dyke.

GABBRO, DIORITE, QUARTZ DIORITE (UNIT 53)

This unit contains a variety of discrete, probably unrelated rock types. They include sills and irregular bodies of diorite/quartz diorite emplaced in Missi Group rocks, and a distinctive suite of small gabbro bodies which intrude P5 faults.

The gabbros (unit 53a) weather green and white and are dark grey and white on fresh surfaces. They are homogeneous, have a 1 — 2 mm diabasic texture and are composed of 50 — 60% lath-shaped plagioclase (0.5 — 2 mm) and 40 — 50% anhedral to subhedral pyroxene (0.4 — 2 mm) replaced by tremolite-actinolite and chlorite. Accessories include Fe-Ti oxides and apatite. The intrusions are unfoliated and are commonly emplaced within sheared, schistose rocks within fault zones.

WHITEFISH LAKE QUARTZ MONZODIORITE AND RELATED INTRUSIONS (UNIT 54)

Three quartz monzodiorite and quartz diorite intrusions are spatially associated with the group of closely spaced post-Missi faults that extends from Athapapuskow Lake, along the Pineroot River, through Whitefish Lake to Mikanagan Lake. The two largest intrusions, east and north of Whitefish Lake, appear to have been emplaced into the zone of faults and are therefore considered to be post-Missi in age. These intrusions display minor offsets and some shearing along extensions of the faults; however, displacements are limited and most movement along the faults must have predated emplacement of the intrusions. The third body in this group, east of Mikanagan Lake, intrudes Amisk Group rocks and does not appear to be directly related to faulting.

Whitefish Lake quartz monzodiorite (unit 54a)

The largest intrusion in this group, a relatively homogeneous, single-phase quartz monzodiorite, occurs north of Whitefish Lake. It is about 2.5 km long and 300 — 600 m wide. The intrusion is flanked to the east by well bedded southeast-facing mafic tuffs of unit 20, and to the west by mafic flows and gabbro. The lack of stratigraphic continuity in the Amisk Group host rocks, from one side of the intrusion to the other, suggests that the intrusion occupies a major fault zone.

The contact zone of the intrusion is characterized by swarms of porphyritic dykes in the wall rocks and abundant volcanic xenoliths in the intrusion. Dykes are generally limited to within 50 m of the contact; they are 0.3 — 3 m in width and do not display chilled margins. Dykes trend subparallel to the margin of the intrusion in the north but have no preferred orientation in the south. Volcanic xenoliths at the margin of the intrusion are angular to tabular in shape and range in size from 5 cm to several metres. Highly elongate tabular xenoliths are oriented with long axes parallel to the margin of the intrusion. Some smaller xenoliths are partially assimilated. Host volcanic rocks in the contact zone are locally epidotized and gossaned; pyrite and epidote occur along irregular fractures.

The quartz monzodiorite weathers white, light pinkish buff to light buff and is pale grey to mottled pink and green on fresh surface. In the core of the intrusion the texture is approximately hypidiomorphic equigranular (1 — 3 mm; Fig. 271); towards the margins the range of plagioclase and amphibole size increases (to 6 mm) and the rock has a seriate/porphyritic texture (Fig. 272).

Plagioclase (0.2 — 6 mm, 35 — 60%) is euhedral, tabular to equant, oscillatory zoned, and partially replaced by sericite and epidote. Amphibole (0.2 — 3 mm, 15 — 30%) is euhedral, prismatic and partially to completely replaced by chlorite, epidote, tremolite-actinolite, carbonate and Fe-oxides. Both plagioclase and amphibole have a moderate preferred (igneous) orientation. Potassium feldspar (0.2 — 1.5 mm, 3 — 18%) in the form of orthoclase is anhedral, poikilitic to interstitial. Quartz (0.1 — 0.5 mm, 5 — 15%) is anhedral interstitial. Fe-Ti oxides (0.1 — 0.5 mm, up to 3%) are anhedral equant to subhedral and are replaced by leucoxene,

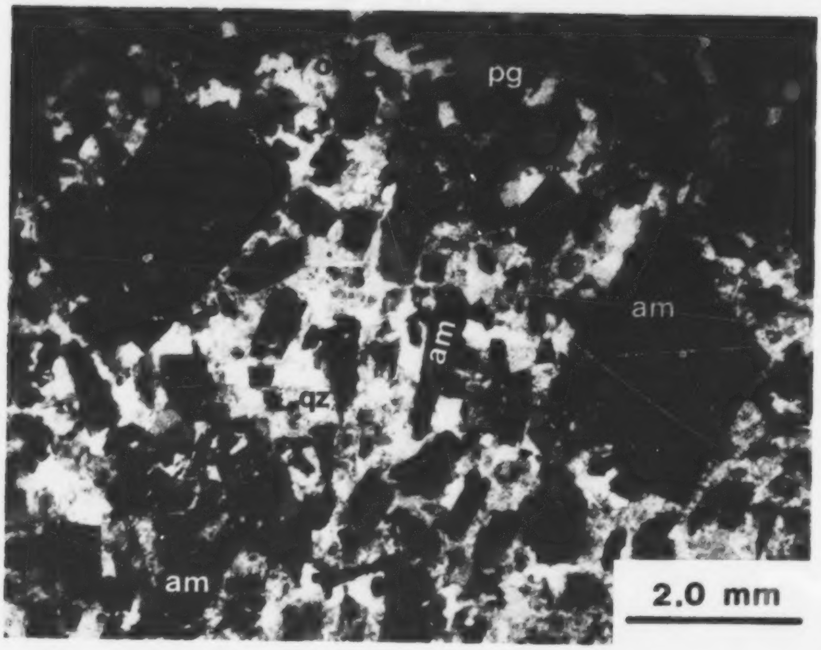

Figure 271: *Hypidiomorphic phase of Whitefish Lake quartz monzodiorite (unit 54). Small to large, euhedral phenocrysts of amphibole (am, dark) and plagioclase (pg, pseudomorphed by fine grained epidote and minor albite). The phenocrysts are set in a ''matrix'' of quartz (qz, clear), orthoclase (or, grey) and plagioclase. Sample 2205-1, plane polarized light.*

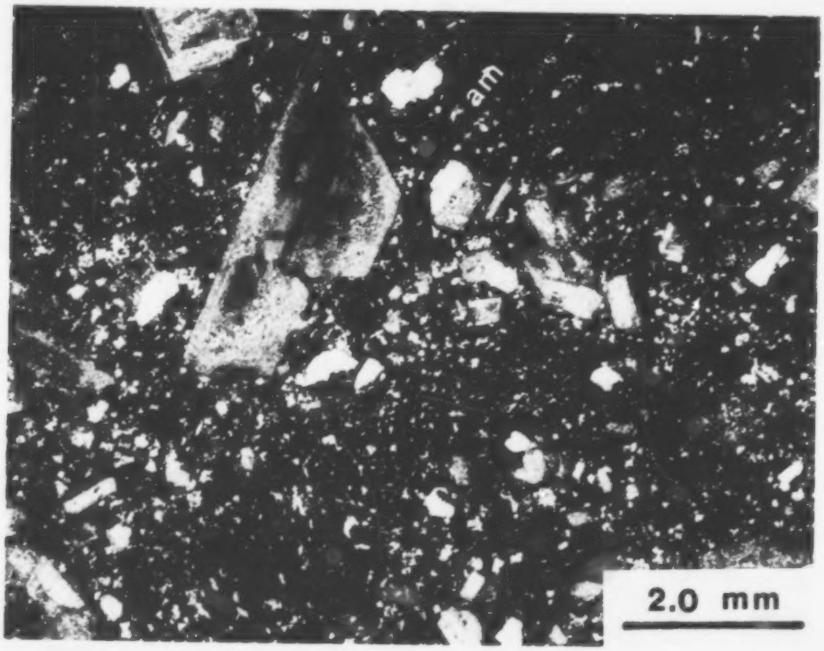

Figure 272: *Porphyritic phase of Whitefish Lake quartz monzodiorite (unit 54a). Small to large euhedral phenocrysts of plagioclase (pg) are twinned and are partially replaced by fine grained sericite. Amphibole phenocrysts (am, AM) are pseudomorphed by epidote, chlorite and feldspar. Groundmass consists of feldspar, chlorite, epidote and quartz. Sample 2336-1, crossed polarizers.*

sphene, magnetite and hematite; some oxides occur as inclusions in amphibole but most are interstitial, and associated with quartz and orthoclase. Apatite (0.1 — 1 mm, up to 2%) is euhedral, prismatic, and occurs both as inclusions in amphibole as and interstitial crystals. Sphene (0.2 mm, trace) and zircon (to 0.1 mm, trace) are both euhedral.

In the southern part of the intrusion widespread alteration takes the form of more complete epidotization of plagioclase and numerous closely spaced fractures with introduction of sericite, epidote and disseminated hematite. Chalcopyrite and pyrite occur as films and blebs on some fractures. A further discussion of the mineralization in this intrusion is given in the section on Economic Geology and by Baldwin (1980).

Related intrusions

The plagioclase-phyric quartz diorite on the southeast shore of Whitefish Lake (unit 54b) is bounded on the west by a major fault, which separates it from the Missi Group. The east contact, with Amisk Group rocks, is also largely fault controlled. The intrusion weathers pink to medium buff, and is pink and green to light grey on fresh surfaces. It is similar to the quartz monzodiorite north of Whitefish Lake in that it has a seriate-porphyritic texture, with plagioclase crystals up to 4 mm composing about 40 — 50% of the rock. Amphibole phenocrysts (to 5 mm, 5%) are commonly not visible on weathered surfaces. Mafic (chlorite plus amphibole) xenoliths 5 — 30 mm are strongly flattened into the plane of weak foliation; they compose up to 5% of the rock. The intrusion differs from the quartz monzodiorite in that it does not contain potassium feldspar, the quartz is very fine grained, and plagioclase phenocrysts are more abundant and generally rhomb-shaped.

The intrusion east of Mikanagan Lake (unit 54) is 210 m wide and exposed for 1350 m within the map area. It is close to the fault through Sawmill Lake, but unlike the Whitefish Lake intrusions, is not emplaced directly in the Pineroot fault zone. The intrusion is strongly seriate-porphyritic quartz diorite with phenocyrsts of plagioclase (up to 7 mm), pyroxene (pseudomorphed by amphiboles and chlorite; up to 5 mm) and, locally, quartz (up to 2 mm). Similar to the Whitefish Lake intrusion this body locally contains small amounts of potassium feldspar and trace amounts of apatite; it differs in that it contains pyroxene as the primary mafic mineral (rather than amphibole) and quartz has a large grain size.

QUARTZ-MEGACRYSTIC TONALITE (UNIT 55)

This unit of quartz-megacrystic tonalite occurs as small elongate bodies within and adjacent to the One Portage Lake Fault. They are placed into the post-Missi intrusive suite because of their spatial relationship with P5 (post-Missi) faults; however, all of these rocks contain strong cataclastic fabrics and the possibility exists that they may be pre-P5 and pre-Missi.

The intrusions are up to 120 x 500 m, white to pale pink weathering and are light grey on fresh surfaces. They are composed of 20 — 30% flattened quartz megacrysts (2 — 10 mm), 60 — 70% plagioclase, and less than 5% chlorite. Deformation textures include granulation of quartz megacrysts, development of sericite and epidote foliation, and local cataclastic foliation.

QUARTZ-PLAGIOCLASE PORPHYRY DYKES (UNIT 56)

Quartz-plagioclase porphyry dykes occur sporadically between the west shore of White Lake and the west shore of Northeast Arm (Schist Lake). The dykes are the youngest intrusive phase in this area. Their orientation is parallel to the axial plane of the Northeast Arm Syncline, and they cut across the Northeast Arm Fault.

The dykes are rhyolitic in composition and texture, weather white, pink or pale green and are white to light pink on fresh surfaces. They range in width from 0.5 — 10 m; most are less than 3 m wide. In places they can be traced along strike for over 500 m. On the west shore of White Lake the dykes are stepped, in linked *en echelon* segments.

The rhyolite dykes are all porphyritic, with euhedral quartz (5 — 10%, 1 — 3 mm) and plagioclase (0 — 5%, 1 — 2 mm) phenocrysts in a very fine grained, leucocratic, recrystallized groundmass of quartz, feldspar, and subordinate white mica.

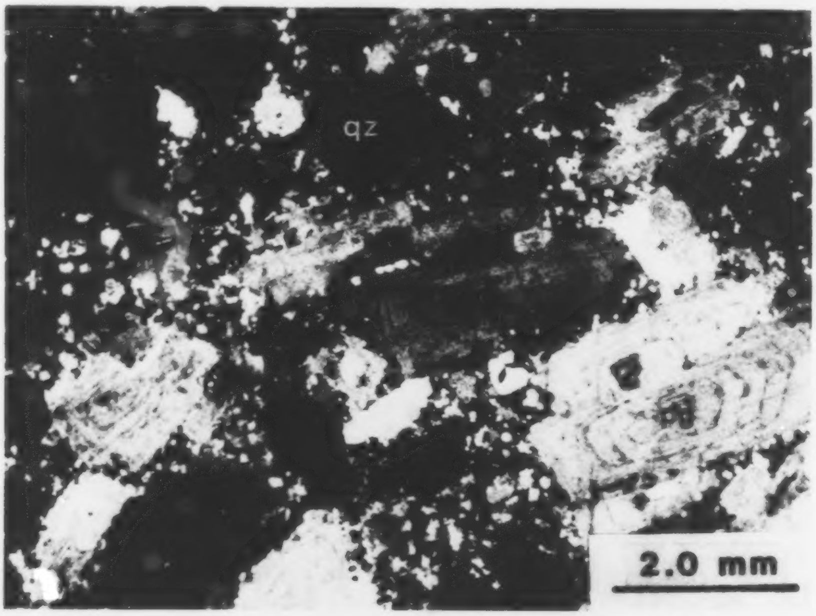

Figure 273: Porphyritic granodiorite (unit 57), Northwest Arm of Schist Lake. Plagioclase phenocrysts (pg) are euhedral, albite-twinned, and oscillatory zoned. Quartz phenocrysts (qz) are anhedral oval. The phenocrysts are set in a fine grained groundmass of quartz and plagioclase. Sample 4225-1, crossed polarizers.

PORPHYRITIC GRANODIORITE (UNIT 57)

Porphyritic granodiorite dykes occur sporadically through the Flin Flon and Hook Lake blocks. They are emplaced in both Amisk and Missi Group rocks. The largest mappable body of porphyritic granodiorite occurs on the east shore of Northwest Arm, east of Mandy Mine. This body weathers pink and is pink on fresh surfaces; locally a reddish alteration (hematization) occurs in the outermost 4 m of the intrusion. Amisk Group wall rocks are epidotized and metasomatized adjacent to the contact. Numerous straight walled dykes and dyke stockworks cut the Amisk rocks in the vicinity of the larger body.

Porphyritic granodiorite (Fig. 273) contains up to 10% euhdedral microcline phenocrysts (0.5 — 4 cm), 50% euhedral oscillatory zoned plagioclase phenocrysts (1 — 6 mm) and 10% oval to embayed quartz phenocrysts (2 — 4 mm). The groundmass is fine grained (0.1 — 0.4 mm) and composed of quartz, feldspar, chlorite and epidote after primary amphibole microphenocrysts (3%), chlorite after biotite (1%), common euhedral sphene (1 — 2%), and trace apatite. Petrographically it is identical to the Phantom Lake granite 3 km west (in Saskatchewan), which has been dated by the U-Pb zircon method at 1.82 Ga (MacQuarrie, pers. comm. 1981).

FOLDS

INTRODUCTION

Five phases of folding were recognized in the Flin Flon-White Lake area (P1 to P5, Table 25). These include one phase of pre-Missi folding and four phases that postdate the Missi Group.

P1 folds (Burley Lake Syncline, Cope Lake Syncline) are overprinted by P3 schistosity, which locally crosses P1 axial planes at a high angle (e.g. south of Louis Lake (Stockwell, 1960) and at Cope Lake). Schistosity is parallel to the P1 axial planes only where they are parallel to P3 axial planes. The P1 folds are intruded by a host of pre-Missi intrusions, including Mikanagan Lake type differentiated gabbroic sills that face both the same as, and opposite to, host volcanic rocks. This relationship suggests that the sills were intruded into recumbent P1 folds. Prior to deposition of the Missi Group the tightly folded Amisk rocks were tilted and deeply eroded; west of Ross Lake between 2.5 and 3 km of Amisk section is truncated at this unconformity.

The second phase of folding (P2, Table 25) is observed only in the Missi Group, as approximately east-trending folds (Fig. 274); these are described by Stauffer and Mukherjee (1971). The folds do not have an axial plane schistosity and have no expression in the Amisk Group. They are overprinted by P4 axial planar schistosity.

The third phase of folding (P3, Table 25) includes a number of major north- and northeast-trending folds in the Amisk Group (Hidden Lake Synform, Milliken Lake Syncline, Northeast Arm Syncline). All of these folds are characterized by a moderate to strong axial planar schistosity that remains parallel to the axial planes regardless of variations in their attitude. Only the Hidden Lake Synform provides information on the age of these folds relative to other folds both in Amisk and Missi rocks. South of Louis Lake the Hidden Lake Synform clearly folds the P1 Burley Lake Syncline. Its age relationships to the Missi Group and folds in the Missi Group are, however, ambiguous. The preferred interpretation is that these folds are post-Missi and post-P2; a full discussion of age relationships is given in a following section.

The north-trending P4 Pipe Line and Mud Lake synclines have a strong associated axial planar schistosity and lineation in the Missi Group (Stauffer and Mukherjee, 1971). Only rarely is this P4 schistosity present in Amisk Group rocks. South of Ross Lake schistosities in the Amisk and Missi are parallel but, based on crosscutting fabrics northwest of Ross Lake, the Amisk fabric is interpreted to be P3 and the Missi fabric P4.

The P5 Embury Lake Antiform is a very large structure which causes bedding and P4 structures to bend to the west, north of the map area. Stauffer and Mukherjee (1971) describe this fold as a cylindrical structure that plunges approximately 30° at 096° azimuth; its axial plane strikes 078° and dips about 70° south. It has no well developed axial planar schistosity.

BURLEY LAKE SYNCLINE

The dominantly north-northwest-trending Burley Lake Syncline is a P1 isoclinal fold developed in Amisk Group rocks. The axial trace of this structure is for the most part located outside the map area, between Burley Lake and Louis Lake in Saskatchewan (Stockwell, 1960). Southeast of Louis Lake the axial trace is shown truncated at the Amisk-Missi unconformity; the distribution of rock units clearly indicates that the fold is pre-Missi in age (Stockwell, 1960). The change in axial plane orientation south of Louis Lake is here interpreted to be due to refolding about the Hidden Lake Synform (Fig. 171).

Structural data on this fold are limited to the area around Burley Lake bounded by the Phantom Lake Fault and Ross Lake Fault. Poles to stratification do not define a girdle on a π diagram (Fig. 275), consequently the orientation of the fold axis is unknown. Schistosity is parallel to bedding in the Burley Lake area (Fig. 275); however, northwest of Carlisle Lake, Stockwell (1960) shows a schistosity at a high angle to both bedding and axial trace of the Burley Lake Syncline. If these schistosities are the same generation, then this foliation postdates the Burley Lake Syncline and is probably axial planar to the P3 Hidden Lake Synform.

East of Green Lake the axial trace of the Burley Lake Syncline is offset along the Phantom Lake fault. Structural data from the area east of Mitt Lake indicate that in this area the syncline trends northerly and probably plunges moderately to the south. A weak schistosity is subparallel to stratification and to the axial trace.

COPE LAKE SYNCLINE

The southeast-trending P1 Cope Lake Syncline is a moderately open, upright structure truncated to the east and west by major faults. It is defined by the distribution of pillow basalt units with contrasting phenocryst populations, and by orientation of flow contacts and primary pillow attitudes. A moderately strong foliation, which trends north and dips steeply to the east, cuts across the axial trace at a high angle and is consequently younger than the fold. The only other fold that predates a strong foliation is the pre-Missi Burley Lake Syncline. For this reason the Cope Lake Syncline is also considered to be pre-Missi.

HIDDEN LAKE SYNFORM

The Hidden Lake Synform is best expressed in Amisk Group basalt flows, northwest of Ross Lake. The axial planar schistosity of this relatively open fold trends 341° and dips 80° east; the hinge plunges 46° at 133° azimuth (Fig. 276). The Hidden Lake Synform is significant because it provides virtually the only link between deformational features observed in the Amisk and Missi Groups.

The synform is defined by the attitudes of bedding, flow contacts and primary pillow orientations (Fig. 276). A well developed schistosity (S_3, Fig. 276c) trends parallel to the axial plane of the fold. Primary structures in the basalt flows (e.g. pillows (Fig. 277 and 278), amygdales) are deformed into rod-shaped linear structures (Fig. 276b), the long axes of which are similar to but not exactly parallel to the axis of the synform (as defined by β on Fig. 276a). Minor folds developed in inter-pillow laminated tuff/sediment (Fig. 279) and in pillow selvages have axial planes and fold axes parallel to those in the major structure (Fig. 276a and c).

In contrast to other folds in the Amisk Group, the Hidden Lake Synform can be related to other structures in the Amisk and Missi groups. The following observations have a bearing on any interpretation on the age of the Hidden Lake Synform:

1) Northeast of the HBMS smelter, basalts locally contain two foliations, one axial planar to the Hidden Lake Synform and a later, superimposed weaker schistosity that is parallel to the axial plane of the P4 Pipe Line Syncline developed in Missi Group rocks.
2) The Hidden Lake Synform P3 axial planar schistosity does not occur in Missi rocks north of the Club Lake Fault.
3) Lineations defined by long axes of deformed primary structures (pillows, amygdales) and hinges of minor folds in Amisk rocks are parallel to long axes of deformed pebbles in Missi rocks.

Table 25:
Summary of major deformational events, Flin Flon-White Lake area

DEFORMATION			OTHER EVENTS	RELEVANT U/Pb ZIRCON AGES
EVENT	DESCRIPTION	SCHISTOSITY AXIAL PLANAR TO FOLDS		
P5	Large, open, ENE-trending cylindrical Embury Lake antiform; major fault displacements (includes block-bounding faults) initiated at different times during P5 folding (amount of flexure about Embury Lake antiform varies from one fault to another)	Not well developed	Units 52, 53, 54, 55(?) and 56 emplaced in or across P5 fault structures	Kaminis granodiorite (unit 57), 1.82 Ga (MacQuarrie, pers. comm., 1981)
P4	N-trending, moderately open folds in Missi Group rocks (eg. Pipe Line and Mud Lake synclines)	Strong in Missi Group rocks; only rarely present in Amisk Group rocks	↑ Regional metamorphism	Anatectic granitoids produced during peak regional metamorphism in Kisseynew Belt, 1841 + 35/-15, 1814 + 17/-11, 1816 + 23/-12 Ma (Gordon et al., 1989)
P3	N- and NE-trending, open to tight folds in Amisk Group rocks (eg. Hidden Lake synform)	Moderate to strong		
P2	E- to ESE-trending, open to tight folds in Missi Group rocks	Absent	↓	
			Deposition of Missi Group in subaerial alluvial fan(s)	Missi Group volcanic rocks at Wekusko Lake, 1832 +/-2 Ma (Gordon et al., 1989)
			Uplift and erosion of folded Amisk Group volcanic rocks and contained intrusions ↑	
P1	N- to NE-trending tight isoclinal folds in Amisk Group rocks (eg. Burley Lake and Cope Lake synclines)	Absent	Units 40-49 emplaced ↓	Lynx Lake pluton, 1847 +/-4 Ma (Syme et al., 1987) Cliff Lake pluton, 1874 + 32/-25 Ma (Gordon et al., 1989)

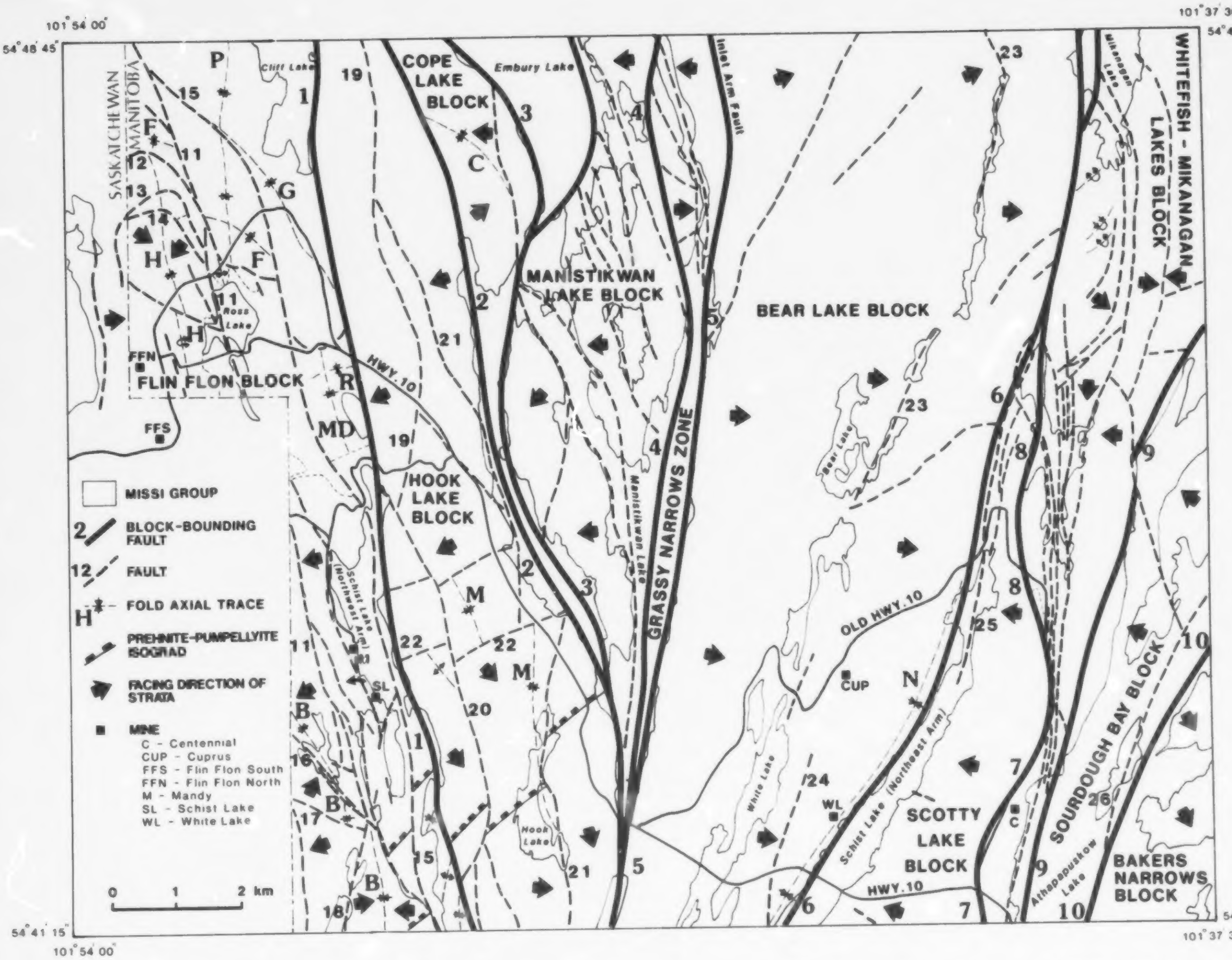
101°54'00"
54°48'45"
101°37'30"
54°48'45"
54°41'15"
101°54'00"
54°41'15"
101°37'30"
SASKATCHEWAN
MANITOBA
Cliff Lake
Embury Lake
Inlet Arm Fault
COPE LAKE BLOCK
MANISTIKWAN LAKE BLOCK
BEAR LAKE BLOCK
WHITEFISH - MIKANAGAN LAKES BLOCK
FLIN FLON BLOCK
HOOK LAKE BLOCK
GRASSY NARROWS ZONE
SCOTTY LAKE BLOCK
SOURDOUGH BAY BLOCK
BAKERS NARROWS BLOCK
Ross Lake
HWY. 10
OLD HWY. 10
Bear Lake
Manistikwan Lake
Schist Lake (Northwest Arm)
Schist Lake (Northeast Arm)
White Lake
Hook Lake
Athapapuskow Lake
Mikanagan Lake
FFN
FFS
CUP
WL
SL
MISSI GROUP
BLOCK-BOUNDING FAULT
FAULT
FOLD AXIAL TRACE
PREHNITE-PUMPELLYITE ISOGRAD
FACING DIRECTION OF STRATA
MINE
C - Centennial
CUP - Cuprus
FFS - Flin Flon South
FFN - Flin Flon North
M - Mandy
SL - Schist Lake
WL - White Lake
0 1 2 km

Figure 274: Disposition of folds, faults and the prehnite-pumpellyite isograd. Metamorphic biotite is present in northern one third of area but is not distributed widely enough to accurately define an isograd.

BLOCK BOUNDING FAULTS

1 Cliff Lake fault
2 Manistikwan Lake fault
3 Big Island and Embury Lake faults
4 Rosenberg Lake fault
5 Inlet Arm fault
6 Northeast Arm fault
7 Old Highway 10 fault
8 Scotty Lake fault
9 Sourdough Bay fault
10 North Arm fault

INTERNAL FAULTS

11 Ross Lake fault
12 Club Lake fault
13 Railway fault
14 South Railway fault
15 Channing fault
16 Phantom Lake fault
17 Green Lake fault
18 Mitt Lake fault
19 Big Charlie Lake fault
20 Insole Lake fault
21 Hook Lake fault
22 Milliken Lake fault
23 Vick Lake fault
24 Bazinet Lake fault
25 One Portage Lake fault
26 Post Island fault

FOLDS

B Burley Lake syncline
C Cope Lake syncline
F Flin Flon Creek syncline
G Grant Lake syncline
H Hidden Lake synform
M Milliken Lake syncline
MD Mud Lake syncline
N Northeast Arm syncline
P Pipe Line syncline
R Ross Creek syncline

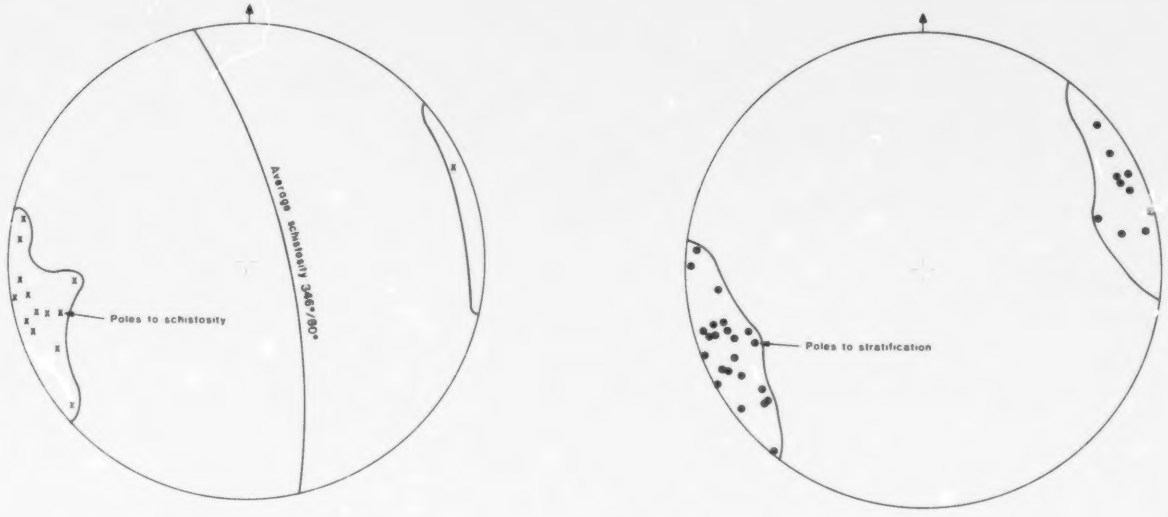
Average schistosity 346°/80°
Poles to schistosity
Poles to stratification

Figure 275: Lower hemisphere stereographic plots of structural fabric elements of the pre-Missi, P1 Burley Lake syncline:
(a) stratification
(b) schistosity (age uncertain, refer to text)

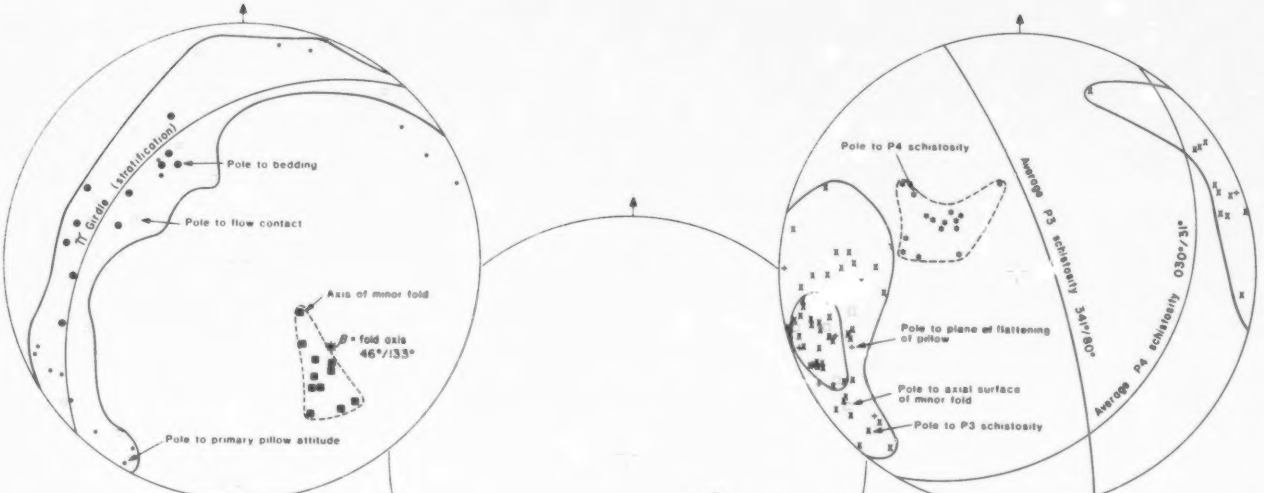
π Girdle (stratification)
Pole to bedding
Pole to flow contact
Axis of minor fold
β = fold axis 46°/133°
Pole to primary pillow attitude
Long axis of deformed structure
Mineral lineation
Average lineation 33°/138°
Pole to P4 schistosity
Average P3 schistosity 341°/80°
Average P4 schistosity 030°/31°
Pole to plane of flattening of pillow
Pole to axial surface of minor fold
Pole to P3 schistosity

Figure 276: Lower hemisphere stereographic plots of structural fabric elements of the P3 Hidden Lake synform.
(a) stratification
(b) lineations
(c) P3 schistosity, plane of flattening of pillows, axial surfaces of minor folds, P4 schistosity

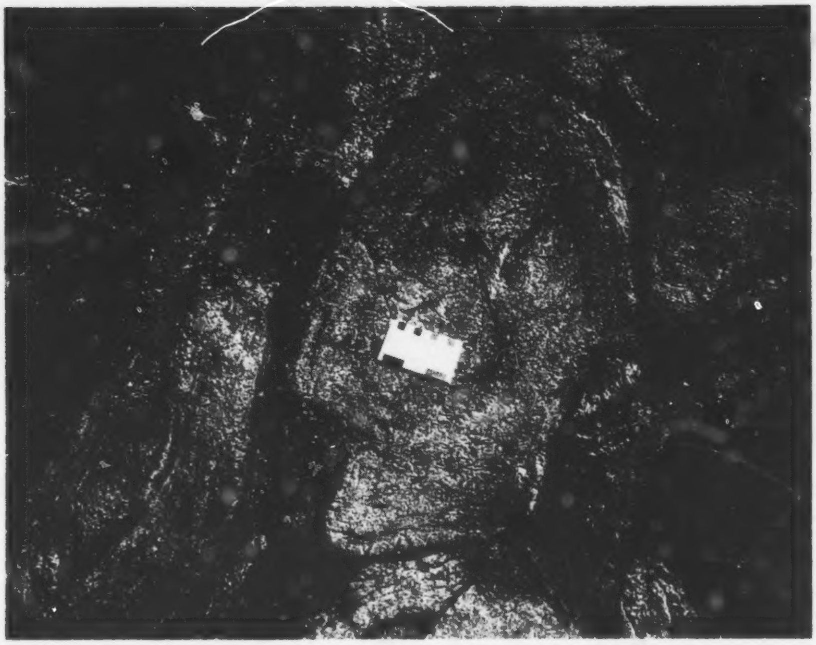

Figure 277: *Deformed pillow in Hidden Lake basalt (unit 2a), near the axial trace of Hidden Lake synform, 460 m northwest of Little Cliff Lake. Pillows are strongly rodded (plunge 35° at 140° azimuth — shown by arrow), and are flattened almost perpendicular to primary stratification.*

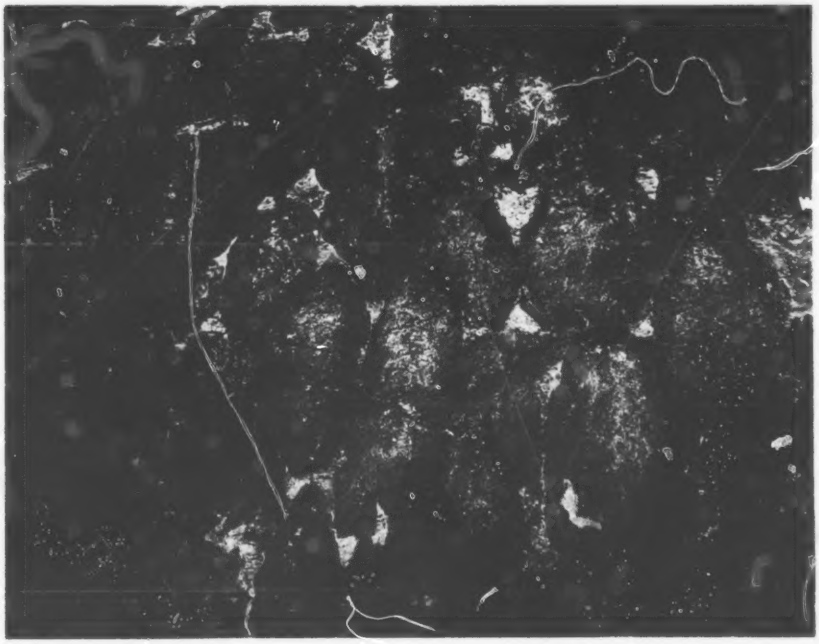

Figure 278: *Deformed pillows in Hidden Lake basalt (unit 2a), south end of Hidden Lake. Stratigraphic tops are towards top of photograph. The pillows have been flattened parallel to the axial trace of the Hidden Lake synform, and are rodded parallel to the axis of the fold.*

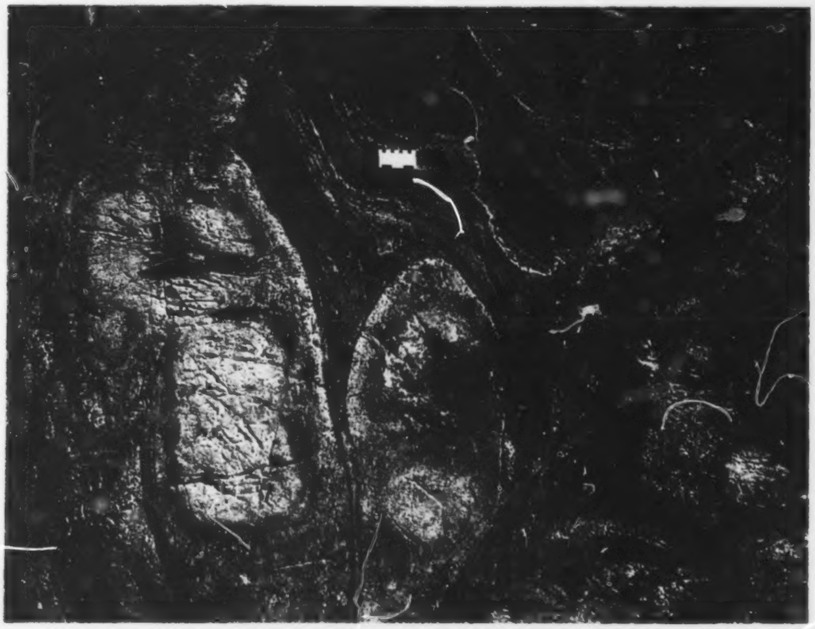

Figure 279: Deformed pillowed flow (unit 9) and interflow sediments, near axial trace of Milliken Lake syncline, 820 m northwest of Milliken Lake. Stratigraphic tops are towards the top of the photograph. Pillows have been flattened almost perpendicular to stratification, resulting in bullet to pear-shaped structures (compare Fig. 134) elongate parallel to the fold axial plane.

4) The Club Lake, Railway and South Railway faults are curved structures broadly symmetrical about the axial trace of the Hidden Lake Synform.
5) Folds in the Club Lake Fault surface, northwest of Little Cliff Lake, have axial planes and axes parallel to those in the Hidden Lake Synform.
6) Tight folds in the Amisk-Missi unconformity, between Railway and South Railway faults, are coaxial and coplanar to the Hidden Lake Synform.
7) The P2 Flin Flon Creek Syncline is broadly curved and coincident with the northern extension of the Hidden Lake Synform axial trace.

From these observations it is clear that the Hidden Lake Synform postdates P1 structures in the Amisk and predates P4 structures in the Missi. Folds in the Amisk-Missi unconformity appear to be related to the Hidden Lake Synform and therefore indicate that the synform must be post-Missi in age. The Club Lake Fault, Railway Fault, South Railway Fault and P2 Flin Flon Creek Syncline are considered to be folded by the Hidden Lake Synform.

The absence of P3 axial planar schistosity in Missi rocks north of the Club Lake Fault is the only piece of evidence that contradicts a post-Missi age for the Hidden Lake Synform. This observation can be explained in at least two ways: the P3 schistosity was either not strongly developed in the Missi and was masked by the subsequent strong P4 fabric, or the fold is pre-Missi in age. In this report the former interpretation is preferred.

Lineations in the Amisk Group are parallel to those in the Missi Group, even though in the preferred interpretation those in the Amisk are P3 and those in the Missi are P4. This relationship can be interpreted to mean that these folds, although clearly not coplanar, must be coaxial.

NORTHEAST ARM SYNCLINE

The stratigraphic sequence in the Bear Lake Block is folded in a tight, north-plunging P3 syncline with an axial trace parallel to the west shore of Northeast Arm (Schist Lake) (Fig. 280). This structure is particularly significant because it folds the stratiform zone hosting the Cuprus and White Lake Cu-Zn massive sulphide deposits.

Poles to bedding, largely from the Vick Lake tuff (unit 25), define a weak girdle indicating plunge of the fold is 36° at azimuth 008° (Fig. 280a). The plunges of minor folds are clustered around the fold axis delineated by bedding (Fig. 280a). These minor folds have an average axial plane schistosity that strikes 202° and dips 74° west. The minor folds contain an axial planar foliation and fold an earlier foliation (Fig. 280b). Where minor folds are absent (the general situation) these two foliations are indistinguishable; presumably the more steeply dipping foliations are earlier.

Minor folds associated with the Northeast Arm Syncline are commonly chevron-type with sharp hinge zones (Fig. 281 and 282). Interlimb angles of these folds are 5° — 60° and average 25° — 35°, similar to the interlimb angle displayed by the major structure.

Quartz and pink-weathering quartz-feldspar veins and stockworks are localized in the hinge zone of the major fold and coincide with the zone of strongest deformation (Fig. 52). These veins are up to only a few centimetres wide and are commonly axial planar.

The Cuprus and White Lake deposits occur in large minor folds in the west limb and hinge zone, respectively, of the Northeast Arm Syncline. The orebodies are localized in the hinges of synforms and plunge parallel to the major structure. The plunge of the White Lake orebody is 35° — 40° (at azimuth 030°) at surface, and flattens with depth to 23° (at azimuth 015° — 020°) at the 2110 foot level in the mine (N. Provins, pers. comm. 1981). The Cuprus orebody plunges 10° — 20° to the north (HBMS Co. Ltd. Geological Staff, 1957); the plunge of this orebody also flattens with depth. These relationships suggest that the general plunge of the Northeast Arm Syncline similarly flattens at depth to the north.

The Northeast Arm Syncline is truncated on its eastern limb by the

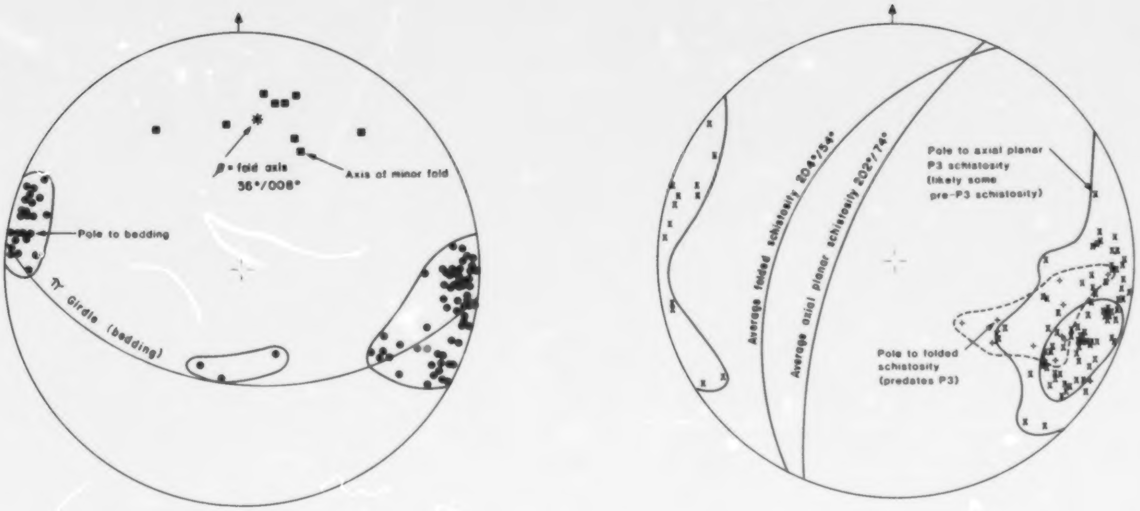

Figure 280: Lower hemisphere stereographic plots of structural fabric elements of the P3 Northeast Arm syncline.
(a) bedding, minor fold axes
(b) schistosity

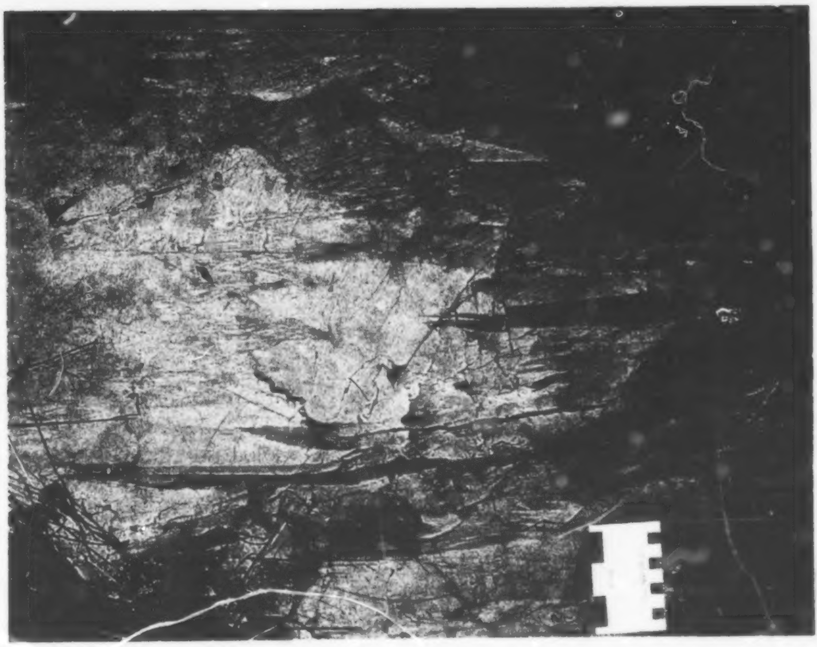

Figure 281: Tight, chevron-shaped minor folds developed in Vick Lake andesitic tuff (unit 25c), 1370 m northeast of White Lake mine, on the shore of Northeast Arm. These minor folds are associated with the Northeast Arm syncline, the axial trace of which passes 120 m to the west of this locality.

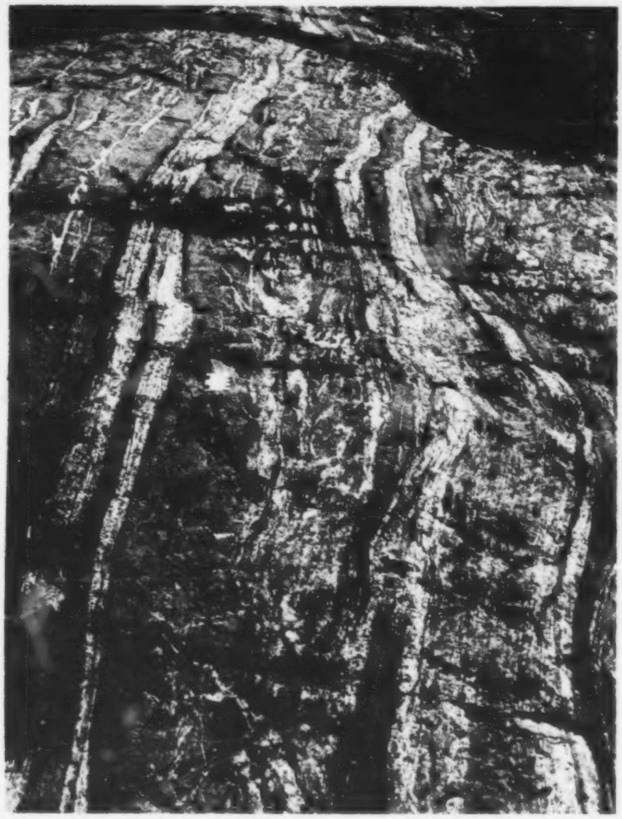

Figure 282: Isoclinal folds in axial trace of Northeast Arm syncline, 400 m south of Highway 10. Folds are defined by chert layers in Little Spruce Lake sediments and tuff (unit 24a, 38a).

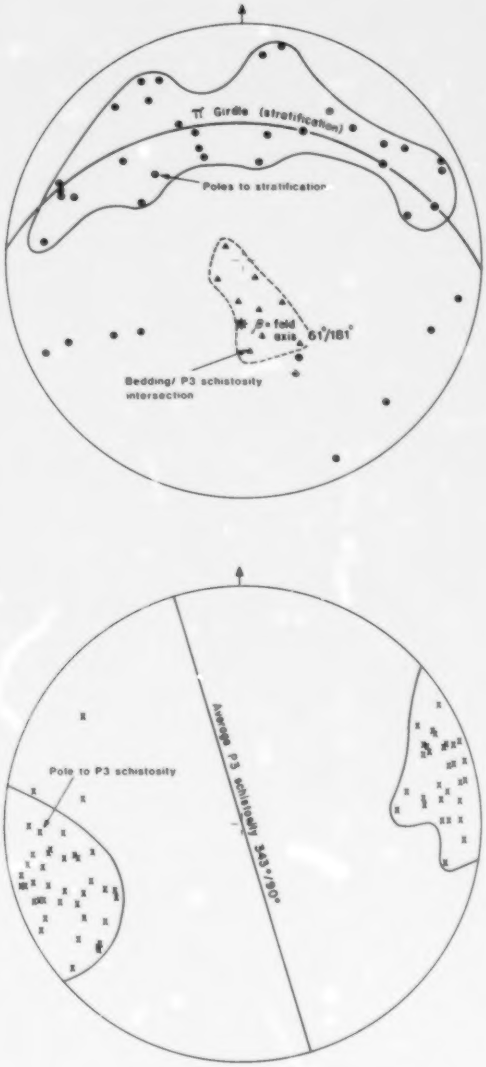
π Girdle (stratification)
Poles to stratification
β = fold axis 61°/181°
Bedding/ P3 schistosity intersection
Pole to P3 schistosity
Average P3 schistosity 343°/90°

Figure 283: Lower hemisphere stereograhic plots of structural fabric elements of the P3 Milliken Lake syncline.
(a) stratification, intersections of bedding and P3 schistosity
(b) P3 schistosity

Northeast Arm Fault, and on its western limb by the Bazinet Lake Fault (Map GR87-1-1). The synvolcanic White Lake Sill displays minor folds east of White Lake, which plunge and trend parallel to the Northeast Arm Syncline. The fold is intruded by a number of intrusions that trend parallel to the axial plane; these include Cuprus diorite sill (unit 42a), gabbro (unit 42a) and quartz-plagioclase porphyry (unit 56). The age of the fold with respect to the Mikanagan Lake Sill is unknown, but the fold is presumed to be younger (Table 20).

MILLIKEN LAKE SYNCLINE

The Milliken Lake Syncline is an open, north-trending P3 fold developed in Amisk Group rocks in the Hook Lake Block. The fold is truncated on the west by the Insole Lake Fault and on the east by the Hook Lake Fault; its axial trace is offset 750 m along the left lateral, east-trending Milliken Lake Fault. A complementary anticline occurs between the Cliff Lake Fault and Insole Lake Fault; its orientation is similar to the Milliken Lake Syncline.

The syncline is defined by bedding, flow contacts and primary pillow orientations (Fig. 283a). The fold axis plunges 60° at azimuth 183°. The average schistosity strikes 343° and dips between 85° and 90° east; it is parallel to the axial plane of the fold. Because the fold is relatively open, schistosity is commonly at a high angle to stratification on the west limb of the fold.

The age of the fold relative to other major folds in the area cannot be directly determined. It has a similar orientation to the post-Missi Hidden Lake Synform and also contains a similar well defined axial planar foliation, and is therefore considered to be a P3 structure.

FOLDS SOUTHEAST OF STITT ISLAND

Amisk Group bedded tuffs, flows and breccias exposed on the west shore of Northwest Arm are folded by north-trending synclines and an intervening anticline. The folds occur in the narrow fault-bounded panel between the C̄liff Lake and Channing faults.

Poles to stratification define the fold axes which plunge 60° at azimuth 181° (Fig. 284a). The average schistosity trends 174° and dips 87° west; it is axial planar to the fold structures (Fig. 284b). Bedding/cleavage intersections are parallel to the plunge of the fold axes.

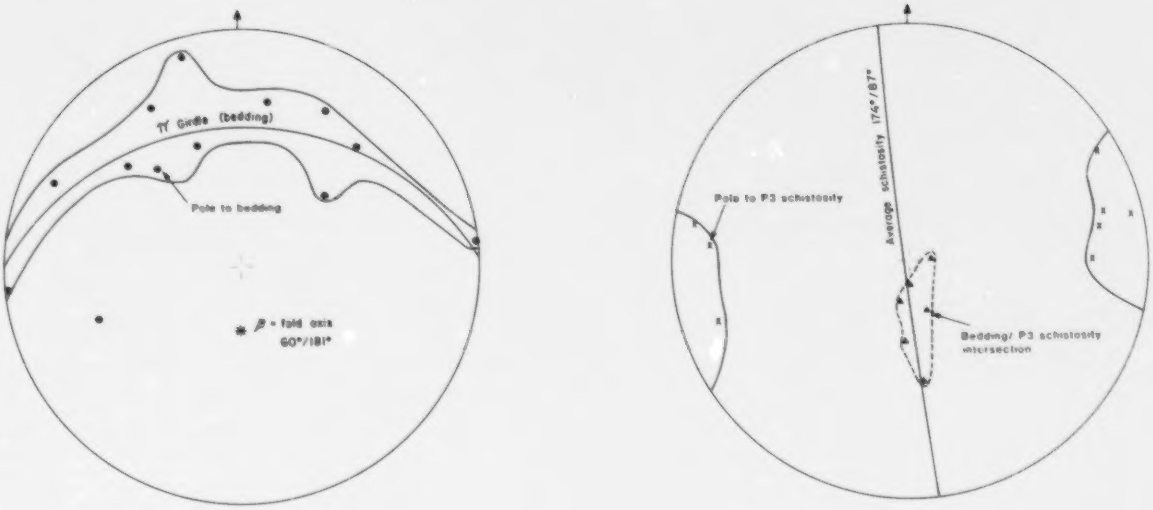
π Girdle (bedding)
Pole to bedding
β = fold axis
60°/181°
Average schistosity 174°/87°
Pole to P3 schistosity
Bedding/ P3 schistosity intersection

Figure 284: Lower hemisphere stereographic plots of structural fabric elements of the P3 folds southeast of Stitt Island.
(a) bedding
(b) P3 schistosity, intersections of bedding and P3 schistosity

FAULTS

INTRODUCTION

Faults dominate the structural fabric of the Flin Flon-White Lake area. Two groups of faults are recognized, those that bound major stratigraphic blocks and those that occur within the blocks (Fig. 3). Stratigraphic correlations cannot be made across block-bounding faults whereas either correlation or similarity of sequences can be observed across internal faults. In other respects (e.g. physical expression, age, displacement) the block-bounding and internal faults are indistinguishable. Orientations of faults can be related to geographic location with respect to the north-northeast-trending Inlet Arm Fault, the most significant fault in the map area. West of the Inlet Arm structure most faults trend north-northwest, whereas east of this structure faults trend northeast to north-northeast. Where dips of faults have been observed they are invariably steep. Many faults are not simple isolated structures, but tend to splay or occur in clusters, resulting in numerous lens-shaped fault-bounded domains of all sizes (Fig. 3).

The age of every fault cannot be precisely established. With the exception of early faults folded by P3 structures (e.g. Club Lake, Railway and South Railway faults) most faults appear to have been initiated during the P5 deformation event (Table 25). Evidence for P5 faulting includes offset of P4 metamorphic isograds, truncation of most intrusions, offset of P3 and P4 folds and truncation of P3 and P4 schistosity. Faults were initiated at different times during P5 folding, and as a result display different degrees of flexure about the P5 Embury Lake Antiform. This is consistent with the findings of Stauffer and Mukherjee (1971), who studied faults in the Missi Group at Flin Flon.

The physical expression of faults in outcrop varies widely between different faults and may also vary at different locations on a single fault. Many faults are marked by a several metre wide zone of intense shear foliation, commonly accompanied by quartz and/or carbonate veins, that grades out of the fault zone into less foliated rocks. Some faults display more brittle deformation features, comprising a breccia of angular fragments "cemented" by carbonate, quartz and chlorite (Fig. 285). Commonly these brittle fault zones are overprinted by discrete zones of more ductile shear deformation, resulting in moderate to extreme flattening and foliation of fragments. A few faults, including some with major displacements, have very little outcrop expression apart from a chlorite-quartz-filled break 1 — 2 cm wide. In the following sections individual block-bounding faults are described in detail, and internal faults are individually described according to block.

BLOCK-BOUNDING FAULTS

Cliff Lake Fault

The Cliff Lake Fault separates the Hook Lake and Flin Flon blocks (Fig. 3). Within the map area it is a north-northwest-trending structure which follows the east shore of Cliff Lake and Northwest Arm (Schist Lake). North of the map area this fault curves to the west and is offset by the younger Channing and Ross Lake faults; the curvature is attributed to folding about the Embury Lake Antiform (Stauffer and Mukherjee, 1971).

The portion of the fault north of Schist Lake differs in appearance from the portion along the east shore of Schist Lake. The best exposure of the northern part of the fault is in a gravel pit adjacent to Highway 10, 400m east of the intersection with the perimeter highway. There, Missi Group and Amisk Group rocks are strongly foliated, mylonitized and hema-

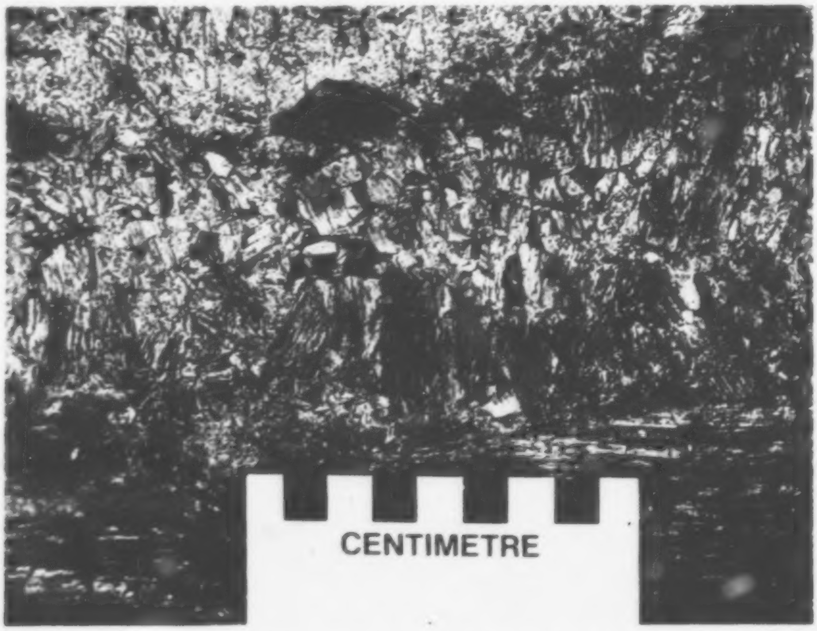

Figure 285: Fault breccia associated with late brittle deformation of strongly foliated White Lake dacite tuff, 200 m west of Little Spruce Lake.

tized in a 15 m wide zone; the schistosity dips 63° to the east. From that locality northwards the fault is covered and occurs at the base of a prominent, west-facing escarpment. Amisk Group rocks exposed in the cliff commonly show only minor deformation features associated with the nearby fault.

The exact location of the southern portion of the fault is uncertain. It follows either the centre of Northwest Arm (Schist Lake) or the east shore. A fault is known to occur along the east shore: it is exposed in several localities, separates closely folded rocks in the west from broadly folded rocks in the east, truncates stratigraphy, and offsets the prehnite-pumpellyite isograd. This fault must have a significant offset and is accordingly considered to be the southern extension of the Cliff Lake Fault. It differs from the northern portion in that it does not have an associated wide zone of strongly deformed rocks. The fault, where observed, comprises 20 — 50 cm of hematized fault gouge or strongly foliated, crumpled and veined material separating completely different lithologies. The fault plane dips 60° — 90° east.

Offset on the Cliff Lake Fault must be significant to explain the complete absence of the Missi Group east of the fault. Stauffer and Mukherjee (1971) estimate the minimum net slip to be 1525 m, with the east side up and to the north.

Manistikwan Lake Fault

The Manistikwan Lake Fault separates the Hook Lake Block from the Cope Lake and Manistikwan Lake blocks (Fig. 3). It apparently splays from the Big Island Fault west of Big Island. The Manistikwan Lake Fault cuts across regional schistosity and truncates the Cope Lake Syncline.

The fault coincides with a very strong topographic linear low between the north end of Manistikwan Lake and Little Charlie Lake. Outcrops adjacent to this linear feature display a strong schistosity that dips steeply east. North of Little Charlie Lake the fault does not have a well defined topographic expression, and is exposed as three discrete zones exposed over 70 m. These zones are characterized by intense schistosity and carbonate veining, and dip 70° east. The width of the entire zone is comparable to the width of the topographic linear south of Little Charlie Lake.

Big Island Fault

The Big Island Fault splays from Inlet Arm Fault, and separates the Manistikwan Lake Block from the Cope Lake and Hook Lake blocks (Fig. 3). On Embury Lake the Big Island Fault joins at least three faults and it is not certain which, if any, of these represent its northern extension.

The near vertical fault is exposed at several localities on the west shore of Big Island. The fault zone is several metres wide and comprises brecciated rocks with carbonate, hematite, quartz and chlorite introduced between tectonic fragments.

Rosenberg Lake Fault

The Rosenberg Lake Fault is a curving structure separating the Grassy Narrows Zone on the east from the Manistikwan Block on the west (Fig. 3). For much of its length, west of Grassy Narrows, it coincides with a steep-sided topographic linear low and consequently is not exposed. 'Evidence for the fault lies in the juxtaposition of distinctly different rock types across the linear. Where observed the fault zone is characterized by intense schistosity, carbonate veining, and intrusion of late, undeformed gabbro (unit 53a). Displacement on this fault must be significant because in the east arm of Manistikwan Lake stratigraphic tops are opposite on either side of the fault. The Rosenberg Lake Fault probably joins the Inlet Arm Fault at the south end of Manistikwan Lake.

Inlet Arm Fault

The Inlet Arm Fault is the largest fault in the map area. For much of its length in the map area it follows the linear east shoreline of Manistikwan Lake. It separates the Bear Lake Block in the east from both the Manistikwan Lake and Hook Lake blocks in the west (Fig. 3). More importantly, the fault separates two larger domains (each composed of several blocks) with significantly different characteristics. The domain west of the Inlet Arm fault has a north-northwest structural grain, consists mainly of folded stratigraphic sequences, and contains a diverse intrusive suite including rhyolite (unit 49), quartz and quartz-plagioclase porphyry (units 48a and b) and abundant diorites (unit 42). The domain east of the fault has a north-northeast structural gain, is composed dominantly of homoclinal stratigraphic sequences, and does not contain the diverse intrusive suite present west of the fault.

The Inlet Arm Fault is characterized by a wide zone of intense deformation on the east side, and a much narrower zone of weak deformation on the west. The intensely deformed rocks are epidotized and foliated Bear Lake basaltic andesite flows (unit 1). Within 30 m of the fault the flows have been transformed into banded, laminated tectonites in which all primary structures are destroyed. Flattening, foliation and boudinage, apparently related to the fault, decrease in intensity eastward for about 1 km. This zone is also characterized by strong epidotization of the flows (Fig. 52). West of the fault the rocks are virtually undeformed and display insignificant epidotization.

Several faults, some of them major, splay from the Inlet Arm Fault. These splays are localized at the south end of Manistikwan Lake and south of Grassy Narrows. The degree of deformation associated with the Inlet Arm Fault decreases northward, as the number of splays increases. For example, northeast of Grassy Narrows the Inlet Arm Fault separates relatively undeformed and unepidotized Grassy Narrows basalt (unit 7) from more deformed and epidotized Bear Lake basaltic andesite (unit 1). However, the basaltic andesites are only moderately deformed compared to those at the south end of Manistikwan Lake, and the zone of deformation is at most 300 m wide. The fault plane and adjacent laminated tectonites are not observed; the fault occupies a linear topographic depression.

The dip of the fault plane can be estimated from that of the adjacent laminated tectonites, which is 75° — 85° east. The horizontal component of the net slip can be partially determined by the observed offset of the prehnite-pumpellyite isograd. Greenschist facies rocks are juxtaposed against prehnite-pumpellyite facies rocks for at least 11 km, to the south end of Schist Lake (Syme, 1985). Thus the horizontal component of displacement on the fault is at least 11 km, with a right lateral sense of movement.

Northeast Arm Fault

The Northeast Arm Fault separates the Bear Lake Block from both the Scotty Lake Block and Whitefish-Mikanagan Lake Block (Fig. 3). North of Whitefish Lake this fault is joined by the One Portage Lake Fault and Centennial Fault. Although the fault plane itself is inconspicuous, it brings into juxtaposition three completely different stratigraphic sequences and is one of the most important faults in the area.

The Northeast Arm Fault truncates the east limb of the Northeast Arm Syncline, and thereby cuts across several kilometres of Bear Lake Block stratigraphy. The fault is conformable with stratigraphy in the homoclinal Scotty Lake Block.

The fault plane is a chloritic dislocation surface a few millimetres wide, dipping steeply (65° — 85°) to the west. East of the fault plane mafic mudstone and siltstone (unit 33) are strongly foliated, contain quartz-ankerite veins and pods, and are locally tightly folded. The axial planar schistosity is parallel to the fault plane. This zone of intense deformation on the eastern side of the fault is about 100 m wide. In contrast, rocks on the west side of the fault show few features that can be attributed to deformation associated with the fault.

The direction and amount of net slip on the fault is unknown. The offset must be at least several kilometres because the entire Bear Lake stratigraphic section (5 km), plus the Mikanagan Lake Sill (1.2 km) are absent on the east side of the fault.

Boundary between Scotty Lake and Whitefish-Mikanagan Lakes blocks

The boundary between the Scotty Lake Block and the Whitefish-Mikanagan Lake Block comprises segments of four faults: old Highway 10 fault, Centennial Fault, Scotty Lake Fault and an unnamed fault on Mikanagan Lake.

The old Highway 10 fault represents the sheared contact between Scotty Lake basalt (unit 4) and Centennial Mine leucogranite-leucogranodiorite (unit 47). The fault is characterized by a wide zone (20 — 25 m) of schistose basalt and foliated, crushed leucogranodiorite that dips 70° — 85° to the west. Augen of less deformed rocks locally occur within the fault zone. At one locality 1.0 km north-northeast of Centennial Mine a trench 24 m long cuts across the fault zone. There, the rocks are sericite-chlorite schists locally containing abundant ankerite and up to 30% disseminated pyrite.

West of Pineroot River, where the Centennial Fault forms the eastern boundary of the Scotty Lake Block, Missi Group conglomerate and pebbly sandstone is in fault contact with an intrusive complex composed of high level dykes specific to the Scotty Lake basalt suite (unit 4); both Missi and intrusive rocks are well foliated in a narrow (2 — 3 m) zone adjacent to the fault. The Centennial Fault appears to truncate and post-date both the old Highway 10 fault and Scotty Lake Fault.

The Scotty Lake Fault is exposed at the northwest end of Scotty Lake and again 1 km to the north. The fault is characterized by a wide zone of strongly foliated rocks that dip 80° — 90° west. Quartz-feldspar veins and pods are abundant in the core of the foliated zone. This fault may be the northern extension of the old Highway 10 fault. The fault is post-Missi in age as it cuts across folded Missi sandstones (unit 50a) east of Scotty Lake.

Sourdough Bay Fault

The Sourdough Bay Fault forms the western margin of the Sourdough Bay Block. The Sourdough Bay Fault is offset 400 m left laterally by a northwest-trending fault at Sourdough Bay (Fig. 3).

The northern segment of the fault truncates gabbro and quartz diorite intrusions along the topographic linear occupied by the Northstar Road. A single small exposure of the fault zone comprises chlorite schist that dips 85° east. Intrafolial folds in the schist are S-asymmetrical and plunge 49° at azimuth 028°.

The southern segment of the fault truncates the same gabbro and quartz diorite units as the northern segment and cuts across volcanic conglomerate (unit 31) of the Whitefish-Mikanagan Lakes Block. The fault follows a well defined topographic lineament; where exposed it comprises rusty weathering quartz-ankerite-sericite schist dipping steeply to the west. Near the fault zone the rocks are brecciated, with introduction of quartz and ankerite along and adjacent to randomly oriented fractures. This zone of alteration extends 30 — 40 m away from the fault.

North Arm Fault

The North Arm Fault, between Post Island and the east shore of Athapapuskow Lake, forms the west boundary of the Bakers Narrows Block. The displacement on this fault must be very large because it juxtaposes thick stratigraphic sequences with opposing facing directions. The fault is not exposed at surface in the map area.

INTERNAL FAULTS

Flin Flon Block

Faults that cut the Missi Group, in the northern part of the Flin Flon Block, are described in detail by Stauffer and Mukherjee (1971). They show the faults to be high-angle, oblique-slip reverse faults, all of which are interpreted to have formed during a single "orogenic event" (P3, Table 25). Differences in degree of curvature shown by the faults are interpreted to reflect initiation at different times during that (P3) folding event. Stauffer and Mukherjee (1971) did not examine these faults where they cut the Amisk Group. In the following paragraphs a number of features are described where the faults *do* cut the Amisk Group, in some examples altering or contributing to previous interpretations of the faults. Refer to Map GR87-1-1 for locations of all named faults.

The *Ross Lake Fault* trends generally north-northwest and dips 65° — 85°E (Byers et al., 1965); it has been traced (north of the Paleozoic cover) for a distance of 65 km (Saskatchewan 1:1 000 000 gological map). Rocks within the fault zone have been brecciated, mylonitized, crenulated, veined and altered by retrograde quartz-albite-chlorite grade metamorphism (Stauffer and Mukherjee, 1971; Byers et al., 1965). For most of its length the fault zone occupies a series of topographic valleys and is not exposed. At a locality 960 m south of Little Cliff Lake the Ross Lake Fault is exposed as a 5 m wide brecciated zone in Amisk Group pillowed flows; quartz, carbonate and chlorite fill the spaces between angular tectonic fragments and occur on planar slip surfaces. There, the Ross Lake Fault clearly truncates the South Railway Fault. In contrast, south of Carlisle Lake the precise location of the Ross Lake fault is uncertain because it has virtually no outcrop expression and trends parallel to Amisk stratigraphy. The position of the fault shown on the geological map is modified from Stockwell (1960). The subdued expression of the fault south of Carlisle Lake may reflect translation of most of the displacememt to a nearby, parallel structure exposed on the west shore of Northwest Arm (Schist Lake). This parallel structure is marked by a zone of strong, steeply dipping schistosity. Net slip on the Ross Lake Fault is reported by Stauffer and Mukherjee (1971) to increase from 762 m south of Ross Lake to 1372 — 1525 m in the vicinity of Little Cliff Lake, with east side up and to the north.

The *Club Lake Fault* is the northernmost of three curved, south-dipping faults folded by the Hidden Lake Synform. The fault zone is marked by a sharp contact between Amisk rocks to the south and Missi rocks to the north; both Amisk and Missi rocks are strongly schistose for about 1 m adjacent to the fault (Fig. 286). The fault contact is locally tightly folded, and these minor folds are coaxial and coplanar with the Hidden Lake Synform, indicating that the fault is older than, and is folded by, the Hidden Lake Synform (Table 24). However, movement along the fault continued after formation of the Hidden Lake Synform, because a post-Missi Boundary Intrusion east of the map area contains a 15 m wide shear zone along the extension of the Club Lake Fault (Syme, 1975). Stauffer and Mukherjee (1971) estimate displacement on the Club Lake Fault to be between 1067 and 1830 m, with the southeast (Amisk) block thrust relatively up and northwest over the Missi.

The *Railway* and *South Railway Faults* are curving structures which are truncated by the Ross Lake Fault north of Ross Lake, and join to become a single fault north of Flin Flon Mine. The South Railway Fault is exposed in several localities southwest of Little Cliff Lake. There, it is expressed in Amisk Group rocks as a 3 — 4 m wide, bluish green schistose zone containing carbonate pods and disseminated hematite. Lineations in the foliation plane (hinges of intrafolial folds, deformed carbonate pods) are coaxial with the axis of Hidden Lake Synform, and are parallel to lineations (deformed clasts) in the Missi Group. The axial trace of the Hidden Lake Synform crosses both faults without displacement, indicating that, like the Club Lake Fault, these structures pre-date the Hidden Lake fold. Dip of the South Railway Fault varies with position in the fold; it is 55° east on the west limb, 34° south in the fold nose, and 57° — 72° east on the east limb.

The *Channing Fault* offsets the Amisk-Missi unconformity and the pre-Missi Channing granodiorite (unit 44), south of Mud Lake. The fault was not observed in outcrop. Stauffer and Mukherjee (1971) suggest that it is cogenetic with and similar to the Ross Lake Fault, but is slightly older because it is moderately folded by the Embury Lake Antiform and offset by the Ross Lake Fault. They calculate that the net slip of this steeply east dipping fault is in the range of 610 — 1220 m, with the east side relatively up and to the north. The southern extension of Channing Fault is consi-

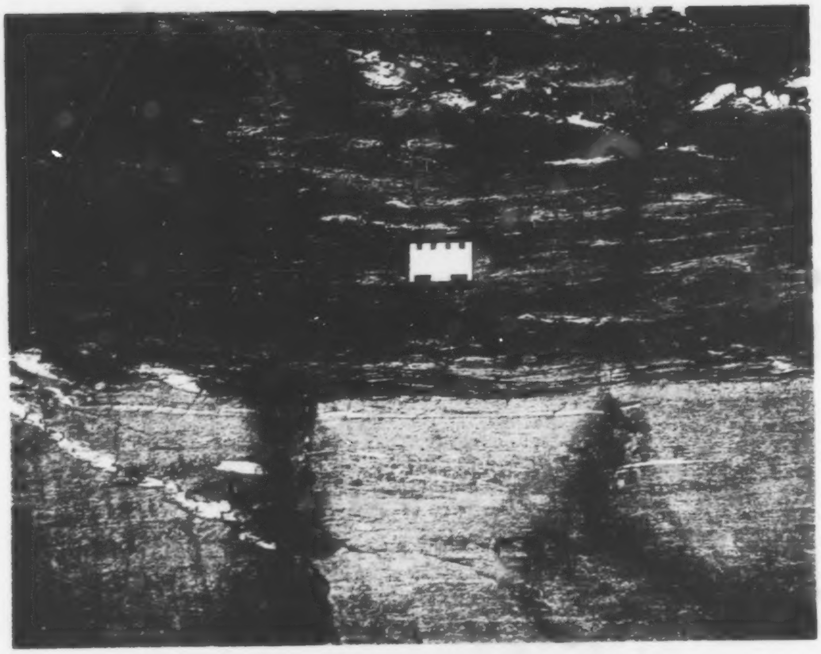

Figure 286: Trace of the Club Lake fault, separating schistose Amisk Group rocks (top; derived from pillowed unit 2 basalt) and foliated Missi Group pebbly sandstone (bottom; unit 50a). The schistose zone is up to 1.5 m wide, passing abruptly into unsheared Amisk rocks to the southwest. The fault plane is subvertical at this locality, and is locally tightly folded parallel to the Hidden Lake synform, indicating the fault predates the fold. 520 m northwest of Little Cliff Lake.

dered to follow the centre of Northwest Arm (Schist Lake).

The *Phantom Lake, Green Lake* and *Mitt Lake faults* separate subblocks with differing facing directions and/or stratigraphic components. The amount of displacement on the faults has not been determined but must be significant. The Phantom Lake and Green Lake faults have little outcrop expression apart from a narrow zone (1 — 2 m) of increased schistosity; these faults occupy a pronounced topographic lineament. The Phantom Lake Fault joins Ross Lake Fault south of Stitt Island, where a major escarpment along the shore of Schist Lake marks the position of the combined structure. The Mitt Lake Fault is marked by a wider zone of intense schistosity, quartz veining, and local intrafolial folds. The Mitt Lake Fault cuts the Green Lake Fault and is itself cut by the Phantom Lake Fault.

Hook Lake Block

The Hook Lake Block is internally subdivided by a number of dominantly north-northwest-trending faults. These faults differ from those in the Flin Flon Block as they have little associated deformation and stratigraphic units can be correlated across them (Fig. 150). The faults postdate folds in the Amisk Group and the imposition of regional axial planar foliation; they may also produce minor offsets of the prehnite-pumpellyite isograd.

The *Big Charlie Lake Fault* is a major, generally north-trending structure that is responsible for 1280 m of right-lateral displacement on the contact between units 45b and 45c in the Cliff Lake Pluton. The fault forms the western boundary of the southern part of the pluton and from there curves to the southwest to produce significant truncation of Amisk stratigraphy. The south end of the fault terminates against the Insole Lake Fault. The Big Charlie Lake Fault is observed in outcrop only within the Cliff Lake Pluton, where it locally occupies a topographic lineament. Near Big Charlie Lake the fault zone is several metres wide and comprises a number of discrete shear zones in which the primary texture of the tonalite is destroyed. Aplite dykes within the fault zone are displaced across cross-foliation slip surfaces. Tonalite adjacent to the fault is hematized and foliated. East of Grant Lake the fault zone is marked by less than 1 m of intense schistosity. Large mafic xenoliths in unit 45b are truncated abruptly at the fault, and a 1 — 2 m wide quartz diorite dyke follows the fault surface for several hundred metres. South of the Cliff Lake Pluton the fault was not directly observed in Amisk Group rocks.

The *Insole Lake Fault* is a north-northwest-trending structure truncated at its northern end by the Cliff Lake Fault. The fault displays approximately 300 m right-lateral displacement, measured on offset of: Amisk lithologic contacts, an abrupt change in amygdale filling in unit 7 flows, and the Milliken Lake Fault. For most of its length the fault occupies a well defined topographic lineament. In the vicinity of Insole Lake, rocks develop a greenish colour and increasing intensity of foliation within several metres of the fault plane, which consists of about 1 m of extremely schistose material. At its northern end the fault is marked by a zone of schistosity at least 30 m wide. The fault dips 71° — 87° east.

The *Hook Lake Fault* is a north-trending structure which passes through the east side of Hook Lake and is offset along the Milliken Lake Fault. To the north it forms the eastern boundary of unit 45b at the south end of the Cliff Lake Pluton before joining or being truncated by the Big Charlie Fault about 1 km south of Big Charlie Lake. Displacement on the fault, measured from left-lateral offset of Amisk Group stratigraphy on Hook Lake, is about 1300 m; the fault truncates the Milliken Lake Syncline. The offset portion of the fault north of Milliken Lake is defined by juxtaposition of two significantly different basalt units: north-trending massive and pillowed flows (unit 7) and north-northwest-trending pillowed flows with abundant amoeboid pillow breccia. The fault is exposed along the west shore of Kinsella Lake, where there is a wide (up to 14 m) zone of schistosity and quartz net-veining that increases in intensity towards the fault. The fault is marked by a 1 m wide zone of strongly schistose rocks intruded by narrow rhyolite veins; dip is 85° to the west. The north end of the Hook Lake Fault follows a distinct topographic linear; where exposed it is marked by a zone of strong schistosity and local hematization of the Cliff Lake Pluton. In Amisk rocks south of the pluton the fault displays a strong shear foliation and locally contains quartz veins with disseminated pyrite and chalcopyrite.

The *Milliken Lake Fault* is an east-northeast-trending structure which offsets Amisk Group stratigraphy, the Milliken Lake Syncline and the Hook Lake Fault. The fault has 760 m of left-lateral displacement. A report in cancelled assessment files identifies this fault and describes it as a 30 cm wide zone of brecciated rock. It is offset along the Insole Lake Fault and truncated by the Cliff Lake Fault. A similarly oriented fault through Hartnett Lake is interpreted to explain the abrupt northern truncation of the Milliken Lake syncline and truncation of some rock units. This structure is also offset to the north across the Insole Lake Fault.

Manistikwan Lake Block

The Manistikwan Lake Block is cut by many north-northwest-trending, steeply dipping faults oriented subparallel to Amisk stratigraphy. The magnitude of displacement along faults could rarely be determined. Many faults are marked by topographic lineaments.

The fault, which is interpreted to trend parallel to the east shore of Big Island, is marked by brecciation, introduction of open-space filling carbonate, and a local strong schistosity. Dip on this fault ranges from 70° — 90° to the west. Although there is no outcrop expression of the fault along the northeast side of the island its presence is indicated by the truncation of pillow fragment breccia (unit 8a) and diorite (unit 42b) units, which do not appear on the mainland. The fault probably joins the Big Island Fault at the north and south ends of Manistikwan Lake; the lensoid shape of Big Island is controlled by these two major structures.

Other faults in the block are broadly similar to the fault east of Big Island in that they display brecciation, carbonate veining, introduction of abundant open-space filling carbonate, and varying degrees of imposed schistosity within fault zones up to 30 m wide. Some fault breccias contain discrete zones of intense schistosity; other faults are marked only by zones of schistosity. Bleaching of rocks adjacent to and within fault zones, carbonate blastesis, and pervasive carbonatization occur along some faults or fault segments. An example of particularly intense carbonatization occurs along the fault that terminates the gabbro (unit 41b) at the south end of Embury Lake. There, the carbonatized zone is at least 12 m wide; within the zone primary textures are completely obliterated and the unfoliated Fe- carbonate-rich material is crossed by irregular, grey veins of amphibole + carbonate.

Faults in the Manistikwan Lake Block are distinctly more carbonate impregnated than most other faults in the Flin Flon-White Lake area. The only other area with faults of this character is the adjacent Grassy Narrows Zone.

Grassy Narrows Zone

The Grassy Narrows Zone is a geologically complex area in which primary Amisk stratigraphy is completely disrupted by easterly-trending faults and later, major north-northwest-trending faults. The structural complexity of this zone is comparable to that in the Whitefish-Mikanagan Lakes Block; both are marked by relatively narrow zones of closely spaced faults across which are abrupt reversals in stratigraphic facing.

Easterly trending faults in this zone have virtually no expression in outcrop. At one locality one of these faults is simply a quartz- and chlorite-filled fracture. Major displacement has occurred on these faults, however, because they juxtapose opposite-facing sequences and truncate some intrusions.

The Grassy Narrows Zone contains two major north-northwest-trending faults in addition to the Rosenberg Lake and Inlet Arm faults previously described (Fig. 3). The western fault follows an elongate valley north of Grassy Narrows; it is truncated east of Rosenberg Lake by the Rosenberg Lake Fault. Adjacent to the fault a massive rhyolite flow (unit 18b) has been moderately foliated, hematized and veined by carbonate, whereas graphitic pyritic mudstone (unit 36) at Grassy Narrows is strongly schistose over a width of at least 50 m. The eastern fault clearly truncates a number of gabbroic intrusions on the east side of Manistikwan Lake. Adjacent to the fault are subsidiary narrow shears; schistosity increases towards the fault. At the entrance to Grassy Narrows, where the eastern and western faults must be at most 60 m apart, the rocks are bleached, veined by carbonate, and contain abundant 0.5 mm carbonate blasts. Schistosity on both east and west faults dips 60° to 86° east.

Bear Lake Block

The Bear Lake Block has few major internal faults. It contains two significant, north-northeast-trending faults which cut across stratigraphy at a shallow angle (Vick Lake and Bazinet Lake faults), and several minor northeast-trending faults with small displacements.

The *Vick Lake Fault* has been traced from the south end of Bear Lake, north through the chain of lakes including Vick Lake, to the northern boundary of the map area. The fault cuts slightly up-section from Bear Lake to Vick Lake, resulting in successive northward omission of formations. At Vick Lake, Vick Lake tuff (unit 25) is juxtaposed against Bear Lake basaltic andesite (unit 1), representing omission of about 850 m of volcanic section. Deformation associated with the fault is exposed on Bear Lake and Solodiuk Lake. The entire zone of deformation is approximately 100 m wide and is cored by 30 m of intensely sheared, crenulated and veined (quartz and carbonate) rocks. Adjacent to the central zone the rocks are strongly foliated and primary structures are flattened; deformation decreases away from the fault.

The Vick Lake Fault is shown on Map GR87-1-1 to be cut by the Benn Lake gabbronorite (unit 41a) between Vick Lake and Solodiuk Lake. However, there is a weak topographic linear, with adjacent strongly foliated outcrops, within the intrusion along strike from known positions of the Vick Lake Fault. Thus the gabbronorite may indeed pre-date the fault, in accord with the general relationships established among intrusions, metamorphism and faults.

The Vick Lake Fault can be traced in outcrop to the south shore of Bear Lake. From this point south the fault cannot be reliably traced due to the general increase in deformation (Fig. 6) and the absence of well defined stratigraphy within Bear Lake basaltic andesite (unit 1). However, the fault may extend along a strong topographic lineament extending through Sleep, Wonderland and We lakes. The linear coincides with apparent truncation of pillow fragment breccia units on and north of Wonderland Lake.

The *Bazinet Lake Fault* is a slightly curved, north-northeast-trending structure east of White Lake; it is exposed only adjacent to a topographic linear west of Bazinet Lake. There, the quartz diorite top of the White Lake Sill is strongly sheared over a width of at least 6 m. The fault truncates the top of the White Lake Sill, produces repetition of stratigraphy, and offsets the Northeast Arm Syncline.

Northeast-trending faults in the Bear Lake Block generally have a left-lateral sense of offset. None of the faults have significant expression in outcrop and only the faults north of Benn Lake coincide with topographic linears. The faults with maximum horizontal components of offset are the large fault northwest of Benn Lake (670 m of left-lateral offset) and the fault south of Bear Lake (520 m of right-lateral offset). The faults cut the Mikanagan Lake Sill and Benn Lake gabbro plug and are truncated against the Northeast Arm Fault.

Scotty Lake Block

The only internal fault in the Scotty Lake Block is the One Portage Lake Fault. This fault occurs in the Northeast Arm of Schist Lake, and trends north-northeast to join the block-bounding Northeast Arm fault in Whitefish Lake. It trends subparallel to stratigraphy in Scotty Lake Block; consequently the amount and sense of offset on this fault is not known. The One Portage Fault is intruded by small bodies of quartz-megacrystic tonalite (unit 55). Both the tonalite and mafic volcanic rocks within the fault zone (several tens of metres wide) are strongly foliated; mafic schists are commonly also crenulated.

Whitefish-Mikanagan Lakes Block

Internal faults in the Whitefish-Mikanagan Lakes Block are abundant. They fall into three broad categories:

1) gently curved, north-northeast-trending faults northeast of Whitefish Lake (e.g. the fault along Pineroot River);
2) straight, north-trending faults on and south of Whitefish Lake; these bound slivers of Missi Group rocks;
3) a north-northwest-trending fault that offsets the block-bounding Sourdough Bay Fault.

The north-northeast-trending faults commonly coincide with topographic linears. Some have associated zones of intense deformation: schistosity, tight folding and transposition of bedding, and obliteration of primary structures. Others appear to have only minor expression. Dips are generally steep; the Pineroot River Fault dips 75° — 90° west. The faults must have significant displacements because they commonly separate narrow panels with opposing facing directions. However, they produce only minor offsets in the contact between the Whitefish quartz monzodiorite (unit 54) and Amisk volcanic rocks. These relationships indicate that most of the movement on the faults predates the intrusion; post-intrusion displacements are minor.

The north-trending faults on Whitefish Lake and south along the Pineroot River are marked by zones of steeply dipping schistosity less than 2 m wide. They separate narrow panels of Missi Group sandstone and conglomerate that have opposing facing directions and different clast populations (reflected in weathering colours of purple and grey). At least one of the faults can be traced through the Whitefish Lake quartz monzodiorite, and two other faults clearly juxtapose Missi against both bodies of quartz monzodiorite on Whitefish Lake. Most movement along this set of faults, however, probably predates emplacement of the intrusions. The faults postdate the regional foliation in the Missi Group; the foliations trend 192° — 203° compared to faults trending about 180°.

The northwest-trending fault between Pineroot River and Sourdough Bay is truncated against the north-northeast-trending fault along Pineroot River but offsets the block-bounding Sourdouth Bay. This is the only fault in the area known to offset a block-bounding fault. There is no outcrop expression of this fault, but it does coincide with a topographic linear and must involve significant displacement. The offset of the Sourdough Bay Fault is left-lateral with approximately 450 m of displacement.

METAMORPHISM

INTRODUCTION

All supracrustal and intrusive rocks in the Flin Flon-White Lake area are metamorphosed. Regional metamorphism increases in grade from subgreenschist (prehnite-pumpellyite) in the southwest to middle greenschist (biotite present) in the northwest. Most rocks in the area belong to the lower greenschist facies (biotite absent). Primary igneous minerals and textures are commonly well preserved in the subgreenschist zone. In the greenschist zone primary minerals are generally absent and primary textures, although locally well preserved, are commonly obscured due to recrystallization. Contact metamorphism adjacent to intrusions is of limited extent and is overprinted by regional metamorphic mineral assemblages.

CONTACT METAMORPHISM

The immediate Flin Flon-White Lake area is devoid of major felsic plutons and consequently significant contact metamorphism of the Amisk and Missi supracrustal rocks is limited. Relatively minor contact metamorphism occurs adjacent to the Cliff Lake Pluton (unit 45), Benn Lake gabbro (unit 41), Mikanagan Lake Sill (unit 41) and a tonalite pluton that occurs outside the map area to the southeast. Other intrusions either do not have a thermal aureole or the effects are limited to, at most, a metre or two.

Adjacent to the unfaulted western margin of the *Cliff Lake Pluton* two types of alteration and recrystallization are developed. The first is simple static recrystallization in which pillowed basalt within 30 — 50 m of the contact is transformed into a dark grey, unfoliated, very fine grained mosaic of actinolite, epidote and relict plagioclase microlites. The second type is an irregularly developed hydrothermal alteration spatially associated with the margin of the intrusion. Rocks within 300 m of the contact have been bleached, epidotized and locally pyritized; similar alteration occurs at the extreme south end of the intrusion. Contact metamorphic effects were not noted adjacent to unit 45d of the Cliff Lake Pluton.

Contact metamorphism related to the *Benn Lake gabbro* (unit 41) varies from relatively minor, on the western margin of the body, to a wide zone of alteration on the southern and northeastern margins. Basaltic andesite flows within 30 — 50 m of the western contact weather rusty buff to dark grey or green, and are completely recrystallized to very fine grained actinolite, chlorite, epidote, feldspar, quartz and magnetite. Despite the obliteration of primary microscopic textures, primary structures such as pillows and amygdales are well preserved and undeformed. At the southern margin, the normally buff weathering basaltic andesite flows are grey-green, unfoliated, pervasively epidotized and locally pyritized in a zone up to 250 m wide. They are composed of fine grained epidote and actinolite, with minor quartz and feldspar. Amygdales in this contact zone are filled with dark green chlorite, pyrite and epidote. Similar dark weathering, undeformed, weakly epidotized rocks occur on the northeastern margin of the intrusion.

The *Mikanagan Lake Sill* (unit 41) is emplaced predominantly within Vick Lake andesitic tuff (unit 25). The tuff within 1 — 3 m of the western, basal contact of the sill weathers pale green rather than the usual buff colour, and contains numerous epidote-filled fractures. The contact metamorphic zone at the top of the sill is much wider, locally up to 30 m. In this zone the tuff is grey-green, massive and recrystallized. Primary structures such as bedding and pumice fragments are largely obliterated. At one locality in the southwest bay of Mikanagan Lake the tuff contains 15 — 20% retrograded garnet porphyroblasts up to 1 mm across; the porphyroblasts are composed of a chlorite-actinolite-epidote core and fine grained epidote rim.

Contact metamorphism presumably due to a *felsic pluton* occurs in the extreme southeast corner of the map area (south shore of Sharpe Bay, Athapapuskow Lake). There, felsic rocks (unit 18) contain fine grained biotite; other rocks in the Bakers Narrows Block are biotite-free. The slightly higher grade in this southeast corner is interpreted to be due to the thermal effects of a nearby (1.2 km) tonalite pluton.

REGIONAL METAMORPHISM

Regional metamorphism in the Flin Flon belt increases in grade towards the Kisseynew metasedimentary gneiss belt (Bailes and McRitchie, 1978; Harrison, 1951). In the Flin Flon-White Lake area, metamorphic grade increases from subgreenschist (prehnite-pumpellyite) at Hook Lake to middle greenschist (biotite) at Ross Lake (Fig. 274). More than three-quarters of the area is within the lower greenschist facies, characterized by mineral assemblages that include chlorite, tremolite-actinolite, epidote, albite, muscovite and quartz.

The age of regional metamorphism of the Flin Flon and Kisseynew belts is estimated by Gordon et al. (1987, 1988) to be between 1815 and 18[illegible] on the basis of U-Pb zircon ages. This metamorphism postdates deposition of the Missi Group and emplacement of all intrusions, and took place with the development of schistosity (Stauffer and Mukherjee, 1971) during the fourth phase of deformation (P4, Table 25). Metamorphic zones are offset by faults developed during P5. In higher grade areas to the north of Flin Flon, retrograde lower greenschist mineral assemblages are reported in P5 fault zones (Stauffer and Mukherjee, 1971; Byers et al., 1965).

Subgreenschist facies (prehnite-pumpellyite)

Subgreenschist facies mineral assemblages occur in rocks in the southern parts of the Hook Lake Block and Flin Flon Block (Fig. 287). The zone is bounded on the east by the Inlet Arm Fault and is offset by the Hook Lake, Insole Lake, Cliff Lake, Channing and Ross Lake faults (Fig. 287). Within this zone most of the rocks contain prehnite and/or pumpellyite; the upper stability limit of these minerals marks the boundary between the subgreenschist facies to the south and lower greenschist facies to the north. The subgreenschist facies zone is further characterized by excellent preservation of primary structures and textures, and abundant primary clinopyroxene. In the following paragraphs, metamorphic mineral parageneses are discussed according to major rock types: mafic flows, mafic fragmental units, felsic flows, and intrusive rocks.

Mafic flows (basalt and basaltic andesite) are the most common rock type in the subgreenschist zone. Many of the flows contain phenocrysts of plagioclase and/or clinopyroxene, as well as polymineralic amygdales. Primary calcic plagioclase is commonly pseudomorphed by albite with or without polysynthetic twinning, plus variable amounts of very fine grained epidote, sericite and carbonate. Minor amounts of chlorite, tremolite-actinolite and pumpellyite occur in some albite pseudomorphs. Less commonly, calcic plagioclase is pseudomorphed by epidote + sericite, prehnite + quartz + carbonate + epidote, or quartz alone. Primary clinopyroxene phenocrysts vary from relatively unaltered (Fig. 288) to completely pseudomorphed by secondary assemblages. Less altered clinopyroxenes have minor colourless chlorite developed along fractures and cleavages, and overgrowths of pale green, fibrous tremolite-actinolite. More altered clinopyroxenes are pseudomorphed by chlorite, tremolite-actinolite, or both.

The groundmass of mafic flows is composed of albite pseudo-

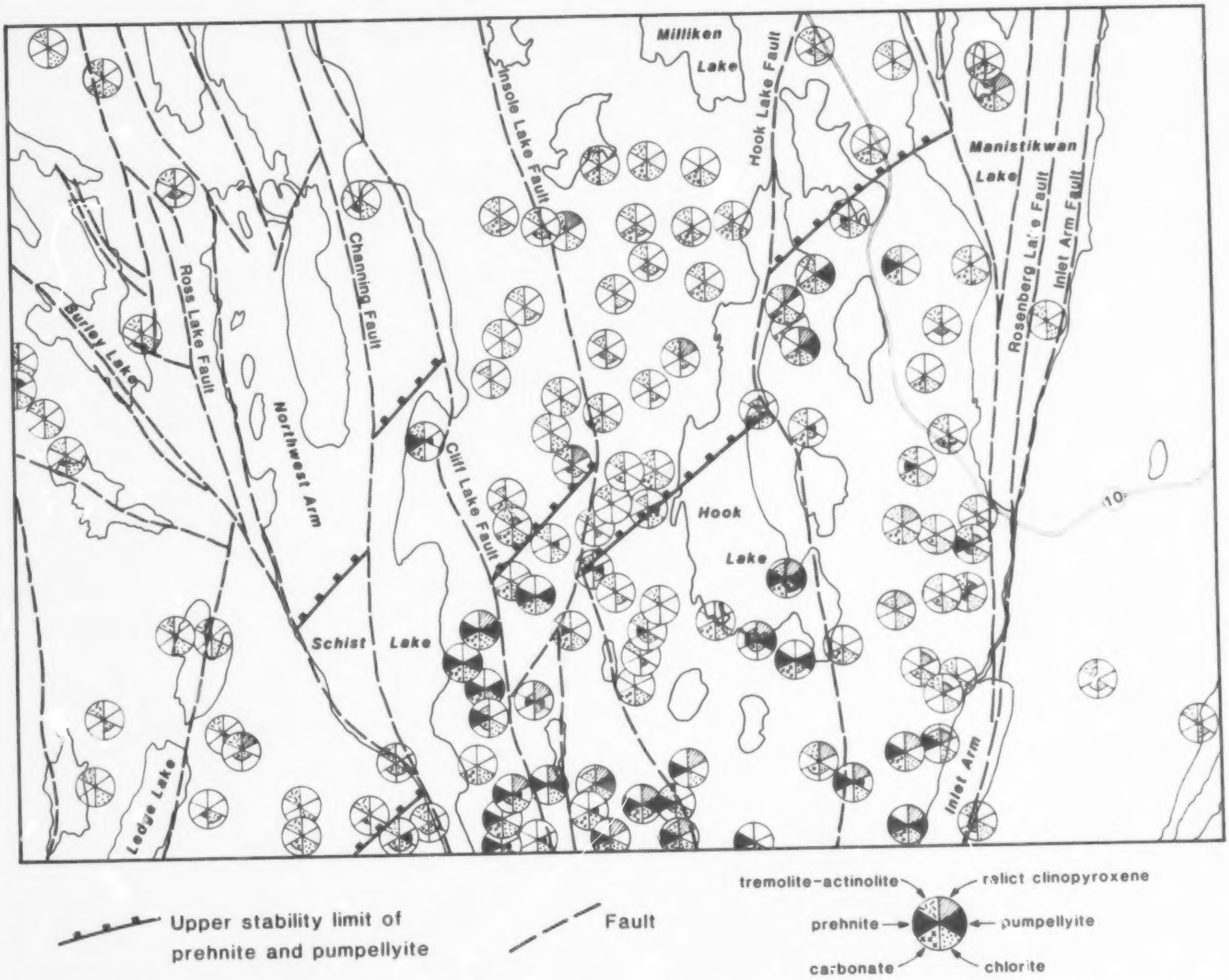
Milliken Lake
Hook Lake Fault
Manistikwan Lake
Rosenberg Lake Fault
Inlet Arm Fault
Insole Lake Fault
Channing Fault
Ross Lake Fault
Burley Lake
Northwest Arm
Cliff Lake Fault
Hook Lake
Schist Lake
Ledge Lake
Inlet Arm
10
Upper stability limit of prehnite and pumpellyite
Fault
tremolite-actinolite
relict clinopyroxene
prehnite
pumpellyite
carbonate
chlorite

Figure 287: Mineral assemblages in the Hook Lake area. Each circle represents the assemblage observed in one thin section: all thin sections from the subgreenschist zone are plotted whereas representative sections only are plotted for the greenschist zone. Filled sectors indicate phase is relatively abundant; partially filled sectors indicate phase is present as a minor component. Unfilled sectors indicate absence of that mineral.

morphs after primary calcic plagioclase microlites, and interstitial mafic minerals. In least altered rocks the groundmass mafic mineral is clinopyroxene partly replaced by chlorite and epidote. Throughout most of the subgreenschist facies zone, however, primary groundmass clinopyroxene is completely replaced by chlorite, epidote, and, in the northern part of the zone, pale green tremolite-actinolite. Prehnite, pumpellyite, carbonate and leucoxene occur in the groundmass of some flows.

Amygdales in mafic flows are filled by a wide variety of secondary assemblages and display an equally wide variety of textures (Fig. 289). Most amygdales are polymineralic and zoned; some appear to contain pseudomorphs after earlier zeolites. Prehnite and pumpellyite are common in amygdales; other minerals include epidote, quartz, carbonate, chlorite, albite and pyrite.

Mafic fragmental rocks include pillow fragment breccias, scoria-rich tuff and lapilli tuff. Pillow fragments in breccias are identical in textural preservation and mineralogy to mafic flows. Matrix in the breccias is a foliated mass of epidote, chlorite, carbonate and pumpellyite; clastic granules are locally entirely replaced by fine grained pumpellyite. Scoriaceous fragments in tuff contain plagioclase and clinopyroxene phenocrysts in a non-microlitic groundmass in which relict axiolitic and spherulitic textures are locally preserved, indicating that the primary groundmass was vitreous. The phenocrysts are replaced by the same minerals as in mafic flows. The primary vitreous groundmass has been recrystallized to a very fine grained, brownish mixture of epidote and chlorite. The tuffs are grain-supported with very little matrix; inter-fragment spaces are filled with abundant carbonate, local prehnite and minor quartz. Amygdales in some fragments are polymineralic and filled by the same suite of minerals as in the mafic flows.

Rhyolite in the subgreenschist facies zone is entirely intrusive (unit 49). Plagioclase phenocrysts are pseudomorphed by albite with a weak to moderate alteration to very fine grained sericite, minor epidote and minor carbonate. The groundmass was originally glass and devitrified to

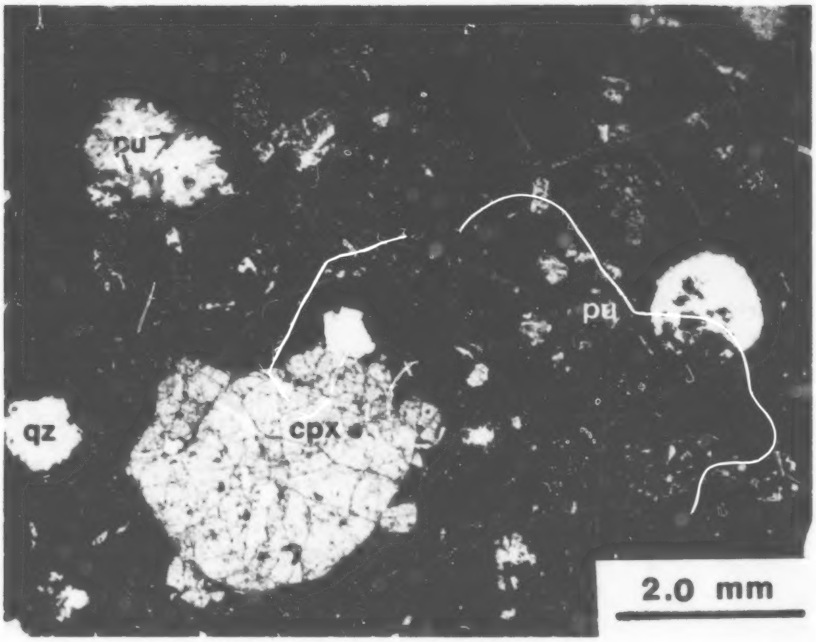

Figure 288: *Plagioclase-pyroxene-phyric mafic flow (unit 9), west of Hook Lake. Clinopyroxene phenocrysts (cpx) are fresh and unaltered. Plagioclase phenocrysts (pg) are altered to albite, epidote and pumpellyite. Groundmass consists of plagioclase microlites and fine grained prehnite, epidote and chlorite (dark). Amygdales are filled with quartz (qz; white) and pumpellyite (pu; grey). Sample 4158-1, plane polarized light.*

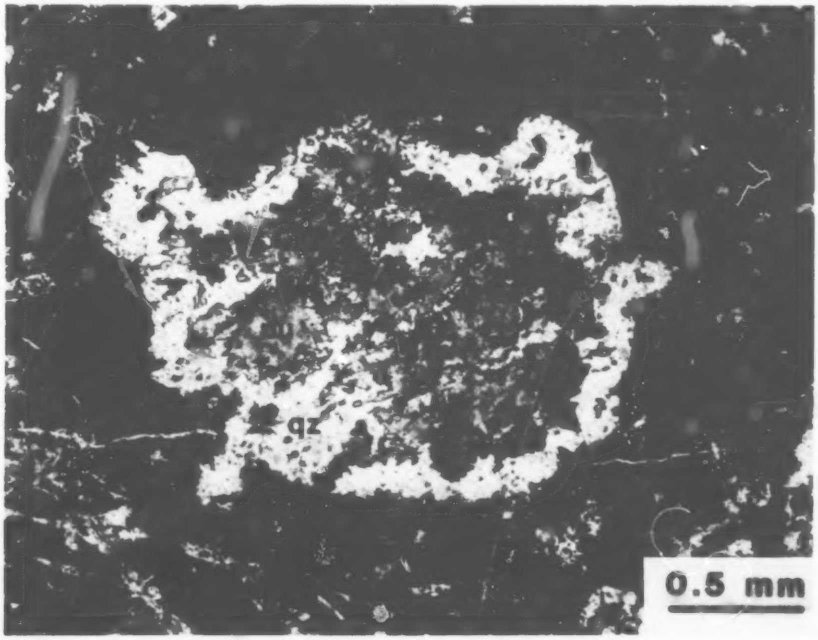

Figure 289: *Detail of amygdale in porphyritic mafic flow (unit 9), west of Hook Lake. Amygdale has a rim of very fine grained epidote (dark) and is filled with quartz (qz; white) and pumpellyite (pu; grey). Sample 4158-1, plane polarized light.*

abundant small feldspar spherulites; some rhyolites are flow banded. The remaining glass between spherulites has recrystallized to a very fine grained mosaic of feldspar, quartz, sericite, minor chlorite and minor epidote. Chlorite is locally abundant in some flow bands and along fine-scale primary perlitic fractures. Sericite also occurs concentrated in some flow bands and in a later generation of fine fractures.

Intrusive rocks in the subgreenschist facies zone include the Hook Lake quartz diorite (unit 42a), Hook Lake differentiated gabbronorite-ferrogabbro (unit 41), gabbro intrusive into rhyolite (unit 42) and minor mafic dykes.

Hook Lake quartz diorite is the only intrusion that contains the indicator minerals (prehnite and pumpellyite). Plagioclase laths are pseudomorphed by albite, fine grained brownish epidote, pale green chlorite, prehnite and pumpellyite. Clinopyroxene is partly replaced by tremolite-actinolite, chlorite, epidote, and rare pumpellyite. Fe-Ti oxides are pseudomorphed by leucoxene and magnetite, which is locally further oxidized to hematite.

Hook Lake gabbronorite-ferrogabbro is mineralogically identical to similar bodies in the greenschist facies. Pumpellyite was observed in a veinlet in one locality. Other mafic intrusions in the subgreenschist zone contain mineral assemblages indistinguishable from those in the greenschist zone.

Lower greenschist facies

Most rocks in the Flin Flon-White Lake area are within the lower greenschist facies. This zone is bounded to the south, at Hook Lake, by the well constrained upper stability limit of prehnite and pumpellyite. To the north it is bounded by a poorly constrained lower stability limit of biotite (Fig. 274).

Rocks in the lower greenschist zone differ from those in the subgreenschist facies only in that they contain no prehnite or pumpellyite, primary clinopyroxene is generally absent, and primary textures are not always as well preserved. Primary calcic plagioclase is replaced by highly variable proportions of albite, epidote, carbonate, sericite and chlorite. Clinopyroxene is preserved sporadically throughout the zone but is relatively abundant only in coarse grained mafic intrusions and in volcanic rocks near the lower boundary of the zone (Fig. 287). Groundmass pyroxene is totally replaced by variable proportions of pleochroic tremolite-actinolite, chlorite and epidote. Fe-Ti oxides are replaced by leucoxene, magnetite and hematite, and white mica is a common constituent in felsic rocks. Polymineralic amygdales are similar to those in the subgreenschist zone but lack prehnite and pumpellyite.

Stilpnomelane is a prominent component in a wide variety of rock types in the Bear Lake, Scotty Lake and Manistikwan Lake blocks. It is virtually absent in other blocks, and is known in only one locality in the subgreenschist zone. Stilpnomelane forms pleochroic (golden brown to very dark brown or reddish brown) flakes, aggregates and rosettes that overprint all other metamorphic minerals. It occurs preferentially in Fe-rich rocks such as Two Portage ferrobasalt (unit 5), Scotty Lake ferrobasalt (unit 4), ferrotonalite and quartz ferrodiorite (unit 41g). It also occurs in Vick Lake andesitic tuff, which is not particularly Fe-rich. Stilpnomelane occurs irregularly in phenocrysts, groundmass, matrix and amygdales, and in late fractures and veinlets. Commonly it is concentrated in the ferromagnesian phases but it is not confined to Fe-bearing minerals.

Middle greenschist facies

The middle greenschist facies, present in the northern one-third of the map area, is distinguished from the lower greenschist facies by the sporadic occurrence of brown biotite. In other respects the mineral assemblages in the two zones are identical and in the absence of biotite cannot be distinguished. Biotite is relatively common in the middle greenschist zone between Flin Flon town and Cliff Lake. East of the Cliff Lake Fault, however, biotite has only a very sporadic distribution and the lower boundary of this zone is poorly constrained. The boundary between the lower and middle greenschist facies is probably offset across faults but there are insufficient biotite-bearing rocks to determine the amount and sense of offset.

In the Hidden Lake area, biotite composes 0 — 5% of mafic rocks and 1 — 2% of felsic rocks. In basalts, biotite is associated with, and appears to be growing at the expense of, green chlorite. It occurs in amygdales (with chlorite, epidote and quartz), as an alteration product of plagioclase, and in minor amounts in the groundmass. In felsic rocks, biotite has sharp boundaries with chlorite; it occurs in the groundmass of rhyolite flows, matrix of rhyolite breccias, in the pressure shadows around phenocrysts (associated with green chlorite, white mica and carbonate), and as an alteration product in plagioclase phenocrysts.

In the Cliff Lake Pluton, biotite is restricted to the area north of Grant Lake, clearly indicating that the pluton is pre-metamorphic in age. Biotite is present sporadically and in small amounts, replacing chlorite.

Throughout the remainder of the biotite zone, biotite is an uncommon constituent in basalt and occurs sporadically in more potassic rocks such as rhyolite intrusions and volcanic conglomerate.

ECONOMIC GEOLOGY

INTRODUCTION

The area around present-day Flin Flon has been actively explored for base metals and gold since the early part of the century; exploration accelerated following discovery of the Flin Flon Cu-Zn deposit in 1914. There are six current and past producing Cu-Zn mines within the map area (Map GR87-1-2, in pocket); still active are the Flin Flon and Centennial mines, whereas Mandy, Schist Lake, Cuprus and White Lake mines are no longer in production (Table 26). Although occurrences of Au and Mo are known, none are of present economic interest. However, north of the map area, at Tartan Lake, a recently discovered Au deposit was brought into production in 1987.

Map GR87-1-2 shows mineral occurrences and conductors referred to in cancelled assessment files, and alteration zones and minor mineral occurrences encountered during mapping. More information (primarily drill holes and logs) is in confidential files and cannot be shown on the map. The more important deposits and occurrences are described, with references, on Mineral Inventory cards available for inspection at Manitoba Department of Energy and Mines. Gale and Eccles (1988a, 1988b) give descriptions and locations of mineral deposits and occurrences for the northern half of the Flin Flon-White Lake area.

Mineral deposits and occurrences have been subdivided into five different types:

1. *Disseminated to massive stratabound sulphide deposits:* volcanogenic sulphides (Sangster, 1972) including Cu-Zn orebodies and subeconomic to barren sulphide layers. Some deposits are directly associated with volcanic rocks and others are associated with minor sedimentary intercalations within the volcanic pile. Discordant alteration zones with stringer and disseminated sulphides are also included in this group.

2. *Disseminated sulphides in sedimentary rocks:* pyritiferous and/or graphitic siltstones and mudstones commonly associated with thicker sedimentary units.

3. *Conductive zones identified by electromagnetic surveys and tested by diamond drilling:* graphite +/- sulphide zones of uncertain origin and schistose zones of probable fault derivation. Some of the graphite + sulphide zones may be sedimentary (2, above) whereas others may be simply seams associated with faults.

4. *Vein/fracture-filling deposits:* Au-bearing quartz veins and Mo-Cu-sulphide-filled fractures, mainly associated with brittle deformation structures in Cliff Lake tonalite and Whitefish Lake quartz monzodiorite, respectively.

5. *Oxide facies iron formation:* exposed at only one locality in the map area, at the northeast end of Schist Lake.

An important objective of metallogenic investigations is to define the origin of a deposit, or class of deposits, in time and space. For volcanogenic Cu-Zn sulphide deposits this includes the stratigraphic setting in which the sulphides were deposited. In the Flin Flon-White Lake area, the stratigraphy of host rocks containing each major Cu-Zn deposit has been determined and is described below. However, the block-faulting pattern that dominates the structure of the area precludes correlation of stratigraphy, and consequently correlation of mineralizing events, across block boundaries. It is therefore unlikely that relative ages of the various orebodies can be determined in the absence of precise radiometric dating. The fact that the sulphide deposits have very different stratigraphic settings strongly suggests that they are separated in both time and paleoenvironment.

Faults that occur within fault blocks also have a significant effect on stratigraphy; an excellent example is the Hook Lake Block. There, the more than 7.5 km of Amisk Group section has been folded and subsequently faulted, resulting in polygonal fault-bounded domains each containing part of the stratigraphic sequence (Fig. 150). Stratigraphic orientation varies in adjacent sub-blocks — an important fact to consider when planning electromagnetic surveys.

VOLCANOGENIC MASSIVE SULPHIDE DEPOSITS

Two types of volcanogenic massive sulphide deposits are recognized: proximal deposits, which have a closely associated alteration zone (Flin Flon, Schist Lake, Mandy, Centennial), and distal deposits, which lack closely associated alteration zones (White Lake, Cuprus). Proximal deposits are hosted by coarse felsic fragmental rocks whereas distal deposits are hosted by fine grained graphitic mudstones. Despite these differences both deposit types are stratigraphically associated with felsic volcanic rocks.

Flin Flon Mine

Flin Flon Mine is the largest deposit (almost 63 million tonnes) in the Flin Flon volcanic belt, an order of magnitude larger than the next largest deposit. The stratigraphic sequence hosting the orebody is described in detail in a previous chapter (Flin Flon Block), and is briefly summarized below.

The Flin Flon massive sulphide orebody was deposited during a hiatus in basaltic volcanism. The immediate footwall of the deposit comprises South Main pillowed basalt flows (unit 6a) and pillow fragment breccias (unit 6b). A lateral facies change from pillowed flows at South Main shaft, northwards into a thick sequence of now-altered pillow fragment breccias underlying the orebody, indicates that the source area for the footwall mafic pile lay to the south of South Main shaft (Fig. 170). The breccias presumably accumulated on the flank of a subaqueous basalt volcano or in a basin adjacent to the volcano. The uppermost part of the South Main basalt shows evidence of relatively shallow water emplacement, including abundance and large size of amygdales and local profusion of radial pipe vesicles.

Following cessation of South Main basaltic volcanism, volcanic activity shifted to intrusion of high level rhyolite domes (unit 16), extrusion of the Mine rhyolite flow (unit 15), and development of a large-scale hydrothermal convection system that altered both the footwall basaltic sequence and Mine rhyolite, and led to deposition of the stratiform volcanogenic Flin Flon orebody contemporaneous with the Mine rhyolite. An unconformity exposed in footwall rocks may be one expression of a synvolcanic fault which may have acted as a focus for hydrothermal discharge. Bedded volcaniclastic rocks (unit 30a) that overlie the Mine rhyolite and orebody represent the final depositional unit that accumulated during the hiatus in basaltic volcanism.

The resumption of basaltic volcanism following deposition of the Flin Flon orebody is represented by the Hidden Lake basalt (unit 2), more than 3.3 km in total thickness. These rocks are chemically and petrographically different from the underlying South Main basalt, and do not show evidence of hydrothermal alteration. At South Main shaft they directly over-

Table 26:
Copper-zinc and gold deposits, Flin Flon District

Deposit	Production Dates	Commodities	Production (P) + Reserves (R) x 000 Tonnes	Average Grades
Flin Flon	1930-	Cu,Zn,Au,Ag Se,Te,Cd	62 927 (P + R)[1]	2.2% Cu, 4.1% Zn
Centennial	1977-	Cu,Zn,Au,Ag	2 366 (P + R)[1]	1.5% Cu, 2.2% Zn
Westarm	1978-85	Cu,Zn,Au, Ag	1 702 P + R)[1]	3.7% Cu, 1.5% Zn
White Lake	1972-83	Cu,Zn,Au,Ag	850 (P)[1]	2.0% Cu, 4.8% Zn
Trout Lake	1982-	Cu,Zn,Au,Ag	5 697 (P + R)[1]	3.1% Cu, 4.5% Zn
Mandy	1916-19 1943-44	Cu,Zn,Au,Ag	23 (P) 102 (P)	20.2% Cu 5.6% Cu, 14.0% Zn
Schist Lake	1950-76	Cu,Zn,Au,Ag	1 871 (P)	4.3% Cu, 7.3% Zn
Cuprus	1948-54	Cu,Zn,Au,Ag	462 (P)	3.3% Cu, 6.4% Zn
North Star	1945-58	Cu,Zn	242 (P)	6.1% Cu
Don Jon	1955-57	Cu,Zn	79 (P)	3.1% Cu
Laguna	1920, 1924-25 1936-40	Au	98 (P)	17.7 g/t Au
Gurney	1937-39	Au,Ag	92 (P)	8.5 g/t Au, 24.2 g/t Ag
Vamp Lake	Drilling 1984	Cu,Zn,Au,Ag	421 (R)	1.7% Cu, 2.2% Zn, 4.3 g/t Au, 14.7 g/t Ag
Callinan	Drilling 1986	Cu,Zn,Au,Ag	1 542 (R)	1.4% Cu, 4.0% Zn, 1.9 g/t Au, 20.9 g/t Ag
Pine Bay	Inactive	Cu	1 361 (R)	1.3% Cu
Tartan	1987	Au	544 (R)	13.0 g/t Au
Puffy Lake	Under Development	Au	603 (R)	6.5 g/t Au
Nokomis Lake	Drilling 1985	Au	91 (R)	10.3 g/t Au
Namew Lake	Under Development	Ni,Cu	2 340 (R)	2.4% Ni, 0.9% Cu

---

[1] Production and Reserves figures as of December 31, 1984
Sources of information: Fogwill (1983), Esposito (1986), Hosain (1986)

lie South Main basalt whereas to the north 180 m of Mine rhyolite and volcaniclastic rocks occur between the two basalt units (Fig. 170). Like the South Main basalt, Hidden Lake basalt was probably extruded in shallow water, shown by the presence of abundant amygdales up to 1 cm in diameter.

Koo and Mossman (1975) outlined a chloritic alteration zone 2000 x 1000 x 200 m which transects the underlying pillow fragment breccia and Mine rhyolite and terminates against Hidden Lake basalt in the stratigraphic hanging wall. This intense chloritization is not exposed at surface. Exposed alteration (Map GR87-1-2) takes a variety of forms but most commonly consists of intense epidotization accompanied by local zones of chloritization and sericitization. Local zones of "bleaching", due to introduction of silica, and gossan zones characterized by anastomosing chlorite-pyrite-filled fractures, are also present. Within the mine workings the alteration zone is characterized by abundant dark green chlorite, that contains local remnants of quartz phenocrysts (altered Mine rhyolite) and quartz amygdales (altered South Main basalt).

The Flin Flon sulphide orebody is predominantly massive with chalcopyrite concentrated near the footwall and sphalerite, sometimes banded with pyrite, more common toward the hanging wall. Disseminated chalcopyrite and pyrite occur in the altered footwall and form approximately 30% of the ore mined. Six ore zones strike 330° and dip 70° E for 1650 m along plunge. The zones are an average of 270 m long, 21 m thick and 450 m in vertical extent.

First production from the Flin Flon Mine was in 1930. Peak production was reached in 1943. Production after 1976 has been mainly from pillars and remnants.

The Callinan deposit, approximately 2 km north of the Flin Flon deposit (Map GR87-1-2), occurs at the same stratigraphic level as the Flin Flon orebody. Early exploration began in 1927 with Cu-Zn mineralization identified in 1938 (Byers et al., 1965). Recent drilling by HBMS has outlined a deposit of 1.5 million tonnes (Table 26).

Schist Lake and Mandy mines

The Schist Lake and Mandy mines are located 5 km southeast of Flin Flon (Map GR87-1-2). Neither mine is presently producing; past production totaled approximately 2 million tonnes (Table 26). These deposits consist of several ore lenses that occur within the same stratigraphic interval. Host rocks for the deposits are sericite-carbonate schists derived from heterolithologic felsic volcanic breccia (unit 30); the rocks face west and occur within a fault-bounded panel, thus stratigraphic relationships with other deposits are unknown. Although the two massive sulphide deposits are about 1 km apart on surface, they are as close as 300 m in underground workings.

Hydrothermally altered breccias occur in the footwall of the ore zone. The rocks are strongly foliated and are variably chloritized, silicified and pyritized. At one locality (Map GR87-1-2) the breccias are traversed by irregularly branching veins and patches of dark green chlorite; contacts between the chlorite veins and volcaniclastics are sharp.

The Mandy orebody was 30 m long, 4 m wide and extended to a depth of 60 m. The orebody had a chalcopyrite-rich core, surrounded by a zone of mixed sulphides (predominantly sphalerite), and an outer zone in which pyrite was the most abundant sulphide (Davies et al., 1962). The Mandy Mine was in production 1916-1919 and again between 1943 and 1944.

The Schist Lake orebodies occur in north and south zones 300 m apart. The north zone contains 3 lenses which have maximum strike lengths of 60 m and extend 300 m down plunge. The south zone consists of 4 lenses that are 60 — 120 m in strike length and extend 300 — 600 m along plunge. Howkins and Martin (1970) report that a series of faults cut the zones obliquely, with displacements of tens of metres. They suggest that the Mandy and Schist Lake deposits may originally have formed a single sheet of sulphide. Metal zoning results in increasing Zn/Cu ratio from stratigraphic footwall to hanging wall (Howkins and Martin, 1970). The deposits are considered by HBMS and HBED geologists to top to the west (C.B. Ko and J. Percel, pers. comm. 1987).

Centennial Mine

The Centennial orebody subcrops under about 50 m of water and overburden some 400 m from the west shore of Athapapuskow Lake, about 1.5 km north of the Flin Flon airport at Bakers Narrows. It contains approximately 2.3 million tonnes of ore (Table 26). The Centennial deposit was discovered in 1970 by ground electromagnetic methods, and production was begun in 1977. The mine closed during 1983-84 and resumed production in 1985.

The deposit as described by Provins (1980) is a tabular sheet 100 m long and 10 m thick, with a near vertical pitch. The orebody is hosted within a unit of quartz-phyric felsic fragmental rocks. The fragmental rocks are overlain to the west by 30 m of pyritic argillite and 50 m of felsic lapilli tuff and flow breccias (Fig. 290).

The orebody is a single sulphide lens consisting of alternating beds of sulphide and siliceous gangue; it is zoned wih a Cu-rich stratigraphic footwall, a pyrite-rich centre and a zinc-rich hanging wall. A discordant alteration zone underlies the sulphide lens (Fig. 291). The most intensely altered material is represented by a chlorite-rich pipe (Fig. 291). Fe-Mg carbonates occur in a broad halo in the stratigraphic footwall of the orebody, south of the chlorite pipe. Element redistribution in the vicinity of the orebody is shown on Fig. 292.

The Centennial deposit occurs within the Sourdough Bay Block and is considered to be stratigraphically equivalent to the Pine Bay and possibly the Sourdough Bay deposits. The Sourdough Bay Block contains a stratified mafic sequence of subaqueous flows, volcaniclastic rocks and subordinate sedimentary rocks. The proportion of flows to volcaniclastics increases to the northeast, suggesting an increasingly more proximal environment in that direction. The sulphide zones are associated with graphitic and pyritic mudstones, siliceous mudstone and felsic volcaniclastics, indicating that the deposition of the Sourdough Bay mafic sequence was punctuated by eposides of felsic volcanism, sedimentation, and sulphide deposition.

White Lake and Cuprus mines

The White Lake and Cuprus deposits, 11 km southeast of Flin Flon (Map GR87-1-2), produced a total of about 1.3 million tonnes of ore. Initial prospecting on the showings that would become the White Lake and Cuprus deposits began in 1919. Cuprus Mine was brought into production in 1948 and peak production occurred in 1953; by 1954 the orebody was exhausted. Production began at White Lake Mine in 1972 and the mine closed in 1982 due to ore depletion.

The orebodies consist of a complex series of elongate lenses that plunge northwards, parallel to the axis of the Northeast Arm Syncline. Both the White Lake and Cuprus deposits are interpreted to occur within a single 25 m thick interval consisting of graphitic mudstone, siliceous mudstone and minor chert (unit 36).

The stratigraphic setting of these deposits can be unambiguously placed within the well defined Bear Lake Block sequence (Fig. 5). Reconstruction of the volcanic events that produced the sequence are fully described in the Bear Lake Block chapter, and are summarized below.

Bear Lake basaltic andesite (unit 1) forms the base of the block succession, and represents a shoaling subaqueous shield volcano at least 3.3 km thick. The volcano was covered by more than 1650 m of dominantly volcaniclastic rocks, suggesting that either a large summit caldera formed in the final stages of Bear Lake volcanism, or the entire volcano underwent isostatic sinking. The cessation of Bear Lake basaltic andesite volcanism was abruptly succeeded by eruption of Solodiuk Lake subaqueous rhyolite flows (unit 13) and contemporaneous infilling of a southward-deepening basin by volcaniclastic rocks. These volcaniclastic rocks include (1) a proximal heterolithologic breccia derived in part from

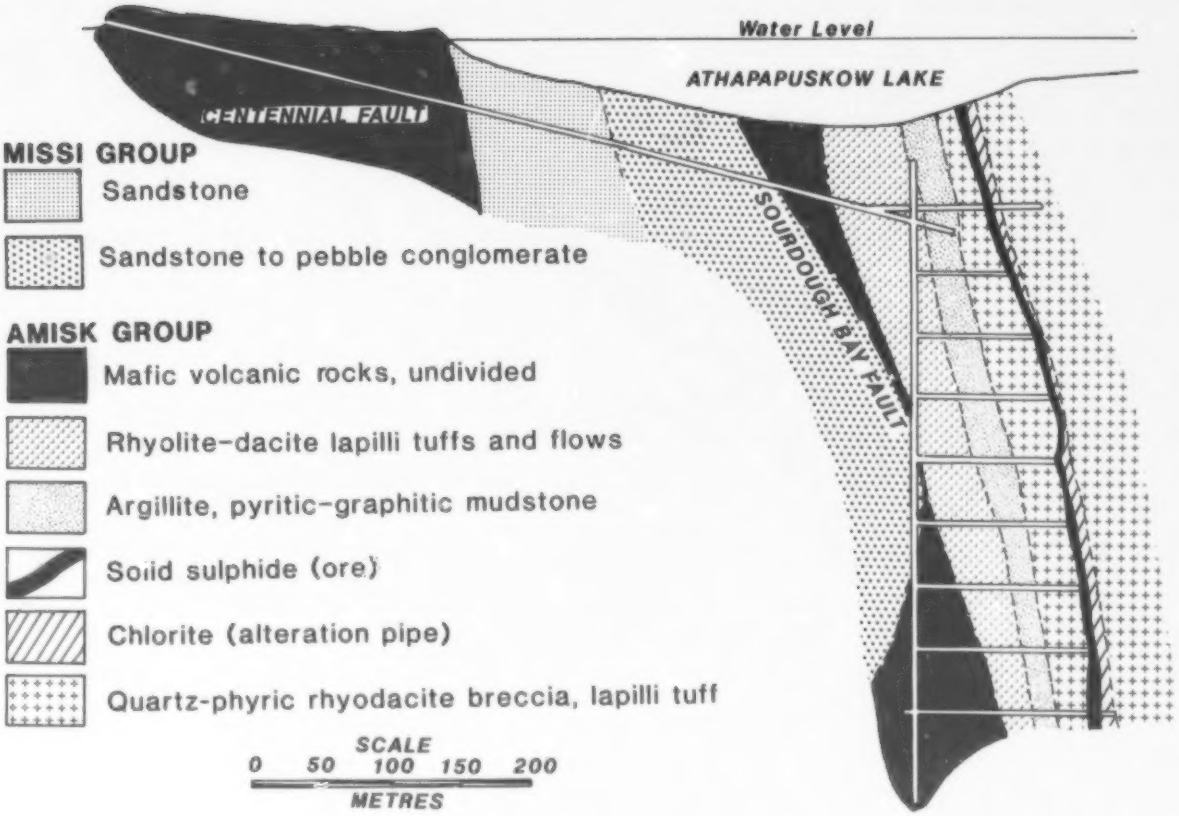
Water Level
ATHAPAPUSKOW LAKE
CENTENNIAL FAULT
SOURDOUGH BAY FAULT
MISSI GROUP
Sandstone
Sandstone to pebble conglomerate
AMISK GROUP
Mafic volcanic rocks, undivided
Rhyolite-dacite lapilli tuffs and flows
Argillite, pyritic-graphitic mudstone
Solid sulphide (ore)
Chlorite (alteration pipe)
Quartz-phyric rhyodacite breccia, lapilli tuff
SCALE
0 50 100 150 200
METRES

Figure 290: Cross-section of the Centennial Mine (from Provins, 1982).

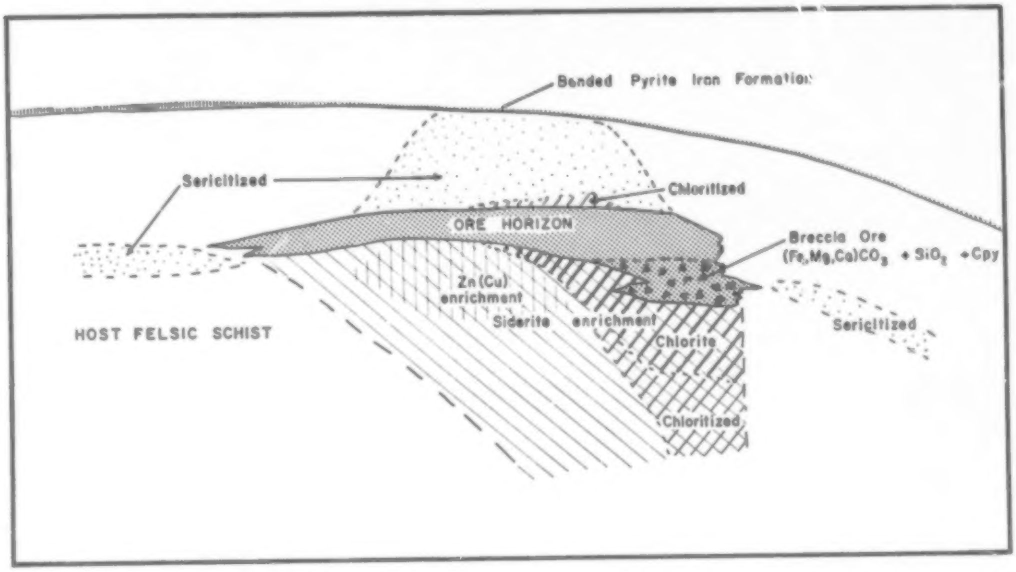
Banded Pyrite Iron Formation
Sericitized
Chloritized
ORE HORIZON
Breccia Ore
(Fe,Mg,Ca)CO3 + SiO2 + Cpy
Zn (Cu) enrichment
Siderite enrichment
Chlorite
HOST FELSIC SCHIST
Sericitized
Chloritized

Figure 291: Generalized distribution of alteration types in host rocks of the Centennial Cu-Zn massive sulphide orebody (from Provins, 1982).

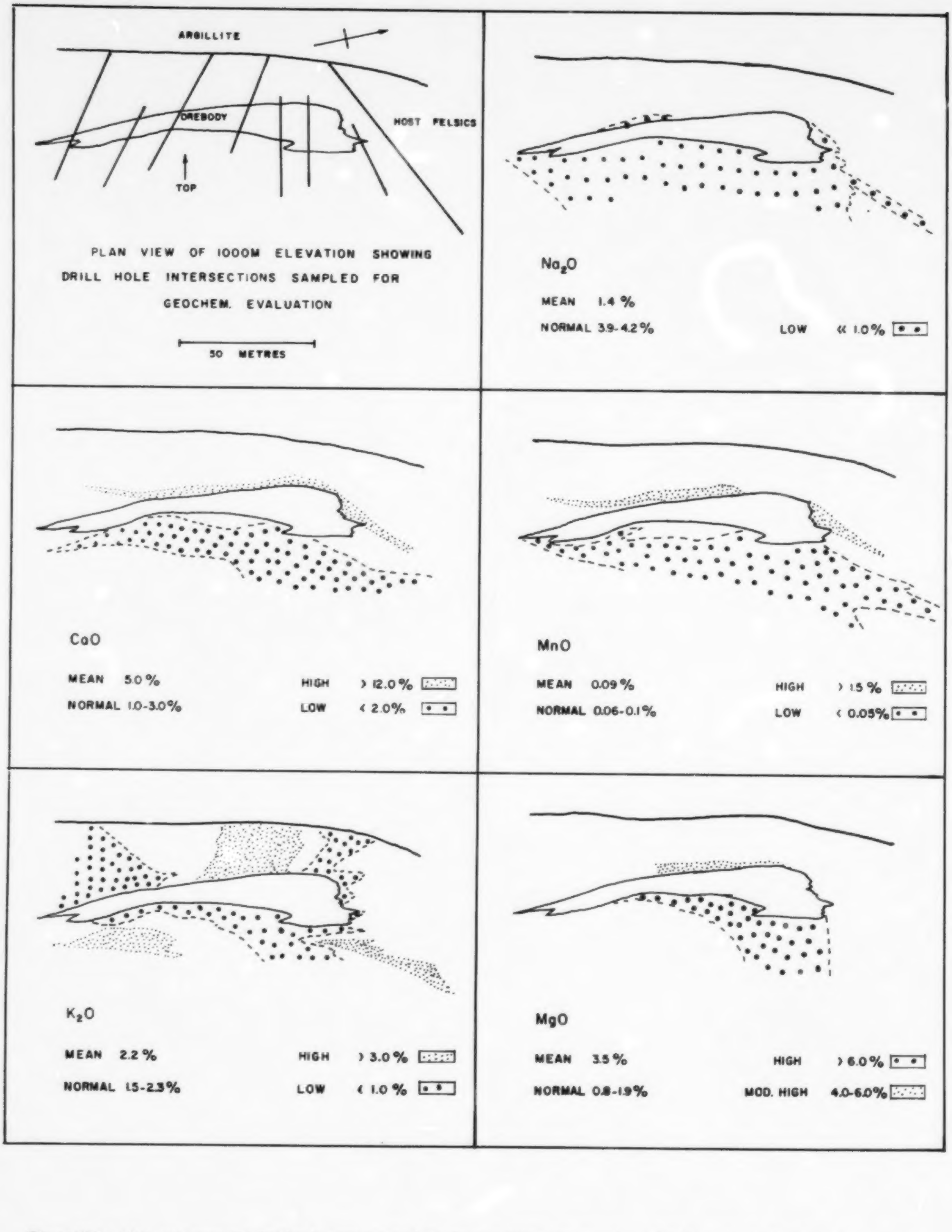
ARGILLITE
OREBODY
HOST FELSICS
TOP
PLAN VIEW OF 1000M ELEVATION SHOWING DRILL HOLE INTERSECTIONS SAMPLED FOR GEOCHEM. EVALUATION
50 METRES
Na₂O
MEAN 1.4 %
NORMAL 3.9-4.2%
LOW « 1.0%
CaO
MEAN 5.0 %
NORMAL 1.0-3.0%
HIGH › 12.0 %
LOW ‹ 2.0%
MnO
MEAN 0.09 %
NORMAL 0.06-0.1%
HIGH › 1.5 %
LOW ‹ 0.05%
K₂O
MEAN 2.2 %
NORMAL 1.5-2.3%
HIGH › 3.0 %
LOW ‹ 1.0 %
MgO
MEAN 3.5 %
NORMAL 0.8-1.9%
HIGH › 6.0 %
MOD. HIGH 4.0-6.0%

Figure 292: Major element distribution in host rocks of the Centennial Cu-Zn massive sulphide orebody (from Provins, 1982).

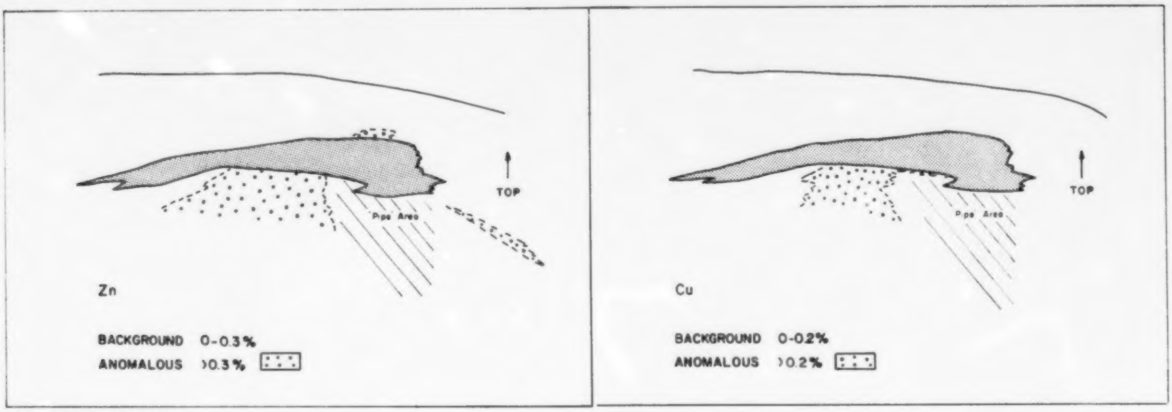

Figure 292 (Cont'd)

the rhyolite (unit 30), (2) White Lake dacite tuff and reworked tuff (unit 26), in large part derived from pyroclastic components of rhyolitic volcanism, and (3) redeposited andesite lapilli tuff (unit 24) derived from a volcanic centre not exposed in the present sequence (Fig. 5).

The period of rhyolite volcanism and deposition of volcaniclastic rocks ended in a period of volcanic quiescence, during which graphitic pelagic mudstones (unit 36), cherts and stratabound massive sulphides were deposited. The massive sulphides are of the "distal" type, lacking a directly associated discordant hydrothermal alteration zone.

The interval of volcanic quiescence, during which the Cuprus and White Lake deposits were formed, ended with the effusion of Two Portage Lake subaqueous ferrobasalt flows (unit 5) and intercalated rhyolite crystal tuffs (unit 27). The Bear Lake succession is topped by more than 900 m of Vick Lake andesitic tuffs (unit 25), representing shallow water or subaerial phreatomagmatic and plinian eruptions.

Other deposits and showings

A number of presently uneconomic sulphide deposits occur in the Flin Flon-White Lake area (Map GR87-1-2). Some of the more significant of these are discussed briefly below.

The *Iron Horse* deposit is located south of Hook Lake (Map GR87-1-2). A zone of massive sulphides 6 m thick and up to 1500 m long strikes north within a sequence of graphitic and siliceous pyritic mudstones. Sulphides include pyrite, pyrrhotite, chalcopyrite, sphalerite and arsenopyrite; associated disseminated mineralization occurs over a width of about 50 m. Numerous large trenches and five shallow exploration "shafts" occur on this property. Assays of selected sulphide samples are reported to have contained up to 12% Cu, 2% Zn and minor Au and Ag but generally Cu and Zn values are less than 1%.

The *Burnt Island* deposit occurs beneath Manistikwan Lake, between Burnt Island and the west shore of the lake (Map GR87-1-2). Massive sulphides interbedded with graphitic "tuff" form a lens-shaped body 975 m long and up to 45 m wide, trending 139°. The sulphide is predominantly pyrite with only trace amounts of Cu and Zn reported. An electromagnetic anomaly coincident with the sulphide zone crosses the projected position of the Hook Lake Fault (Maps GR87-1-1 and 2). The portion of the fault between Burnt Island and the mainland may therefore run closer to the shore than is shown on the geological map.

The *Now* showing is located near the western shore of Manistikwan Lake (Map GR87-1-2). It consists of a massive sulphide body 23 m long and 8 m wide. The main constituents are pyrite and pyrrhotite, with minor chalcopyrite. The showing occurs within a sequence of massive mafic flows intruded by diorite and rhyolite. A pyritiferous alteration zone in the stratigraphic footwall of the sulphide body can be traced 335 m north-northwest; it has a width of 30 m.

The *South Embury* showing lies east of the portage between Embury Lake and Manistikwan Lake (Map GR87-1-2). The showing occurs within an extensive alteration zone developed in mafic flows and interflow heterolithologic breccias. The altered rocks are in sharp, possibly unconformable contact with an overlying group of pebbly sandstones and grits (unit 32) which display no evidence of alteration. Drill holes in the area penetrated the coarse sediments and encountered minor chalcopyrite mineralization in the structurally underlying altered volcanic rocks.

The *Levasseur* showing is located on the northwest tip of the Northeast Arm of Schist Lake (Map GR87-1-2). Disseminated mineralization (pyrite, chalcopyrite, malachite) occurs in sericite-chlorite schist approximately at the contact between units 19 (intermediate to mafic volcaniclastics) and 35 (interbedded mafic and felsic mudstone). The zone can be traced from the north shore of the lake, 670 m north (adjacent to old Highway 10). Massive pyrite and minor chalcopyrite is reported in shallow exploration pits along the zone.

The newly discovered *Big Island* showing belonging to Westfield Minerals and Goldbrae Resources (Northern Miner, Nov. 23, 1987) is a gold- and silver-rich base metal sulphide zone located 600 m east-northeast of the north end of Shore Lake. One drill hole on the property has intersected a mineralized zone 12.4 m wide grading, 4.9 grams gold per tonne, 78.6 grams silver per tonne, 0.58% copper and 22.44% zinc. Trenching on the property exposed a 6 to 12 m wide gossan zone which assayed 7.8 grams gold per tonne across 3.7 m. A detailed description of the geological setting of the deposit is given by Ferreira and Gale (1988). They have identified thin discontinuous rhyolite flows and a 60 m thick unit of mafic tuff and lapilli tuff in the stratigraphic footwall to this sulphide deposit.

Cu-Mo MINERALIZATION IN FELSIC INTRUSIONS

Whitefish Lake quartz monzodiorite

Whitefish Lake quartz monzodiorite (unit 54) is a single-phase intrusion 2.5 km long and 300 — 600 m wide, emplaced into Amisk Group rocks north of Whitefish Lake (Map GR87-1-2). The stock is intruded into a large north-trending post-Missi fault system which parallels Pineroot River, through Whitefish Lake to Mikanagan Lake. The intrusion is itself cut by north- and northeast-trending faults, some possibly representing reactivated pre-intrusion faults in the system. The core of the intrusion is approximately hypidiomorphic equigranular; towards the margins the range of plagioclase and amphibole size increases and the rock has a seriate/porphyritic texture (complete petrographic description given previously). The contact zone of the intrusion is characterized by swarms of porphyritic dykes in the wall rocks and abundant volcanic xenoliths in the intrusion.

Mineralization at the main trench within the intrusion (Map GR87-1-2) consists of pyrite, chalcopyrite, minor molybdenite and secondary malachite along generally north-trending, steeply east-dipping fractures (range of trends 020° — 355°, dips 65° — 75°) and in tight, subhorizontal fractures. Disseminated sulphides are associated with the fracture-controlled mineralization. Fractures in which only sulphides occur are 1 — 3 mm thick. Fractures filled with sulphides and associated quartz, epidote and chlorite are more open vein systems, commonly about 1 cm wide but locally up to 30 cm. The fractures are spaced 1 — 40 cm apart in the trench but are more widely spaced to the east.

Twenty metres west of the main trench there is a major north-trending shear zone, parallel to mineralized fractures in the trench. Similar fault/fracture-controlled mineralization is exposed sporadically for 1 km south along the major structure. Associated alteration comprises epidotization of plagioclase and local carbonatization; the rocks are unfoliated.

The mineralization is interpreted to represent remobilization of disseminated sulphides into late, fault-associated fractures. The concentration of Cu and Mo in the intrusion (Baldwin, 1980) is highest in the vicinity of the north-trending fault, but the area of anomalous metal values is not exactly coincident with the fault. In addition, there are two Cu occurrences in the country rocks, near the margin of the intrusion. These facts suggest a primary "porphyry-type" component to the mineralization, which was subsequently remobilized into later fractures.

Cliff Lake Pluton

The Cliff Lake Pluton is a multiphase, quartz-megacrystic tonalite stock that intrudes the Amisk Group, east of Cliff Lake (Map GR87-1-2). The pluton is 6.2 km long and up to 1.8 km wide; its elongate shape is partly due to displacement of up to 1.2 km along north- and northwest-trending faults. Petrographic descriptions of the various phases in the pluton are given in a previous section.

Baldwin (1980) reports local minor disseminated pyrite and chalcopyrite, and very minor molybdenite and chalcopyrite in fractures, and traces of gold in poorly developed stockworks and veinlets.

Tourmaline-filled breccia pipes occcur at two localities (Baldwin, 1980; Map GR87-1-2). The pipes are 10 — 20 m^2 and contain fragments of tonalite and broken crystals of plagioclase and quartz set in a fine grained matrix dominated by black tourmaline. Similar breccia zones occur in porphyry-copper type granitoids and are considered to occur in high-level intrusions (Baldwin, 1980).

GOLD DEPOSITS

Nine Au occurrences are present in the map area; eight are within or on the border of the Cliff Lake Pluton and one is adjacent to the upper margin of the Mikanagan Lake Sill (Map GR87-1-2).

Six of the occurrences in the Cliff Lake Pluton are aligned on a north-trending zone. These occurrences are composed of small quartz-tourmaline +/- chlorite and carbonate veinlets with very minor Au values. The occurrences on the border of the pluton consist of silicified mafic volcanics with quartz-carbonate-pyrite-filled fractures.

The gold occurrence on the west shore of Mikanagan Lake has been described by Bateman (1945). At this location the leucotonalite top of the Mikanagan Lake Sill is in intrusive contact with Vick Lake andesitic tuff. This area is near the axis of the northeast-trending P5 Embury Lake antiform, and the Northeast Arm Fault lies approximately 120 m to the east. Gold is associated with quartz stringers (striking 057° — 063°) in the leucotonalite. The stringers occur *en echelon* and form a short mineralized lens that strikes across a tongue of leucotonalite for an exposed length of 30 x 6 m. Between the quartz stringers the intrusive rock is impregnated with rusty weathering carbonate, acicular arsenopyrite and a small amount of cubic pyrite. Pyrite also occurs in the quartz. Gold is reported to assay about 5.5 g/tonne over widths up to 5 m, and is considered to be associated with the arsenopyrite.

Gold potential in the Flin Flon-White Lake area

The setting of gold deposits in the area has been described in detail by Bateman (1945). More recent investigations (eg. Peloquin et al., 1986) are consistent with the original observations of Bateman. Favourable sites for gold mineralization are shear zones and faults, both in mafic intrusive and volcanic rocks. The gold occurs with quartz veins or stringers within the shear zones or in adjacent related tension fractures. The shear zones are impregnated with rusty-weathering carbonate, and the host country rocks are altered to an assemblage containing chlorite and sericite. Associated minerals include sulphides (pyrite, chalcopyrite, arsenopyrite in places), tourmaline, and fuchsite. Peloquin et al. (1986) describes the typical zonation in shear zones (in gabbro) at Tartan Lake as characterized by a central zone of chlorite-carbonate-quartz +/- fuchsite +/- tourmaline +/- sericite, a marginal zone of weakly schistose chlorite-carbonate-quartz and an outermost zone of weakly schistose chloritic rock with pink feldspar blasts. These authors found that it is possible to predict the presence of shear zones on the basis of small exposures of altered host rocks.

It would appear that favourable sites for gold mineralization require both (a) a fault or shear zones, and (b) dilational structures within the shear zones. Shear zones and faults are abundant in the Flin Flon-White Lake area, yet significant showings have not been identified along or adjacent to them despite many years of prospecting. Most of the northerly trending faults in the area do not contain zones of dilation, possibly explaining this lack of Au mineralization. Northwest-trending dilational structures, filled wih carbonate and minor quartz, are common in the Manistikwan Lake block south of Embury Lake. Mineralized shears at Tartan Lake, Albert Lake, Neso Lake and Twin-Payuk Lakes are east to northeasterly trending, suggesting that dilation zones occur preferentially in faults with these orientations.

ALTERATION

In the Flin Flon-White Lake area, hydrothermal alteration occurs predominantly in fault blocks west of the Inlet Arm Fault. Although there are probably several ages of alteration, most appear to be synvolanic. The varieties of alteration recognized and identified on Map GR87-1-2 are:

1. *Epidotization:* The intensity of epidotization is highly variable and takes two forms — first as large-scale pervasive epidotization (e.g. Bear Lake Block, Hook Lake Block), and secondly, smaller zones of intense epidotization associated with other types of hydrothermal alteration. In volcanic rocks epidotization takes the form of pervasive conversion to epidote-quartz or epidote-actinolite assemblages and partial to complete obliteration of primary structures and textures. Epidote also occurs as straight walled to anastomosing vein systems, and in alteration envelopes adjacent to fractures (particularly in intrusive rocks). Ovoid epidote +/- quartz structures (some with a concentric internal zonation) are up to 15 cm across and are common in some alteration zones (e.g. South of Embury Lake); they occur in both metavolcanic and mafic intrusive rocks (Fig. 293, 294). In the Cliff Lake tonalite pluton epidotizaton occurs adjacent to fractures and also in a more pervasive, less localized manner that affects large areas in the core of unit 45d.
2. *Silicification:* Low intensity silicification locally accompanies epidotization but is difficult to distinguish in the field. It also locally accompanies carbonatization, producing, for example, "bleached"-looking pillowed mafic flows. Pervasive silicification is locally accompanied by fine-scale quartz stockworks. The two main areas in which the quartz networks occur are in the footwall to the Schist Lake Mine and in a wide alteration zone at the south end of Embury Lake.
3. *Chloritization:* Pervasive conversion of metavolcanic rocks to chlorite is prominent in the footwalls of major "proximal" stratiform sulphide deposits (e.g. Flin Flon Mine, Centennial Mine). Chlorite and chlorite-sulphide veins and transposed veinlets occur in many of the alteration zones and are conspicuous in the footwall to the Schist Lake Mine (Fig. 295) and in the alteration zone south of Embury Lake (Fig. 296).

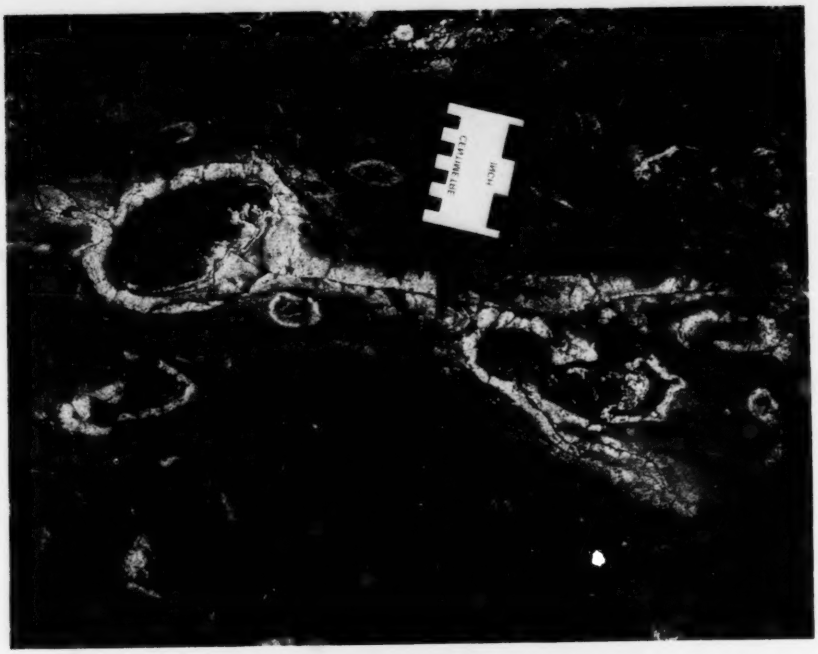

Figure 293: *Zoned polymineralic alteration structures in unit 7 mafic flow; island in Manistikwan Lake, 640 m west of Steeves Lake. The structures have an epidote-rich rim (white), chlorite plus carbonate core (dark). Many have a concentric structure. Similar alteration structures occur southwest of Steeves Lake, in mafic flows and mafic dykes.*

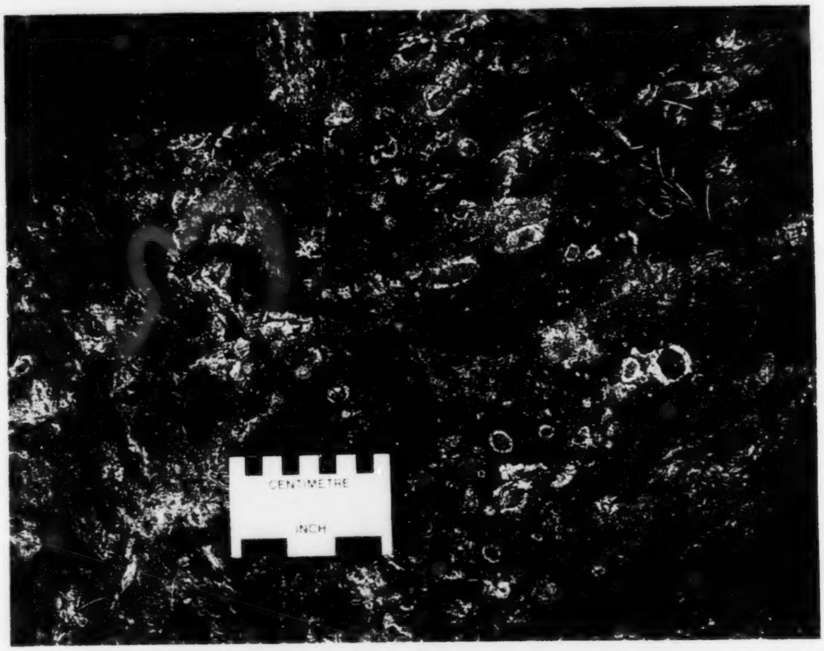

Figure 294: *Spherical hydrothermal alteration structures of uncertain genesis in fine grained quartz diorite dyke 1200 m north of Cope Lake near west shore of Embury Lake. These structures are cored by epidote and rimmed by quartz.*

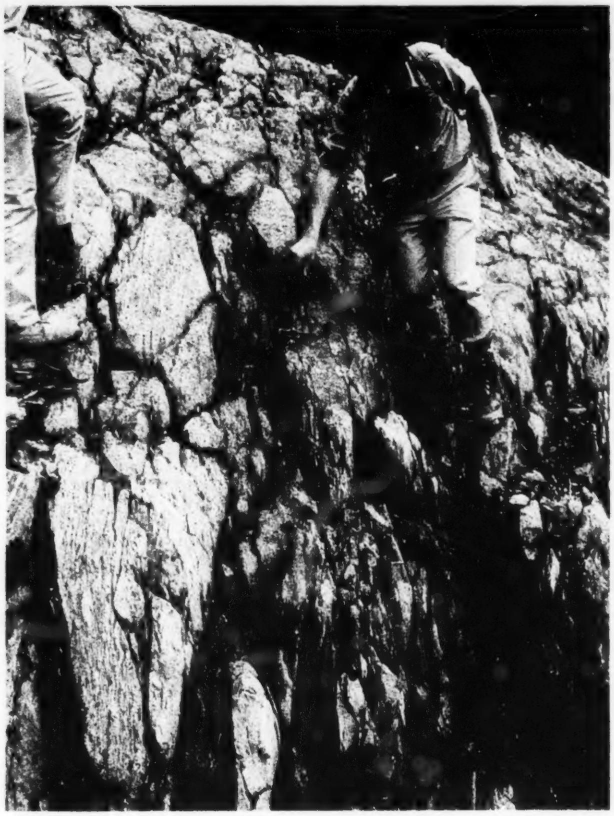

Figure 295: Anastomosing chlorite-filled veins in foliated, heterolithologic felsic breccias, Schist Lake Mine area. Chloritic alteration such as this typically occurs in the footwall beneath proximal volcanogenic massive sulphide deposits.

Figure 296: South Embury alteration zone (see Map GR87-1-2). Primary structures in mafic flows and fragmentals are almost completely obliterated. Anastomosing, sulphide-chlorite veinlets (dark) are common; these weather rusty brown on outcrop.

4. *Pyritization:* The degree to which rocks have developed disseminated or fracture-filling pyrite varies considerably. Small amounts of disseminated fine grained pyrite commonly accompany epidotization and silicification. Pyrite also occurs remobilized into veins and fractures, and as disseminated large cubic crystals (porphyroblasts). Intense pyritization of metavolcanic rocks is generally of local extent, identified by patches of rusty gossan. On Map GR87-1-2, pyritization is shown only where the sulphide has been identified; where the sulphides have been completely oxidized the alteration is simply shown as a "gossan zone". Some units of mudstone are characterized by abundant pyrite (e.g. south end of Embury Lake, Manistikwan Lake (unit 36)); the sulphide in these rocks is probably primary and not introduced.
5. *Carbonatizaton:* This common form of alteration has a variable expression, including: (1) small discrete carbonate blasts comprising up to 40% of the rock, (2) rusty weathering veins and pods (Fig. 297), and (3) carbonate matrix in brecciated rocks. Vein-type carbonate also occurs associated with some fault zones but is associated with tectonism rather than volcanism. Three main areas showing carbonatization are (a) in the Stitt Island rhyolite and in the footwall to the Schist-Mandy ore zone, (b) along the west shore of the east arm of Manistikwan Lake, and (c) small areas in the north-central part of Big Island.
6. *Discordant zones of spherulites:* Zones of spherulites which crosscut stratigraphy at a high angle occur in mafic flows at several locations west-northwest of Hook Lake (Fig. 298 and 299). The spherulites are between 5 mm and 6 cm in diameter and are locally restricted to sharply bounded zones that are several metres wide. These zones are locally accompanied by weak pyritization.
7. *Sericitization:* Sericite schist occurs in the footwall to the Flin Flon Mine and is the host rock of the Schist Lake-Mandy deposits. Widespread sericitization is not a prominent alteration type in the area.
8. *Oxide alteration:* Hematization occurs in the Cliff Lake Pluton, accompanying epidotization. It produces pink feldspar and quartz crystals, in part due to the presence of finely divided hematite along intergranular fractures. Disseminated magnetite blasts are common in the outer portion of this alteration zone.
9. *Tourmalinization:* Quartz-tourmaline veins are associated with the Cliff Lake Pluton and adjacent host rocks. Tourmaline blastesis occurs adjacent to some veins (Fig. 300). Baldwin (1980) reports tourmaline-filled breccias in two localities within the pluton.

CONTROLS ON DEPOSITION OF BASE METAL MASSIVE SULPHIDE DEPOSITS

The generally well defined stratigraphic setting of the base metal massive sulphide deposits in the Flin Flon area indicates that all deposits (a) are associated with felsic volcanism, (b) are hosted and underlain by coarse volcaniclastic rocks, (c) occur in basin structures of varying sizes, and (d) occur at major breaks in the volcanic sequence. These factors can be taken into account in exploration for new deposits along known mineralized intervals, as well as in areas where there is no known mineralization.

The first common rock association is the occurrence of rhyolite at the same stratigraphic level as massive sulphide deposits. Flin Flon and Callinan deposits occur within a single 30 — 150 m thick rhyolite flow and flow breccia unit. Cuprus and White Lake orebodies are "distal" deposits within fine grained sediments in what is interpreted as an intravolcanic basin; they are, however, at exactly the same stratigraphic position as Solodiuk Lake rhyolite, 3 — 4 km to the north. Centennial and Pine Bay deposits are hosted directly by felsic volcaniclastics. Similarly, Schist Lake and Mandy deposits occur within heterolithologic breccias with a prominent felsic component. Since these last two deposits occur in a fault-bounded panel, it is not known whether there is a major rhyolite complex along strike.

Figure 297: Rusty-brown weathering carbonate vein cutting Stitt Island dacite (unit 14).

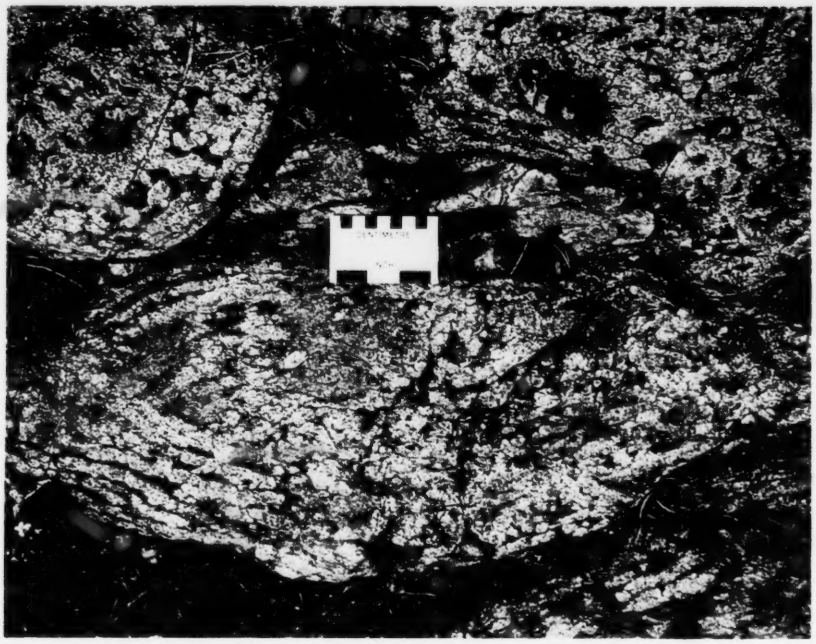

Figure 298: Spherulitic pillowed mafic flow (unit 7). Spherulites define an alteration zone which cuts across stratigraphy at a high angle, 700 m south southeast of Insole Lake. Note concentric zonation of spherulites, possibly formed by devitrification sited on permeable thermal contraction cracks.

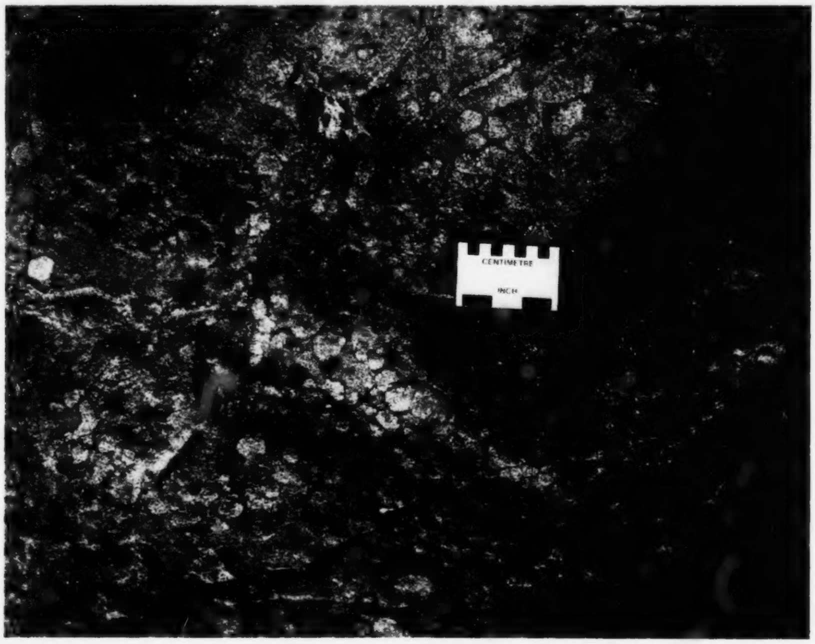

Figure 299: Spherulitic alteration structures (light, with dark rims) nucleated on fractures and selvages in unit 7 mafic pillowed flow, 300 m northwest of Hook Lake.

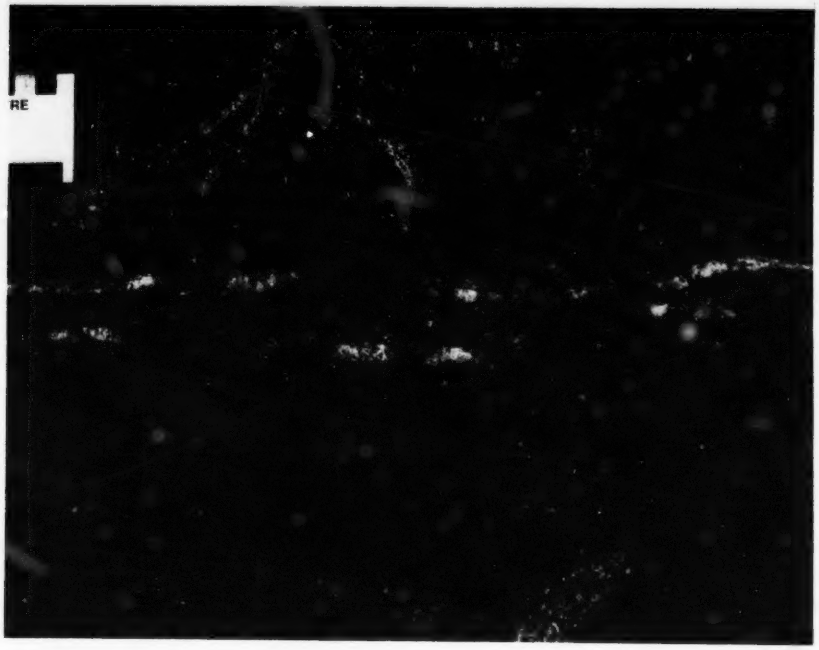

Figure 300: Tourmalinization adjacent to vein in gabbro; north end of Big Charlie Lake. The vein has quartz at margins and a core of chlorite; black tourmaline blasts are concentrated in an envelope about 5 cm wide adjacent to the vein.

The second common association is that all of the massive sulphide bodies occur within, and are underlain by, volcaniclastic rocks. Flin Flon (and Callinan?) deposits are hosted by rhyolite flow breccia and are underlain by a thick (at least 400 m) sequence of basalt pillow fragment breccia. Centennial and Pine Bay deposits are hosted by felsic fragmental rocks that are part of a larger sequence dominated by mafic and felsic volcaniclastics. Schist Lake and Mandy also occur in a heterolithologic sequence of volcaniclastic rocks, including pillow fragment breccias. Cuprus and White Lake, although not directly hosted by coarse volcaniclastic rocks, occur in fine grained sediments at or near the top of an andesitic volcaniclastic unit 350 m thick.

All deposits for which paleotopography can be reasonably interpreted, occur within topographic lows. The Flin Flon massive sulphide body occurs on the flank of, or within a basin adjacent to, the South Main subaqueous basalt volcano. This environment is indicated by a lateral facies change from proximal pillowed flows northwards into a thick sequence of now altered pillow fragment beccias underlying the orebody. Cuprus and White Lake deposits appear to occur in a sediment-filled subbasin within a much larger basinal structure. This large basin, filled with volcaniclastic rocks, may represent a summit caldera in the Bear Lake basaltic andesite shield volcano. The setting of the Centennial and Pine Bay deposits, although somewhat less clearly defined, nevertheless fits the pattern in that a lateral, southwards facies change from proximal basalt flows to volcaniclastics is recognized. The massive sulphides occur in the volcaniclastic package.

Four of the deposits occur at well defined breaks in volcanism. The Flin Flon and Callinan deposits were deposited in a hiatus between two major, petrographically and geochemically different basalt piles. During this hiatus volcanic activity shifted to intrusion of high level rhyolite domes, extrusion of a rhyolite flow, and development of a large-scale hydrothermal convection system which altered the footwall basaltic sequence and led to deposition of stratiform volcanogenic massive sulphides contemporaneous with the rhyolite. An unconformity in footwall rocks may be one expression of a synvolcanic fault that acted as a focus for hydrothermal discharge. The Cuprus and White Lake deposits were deposited during a hiatus in volcanism represented by the change from rhyolitic volcanism (Solodiuk Lake rhyolite) to extrusion of ferrobasalt flows (Two Portage Lake ferrobasalt). Within the volcaniclastic basin, with which the deposits are associated, this hiatus is marked by graphitic pelagic mudstones and cherts which host the massive sulphides. This suite of pelagic and chemical sedimentary rocks at the top of the volcaniclastic section indicates that at this time the basin was starved of detrital material. Again, a synvolcanic fault may have acted to focus the discharge of metalliferous hydrothermal fluids.

REGIONAL CONSIDERATIONS

INTRODUCTION

The Flin Flon-White Lake area provides a type locality for the Amisk Group. Metamorphic grade is low, primary structures are well preserved, and there is a high percentage of clean exposure, facilitating detailed stratigraphic mapping. This investigation has shown that the Amisk Group is dominated by basalt and basaltic andesite flows and breccias, all of which were emplaced in a subaqueous environment. Some thick mafic piles have features that indicate they formed by upward construction of broad subaqueous volcanoes into a shallow water environment (e.g. Bear Lake basaltic andesite, unit 1). Certain pyroclastic units (e.g. Vick Lake tuff, unit 25; scoria-rich mafic tuff, unit 23) are interpreted, on the basis of well preserved primary structures, to have been erupted in a very shallow marine or subaerial environment and immediately redeposited by subaqueous density currents. Rhyolite flows, breccias and tuffs form about 5% of the Amisk Group at Flin Flon. Sedimentary rocks (conglomerate, greywacke-mudstone) similarly constitute a small proportion of the Amisk Group; however, their true proportion may be somewhat greater than is evident because they tend to form recessive units covered by lakes or swamps. The various stratigraphic sequences that occur in fault-bounded blocks are all characteristic of the proximal and central (vent) facies of central-vent composite volcanoes (Williams and McBirney, 1979; Easton and Johns, 1986): lava flows, pyroclastic rocks and synvolcanic intrusions dominate. Volcaniclastic rocks are interpreted to form flank deposits on central vent complexes and, in some places, probably represent intravolcanic basin-fill deposits.

The maximum stratigraphic thickness of the Amisk Group within the map area is 7.5 km, in the Hook Lake Block. However, because each of the ten fault-bounded blocks displays a unique stratigraphic sequence, with no repetition from one block to another, it can be assumed that the total thickness is considerably greater that 7.5 km. Inasmuch as all of the sequences in the Flin Flon-White Lake area are proximal in nature, and share common geochemical characteristics, it is likely that the late faulting juxtaposed different portions of a single major volcanic pile rather than random tectonic slices from unrelated volcanic packages.

In the following sections, the Amisk Group stratigraphy in other portions of the Flin Flon belt (at Amisk Lake, Saskatchewan and Snow Lake, Manitoba) are briefly reviewed to provide comparison with the Amisk Group in the Flin Flon-White Lake area.

AMISK LAKE

Byers and Dahlstrom (1954) estimated the thickness of Amisk Group rocks on Amisk Lake to be in the order of 6.4 km, composed of a dominantly mafic volcanic sequence overlain by felsic to intermediate flows and breccias, in turn overlain by clastic sediments. East of Amisk Lake, Byers et al. (1965) measured 4.3 km of Amisk Group rocks. Fox (1976) mapped the area west of Amisk Lake and proposed a two-fold subdivision of the Amisk, similar to Byers and Dahlstrom (1954). The lower unit comprises tholeiitic basalt which evolves upwards from olivine-normative to quartz-normative compositions. The upper unit is characterized by calc-alkaline andesite, high-alumina basalt, dacite and rhyolite. Volcanogenic sediments top the upper unit and are intruded (and overlain) by the "Missi Island Vent Suite" composed of plutonic, hypabyssal and extrusive rocks.

Recent detailed investigations in the Amisk Lake area have been conducted by Ayres (1982), and Van Wagoner and Van Wagoner (1982). These workers describe a 9 km thick Amisk Group section that contains two transitions (surf zones) between subaerial and subaqueous conditions. The lower transition represents submergence of the volcano due to decrease in volcanism accompanied by isostatic sinking, and the upper transition represents emergence of the volcano due to increasing volcanism. Van Wagoner and Van Wagoner (1982) and Ayres et al. (1982) report that the 9 km sequence consists of a lower 6.5 — 7 km section of mafic to intermediate rocks and an upper 2 — 2.5 km section of felsic to intermediate rocks.

Parslow and Gaskarth (1984) conducted a regional geochemical survey of the east Amisk Lake area and reported that some of the basalts are of ocean floor affinity.

There are many differences and few similarities between the Amisk Group at Amisk Lake and at Flin Flon. The two areas are at least 30 km apart, separated by lobes of the Kaminis Lake and Annabel Lake plutons, and may also be separated by faults similar to block-bounding faults in the Flin Flon-White Lake area. The well defined subdivison at Amisk Lake between a lower, mafic tholeiitic sequence and an upper, intermediate to felsic calc-alkaline sequence topped by clastic sediments has no counterpart at Flin Flon. All basalts and basaltic andesites in Flin Flon have arc tholeiite characteristics, intermediate to felsic rocks are not common, calc-alkaline rocks are absent, subaerial volcanics are not present and sediments occur in minor amounts throughout the sequence. This implies that Amisk Lake and Flin Flon probably represent two distinct volcanic centres.

SNOW LAKE

Harrison (1949) mapped the entire Snow Lake area, established a basic subdivision of the supracrustal rocks, and recognized most of the major intrusive bodies and structures in the area. Froese and Moore (1980) established the now-accepted stratigraphic division into Amisk and Missi Groups, and defined several major metamorphic isograd reactions. Walford and Franklin (1982), Bailes (1987, 1988) and Skirrow (1987) provide a stratigraphic subdivision of the Amisk Group. The 5 km section includes (from base to top): more than 2500 m of pillowed mafic flows, 100 — 350 m of stratified, thick bedded, felsic volcanic breccia and wacke, 150 — 500 m of strongly porphyritic subaqueous mafic flows, approximately 1000 m of mixed mafic and felsic volcanic breccia and wacke, 250 — 350 m of felsic volcanic rocks, 600 m of mafic volcaniclastics and minor flows and an upper 300 m of greywacke-mudstone turbidites. Major block-bounding faults of the type that characterize the Flin Flon area do not appear to be present. A large subvolcanic tonalite sill intrudes the lower portion of the sequence and is apparently the "heat engine" that drove a large-scale hydrothermal system which has altered a significant portion of the overlying Amisk volcanic sequence.

In comparison with the Amisk Group at Flin Flon, the Snow Lake sequence contains a much greater percentage of felsic volcanic rocks, volcaniclastics, and sedimentary rocks. The two areas are 110 km apart and likely represent different volcanic centres. Basalt and basaltic andesites in the Snow Lake area have arc tholeiite characteristics similar to the prominent basalt and basaltic andesite sequences at Flin Flon, and like the latter have low Zr contents.

SIGNIFICANCE OF FLIN FLON BELT IN TRANS-HUDSON OROGEN

The major geological features of the Churchill Province (Fig. 1) have been outlined by Hoffman (1988, 1989), Green et al. (1985) and Lewry and

Sibbald (1980). The area consists of three Archean crustal blocks, the Rae Province, Hearne Province and Superior Province (terminology after Hoffman, 1988). These blocks were assembled in their present configuration between 1.9 Ga and 1.8 Ga. Proterozoic crust was created concurrently and forms the Trans-Hudson Orogen, sandwiched between the Superior Province to the southeast and Hearne Province to the northwest. The Flin Flon belt represents juvenile Proterozoic crust developed within the orogen at approximately 1.9 Ga (Table 1).

Mafic rocks in the Flin Flon-White Lake area have arc tholeiite geochemical characteristics and the Amisk Group as a whole contains lithologies and stratigraphic sequences comparable to those described in Cenozoic island arcs. Detailed mapping in scattered portions of the Flin Flon belt suggests that there were probably a number of volcanic centres in the belt, each with different lithologic and stratigraphic make-up. Belt-wide geochemical variation has yet to be established, but considering the probable existence of several volcanic centres separated by both time and space it is unlikely that a single geochemical "type" Amisk, or "type" Amisk stratigraphic sequence, exists.

The relationships of major structural blocks in the Churchill Province and the nature of the juvenile Proterozoic material within the Trans-Hudson orogen provides strong evidence for the existence of plate tectonic processes at least as early as the Early Proterozoic. The Flin Flon belt is presently best interpreted as an intra-oceanic island arc assemblage which was constructed above a subduction zone within the Trans-Hudson Orogen.

REFERENCES

Allen, C.C.
1979: Icelandic subglacial volcanism: thermal and physical studies; Journal of Geology, v. 88, p. 108-117.

Ambrose, J.W.
1936a: Progressive kinetic metamoprhism in the Missi Series, near Flin Flon, Manitoba; American Journal of Science, v. 32, 5th ser. p. 257-286.
1936b: Structures in the Missi Series near Flin Flon, Manitoba, Transactions of the Royal Society of Canada, ser. 3, sec. IV, v. 30, p. 81-98, 4 figs.

Ayres, L.D.
1978: A transition from subaqueous to subaerial eruptive environments in the middle Precambrian Amisk Group at Amisk Lake, Saskatchewan — A progress report; 1977 Annual Report, Centre for Precambrian Studies, University of Manitoba, p. 36-51.
1982: A subaqueous to subaerial transition zone in the Early Proterozoic metavolcanic sequence, Amisk Lake, Saskatchewan; 1981 Annual Report, Centre for Precambrian Studies, p. 49-61.

Bailes, A.H.
1980: Geology of the File Lake area; Manitoba Mineral Resources Division, Geological Report 78-1, 134 p.
1987: Chisel-Morgan Lakes project, Manitoba; Manitoba Energy and Mines, 1987 Report of Field Activities, p. 70-79.
1988: Chisel-Morgan Lakes project, Manitoba; Manitoba Energy and Mines, 1988 Report of Field Activities, p. 53-61.

Bailes, A.H. and McRitchie, W.D.
1978: The transition from low to high grade metamorphism in the Kisseynew sedimentary gneiss belt, Manitoba; *in* Metamorphism in the Canadian Shield, Geological Survey of Canada, Paper 78-10, p. 158-178.

Bailes, A.H., Syme, E.C., Galley, A. and Skirrow, R.
1987: Early Proterozoic volcanism, hydrothermal activity, and associated ore deposits at Flin Flon and Snow Lake, Manitoba; Geological Association of Canada/Mineralogical Association of Canada, 1987 Annual Meeting, Field Trip Guidebook No. 1, 95 p.

Bailes, A.H., Gordon, T.M., and Hunt, P.A.
1988: U-Pb zircon geochronology of the Richard Lake tonalite, a possible synvolcanic pluton in the Snow Lake area; Manitoba Energy and Mines, Report of Field Activities 1988, p. 63-65.

Baldwin, D.A.
1980: Porphyritic intrusions and related mineralization in the Flin Flon volcanic belt; Manitoba Mineral Resources Division, Economic Geology Report ER79-4, 23 p.

Bateman, J.D.
1945: Gold deposits east of Flin Flon, Manitoba; Geological Survey of Canada, Paper 45-14, 34 p.

Bateman, J.D. and Harrison, J.M.
1945: Mikanagan Lake, Manitoba; Geological Survey of Canada Map 832A with descriptive notes.

Bruce, E.V.
1918: Amisk-Athapapuskow Lake district; Geological Survey of Canada, Memoir 105, 91 p.

Buckham, A.F.
1944: Athapapuskow Lake, Manitoba; Geological Survey of Canada Map 807A with descriptive notes.

Byers, A.R.
1953: Missi Series, Amisk Lake area, northern Saskatchewan; Transactions of the Royal Society of Canada, ser. 3, v. 47, sec. 4, p. 1-10.

Byers, A.R. and Dahlstrom, C.D.A.
1954: Geology and mineral deposits of the Amisk-Wildnest Lakes area, Saskatchewan; Saskatchewan Department of Mineral Resources, Report No. 14, 177 p.

Byers, A.R., Kirkland, S.J.T., and Pearson, W.J.
1965: Geology and mineral deposits of the Flin Flon area, Saskatchewan; Saskatchewan Department of Mineral Resources, Report No. 62, 95 p.

Campbell, I.H., Lesher, C.M., Coad, P., Franklin, J.M., Goodwin, A.M., Gorton, M.P., Hart, T.R., Scott, S.D., Sowa, J.M., and Thurston, P.C.
1983: Ontario Geoscience Research Grant Program, Grant No. 80 — Rare earth elements in felsic volcanic rocks associated with Cu-Zn massive sulphide mineralization; Ontario Geological Survey Open File Report 5485, 35 p.

Condie, K.C.
1986: Geochemistry and tectonic setting of Early Proterozoic supracrustal rocks in the Southwest United States; Journal of Geology, v. 94, p. 845-864.

De Rosen-Spence, A.F., Provost, G., Dimroth, E., Gochnauer, K., and Owen, V.
1980: Archean subaqueous felsic flows, Rouyn-Noranda, Quebec, Canada, and their Quaternary equivalents; Precambrian Research, v. 12, p. 43-77.

Dolozi, M.B. and Ayres, L.D.
1987: A Proterozoic, shallow water, basaltic scoria cone near Flin Flon, Manitoba; Program with Abstracts, Joint Annual Meeting Geological Association of Canada-Mineralogical Association of Canada, 1987, v. 12, p. 37.

Dimroth, E., Cousineau, P., Leduc, M., and Sanschagrin, Y.
1978: Structure and organization of Archean subaqueous basalt flows, Rouyn-Noranda area, Quebec, Canada; Canadian Journal of Earth Science, v. 15, No. 6, p. 902-918.

Dimroth, E., and Lichtblau, A.P.
1979: Metamorphic evolution of Archean hyaloclastites, Noranda area, Quebec, Canada. Part I: Comparison of Archean and Cenozoic seafloor metamorphism; Canadian Journal of Earth Science, v. 16, pp. 1315-1340.

Easton, R.M. and Johns, G.W.
1986: Volcanology and mineral exploration: the application of physical volcanology and facies studies; *in* Volcanology and Mineral Deposits, ed. J. Wood and H. Wallace; Ontario Geological Survey Miscellaneous Paper 129, p. 2-40.

Esposito, B.
1986: Copper and zinc in Manitoba (revised and expanded); Manitoba Energy and Mines, Mines Branch, Mineral Education Series, 24 p.

Ewart, A. and Hawkesworth, C.J.
1987: The Pleistocene-Recent Tonga-Kermadec arc lavas: interpretation of new isotopic and rare earth data in terms of a depleted mantle source model; Journal of Petrology, v. 28, p. 495-530.

Ferreira, K. and Gale, G.H.
1988: Geological setting of the Big Island zinc property, Shore Lake area, Flin Flon; Manitoba Energy and Mines, 1988 Report of Field Activities, p. 66-71.

Fink, J.H. and Pollard, D.D.
1983: Structural evidence for dykes beneath silicic domes, Medicine Lake Highland Volcano, California; Geology, v. 11, p. 458-461.

Fisher, R.V.
1961: Proposed classification of volcaniclastic sediment and rocks; Geological Society of America, v. 72, p. 1409-1414.
1966: Rocks composed of volcanic fragments and their classification, Earth Science Reviews, v. 1, pp. 287-298.

Fisher, R.V. and Schmincke, H.-U.
1984: Pyroclastic rocks; Springer-Verlag, Berlin, Heidelberg, New York, Tokoyo; 472 p.

Fogwill, W.D.
1983: Mining in Manitoba: past and present; *in* Canadian Institute of Mining and Metallurgy Directory Feature, Manitoba Department of Mines and Natural Resources, Mines Branch, p. 75-91.

Fox, J.S.
1976: Some comments on the volcanic stratigraphy and economic potential of the West Amisk Lake area, Saskatchewan; Geology Division, Saskatchewan Research Council, Circular 9.

Froese, E. and Moore, J.M.
1980: Metamorphism in the Snow Lake area, Manitoba; Geological Survey of Canada, Paper 78-27, 16 p.

Furnes, H., Fridleifsson, I.M., and Atkins, F.B.
1980: Subglacial volcanics — on the formation of acid hyaloclastites; Journal of Volcanology and Geothermal Research, v. 8, p. 95-110.

Gale, G.H., Baldwin, D.A. and Koo, J.
1980: A geological evaluation of Precambrian massive sulphide deposit potential in Manitoba; Manitoba Energy and Mines, Economic Geology Report ER79-1, 137 p.

Gale, G.H. and Eccles, D.R.
1988a: Mineral deposits and occurrences in the Flin Flon area NTS 63K/13: Part I, Mikanagan Lake area (63K/13SE); Manitoba Energy and Mines, Mineral Deposit Series, Report No. 1, 133 p.
1988b: Mineral deposits and occurrences in the Flin Flon area NTS 63K/13: Part II, Flin Flon area (63K/13SW); Manitoba Energy and Mines, Mineral Deposit Series, Report No. 2, 98 p.

Gelinas, L., Lajoie, J., Bouchard, M., Simard, A., Verpaelst, P., and Sansfacon, R.
1978: Les complexes rhyolitiques de la region de Rouyn-Noranda; Rapp. Prelim., D.P.V. 583, Quebec Dep. Natural Resources.

Gill, J.B.
1981: Orogenic andesite and plate tectonics; Springer-Velag, Berlin, Heilelberg, New York, 390 p.
1987: Early geochemical evoluation of an oceanic island arc and backarc: Fiji and the South Fiji basin; Journal of Geology, v. 95, p. 589-615.

Goetz, P.A.
1980: Depositional environment of the Sherridon Group and related mineral deposits near Sherridon, Manitoba; Unpublished Ph.D. thesis, Carleton University, Ottawa, 248 p.

Gordon, T.M., Hunt, P.A., Loveridge, W.D., Bailes, A., and Syme, E.
1987: U-Pb zircon ages from the Flin Flon and Kisseynew belts, Manitoba: Chronology of Early Proterozoic crust formation; Program with Abstracts, Joint Annual Meeting Geological Association of Canada-Mineralogical Association of Canada, 1987, v.12, p. 48.

Gordon, T.M., Hunt, P.A., Bailes, A. and Syme, E.
1989: U-Pb zircon ages from the Flin Flon and Kisseynew belts, Manitoba: Chronology of crust formation at an Early Proterozoic accretionary margin; *in* The Early Proterozoic Trans-Hudson Orogen: Lithotectonic correlations and evolution, eds. J.F. Lewry and M.R. Stauffer; Geological Association of Canada, Special Paper (in press).

Green, A.G., Hajnal, Z., and Weber, W.
1985: An evolutionary model of the Western Churchill Province and Western margin of the Superior Province in Canada and north-central United Sates; Tectonophysics, v. 116, pp. 281-322.

Guber, A.L. and Ohmoto, H.
1978: Deep sea environment of Kuroko formation as indicated by the Benthic foraminifera from the Hokuroku district, Japan; Mining Geology, v. 28, pp. 245-255.

Harrison, J.M.
1949: Geology and mineral deposits of the File-Tramping Lakes area, Manitoba; Geological Survey of Canada, Memoir 250.

1951: Precambrian correlation and nomenclature, and problems of the Kisseynew gneisses in Manitoba; Geological Survey of Canada, Bulletin 20: 53 pp.

Heywood, W.W.
1966: Ledge Lake area, Manitoba and Saskatchewan; Geological Survey of Canada, Memoir 337, 43 p.

Heiken, G.
1972: Morphology and petrography of volcanic ashes; Geological Society of America Bulletin, v. 83, pp. 1961-1988.

Heinrichs, T.
1984: The Umsoli chert, turbidite testament for a major phreatoplinian event of the Onverwacht/Fig Tree transition (Swaziland Supergroup, Archean, South Africa); Precambrian Research, v. 24, p. 237-283.

Hoffman, P.F.
1988: United Plates of America, the birth of a craton: Early Proterozoic assembly and growth of Laurentia; Annual Review of Earth and Planetary Sciences, v. 16, p. 543-603.
1989: The extent of Trans-Hudson Orogen and subdivison of the Churchill province; *in* The Early Proterozic Trans-Hudson Orogen: Lithotectonic correlations and evolution, eds. J.F. Lewry and M.R. Stauffer; Geological Association of Canada, Special Paper (in press).

Honnorez, H.D.
1972: La palagonitization, l'alteration sous-marine du verre volcanique basique de Palogonia (sicile); Volkaninstitut Immanuel Friedlander, No. 9, Birkhauser Verlag, Basel.

Hosain, I.T.
1986: Mineral producers, past prodcuers and significant deposits in Manitoba (MINPROP FILE); Manitoba Energy and Mines; Mines Branch, 32 p.

Howkins, J.B. and Martin, P.L.
1970: A comparsion between the Flin Flon and Snow Lake orebodies of Hudson Bay Mining and Smelting Co. Ltd.; Unpublished paper presented at Annual Convention, Canadian Institute of Mining and Metallurgy, April 1970.

Irvine, T.N. and Baragar, W.R.A.
1971: A guide to the chemical classification of common volcanic rocks; Canadian Journal of Earth Sciences, v. 8: 523-548.

Jensen, L.S.
1976: A new cation plot for classifying subalkalic volcanic rocks; Ontario Divsion Mines, Miscellaneous Paper 66, 22 p.

Jones, J.G.
1969: Pillow lavas as depth indicators; American Journal of Science, v. 267: 181-195.
1970: Intraglacial volcanoes of the Laugarvatn region, southwest Iceland, II; Journal of Geology, v. 78, p. 127-140.

Koo, J. and Mossman, D.J.
1975: Origin and metamorphism of the Flin Flon stratabound Cu-Zn sulphide deposit, Saskatchewan and Manitoba; Economic Geology, v. 70: 48-62.

Lewry, J.F. and Sibbald, T.I.I.
1980: Thermotectonic evolution of the Churchill Province in northern Saskatchewan; Tectonophysics, v. 68, p. 45-82.

Lofgren, G.
1974: An experimental study of plagioclase crystal morphology: Isothermal crystallization; American Journal of Science, v. 274, pp. 243-273.
1983: Effect of heterogeneous nucleation on basaltic textures: a dynamic crystallization study; Journal of Petrology, v. 24, pp. 229-255.

MacPherson, G.J.
1984: A model for predicting the volumes of vesicles in submarine basalts; Journal of Geology, v. 92, p. 73-82.

MacQuarrie, R.
1980: Absolute age of the Flin Flon deposit. Bulletin of the Canadian Institute of Mining and Metallurgy, abstract, No. 4 District Meeting, v. 73, p. 53.

Moore, J.G.
1970: Water content of basalt erupted on the ocean floor; Contributions to Mineralogy and Petrology, v. 28, p. 272-279.

Moore, J.G. and Schilling, J.G.
1973: Vesicles, water and sulphur in Reykjanes Ridge basalts; Contributions to Mineralogy and Petrology, v. 41, p. 105-118.

Mukherjee, A.C.
1971: The Precambrian geology of the Flin Flon area, northern Saskatchewan and Manitoba; University of Saskatchewan, Saskatoon, Ph.D. thesis (unpublished), 161 p.

Mukherjee, A.C., Stauffer, M.R., and Baadsgaard, H.
1971: The Hudsonian orogeny near Flin Flon, Manitoba: A tentative interpretation of Rb/Sr and K/Ar ages; Canadian Journal of Earth Sciences, v. 8, no. 8: 939-946.

Parslow, G.R. and Gaskarth, J.W.
1984: Geochemistry of the East Amisk area; Saskatchewan Energy and Mines, Open File Report OF84-23, 79 p.

Pearce J.A.
1982: Trace element characteristics of lavas from destructive plate boundaries; *in* Andesites (R.S. Thorpe, editor); John Wiley and Sons; p. 525-548.

Pearce, J.A. and Cann, J.R.
1973: Tectonic setting of basic volcanic rocks determined using trace element analyses: Earth and Planetary Science Letters, v. 19, p. 290-300.

Pearce, J.A., Alabaster, T., Shelton, A.W., and Searle, M.P.
1981: The Oman ophiolite as a Cretaceous arc-basin complex: evidence and implications; Philosophical Transactions of the Royal Society, A300, p. 299-317.

Peloquin, A.S.
1981: The morphology of an Aphebian rhyolite flow and associated fragmental rocks in the White Lake-Mikanagan Lake area, northwest Manitoba; B.Sc. thesis, University of Manitoba, 39 p.

Peloquin, A.S., Ayres, L.D., and Nikols, C.A.
1982: Morphology of an early Proterozoic rhyolite flow and associated fragmental unit near Flin Flon, Manitoba; Centre for Precambrian Studies, University of Manitoba, 1981 Annual Report, pp.62-70.

Peloquin, A.S., Tannahill, B., and Gale, G.H.
1986: Geology of the Tartan Lake gold deposits; Manitoba Energy and Mines, 1986 Report of Field Activities, p. 56-64.

Pharoah, T.C. and Pearce, J.A.
1984: Geochemical evidence for the geotectonic setting of Early Proterozic metavolcanic sequences in Lapland; Precambrian Research, v. 25, p. 283-308.

Philpotts, A.R. and Lewis, C.L.
1987: Pipe vesicles — an alternate model for their origin; Geology, v.15, p. 971-974.

Plimer, I.R.
1979: Sulphide zonation and hydrothermal alteration at Broken Hill, Australia,; Transactions of the Institution of Mining and Metallurgy, Section B: Applications to Earth Sciences, v. 88, p. B161-B176.

Price, D.P.
1978: Geology and economic potential of the Flin Flon-Snow Lake area; Centre for Precambrian Studies, University of Manitoba, 1977 Annual Report, pp. 52-83.

Provins, N.M.
1980: Geology of the Centennial Copper-Zinc deposit, Flin Flon, Manitoba; CIM 5th Annual District Four Meeting, Flin Flon, Manitoba, September, 1980.

Ridley, W.I., Rhodes, J.M., Reid, A.M., Jakes, R., Shih, C., and Bass, M.N.
1974: Basalts from Leg 6 of the deep-sea drilling project; Journal of Petrology, v. 15, p. 140-159.

Rittman, A.
1958: Il meccanismo di formazione delle lave a pillows e dei cosidetti tufi palagonitici; Atti Acc. Geioenia, v. 4, p. 310-317.
1962: Volcanoes and their activity; Wiley-Interscience Publishers, New York, 305 p.

Sangster, D.F.
1972: Precambrian volcanogenic massive sulphide deposits in Canada: A review; Geological Survey of Canada, Paper 72-22.
1978: Isotopic studies of ore-leads in the circum-Kisseynew volcanic belt of Manitoba and Saskatchewan; Canadian Journal of Earth Sciences, v. 15, pp. 1112-1121.

Saunders, A.D., Tarney, J. , and Weaver, S.D.
1980: Transverse geochemical variations across the Antarctic Peninsula: implications for the genesis of calc-alkaline magmas; Earth and Planetary Sciences Letters, v. 46, p. 344-360.

Sigurdson, H.
1982: Subaqueous volcanogenic sediments in ocean basins; *in* Geological Association of Canada Short Course Notes Volume 2: Pyroclastic volcanism and deposits of Cenozoic intermediate to felsic volcanic islands with implications for Precambrian greenstone-belt volcanoes, ed. L.D. Ayres; p. 294-342.

Sigvaldson, G.E.
1968: Structure and products of subaquatic volcanoes in Iceland; Contributions Mineralogy and Petrology, No. 18, pp. 1-18.

Skirrow, R.G.
1987: Silicification in a semi-conformable alteration zone below the Chisel massive sulphide deposit, Manitoba; unpublished M.Sc. thesis, Carleton University, Ottawa, 171 p.

Staudigel, H. and Schmincke, H.-U.
1984: The Pliocene seamount series of La Palma/Canary Islands; Journal of Geophysical Research, v. 89, no. B13, p. 11195-11215.

Stauffer, M.R.
1974: Geology of the Flin Flon area; a new look at the sunless city; Geoscience Canada, v. 1, no. 3, pp. 30-35.

Stauffer, M.R. and Mukherjee, A.
1971: Superimposed deformation in the Missi metasedimentary rocks near Flin Flon, Manitoba; Canadian Journal of Earth Scinece, v. 8, pp. 217-242.

Stauffer, M.R., Mukherjee, A.C., and Koo, J.
1975: The Amisk Group: an Aphebian(?) island arc deposit; Canadian Journal of Sciences, v. 12, pp. 2021-2035.

Stockwell, C.H.
1946: Flin Flon-Mandy Area, Manitoba and Saskatchewan; Geological Survey of Canada Paper 46-14.
1960: Flin Flon-Mandy Lake area, Manitoba and Saskatchewan; Geological Survey of Canada Map 17078A, with descriptive roles.

Streckeisen, A.
1976: To each plutonic rock its proper name; Earth-Science Reviews, v. 12, p. 1-33.

Syme, E.C.
1985: Geochemistry of metavolcanic rocks in the Lynn Lake belt; Manitoba Energy and Mines, Geological Report GR84-1, 84 p.
1987: Athapapuskow Lake Project; *in* Manitoba Energy and Mines Report of Field Acivities, 1987, p. 30-40.
1989: Stratigraphy and geochemistry of the Lynn Lake and Flin Flon metavolcanic belts, Manitoba; *in* The Early Proterozoic Trans-Hudson Orogen: Lithotectonic correlations and evolution, eds. J.F. Lewry and M.R. Stauffer; Geological Association of Canada, Special Paper (in press).

Syme, E.C. and Forester, R.W.
1977: Petrogenesis of the Boundary intrusions in the Flin Flon area of Saskatchewan and Manitoba; Canadian Journal of Earth Sciences, v. 14, p. 444-455.

Syme, E.C., Bailes, A.H., Price, D.P. and Ziehlke, D.V.
1982: Flin Flon volcanic belt: Geology and ore deposits at Flin Flon and Snow Lake, Manitoba; Geological Association of Canada/Mineralogical Association of Canada, 1982 Annual Meeting, Field Trip Guidebook no. 6, 91 p.

Syme, E.C., Bailes, A.H., Gordon, T.M., and Hunt, P.A.
1987: U-Pb zircon geochronology in the Flin Flon belt: age of Amisk volcanism; Manitoba Energy and Mines, Report of Field Activities 1987, p. 105-107.

Tanton, T.L.
1941a: Flin Flon, Saskatchewan and Manitoba; Geological Survey of Canada Map 632A, with descriptive notes.
1941b: Schist Lake, Saskatchewan and Manitoba; Geological Survey of Canada, Map 633A with descriptive notes.

Tarney, J., Saunders, A.D., Mattey, D.P., Wood, D.A., and Marsh, N.G.
1981: Geochemical aspects of backarc spreading in the Scotia Sea and Western Pacific; Philosophical Transactions of the Royal Society of London, A300, p. 263-285.

Van Wagoner, N. and Van Wagoner, S.
1982: Shallow water volcanism and sedimentation in a portion of the Flin Flon-Snow Lake greenstone belt: A preliminary report; Centre for Precambrian Studies, 1981 Annual Report, p. 71-88.

Walford, P.C. and Franklin, J.M.
1982: The Anderson Lake Mine, Snow Lake, Manitoba, Geological Association of Canada, Robinson Symposium Volume, p. 481-523.

Weaver, B.L., Tarney, J., Windley, B.F., and Leake, B.E.
1982: Geochemistry and petrogenesis of Archean metavolcanic amphibolites from Fiskanaesset, S.W. Greenland; Geochemica et Cosmochimica Acta, v. 46, p. 2203-2215.

Wentworth, C.K.
1922: A scale of grade and class terms for clastic sediments; Journal of Geology, v. 30, p. 377-392.

Williams, H. and McBirney, A.R.
1979: Volcanology; Freeman, Cooper and Co., San Francisco, 397 pp.

APPENDIX

The Appendix lists 215 whole rock major and trace element analyses for various rocks in the Flin Flon-White Lake area. The analyses are listed in order according to unit number; not all units have analyses. Individual analyses are identified by a column number (1 to 215) and a field sample number (e.g. 1268-C1). Short descriptions of analysed rocks, including rock type and unit number, appear at the foot of each page of analyses. Locations of samples are given on Map GR87-1-2 (in pocket), listed by field sample number.

Analyses were performed in more than one lab; identification of analytical method is indicated by asterisks (*) preceeding column numbers in the sample descriptions. Samples with asterisks were analysed by XRF at the University of Ottawa in 1983 (SiO_2, TiO_2, Al_2O_3, Fe_2O_3(T), MnO, MgO, CaO, Na_2O, K_2O, S, Ni, Cr, Zn, Rb, Sr, Ba, Zr, Y) and at the Manitoba Energy and Mines Analytical Laboratory (FeO, P_2O_5, H_2O, CO_2, Cu). Samples with no asterisks were analysed at the Manitoba Energy and Mines Analytical Laboratory (SiO_2, TiO_2, Al_2O_3, Fe_2O_3, FeO, MnO, MgO, CaO, Na_2O, K_2O, P_2O_5, H_2O, S, CO_2, Ni, Cr, Cu, Zn, Rb, Sr, Ba) and by XRF at Bondar Clegg (Zr, Y). Analytical methods at the Energy and Mines Lab include colorimetry (for SiO_2, Al_2O_3, TiO_2 and P_2O_5), atomic absorption (for Fe_2O_3, FeO, CaO, MgO, Na_2O, K_2O, MnO, Ni and Cr). Rare earth elements, Th and U were done by INAA at Nuclear Activation Services in 1984. Sc, Th, U, Ta and Hf were done by INAA at Becquerel Laboratory in 1987. The value listed as "OTHER" was calculated in the Energy and Mines Lab as the sum of analysed trace elements in oxide form. Precisions and/or detection limits are listed in the following tables.

TABLES OF PRECISIONS AND DETECTION LIMITS FOR ANALYSES

Analytical Precision and Detection Limits
Manitoba Energy and Mines Analytical Laboratory

Oxide or Element	Concentration Range (%)	Absolute Precision (%)	
		Precise Method[1]	Rapid Method
SiO_2	30.0 - 80.0	± 1.0	± 1.5
TiO_2	0.01 - 2.50	± 0.05	± 0.2
Al_2O_3	3.0 - 25.0	± 0.3	± 0.8
FeO*	0.5 - 20.0	± 0.15	± 0.5
FeO	0.20 - 13.0	± 0.05	N.A.
MnO	0.01 - 1.00	± 0.02	± 0.03
MgO	0.4 - 40.0	± 0.3	± 0.3
CaO	0.4 - 20.0	± 0.2	± 0.2
Na_2O	0.1 - 10.0	± 0.2	± 0.2
K_2O	0.1 - 10.0	± 0.2	± 0.2
P_2O_5	0.01 - 1.00	± 0.03	± 0.03
H_2O(T)	0.01 - 5.00	± 0.15	N.A.
S	0.00 - 0.5	± 0.02	N.A.
CO_2	0.00 - 5.0	± 0.15	N.A.

	Detection Limit
Ni	2 ppm
Cr	3 ppm
Cu	2 ppm
Zn	10 ppm
Rb	2 ppm
Sr	6 ppm
Ba	20 ppm

[1] All of the analyses performed at the Manitoba Analytical Laboratory were done by the "Precise Method", except for analyses 132, 138, 174 and 175.

Analytical Precision — University of Ottawa XRF

Oxide or Element	Concentration Range	Precision (as % of concentration)
SiO_2	50 — 100%	± 1.3
TiO_2	0.1 — 1%	± 3.0
	1 — 3%	± 1.0
Al_2O_3	10 — 20%	± 2.0
Fe_2O_3(T)	1 — 20%	± 2.0
MnO	0.1 — 1%	± 10.0
MgO	0.1 — 1%	± 25.0
	1 — 10%	± 4.0
CaO	0.1 — 1%	± 7.0
	10 — 20%	± 2.0
Na_2O	0.1 — 2%	± 25.0
	2 — 5%	± 4.5
K_2O	0.1 — 2%	± 3.0
	2 — 5%	± 1.0
S	0.1 — 1%	± 10.0
Ni	< 40 ppm	± 100
	40 — 100 ppm	± 50
	> 100 ppm	± 10
Cr	< 20 ppm	± 100
	20 — 50 ppm	± 50
	50 — 500 ppm	± 15
	> 500 ppm	± 10
Zn	< 20 ppm	± 100
	20 — 40 ppm	± 50
	> 50 ppm	± 10
Rb	< 20 ppm	± 100
	20 — 40 ppm	± 50
	> 50 ppm	± 10
Sr	< 20 ppm	± 100
	20 — 40 ppm	± 50
	> 50 ppm	± 10
Ba	< 20 ppm	± 100
	10 — 40 ppm	± 50
	> 40 ppm	± 10
Zr	< 20 ppm	± 100
	20 — 50 ppm	± 50
	50 — 500 ppm	± 15
Y	< 40 ppm	± 100
	40 — 100 ppm	± 25

Detection Limits — Nuclear Activation Services (INAA)

Th	0.2 ppm
U	0.1 ppm
La	0.1 ppm
Ce	1 ppm
Nd	3 ppm
Sm	0.01 ppm
Eu	0.05 ppm
Tb	0.1 ppm
Dy	0.5 ppm
Tb	0.05 ppm
Lu	0.01 ppm

Detection Limits — Becquerel (INAA)

Sc	0.2 ppm
Th	0.2 ppm
U	0.2 ppm
Ta	0.5 ppm
Hf	1 ppm

TABLE OF WHOLE ROCK CHEMICAL ANALYSES

	1	2	3	4	5	6	7	8	
	1268-C1	1362-C1	1388-F2	1388-F7	1388-F8	1510-C1	399-C1	3363-2	
SiO_2	50.80	54.65	53.60	53.85	51.75	53.00	51.90	53.05	SiO_2
TiO_2	0.93	0.47	0.49	0.51	0.48	0.39	0.26	0.35	TiO_2
Al_2O_3	15.82	15.46	16.11	15.78	16.15	14.69	14.45	15.04	Al_2O_3
Fe_2O_3	3.15	2.04	2.09	3.22	2.84	3.00	1.53	2.97	Fe_2O_3
FeO	7.52	8.60	7.77	7.77	7.40	6.85	8.93	6.69	FeO
MnO	0.17	0.19	0.18	0.18	0.18	0.17	0.21	0.16	MnO
MgO	5.82	5.03	5.35	4.48	6.09	6.60	8.51	6.42	MgO
CaO	10.37	4.52	7.42	8.49	8.42	7.97	6.35	9.23	CaO
Na_2O	1.93	5.06	3.44	2.29	2.39	3.31	3.45	1.29	Na_2O
K_2O	0.17	0.61	0.89	0.54	1.02	0.78	1.04	1.00	K_2O
P_2O_5	0.16	0.14	0.14	0.13	0.13	0.12	0.12	0.14	P_2O_5
H_2O	3.25	3.03	2.81	3.16	3.47	2.94	3.41	3.44	H_2O
S	0.09	0.02	0.02	0.01	0.01	0.01	0.02	0.00	S
CO_2	0.15	0.42	0.14	0.05	0.15	0.58	0.15	0.11	CO_2
OTHER	0.10	0.08	0.11	0.09	0.11	0.08	0.10	0.11	OTHER
O≡S	-0.04	-0.01	-0.01	-0.01			-0.01		O≡S
TOTAL	100.39	100.31	100.55	100.54	100.59	100.49	100.42	100.00	TOTAL
Ni	82	10	18	10	19	20	30	39	Ni
Cr	272	25	46	8	36	129	142	150	Cr
Sc			33.2			34.9			Sc
Cu	74	126	129	87	90	72	99	31	Cu
Zn	108	117	109	98	85	75	95	82	Zn
Rb				8	18	18		18	Rb
Sr	125	105	130	305	265	145	80	355	Sr
Ba	70	250	510	220	420	230	390	230	Ba
Th			0.38			0.30			Th
U			<0.2			0.26			U
Ta			0.78			0.63			Ta
Hf			1.6			1.1			Hf
Zr	34	25	18	21	19	20	13	22	Zr
Y	25	17	14	16	15	14	13	19	Y
La				4.2		4.8			La
Ce				11		13			Ce
Nd				7		7			Nd
Sm				2.01		1.60			Sm
Eu				0.68		0.55			Eu
Tb				0.4		0.3			Tb
Dy				2.8		1.8			Dy
Yb				2.14		1.54			Yb
Lu				0.34		0.26			Lu
FeO^*	10.35	10.44	9.65	10.67	9.96	9.55	10.31	9.36	FeO^*

1 1268-C1 Bear Lake basaltic andesite (unit 1), from the unepidotized portion of a pillow 0.3 x 1.9 m. Rare chlorite pseudomorphs after pyroxene phenocrysts.

2 1362-C1 Bear Lake basaltic andesite (unit 1), from a 3.7 m thick compound (massive base, pillowed top) flow. Sample C1 located 0.9 m above base of flow, and represents least epidotized material. 2% plagioclase phenocrysts.

2 1388-F2 Bear Lake basaltic andesite (unit 1), from the core of a megapillow in a 4.8 m thick pillowed flow. 5% plagioclase phenocrysts.

4 1388-F7 Bear Lake basaltic andesite (unit 1), from 2.8 m above base of an 8.4 m thick compound flow. Sample F7 is from the massive portion of the flow. Aphyric.

5 1388-F8 Bear Lake basaltic andesite (unit 1), from 2.5 m above base of a 5.0 m thick massive flow. Rare small plagioclase phenocrysts.

6 1510-C1 Bear Lake basaltic andesite (unit 1), from 3 m above base of 4.5 m thick massive flow. Aphyric.

7 399-C1 Bear Lake basaltic andesite (unit 1a), pillowed flow. Relatively unaltered sample from centre of partially epidotized pillow. Aphyric.

8 3363-1 Bear Lake basaltic andesite (unit 1a), massive division of 26 m thick compound flow. Aphyric.

	9	**10**	**11**	**12**	**13**	**14**	**15**	**16**	
	3231-1	1268-C2	1362-C2	1362-C3	399-C2	6034-C1	6036-C1	6036-C2	
SiO_2	55.10	47.85	54.00	46.50	51.75	49.20	48.47	49.37	SiO_2
TiO_2	0.37	0.75	0.44	0.55	0.18	0.69	0.32	0.54	TiO_2
Al_2O_3	15.39	16.41	15.55	17.89	13.23	17.52	19.16	16.11	Al_2O_3
Fe_2O_3	1.34	6.51	4.46	5.83	3.74	3.45	3.31	1.54	Fe_2O_3
FeO	8.17	3.90	5.95	6.22	4.45	8.44	5.93	10.62	FeO
MnO	0.16	0.14	0.17	0.19	0.16	0.19	0.17	0.62	MnO
MgO	5.58	3.78	4.20	4.50	6.63	3.61	4.44	6.33	MgO
CaO	4.97	17.23	9.23	13.28	15.53	9.42	11.84	6.26	CaO
Na_2O	3.75	0.05	2.45	1.03	0.23	3.61	2.83	3.92	Na_2O
K_2O	2.09	0.11	0.28	0.21	0.26	0.24	0.34	0.22	K_2O
P_2O_5	0.14	0.13	0.13	0.15	0.10	0.12	0.06	0.06	P_2O_5
H_2O	2.82	1.97	2.91	3.37	1.75	2.82	2.70	3.51	H_2O
S	0.10	0.22	0.01	0.02	0.00	0.00	0.01	0.00	S
CO_2	0.35	0.95	0.25	0.43	1.98	0.93	0.54	0.29	CO_2
OTHER	0.13	0.03	0.08	0.11	0.01	0.07	0.08	0.11	OTHER
O≡S	-0.04	-0.09		-0.01					O≡S
TOTAL	100.42	99.94	100.11	100.27	100.00	100.31	100.20	99.50	TOTAL
Ni	20	38	10	12	20	0	5	9	Ni
Cr	37	223	25	29	96	60	67	80	Cr
Sc								51.3	Sc
Cu	84	71	129	178	11	157	145	120	Cu
Zn	122	48	100	104	48	85	48	473	Zn
Rb	24					1	<1	<1	Rb
Sr	150	200	275	475	185	117	164	73	Sr
Ba	700	60	120	90	170	134	192	130	Ba
Th								<0.2	Th
U								<0.2	U
Ta								1.10	Ta
Hf								<1.0	Hf
Zr	28	11	11	14	10	17	14	11	Zr
Y	23	21	19	18	10	15	14	15	Y
La								1.8	La
Ce								7	Ce
Nd								4	Nd
Sm								0.99	Sm
Eu								0.49	Eu
Tb								0.3	Tb
Dy								<3.0	Dy
Yb								1.45	Yb
Lu								0.22	Lu
FeO^*	9.38	9.76	9.96	11.47	7.82	11.54	8.91	12.01	FeO^*

9	3231-1	Bear Lake basaltic andesite (unit 1a), massive base of 6 m thick compound flow. Aphyric.
10	1268-C2	Bear Lake basaltic andesite (unit 1), from an oval, 20 x 36 cm epidosite domain within a 0.3 x 1.9 m pillow. Sampled 36 cm from 1268-C1.
11	1362-C2	Bear Lake basaltic andesite (unit 1), from a 3.7 m thick compound flow. Sample C2 located 1.7 m above base of flow, from a moderately epidotized zone in the massive portion of the flow.
12	1362-C3	Bear Lake basaltic andesite (unit 1), from a 3.7 m thick compound flow. Sample C3 located 2.1 m above base of flow, from one of the more epidote-rich epidosite domains that occur in the top 1 m of the flow.
13	399-C2	Bear Lake basaltic andesite (unit 1a), pillowed flow. Sample from epidosite domain in same altered pillow as sample 399-C1. Aphyric, 2% quartz amygdales.
***14**	6034-C1	Hidden Lake basalt (unit 2), from the core of a 1 x 3 m megapillow; contains about 5% 2 - 3 mm epidote-quartz amygdales. 10% plagioclase phenocrysts.
***15**	6036-C1	Hidden Lake basalt (unit 2), from megapillow at base of a pillowed flow. Plagioclase-pyroxene (pseudomorph)-phyric.
***16**	6036-C2	Hidden Lake basalt (unit 2), from core of megapillow. 1% amygdales, plagioclase-pyroxene (pseudomorph)-phyric.

	17	18	19	20	21	22	23	24	
	6083-C1	6113-C1	6164-C1	6204-C1	6204-C2	7034-C1	7034-C2	7042-C1	
SiO_2	48.33	51.96	47.65	49.89	49.55	51.33	48.39	52.88	SiO_2
TiO_2	0.59	0.46	0.83	0.59	0.60	0.74	0.58	0.69	TiO_2
Al_2O_3	16.30	15.96	15.15	16.25	16.60	15.21	18.50	14.55	Al_2O_3
Fe_2O_3	3.80	1.82	2.04	3.20	3.20	2.86	2.76	3.77	Fe_2O_3
FeO	7.47	9.28	13.66	8.48	8.49	10.88	8.30	10.41	FeO
MnO	0.22	0.17	0.29	0.21	0.19	0.24	0.20	0.24	MnO
MgO	4.03	6.82	7.10	4.87	4.96	4.44	4.37	4.40	MgO
CaO	11.80	5.71	6.41	8.43	8.76	9.15	8.31	8.90	CaO
Na_2O	2.98	4.44	3.21	2.89	3.26	2.81	3.51	2.09	Na_2O
K_2O	0.28	0.51	0.14	0.65	0.47	0.32	1.25	0.28	K_2O
P_2O_5	0.05	0.10	0.13	0.11	0.11	0.11	0.11	0.11	P_2O_5
H_2O	2.34	3.17	4.20	3.09	3.20	2.51	2.59	2.71	H_2O
S	0.01	0.00	0.01	0.00	0.02	0.01	0.01	0.01	S
CO_2	1.73	0.08	0.08	0.60	0.86	0.15	0.07	0.12	CO_2
OTHER	0.10	0.09	0.06	0.11	0.11	0.07	0.14	0.08	OTHER
O≡S					-0.01				O≡S
TOTAL	100.03	100.57	100.96	99.37	100.37	100.83	99.09	101.24	TOTAL
Ni	5	24	6	<1	6	<1	<1	<1	Ni
Cr	53	128	90	79	82	60	63	52	Cr
Sc	34.6								Sc
Cu	115	43	127	131	266	138	112	104	Cu
Zn	71	64	131	88	81	108	70	98	Zn
Rb	5	<1	<1	8	<1	<1	17	<1	Rb
Sr	429	92	46	327	235	86	182	199	Sr
Ba	140	362	59	248	195	115	715	152	Ba
Th	0.35								Th
U	<0.2								U
Ta	0.72								Ta
Hf	1.1								Hf
Zr	28	19	16	24	21	15	17	26	Zr
Y	16	14	16	12	13	15	15	18	Y
La	3.2								La
Ce	8								Ce
Nd	5								Nd
Sm	1.35								Sm
Eu	0.64								Eu
Tb	0.3								Tb
Dy	2.3								Dy
Yb	1.70								Yb
Lu	0.27								Lu
FeO^*	10.89	10.92	15.50	11.36	11.37	13.45	10.78	13.80	FeO^*

***17**	6083-C1	Hidden Lake basalt (unit 2), from interior of a large megapillow. Less than 2% amygdales; pyroxene (pseudomorph)-phyric.
***18**	6113-C1	Hidden Lake basalt (unit 2), from non-vesicular portion of massive flow. 20% plagioclase phenocrysts.
***19**	6164-C1	Hidden Lake basalt (unit 2), from 1 x 2.5 m pillow. Aphyric.
***20**	6204-C2	Hidden Lake basalt (unit 2), from centre of a 2.5 x 9 m megapillow, 5 m stratigraphically above 6204-C1. Plagioclase-phyric
***21**	6204-C1	.Hidden Lake basalt (unit 2), from core of 2 x 6 m megapillow. 20% plagioclase phenocrysts.
***22**	7034-C1	Hidden Lake basalt (unit 2), centre of 1.5 x 4 m megapillow. 2% pseudomorphs after pyroxene phenocrysts, 0.5% quartz amygdales.
***23**	7034-C2	Hidden Lake basalt (unit 2), centre of 2 x 5 m megapillow. 10% plagioclase phenocrysts.
***24**	7042-C1	Hidden Lake basalt (unit 2a), 1 m above base of 15 m thick compound flow. Aphyric.

	25	26	27	28	29	30	31	32	
	7040-C1	6095-C1	6098-C1	6108-C2	5546-C1	5546-C2	5551-C1	6183-C1	
SiO_2	52.78	49.51	57.50	54.76	54.72	51.76	53.74	49.73	SiO_2
TiO_2	0.69	0.52	0.63	0.61	0.65	0.60	0.68	0.56	TiO_2
Al_2O_3	14.58	17.70	14.46	14.11	13.24	15.00	13.83	15.71	Al_2O_3
Fe_2O_3	2.91	1.77	2.70	2.58	3.65	2.67	4.02	3.10	Fe_2O_3
FeO	10.45	8.42	7.81	11.04	9.05	10.13	8.61	9.05	FeO
MnO	0.23	0.18	0.16	0.22	0.22	0.21	0.22	0.20	MnO
MgO	4.92	4.90	2.72	4.06	4.48	4.34	3.94	5.24	MgO
CaO	7.91	6.01	5.65	5.51	9.57	7.94	9.24	8.76	CaO
Na_2O	2.91	4.48	4.29	3.61	0.54	2.82	1.59	3.54	Na_2O
K_2O	0.29	0.69	0.80	0.43	0.12	0.37	0.28	0.21	K_2O
P_2O_5	0.13	0.06	0.16	0.23	0.11	0.11	0.10	0.08	P_2O_5
H_2O	2.84	3.30	2.19	3.07	3.27	3.22	3.26	2.90	H_2O
S	0.02	0.00	0.01	0.02	0.03	0.01	0.00	0.01	S
CO_2	0.33	0.12	0.10	0.07	0.40	0.89	0.22	0.29	CO_2
OTHER	0.11	0.10	0.10	0.09	0.08	0.08	0.09	0.07	OTHER
O≡S	-0.01			-0.01	-0.01				O≡S
TOTAL	101.09	97.76	99.28	100.40	100.12	100.15	99.82	99.45	TOTAL
Ni	7	15	5	7	<1	<1	<1	10	Ni
Cr	78	74	41	63	61	51	47	87	Cr
Sc				35.0					Sc
Cu	280	85	141	199	303	86	178	123	Cu
Zn	104	65	73	103	94	85	76	77	Zn
Rb	<1	7	10	<1	<1	1	1	<1	Rb
Sr	178	157	152	127	78	164	289	184	Sr
Ba	187	390	303	175	68	247	140	70	Ba
Th				2.40					Th
U				1.10					U
Ta				0.80					Ta
Hf				1.9					Hf
Zr	25	22	46	40	21	19	28	16	Zr
Y	22	14	24	15	20	14	17	16	Y
La				16.0					La
Ce				36					Ce
Nd				17					Nd
Sm				3.36					Sm
Eu				0.95					Eu
Tb				0.5					Tb
Dy				3.5					Dy
Yb				2.33					Yb
Lu				0.38					Lu
FeO*	13.07	10.01	10.24	13.36	12.33	12.53	12.23	11.84	FeO*

***25**	7040-C1	Fine grained, equigranular mafic synvolcanic dyke in Hidden Lake basalt sequence.
***26**	6095-C1	Burley Lake basaltic andesite (unit 3), from pillowed flow. 20% plagioclase phenocrysts, 3% chlorite after pyroxene phenocrysts.
***27**	6098-C1	Burley Lake andesite (unit 3), from 7 m above base of thick massive flow. Aphyric.
***28**	6108-C2	Burley Lake basaltic andesite (unit 3), from 1 x 1.5 m partially epidotized pillow. 3% small plagioclase phenocrysts.
***29**	5546-C1	Burley Lake basaltic andesite (unit 3b), 2.5 m above base of 9.5 m thick compound flow (see Flow 1 in Fig. 186). Aphyric, 1% quartz-carbonate amygdales.
***30**	5546-C2	Burley Lake basaltic andesite (unit 3b), 5 m above base of 7 m thick massive flow. Aphyric, 1 - 2% of quartz-carbonate amygdales.
***31**	5551-C1	Burley Lake basaltic andesite (unit 3b), 0.7 m above base of 15 m thick compound flow. Aphyric, 1% quartz-carbonate amygdales.
***32**	6183-C1	Burley Lake basaltic andesite (unit 3), from centre of megapillow. 1% quartz amygdales. 1% each of plagioclase and pseudomorphs after pyroxene phenocrysts.

	33	34	35	36	37	38	39	40	
	6182-C1	81-1	1111-C1	1112-C1	1112-C2	1112-C3	1112-C4	1112-C5	
SiO_2	52.42	53.90	50.60	50.55	54.50	54.20	58.10	53.15	SiO_2
TiO_2	0.74	0.44	1.44	1.28	1.26	1.27	1.08	1.27	TiO_2
Al_2O_3	14.50	15.22	14.30	14.89	14.48	14.93	13.61	14.95	Al_2O_3
Fe_2O_3	3.04	2.25	2.08	1.54	1.47	1.58	1.26	1.06	Fe_2O_3
FeO	10.62	8.61	10.91	10.38	8.38	8.19	7.67	8.78	FeO
MnO	0.23	0.18	0.24	0.24	0.20	0.19	0.16	0.20	MnO
MgO	4.30	5.24	5.21	5.78	5.12	5.21	4.94	5.84	MgO
CaO	7.36	7.93	9.04	7.68	6.43	6.92	5.45	6.14	CaO
Na_2O	2.67	3.11	2.94	3.24	4.01	3.53	3.63	3.62	Na_2O
K_2O	0.52	0.76	1.01	1.33	1.16	1.13	1.01	2.02	K_2O
P_2O_5	0.09	0.08	0.17	0.20	0.20	0.22	0.21	0.21	P_2O_5
H_2O	3.28	2.87	3.29	2.50	2.25	2.52	2.54	2.53	H_2O
S	0.01	0.01	0.11	0.00	0.01	0.01	0.01	0.00	S
CO_2	0.04	0.18	0.14	0.07	0.08	0.08	0.17	0.17	CO_2
OTHER	0.09	0.09	0.09	0.13	0.11	0.10	0.10	0.14	OTHER
O≡S			-0.05						O≡S
TOTAL	99.91	100.87	101.52	99.81	99.66	100.08	99.94	100.08	TOTAL
Ni	<1	4	18	32	30	24	38	22	Ni
Cr	54	<3	26	163	159	137	148	167	Cr
Sc						31.7			Sc
Cu	194	90	38	6	7	10	40	3	Cu
Zn	105	99	120	158	81	86	72	77	Zn
Rb	5	9	24			<2			Rb
Sr	90	150	210	245	210	250	160	195	Sr
Ba	220	390	300	480	380	320	320	720	Ba
Th						3.4			Th
U						1.4			U
Ta						1.2			Ta
Hf						3.9			Hf
Zr	22	18	84	87	85	99	94	102	Zr
Y	17	18	35	27	28	32	27	27	Y
La						14.5			La
Ce						34			Ce
Nd						17			Nd
Sm						4.50			Sm
Eu						1.46			Eu
Tb						0.8			Tb
Dy						4.8			Dy
Yb						3.00			Yb
Lu						0.46			Lu
FeO^*	13.36	10.63	12.78	11.77	9.70	9.61	8.80	9.73	FeO^*

***33** 6182-C1 Burley Lake basaltic andesite (unit 3), from centre of a 2.5 x 3 m megapillow. Aphyric, 2% small quartz amygdales.

34 81-1 Burley Lake basaltic andesite (unit 3), from pillowed flow with prominent concentric thermal contraction cracks. Aphyric.

35 1111-C1 Scotty Lake basalt (unit 4), from massive flow.

36 1112-C1 Scotty Lake basalt (unit 4), 10 cm above base of aphyric massive flow (Fig. 79).

37 1112-C2 Scotty Lake basalt (unit 4), 75 cm above base of massive flow (Fig. 79).

38 1112-C3 Scotty Lake basalt (unit 4), 155 cm above base of massive flow (Fig. 79).

39 1112-C4 Scotty Lake basalt (unit 4), 240 cm above base of massive flow (Fig. 79).

40 1112-C5 Scotty Lake basalt (unit 4), 340 cm above base of massive flow (Fig. 79).

	41	**42**	**43**	**44**	**45**	**46**	**47**	**48**	
	1112-C6	1112-C7	1112-C8	1114-C1	1116-C1	1117-C1	117-C1	117-C2	
SiO_2	55.50	56.05	53.40	51.05	54.40	48.00	48.55	50.30	SiO_2
TiO_2	1.14	1.21	1.30	1.56	1.83	1.47	1.31	1.30	TiO_2
Al_2O_3	14.47	13.93	15.16	13.49	13.53	14.83	15.19	14.16	Al_2O_3
Fe_2O_3	1.17	0.91	1.83	3.08	6.48	3.35	3.05	0.00	Fe_2O_3
FeO	8.31	8.59	8.04	11.03	8.41	12.14	8.80	8.35	FeO
MnO	0.19	0.19	0.19	0.21	0.21	0.23	0.23	0.23	MnO
MgO	5.49	5.28	5.09	5.07	3.00	4.50	6.02	6.13	MgO
CaO	5.64	5.68	6.47	8.22	4.65	7.44	9.87	10.50	CaO
Na_2O	3.81	3.58	3.42	2.31	3.08	2.48	2.27	2.44	Na_2O
K_2O	1.23	1.57	1.79	0.32	0.59	0.93	0.22	0.18	K_2O
P_2O_5	0.21	0.19	0.21	0.17	0.31	0.19	0.15	0.15	P_2O_5
H_2O	2.56	2.32	2.66	3.70	4.02	3.86	3.58	2.97	H_2O
S	0.03	tr.	0.00	0.15	0.03	0.00	0.08	0.05	S
CO_2	0.17	0.27	0.27	0.10	0.15	0.90	0.89	0.17	CO_2
OTHER	0.11	0.13	0.14	0.07	0.05	0.08	0.08	0.07	OTHER
O≡S	-0.01			-0.07	-0.01		-0.03	-0.02	O≡S
TOTAL	100.02	99.90	99.97	100.44	100.73	100.40	100.26	96.98	TOTAL
Ni	30	22	26	14	<2	<2	20	18	Ni
Cr	170	148	167	8	<3	<3	64	50	Cr
Sc								37.3	Sc
Cu	36	9	16	53	22	4	41	34	Cu
Zn	98	77	74	128	100	134	149	113	Zn
Rb				4	10	16		<2	Rb
Sr	200	175	240	230	150	180	210	210	Sr
Ba	340	640	610	140	150	370	140	110	Ba
Th								2.3	Th
U								0.73	U
Ta								1.1	Ta
Hf								4.0	Hf
Zr	96	93	99	72	143	65	77	70	Zr
Y	28	28	36	33	53	34	30	28	Y
La								10.3	La
Ce								25	Ce
Nd								13	Nd
Sm								3.80	Sm
Eu								1.36	Eu
Tb								0.8	Tb
Dy								5.6	Dy
Yb								2.93	Yb
Lu								0.44	Lu
FeO^*	9.36	9.41	9.69	13.80	14.24	15.15	11.54	8.35	FeO^*

41	1112-C6	Scotty Lake basalt (unit 4), 460 cm above base of massive flow (Fig. 79).
42	1112-C7	Scotty Lake basalt (unit 4), 520 cm above base of massive flow (Fig. 79).
43	1112-C8	Scotty Lake basalt (unit 4), 540 cm above base of massive flow, representing spherulitic top of massive division (Fig. 79).
44	1114-C1	Scotty Lake basalt (unit 4), pillowed flow.
45	1116-C1	Scotty Lake basalt (unit 4), massive flow.
46	1117-C1	Scotty Lake basalt (unit 4), pillowed flow.
47	117-C1	Scotty Lake basalt (unit 4), 0.3 m above base of 15 m thick compound flow (Fig. 86). Aphyric, 3 - 4% chlorite-, epidote, quartz- and muscovite-filled fractures.
48	117-C2	Scotty lake basalt (unit 4), 3.2 m above base of 15 m thick compound flow (Fig. 86). Aphyric, 1% carbonate-filled fractures.

	49	50	51	52	53	54	55	56	
	117-C3	117-C4	117-C5	1519-C1	1519-C2	1519-C3	1519-C4	563-C1	
SiO_2	52.90	50.70	47.35	48.45	47.65	46.40	47.35	47.30	SiO_2
TiO_2	1.40	1.16	1.35	1.49	2.65	2.26	2.37	1.85	TiO_2
Al_2O_3	13.90	14.36	15.64	13.94	11.94	12.78	12.56	14.16	Al_2O_3
Fe_2O_3	3.05	2.23	1.99	2.58	2.20	2.71	2.59	3.25	Fe_2O_3
FeO	8.74	8.56	10.31	10.58	16.07	14.48	14.76	10.91	FeO
MnO	0.19	0.20	0.20	0.22	0.22	0.24	0.24	0.19	MnO
MgO	5.33	6.43	7.69	7.55	4.25	5.32	5.06	5.03	MgO
CaO	8.83	9.47	7.13	8.64	7.91	9.22	8.35	9.46	CaO
Na_2O	2.65	3.33	3.36	2.89	3.55	2.61	2.73	1.70	Na_2O
K_2O	0.20	0.56	0.38	0.68	0.41	0.39	0.96	0.17	K_2O
P_2O_5	0.17	0.14	0.16	0.13	0.41	0.30	0.31	0.24	P_2O_5
H_2O	3.09	2.82	4.00	3.03	2.74	3.06	2.83	3.54	H_2O
S	0.08	0.08	0.28	0.03	0.48	0.12	0.08	0.21	S
CO_2	0.12	0.10	0.12	0.29	0.40	0.32	0.21	1.53	CO_2
OTHER	0.06	0.08	0.07	0.09	0.05	0.08	0.11	0.08	OTHER
O=S	-0.03	-0.03	-0.11	-0.01	-0.19	-0.05	-0.03	-0.08	O=S
TOTAL	100.68	100.19	99.92	100.58	100.74	100.24	100.49	99.54	TOTAL
Ni	8	26	28	58	8	70	64	77	Ni
Cr	15	46	53	92	<3	85	92	80	Cr
Sc						41.3			Sc
Cu	36	29	78	100	80	70	80	97	Cu
Zn	101	101	125	101	84	73	58	132	Zn
Rb	4			13	<2	<2	<2	<2	Rb
Sr	240	205	160	155	120	200	190	190	Sr
Ba	130	240	160	180	140	120	460	60	Ba
Th						<0.2			Th
U						<0.2			U
Ta						0.56			Ta
Hf						3.7			Hf
Zr	79	63	74	59	111	84	95	60	Zr
Y	31	27	29	25	43	33	32	31	Y
La						6.6			La
Ce						21			Ce
Nd						14			Nd
Sm						4.40			Sm
Eu						1.78			Eu
Tb						0.9			Tb
Dy						5.6			Dy
Yb						3.67			Yb
Lu						0.56			Lu
FeO^*	11.48	10.57	12.10	12.90	18.05	16.92	17.09	13.83	FeO^*

49 117-C3 Scotty Lake basalt (unit 4), 8.2 m above base of 15 m thick compound flow (Fig. 86). Aphyric.

50 117-C4 Scotty Lake basalt (unit 4), 1.5 m from top of 12.5 m massive division of 15 m thick compound flow (Fig. 86). Aphyric, 4% disseminated pyrite.

51 117-C5 Scotty Lake basalt (unit 4), 0.2 m from top of 12.5 m massive division of 15 m compound flow (Fig. 86). Aphyric, 3 - 4% disseminated pyrite and 1% epidote-, chlorite- and sericite-filled fractures.

52 1519-C1 Two Portage Lake ferrobasalt (unit 5), 5 m below top of flow 1 (Fig. 49).

53 1519-C2 Two Portage Lake ferrobasalt (unit 5), 13 m above base of flow 2 (Fig. 49).

54 1519-C3 Two Portage Lake ferrobasalt (unit 5), 5 m above base of flow 3 (Fig. 49).

55 1519-C4 Two Portage Lake ferrobasalt (unit 5), 3 m above base of flow 4 (Fig. 49).

56 563-C1 Two Portage Lake ferrobasalt (unit 5), strongly foliated and recrystallized, with no primary textures or structures. Aphyric, trace pyrite and minor (less than 0.5%) carbonate-filled fractures.

	57	58	59	60	61	62	63	64	
	6197-C1	6197-C2	4174-C2	4174-C1	4183-C1	5177-C1	4062-C1	4058-C1	
SiO_2	50.64	52.55	54.25	53.24	53.01	48.72	59.11	45.78	SiO_2
TiO_2	0.83	0.83	0.66	0.63	1.10	0.19	0.71	0.54	TiO_2
Al_2O_3	14.12	14.06	15.73	15.66	15.02	14.31	13.99	15.26	Al_2O_3
Fe_2O_3	3.56	3.50	1.46	2.57	3.01	2.24	3.03	1.60	Fe_2O_3
FeO	11.41	11.00	8.72	7.04	8.93	5.95	8.53	9.48	FeO
MnO	0.24	0.24	0.18	0.15	0.26	0.13	0.21	0.22	MnO
MgO	4.01	4.23	5.85	5.41	3.48	10.31	1.89	10.85	MgO
CaO	7.32	7.19	5.33	8.25	6.57	12.80	7.56	8.56	CaO
Na_2O	3.06	3.75	4.07	3.19	3.05	0.92	1.61	2.10	Na_2O
K_2O	0.88	0.24	0.62	0.19	0.27	0.47	0.12	1.11	K_2O
P_2O_5	0.14	0.10	0.14	0.12	0.18	0.06	0.12	0.06	P_2O_5
H_2O	2.91	2.79	3.55	2.93	3.46	3.03	3.14	4.18	H_2O
S	0.01	0.02	0.01	0.01	0.05	0.01	0.04	0.02	S
CO_2	0.67	0.29	0.40	0.53	1.56	0.44	0.86	0.77	CO_2
OTHER	0.13	0.08	0.09	0.07	0.06	0.15	0.07	0.18	OTHER
O≡S		-0.01			-0.02		-0.02	-0.01	O≡S
TOTAL	99.93	100.86	101.06	99.99	99.99	99.73	100.97	100.70	TOTAL
Ni	1	25	21	17	<1	76	<1	146	Ni
Cr	58	55	56	57	41	487	33	444	Cr
Sc	42.8					36.3			Sc
Cu	200	169	137	106	46	75	168	142	Cu
Zn	103	99	73	75	98	55	57	119	Zn
Rb	20	<1	5	<1	4	6	<1	15	Rb
Sr	113	101	150	184	175	228	153	128	Sr
Ba	526	131	250	40	56	200	106	357	Ba
Th	0.61					0.60			Th
U	0.40					<0.2			U
Ta	1.1					0.71			Ta
Hf	1.9					<1.0			Hf
Zr	22	23	51	48	50	12	54	13	Zr
Y	17	23	29	24	26	9	17	17	Y
La		3.7				3.4			La
Ce		13				9			Ce
Nd		8				4			Nd
Sm		1.69				0.88			Sm
Eu		0.79				0.56			Eu
Tb		0.5				0.2			Tb
Dy		3.4				1.5			Dy
Yb		2.38				0.72			Yb
Lu		0.38				0.11			Lu
FeO^*	14.61	14.15	10.03	9.35	11.64	7.97	11.26	10.92	FeO^*

***57**	6197-C1	South Main basalt (unit 6), from centre of megapillow. 3% pseudomorphs after pyroxene microphenocrysts.
***58**	6197-C2	South Main basalt (unit 6), from centre of megapillow. 3% pseudomorphs after pyroxene microphenocrysts.
***59**	4174-C1	Aphyric basalt (unit 7), unit "C", Hook Lake Block. Sample from 70 cm above base of 5 m thick massive flow.
***60**	4174-C2	Aphyric basalt (unit 7), unit "C", Hook Lake Block. Sample from pillowed flow 20 m stratigraphically above 4714-C1. 1% quartz amygdales.
***61**	4183-C1	Aphyric basalt (unit 7), unit "C", Hook Lake Block. Sample from core of 1 x 1.5 m pillow.
***62**	5177-C1	Aphyric basalt (unit 7), unit "E", Hook Lake Block. Massive division of compound (massive base, pillowed top) flow. Subophitic texture.
***63**	4062-C1	Synvolcanic dyke 1.2 m wide emplaced in aphyric basalt (unit 7), unit "E", Hook Lake Block. Equigranular, aphyric, weakly banded margins.
***64**	4058-C1	Aphyric basalt (unit 7), unit "E", Hook Lake Block. Sample from center of large pillow. 3% pyroxene phenocrysts.

	65	66	67	68	69	70	71	72	
	4003-C1	4003-C2	4027-C1	4022-C3	4022-C1	4022-C4	4022-C5	4022-C2	
SiO_2	50.71	51.05	52.78	50.51	47.70	51.66	48.00	47.63	SiO_2
TiO_2	0.68	0.42	0.99	0.68	0.41	0.70	0.67	0.42	TiO_2
Al_2O_3	14.78	16.86	16.98	15.18	19.61	15.55	18.51	19.33	Al_2O_3
Fe_2O_3	2.32	1.07	1.21	1.93	1.15	2.16	1.70	1.10	Fe_2O_3
FeO	10.94	7.13	9.74	10.84	7.55	10.84	9.20	7.92	FeO
MnO	0.23	0.16	0.25	0.24	0.15	0.22	0.15	0.16	MnO
MgO	4.74	6.19	4.38	4.60	4.52	4.68	5.81	4.83	MgO
CaO	7.79	5.77	4.51	6.97	9.19	7.09	9.13	8.99	CaO
Na_2O	3.91	4.75	5.02	4.43	2.89	4.30	1.89	3.57	Na_2O
K_2O	0.22	0.40	0.56	0.12	1.50	0.16	0.49	0.97	K_2O
P_2O_5	0.14	0.11	0.14	0.10	0.07	0.13	0.10	0.07	P_2O_5
H_2O	2.86	2.95	3.37	3.05	2.75	2.76	3.45	3.20	H_2O
S	0.01	0.16	0.11	0.05	0.04	0.02	0.04	0.08	S
CO_2	0.99	0.59	0.34	1.13	1.15	0.38	0.36	1.58	CO_2
OTHER	0.06	0.07	0.08	0.14	0.08	0.07	0.08	0.10	OTHER
O≡S		-0.06	-0.05	-0.02	-0.02	-0.01	-0.02	-0.03	O≡S
TOTAL	100.38	97.62	100.41	99.95	98.74	100.71	99.56	99.92	TOTAL
Ni	4	27	6	<1	9	8	12	12	Ni
Cr	59	52	53	49	58	59	73	55	Cr
Sc						42.9			Sc
Cu	142	105	67	170	133	137	133	122	Cu
Zn	119	40	176	173	71	90	96	76	Zn
Rb	15	<1	<1	<1	16	<1	4	11	Rb
Sr	128	154	74	116	207	135	204	171	Sr
Ba	357	160	186	62	652	116	96	323	Ba
Th						0.23			Th
U						0.43			U
Ta						0.63			Ta
Hf						1.7			Hf
Zr	13	26	32	22	16	25	24	16	Zr
Y	17	20	28	20	13	19	21	13	Y
La						3.7			La
Ce						10			Ce
Nd						6			Nd
Sm						1.88			Sm
Eu						0.74			Eu
Tb						0.5			Tb
Dy						4.0			Dy
Yb						2.59			Yb
Lu						0.40			Lu
FeO^*	10.92	8.09	10.83	12.58	8.58	12.78	10.73	8.91	FeO^*

***65** 4003-C1 Aphyric basalt (unit 7), unit "I", Hook Lake Block. Sample from massive flow with 1% plagioclase phenocrysts.

***66** 4003-C2 Aphyric basalt (unit 7), unit "I", Hook Lake Block. Sample from pillowed flow with 1% pseudomorphs after pyroxene phenocrysts.

***67** 4027-C1 Aphyric basalt (unit 7), unit "I", Hook Lake Blok. Sample from massive flow with sparse plagioclase microphenocrysts.

***68** 4022-C1 Porphyritic basalt (unit 9), unit "J", Hook Lake Block (Fig. 161). Sample from centre of a pillow. 25% plagioclase phenocrysts, 3% pseudomorphs after pyroxene microphenocrysts, 2% carbonate amygdales.

***69** 4022-C3 Porphyritic basalt (unit 9), unit "J", Hook Lake Block (Fig. 161). Sample from centre of pillow, 1.2 m below flow top. 5% plagioclase phenocrysts, 1% pseudomorphs after pyroxene microphenocrysts.

***70** 4022-C4 Porphyritic basalt (unit 9), unit "J", Hook Lake Block (Fig. 161). Sample from base of pillowed flow. 5% plagioclase phenocrysts, 1% pseudomorphs after pyroxene phenocrysts.

***71** 4022-C5 Porphyritic basalt (unit 9), unit "J", Hook Lake Block (Fig. 161). Sample from pillow 18 m below flow top. 15% plagioclase phenocrysts, 2% pseudomorphs after pyroxene phenocrysts.

***72** 4022-C2 Porphyritic basalt (unit 9), unit "J", Hook Lake Block (Fig. 161). Same flow as 4022-C1.

	73	74	75	76	77	78	79	80	
	4022-C6	5029-C1	5057-C1	5032-C1	5043-C1	2431-C1	2442-C1	2444-C1	
SiO_2	52.41	51.50	56.50	53.30	52.00	53.50	51.60	55.10	SiO_2
TiO_2	0.56	0.62	0.52	0.48	0.53	0.38	0.36	0.46	TiO_2
Al_2O_3	15.92	14.68	14.62	14.70	15.62	15.24	16.37	14.71	Al_2O_3
Fe_2O_3	1.99	2.86	1.75	1.98	2.14	2.39	2.98	3.00	Fe_2O_3
FeO	9.62	10.62	6.68	9.41	9.26	7.71	7.73	6.97	FeO
MnO	0.16	0.22	0.18	0.21	0.21	0.10	0.15	0.17	MnO
MgO	6.28	4.99	4.25	4.53	4.39	7.00	6.22	6.04	MgO
CaO	6.79	7.59	6.53	7.16	6.34	5.82	5.67	6.45	CaO
Na_2O	3.25	2.51	4.20	3.18	4.12	2.07	4.88	3.45	Na_2O
K_2O	0.38	0.62	0.73	1.25	0.67	1.02	0.49	0.20	K_2O
P_2O_5	0.11	0.14	0.14	0.15	0.14	0.09	0.05	0.07	P_2O_5
H_2O	3.15	3.59	2.40	2.99	3.18	4.04	3.18	3.24	H_2O
S	0.01	0.00	0.01	0.03	0.00	0.00	0.01	0.00	S
CO_2	0.21	0.62	0.49	0.75	0.75	0.07	0.00	0.09	CO_2
OTHER	0.07	0.13	0.10	0.11	0.10	0.10	0.09	0.07	OTHER
O≡S				-0.01					O≡S
TOTAL	100.91	100.69	99.10	100.22	99.45	99.53	99.78	100.02	TOTAL
Ni	19	9	7	14	8	16	11	20	Ni
Cr	79	66	50	81	62	60	20	122	Cr
Sc									Sc
Cu	112	140	108	95	102	35	109	59	Cu
Zn	180	93	104	97	116	68	84	70	Zn
Rb	<1	7	9	12	3	9	4	4	Rb
Sr	166	214	143	103	122	150	215	155	Sr
Ba	112	537	367	492	355	480	350	90	Ba
Th									Th
U									U
Ta									Ta
Hf									Hf
Zr	18	25	24	28	23	20	6	13	Zr
Y	16	9	18	18	18	9	6	8	Y
La									La
Ce									Ce
Nd									Nd
Sm									Sm
Eu									Eu
Tb									Tb
Dy									Dy
Yb									Yb
Lu									Lu
FeO^*	11.41	13.19	8.25	11.19	11.19	9.86	10.41	9.67	FeO^*

***73**	4022-C6	Porphyritic basalt (unit 9), unit "J", Hook Lake Block (Fig. 161). Sample from pillow 12 m above base of pillowed flow. 15% plagioclase phenocrysts, 5% pseudomorphs after pyroxene phenocrysts.
***74**	5029-C1	Sparsely porphyritic basaltic andesite (unit 9), unit "L", Hook Lake Block. Centre of large pillow, 0.5% small clinopyroxene phenocrysts.
***75**	5057-C1	Porphyritic andesite (unit 10), unit "M", Hook Lake Block. 1 m above massive base of compound flow, 13% plagioclase phenocrysts and glomerocrysts, 0.5% clinopyroxene phenocrysts, 0.5% carbonate-chlorite filled vesicles.
***76**	5032-C1	Sparsely porphyritic basaltic andesite (unit 10), unit "M", Hook Lake Block. Combined sample from centre of two pillows, 1% small plagioclase phenocrysts, minor (less than 0.5%) epidote-filled fractures.
***77**	5043-C1	Porphyritic basaltic andesite (unit 10), unit "M", Hook Lake Block. Centre of pillow, 10% plagioclase glomerocrysts, 3% prehnite-, carbonate-, quartz-filled vesicles.
78	2431-C1	Aphyric basalt (unit 7), unit "BC", Bakers Narrows Block. Sample from 14 m thick massive flow.
79	2442-C1	Aphyric basalt (unit 7), unit "BB" (Wright Bay basalt). Sample from massive flow.
80	2444-C1	Porphyritic basalt (unit 9), unit "BC", Bakers Narrows Block. 5% plagioclase phenocrsyts, 2% pseudomorphs after plagioclase phenocrysts.

	81	82	83	84	85	86	87	88	
	2522-C1	3486-C1	7116-C1	3394-C1	5367-C1	5397-C1	4393-C1	1007-C1	
SiO_2	50.60	47.98	51.89	49.05	52.40	52.90	53.76	49.10	SiO_2
TiO_2	0.35	0.90	1.28	1.03	0.42	0.39	0.48	0.82	TiO_2
Al_2O_3	14.97	14.71	16.02	13.49	15.44	14.16	13.67	14.39	Al_2O_3
Fe_2O_3	0.95	1.78	1.25	2.15	2.48	3.05	1.88	2.02	Fe_2O_3
FeO	8.69	9.98	7.04	9.67	10.52	8.75	11.37	9.57	FeO
MnO	0.15	0.18	0.14	0.18	0.20	0.19	0.21	0.20	MnO
MgO	9.10	8.52	5.39	7.80	4.91	4.28	4.79	8.67	MgO
CaO	5.86	9.49	8.52	11.06	6.28	5.88	5.84	7.96	CaO
Na_2O	3.80	2.43	4.30	2.38	3.91	5.17	2.70	3.20	Na_2O
K_2O	1.34	0.15	0.20	0.10	0.36	0.61	0.53	0.35	K_2O
P_2O_5	0.05	0.11	0.11	0.10	0.08	0.08	0.13	0.10	P_2O_5
H_2O	3.78	3.48	2.33	2.90	3.09	2.30	1.11	3.51	H_2O
S	0.01	0.00	0.00	0.04	0.01	0.01	0.01	0.02	S
CO_2	0.46	0.49	0.12	0.12	0.14	0.95	1.10	0.24	CO_2
OTHER	0.17	0.10	0.08	0.09	0.07	0.09	0.08	0.10	OTHER
$O\equiv S$				-0.02				-0.01	$O\equiv S$
TOTAL	100.28	100.30	98.67	100.14	100.31	98.81	97.66	100.24	TOTAL
Ni	86	67	12	91	3	14	5	86	Ni
Cr	500	324	179	237	61	53	52	184	Cr
Sc		44.9							Sc
Cu	90	85	91	73	107	172	152	142	Cu
Zn	76	88	88	110	93	84	114	100	Zn
Rb	13	1	<1	<2	1	<1	1		Rb
Sr	115	134	163	110	123	167	64	125	Sr
Ba	490	29	22	40	140	188	208	160	Ba
Th		0.20							Th
U		<0.2							U
Ta		0.74							Ta
Hf		2.0							Hf
Zr	4	39	51	42	24	24	15	51	Zr
Y	6	23	27	25	12	12	14	24	Y
La		2.5							La
Ce		11							Ce
Nd		7							Nd
Sm		1.84							Sm
Eu		0.66							Eu
Tb		0.5							Tb
Dy		2.9							Dy
Yb		2.28							Yb
Lu		0.35							Lu
FeO^*	9.54	11.58	8.16	11.60	12.75	11.49	13.06	11.39	FeO^*

81	2522-C1	Aphyric basalt (unit 7), unit "BA", Bakers Narrows Block. Sample from pillowed flow.
***82**	3486-C1	Aphyric basalt (unit 7), Grassy Narrows Zone. Centre of pillow, trace epidote-carbonate-filled fractures.
***83**	7116-C1	Aphyric basalt (unit 7), Grassy Narrows Zone. Centre of non-vesicular pillow, minor pyrite-filled fractures (less than 0.5%).
84	3394-C1	Sparsely porphyritic basalt (unit 7), Grassy Narrows Zone. Centre of pillow, 0.5% small plagioclase phenocrysts, trace pyrite.
***85**	5367-C1	Porphyritic basaltic andesite (unit 8), Manistikwan Lake Block. Centre of megapillow, 10% plagioclase glomerocrysts and 1% 0.5 mm pyroxene phenocyrsts.
***86**	5397-C1	Porphyritic basaltic andesite (unit 8), Manistikwan Lake Block. Centre of large pillow, 10% plagioclase phenocrysts, 1 - 2% quartz amygdales.
***87**	4393-C1	Porphyritic basalt (unit 8), Manistikwan Lake Block. Sample from centre of pillow. 3% plagioclase microphenocrysts, 1% pseudomorphs after pyroxene microphenocrysts.
88	1007-C1	Aphyric basalt (unit 7) within unit 34a, Scotty Lake Block. Sample from centre of 27 x 80 cm pillow.

	89	**90**	**91**	**92**	**93**	**94**	**95**	**96**	
	429-C1	6139-C1	6141-C1	7127-C1	3441-C1	3440-C1	3438-C1	3438-C4	
SiO_2	75.65	81.05	77.48	76.10	74.75	76.85	79.90	78.45	SiO_2
TiO_2	0.26	0.17	0.14	0.09	0.12	0.13	0.12	0.15	TiO_2
Al_2O_3	11.86	8.38	11.70	11.58	11.41	11.49	10.31	11.10	Al_2O_3
Fe_2O_3	0.27	0.41	0.08	1.26	0.64	0.58	0.11	0.16	Fe_2O_3
FeO	1.24	1.81	0.66	0.61	1.36	0.55	0.08	1.21	FeO
MnO	0.02	0.06	0.03	0.02	0.02	0.02	0.00	0.02	MnO
MgO	0.53	0.13	0.01	0.17	1.32	0.66	0.12	0.66	MgO
CaO	0.55	1.41	1.01	4.11	0.88	0.63	0.32	0.66	CaO
Na_2O	2.76	2.28	5.80	0.87	0.52	1.23	2.37	5.60	Na_2O
K_2O	5.03	1.10	0.39	2.06	6.03	5.09	5.43	0.36	K_2O
P_2O_5	0.10	0.03	0.01	0.02	0.03	0.06	0.03	0.03	P_2O_5
H_2O	0.52	0.81	0.28	1.08	1.08	0.85	0.22	0.48	H_2O
S	0.04	0.01	0.01	0.01	0.00	0.00	0.02	0.00	S
CO_2	0.44	0.88	0.70	0.51	1.24	0.98	0.37	0.69	CO_2
OTHER	0.26	0.06	0.04	0.08	0.02	0.09	0.14	0.03	OTHER
O≡S	-0.02						-0.01		O≡S
TOTAL	99.51	98.59	98.34	98.57	99.42	99.21	99.53	99.60	TOTAL
Ni	<2	1	4	<1	<2	<2	<2	<2	Ni
Cr	<3	25	26	22	<4	4	<4	4	Cr
Sc									Sc
Cu	283	<4	21	20	14	6	3	10	Cu
Zn	32	52	54	18	48	60	43	58	Zn
Rb	57	11	6	31	95	123	64	2	Rb
Sr	65	53	30	91	20	15	60	110	Sr
Ba	1830	327	105	301	60	570	1110	50	Ba
Th	1.6		2.1			12			Th
U	0.9		1.4			3.2			U
Ta									Ta
Hf									Hf
Zr	45	49	75	108	281	310	174	349	Zr
Y	14	28	39	65	90	82	42	85	Y
La	12.0		11.0			53.7			La
Ce	27		26			110			Ce
Nd	13		16			50			Nd
Sm	3.21		4.13			11.0			Sm
Eu	0.70		1.00			2.03			Eu
Tb	0.5		0.9			2.0			Tb
Dy	2.6		6.6			13.2			Dy
Yb	1.10		5.64			7.23			Yb
Lu	0.15		0.86			1.04			Lu
FeO^*	1.48	2.18	0.73	1.74	1.94	1.07	0.18	1.35	FeO^*

89	429-C1	Solodiuk Lake rhyolite (unit 13), strongly spherulitic and massive. 0.5% quartz phenocrysts; trace sericite, pyrite, and chalcopyrite along fractures.
***90**	6139-C1	Mine rhyolite (unit 15a). 2% each of plagioclase and quartz phenocrysts.
***91**	6141-C1	Mine rhyolite (unit 15b), from the massive, flow-banded portion of the flow. 5% quartz phenocrysts, 3% plagioclase phenocrysts.
***92**	7127-C1	South Main rhyolite dome (unit 16). 5% 0.3 - 1 mm embayed quartz phenocrysts, patchy seritization.
93	3441-C1	Sparsely porphyritic rhyolite, northern flow (Fig. 137), Grassy Narrows Zone. Massive, strongly spherulitic, with 0.5% plagioclase phenocrysts and 2 - 3% fracture-filling quartz and calcite.
94	3440-C1	Porphyritic rhyolite, northern flow (Fig. 137), Grassy Narrows Zone. Massive, strongly spherulitic, with 1 - 2% plagioclase phenocrysts and 2 - 3% fracture-filling quartz, sericite and calcite.
95	3438-C1	Porphyritic rhyolite, massive lobe, southern flow (Fig. 137), Grassy Narrows Zone. 10 - 15% quartz phenocrysts, 5% plagioclase phenocrysts, 1% calcite-filled fractures and irregular zones. Strong, pervasive silicification.
96	3438-C4	Aphyric rhyolite, massive lobe, southern flow (Fig. 137), Grassy Narrows Zone. Minor small veinlets and domains of calcite and rare epidote. Pervasively silicified.

	97	98	99	100	101	102	103	104	
	3438-C5	3438-C3	3438-C2	2421-C1	2465-C1	1552-C1	6108-C1	1051-C1	
SiO_2	78.25	75.50	74.95	73.40	73.40	62.80	83.44	50.86	SiO_2
TiO_2	0.13	0.16	0.14	0.27	0.27	0.62	0.14	0.45	TiO_2
Al_2O_3	11.28	12.32	14.22	12.32	11.46	16.02	7.19	15.88	Al_2O_3
Fe_2O_3	0.39	0.79	0.52	0.51	0.93	0.27	0.39	1.76	Fe_2O_3
FeO	1.79	1.36	0.68	2.50	2.54	4.26	1.73	7.85	FeO
MnO	0.03	0.03	0.02	0.03	0.05	0.07	0.05	0.15	MnO
MgO	0.55	1.67	1.56	1.53	1.03	2.11	0.11	8.95	MgO
CaO	0.30	0.68	0.49	0.79	0.94	3.68	0.84	6.68	CaO
Na_2O	5.51	0.08	0.69	5.21	3.24	7.92	2.83	1.96	Na_2O
K_2O	0.18	4.09	4.73	0.81	3.20	0.26	0.63	1.03	K_2O
P_2O_5	0.03	0.03	0.01	0.07	0.05	0.24	0.04	0.10	P_2O_5
H_2O	0.67	1.83	1.73	1.06	1.08	0.82	0.61	4.41	H_2O
S	0.00	0.00	0.00	0.19	0.01	0.07	0.01	0.00	S
CO_2	0.34	0.81	0.38	0.82	1.08	0.15	0.58	0.15	CO_2
OTHER	0.03	0.09	0.06	0.05	0.14	0.06	0.05	0.11	OTHER
O≡S				-0.08		-0.03			O≡S
TOTAL	99.48	99.44	100.18	99.48	99.42	99.32	98.64	100.34	TOTAL
Ni	<2	<2	<2	<2	<2	20	2	44	Ni
Cr	4	<4	<4	<3	<3	68	26	254	Cr
Sc									Sc
Cu	7	16	14	68	33	11	39	45	Cu
Zn	62	52	65	44	57	23	46	88	Zn
Rb	<2			9	36	4	<1		Rb
Sr	100	15	30	90	80	280	44	190	Sr
Ba	50	370	390	250	1040	60	163	280	Ba
Th				2.7					Th
U				1.5					U
Ta									Ta
Hf									Hf
Zr	343	351	250	124	161	146	44	25	Zr
Y	94	70	65	30	30	41	17	9	Y
La				8.9					La
Ce				20					Ce
Nd				11					Nd
Sm				2.76					Sm
Eu				0.76					Eu
Tb				0.6					Tb
Dy				4.3					Dy
Yb				2.36					Yb
Lu				0.37					Lu
FeO^*	2.14	2.07	1.15	2.96	3.38	4.50	2.08	9.43	FeO^*

97	3438-C5	Plagioclase-phyric rhyolite, massive lobe, southern flow (Fig. 137), Grassy Narrows Zone. Spherulitic with 2 - 4% plagioclase phenocrysts. Minor (less than 1%) quartz-filled fractures. Pervasively silicified.
98	3438-C3	Rhyolite hyaloclastite adjacent to aphyric rhyolite lobe (3438-C4), southern flow (Fig. 137), Grassy Narrows zone. 2 - 3% calcite in veinlets and small domains.
99	3438-C2	Rhyolite hyaloclastite adjacent to porphyritic rhyolite lobe (3438-C1), southern flow (Fig. 137), Grassy Narrows Zone. 10 - 15% quartz phenocrysts, 10% plagioclase phenocrysts, pervasive fine grained sericite.
100	2421-C1	Porphyritic rhyolite (unit 18d), Bakers Narrows Block. Sample from massive zone of a flow with a brecciated top. 5% plagioclase phenocrysts, 2% quartz phenocrysts.
101	2465-C1	Porphyritic rhyolite dyke (unit 17c) emplaced in felsic tuff and felsic flow, Sourdough Bay Block. Dyke contains mafic xenoliths in margins. 12% quartz phenocrysts, 5% plagioclase phenocrysts.
102	1552-C1	Felsic flow (unit 18a), Bear Lake Block. Aphyric.
***103**	6108-C1	Burley Lake rhyolite (unit 18a), massive flow-banded flow. 3% plagioclase phenocrysts, pumiceous texture (vesicles filled with quartz).
104	1051-C1	Northeast Arm mafic volcaniclastics (unit 19). Sample from centre of 41 cm thick tuff bed with 25% plagioclase crystals and 20% strongly flattened mafic lapilli.

	105	106	107	108	109	110	111	112	
	626-C1	1006-C1	441-C1	2541-C1	1548-C1	355-C1	442-C1	1417-C1	
SiO_2	51.15	57.25	54.25	54.60	57.20	58.30	45.55	53.00	SiO_2
TiO_2	0.54	0.44	0.43	0.43	0.42	0.38	0.60	0.64	TiO_2
Al_2O_3	16.37	15.10	14.86	14.81	14.85	14.05	15.24	19.35	Al_2O_3
Fe_2O_3	1.97	2.71	2.60	3.03	3.26	2.83	1.73	2.09	Fe_2O_3
FeO	7.75	6.11	9.47	8.51	7.94	7.30	14.33	5.05	FeO
MnO	0.16	0.16	0.20	0.20	0.18	0.19	0.19	0.12	MnO
MgO	7.20	4.46	4.79	4.54	3.56	4.03	9.91	2.90	MgO
CaO	5.93	7.20	5.16	5.97	5.71	6.44	1.81	4.98	CaO
Na_2O	2.69	3.19	1.63	2.07	1.51	1.10	0.05	3.54	Na_2O
K_2O	0.83	0.35	1.65	1.54	1.37	1.50	1.83	4.79	K_2O
P_2O_5	0.11	0.12	0.30	0.28	0.34	0.23	0.08	0.40	P_2O_5
H_2O	4.26	2.61	3.87	3.57	3.59	3.13	7.04	2.52	H_2O
S	0.02	0.10	0.03	0.02	0.03	0.03	0.01	0.01	S
CO_2	0.89	0.20	1.23	0.41	0.24	0.86	2.06	0.09	CO_2
OTHER	0.12	0.07	0.13	0.12	0.12	0.11	0.11	0.31	OTHER
O≡S	-0.01	-0.04	-0.01	-0.01	-0.01	-0.01			O≡S
TOTAL	99.98	100.03	100.59	100.09	100.31	100.47	100.54	99.79	TOTAL
Ni	38	18	<2	<2	2	2	101	19	Ni
Cr	184	120	8	12	15	23	244	70	Cr
Sc									Sc
Cu	64	73	184	189	146	166	143	97	Cu
Zn	94	77	106	113	90	87	108	62	Zn
Rb			24	23	23	36	15	108	Rb
Sr	255	165	280	345	325	305	10	690	Sr
Ba	220	130	480	370	380	350	200	1630	Ba
Th									Th
U									U
Ta									Ta
Hf									Hf
Zr	20		11	13	14	11	11	29	Zr
Y	9		15	14	13	12	16	18	Y
La									La
Ce									Ce
Nd									Nd
Sm									Sm
Eu									Eu
Tb									Tb
Dy									Dy
Yb									Yb
Lu									Lu
FeO^*	9.52	8.55	11.81	11.24	10.87	9.85	15.89	6.93	FeO^*

105	626-C1	Northeast Arm mafic volcaniclastics (unit 19) from 1.1 m thick lapilli tuff bed. Strongly foliated, 30 - 35% fragments, 10 - 15% plagioclase crystals.
106	1006-C1	Northeast Arm mafic volcaniclastics (unit 19). Sample from centre of a 21 cm thick tuff bed with 25% plagioclase crystals and 15% granule-size rock fragments.
107	441-C1	Little Spruce Lake andesite tuff and lapilli tuff (unit 24), crudely layered and composed of scoria clasts in a granular tuffaceous matrix. Strongly recrystallized. Analysis represents chip samples collected from least altered material at several locations on outcrop.
108	2541-C1	Little Spruce Lake andesitic lapilli tuff (unit 24). 10 - 15% plagioclase crystals, lens-shaped mafic lapilli.
109	1548-C1	Little Spruce Lake andesitic lapilli tuff (unit 24) with lens-shaped mafic lapilli.
110	355-C1	Little Spruce Lake andesitic lapilli tuff (unit 24). Analysis represents chip samples over a 1 m diameter area.
111	442-C1	Altered Little Spruce andesitic lapilli tuff (unit 24) directly below Cuprus-White Lake base metal mineralized zone.
112	1417-C1	Vick Lake andesitic tuff, member 2 (unit 25b).

	113	114	115	116	117	118	119	120	
	1212-C1	1212-C3	2544-C1	1036-C1	1036-C2	1036-C3	1045-C1	1045-C2	
SiO_2	55.20	58.70	56.60	57.40	56.05	54.50	52.10	52.95	SiO_2
TiO_2	0.54	0.55	0.70	0.73	0.66	0.76	0.64	0.72	TiO_2
Al_2O_3	16.61	15.86	16.57	16.79	17.20	17.89	20.00	19.25	Al_2O_3
Fe_2O_3	2.02	1.89	1.47	2.36	2.68	2.95	3.28	3.41	Fe_2O_3
FeO	6.41	5.60	6.58	5.83	5.36	5.57	4.27	4.31	FeO
MnO	0.16	0.12	0.18	0.17	0.18	0.19	0.12	0.13	MnO
MgO	3.69	2.59	2.22	2.48	2.50	2.69	2.94	2.84	MgO
CaO	6.67	4.56	4.03	5.57	6.57	6.45	6.02	6.69	CaO
Na_2O	4.25	0.92	2.14	3.38	3.69	3.61	4.43	4.77	Na_2O
K_2O	2.24	6.19	6.18	2.79	2.36	2.39	3.23	2.25	K_2O
P_2O_5	0.28	0.30	0.45	0.32	0.36	0.38	0.37	0.42	P_2O_5
H_2O	2.14	2.42	2.24	2.49	2.51	2.51	2.75	2.55	H_2O
S	0.03	0.18	0.45	0.03	0.07	0.02	0.01	0.01	S
CO_2	0.12	0.24	0.30	0.10	0.14	0.08	0.12	0.08	CO_2
OTHER	0.18	0.35	0.38	0.22	0.22	0.24	0.25	0.20	OTHER
O≡S	-0.01	-0.07	-0.18	-0.01	-0.02	-0.01			O≡S
TOTAL	100.53	100.40	100.31	100.65	100.53	100.22	100.53	100.58	TOTAL
Ni	22	14	2	4	10	7	28	20	Ni
Cr	112	38	8	23	34	34	85	59	Cr
Sc									Sc
Cu	121	166	270	138	175	164	139	140	Cu
Zn	85	116	138	72	67	74	83	75	Zn
Rb	54	150	123	62	50	50	76	54	Rb
Sr	385	560	800	615	640	725	705	680	Sr
Ba	770	1970	1920	960	940	1050	1060	640	Ba
Th									Th
U									U
Ta									Ta
Hf									Hf
Zr	49	69	58	64	52	63	27	55	Zr
Y	21	26	28	33	25	28	22	28	Y
La									La
Ce									Ce
Nd									Nd
Sm									Sm
Eu									Eu
Tb									Tb
Dy									Dy
Yb									Yb
Lu									Lu
FeO^*	8.23	7.30	7.90	7.95	7.77	8.22	7.22	7.38	FeO^*

113	1212-C1	Vick Lake andesitic tuff, member 3 (unit 25c). Sampled in A division, 20 cm above base of 4.15 m thick ABE bed.
114	1212-C3	Vick Lake andesitic tuff, member 3 (unit 25c). Sampled in B division, 3.65 m above base of 4.15 m thick ABE bed.
115	2544-C1	Vick Lake andesitic tuff, member 5 (unit 25e). Sample from a 2 m thick unit of thin AB beds; very fine grained porcellanous tuff representative of material that occurs as layers sporadically distributed throughout the unit.
116	1036-C1	Vick Lake andesitic tuff, member 5 (unit 25e). Sampled in A division, 20 cm above base of 5.65 m thick AB bed.
117	1036-C2	Vick Lake andesitic tuff, member 5 (unit 25e). Sampled in A division, 2.0 m above base of 5.65 m thick AB bed.
118	1036-C3	Vick Lake andesitic tuff, member 5 (unit 25e) Sampled in A division, 5.2 m above base of 5.65 m thick AB bed.
119	1045-C1	Vick Lake andesitic tuff, member 6 (unit 25f). Sampled in A division 5 cm above base of 5.26 m thick AB bed.
120	1045-C2	Vick Lake andesitic tuff, member 6 (unit 25f). Sampled in A division 2.8 m above base of 5.26 m thick AB bed.

	121	**122**	**123**	**124**	**125**	**126**	**127**	**128**	
	1045-C3	1321-C1	254-C1	1569-C1	2385-C1	453-C1	453-C2	1010-C1	
SiO_2	54.15	66.30	66.90	67.35	68.20	71.55	73.65	55.00	SiO_2
TiO_2	0.74	0.32	0.31	0.30	0.28	0.19	0.17	0.70	TiO_2
Al_2O_3	17.96	12.81	12.76	12.89	12.69	12.08	12.17	17.15	Al_2O_3
Fe_2O_3	2.98	1.40	2.28	2.70	2.80	1.14	0.39	1.40	Fe_2O_3
FeO	4.56	6.33	5.55	5.56	5.18	4.27	2.06	6.56	FeO
MnO	0.14	0.16	0.10	0.12	0.12	0.12	0.04	0.06	MnO
MgO	2.54	2.62	1.71	1.13	1.73	1.10	0.99	3.94	MgO
CaO	6.56	1.36	3.13	3.90	1.56	1.53	1.17	1.68	CaO
Na_2O	4.22	2.51	2.29	2.56	2.46	3.15	3.06	6.05	Na_2O
K_2O	3.24	2.62	2.39	1.61	2.95	2.43	4.65	1.54	K_2O
P_2O_5	0.43	0.16	0.18	0.16	0.13	0.06	0.05	0.24	P_2O_5
H_2O	2.16	2.45	2.04	1.75	2.03	1.60	0.82	2.94	H_2O
S	0.03	0.05	0.01	0.00	0.00	0.02	0.02	0.20	S
CO_2	0.07	0.70	0.79	0.20	0.24	0.64	0.86	1.98	CO_2
OTHER	0.24	0.17	0.15	0.11	0.12	0.11	0.12	0.21	OTHER
O≡S	-0.01	-0.02				-0.01	-0.01	-0.08	O≡S
TOTAL	100.01	99.94	100.59	100.34	100.49	99.98	100.21	99.57	TOTAL
Ni	14	<2	<2	<2	<2	<2	<2	30	Ni
Cr	38	4	<3	<3	<3	<3	<3	128	Cr
Sc									Sc
Cu	189	562	90	27	6	6	12	216	Cu
Zn	63	159	110	75	67	28	29	78	Zn
Rb	78		34	39	56	39	66		Rb
Sr	635	130	340	365	245	125	110	120	Sr
Ba	1040	550	720	430	680	730	860	330	Ba
Th									Th
U									U
Ta									Ta
Hf									Hf
Zr	59		34	26	35	263	324		Zr
Y	25		18	23	21	82	112		Y
La									La
Ce									Ce
Nd									Nd
Sm									Sm
Eu									Eu
Tb									Tb
Dy									Dy
Yb									Yb
Lu									Lu
FeO^*	7.24	7.59	7.60	7.99	7.70	5.30	2.41	7.82	FeO^*

121 1045-C3 Vick Lake andesitic tuff, member 6 (unit 25e). Sampled at top of A division, 4.6 m above base of 5.26 m thick AB bed.

122 1321-C1 White Lake dacite tuff (unit 26c). Fine grained indistinctly bedded reworked tuff/greywacke with 15% fine grained quartz.

123 254-C1 White Lake dacite tuff (unit 24b), oligomictic clast population, strongly foliated, 2 - 3% quartz grains.

124 1569-C1 White Lake dacite tuff (unit 26a) with weakly defined layering, 20% fine grained quartz, sporadic pumice fragments.

125 2385-C1 White Lake dacite tuff (unit 26b) with approximately 20% strongly flattened pumice fragments.

126 453-C1 Two Portage Lake rhyolite crystal tuff (unit 27) 0.85 m above base of 5.9 m thick bed (Fig. 51c). 20 - 25% quartz phenocrysts, 15% plagioclase phenocrysts, and 0.5% fracture-filling quartz, calcite and sericite.

127 453-C2 Two Portage Lake rhyolite crystal tuff (unit 27) 4.5 m above base of 5.9 m thick bed (Fig. 51c). Same bed as 453-C1. 4% quartz phenocrysts, 3% plagioclase phenocrysts, and 0.5% fracture-filling quartz.

128 1010-C1 Chloritic mudstone (unit 33), Scotty Lake Block. Bedding 0.1 - 15 cm defined by colour, from light grey to dark green. Sample represents a single homogeneous layer.

	129	**130**	**131**	**132**	**133**	**134**	**135**	**136**	
	1002-C1	599-C1	1009-C1	254-8	1312-1	1241-C1	1230-C1	1232-C1	
SiO_2	63.75	52.77	45.35	47.3	47.70	46.38	46.92	47.10	SiO_2
TiO_2	0.36	1.43	1.74	1.80	1.92	1.55	2.91	2.64	TiO_2
Al_2O_3	15.44	14.29	13.19	13.4	13.2	15.19	12.03	11.10	Al_2O_3
Fe_2O_3	1.77	4.04	1.06	2.9	4.3	2.72	8.90	5.58	Fe_2O_3
FeO	3.93	7.09	12.57	11.4	10.1	11.08	11.06	12.59	FeO
MnO	0.13	0.19	0.17	0.19	0.15	0.21	0.25	0.25	MnO
MgO	1.13	4.28	4.23	6.6	6.9	7.17	4.76	3.41	MgO
CaO	1.49	8.45	5.99	8.8	8.6	8.14	7.26	6.78	CaO
Na_2O	6.18	3.09	2.61	1.9	2.3	3.03	4.05	2.81	Na_2O
K_2O	2.83	0.33	0.88	0.4	0.8	0.32	0.42	0.33	K_2O
P_2O_5	0.13	0.25	0.19	0.16	0.19	0.14	0.22	0.30	P_2O_5
H_2O	1.76	2.94	3.49	3.22	3.06	4.08	3.18	3.18	H_2O
S	0.18	0.10	0.12	0.1	0.01	0.00	0.00	0.01	S
CO_2	0.73	0.71	8.37	0.9	0.22	0.67	0.09	4.67	CO_2
OTHER	0.13	0.09	0.13	0.13	0.12	0.07	0.08	0.06	OTHER
O≡S	-0.07	-0.04	-0.05	-0.04					O≡S
TOTAL	99.87	100.01	100.04	99.16	99.57	100.75	102.13	100.81	TOTAL
Ni	6	28	16			37	13	<1	Ni
Cr	12	50	25			55	73	36	Cr
Sc									Sc
Cu	66	76	47			82	90	15	Cu
Zn	105	117	158			85	151	100	Zn
Rb						<1	<1	<1	Rb
Sr	120	305	130			161	191	165	Sr
Ba	800	210	290			36	<15	<15	Ba
Th									Th
U									U
Ta									Ta
Hf									Hf
Zr		168		66	91	81	123	143	Zr
Y		33		27	31	25	32	31	Y
La									La
Ce									Ce
Nd									Nd
Sm									Sm
Eu									Eu
Tb									Tb
Dy									Dy
Yb									Yb
Lu									Lu
FeO^*	5.52	10.73	13.52	14.01	13.97	13.53	19.07	17.61	FeO^*

129	1002-C1	Laminated siltstone-mudstone (unit 33), Scotty Lake Block. Laminae 1 - 3 mm, reddish brown and light grey-green, defined by the abundance of fine grained stilpnomelane.
130	599-C1	Mafic siltstone (unit 34a) from base of a 25 cm thick normally size graded bed, Scotty Lake Block. 0.5% fracture-filling calcite.
131	1009-C1	Ankerite-quartz-chlorite schist (unit 37a), Scotty lake Block. Laminated, microfolded, alternating laminae of carbonate-quartz and chlorite-epidote-quartz.
132	254-8	White Lake Sill (unit 39); fine grained chilled margin.
133	1312-C1	White Lake Sill (unit 39); fine grained chilled margin.
***134**	1241-C1	Gabbro, White Lake Sill (unit 39a).
***135**	1230-C1	Ferrogabbro, White Lake Sill (unit 39b).
***136**	1232-C1	Ferrodiorite, White Lake Sill (unit 39c). 4% quartz.

	137	**138**	**139**	**140**	**141**	**142**	**143**	**144**	
	1229-C1	276-1	2084-1	3401-C1	3419-C1	3146-C1	2086-1	2083-1	
SiO_2	45.94	51.6	48.70	48.89	49.77	49.96	48.05	46.90	SiO_2
TiO_2	1.86	0.2	0.58	0.73	0.78	0.72	0.31	0.29	TiO_2
Al_2O_3	14.42	4.4	14.02	13.40	13.46	14.78	12.97	12.42	Al_2O_3
Fe_2O_3	3.83	1.2	1.54	1.40	1.55	2.54	1.27	1.47	Fe_2O_3
FeO	10.11	8.01	7.55	8.83	9.05	7.47	5.60	5.77	FeO
MnO	0.18	0.20	0.17	0.18	0.21	0.16	0.14	0.14	MnO
MgO	6.63	19.1	10.91	8.86	8.00	7.31	12.74	13.67	MgO
CaO	10.74	14.1	10.35	9.40	9.39	10.23	14.57	14.38	CaO
Na_2O	2.39	0.3	2.41	2.79	2.64	2.43	0.61	0.50	Na_2O
K_2O	0.16	0.1	0.31	0.47	0.92	0.86	0.04	0.04	K_2O
P_2O_5	0.17	0.02	0.06	0.08	0.10	0.05	0.04	0.03	P_2O_5
H_2O	3.42	2.79	3.23	3.23	2.46	2.88	3.19	3.45	H_2O
S	0.05	0.00	0.01	0.00	0.01	0.01	0.03	0.02	S
CO_2	0.09	0.08	0.17	1.48	0.70	0.48	0.14	0.24	CO_2
OTHER	0.07	0.14	0.20	0.13	0.16	0.09	0.28	0.27	OTHER
O≡S	-0.02						-0.01	-0.01	O≡S
TOTAL	100.04	102.24	100.21	99.87	99.20	99.97	99.97	99.58	TOTAL
Ni	35	131	186	83	80	45	242	256	Ni
Cr	108	520	820	111	316	88	1440	1440	Cr
Sc									Sc
Cu	90	68	86	111	178	44	72	45	Cu
Zn	40	112	100	64	93	39	56	60	Zn
Rb	<1	9	2	11	22	11	<2	<2	Rb
Sr	198	89	190	203	288	228	75	75	Sr
Ba	<15	160	100	131	263	249	80	70	Ba
Th			0.2						Th
U			0.1						U
Ta									Ta
Hf									Hf
Zr	70	1	27	31	40	22	8	8	Zr
Y	25	5	15	18	17	18	9	9	Y
La			2.5						La
Ce			8						Ce
Nd			5						Nd
Sm			1.29						Sm
Eu			0.51						Eu
Tb			0.4						Tb
Dy			2.8						Dy
Yb			1.50						Yb
Lu			0.24						Lu
FeO^*	13.56	9.09	8.94	10.09	10.44	9.76	6.74	7.09	FeO^*

***137**	1229-C1	Pyroxene-phyric gabbro, White Lake Sill (unit 39d). 3 m below top of sill.
138	276-1	Pyroxenite (unit 40b), small body west of Wonderland Lake, Bear Lake Block.
139	2084-1	Chilled base, Mikanagan Lake Sill (unit 41). Within 4 m of west contact of sill.
***140**	3401-1	Chilled base, Mikanagan Lake Sill (unit 41), 3 cm from western contact. 2% fracture-filling epidote, calcite and chlorite.
***141**	3419-1	Chilled base, Mikanagan Lake Sill (unit 41), within 0.5 m of western contact.
***142**	3146-1	Chilled upper margin, Mikanagan Lake Sill (unit 41), within 1.5 m of eastern contact.
143	2086-1	Gabbronorite, Mikanagan Lake Sill (unit 41a). 75 m above base of sill.
144	2083-1	Gabbronorite, Mikanagan Lake Sill (unit 41a). 150 m above base of sill.

	145	**146**	**147**	**148**	**149**	**150**	**151**	**152**	
	2087-1	2088-1	2082-1	2081-1	2089-1	2090-1	2090-2	2079-1	
SiO_2	47.90	46.30	45.10	46.90	48.60	48.10	47.80	46.00	SiO_2
TiO_2	0.25	0.22	0.26	0.23	0.28	0.55	1.04	1.25	TiO_2
Al_2O_3	13.87	21.34	19.68	20.83	16.87	16.90	15.55	15.40	Al_2O_3
Fe_2O_3	1.54	1.39	1.57	1.58	1.34	2.59	3.50	5.09	Fe_2O_3
FeO	5.09	4.71	4.34	3.92	6.67	8.20	10.59	10.02	FeO
MnO	0.13	0.11	0.11	0.11	0.16	0.17	0.18	0.17	MnO
MgO	12.08	9.41	9.16	7.42	9.16	7.61	6.33	6.00	MgO
CaO	15.15	8.93	15.02	14.70	12.27	9.13	9.49	9.89	CaO
Na_2O	0.51	2.53	1.47	1.66	1.28	2.44	1.54	2.59	Na_2O
K_2O	0.01	0.61	0.05	0.10	0.11	0.13	0.06	0.40	K_2O
P_2O_5	0.01	0.02	0.01	0.01	0.03	0.06	0.06	0.05	P_2O_5
H_2O	3.05	4.72	3.36	2.81	3.44	3.71	3.89	2.91	H_2O
S	0.03	0.00	tr.	0.00	0.03	0.03	0.07	0.06	S
CO_2	0.07	0.12	0.10	0.10	0.10	0.19	0.38	0.17	CO_2
OTHER	0.21	0.07	0.10	0.07	0.07	0.08	0.12	0.09	OTHER
O≡S	-0.01				-0.01	-0.01	-0.03	-0.02	O≡S
TOTAL	99.89	100.48	100.33	100.44	100.40	99.88	100.57	100.07	TOTAL
Ni	208	92	118	83	58	68	63	38	Ni
Cr	1050	152	267	119	27	38	18	11	Cr
Sc									Sc
Cu	50	10	146	53	230	277	700	414	Cu
Zn	53	60	45	42	64	72	70	83	Zn
Rb	<2	2	<2	<2	<2	<2	<2	<2	Rb
Sr	75	145	130	140	100	105	95	115	Sr
Ba	40	60	60	80	50	80	40	70	Ba
Th									Th
U									U
Ta									Ta
Hf									Hf
Zr	6	14	6	6	7	12	16	6	Zr
Y	6	9	8	8	9	12	11	8	Y
La									La
Ce									Ce
Nd									Nd
Sm									Sm
Eu									Eu
Tb									Tb
Dy									Dy
Yb									Yb
Lu									Lu
FeO^*	6.48	5.96	5.75	5.34	7.88	10.53	13.74	14.60	FeO^*

145	2087-1	Gabbronorite, Mikanagan Lake Sill (unit 41a). 205 m above base of sill.
146	2088-1	Gabbro, Mikanagan Lake Sill (unit 41b). 305 m above base of sill.
147	2082-1	Gabbro, Mikanagan Lake Sill (unit 541b). 395 m above base of sill.
148	2081-1	Gabbro, Mikanagan Lake Sill (unit 41b). 535 m above base of sill.
149	2089-1	Oikocrystic gabbronorite, Mikanagan Lake Sill (unit 41c). 650 m above base of sill.
150	2090-1	Transition gabbro, Mikanagan Lake Sill (unit 41d). 730 m above base of sill.
151	2090-2	Ferrogabbro, Mikanagan Lake Sill (unit 41f). 740 m above base of sill.
152	2079-1	Ferrogabbro, Mikanagan Lake Sill (unit 41f). 790 m above base of sill.

	153	154	155	156	157	158	159	160	
	2065-1	2292-1	2078-1	2092-2	2092-1	2077-1	2112-2	2112-1	
SiO_2	42.05	47.35	63.95	65.55	62.60	72.30	68.20	73.70	SiO_2
TiO_2	2.88	2.76	1.19	0.71	0.92	0.32	0.51	0.29	TiO_2
Al_2O_3	12.68	11.45	10.89	11.90	12.06	11.32	11.39	11.40	Al_2O_3
Fe_2O_3	7.99	4.74	6.51	6.14	4.51	2.12	1.35	0.74	Fe_2O_3
FeO	13.02	14.60	6.07	4.56	8.44	3.89	5.87	3.89	FeO
MnO	0.24	0.28	0.21	0.15	0.14	0.07	0.08	0.05	MnO
MgO	6.04	2.47	0.53	0.19	0.43	0.18	0.07	0.05	MgO
CaO	10.12	10.61	4.26	4.46	5.43	2.79	3.44	1.88	CaO
Na_2O	1.99	3.08	3.50	4.02	3.84	4.48	4.18	4.85	Na_2O
K_2O	0.16	0.45	0.64	0.54	0.43	0.44	0.37	0.37	K_2O
P_2O_5	0.05	0.84	0.34	0.17	0.34	0.04	0.09	0.06	P_2O_5
H_2O	2.99	1.88	1.96	1.57	1.46	1.06	1.61	1.01	H_2O
S	0.23	0.00	0.00	0.00	0.00	0.02	0.08	0.08	S
CO_2	0.12	0.12	0.64	0.14	0.14	0.56	2.49	1.35	CO_2
OTHER	0.05	0.05	0.04	0.05	0.04	0.03	0.07	0.03	OTHER
O≡S	-0.09					-0.01	-0.03	-0.03	O≡S
TOTAL	100.52	100.68	100.73	100.15	100.78	99.61	99.77	99.72	TOTAL
Ni	26	<2	<2	<2	<2	<2	<2	4	Ni
Cr	5	<3	<3	3	3	<3	<3	8	Cr
Sc									Sc
Cu	147	8	4	3	8	5	38	9	Cu
Zn	112	62	56	60	45	30	36	22	Zn
Rb	<2	<2	9	2	2	<2	<2	2	Rb
Sr	90	250	120	195	200	155	390	170	Sr
Ba	70	80	110	130	90	40	90	70	Ba
Th									Th
U									U
Ta									Ta
Hf									Hf
Zr	<1	22	135	240	166	397	283	348	Zr
Y	6	27	55	107	80	132	108	109	Y
La									La
Ce									Ce
Nd									Nd
Sm									Sm
Eu									Eu
Tb									Tb
Dy									Dy
Yb									Yb
Lu									Lu
FeO^*	20.21	18.87	11.93	10.08	12.50	5.80	7.08	4.56	FeO^*

153	2065-1	Ferrogabbro, Mikanagan Lake Sill (unit 41f). 830 m above base of sill.
154	2292-1	Ferrogabbro, Mikanagan Lake Sill (unit 41f). 905 m above base of sill.
155	2078-1	Ferrotonalite, Mikanagan Lake Sill (unit 41g). 975 m above base of sill.
156	2092-2	Ferrotonalite, Mikanagan Lake Sill (unit 41g). 1100 m above base of sill. Possibly pegmatoid; characterized by very large (up to 5 cm) elongate pyroxenes.
157	2092-1	Ferrotonalite, Mikanagan Lake Sill (unit 41g). 1100 m above base of sill.
158	2077-1	Ferrotonalite, Mikanagan Lake Sill (unit 41g). 1160 m above base of sill.
159	2112-2	Ferrotonalite, Mikanagan Lake Sill (unit 41g). 1185 m above base of sill. Represents top of ferrotonalite zone; grades to 2112-1 over 3 m.
160	2112-1	Micrographic leucotonalite, Mikanagan Lake Sill (unit 41h). 1195 m above base of sill.

	161	**162**	**163**	**164**	**165**	**166**	**167**	**168**	
	2096-1	2076-1	2312-2	2317-2	4384-2	4376-C1	4391-1	4088-C2	
SiO_2	73.80	75.15	48.3	54.2	47.96	48.10	49.41	45.90	SiO_2
TiO_2	0.34	0.35	1.78	0.43	0.44	0.35	1.27	0.08	TiO_2
Al_2O_3	11.22	11.21	13.6	14.7	14.82	11.10	14.69	20.15	Al_2O_3
Fe_2O_3	1.10	1.88	3.0	2.7	1.88	1.55	2.50	1.57	Fe_2O_3
FeO	3.12	1.76	11.17	9.83	6.70	6.54	9.66	4.81	FeO
MnO	0.05	0.05	0.22	0.15	0.15	0.16	0.18	0.12	MnO
MgO	0.13	0.15	6.3	4.5	9.58	12.47	6.07	7.72	MgO
CaO	3.08	1.90	8.9	6.6	13.01	16.37	10.67	15.07	CaO
Na_2O	4.84	5.86	2.0	1.8	1.41	0.82	2.22	1.18	Na_2O
K_2O	0.17	0.30	0.6	0.3	0.11	0.08	0.18	0.13	K_2O
P_2O_5	0.04	0.01	0.15	0.19	0.04	0.02	0.13	0.00	P_2O_5
H_2O	0.93	0.39	2.88	3.36	2.90	2.30	3.81	3.23	H_2O
S	tr.	tr.	0.01	0.01	0.03	0.00	0.00	0.00	S
CO_2	1.47	0.90	0.06	0.17	0.36	0.02	0.26	0.24	CO_2
OTHER	0.03	0.04	0.11	0.10	0.11	0.13	0.08	0.07	OTHER
O≡S					-0.01				O≡S
TOTAL	100.32	99.95	99.08	99.04	99.49	100.01	101.13	100.27	TOTAL
Ni	<2	<2	54	12	116	161	41	52	Ni
Cr	5	<3	79	20	348	479	129	215	Cr
Sc									Sc
Cu	8	5	94	184	50	96	123	7	Cu
Zn	20	22	120	137	66	66	95	34	Zn
Rb	<2	4	14	8	<1	<1	<1	<1	Rb
Sr	150	160	206	276	140	119	164	104	Sr
Ba	30	180	380	240	31	58	15	115	Ba
Th	3.3								Th
U	1.2								U
Ta									Ta
Hf									Hf
Zr	373	377	73	12	21	14	54	5	Zr
Y	120	123	29	15	16	12	25	3	Y
La	20.0								La
Ce	58								Ce
Nd	32								Nd
Sm	9.83								Sm
Eu	2.04								Eu
Tb	2.5								Tb
Dy	16.9								Dy
Yb	11.0								Yb
Lu	1.65								Lu
FeO^*	4.11	3.45	13.87	12.26	8.39	7.93	11.91	6.22	FeO^*

161	2096-1	Micrographic leucotonalite, Mikanagan Lake Sill (unit 41h). 1220 m above base of sill.
162	2076-1	Porphyritic micrographic leucotonalite, Mikanagan Lake Sill (unit 41h). 1235 m above base of sill.
163	2312-2	Chilled margin, Benn Lake intrusion (unit 41). Sample from east margin of the intrusion, 25 cm from contact with basaltic andesite host rocks (unit 1a).
164	2317-2	Chilled margin, Benn Lake intrusion (unit 41). Sample from west margin of the intrusion.
***165**	4384-1	Chilled margin, Embury Lake intrusion (unit 41).
***166**	4376-C1	Gabbro, Embury Lake intrusion (unit 41b).
***167**	4391-1	Quartz ferrodiorite, Embury Lake intrusion (unit 41g).
***168**	4088-C2	Gabbronorite, Hook Lake intrusion (unit 41a).

	169	170	171	172	173	174	175	176	
	4093-C1	566-C1	4077-C1	4013-C1	7163-C1	273-1	279-3	4345-C1	
SiO_2	43.91	47.15	49.27	55.77	49.85	49.8	56.2	49.76	SiO_2
TiO_2	0.65	1.35	0.36	0.67	0.26	0.19	1.18	1.12	TiO_2
Al_2O_3	16.54	13.91	13.86	14.45	14.76	13.2	12.7	13.14	Al_2O_3
Fe_2O_3	4.26	2.38	1.38	2.20	3.22	2.6	5.0	7.29	Fe_2O_3
FeO	11.96	10.01	9.14	10.64	8.65	7.32	10.29	11.02	FeO
MnO	0.22	0.18	0.16	0.19	0.21	0.18	0.16	0.23	MnO
MgO	6.32	7.55	10.66	3.64	6.74	10.7	2.4	4.99	MgO
CaO	10.56	10.65	8.39	5.31	11.60	11.0	5.3	6.39	CaO
Na_2O	1.32	2.50	2.42	3.60	1.97	0.7	2.7	2.87	Na_2O
K_2O	0.31	0.20	0.37	0.64	0.29	0.5	0.6	0.40	K_2O
P_2O_5	0.02	0.13	0.03	0.17	0.10	0.04	0.44	0.11	P_2O_5
H_2O	4.09	3.06	4.44	3.15	2.73	3.29	2.48	3.56	H_2O
S	0.01	0.03	0.00	0.02	0.01	0.01	0.00	0.00	S
CO_2	0.07	1.09	0.41	0.69	0.08	0.39	0.23	0.09	CO_2
OTHER	0.09	0.08	0.16	0.12	0.08	0.11	0.05	0.06	OTHER
O≡S		-0.01		-0.01					O≡S
TOTAL	100.33	100.26	101.05	101.25	100.55	100.03	99.73	101.03	TOTAL
Ni	<1	56	167	16	3	65	<2	<1	Ni
Cr	81	88	690	48	58	129	11	67	Cr
Sc									Sc
Cu	326	127	57	191	20	47	17	83	Cu
Zn	37	74	32	82	77	94	111	123	Zn
Rb	<1	<2	<1	<1	1	11	13	<1	Rb
Sr	105	220	48	151	303	280	92	93	Sr
Ba	143	80	154	424	140	250	200	67	Ba
Th									Th
U									U
Ta									Ta
Hf									Hf
Zr	10	64	11	34	22	<1	56	24	Zr
Y	8	27	1	22	11	6	37	18	Y
La									La
Ce									Ce
Nd									Nd
Sm									Sm
Eu									Eu
Tb									Tb
Dy									Dy
Yb									Yb
Lu									Lu
FeO^*	15.79	12.15	10.38	12.62	11.55	9.66	14.79	17.58	FeO^*

***169**	4093-C1	Ferrograbbro, Hook Lake intrusion (unit 41f).
170	566-C1	Gabbro, Johnson Lake sill (unit 42a). Strongly foliated.
***171**	4077-C1	Equigranular diorite, Hook Lake diorite (unit 42a). Subequal amounts of clinopyroxene and lath-shaped plagioclase.
***172**	4013-C1	Equigranular diorite (unit 42b) representative of the type commonly associated with, and younger than, unit 49 rhyolite intrusions. Hook Lake.
***173**	7163-C1	Town diorite (unit (42b).
174	273-1	Wonderland Lake gabbro unit 42b).
175	279-3	Wonderland Lake quartz diorite (unit 42b). Quartz- and magnetite-rich.
***176**	4345-C1	Big Island diorite (unit 42b).

	177	**178**	**179**	**180**	**181**	**182**	**183**	**184**	
	5330-C1	3722-C1	4368-C1	5427-C1	6189-C1	4440-C2	4440-C3	4440-C4	
SiO_2	51.18	49.60	54.20	55.38	70.83	50.40	49.93	48.47	SiO_2
TiO_2	0.62	1.16	1.00	0.98	0.18	0.66	0.61	0.57	TiO_2
Al_2O_3	14.06	13.95	12.29	12.81	11.30	17.51	17.31	18.85	Al_2O_3
Fe_2O_3	1.97	2.18	6.60	5.47	0.65	2.82	2.37	2.49	Fe_2O_3
FeO	12.22	10.19	10.19	10.54	2.31	10.23	8.42	8.26	FeO
MnO	0.23	0.17	0.18	0.23	0.07	0.27	0.22	0.20	MnO
MgO	5.92	7.18	3.31	1.93	0.69	4.05	4.19	4.07	MgO
CaO	7.64	9.19	3.12	4.48	2.55	5.96	7.78	7.20	CaO
Na_2O	3.17	2.33	3.45	3.37	1.81	3.16	3.34	3.51	Na_2O
K_2O	0.17	0.14	0.82	0.35	3.33	0.64	1.08	0.72	K_2O
P_2O_5	0.09	0.12	0.37	0.49	0.05	0.10	0.05	0.05	P_2O_5
H_2O	3.34	3.39	2.93	2.75	1.16	3.27	3.27	3.65	H_2O
S	0.01	0.05	0.00	0.00	0.00	0.00	0.01	0.00	S
CO_2	0.08	0.28	1.85	2.08	3.72	1.04	1.47	1.06	CO_2
OTHER	0.06	0.07	0.08	0.06	0.10	0.06	0.10	0.07	OTHER
O≡S		-0.02							O≡S
TOTAL	100.76	99.98	100.39	100.92	98.75	100.17	100.15	99.17	TOTAL
Ni	14	68	<1	<1	<1	<1	51	2	Ni
Cr	60	147	36	26	23	42	62	54	Cr
Sc									Sc
Cu	107	99	65	43	31	22	67	46	Cu
Zn	120	103	165	120	49	127	95	88	Zn
Rb	<2	<2	<1	1	26	7	19	6	Rb
Sr	73	130	86	143	64	170	163	188	Sr
Ba	98	30	227	102	509	135	323	197	Ba
Th									Th
U									U
Ta									Ta
Hf									Hf
Zr	20		36	41	105	12	22	11	Zr
Y	17		20	24	23	17	24	14	Y
La									La
Ce									Ce
Nd									Nd
Sm									Sm
Eu									Eu
Tb									Tb
Dy									Dy
Yb									Yb
Lu									Lu
FeO^*	13.99	12.15	16.13	15.46	2.89	12.77	10.55	10.50	FeO^*

177	5330-C1	Big Island diorite (unit 42b).
178	3722-C1	Quartz diorite (unit 42g), Sourdough Bay Block.
***179**	4368-C1	Big Island magnetiferous quartz diorite (unit 42j).
***180**	5427-C1	Big Island magnetiferous quartz diorite (unit 42j; Fig. 220).
***181**	6189-C1	Channing tonalite (unit 44).
***182**	4440-C2	Mafic volcanic xenolith displaying incipient recrystallization, Cliff Lake tonalite (unit 45b). Xenolith is angular, 45 cm across and contains few plagioclase, hornblende and quartz blasts.
***183**	4440-C3	Mafic volcanic xenolith displaying moderate recrystallization, Cliff Lake tonalite (unit 45b). Xenolith is angular, 50 x 80 cm with abundant plagioclase and hornblende blasts and rare quartz blasts.
***184**	4440-C4	Mafic volcanic xenolith displaying high degree of recrystallization, Cliff Lake tonalite (unit 45b). Xenolith is 60 x 100 cm with blocky plagioclase blasts and acicular hornblende.

	185	186	187	188	189	190	191	192	
	5445-C2	5451-C1	5445-C1	4440-C1	5359-C1	7174-C1	4448-C1	4526-C1	
SiO_2	50.30	50.44	67.23	72.97	76.11	63.38	69.43	70.39	SiO_2
TiO_2	0.57	0.09	0.40	0.25	0.15	0.50	0.26	0.27	TiO_2
Al_2O_3	16.47	15.73	13.48	12.72	12.21	15.81	13.08	13.45	Al_2O_3
Fe_2O_3	2.61	1.50	1.70	1.02	0.43	1.67	0.84	1.38	Fe_2O_3
FeO	8.99	8.16	4.22	2.51	1.10	4.67	3.31	2.90	FeO
MnO	0.20	0.23	0.10	0.07	0.03	0.11	0.09	0.08	MnO
MgO	5.85	5.28	1.15	0.51	0.44	1.30	1.89	1.13	MgO
CaO	9.27	8.55	4.57	2.84	2.01	5.66	2.35	3.96	CaO
Na_2O	2.61	1.93	3.12	3.93	4.21	2.95	4.19	3.45	Na_2O
K_2O	0.23	0.32	0.42	0.81	0.69	0.68	0.71	0.70	K_2O
P_2O_5	0.06	0.07	0.11	0.08	0.02	0.12	0.08	0.08	P_2O_5
H_2O	2.90	4.20	1.78	4.12	0.66	2.17	1.73	1.47	H_2O
S	0.01	0.01	0.00	0.00	0.22	0.01	0.00	0.00	S
CO_2	0.22	3.53	0.73	0.36	0.03	0.24	0.49	0.31	CO_2
OTHER	0.07	0.07	0.06	0.06	0.06	0.06	0.06	0.08	OTHER
O≡S					-0.09				O≡S
TOTAL	100.36	100.11	99.07	102.25	98.28	99.33	98.51	99.65	TOTAL
Ni	7	28	<1	1	12	<1	7	<1	Ni
Cr	73	77	26	38	23	32	62	44	Cr
Sc									Sc
Cu	95	49	49	<4	50	39	27	16	Cu
Zn	84	98	58	39	15	40	45	61	Zn
Rb	<1	<1	<1	4	4	4	3	8	Rb
Sr	186	132	145	117	75	178	93	162	Sr
Ba	59	118	136	222	215	124	189	238	Ba
Th					3.6				Th
U					2.1				U
Ta									Ta
Hf									Hf
Zr	26	13	31	71	85	51	59	64	Zr
Y	23	17	19	14	14	19	23	27	Y
La					7.7				La
Ce					16				Ce
Nd					6				Nd
Sm					1.36				Sm
Eu					0.35				Eu
Tb					0.3				Tb
Dy					2.2				Dy
Yb					2.63				Yb
Lu					0.47				Lu
FeO^*	11.34	9.51	5.75	3.43	1.49	6.17	4.07	4.14	FeO^*

***185**	5445-C2	Cliff Lake quartz diorite (unit 45a) from 10 m wide tabular xenolith in unit 45b tonalite. Mafic minerals altered to chlorite.
***186**	5451-C1	Cliff Lake quartz diorite (unit 45a) from large xenolith in unit 45b tonalite. Altered, mafic mineral to chlorite and 7% calcite as veinlets and irregular domains.
***187**	5445-C1	Cliff Lake tonalite (unit 45b). Relatively inclusion-free sample of a phase of the pluton characterized by abundant large xenolites. 10% mafic clots are considered to be assimilated xenoliths.
***188**	4440-C1	Cliff Lake tonalite (unit 45b). Inclusion-free sample of a phase of the pluton characterized by abundant large xenoliths.
***189**	5359-C1	Cliff Lake tonalite (unit 45b). Inclusion-free sample from 25 cm wide dyke.
***190**	7174-C1	Cliff Lake tonalite (unit 45c). Inclusion-free sample 2 m from chilled contact with xenolith - rich tonalite (unit 45b).
***191**	4448-C1	Cliff Lake tonalite (unit 45c), characterized by abundant small, almost completely assimilated xenoliths.
***192**	4526-C1	Cliff Lake tonalite (unit 45c) with about 20% 0.5 - 5 cm, rounded, almost completely assimilated xenoliths.

	193	194	195	196	197	198	199	200	
	6184-C1	7169-C1	4503-C1	4449-C1	4459-C1	4447-C1	5382-C1	4346-C1	
SiO_2	76.58	73.41	73.50	74.80	73.18	77.49	71.03	76.02	SiO_2
TiO_2	0.14	0.19	0.18	0.18	0.15	0.03	0.23	0.17	TiO_2
Al_2O_3	11.90	11.76	11.97	12.17	11.37	11.68	13.11	10.65	Al_2O_3
Fe_2O_3	0.88	1.15	1.54	0.87	0.43	0.37	0.87	0.82	Fe_2O_3
FeO	0.75	2.44	2.68	1.89	1.02	0.41	3.39	3.51	FeO
MnO	0.02	0.05	0.03	0.04	0.04	0.02	0.06	0.03	MnO
MgO	0.20	0.38	0.26	0.33	0.55	0.01	1.87	1.55	MgO
CaO	1.31	2.13	2.06	1.97	3.14	1.55	0.77	0.41	CaO
Na_2O	3.95	3.96	3.84	4.48	4.92	5.14	1.69	0.44	Na_2O
K_2O	1.38	1.14	0.95	0.73	0.80	0.61	3.35	3.31	K_2O
P_2O_5	0.02	0.07	0.07	0.04	0.06	0.01	0.11	0.09	P_2O_5
H_2O	0.66	1.01	1.16	0.87	0.80	0.31	2.19	2.14	H_2O
S	0.05	0.00	0.00	0.01	0.04	0.03	0.00	0.00	S
CO_2	0.12	0.30	0.58	0.34	1.93	0.22	0.82	0.17	CO_2
OTHER	0.11	0.09	0.08	0.07	0.05	0.15	0.07	0.07	OTHER
O=S	-0.02				-0.02	-0.01			O=S
TOTAL	98.05	98.08	98.90	98.79	98.46	98.02	99.56	99.38	TOTAL
Ni	<1	<1	<1	<1	<1	4	1	<1	Ni
Cr	23	28	23	23	21	27	27	26	Cr
Sc									Sc
Cu	32	13	27	30	30	731	75	73	Cu
Zn	<15	19	26	39	26	19	108	56	Zn
Rb	11	10	13	3	6	5	35	25	Rb
Sr	77	144	122	105	66	69	16	<15	Sr
Ba	620	449	343	260	230	275	284	413	Ba
Th									Th
U									U
Ta									Ta
Hf									Hf
Zr	126	73	67	67	51	90	43	32	Zr
Y	30	28	36	39	27	34	21	14	Y
La									La
Ce									Ce
Nd									Nd
Sm									Sm
Eu									Eu
Tb									Tb
Dy									Dy
Yb									Yb
Lu									Lu
FeO^*	1.54	3.47	4.07	2.67	1.41	0.74	4.17	4.25	FeO^*

***193**	6184-C1	Cliff Lake tonalite (unit 45c), from the chilled margin of an internal intrusive contact. Represents uncontaminated composition of unit 45c, that elsewhere contains abundant assimilated xenoliths.
***194**	7169-C1	Cliff Lake tonalite (unit 45d) representing least altered material on the outcrop. 5% mafic clots are considered to be assimilated xenoliths.
***195**	4503-C1	Cliff Lake tonalite (unit 45d), representing the least altered material on the outcrop. 15% mafic clots, considered to be assimilated xenoliths.
***196**	4449-C1	Fine grained, quartz-phyric, micrographic tonalite, Cliff Lake tonalite (unit 45e). From an oval body of similar material intrusive into unit 45c tonalite.
***197**	4459-C1	Leucotonalite margin phase, Cliff Lake tonalite (unit 45f).
***198**	4447-C1	Aplite dyke cutting unit 45c tonalite, Cliff Lake pluton. Dyke is 15 - 25 cm wide.
***199**	5382-C1	Quartz porphyry (unit 48a). 5% quartz phenocrysts, slightly fractured with 0.5% fracture-filling ankerite.
***200**	4346-C1	Quartz porphyry (unit 48a). 15% quartz phenocrysts in a spherulitic groundmass.

	201	202	203	204	205	206	207	
	6181-C1	4015-C1	4002-C1	7170-C1	4592-C1	4589-C1	2358-C1	
SiO_2	68.95	75.57	76.30	72.22	72.59	75.70	54.00	SiO_2
TiO_2	0.20	0.14	0.17	0.14	0.22	0.24	1.27	TiO_2
Al_2O_3	12.71	11.17	10.90	13.55	10.17	10.50	19.63	Al_2O_3
Fe_2O_3	0.73	0.43	0.41	0.57	0.37	0.29	15.81	Fe_2O_3
FeO	2.93	1.57	1.58	2.94	2.96	4.06	0.52	FeO
MnO	0.05	0.04	0.04	0.04	0.11	0.07	0.02	MnO
MgO	1.05	0.37	0.41	0.60	1.31	1.30	0.33	MgO
CaO	2.04	1.33	1.21	1.12	2.18	0.55	0.67	CaO
Na_2O	3.17	3.82	3.81	6.39	3.11	2.54	1.79	Na_2O
K_2O	2.68	1.68	1.17	0.33	1.65	2.28	2.86	K_2O
P_2O_5	0.07	0.02	0.04	0.07	0.05	0.07	0.43	P_2O_5
H_2O	1.34	0.78	0.87	1.08	1.17	1.57	2.76	H_2O
S	0.02	0.01	0.00	0.01	0.10	0.01	0.00	S
CO_2	2.76	1.72	0.71	0.62	3.07	0.60	0.08	CO_2
OTHER	0.13	0.07	0.09	0.05	0.13	0.07	0.19	OTHER
O≡S	-0.01				-0.04			O≡S
TOTAL	98.82	98.72	97.71	99.73	99.15	99.85	100.36	TOTAL
Ni	16	6	4	<1	<1	<1	<1	Ni
Cr	31	19	25	25	21	27	<3	Cr
Sc								Sc
Cu	114	11	40	26	92	32	6	Cu
Zn	81	83	74	20	418	88	32	Zn
Rb	27	23	20	1	20	29	79	Rb
Sr	77	53	85	51	44	32	205	Sr
Ba	675	227	316	136	356	268	1340	Ba
Th		1.4						Th
U		0.8						U
Ta								Ta
Hf								Hf
Zr	57	82	107	97	116	60		Zr
Y	20	47	51	32	26	16		Y
La		10.4						La
Ce		28						Ce
Nd		17						Nd
Sm		4.40						Sm
Eu		1.17						Eu
Tb		1.0						Tb
Dy		7.7						Dy
Yb		6.10						Yb
Lu		0.91						Lu
FeO^*	3.59	1.96	1.95	3.45	3.29	4.32	14.75	FeO^*

***201**	6181-C1	Quartz-plagioclase porphyry (unit 48b), Big Island.
***202**	4015-C1	Borne Lake rhyolite (unit 49c), with 10% quartz and plagioclase phenocrysts in a spherulitic groundmass.
***203**	4002-C1	Borne Lake rhyolite (unit 49c), with 7% plagioclase and 5% quartz phenocrysts in spherulitic, flow banded groundmass.
***204**	7170-C1	Aphyric rhyolite (unit 49). 1% fracture-filling quartz and calcite.
***205**	4592-C1	Porphyritic rhyolite dyke (unit 49c), Manistikwan Lake Block. 7% quartz and 2% plagioclase phenocrysts in a spherulitic groundmass.
***206**	4589-C1	Porphyritic rhyolite dyke (unit 49C), Manistikwan Lake Block. Dyke is 1.2 m wide.
***207**	2358-C1	Hematiferous regolith developed in Amisk Group pillowed flow, at contact with Missi Group. Old Highway 10 at Northstar Road.

	208	**209**	**210**	**211**	**212**	**213**	**214**	**215**	
								2352-C1	
SiO_2	58.0	50.5	49.6	62.5	47.7	49.6	54.2	74.10	SiO_2
TiO_2	0.79	0.73	0.70	0.96	0.71	0.63	0.96	0.63	TiO_2
Al_2O_3	19.5	17.4	15.1	14.9	16.2	15.4	15.0	10.71	Al_2O_3
Fe_2O_3	11.0	8.0	2.8	7.3	1.8	2.0	1.8	5.52	Fe_2O_3
FeO	2.0	5.2	7.2	5.3	9.7	9.1	10.5	1.19	FeO
MnO	0.06	0.21	0.28	0.11	0.18	0.18	0.18	0.05	MnO
MgO	1.20	4.81	5.85	2.48	5.30	5.37	4.09	2.56	MgO
CaO	0.00	1.93	3.96	0.55	4.83	7.04	4.00	0.69	CaO
Na_2O	1.9	2.6	3.5	1.0	2.2	2.4	3.1	0.68	Na_2O
K_2O	2.40	2.29	1.98	1.48	1.76	0.29	0.14	1.02	K_2O
P_2O_5	0.04	0.06	0.07	0.32	0.05	0.06	0.18	0.19	P_2O_5
H_2O	2.9	1.5	2.3	1.1	4.4	3.8	2.6	2.66	H_2O
S	0.00	2.9	4.8	0.2	4.1	3.8	3.8	0.00	S
CO_2								0.34	CO_2
OTHER								0.11	OTHER
O≡S									O≡S
TOTAL	99.79	98.13	98.14	98.20	98.93	99.67	100.55	100.45	TOTAL
Ni								60	Ni
Cr								258	Cr
Sc									Sc
Cu								15	Cu
Zn								54	Zn
Rb								27	Rb
Sr								90	Sr
Ba								340	Ba
Th									Th
U									U
Ta									Ta
Hf									Hf
Zr									Zr
Y									Y
La									La
Ce									Ce
Nd									Nd
Sm									Sm
Eu									Eu
Tb									Tb
Dy									Dy
Yb									Yb
Lu									Lu
FeO^*	11.90	12.40	9.72	11.87	11.32	10.90	12.12	6.16	FeO^*

208-214 Samples form traverse across 20 m thick regolith beneath the Missi Group and developed on Amisk Group aphyric basalt (unit 7). Samples collected by D. Price, analyzed by the Geological Survey of Canada in Ottawa, and reported by Goetz (1980). Depths of samples below Amisk-Missi contact as follows:

208 -- 2 m

209 -- 2.5 m

210 -- 6 m

211 -- 10 m

212 -- 8 m

213 -- 20 m

214 -- 30 m

215 2352-C1 Mauve-weathering Missi Group pebbly sandstone (unit 50mb), Scotty Lake.

MAPS
NOT
FILMED

CARTES
OMISES